IMMUNE CELL MIGRATION IN HEALTH AND DISEASE

EDITED BY: Hélène D. Moreau, Jörg Renkawitz and Emmanuel Donnadieu
PUBLISHED IN: Frontiers in Immunology

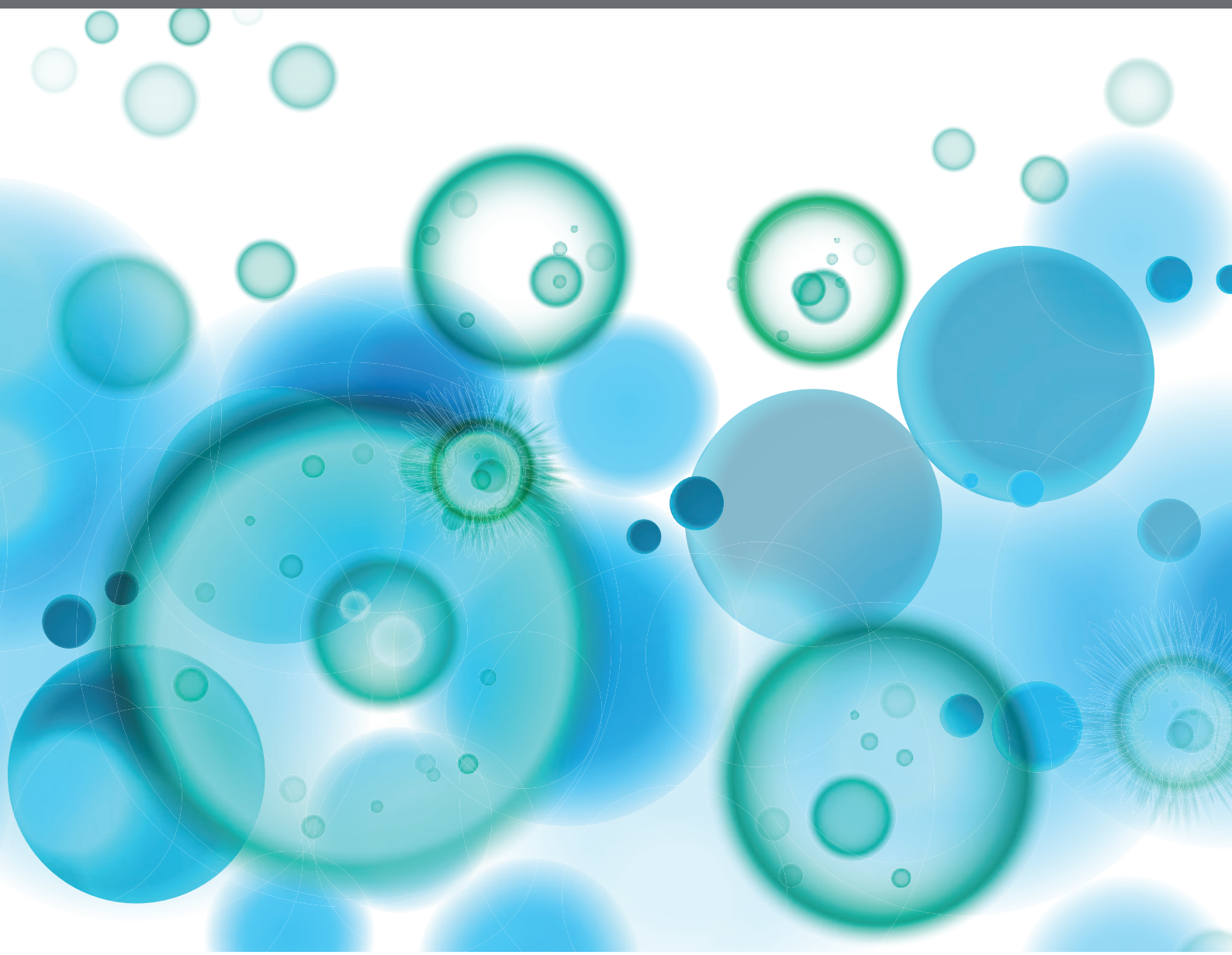

frontiers Research Topics

ISSN 1664-8714
ISBN 978-2-88976-088-6
DOI 10.3389/978-2-88976-088-6

About Frontiers

Frontiers is more than just an open-access publisher of scholarly articles: it is a pioneering approach to the world of academia, radically improving the way scholarly research is managed. The grand vision of Frontiers is a world where all people have an equal opportunity to seek, share and generate knowledge. Frontiers provides immediate and permanent online open access to all its publications, but this alone is not enough to realize our grand goals.

Frontiers Journal Series

The Frontiers Journal Series is a multi-tier and interdisciplinary set of open-access, online journals, promising a paradigm shift from the current review, selection and dissemination processes in academic publishing. All Frontiers journals are driven by researchers for researchers; therefore, they constitute a service to the scholarly community. At the same time, the Frontiers Journal Series operates on a revolutionary invention, the tiered publishing system, initially addressing specific communities of scholars, and gradually climbing up to broader public understanding, thus serving the interests of the lay society, too.

Dedication to Quality

Each Frontiers article is a landmark of the highest quality, thanks to genuinely collaborative interactions between authors and review editors, who include some of the world's best academicians. Research must be certified by peers before entering a stream of knowledge that may eventually reach the public - and shape society; therefore, Frontiers only applies the most rigorous and unbiased reviews.
Frontiers revolutionizes research publishing by freely delivering the most outstanding research, evaluated with no bias from both the academic and social point of view. By applying the most advanced information technologies, Frontiers is catapulting scholarly publishing into a new generation.

What are Frontiers Research Topics?

Frontiers Research Topics are very popular trademarks of the Frontiers Journals Series: they are collections of at least ten articles, all centered on a particular subject. With their unique mix of varied contributions from Original Research to Review Articles, Frontiers Research Topics unify the most influential researchers, the latest key findings and historical advances in a hot research area! Find out more on how to host your own Frontiers Research Topic or contribute to one as an author by contacting the Frontiers Editorial Office: frontiersin.org/about/contact

IMMUNE CELL MIGRATION IN HEALTH AND DISEASE

Topic Editors:
Hélène D. Moreau, INSERM U932 Immunité et Cancer, France
Jörg Renkawitz, Ludwig Maximilian University of Munich, Germany
Emmanuel Donnadieu, Institut National de la Santé et de la Recherche Médicale (INSERM), France

Citation: Moreau, H. D., Renkawitz, J., Donnadieu, E., eds. (2022). Immune Cell Migration in Health and Disease. Lausanne: Frontiers Media SA.
doi: 10.3389/978-2-88976-088-6

Table of Contents

frontiers | Frontiers in Immunology

EDITORIAL
published: 13 April 2022
doi: 10.3389/fimmu.2022.897626

Editorial: Immune Cell Migration in Health and Disease

Jörg Renkawitz[1], *Emmanuel Donnadieu*[2] *and Hélène D. Moreau*[3*]

[1] Biomedical Center (BMC), Walter Brendel Center of Experimental Medicine, Institute of Cardiovascular Physiology and Pathophysiology, Klinikum der Universität, Ludwig-Maximilians University (LMU) Munich, Munich, Germany, [2] Université de Paris, Institut Cochin, INSERM, CNRS, Paris, France, [3] Institut Curie, PSL University, Inserm U932, Immunity and Cancer, Paris, France

Keywords: cell migration, cytoskeleton, adhesion, monocytes, macrophages, neutrophils, T cells, dendritic cells

Editorial on the Research Topic

Immune Cell Migration in Health and Disease

Migration of immune cells is essential to virtually every step of their surveillance function (1–6). In this Research Topic, we gather reviews and original research articles that emphasize the wide variety of both physiological and pathological contexts in which immune cell migration is either favored or impeded and exemplify the latest mechanistic insights in immune cell migration.

The surveillance function of immune cells requires both long-range patrolling throughout the body and local scanning of cells and molecular cues in tissues. For long-distance displacement, immune cells take advantage of the systemic blood and lymphatic circulation. Importantly, in the circulation, immune cells are also ensuring vessels integrity but how they detect anomalies and restore homeostasis remains poorly understood. In this Research Topic, Moreno-Cañadas et al. propose that intravascular crawling monocytes are switching from random migration to Levy-like motility upon detection of damaged endothelium. This motility mode alternates between fast & directed and slow & random migration phases, which enhances local patrolling. Interestingly, this type of motility has been previously reported as an optimal search strategy for T cells in infected brains (7). Adaptation of migratory behavior to local context in both health and disease is a common feature of immune cells. Tomas et al. review how the trafficking of monocytes and macrophages in arteries is altered during atherosclerosis as well as their contribution to return to homeostasis, highlighting the dual role of macrophages in both establishment and regression of the plaque. The role of immune cell circulation and adhesion to damaged vessels in disease onset is also illustrated in this topic by Morikis et al., who review the implication of neutrophils in vaso-occlusive crisis in sickle cell disease. Uncovering the molecular mechanisms linking immune cell migration and disease onset can help foster new therapeutic strategies, as suggested by these two reviews.

Exiting the systemic circulation requires immune cells to first detect exit signals, then adhere, roll and transmigrate from the circulation to the tissue interstitium (8). These processes are known to depend on integrin activation and conformational changes, but how integrin activation is fine-tuned remains to be fully understood (9, 10). Bromberger et al. investigate the role of the Rap1 and Riam pathways, converging to Talin1, on β2 integrin-mediated rolling, adhesion and emigration of leukocytes. After transmigration, immune cells crawl under the endothelium before diving into the interstitial tissue. Arts et al. focus on this poorly-investigated step of immune cell migration and show that focal adhesions are avoided by neutrophils, hence determining their path underneath the epithelium.

Edited and reviewed by:
Francesca Granucci, University of Milano-Bicocca, Italy

****Correspondence:***
Hélène D. Moreau
helene.moreau@curie.fr

Specialty section:
This article was submitted to Molecular Innate Immunity, a section of the journal Frontiers in Immunology

Received: *16 March 2022*
Accepted: *25 March 2022*
Published: *13 April 2022*

Citation:
Renkawitz J, Donnadieu E and Moreau HD (2022) Editorial: Immune Cell Migration in Health and Disease. Front. Immunol. 13:897626. doi: 10.3389/fimmu.2022.897626

Cues to exit the circulation and enter the interstitium are not only delivered by the vessels but also by the tissue calling for help. SenGupta et al. here review the secretome of cancer cells and its importance in triggering neutrophil invasion. Understanding how this secretome is generated and how neutrophils integrate the different cues to migrate could open new therapeutic options. Once in the tissue, the environment could drastically impact immune cell migration and function. This is particularly the case in tumors, where the stroma negatively modulates dendritic cell migration hence dampening T cell antitumoral activities, as reviewed by Gupta et al.

As evidenced in this topic, immune cells are facing highly distinct environments during their migratory journey throughout the organism. Yet a common denominator emerges, from hematopoiesis in primary lymphoid organs, to homing and local patrolling in secondary lymphoid organs and peripheral tissues. The extracellular cues of the tissue environment are finely integrated by immune cells through the actin cytoskeleton that controls their migration patterns. Kamnev et al. review how the study of immune actinopathies has contributed to our understanding of immune cell migration at the organism, tissue, cellular and molecular levels, highlighting the central role of the actin cytoskeleton and its regulators. The actin-related protein Arp2/3 complex is implicated in the coordination of migration and environment sensing in many different immune cell types (11–16). Investigating neutrophils from immunodeficiency patients with mutations in the Arp2/3 subunit ARPC1B, Kempers et al. here provide evidence for a differential role of ARPC1B in transmigration under flow shear stress and during interstitial human neutrophil migration. But actin is not the only important player, and the fine regulation of immune cell migration also lies in its interplay with the microtubule network. In this topic, Fazil et al. report the role of Glycogen synthase kinase 3β in T cell motility through interactions with the cytoskeletal regulator CRMP2.

Another important question addressed in this Research Topic is how very diverse extracellular cues are integrated by immune cells to turn on their cytoskeleton? Harcha et al. propose the pannexin channels as central sensors for both physical and chemical signals during inflammation. Having common receptors for distinct cues and converging signaling pathways could facilitate integration of information by immune cells.

Reviews and original articles in this Research Topic illustrate how advances in imaging microscopy over the last 20 years have shed light on the complex behavior of immune cells *in vivo* and contributed to our better understanding of molecular mechanisms underlying immune cell migration. Yet, a lot remains to be investigated and new models are a never-ending demand. First, primary immune cells present some limitations for mechanistic studies, as they may not survive well *in vitro*, or may not be amenable for genetic engineering. Uetz-von Allmen et al. propose a human neoplastic cell line CAL-1 as a good proxy for human dendritic cell signaling and migration. On the other hand, "just" observing cells is no longer sufficient to uncover molecular mechanisms underlying immune cell migration. The opto-genetic revolution offers new tools to fine-tune molecular activity that will be instrumental for deeper investigation. Amitrano et al. develop such a tool based on light stimulation to remotely control mitochondria activity and take advantage of it to reveal the role of mitochondrial ATP-production in CD8 T cell migration and function.

This Research Topic stresses the importance of better understanding immune cell migration in health and disease. A lot is known but a lot remains to be understood. Gaining mechanistic insights in the different physio-pathological contexts will open new avenues for innovative therapeutic strategies.

AUTHOR CONTRIBUTIONS

HM wrote the first draft of the editorial. JR and ED edited the manuscript. All authors contributed to the article and approved the submitted version

FUNDING

HM is supported by the program "Investissements d'Avenir" launched by the French Government and Agence Nationale de la Recherche (ANR-20-CE15-0023 *InfEx*). ED is supported by the French Ligue Nationale contre le Cancer (Equipes labellisées). JR is supported by the Stiftung Experimentelle Biomedizin (Peter Hans Hofschneider Professorship), the LMU Institutional Strategy LMU-Excellent within the framework of the German Excellence Initiative, and the Deutsche Forschungsgemeinschaft (DFG; German Research Foundation; Collaborative Research Center SFB914, project A12; Priority Programme SPP2332, project 492014049).

ACKNOWLEDGMENTS

The authors would like to thank all contributors of this research topic as well as the reviewers for their insightful comments.

REFERENCES

1. Nourshargh S, Hordijk PL, Sixt M. Breaching Multiple Barriers: Leukocyte Motility Through Venular Walls and the Interstitium. *Nat Rev Mol Cell Bio* (2010) 11:366–78. doi: 10.1038/nrm2889
2. Girard J-P, Moussion C, Förster R. HEVs, Lymphatics and Homeostatic Immune Cell Trafficking in Lymph Nodes. *Nat Rev Immunol* (2012) 12:762–73. doi: 10.1038/nri3298
3. Lämmermann T, Germain RN. The Multiple Faces of Leukocyte Interstitial Migration. *Semin Immunopathol* (2014) 36:227–51. doi: 10.1007/s00281-014-0418-8
4. Moreau HD, Piel M, Voituriez R, Lennon-Duménil A-M. Integrating Physical and Molecular Insights on Immune Cell Migration. *Trends Immunol* (2018) 39:632–43. doi: 10.1016/j.it.2018.04.007
5. Kameritsch P, Renkawitz J. Principles of Leukocyte Migration Strategies. *Trends Cell Biol* (2020) 30:818–32. doi: 10.1016/j.tcb.2020.06.007

6. Donnadieu E, Dupré L, Pinho LG, Cotta-de-Almeida V. Surmounting the Obstacles That Impede Effective CAR T Cell Trafficking to Solid Tumors. *J Leukocyte Biol* (2020) 108:1067–79. doi: 10.1002/jlb.1mr0520-746r
7. Harris TH, Banigan EJ, Christian DA, Konradt C, Tait Wojno ED, Norose K, et al. Generalized Lévy Walks and the Role of Chemokines in Migration of Effector CD8+ T Cells. *Nature* (2012) 486(7404):545–8. doi: 10.1038/nature11098
8. Vestweber D. How Leukocytes Cross the Vascular Endothelium. *Nat Rev Immunol* (2015) 15:692–704. doi: 10.1038/nri3908
9. Sun Z, Costell M, Fässler R. Integrin Activation by Talin, Kindlin and Mechanical Forces. *Nat Cell Biol* (2019) 21:25–31. doi: 10.1038/s41556-018-0234-9
10. Margadant C, Monsuur HN, Norman JC. Sonnenberg, A. Mechanisms of Integrin Activation and Trafficking. *Curr Opin Cell Bio* (2011) 23(5):607-14. doi: 10.1016/j.ceb.2011.08.005
11. Thiam H-R, Vargas P, Carpi N, Crespo CL, Raab M, Terriac E, et al. Perinuclear Arp2/3-Driven Actin Polymerization Enables Nuclear Deformation to Facilitate Cell Migration Through Complex Environments. *Nat Commun* (2016) 7:10997. doi: 10.1038/ncomms10997
12. Leithner A, Eichner A, Müller J, Reversat A, Brown M, Schwarz J, et al. Diversified Actin Protrusions Promote Environmental Exploration But are Dispensable for Locomotion of Leukocytes. *Nat Cell Biol* (2016) 18:1253–9. doi: 10.1038/ncb3426
13. Vargas P, Maiuri P, Bretou M, Sáez PJ, Pierobon P, Maurin M, et al. Innate Control of Actin Nucleation Determines Two Distinct Migration Behaviours in Dendritic Cells. *Nat Cell Biol* (2016) 18:43–53. doi: 10.1038/ncb3284
14. Fritz-Laylin LK, Riel-Mehan M, Chen B-C, Lord SJ, Goddard TD, Ferrin TE, et al. Actin-Based Protrusions of Migrating Neutrophils are Intrinsically Lamellar and Facilitate Direction Changes. *Elife* (2017) 6:e26990. doi: 10.7554/elife.26990
15. Rotty JD, Brighton HE, Craig SL, Asokan SB, Cheng N, Ting JP, et al. Arp2/3 Complex Is Required for Macrophage Integrin Functions But Is Dispensable for FcR Phagocytosis and *In Vivo* Motility. *Dev Cell* (2017) 42:498–513.e6. doi: 10.1016/j.devcel.2017.08.003
16. Stahnke S, Döring H, Kusch C, de Gorter DJJ, Dütting S, Guledani A, et al. Loss of Hem1 Disrupts Macrophage Function and Impacts Migration, Phagocytosis, and Integrin-Mediated Adhesion. *Curr Biol* (2021) 31 (10):2051–64.e8. doi: 10.1016/j.cub.2021.02.043

Conflict of Interest: The authors declare that the research was conducted in the absence of any commercial or financial relationships that could be construed as a potential conflict of interest.

Publisher's Note: All claims expressed in this article are solely those of the authors and do not necessarily represent those of their affiliated organizations, or those of the publisher, the editors and the reviewers. Any product that may be evaluated in this article, or claim that may be made by its manufacturer, is not guaranteed or endorsed by the publisher.

frontiers in Immunology

REVIEW
published: 28 April 2021
doi: 10.3389/fimmu.2021.663886

Targeting Neutrophil Adhesive Events to Address Vaso-Occlusive Crisis in Sickle Cell Patients

Vasilios A. Morikis[1], *Alfredo A. Hernandez*[1], *John L. Magnani*[2], *Markus Sperandio*[3] *and Scott I. Simon*[1]*

[1] Department of Biomedical Engineering, University of California-Davis, Davis, CA, United States, [2] GlycoMimetics Inc., Rockville, MD, United States, [3] Institute for Cardiovascular Physiology and Pathophysiology, Walter Brendel Center for Experimental Medicine Biomedical Center, Ludwig Maximilians University, Walter Brendel Center, Munich, Germany

Neutrophils are essential to protect the host against invading pathogens but can promote disease progression in sickle cell disease (SCD) by becoming adherent to inflamed microvascular networks in peripheral tissue throughout the body. During the inflammatory response, leukocytes extravasate from the bloodstream using selectin adhesion molecules and migrate to sites of tissue insult through activation of integrins that are essential for combating pathogens. However, during vaso-occlusion associated with SCD, neutrophils are activated during tethering and rolling on selectins upregulated on activated endothelium that line blood vessels. Recently, we reported that recognition of sLe^x on L-selectin by E-selectin during neutrophil rolling initiates shear force resistant catch-bonds that facilitate tethering to endothelium and activation of integrin bond clusters that anchor cells to the vessel wall. Evidence indicates that blocking this important signaling cascade prevents the congestion and ischemia in microvasculature that occurs from neutrophil capture of sickled red blood cells, which are normally deformable ellipses that flow easily through small blood vessels. Two recently completed clinical trials of therapies targeting selectins and their effect on neutrophil activation in small blood vessels reveal the importance of mechanoregulation that in health is an immune adaption facilitating rapid and proportional leukocyte adhesion, while sustaining tissue perfusion. We provide a timely perspective on the mechanism underlying vaso-occlusive crisis (VOC) with a focus on new drugs that target selectin mediated integrin adhesive bond formation.

Keywords: vaso-occlusion crises, neutrophil, selectin, integrins, sickle cell disease

OPEN ACCESS

Edited by:
Emmanuel Donnadieu, Institut National de la Santé et de la Recherche Médicale (INSERM), France

Reviewed by:
Lubka T. Roumenina, INSERM U1138 Centre de Recherche des Cordeliers (CRC), France
Rostyslav Bilyy, Danylo Halytsky Lviv National Medical University, Ukraine

***Correspondence:**
Scott I. Simon
sisimon@ucdavis.edu

Specialty section:
This article was submitted to Molecular Innate Immunity, a section of the journal Frontiers in Immunology

Received: *03 February 2021*
Accepted: *29 March 2021*
Published: *28 April 2021*

Citation:
Morikis VA, Hernandez AA, Magnani JL, Sperandio M and Simon SI (2021) Targeting Neutrophil Adhesive Events to Address Vaso-Occlusive Crisis in Sickle Cell Patients. Front. Immunol. 12:663886. doi: 10.3389/fimmu.2021.663886

INTRODUCTION

Sickle cell disease (SCD) is an inherited disease characterized by defects in hemoglobin that distorts red blood cells (RBC) into a "sickle" shape (1–3). Clinical manifestations common to this inherited hemoglobinopathy, chronic hemolysis, and erythrocyte adhesion that can lead to vaso-occlusion (4). Vaso-occlusive crisis (VOC) is defined by clinical episodes of severe ischemic pain due to lack of blood flow resulting in cumulative and irreversible organ damage. As such, the occurrence of VOC

is a serious clinical event that is responsible for the increased morbidity and mortality of sickle cell patients. The clinical sequalae associated with VOC often manifests in episodes of pain that vary in intensity and duration as a function of patient comorbidities such as diabetes. Some patients experience only infrequent pain crises each year, while others require acute hospitalization for treatment. Pain management during VOC often includes the prescription of opioids that, while effectively diminishing pain, do not treat the root cause and therefore do not significantly lower the risk of a catastrophic clinical event (5). Thus, treatments to prevent genesis of VOC as opposed to pain management is a primary challenge for scientists aiming to establish effective treatments that target the initiation and block progression (6). In this perspective we review the recent studies highlighting the importance of neutrophil inflammatory recruitment and the role of selectin and integrin adhesive receptors in progression to clinical crisis. We endeavor to illuminate the lessons learned from preclinical studies in mouse models of SCD and how they apply to human disease in order to evaluate the outcome of recent clinical trials that target neutrophil recruitment.

The etiology of VOC involves the innate immune response that enables white blood cells (WBC) predominantly neutrophils to capture on adhesive receptors upregulated on inflamed endothelium. Captured neutrophils become activated during interaction with endothelium at sites of inflamed microvasculature leading to upregulation of additional adhesion molecules on the plasma membrane that serve to recruit additional circulating cells, such as sickle RBC (sRBC) and platelets that aggregate causing rapid occlusion of the microvasculature leading to vessel ischemia (**Figure 1**) (2, 7, 8). Contributing to microvascular occlusion is a greater capacity for neutrophil extracellular trap (NET) formation characterized by decondensed chromatin enriched in citrullinated histones and bound to granular enzymes (9). The pathophysiology and requirement for pain management directly associated with VOC in patients has been extensively reviewed (2, 4, 6, 10, 11). As such, the focus of this review is to highlight the role of neutrophils in the initiation and propagation of VOC, as well as targeted pharmacological interventions against adhesion molecules critical for neutrophil recruitment and heterotypic adhesion with other blood cells during flow within vessels.

Neutrophil capture on inflamed endothelium is initiated by Sialyl Lewis^x (sLe^x) bearing selectin ligands on cells in flow (12–15). Ligand recognition by selectins is an early step in the inflammatory process mediating leukocyte rolling and platelet capture, as such selectins are a primary target for therapeutics to prevent propagation of VOC. Early studies on the specific role of cellular adhesion molecules that induce VOC were carried out in mice due to the availability of genetic knockout models of WBC adhesion *via* selectins and integrins. However, human and mouse genomes have diverged in the past 75 million years and as such selectin function differs between the mouse and human innate immune response (**Table 1**). While selectin targeting has been a major focus in designing VOC treatments,

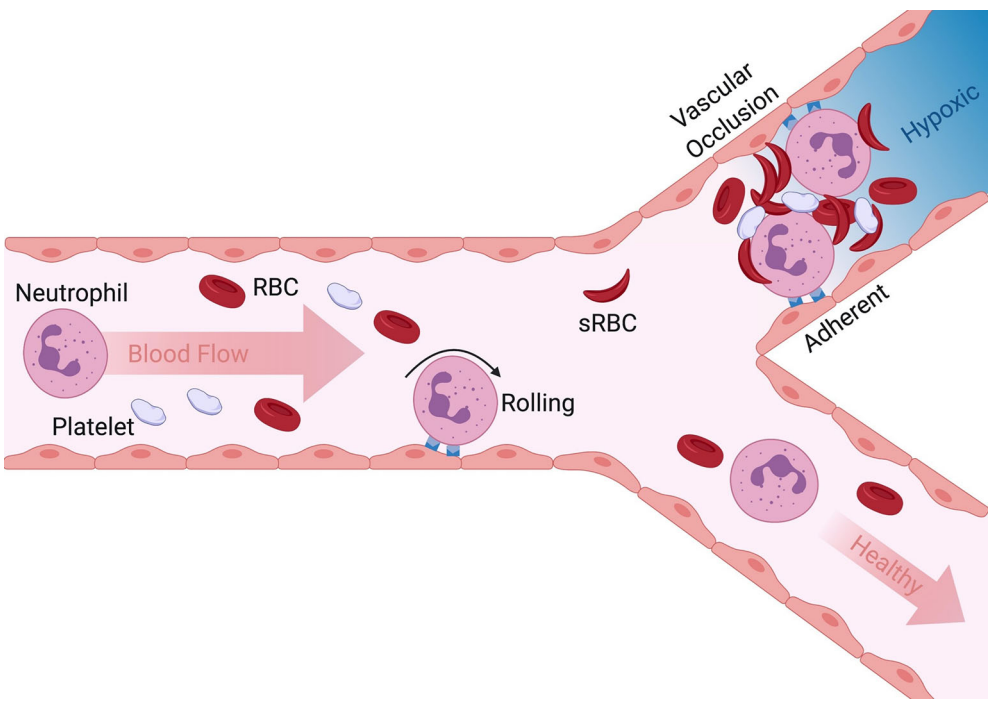

FIGURE 1 | Overview of initiation and progression of VOC in SCD. Neutrophil rolling to arrest on inflamed endothelium is a normal innate immune response to tissue injury. Adherent neutrophils can also capture sickle red blood cells and platelets in post capillary venules leading to vascular occlusion (upper bifurcation). Dramatic reduction in blood flow and lack of oxygen results in hypoxia, episodic painful and often leads to organ failure. When inappropriate neutrophil activation and adhesion is absent and secondary capture of RBC and platelets limited, the vasculature remains perfused and healthy (lower pathway).

TABLE 1 | Differences between mouse and human selectins.

	Human *versus* Mouse
E-selectin	Lectin domain homology: 72% (16) EGF domain homology 60% (17) Mice have a greater interdomain angle (more flexibility, better binding to sLex) (17) ESL-1 is not a functional E-selectin ligand in humans (18)
P-selectin	TNFa, IL1B and LPS increase P-selectin mRNA in mice but decrease it in humans (19)
L-selectin	Human E-selectin binds sLex on L-selectin (mouse L-selectin lacks fucosylation) (18) Fucosyltransferase 9 (FUT9) plays a key role in human L-selectin biosynthesis (20)

there is a need to better understand how selectins participate in precipitating neutrophil recruitment leading to VOC in more accurate models of human SCD in order to design informed therapeutic treatments.

SELECTIN FUNCTION AND BOND MECHANICS IN VASO-OCCLUSIVE CRISIS IN HUMANS

To understand the etiology of VOC in terms of the initiation and development of a congested microvascular bed, selectin function during neutrophil recruitment must be examined. In humans three selectins participate in forming stable but transient adhesive bonds with carbohydrate structures between cells in interactions characterized by fast kinetics that allow cell adhesion to proceed under the shear forces of blood flow (21, 22). Expression of endothelial E-selectin requires *de novo* protein synthesis, and is upregulated within hours of cytokine activation at inflamed sites experiencing disturbed blood flow or focal tissue insult (23, 24). P-selectin is preformed and stored in Weibel Palade Bodies (WPB) of endothelial cells and in α-granules of circulating platelets and is rapidly mobilized from these storage sites by merging with the plasma membrane where it participates in tethering and rolling of leukocytes and platelets on inflamed endothelium (25, 26). Leukocyte expressed L-selectin is a glycoprotein that not only binds sLe^x as its primary carbohydrate recognition motif expressed by PSGL-1 on neutrophils, but it also presents sLe^x to facilitate neutrophil homing and subsequent activation within inflamed venules (27, 28). E-selectin binding to sLe^x supports capture and rolling of human, but not murine neutrophils thereby providing a key event for subsequent mechanosignaling of integrin activation that mediates leukocyte arrest even in absence of chemokine signaling (29). Neutrophil homotypic adhesion is observed as secondary capture of a neutrophil from the blood stream by a rolling or arrested neutrophil *via* L-selectin binding of PSGL-1 between cells (**Figure 2A**) (29–31). While E-selectin and P-selectin both function in the early capture and adhesion of leukocytes to the vascular endothelium, there are some distinct differences. All selectins share a similar structure characterized by a lectin binding domain, epidermal growth factor domain, a variable number of short consensus repeats (9 for P-selectin, 6 for E-selectin, and 2 for L-selectin), a transmembrane domain, and a cytosolic tail (13). Despite the similarities in structure, the binding kinetics and capacity to form durable bonds that mechanotransduce activation of integrins are quite different (22, 32). P-selectin projects the furthest above the endothelial surface and is thought to provide the initial interaction between leukocytes in the free stream through recognition of PSGL-1, although it also can bind additional ligands including sulfated polysaccharides (33). However, P-selectin does not mechanotransduce activation of integrin on bound leukocytes in the same manner as E-selectin binding to L-selectin. E-selectin forms longer-lived shear resistant bonds with L-selectin compared with P-selectin, that is independent of recognition of its other cognate ligands (i.e. PSGL-1, CD44). L-selectin appears to be unique on human neutrophils due to its recognition by E-selectin and capacity to actively condense into bond clusters that mechanotransduce signals leading to β_2-integrin activation and adhesion (29). This function is attributed to E-selectin dependent formation of a high-affinity complex with sLe^x under precise hydrodynamic conditions to form a catch-bond with L-selectin (34). A molecular model of E-selectin binding sLe^x under tension predicts that it adopts an extended conformation, which was verified by small-angle X-ray scattering of it bound to purified ligand (34). Extended E-selectin/sLe^x complexes form shear resistant bonds characterized by adhesive lifetimes that are long lived (~ 500 msec) at sufficiently high hydrodynamic shear stress. Whereas at low shear rates (i.e. < 1 dyne/cm^2) associated with microvascular regions of slow blood flow and ischemia, adhesive bonds are less durable and dissociate more rapidly. This phenomenon is denoted catch-bond behavior (34–38). E-selectin binding to sLe^x results in co-localization of L-selectin and PSGL-1 on the trailing edge of neutrophils, a process associated with β_2-integrin activation and neutrophil arrest (26, 29). A stepwise process depicted in **Figure 2** illustrates how neutrophils tethered on endothelial P-selectin, may facilitate E-selectin and L-selectin to engage and mechanically signal cell activation and arrest. Selectins are a prime target for inhibition of the inflammatory response that initiates VOC, with the rationale that blocking the adhesive steps in the vaso-occlusive process will prevent propagation of congestion and decrease the duration and intensity of painful VOC in patients with SCD.[2]

The importance of selectins in VOC was rigorously studied by Hidalgo et. al., who first reported in a humanized sickle cell mouse model that E-selectin mediated activation of β_2-integrins at the leading edge of a neutrophil promotes transition from rolling to arrest in an inflamed microvascular bed (39). In this model of acute lethal VOC, a proinflammatory state was induced in post capillary venules by injection of tumor necrosis factor-α (TNF-α). This resulted in capture of sRBC by activated $\alpha_M\beta_2$ integrin (macrophage-1 antigen, Mac-1) clustered on the leading edge of arrested neutrophils. Genetic deletion of E-selectin ($Sele^{-/-}$) or P-selectin ($Selp^{-/-}$) provided equivalent inhibition of

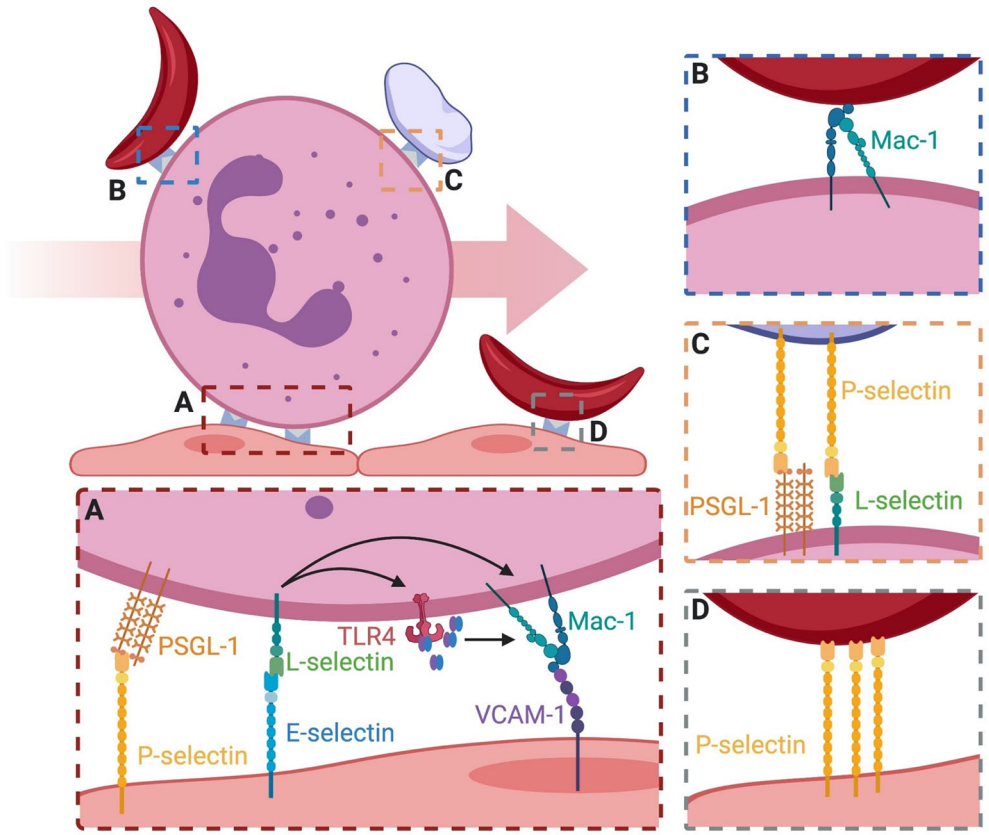

FIGURE 2 | Binding events that lead to vasculature occlusion on inflamed endothelium. **(A)** Neutrophil rolling is mediated by P-selectin and E-selectin binding PSGL-1 and L-selectin. Signaling through E-selectin/L-selectin bonds results in (1) release of MRP8/14 and endogenous activation of surface TLR4 which primes integrin for activation and (2) direct signaling of transition to a high-affinity integrin state capable of binding ligand. High affinity integrin is capable of stable bond formation to VCAM-1 and ICAM-1 on endothelial to mediate neutrophil arrest. **(B)** Secondary capture of sRBC to adherent neutrophils is mediated *via* Mac-1. The mechanism of capture is an active area of research. **(C)** Secondary capture of platelets to adherent neutrophils is mediated through platelet surface P-selectin and its binding to PSGL-1 and L-selectin. **(D)** Direct engagement of sRBC to the surface of endothelial cells has been attributed to P-selectin, similar to secondary capture *via* Mac-1.

neutrophil capture and reduced RBC/WBC aggregates at early time points within 3 hours of TNF-α stimulation. However, E-selectin knockouts exhibited reduced neutrophil arrest and RBC/WBC aggregates were undetected at later time points of 3-5 hours post stimulation. In contrast, P-selectin knockouts had a spike in the occurrence of RBC/WBC aggregates at 3-5 hours post TNF-α stimulation, resulting in VOC equivalent to control WT mice experiencing a VOC. Significant was the observation that E-selectin knockout mice maintained low levels of secondary capture of RBC that maintained higher rates of blood flow (39). One may conclude that inhibition of P-selectin effectively delayed VOC progression within the initial hours of an inflammatory insult, however, the presence of E-selectin that maintains expression on endothelium elicits sustained neutrophil-RBC recruitment that is responsible for long term VOC. Of note, another important difference between the human and the mouse system concerns the transcriptional regulation of P-selectin. While stimulation of endothelial cells with the proinflammatory cytokine TNF-α leads to the transcriptional upregulation of endothelial P-selectin in the mouse system, endothelial P-selectin expression is downregulated following stimulation with TNF-α in human microvasculature. This has been elegantly demonstrated in the TNF- α stimulated cremaster muscle of mice lacking mouse P-selectin, but expressing human P-selectin supporting the concept that P-selectin in humans might be less important in the pathogenesis of VOC progression than E-selectin (19).

E-selectin mediates recruitment by engaging L-selectin on human neutrophils during rolling which results in arrest *via* activation of LFA-1 to bind with ICAM-1 expressed on inflamed endothelium (29). Secondary capture of RBCs can also be observed in parallel plate flow channels that mimic the hydrodynamic conditions observed in normal versus inflamed microcirculation. In such a model, it was confirmed that human neutrophil capture and RBC/WBC heterotypic aggregates are enhanced in sickle cell patients (**Figure 2B**) (40). It is noteworthy that antibodies that block E-selectin mediated activation of Mac-1 on neutrophils, also blocks heterotypic RBC/WBC aggregation. This directly correlates with increased survival compared to isotype nonblocking control antibody (41). Platelet/WBC

aggregates are also significantly reduced in Mac-1 knockout mice during an induced VOC event in mice (41). Thus, both E-selectin and Mac-1 are implicated as primary capture molecules initiating and propagating VOC. However, β_2-integrins including Mac-1 and LFA-1 are not strategic targets for treatment of VOC in SCD, as leukocytes require these integrins to maintain immune surveillance and to combat infection. Complete blockade of integrin subunit function can be dangerous for high risk immunodeficient patients as realized in clinical trials of the CD11a blocker Efalizumab that was associated with viral meningitis and bacterial sepsis in a subset of patients, which triggered it's rapid withdrawal from the market in 2009 (42). Another strategy is to target selectins in order to reduce integrin activation and neutrophil capture. In this manner, integrin activation is maintained *via* alternate pathways such as by chemokine receptor ligation, thereby preserving neutrophil and T cell function necessary to combat infections.

There is evidence that soluble E-selectin levels in serum are higher in SCD patients than in healthy subjects and can increase further during acute VOC in SCD patients (43). Kato et al. measured the level of E-selectin, P-selectin, VCAM-1, and ICAM-1 in the plasma of 160 patients suffering from VOC over a four-year period (44). E-selectin, P-selectin, and the integrin ligand VCAM-1 were all significantly increased in patients suffering from SCD compared to controls. A significant finding was that patients with high levels of soluble E-selectin directly correlated with elevated risk of mortality, while those with high levels of soluble P-selectin did not significantly correlate with increased mortality. This implicates neutrophil binding to E-selectin as a primary means of Mac-1 activation and binding to its ligands as a predominant feature that drives neutrophil adhesion and progression of VOC.

E-selectin and P-selectin recognize a variety of ligands on the neutrophil plasma membrane. L-selectin and PSGL-1 are prominent among these since they can function not only to tether neutrophils to inflamed post capillary venules, but allow function as mechanosignaling receptors that activate rapid cell arrest *via* high affinity β_2-integrin bond formation in shear flow (12). Recruitment of human neutrophils on inflamed endothelium is supported by the preferential recognition of L-selectin by E-selectin and PSGL-1 by P-selectin, respectively (22, 45–47). Studies of neutrophil recruitment using vascular mimetic microfluidic channels under defined hydrodynamic shear on a substrate of recombinant E-selectin revealed that L-selectin and PSGL-1 co-localize into clusters on neutrophil microvilli and spontaneously activate β_2-integrin bond formation on ICAM-1 (48). Recently, it was reported that formation of catch-bonds between E-selectin and L-selectin effectively induce the extension of β_2-integrin that supports its binding to ICAM-1 during neutrophil deceleration that can prime the transition to a high-affinity state (29). A mechanism has been identified that involves the calcium-modulating proteins myeloid related protein-8 (MRP8) and MRP14 (also known as MRP8/14, S100A8/S100A9, and calprotectin). MRP8/14 can modulate myeloid cell function by binding Toll-like receptor-4 to induce calcium signaling and cytoskeletal reorganization (49–51). A complex of MRP8/14 released from leukocytes in mouse and human models of SCD are known to contribute to vascular inflammation and tissue injury. Supporting such a mechanism is the observation that MRP8/14-/- mice exhibited reduced neutrophil accumulation and lesion severity, implicating it in regulation of neutrophil recruitment (52). This mechanism is associated with acute inflammation, as neutrophils captured on E-selectin secrete MRP8/14 which then binds TLR4 on the same cell to initiate integrin extension (29, 49). Blocking TLR4 binding by treatment with antibody, or inhibiting E-selectin/L-selectin bond formation under shear by addition of the sLe^x mimetic Rivipansel, blocked the release of MRP8/14 and significantly reduced integrin extension and transient bond formation with ICAM-1 (29). These data reveal a pathway by which E-selectin/L-selectin bonds induce the release of MRP8/14 that bind TLR4 and in an autocrine manner signal conformational extension of LFA-1. This along with signaling *via* engaged and clustered L-selectin promotes long-lived high-affinity integrin bonds and the efficient arrest of rolling neutrophils in the microcirculation (22, 45, 53). This early step in the multistep process of neutrophil recruitment facilitates deceleration *via* E-selectin mediated rolling that upregulates high-affinity LFA-1 and subsequently Mac-1. When blocked with small molecule antagonists or anti-L-selectin antibody, LFA-1/Mac-1 mediated neutrophil recruitment and secondary capture observed in VOC is prevented (**Figures 2A, B**).

While E-selectin and P-selectin mediate the capture of individual neutrophils, it is important to highlight heterotypic adhesive interactions in the genesis of VOC. Secondary capture of free-flowing neutrophils, platelets and erythrocytes with adherent WBC are implicated in various disease states such as atherosclerotic plaque formation and VOC (54, 55). Homotypic neutrophil-neutrophil adhesion is mediated by L-selectin on one cell and PSGL-1 on the adjacent cell (**Figures 2B, C**). This results in strings of rolling neutrophils aligned along the direction of shear flow, which is thought to be relevant in the pathogenesis of VOC. Cell aggregation leading to microvascular congestion is also mediated by neutrophil-platelet interactions. Activated platelets express P-selectin and can bind free flowing neutrophils, thereby amplifying the surface area and the likelihood of capture on inflamed endothelium or on adherent neutrophils (**Figure 2C**) (56, 57). Adherent platelets help orchestrate diapedesis of neutrophils by Mac-1 binding to platelet GPIIb/IIIa in a fibrinogen dependent manner (58). Cellular crosstalk between platelet P-selectin binding to neutrophil PSGL-1 and Mac-1/fibrinogen/GPIIb/IIIa supports the efficient trafficking of neutrophils to sites of inflammation. Taken together, this implicates Mac-1 and P-selectin as adhesion receptors that may play a central role in the heterotypic platelet adhesive events that occur downstream of E-selectin in the progression of VOC. While the importance of selectins and their ligands cannot be overstated, there are key differences in function between human and mouse models that must be appreciated in order to efficiently develop effective therapeutics to prevent VOC.

OF MICE AND MEN, WHAT ARE THE LESSONS FOR TREATMENT OF VOC

Much of the knowledge base surrounding E-selectin function stems from transgenic mouse models, which indicate that rolling *via* PSGL-1 elicits a distinct mechanosignal that leads to integrin mediated neutrophil arrest. A key difference in mouse E-selectin ligands versus humans stems from fucosyltransferase-9/7 function, which is critical for assembly of the ligands that decorate glycoproteins supporting neutrophil rolling on E-selectin in human microvasculature, but not mice (**Table 1**) (18–20). These fucosyltransferases function to modify O- and N-linked carbohydrates on L-selectin to express the E-selectin ligand sLe^x (18, 20, 59). This adaption in humans enables the sLe^x on L-selectin to be recognized by E-selectin directly, which does not occur for mouse L-selectin. The observation that mouse E-selectin plays a critical role in mechanosignaling during rolling in inflamed venules is accounted for by the finding that recognition of sLe^x on PSGL-1 results in its co-clustering with L-selectin, which in turn elicits outside-in signaling of integrin activation (27). Knockout mice lacking L-selectin do not possess the capacity for direct outside-in signaling of integrin activation, yet they can still roll *via* endothelial selectins. This difference between human and mouse E-selectin ligands may account for the spontaneous vaso-occlusion observed in humans and not mouse microvasculature (60). It is clear that in humans the E-selectin/L-selectin signaling complex represents a primary step in neutrophil adhesion even in the absence of cytokine or chemokine. Targeting this mechanosignaling pathway by antagonizing selectin catch-bond formation could provide a strategic tipping point for therapeutic targets to prevent development of VOC in SCD patients.

Another difference in the regulation of selectin expression between mouse and humans consists in downregulation of human and upregulation of mouse P-selectin expression during TNF-α stimulated inflammation (19). Evidence supporting a primary role for P-selectin in SCD was demonstrated in a mouse model lacking P-selectin that showed a protective effect in pulmonary VOC (61). To further illuminate the contribution of P-selectin in human VOC, the next logical step would be to generate sickle cell mice lacking mouse P-selectin but edited to express human P-selectin. Such a hybrid mouse line could be used to reveal a species difference in P-selectin function.

TARGETED THERAPEUTICS AGAINST LEUKOCYTE AND PLATELET ACTIVATION IN VASO-OCCLUSIVE CRISIS

Mouse models of SCD have been indispensable for dissecting the molecular determinants of cytokine driven and selectin mediated vascular congestion, including to test selectin targeted drug treatments (16, 62). In the case of the small molecule sLe^x mimetic Rivipansel® (GMI-1070), we tested its capacity to antagonize the rolling and activation of neutrophils in blood over time of treatment in a Phase-3 clinical trial for treatment of VOC (29). Employing real-time immunofluorescence imaging of neutrophils in microfluidic channels, we examined the molecular dynamics of selectin-ligand receptor engagement during the transition from cell tethering and rolling to arrest on recombinant E-selectin and ICAM-1 *ex-vivo*. Rivipansel was found to block E-selectin recognition of sLe^x on L-selectin and antagonize the formation of catch-bonds and outside-in signaling of integrin mediated cell arrest in human SCD patient blood. GSnP-6, a novel PSGL-1 mimetic that blocks its recognition by E-selectin and P-selectin, effectively doubled the rolling velocity of neutrophils, but had no effect on L-selectin outside-in signaling of β_2-integrin or the frequency of neutrophil rolling to arrest (29, 63). This differential glycomimetic inhibition of neutrophil rolling versus outside-in activation of integrins *via* selectins reveals a novel mechanosignaling circuit. E-selectin transmitted tension on L-selectin induces clustering and signaling within sites of focal adhesion, which is markedly different than that observed in mouse neutrophils. PSGL-1 is the primary ligand for E-selectin mediated rolling in mouse as compared with L-selectin on human neutrophils. To determine the therapeutic efficacy of antagonists directed at sLe^x recognition by selectins in treatment of VOC, humanized P-selectin mouse models and/or *ex-vivo* assays could be used to quantify MRP8/14 release and TLR4 signaling of integrin activation.

Improving patient quality of life through preventative treatments of VOC occurrence or decreasing the time to crisis resolution are critical goals for long-term care of patients with SCD. Current standards for clinical treatment serve to modify the pathobiology of the disease through blood transfusions and dosing with hydroxyurea which serves to increase circulating Fetal Hemoglobin (HbF) and diminish the polymerization of intracellular sickle cell hemoglobin (HbS) in adults and pediatric populations (59, 60, 63–66). Studies by Frenette et al. demonstrated the importance of elevated plasma heme in a humanized SCD mouse model. In fact, unstimulated neutrophils isolated from SCD patients rapidly begin forming NETs compared to almost no NET formation in age-matched healthy controls, even when under treatment with hydroxyurea (67). This elevated level of heme induces arrested neutrophils to release NETs that have been associated with hypothermia and rapid death. Modulation of plasma heme does alter the NET release and subsequent survival in this mouse model, leaving the underlying issue of the role of elevated neutrophil arrest efficiency and the onset of vaso-occlusion (8, 9). While allogenic hematopoietic stem cell transplants (HSCT) and gene therapies are currently under investigation for their potential long-term curative effects by reversing the defect in hemoglobin function, these have proven to be costly and currently have limited availability for wide spread treatment of SCD.

Activated platelets contribute to vaso-occlusion by participating in intercellular adhesion leading to formation of cell aggregates (6, 10). Pharmacological inhibition of platelet activation has been achieved using receptor antagonists of P2Y12R, the chemoreceptor involved in ADP-stimulated activation of platelets including platelet degranulation (41, 68). Clinical assessment of P2Y12R antagonists including Prasugrel

and Ticagrelor have shown limited efficacy in adolescents and young adults with modest reduction of platelet activity and frequency of VOC (69, 70). These interventions have been ineffective in decreasing the frequency of pediatric VOC, pointing to a more significant role for platelet function on the occurrence of VOC in young adults. Directly targeting platelet adhesion through blocking GPIIbIIIa *via* administration of eptifbatide has been evaluated in a small cohort of subjects undergoing VOC (71). Treatment with eptifbatide did not diminish time to VOC resolution, but did successfully inhibit platelet and leukocyte aggregation, release into circulation, as well as diminished surface expression of P-selectin and serum measures of inflammation such as CD40L, sVCAM-1, sICAM-1, sICAM-3, MIP1α, and TNFα (71, 72).

Current reports link activation of the anaphylatoxin complement- C5a that activates neutrophils, platelets and endothelial cells with induction of vaso-occlusion in SCD mice (73). Blocking P-selectin inhibits C5a-induced vaso-occlusion in liver and skin venules of SCD mice. Moreover, blocking receptor binding with antibody targeting the C5a receptor antagonizes upregulation of endothelial adhesion molecules including VCAM-1, ICAM-1, and E-selectin in liver and lungs. It is noteworthy that a P-selectin deficient SCD mouse model revealed that chronic P-selectin deficiency attenuated liver ischemia but did not resolve cellular senescence and reduced epithelial cell proliferation necessary to maintain hepatic homeostasis (74). Complement from human sera has also been shown to stimulate expression of E-selectin in porcine endothelial cells (75). Likewise, the most abundant enzyme of the complement pathway, MASP-1 induced expression of TNFα, and upregulation of E-selectin on microvascular endothelium (76). Complement activation leads to venous thrombosis, an alternate mechanism driving vaso- occlusion. Interestingly, E-selectin plays a dominant role in venous thrombosis and a specific and potent antagonist of E-selectin adhesive function (GMI-1271; Uproleselan) blocks venous thrombosis, without the need to infuse anti-coagulants such as heparin (77, 78). In addition, blocking E-selectin with Uproleselan also inhibited deep venous thrombosis in a non-human primate model and showed efficacy in treating 2 patients in a case study of calf vein thrombosis (77, 79). Taken together, it appears that complement activation is a viable target to alleviate acute P-selectin and E-selectin dependent mechanisms of microvasculature inflammation that include thrombosis, but may not provide a long-term solution in context of preserving vital organ function.

Numerous anti-adhesive therapies that target RBC-endothelial and leukocyte-endothelial interactions have been completed or are undergoing clinical trials (**Table 2**). Of these, selectin mediating leukocyte and erythrocyte adhesion to the endothelium are prominent targets to limit vaso-occlusion in SCD patients (80–82). Improvement to time of VOC resolution or delay in first incidence of VOC appears to be a common efficacious event in pharmacological inhibitors of selectin binding, such as Rivipansel (5, 83), unfractionated heparin (84, 85), intravenous immunoglobulin (86, 87), and Crizanlizumab (88). Of these, Crizanlizumab® which inhibits P-selectin binding to PSGL-1 currently has completed clinical trials in adults and has the most ongoing trials to assess efficacy in pediatric populations as well as subjects with non-HbSS genotypes (**Table 2**). High dose (5 mg/mL) Crizanlizumab resulted in significant diminishment of the rate of crisis per year and delayed mean time to first or secondary crisis in adults (88). There was, however, no detectable difference in cell hemolysis suggesting that treatment with Crizanlizumab only serves to modify cell adhesion, but not to completely diminish patient systemic inflammation. Antagonism of E-selectin for treatment of VOC using the small molecule Rivipansel did not initially meet the Phase III clinical endpoint of time to readiness for patient discharge. However, subsequent analysis revealed that Rivipansel was efficacious in a subset of patients who were treated earlier from the time of onset of their VOC, with statistical significance demonstrated in both adults and adolescents who received treatment within 26 hours of the initial painful episode of VOC (median difference of 58 hours between Rivipansel and placebo; HR = 0.58; p = 0.03). Importantly, rapid and sustained statistically significant reductions in soluble E-selectin in circulation in this acute setting was observed in the Phase III trial supporting the biological effect of Rivipansel. This raises an important point on the beneficial effects of administering treatment to VOC early in progression and following systemic markers of the capacity of neutrophils to participate in adhesion. Clinical trials on the effects of anti-inflammatory agents such as statins and leukotriene and adenosine receptor inhibitors on resolution of VOC have also been performed (82, 89). Clinical trials assessing the efficacy of simvastatin in adolescents and young adults appear to have a significant effect on occurrence of VOC, as well as a reduction in patient reported pain, and decreased nitric oxide metabolites, human serum C-reactive protein, and soluble cell adhesion molecules ICAM1, VCAM-1, and E-Selectin (89). The data collected over the course of these clinical trials indicates that use of monotherapies targeting selectin expression, activity, and shedding on activated platelet and leukocytes are likely to improve patient quality of life.

CONCLUSIONS

Recurrent painful episodes of VOC severely diminish patient's quality of life and frequently increase the risk of infections and complication of comorbidities that require emergency intervention. There is a need for therapeutics that target the earliest events leading to VOC progression before development of painful crises and end organ damage that typically call for immediate treatment of pain perception rather than the cause of its onset. Neutrophil rolling on E-selectin expressed in the inflamed microvasculature of patients with SCD can initiate integrin activation and firm arrest. Secondary capture of sRBCs and platelet aggregation leads to vascular congestion and tissue ischemia. Targeting these earliest selectin-dependent events in neutrophil recruitment with antagonists that block both initial

TABLE 2 | Current agents being investigated to treat VOC.

General Cascade	VOC Prevention Therapeutics	Trials	Targets/ Response	Patient Demographic	Results	Dose	Reference
anti-platelet/ anti-coagulation	Prasugrel	DOVE (Terminated-lack of efficacy)	P2Y12 receptor antagonist-inhibits adenosine diphosphate (ADP)-mediated platelet adhesion and aggregation	Children 2-17 years old with history of HbSS or HBSβ thalassemia	No significant reduction in the rate of VOC in treatment vs placebo in aggregate. Children 12-17 experienced significant reduction in VOC	Initial dose 0.06 mg/kg with adjusted dosing of 0.04 - 0.12 mg/kg to a maximum of 10 mg	(65)
	Ticagrelor	HESTIA2 (Adults-completed); HESTIA3 (Pediatric-Ongoing)	P2Y12 receptor antagonist-inhibits adenosine diphosphate (ADP)-mediated platelet adhesion and aggregation	Adults 18-30 years, Children 2-18 years	HESTIA2- no reduction in number of days without pain; HESTIA3- not yet reported	Twice daily dose @ 10 to 45 mg (Adults)	(66)
	Epitfbatide	NCT00834899 (Terminated-Low accural, lack of funding)	Synthetic peptide inhibitor of αIIbβ3	Adults 18-55	No significant reduction in median times of discharge or median time of VOC resolution. Lowered serum levels of CD40L, MIP1a, TNFa, and Myoglobin; increases in MMP2/9 and leptin. Transient effect seen post treatment	2 bolus of 180ug/mL 10 min apart, then continous infusion at 2 ug/ kg/min for 6 hours	(67, 68)
	Apixaban	NCT02179177 (Terminated-funding exhausted)	Factor Xa Inhibitor	Adults ~30 years	No considerable effect over placebo	2.5 mg/kg twice daily for 6 months	(70, 71)
	Rivaroxaban	NCT02072668 (Ongoing)	Factor Xa Inhibitor	Adults ~30 years	Not yet reported	20 mg daily for 4 weeks	(70, 71)
RBC and WBC adhesion	Crizanlizumab	SUSTAIN (completed); Ongoing: STAND, SOLACE-adults, SOLACE-kids, STEADFAST, SPARTAN, ADORE	Humanized monoclonal (IgG2κ) to P-selectin. Inhibits interaction with P-selectin glycoprotein ligand-1 (PSGL-1)	Various ages from adolescent to adult	Reduction in the duration of VOC	Effective dose of 5mg/kg	(77)
	Rivipansel	Phase 3, Multiceneter, Randomized, Double-Blind, Placebo-Controlled, Parallel-Group Study to evaluate the efficacy and Safety of Rivipansel (GMI-1070) in the Treatment of Vaso-Occlusive Crisis in Hospitalized Subjects with Sicke Cell Disease [NTC02187003 (Completed)]	sLex mimetic; pan-selectin antagonist	Various ages from adolescent to adult (345 participants)	Primary endpoint not met. Ad hoc analysis, treatment within 26 hours met endpoint. Significant reduction in readiness for discharge, 58 hours, median, p = 0.03	Initial loading dose of 20 mg/ kg, following ~14 subsequent 10mg/kg doses for 12 hours to achieve minimum plasma levels	(5, 72)
	Intravenous Immunoglobulin (IVIG)	NTC01757418(Ongoing)	Inhibition of RBC-Neutrophil interactions and	12-65 (Phase 1); 8-14 (Phase 2)	Not yet reported	Intravenous IgG at 800mg/kg (Phase 1); 400mg/kg	(75, 76)

(Continued)

TABLE 2 | Continued

General Cascade	VOC Prevention Therapeutics	Trials	Targets/ Response	Patient Demographic	Results	Dose	Reference
			neutrophil-endothelial interactions			(Phase 2) at time of crisis	
	Unfractionated Heparin	NTC02098993 (Terminated-Poor enrollment)	Inhibition of P-selectin mediated adhesion	Adults ~30 years	Reduction in the duration of VOC	Initial bolus of 80U/kg followed by 18U/hr IV for 7 days until discharge	(73, 74)
	Propanolol	NCT02012777 (Terminated-lack of results); NCT01077921 (Completed)	Competitive inhibition of βe1-adrenergic receptors; inhibition of RBC binding to the endothelium	Adults ~30 years	Trend in diminished expression of E-selectin, P-selectin, ICAM-1, and VCAM-1. Diminished binding of sickle RBC to the endothelium (ex-vivo)	Standard dose of 40mg every 12 hours for 6 weeks	(56)
Anti-inflammatories	Simvastatin	NCT01702246 (Completed)	HMG-CoA reductase inhibitors, restores eNOS production and reduces CAM expression	Adolescents/ Young Adults ~ 18 years	Significant reduction in pain. Reduction of serum NOx metabolites, hs-CRP, sVCAM-1, sICAM-1, sICAM-3, (s)E-selectin, VEGF	Single oral dose 40mg (>60kg); 30mg (46-60kg), 25mg (35-44kg) daily for 3 months	(78)
	Zileuton	NCT01136941 (Completed)	5-Lipoxigenase inhibitor, inhibits formation of LTB4, LTC4, LTD4	Young adults 12-18 years	No results reported	Initial dosing of 2.4gm/day increased to 3.0 gm/day for 6 weeks	(71)
	Regadenson	NCT01788631 (Ongoing)	Adenosine A2A Receptor (A2AR) Agonist	Adults ~ 25 years	No reduction in iNKT cell activation, no significant reduction in hospital stay, opiod use, or reported pain.	1.44 mcg/kg/ hour over 48 hours	(71)

tethering and signaling of adhesion appear to be clinically effective at mitigating VOC and painful episodes. First clinical trials are promising and should be accompanied by further experimental studies including novel appropriate murine *in vivo* models which address the various differences in the regulation of selectin function between mouse and human and *ex-vivo* analysis of treatment efficacy in inflammatory recruitment especially of neutrophils and sRBC over the course of the disease. Combined, this will shed new light on the role of selectins in the pathogenesis of VOC and hopefully contribute to establishing and refining a potentially beneficial selectin blocking strategy for the treatment of patients suffering from sickle cell disease.

AUTHOR CONTRIBUTIONS

VM contributed his knowledge on selectin function in humans, helped outline and wrote the first draft of the manuscript. AH contributed his knowledge on drug efficacy in treatment of VOC in SCD and wrote corresponding sections. MS and JM contributed their vast knowledge of selectin function and clinical mechanisms of VOC and wrote the corresponding sections. SS contributed his vast knowledge on selectin function and neutrophil recruitment in human and mouse inflammation, outlined the manuscript, and wrote corresponding sections. All authors contributed to the article and approved the submitted version.

FUNDING

The work was supported by National Institute of Health grants AI047294 (SIS), AI103687 (SIS), and by the German research foundation collaborative research center (SFB), project B01 (MS).

REFERENCES

1. Stuart MJ, Nagel RL. Sickle-cell disease. *Lancet* (2004) 364:1343–60. doi: 10.1016/S0140-6736(04)17192-4
2. Frenette PS, Atweh GF. Sickle cell disease: old discoveries, new concepts, and future promise. *J Clin Invest* (2007) 117:850–8. doi: 10.1172/JCI30920
3. Kato GJ, Piel FB, Reid CD, Gaston MH, Ohene-Frempong K, Krishnamurti L, et al. Sickle cell disease. *Nat Rev Dis Primers* (2018) 4:18010. doi: 10.1038/nrdp.2018.10
4. Uwaezuoke SN, Ayuk AC, Ndu IK, Eneh CI, Mbanefo NR, Ezenwosu OU. Vaso-occlusive crisis in sickle cell disease: current paradigm on pain management. *J Pain Res* (2018) 11:3141–50. doi: 10.2147/JPR.S185582
5. Telen MJ, Wun T, McCavit TL, De Castro LM, Krishnamurti L, Lanzkron S, et al. Randomized phase 2 study of GMI-1070 in SCD: reduction in time to resolution of vaso-occlusive events and decreased opioid use. *Blood* (2015) 125:2656–64. doi: 10.1182/blood-2014-06-583351
6. Darbari DS, Sheehan VA, Ballas SK. The Vaso-Occlusive Pain Crisis in Sickle Cell Disease: Definition, Pathophysiology, and Management. *Eur J Haematol* (2020). doi: 10.1111/ejh.13430
7. Okpala I. Investigational selectin-targeted therapy of sickle cell disease. *Expert Opin Investig Drugs* (2015) 24:229–38. doi: 10.1517/13543784.2015.963552
8. Nader E, Romana M, Connes P. The Red Blood Cell-Inflammation Vicious Circle in Sickle Cell Disease. *Front Immunol* (2020) 11:454. doi: 10.3389/fimmu.2020.00454
9. Chen G, Zhang D, Fuchs TA, Manwani D, Wagner DD, Frenette PS. Heme-induced neutrophil extracellular traps contribute to the pathogenesis of sickle cell disease. *Blood* (2014) 123:3818–27. doi: 10.1182/blood-2013-10-529982
10. Ballas SK, Darbari DS. Review/overview of pain in sickle cell disease. *Complement Ther Med* (2020) 49:102327. doi: 10.1016/j.ctim.2020.102327
11. Veluswamy S, Shah P, Denton CC, Chalacheva P, Khoo MCK, Coates TD. Vaso-Occlusion in Sickle Cell Disease: Is Autonomic Dysregulation of the Microvasculature the Trigger? *J Clin Med* (2019) 8(10). doi: 10.3390/jcm8101690
12. Simon SI, Hu Y, Vestweber D, Smith CW. Neutrophil tethering on E-selectin activates beta 2 integrin binding to ICAM-1 through a mitogen-activated protein kinase signal transduction pathway. *J Immunol* (2000) 164:4348–58. doi: 10.4049/jimmunol.164.8.4348
13. Ley K. The role of selectins in inflammation and disease. *Trends Mol Med* (2003) 9:263–8. doi: 10.1016/S1471-4914(03)00071-6
14. Hidalgo A, Peired AJ, Wild M, Vestweber D, Frenette PS. Complete identification of E-selectin ligands on neutrophils reveals distinct functions of PSGL-1, ESL-1, and CD44. *Immunity* (2007) 26:477–89. doi: 10.1016/j.immuni.2007.03.011
15. Sperandio M, Gleissner CA, Ley K. Glycosylation in immune cell trafficking. *Immunol Rev* (2009) 230:97–113. doi: 10.1111/j.1600-065X.2009.00795.x
16. Rocheleau AD, Cao TM, Takitani T, King MR. Comparison of human and mouse E-selectin binding to Sialyl-Lewis(x). *BMC Struct Biol* (2016) 16:10. doi: 10.1186/s12900-016-0060-x
17. Rocheleau AD, Sumagin R, Sarelius IH, King MR. Simulation and Analysis of Tethering Behavior of Neutrophils with Pseudopods. *PloS One* (2015) 10:e0128378. doi: 10.1371/journal.pone.0128378
18. Mondal N, Buffone A Jr, Neelamegham S. Distinct glycosyltransferases synthesize E-selectin ligands in human vs. mouse leukocytes. *Cell Adh Migr* (2013) 7:288–92. doi: 10.4161/cam.24714
19. Liu Z, Miner JJ, Yago T, Yao L, Lupu F, Xia L, et al. Differential regulation of human and murine P-selectin expression and function in vivo. *J Exp Med* (2010) 207:2975–87. doi: 10.1084/jem.20101545
20. Buffone A Jr, Mondal N, Gupta R, McHugh KP, Lau JT, Neelamegham S. Silencing alpha1,3-fucosyltransferases in human leukocytes reveals a role for FUT9 enzyme during E-selectin-mediated cell adhesion. *J Biol Chem* (2013) 288:1620–33. doi: 10.1074/jbc.M112.400929
21. Chen S, Springer TA. Selectin receptor-ligand bonds: Formation limited by shear rate and dissociation governed by the Bell model. *Proc Natl Acad Sci U S A* (2001) 98:950–5. doi: 10.1073/pnas.98.3.950
22. Morikis VA, Simon SI. Neutrophil Mechanosignaling Promotes Integrin Engagement With Endothelial Cells and Motility Within Inflamed Vessels. *Front Immunol* (2018) 9:2774. doi: 10.3389/fimmu.2018.02774
23. Leeuwenberg JF, Smeets EF, Neefjes JJ, Shaffer MA, Cinek T, Jeunhomme TM, et al. E-selectin and intercellular adhesion molecule-1 are released by activated human endothelial cells in vitro. *Immunology* (1992) 77:543–9.
24. Keelan ET, Licence ST, Peters AM, Binns RM, Haskard DO. Characterization of E-selectin expression in vivo with use of a radiolabeled monoclonal antibody. *Am J Physiol* (1994) 266:H278–290. doi: 10.1152/ajpheart.1994.266.1.H279
25. Kiskin NI, Hellen N, Babich V, Hewlett L, Knipe L, Hannah MJ, et al. Protein mobilities and P-selectin storage in Weibel-Palade bodies. *J Cell Sci* (2010) 123:2964–75. doi: 10.1242/jcs.073593
26. Chase SD, Magnani JL, Simon SI. E-selectin ligands as mechanosensitive receptors on neutrophils in health and disease. *Ann BioMed Eng* (2012) 40:849–59. doi: 10.1007/s10439-011-0507-y
27. Stadtmann A, Germena G, Block H, Boras M, Rossaint J, Sundd P, et al. The PSGL-1-L-selectin signaling complex regulates neutrophil adhesion under flow. *J Exp Med* (2013) 210:2171–80. doi: 10.1084/jem.20130664
28. McEver RP. Selectins: initiators of leucocyte adhesion and signalling at the vascular wall. *Cardiovasc Res* (2015) 107:331–9. doi: 10.1093/cvr/cvv154
29. Morikis VA, Chase S, Wun T, Chaikof EL, Magnani JL, Simon SI. Selectin catch-bonds mechanotransduce integrin activation and neutrophil arrest on inflamed endothelium under shear flow. *Blood* (2017) 130:2101–10. doi: 10.1182/blood-2017-05-783027
30. Shimaoka M, Xiao T, Liu JH, Yang Y, Dong Y, Jun CD, et al. Structures of the alpha L I domain and its complex with ICAM-1 reveal a shape-shifting pathway for integrin regulation. *Cell* (2003) 112:99–111. doi: 10.1016/S0092-8674(02)01257-6
31. Riese SB, Kuehne C, Tedder TF, Hallmann R, Hohenester E, Buscher K. Heterotropic modulation of selectin affinity by allosteric antibodies affects leukocyte rolling. *J Immunol* (2014) 192:1862–9. doi: 10.4049/jimmunol.1302147
32. Beste MT, Hammer DA. Selectin catch-slip kinetics encode shear threshold adhesive behavior of rolling leukocytes. *Proc Natl Acad Sci USA* (2008) 105:20716–21. doi: 10.1073/pnas.0808213105
33. Guyer DA, Moore KL, Lynam EB, Schammel CM, Rogelj S, McEver RP, et al. P-selectin glycoprotein ligand-1 (PSGL-1) is a ligand for L-selectin in neutrophil aggregation. *Blood* (1996) 88:2415–21. doi: 10.1182/blood.V88.7.2415.bloodjournal8872415
34. Preston RC, Jakob RP, Binder FP, Sager CP, Ernst B, Maier T. E-selectin ligand complexes adopt an extended high-affinity conformation. *J Mol Cell Biol* (2016) 8:62–72. doi: 10.1093/jmcb/mjv046
35. Sokurenko EV, Vogel V, Thomas WE. Catch-bond mechanism of force-enhanced adhesion: counterintuitive, elusive, but ... widespread? *Cell Host Microbe* (2008) 4:314–23. doi: 10.1016/j.chom.2008.09.005
36. Snook JH, Guilford WH. The Effects of Load on E-Selectin Bond Rupture and Bond Formation. *Cell Mol Bioeng* (2010) 3:128–38. doi: 10.1007/s12195-010-0110-6
37. Pereverzev YV, Prezhdo E, Sokurenko EV. The two-pathway model of the biological catch-bond as a limit of the allosteric model. *Biophys J* (2011) 101:2026–36. doi: 10.1016/j.bpj.2011.09.005
38. Wayman AM, Chen W, McEver RP, Zhu C. Triphasic force dependence of E-selectin/ligand dissociation governs cell rolling under flow. *Biophys J* (2010) 99:1166–74. doi: 10.1016/j.bpj.2010.05.040
39. Hidalgo A, Chang J, Jang JE, Peired AJ, Chiang EY, Frenette PS. Heterotypic interactions enabled by polarized neutrophil microdomains mediate thromboinflammatory injury. *Nat Med* (2009) 15:384–91. doi: 10.1038/nm.1939
40. Finnegan EM, Turhan A, Golan DE, Barabino GA. Adherent leukocytes capture sickle erythrocytes in an in vitro flow model of vaso-occlusion. *Am J Hematol* (2007) 82:266–75. doi: 10.1002/ajh.20819
41. Wun T, Cordoba M, Rangaswami A, Cheung AW, Paglieroni T. Activated monocytes and platelet-monocyte aggregates in patients with sickle cell disease. *Clin Lab Haematol* (2002) 24:81–8. doi: 10.1046/j.1365-2257.2002.t01-1-00433.x
42. Major EO. Progressive multifocal leukoencephalopathy in patients on immunomodulatory therapies. *Annu Rev Med* (2010) 61:35–47. doi: 10.1146/annurev.med.080708.082655
43. Blum A, Yeganeh S, Peleg A, Vigder F, Kryuger K, Khatib A, et al. Endothelial function in patients with sickle cell anemia during and after sickle cell crises. *J Thromb Thrombolysis* (2005) 19:83–6. doi: 10.1007/s11239-005-1377-7

44. Kato GJ, Martyr S, Blackwelder WC, Nichols JS, Coles WA, Hunter LA, et al. Levels of soluble endothelium-derived adhesion molecules in patients with sickle cell disease are associated with pulmonary hypertension, organ dysfunction, and mortality. *Br J Haematol* (2005) 130:943–53. doi: 10.1111/j.1365-2141.2005.05701.x
45. Kuwano Y, Spelten O, Zhang H, Ley K, Zarbock A. Rolling on E- or P-selectin induces the extended but not high-affinity conformation of LFA-1 in neutrophils. *Blood* (2010) 116:617–24. doi: 10.1182/blood-2010-01-266122
46. Sundd P, Pospieszalska MK, Cheung LS, Konstantopoulos K, Ley K. Biomechanics of leukocyte rolling. *Biorheology* (2011) 48:1–35. doi: 10.3233/BIR-2011-0579
47. Shao B, Yago T, Setiadi H, Wang Y, Mehta-D'souza P, Fu J, et al. O-glycans direct selectin ligands to lipid rafts on leukocytes. *Proc Natl Acad Sci U.S.A.* (2015) 112:8661–6. doi: 10.1073/pnas.1507712112
48. Green CE, Pearson DN, Camphausen RT, Staunton DE, Simon SI. Shear-dependent capping of L-selectin and P-selectin glycoprotein ligand 1 by E-selectin signals activation of high-avidity beta2-integrin on neutrophils. *J Immunol (Baltimore Md 1950)* (2004) 172:7780–90. doi: 10.4049/jimmunol.172.12.7780
49. Pruenster M, Kurz AR, Chung KJ, Cao-Ehlker X, Bieber S, Nussbaum CF, et al. Extracellular MRP8/14 is a regulator of beta2 integrin-dependent neutrophil slow rolling and adhesion. *Nat Commun* (2015) 6:6915. doi: 10.1038/ncomms7915
50. Hobbs JA, May R, Tanousis K, McNeill E, Mathies M, Gebhardt C, et al. Myeloid cell function in MRP-14 (S100A9) null mice. *Mol Cell Biol* (2003) 23:2564–76. doi: 10.1128/MCB.23.7.2564-2576.2003
51. Vogl T, Tenbrock K, Ludwig S, Leukert N, Ehrhardt C, van Zoelen MA, et al. Mrp8 and Mrp14 are endogenous activators of Toll-like receptor 4, promoting lethal, endotoxin-induced shock. *Nat Med* (2007) 13:1042–9. doi: 10.1038/nm1638
52. Croce K, Gao H, Wang Y, Mooroka T, Sakuma M, Shi C, et al. Myeloid-related protein-8/14 is critical for the biological response to vascular injury. *Circulation* (2009) 120:427–36. doi: 10.1161/CIRCULATIONAHA.108.814582
53. Lefort CT, Rossaint J, Moser M, Petrich BG, Zarbock A, Monkley SJ, et al. Distinct roles for talin-1 and kindlin-3 in LFA-1 extension and affinity regulation. *Blood* (2012) 119:4275–82. doi: 10.1182/blood-2011-08-373118
54. Eriksson EE, Xie X, Werr J, Thoren P, Lindbom L. Importance of primary capture and L-selectin-dependent secondary capture in leukocyte accumulation in inflammation and atherosclerosis in vivo. *J Exp Med* (2001) 194:205–18. doi: 10.1084/jem.194.2.205
55. Begandt D, Thome S, Sperandio M, Walzog B. How neutrophils resist shear stress at blood vessel walls: molecular mechanisms, subcellular structures, and cell-cell interactions. *J Leukoc Biol* (2017) 102:699–709. doi: 10.1189/jlb.3MR0117-026RR
56. Rossaint J, Zarbock A. Platelets in leucocyte recruitment and function. *Cardiovasc Res* (2015) 107:386–95. doi: 10.1093/cvr/cvv048
57. Rossaint J, Margraf A, Zarbock A. Role of Platelets in Leukocyte Recruitment and Resolution of Inflammation. *Front Immunol* (2018) 9:2712. doi: 10.3389/fimmu.2018.02712
58. Weber C, Springer TA. Neutrophil accumulation on activated, surface-adherent platelets in flow is mediated by interaction of Mac-1 with fibrinogen bound to alphaIIbbeta3 and stimulated by platelet-activating factor. *J Clin Invest* (1997) 100:2085–93. doi: 10.1172/JCI119742
59. Weninger W, Ulfman LH, Cheng G, Souchkova N, Quackenbush EJ, Lowe JB, et al. Specialized contributions by alpha(1,3)-fucosyltransferase-IV and FucT-VII during leukocyte rolling in dermal microvessels. *Immunity* (2000) 12:665–76. doi: 10.1016/S1074-7613(00)80217-4
60. Manwani D, Frenette PS. Vaso-occlusion in sickle cell disease: pathophysiology and novel targeted therapies. *Blood* (2013) 122:3892–8. doi: 10.1182/blood-2013-05-498311
61. Bennewitz MF, Tutuncuoglu E, Gudapati S, Brzoska T, Watkins SC, Monga SP, et al. P-selectin-deficient mice to study pathophysiology of sickle cell disease. *Blood Adv* (2020) 4:266–73. doi: 10.1182/bloodadvances.2019000603
62. Wun T, Styles L, DeCastro L, Telen MJ, Kuypers F, Cheung A, et al. Phase 1 study of the E-selectin inhibitor GMI 1070 in patients with sickle cell anemia. *PloS One* (2014) 9:e101301. doi: 10.1371/journal.pone.0101301
63. Krishnamurthy VR, Sardar MY, Ying Y, Song X, Haller C, Dai E, et al. Glycopeptide analogues of PSGL-1 inhibit P-selectin in vitro and in vivo. *Nat Commun* (2015) 6:6387. doi: 10.1038/ncomms7387
64. Charache S, Dover GJ, Moore RD, Eckert S, Ballas SK, Koshy M, et al. Hydroxyurea: effects on hemoglobin F production in patients with sickle cell anemia. *Blood* (1992) 79:2555–65. doi: 10.1182/blood.V79.10.2555.bloodjournal79102555
65. Steinberg MH, Lu ZH, Barton FB, Terrin ML, Charache S, Dover GJ. Fetal hemoglobin in sickle cell anemia: determinants of response to hydroxyurea. Multicenter Study of Hydroxyurea. *Blood* (1997) 89:1078–88. doi: 10.1182/blood.V89.3.1078
66. Zimmerman SA, Schultz WH, Davis JS, Pickens CV, Mortier NA, Howard TA, et al. Sustained long-term hematologic efficacy of hydroxyurea at maximum tolerated dose in children with sickle cell disease. *Blood* (2004) 103:2039–45. doi: 10.1182/blood-2003-07-2475
67. Barbu EA, Dominical VM, Mendelsohn L, Thein SL. Neutrophils remain detrimentally active in hydroxyurea-treated patients with sickle cell disease. *PloS One* (2019) 14:e0226583. doi: 10.1371/journal.pone.0226583
68. Wun T, Paglieroni T, Rangaswami A, Franklin PH, Welborn J, Cheung A, et al. Platelet activation in patients with sickle cell disease. *Br J Haematol* (1998) 100:741–9. doi: 10.1046/j.1365-2141.1998.00627.x
69. Heeney MM, Hoppe CC, Abboud MR, Inusa B, Kanter J, Ogutu B, et al. A Multinational Trial of Prasugrel for Sickle Cell Vaso-Occlusive Events. *N Engl J Med* (2016) 374:625–35. doi: 10.1056/NEJMoa1512021
70. Kanter J, Abboud MR, Kaya B, Nduba V, Amilon C, Gottfridsson C, et al. Ticagrelor does not impact patient-reported pain in young adults with sickle cell disease: a multicentre, randomised phase IIb study. *Br J Haematol* (2019) 184:269–78. doi: 10.1111/bjh.15646
71. Lee SP, Ataga KI, Zayed M, Manganello JM, Orringer EP, Phillips DR, et al. Phase I study of eptifibatide in patients with sickle cell anaemia. *Br J Haematol* (2007) 139:612–20. doi: 10.1111/j.1365-2141.2007.06787.x
72. Desai PC, Brittain JE, Jones SK, McDonald A, Wilson DR, Dominik R, et al. A pilot study of eptifibatide for treatment of acute pain episodes in sickle cell disease. *Thromb Res* (2013) 132:341–5. doi: 10.1016/j.thromres.2013.08.002
73. Vercellotti GM, Dalmasso AP, Schaid TR, Nguyen J, Chen C, Ericson ME, et al. Critical role of C5a in sickle cell disease. *Am J Hematol* (2019) 94:327–37. doi: 10.1002/ajh.25384
74. Vats R, Kaminski TW, Ju EM, Brzoska T, Tutuncuoglu E, Tejero J, et al. P-selectin deficiency promotes liver senescence in sickle cell disease mice. *Blood* (2021). doi: 10.1182/blood.2020009779
75. Sølvik U, Haraldsen G, Fiane AE, Boretti E, Lambris JD, Fung M, et al. Human serum-induced expression of E-selectin on porcine aortic endothelial cells in vitro is totally complement mediated. *Transplantation* (001) 72:1967–73. doi: 10.1097/00007890-200112270-00017
76. Jani PK, Kajdácsi E, Megyeri M, Dobó J, Doleschall Z, Futosi K, et al. MASP-1 induces a unique cytokine pattern in endothelial cells: a novel link between complement system and neutrophil granulocytes. *PloS One* (2014) 9(1):e87104. doi: 10.1371/journal.pone.0087104
77. Devata S, Angelini DE, Blackburn S, Hawley A, Myers DD, Schaefer JK, et al. Use of GMI-1271, an E-selectin antagonist, *in* healthy subjects and in 2 patients with calf vein thrombosis. *Res Pract Thromb Haemost* (2020) 4(2):193–204. doi: 10.1002/rth2.12279
78. Culmer DL, Dunbar ML, Hawley AE, Sood S, Sigler RE, Henke PK, et al. E-selectin inhibition with GMI-1271 decreases venous thrombosis without profoundly affecting tail vein bleeding in a mouse model. *Thromb Haemost* (2017) 117:1171–81. doi: 10.1160/TH16-04-0323
79. Myers D, Lester P, Adili R, Hawley A, Durham L, Dunivant V, et al. A new way to treat proximal deep venous thrombosis using E-selectin inhibition. *J Vasc Surg Venous Lymphat Disord* (2020) 8:268–78. doi: 10.1016/j.jvsv.2019.08.016
80. De Castro L, Zennadi R, Jonassaint J, Batchvarova M, Telen M. Effect of Propranolol as Anti-Adhesive Therapy in Sickle Cell Disease. *Clin Trans Sci* (2012) 5:437–44. doi: 10.1111/cts.12005
81. Christen JR, Bertolino J, Jean E, Camoin L, Ebbo M, Harlé JR, et al. Use of Direct Oral Anticoagulants in Patients with Sickle Cell Disease and Venous Thromboembolism: A Prospective Cohort Study of 12 Patients. *Hemoglobin* (2019) 43:296–9. doi: 10.1080/03630269.2019.1689997

82. Telen MJ. Beyond hydroxyurea: new and old drugs in the pipeline for sickle cell disease. *Blood* (2016) 127:810–9. doi: 10.1182/blood-2015-09-618553
83. Chang J, Patton JT, Sarkar A, Ernst B, Magnani JL, Frenette PS. GMI-1070, a novel pan-selectin antagonist, reverses acute vascular occlusions in sickle cell mice. *Blood* (2010) 116:1779–86. doi: 10.1182/blood-2009-12-260513
84. Nelson RM, Cecconi O, Roberts WG, Aruffo A, Linhardt RJ, Bevilacqua MP. Heparin oligosaccharides bind L- and P-selectin and inhibit acute inflammation. *Blood* (1993) 82:3253–8. doi: 10.1182/blood.V82.11.3253.bloodjournal82113253
85. Qari MH, Aljaouni SK, Alardawi MS, Fatani H, Alsayes FM, Zografos P, et al. Reduction of painful vaso-occlusive crisis of sickle cell anaemia by tinzaparin in a double-blind randomized trial. *Thromb Haemost* (2007) 98:392–6. doi: 10.1160/Th06-12-0718
86. Chang J, Shi PA, Chiang EY, Frenette PS. Intravenous immunoglobulins reverse acute vaso-occlusive crises in sickle cell mice through rapid inhibition of neutrophil adhesion. *Blood* (2008) 111:915–23. doi: 10.1182/blood-2007-04-084061
87. Turhan A, Jenab P, Bruhns P, Ravetch JV, Coller BS, Frenette PS. Intravenous immune globulin prevents venular vaso-occlusion in sickle cell mice by inhibiting leukocyte adhesion and the interactions between sickle erythrocytes and adherent leukocytes. *Blood* (2004) 103:2397–400. doi: 10.1182/blood-2003-07-2209
88. Ataga KI, Kutlar A, Kanter J, Liles D, Cancado R, Friedrisch J, et al. Crizanlizumab for the Prevention of Pain Crises in Sickle Cell Disease. *N Engl J Med* (2017) 376:429–39. doi: 10.1056/NEJMoa1611770
89. Hoppe C, Styles L, Kuypers F, Larkin S, Vichinsky E. Simvastatin reduces vaso-occlusive pain in sickle cell anaemia: a pilot efficacy trial. *Br J Haematol* (2017) 177:620–9. doi: 10.1111/bjh.14580

Conflict of Interest: JM is Senior Vice-President, for Research and Chief Scientific Officer of GlycoMimetics, Inc. He has a financial interest in clinical development of selectin antagonist currently in clinical trials.

The remaining authors declare that the research was conducted in the absence of any commercial or financial relationships that could be construed as a potential conflict of interest.

frontiers in Immunology

ORIGINAL RESEARCH
published: 18 May 2021
doi: 10.3389/fimmu.2021.667213

Endothelial Focal Adhesions Are Functional Obstacles for Leukocytes During Basolateral Crawling

*Janine J. G. Arts[1,2], Eike K. Mahlandt[2], Lilian Schimmel[1], Max L. B. Grönloh[1], Sanne van der Niet[1], Bart J. A. M. Klein[1], Mar Fernandez-Borja[1], Daphne van Geemen[1], Stephan Huveneers[3], Jos van Rijssel[1], Joachim Goedhart[2] and Jaap D. van Buul[1,2]**

[1] Molecular Cell Biology Lab, Department of Molecular Hematology, Sanquin Research and Landsteiner Laboratory, Amsterdam, Netherlands, [2] Leeuwenhoek Centre for Advanced Microscopy (LCAM), Section of Molecular Cytology, Swammerdam Institute for Life Sciences (SILS), University of Amsterdam, Amsterdam, Netherlands, [3] Department of Medical Biochemistry, Amsterdam Cardiovascular Sciences, Amsterdam University Medical Center (UMC), University of Amsterdam, Amsterdam, Netherlands

OPEN ACCESS

Edited by:
Deirdre R. Coombe,
Curtin University, Australia

Reviewed by:
Britta Engelhardt,
University of Bern, Switzerland
Ruth Lyck,
University of Bern, Switzerland
William A. Muller,
Northwestern University,
United States

***Correspondence:**
Jaap D. van Buul
j.vanbuul@sanquin.nl

Specialty section:
This article was submitted to Molecular Innate Immunity, a section of the journal Frontiers in Immunology

Received: 12 February 2021
Accepted: 27 April 2021
Published: 18 May 2021

Citation:
Arts JJG, Mahlandt EK, Schimmel L, Grönloh MLB, van der Niet S, Klein BJAM, Fernandez-Borja M, van Geemen D, Huveneers S, van Rijssel J, Goedhart J and van Buul JD (2021) Endothelial Focal Adhesions Are Functional Obstacles for Leukocytes During Basolateral Crawling. Front. Immunol. 12:667213. doi: 10.3389/fimmu.2021.667213

An inflammatory response requires leukocytes to migrate from the circulation across the vascular lining into the tissue to clear the invading pathogen. Whereas a lot of attention is focused on how leukocytes make their way through the endothelial monolayer, it is less clear how leukocytes migrate underneath the endothelium before they enter the tissue. Upon finalization of the diapedesis step, leukocytes reside in the subendothelial space and encounter endothelial focal adhesions. Using TIRF microscopy, we show that neutrophils navigate around these focal adhesions. Neutrophils recognize focal adhesions as physical obstacles and deform to get around them. Increasing the number of focal adhesions by silencing the small GTPase RhoJ slows down basolateral crawling of neutrophils. However, apical crawling and diapedesis itself are not affected by RhoJ depletion. Increasing the number of focal adhesions drastically by expressing the Rac1 GEF Tiam1 make neutrophils to avoid migrating underneath these Tiam1-expressing endothelial cells. Together, our results show that focal adhesions mark the basolateral migration path of neutrophils.

Keywords: transmigration, focal adhesions, small GTPase, RhoJ, Tiam1, endothelium, inflammation

INTRODUCTION

Neutrophils in the bloodstream form the first line of defense during an infection. To fulfil their function at the site of inflammation, they must exit the vasculature in a process referred to as transendothelial migration (TEM). To prevent vascular leakage, endothelial cells lining the blood vessels form a tight barrier involving the adherens junction protein VE-cadherin. During inflammation, these junctions allow leukocytes to cross while keeping the barrier intact. The endothelium is activated by pro-inflammatory stimuli, resulting in the upregulation of adhesion molecules such as selectins, ICAM-1 and VCAM-1. Neutrophils slowdown from the circulation and after the multistep process of rolling, adhesion, crawling and diapedesis they enter the subendothelial space (1, 2). Once crossed the endothelium, neutrophils tend to stay between the

endothelium and the basement membrane for up to 20 minutes before penetrating the inflamed tissue (3, 4). It seems that they are actively searching for a spot to enter the tissue. However, the factors that control the crawling of neutrophils at the basolateral level are not well known. Identifying these factors may provide new therapeutic options to promote or reduce tissue infiltration of immune cells.

TEM mainly occurs in post capillary venules which consist of an endothelial cell layer, supporting pericytes and a basement membrane. Endothelial cells are physically attached to the underlying basement membrane through protein complexes called focal adhesions (FAs), linking the actin cytoskeleton to the basement membrane (5). FAs assemble when integrin receptors are activated by the extracellular matrix, resulting in recruitment of multiple FA proteins as paxillin, vinculin, Focal Adhesion Kinase (FAK) and talin (6). Nascent adhesions can rapidly disassemble or mature to focal complexes. Thereafter, focal complexes mature into FAs that are larger and reside at the end of actin fibers (7). The assembly and disassembly of FAs together with the remodeling of the actin cytoskeleton enable cells to migrate and to maintain their barrier function. *En face* imaging of human vascular endothelial beds from different tissues showed the presence of these complexes in arteries as well as venules (8).

It was reported that T-cell TEM preferentially occurred through junctions where near-junction FA density of ECs was low (9). Moreover, the disruption of adhesions was observed, and a transient weakening of the FAs was hypothesized to be necessary to widen subendothelial spaces. Another study showed that disruption of FAK protein or FAK signaling decreased neutrophil transmigration (5). However, if FA dynamics are involved in the efficiency how neutrophils maneuver underneath the endothelium is not known.

The remodeling and turnover of FAs involves the small GTPases RhoJ (10, 11), which has been shown to be expressed in the vasculature *in vivo* (12, 13). RhoJ is a member of the family of Rho GTPases acting as molecular switches cycling from an inactive GDP-bound mode to an active GTP-bound mode. Guanine exchange factors (GEFs) and GTPase activating proteins (GAPs) assist in this switching. Rho GTPases mainly regulate the cell's cytoskeleton, thereby fulfilling a major role in cellular homeostasis. Although several studies have focused on the contribution of the endothelial GTPases RhoA, Cdc42 and Rac1 on leukocyte TEM (14–20), nothing is known about the role of the FA-regulating RhoJ in leukocyte TEM.

Here, we show that neutrophils underneath the endothelium navigate around FAs as physical obstacles. Depletion of RhoJ increased the number of FAs, resulting in a reduction of the speed and motility of basolateral crawling of neutrophils. RhoJ perturbation did not alter apical rolling, crawling or diapedesis of neutrophil TEM. Furthermore, by drastically increasing the number of FAs by expressing an active mutant of the Rac1 GEF Tiam1 (C1199), we were able to steer neutrophil basolateral crawling underneath endothelial cells that displayed lowest number of FAs. This supports our hypothesis that FAs can mark the path for basolateral migration of neutrophils.

MATERIALS AND METHODS

Cell Culture

Human umbilical vein endothelial cells (HUVECs) (Lonza) were cultured in EGM2 medium (Cat.nr C-22110, Promocell) supplemented with 1% penstrep (Invitrogen). The culture flasks, plates (TPP) and coverslips were coated with fibronectin (30 µg/ml; Sanquin Reagents, Amsterdam, Netherlands). HUVECs were used during experiments when at passage 3-4. Blood-outgrowth Endothelial Cells (BOECs) were isolated as described before (21) and cultured in EGM2 medium (Cat.nr C-22110, Promocell) supplemented with 1% penstrep (Invitrogen) and 18% fetal calf serum (Bodinco). The culture flasks, plates (TPP) and coverslips were coated with gelatin (Sigma). Endothelial cells were cultured at 37°C and 5% CO2.

Umbilical Cord

Human umbilical cords were collected from the Department of Obstetrics and Gynaecology of the Amsterdam UMC (VUMC) after obtaining written informed consent from the mothers. 1 to 2-day old human umbilical cords were used for all our experiments. The outer ends of the cord were cut off. A cannula was inserted in the human umbilical vein and it was tied up with a tie-rip. The vein was gently flushed with warm PBS to remove blood and blood clots. Then the vein was either fixed or stained directly. Alternatively, HUVECs were removed (denudation) by 0.05% trypsin-EDTA solution (Sigma cat #59418C) and rinsed with PBS. The vein was cut in pieces of approximately 1 cm^2 and 250.000 BOECs were seeded on the vein in a 12-well plate. After overnight incubation 37°C and 5% CO_2 and 4 hours of TNF-alpha stimulation (10 ng/ml, Peprotech) veins with BOEC were fixed and stained.

Immunofluorescence Staining

Umbilical cords: Umbilical veins were fixed with 4% PFA (Merck Millipore, 104005) in PBS containing 1 mM $CaCl_2$ and 0.5 mM $MgCl_2$ for 15 minutes. Veins were washed with PBS and quenched with 50 mM NH_4Cl in PBS for 10 minutes at RT. Veins were then permeabilized with 0.5% Triton X-100 (Sigma, USA, 9002-93-1) for 5 minutes. Subsequently, unspecific binding sites were blocked with 1% bovine serum albumin (BSA) (PAA laboratories, Austria, Pasching, AFFY10857) in 50mM NH_4Cl in PBS++ for 60 minutes at RT. For immunostaining, 50 µL of primary antibody solution in PBS-BSA was added to the luminal side of the vein and incubated for 60 minutes at RT. After washing with PBS, the veins were incubated with fluorescently labelled secondary antibodies for 60 minutes at RT. After washing with PBS, veins were mounted with the luminal surface facing down on glass-bottom Petri dishes using DAPI Fluoromount-G mounting medium (Southern Biotech, cat #0100-20). For the mesenteric arteries, we used the protocol as described by van Geemen et al. (8). HUVECs were cultured on fibronectin coated coverslips (12mm, Thermo Scientific). Cells were fixed with 4% paraformaldehyde in PBS containing 1mM $CaCl_2$ and 0.5 mM $MgCl_2$ for 10 minutes and washed three times. Thereafter, HUVECs were permeabilized with 0.1%

Triton-X 100 in PBS containing 1mM $CaCl_2$ and 0.5 mM $MgCl_2$ for 5 minutes and blocked using 2% BSA in PBS containing 1mM $CaCl_2$ and 0.5 mM $MgCl_2$ for 30 minutes. Coverslips were incubated with primary antibodies for one hour and washed three times, followed by 1 hour incubation with secondary antibodies. After three times washing, the coverslips were mounted using Mowiol (10% Mowiol®4-88, 2.5% Dabco, 25% Glycerol, pH 8.5). For the lattice light sheet microscopy imaging and processing, we refer to (22).

Antibodies and Imaging

Polyclonal rabbit antibody against phospho-Paxillin (cat# 44-722G), Alexa 488-conugated chicken anti rabbit (cat# A21441) secondary antibody, Alexa 633-conjugated goat anti mouse (cat# A21050) secondary antibody and Phalloidin-Texas Red (cat# T7471) were purchased from Invitrogen. Mouse monoclonal antibody against Fibronectin (cat# 610077) and Alexa 647-conjugated mouse monoclonal antibody against VE-cadherin (cat# 561567) were purchased from BD biosciences. Hoechst 33342 (cat# H-1399) was purchased from Molecular Probes. Goat Polyclonal anti VE-cadherin antibody was purchased from Santa Cruz (cat #SC-6458). Secondary Chicken anti Goat Alexa 647 conjugated antibody was purchased from Invitrogen (cat#A21469). Polyclonal rabbit antibody against Laminin 1αβγ and 2 αβγ was purchased from Novus Biologicals (cat# NB300-177). Monoclonal mouse antibody against Laminin α4 was purchased from R&D Systems (cat# MAB7340). Polyclonal rabbit antibody against Collagen IV was purchased from Abcam (cat# ab6586). Polyclonal rabbit antibody against HA was purchased from Sigma (cat# H6908). Images were acquired using a confocal laser scanning microscope (Leica SP8) using a 20x, 40x, or 63x NA 1.4 oil immersion objective and HyD detectors.

Plasmids

mNeonGreen-Paxillin is available through Addgene (plasmid # 129604) (23). mNeonGreen-Paxillin was PCR amplified with the following primers: FW 5'-AGGTCTATATAAGCAGAGC-3', RV 5'-ATATGCTAGCCTAGCAGAAGAGCTTGAGGAAG-3'. PCR product and lentiviral backbone were restriction digested with AgeI and NheI. The fragments were ligated to create pLV-mNeonGreen-Paxillin. Tiam1-C1199-HA constitutively active mutant was a kind gift of John Collard and was microporated into HUVEC using Neon Transfection System (ThermoFisher) according to manufacturer's protocol (HA tag from Human influenza hemagglutinin). Lentiviral RhoJ short hairpin DNA was a kind gift from Dirk Geerts, AMC (CAACACTTGCTCGGACTGTATCTC).

TIRF Microscopy

Cells were imaged with a Nikon Ti-E microscope equipped with a motorized TIRF Illuminator unit, a 60x TIRF objective (60x Plan Apo, Oil DIC N2, NA =1.49, WD = 120 um) and Perfect Focus System. Images were acquired with an Andor iXon 897 EMCCD camera and the Nikon NIS elements software. mNeonGreen was imaged using the 488 nm laser line and calcein red-orange was imaged using the 561 nm laser line. A quad split dichroic mirror (405 nm, 488 nm, 561 nm, 640 nm) was used in combination with dual band pass emission filter (515 to 545 nm, 600 to 650 nm). To achieve a larger field of view a 3 x 3 tile scans was acquired with 15% overlap stitching on the GFP channel. Time lapse images were taken every 10 s.

Virus Production

Lentiviral particles were produced in HEK293T cells using 3rd generation packing plasmids. 2 and 3 days post transfection, supernatant was harvested and filtered (0.45 um) and concentrated using Lenti-X Concentrator (TaKaRa). Cells were selected with 1.5 ug/ml puromycin and used 2-6 days post transduction.

SDS PAGE Gel and Western Blot

Cells were washed with PBS containing 1mM $CaCl_2$ and 0.5 mM $MgCl_2$, lysed in SDS-sample buffer (Life technologies) containing 4% β-mercaptoethanol (Sigma Aldrich) and denatured at 95 degrees for 10 minutes. Proteins were separated on a 4-12% gradient SDS-PAGE gel (Invitrogen) in MES buffer according to manufacturer's protocol, and transferred to nitrocellulose membrane (Thermo Scientific Cat# 26619) in blot buffer (48 nM Tris, 39 nM Glycine, 0.04% SDS, 20% methanol). Membrane was blocked with 5% (w/v) milk (Campina) in Tris-buffered saline with Tween20 (TBST) for 60 minutes. The immunoblots were analyzed using primary antibodies incubated overnight at 4 degrees, washed three times with TBST, incubated with secondary antibodies linked to HRP (Dako, Aligent Technologies) and washed three times with TBST. HRP signals were visualized by enhanced chemiluminescence (ECL, cat# 32106, Thermo Scientific) for actin antibody and Super ECL (Thermo Scientific) for RhoJ antibody and light sensitive films (Fuji Film). Mouse monoclonal antibodies against RhoJ (cat# WH0057381M1) and actin (cat# A3853) were purchased from Sigma. Secondary HRP-conjugated goat anti-mouse (cat# P0447) antibody was purchased from Dako.

Neutrophil Transendothelial Migration Under Physiological Flow

Blood used for neutrophil isolation was obtained from healthy adult volunteers. Whole blood with heparin was diluted (1:1) with 5% trisodium citrate in PBS, thereafter the diluted blood was pipetted on 12.5 ml Percoll (room temperature) 1.076 g/ml. The blood was centrifuged at 800g (room temperature) with slow start and brake for 20 minutes. The PBMC ring fraction and blood plasma were discarded and erythrocytes were lysed using ice cold lysis buffer (155 nM NH_4CL, 10 mM KHCO, 0.1 mM EDTA). Thereafter, the neutrophils were washed with ice cold PBS. In between the neutrophils were centrifuged for 5 minutes at 450g at 4°C. The neutrophils were suspended in HEPES buffer (20 mM HEPES, 132 mM NaCl, 6 mM KCL, 1 mM $CaCL_2$, 1 mM $MgSO_4$, 1.2 mM K_2HPO_4, 5 mM D-glucose (Sigma-Aldrich), and 0.4% human serum albuman (Sanquin Reagents). Neutrophils were labelled with Calcein red-orange (Invitrogen) according to manufacturer's protocol. Neutrophils were kept at room temperature for a maximum of 4 hours prior to experiment. HUVECs were cultured 48 before the experiment in an Ibidi 6 channel flow slide (μ-Slide VI 0.4, Cat.nr 80606,

Ibidi) coated with fibronectin. HUVECs were stimulated with 10ng/ml TNFα (Peprotech) 4-20 hours prior to the experiment. Isolated neutrophils were activated at 37°C for 30 minutes, 1x10xxx2076 neutrophils were used per channel. A perfusion system was used to reach a flow of HEPES buffer of 0.5ml/minute (0.8 dyne/cm^2) during the experiment, neutrophils were injected in the flow. The transendothelial migration was monitored for 20 minutes with a 10x air objective using a Zeiss Observer Z1 microscope. Live cell imaging was performed at 37°C with 5% CO_2. The percentage of transmigrated neutrophils was calculated by dividing the number of neutrophils underneath the endothelium by the total neutrophil count. These percentages were calculated at 1, 2, 3, 4, 5, 10 and 15 minutes after the first neutrophils were in focus.

Analyses

Images were analyzed using Fiji/ImageJ software. Images with labelled neutrophils were thresholded and analyzed using 'Analyze Particles'. To quantify the tracks of the neutrophils Manual Tracking ImageJ plugin was used. A 'turn' was defined as a more than 90 degrees change in direction in the track of a specific neutrophil. To quantify focal adhesions, the images were thresholded and analyzed using 'Analyze Particles', including only particles with an area between 0.2 and 10 μm^2. The speed of neutrophils underneath the endothelium was measured using MtrackJ, a plugin for Fiji. The neutrophils were tracked from the moment they were underneath the endothelium till the end of the experiment. The total length was divided through the time in seconds of the track. apical crawling was analyzed using Imaris software.

The crawling of neutrophils on top of the endothelium (apical) was measured using TrackMate, a plugin for Fiji, using spot finding, a blob diameter of 10.5 μm and spot threshold of 4000 or 300 depending on the imaging brightness/contrast. Simple LAP tracker was used with a minimal overlap of 10.5 μm, disabling gaps in tracks. All tracks that were not finished before the end of the movie (not finished crawling stage) or with less than 5 spots (to exclude rolling) were removed. Superplots were generated using the Super Plots Of Data web app (24).

RESULTS

Neutrophils Change Shape Extensively During Basolateral Crawling

Endothelial cells are attached to the substratum through FA protein complexes (25). To examine the localization of FAs in cultured Human Umbilical Vein Endothelial Cells (HUVECs), we stained a monolayer of endothelial cells for F-actin and phospho-paxillin, a well-known marker for FAs (26). We observed phospho-paxillin puncta at the end of F-actin stress fibers (**Figure 1A**). Under inflammatory conditions, neutrophils cross the endothelium and stay under the endothelium for several minutes before continuing crossing the basement membrane and enter the underlying tissue (4). When monitoring this in real time using a transendothelial migration (TEM) flow model, neutrophils made several turns as if they were searching for a perfect route to prepare themselves to cross the basement membrane (**Supplementary Movie 1**).

From these observations, we hypothesized that FAs direct the basolateral route for neutrophils. To explore how neutrophils deal with FAs during TEM, we cultured mNeonGreen Paxillin-expressing HUVECs in specialized flow channels. The mNeonGreen-Paxillin is used as a proxy for FAs, enabling us to monitor in real-time FAs during neutrophil TEM under physiological flow conditions. By using TIRF microscopy, we specifically detected the basolateral side of the endothelial cell layer and were able to detect the FAs with high contrast in real-time. When studying both FA and neutrophil behavior at the basolateral side, it seems that neutrophils were trapped by surrounding FAs as if they experienced a physical barrier (**Figure 1B** and **Supplementary Movie 2**). We found that the basement membrane proteins laminin, collagen and fibronectin were deposited by the HUVEC upon culturing (**Supplementary Figure 1A**). These proteins can form a confined surrounding that potentially can be used by neutrophils to migrate underneath the endothelium. For the neutrophils crawling at the basolateral side, we observed a wide variety of neutrophil shapes, ranging from stretched out to bended (**Figure 1C**, **Supplementary Figure 1B** and **Supplementary Movie 3**). These morphological changes were specific for neutrophils at the basolateral side, as we did not observe these changes for neutrophils that were crawling at the apical side of the endothelium prior to crossing the endothelium (**Figure 1D** and **Supplementary Figure 1C**). To illustrate these morphological changes in more detail, we used 3D lattice light sheet imaging (**Figure 1E** and **Supplementary Figure 1D**). These recordings showed the morphological shape transition neutrophils undergo as soon as they cross the endothelium. To measure these morphological changes, neutrophil circularity during basolateral and apical crawling was determined using time-lapse recordings. Circularity was measured by 4π(area/perimeter^2) with 1 being perfectly round. Apical crawling neutrophils showed a circularity of 0.74 (**Figure 1F**), whereas basolateral crawling neutrophils showed a circularity of 0.43 (**Figure 1G**). Thus, neutrophils that crawled underneath the endothelium showed a higher degree of deformation than neutrophils that crawled on the apical surface of the endothelium.

The endothelial cells used are cultured on glass cover slips to allow TIRF microscopy. It is recognized that stiff surfaces can influence structures like FAs (27). To study FAs in endothelial cells on more softer substrates, we used umbilical cord tissue and replated HUVECs onto the umbilical cord substrate that were depleted from endothelial cells first. These experiments showed the presence of FAs in endothelial cells *in vivo* albeit much more at the junctional region. Although endothelial cells of the umbilical cord were smaller in size, the presence and number of FAs per surface area was comparable with what was observed for *in vitro* cultures (**Figures 2A, B** and **Supplementary Figures 1E, F**). These data are in line with previous reports showing the presence of FAs in different vascular beds (8). Additional treatment of the endothelial cells in umbilical cords with TNFα showed similar numbers of FAs compared to the

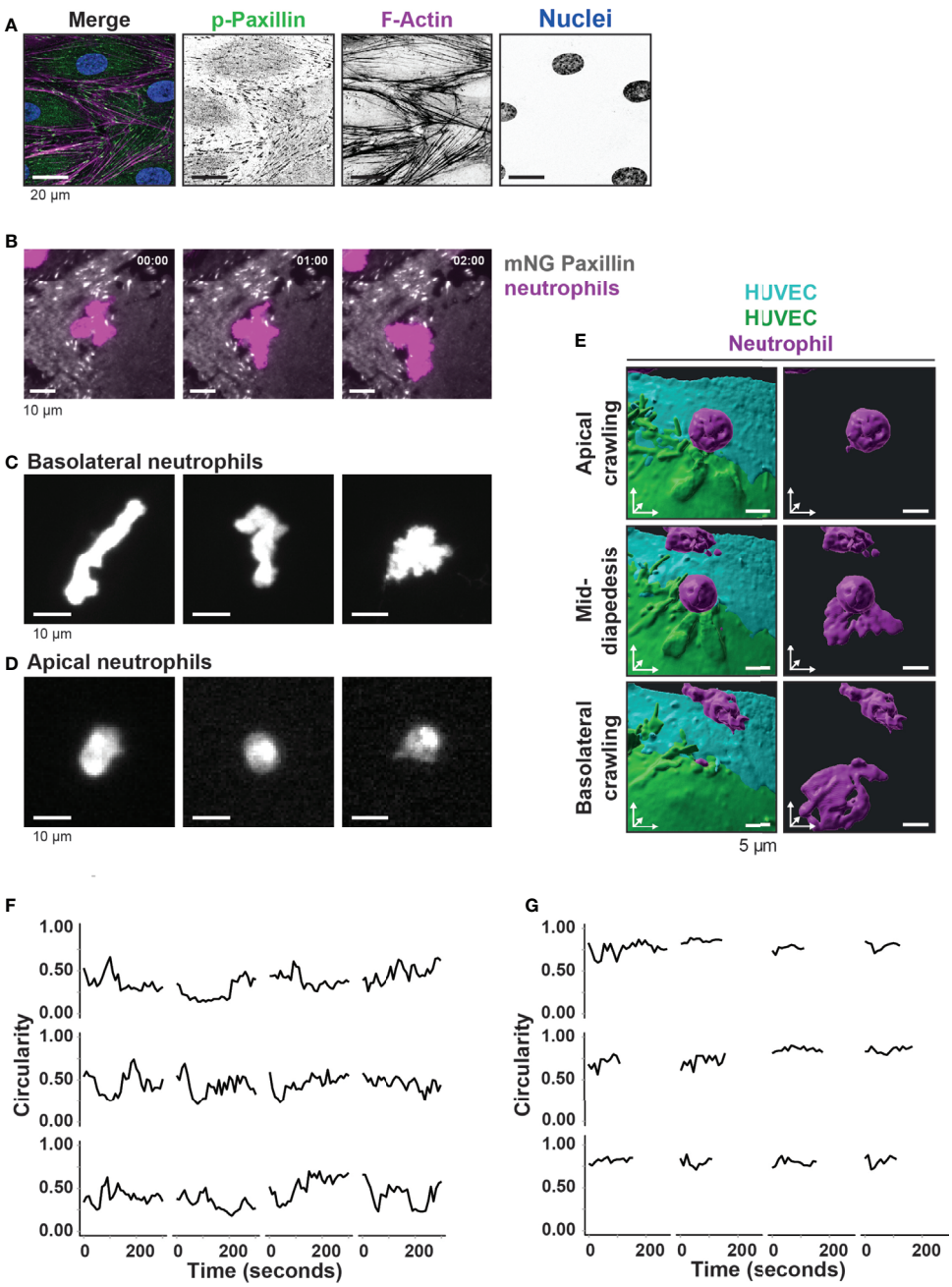

FIGURE 1 | Neutrophil deformation at the basolateral side of the endothelium. **(A)** Immunofluorescent staining for phospho-paxillin (green), F-actin (magenta), and DNA (blue) on HUVECs stimulated for 20h with TNFα. Scale bar, 20 µm. **(B)** Stills from TIRF microscopy time lapse imaging showing neutrophils (magenta) and mNeonGreen-Paxillin (gray). Time indicated in seconds in upper right corner. Bar, 10 µm. **(C)** Stills from TIRF microcopy times lapse imaging showing 3 representative neutrophil shapes during crawling at the basolateral side of the endothelium. Bar, 10 µm. **(D)** Stills from widefield microscopy time lapse imaging showing 3 representative neutrophil shapes during crawling at the apical side of the endothelium. Bar, 10 µm. **(E)** 3D view stills from two ECs (green/turquoise) and a neutrophil (magenta) at three time points (apical crawling, mid-diapedesis, and basolateral crawling). Right panels show only the neutrophil. Bar, 5µm. **(F)** Quantification of the dynamics of circularity of neutrophils at the basolateral side (Basolateral). Each graph represents one neutrophil. **(G)** Quantification of the dynamics of circularity of neutrophils at the apical endothelial side (Apical). Each graph represents one neutrophil.

in vitro setup, namely 0.05 (± 0.01, standard deviation) per μm^2 and an average size of 0.75 (± 0.04, standard deviation) μm^2 and an increase in FAs and stress fibers across the axis of the endothelial cell (**Figure 2C**). FAs have been recognized *in vivo* as well, albeit less prominent (8). To verify FAs under more *in vivo* conditions, we stained human mesenteric vessels and showed the presence of FAs in the endothelium (**Supplementary Figure 2A**).

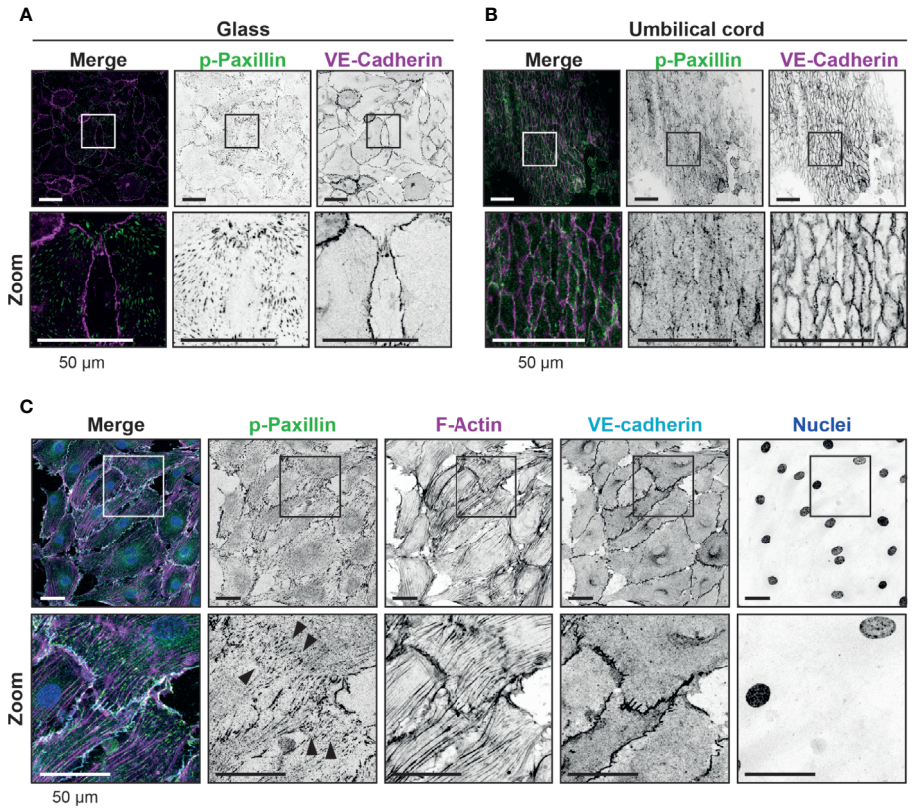

FIGURE 2 | Presence of focal adhesions at endothelium from the umbilical cord. **(A)** Immunofluorescent staining for phospho-paxillin (green) and VE-cadherin (magenta) of HUVECs grown on glass substrate. ROI is indicated in the merge. Images are inverted for clarification. Lower panel shows zoom from ROI. Scale bar, 50 µm. **(B)** Immunofluorescent staining for phospho-paxillin (green) and VE-cadherin (magenta) of HUVECs on an umbilical cord. ROI is indicated in the merge. Images are inverted for clarification. Lower panel shows zoom from ROI. Scale bar, 50 µm **(C)** Immunofluorescent staining for phospho-paxillin (green), F-actin (magenta), VE-cadherin (cyan) and nuclei (blue) of BOEC seeded on umbilical cord, treated with TNF-alpha. ROI is indicated in the merge. Images are inverted for clarification. Lower panel shows zoom from ROI. Black arrowheads indicate focal adhesions. Scale bar, 50 µm.

Neutrophils Navigate Around Focal Adhesions

We hypothesized that neutrophil deformation is imposed by FAs in the subendothelial space. Indeed, neutrophils changed shape to squeeze between FAs (**Figure 3A** and **Supplementary Movie 4**). We quantified the minimum distance between two FAs where a neutrophil can still pass through. This was on average 6 µm, but the minimal distance between two adhesions was as small as 2 µm (**Figure 3B**), indicating that neutrophils underneath the endothelium drastically deform to crawl themselves in between individual FAs.

In addition, neutrophils that crawled at the basolateral level frequently changed their migration direction. To quantify this, we tracked neutrophil migration paths and defined a change in direction as a "turn" when an angle in the migration path was more than 90°. One individual neutrophil was able to change its direction multiple times per minute. We did not see this effect for neutrophils that crawled on the apical surface of the endothelium, as they only occasionally change direction (**Figure 3C**). This suggests that FAs may indeed act as physical obstacles for neutrophils. Related to this finding, we noticed that the basolateral crawling speed of neutrophils is remarkably high, but their net displacement is rather limited (**Figure 3D**). In contrast, the net displacement of apical neutrophils was similar to their total displacement or track length, indicated by a ratio of 1 (**Figure 3D**). By studying the individual crawling tracks, the motion did not occur as directional but rather random (**Figure 3E**). This is in sharp contrast to neutrophils that crawled at the apical side of the endothelium, where migration tracks were often more directional (**Figure 3F**). Together, the findings on the difference of neutrophil crawling either on the apical or basolateral side of the endothelium support the notion that FAs act as physical obstacles for neutrophil basolateral migration.

Neutrophils Navigate Around Focal Adhesions During Basolateral Crawling

As we observed that neutrophils navigated around FAs, we hypothesized that neutrophils did not disrupt or change the turnover of FAs. To test this, we measured the area and perimeter of individual endothelial FAs before and during basolateral crawling of neutrophils. To quantify FA stability, we calculated the total FA area of a region of interest containing one endothelial cell including a neutrophil that was crawling at the

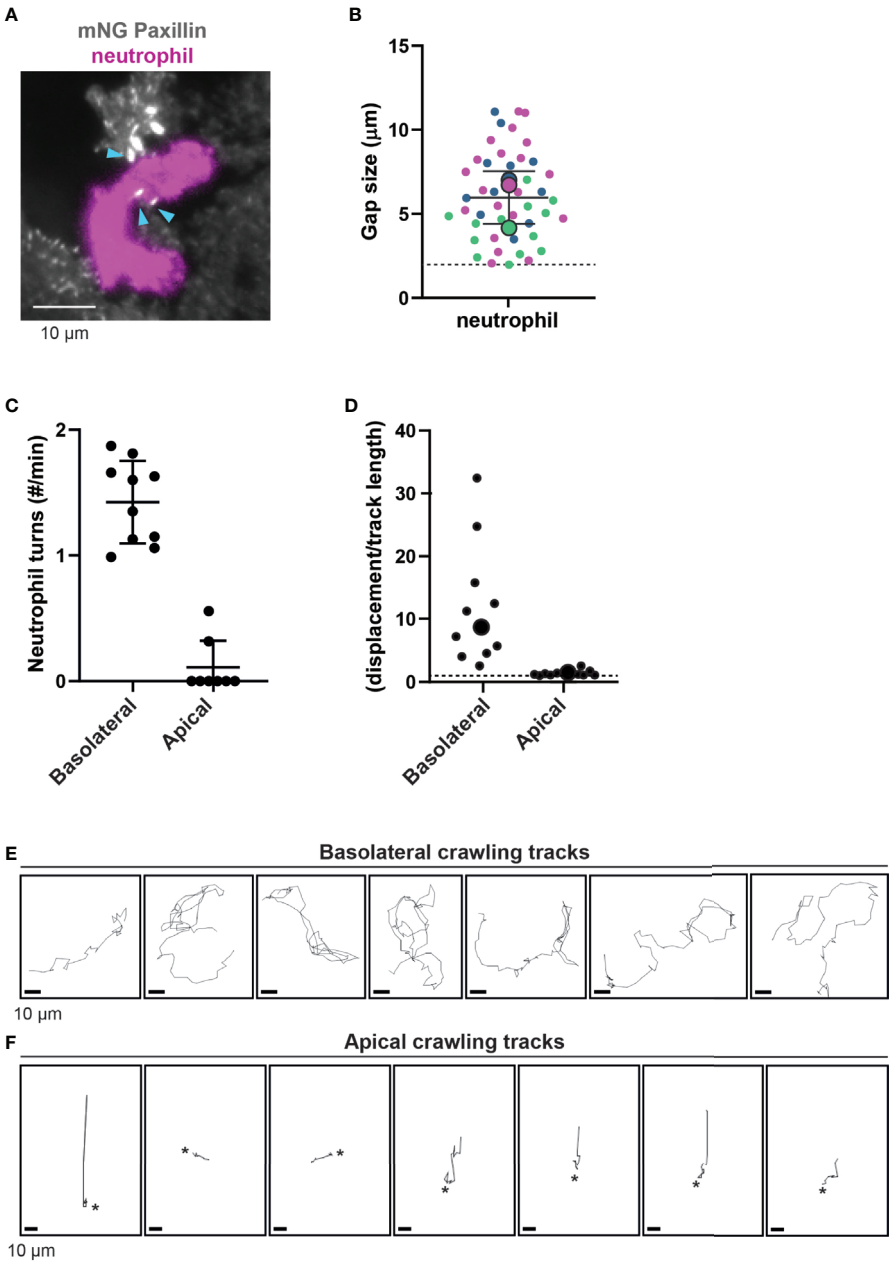

FIGURE 3 | Neutrophil crawling at the apical and basolateral side of the endothelium. **(A)** Still from TIRF microscopy time lapse imaging showing neutrophil (magenta) and mNeonGreen-Paxillin (gray). Neutrophil squeezes through a small gap between three focal adhesions indicated with blue arrowheads. Bar, 10 µm. **(B)** Quantification of gap size between focal adhesions where neutrophils can navigate through. Superplot in which small dots are individual datapoints, large dots represent means from 3 independent experiments (magenta, green, blue). Mean and standard deviation are indicated. Dotted line at 2 µm, indicating the minimum distance between two focal adhesions neutrophils can still migrate through. **(C)** Quantification of the amount of turns (>90°) basolateral and apical neutrophils make per minute. Data from three independent experiments. Each dot represents an individual neutrophil. **(D)** Superplot of ratios of the effective displacement (distance between beginning and end of the migratory track) and the total displacement (length of the migratory track) of basolateral and apical neutrophils. Each dot represents an individual neutrophil. Dotted line represents 1, meaning straight migration paths. Large dots represent means. Welch's T-test p=0.03951772 **(E)** Crawling tracks of neutrophils at the basolateral side of the endothelium. Each frame is about 11 seconds. Bar, 10 µm. **(F)** Crawling tracks of neutrophils at the apical side of the endothelium. Each frame is about 11 seconds. Asterisks indicate start of diapedesis. Bar, 10 µm.

basolateral side. We compared this area before neutrophil arrival at the subendothelial space to the total area after the neutrophil migrated underneath the endothelial cell. This analysis showed that the total FA area did not change upon basolateral crawling of neutrophils (**Figure 4A**). Additionally, the average size of FAs did not change during basolateral crawling of neutrophils (**Figure 4B**). To determine if basolateral crawling of neutrophils changed the shape of FAs, we determined the total

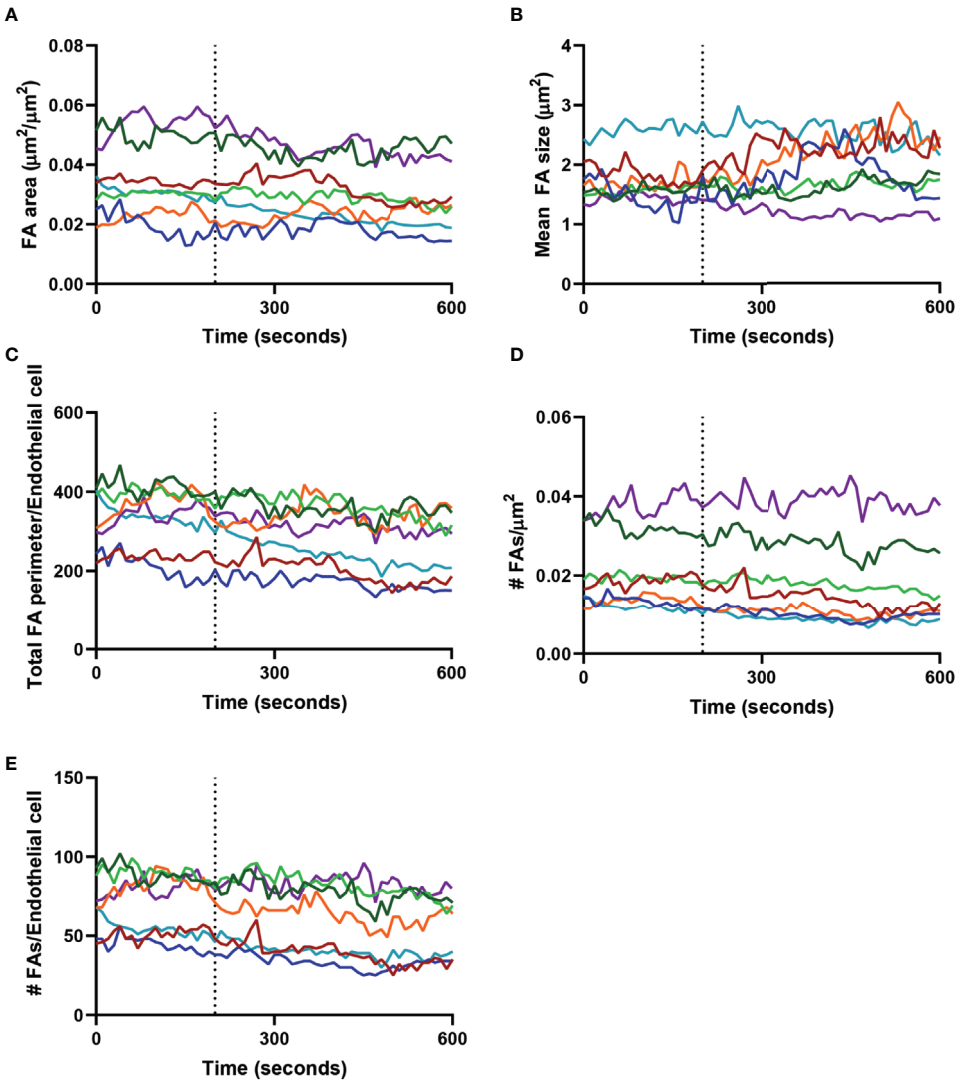

FIGURE 4 | Focal adhesions during neutrophil crawling. Quantification of the focal adhesions (FA) of an endothelial cell with a neutrophil crawling underneath from the dotted line (diapedesis) onwards. Colored lines indicate seven representative neutrophils. **(A)** Graph shows the total focal adhesion area per µm^2. **(B)** Graph shows the mean FA size. **(C)** Graph shows the total perimeter of all the focal adhesions of one endothelial cell. This is a measure for the shape of the focal adhesions. **(D)** Graph shows the number of FAs per µm^2. **(E)** Graph shows the number of FAs per endothelial cell.

perimeter of all FAs in the field of view. Again, we did not find any difference of the FA perimeter upon basolateral crawling of neutrophils (**Figure 4C**). Furthermore, the number of focal adhesions did not change (**Figures 4D**, **E**). Thus, neutrophil TEM including basolateral crawling is a non-destructive process that retains FA integrity. This suggests that FA density can act as barrier for neutrophil migration at the basolateral side.

RhoJ Depletion Results in Reduced Basolateral Crawling Velocity

The small GTPase RhoJ regulates FA turnover, thereby dictating FA density (11). To study if an increase in FA density reduced neutrophil basolateral crawling, we depleted RhoJ from endothelial cells. RhoJ was silenced with an efficacy of >90% (**Supplementary Figures 2B, C**), which resulted in an almost 2-fold increase in the number of FAs (**Figures 5A**, **B**), with no change in FA size (**Figure 5C**). These results enabled us to study if increasing number of FAs perturbed neutrophil TEM and basolateral migration. Indeed, RhoJ silencing reduced neutrophil motility during basolateral crawling (**Figure 5D**), suggesting that increased number of FAs resulted in more obstacles for neutrophils to overcome when migrating underneath the endothelium. To rule out an effect of the underlying matrix that is deposited by the endothelial cells, we performed immunofluorescence staining of the matrix protein fibronectin, known to be involved in inflammation (28). These data showed

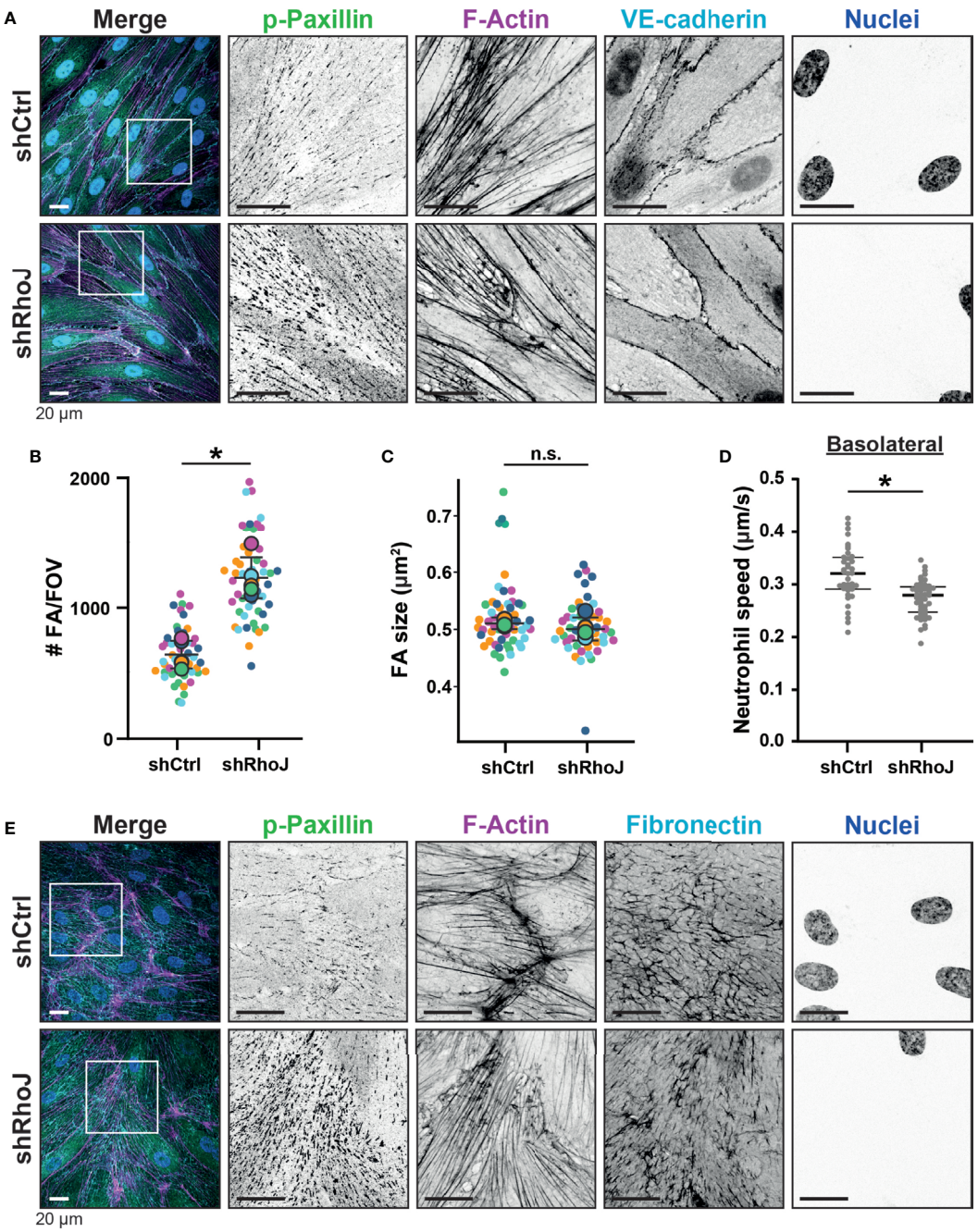

FIGURE 5 | Focal adhesions upon RhoJ silencing. **(A)** Immunofluorescent staining for phospho-paxillin (green), F-actin (magenta), VE-cadherin (Turquoise) and DNA (blue) on HUVECs stimulated for 20h with TNFα. ROI is indicated in the merge. Images are inverted for clarification. Upper panel are control cells (shCtrl), lower panel are cells with RhoJ depletion (shRhoJ). Scale bar, 20 µm. **(B)** Quantification of the number of focal adhesions (FA) per field of view (FOV) for control (shCtrl) and RhoJ knockdown (shRhoJ) conditions. Superplot in which small dots are individual datapoints, large dots represent means from 5 independent experiments (five colors). Mean and standard deviation are indicated. Welch's T-test *p=0.000218. **(C)** Quantification of the size of focal adhesions (FA) for control (shCtrl) and RhoJ knockdown (shRhoJ) conditions. Superplot in which small dots are individual datapoints, large dots represent means from 5 independent experiments (five colors). Mean and standard deviation are indicated. Welch's T-test p=0.2712415, not significant (n.s.). **(D)** Quantification of the speed of basolateral neutrophils under control (shCtrl) and RhoJ knockdown (shRhoJ) endothelial cells. Violin plot in which small dots are individual datapoints. Mann-Whitney U-test: p<0.05.
(E) Immunofluorescent staining for phospho-paxillin (green), F-actin (magenta), Fibronectin (Turquoise) and DNA (blue) on HUVECs stimulated for 20h with TNFα. ROI is indicated in the merge. Images are inverted for clarification. Upper panel are control cells (shCtrl), lower panel are cells with RhoJ depletion (shRhoJ). Scale bar, 20 µm.

no difference in basolateral deposition of fibronectin upon RhoJ depletion (**Figure 5E**). From these experiments we concluded that increasing the number of FAs decreased basolateral crawling speed of neutrophils.

Endothelial RhoJ Depletion Does Not Affect Apical Crawling and Diapedesis of Neutrophils

To study if the number of FAs regulate TEM efficiency, we focused on the different steps of the TEM process under flow conditions. To increase the number of FAs, we used endothelial cells that were silenced for RhoJ or treated with shCtrl. For the apical crawling distance, we did not find any difference of neutrophil crawling between RhoJ-depleted and control endothelial cells (**Figure 6A**). Also, the crawling time, i.e., the time from crawling until diapedesis as well as the speed, did not differ between both endothelial cell treatments (**Figures 6B**, **C**). In line with these findings, RhoJ-deficient endothelial cells did not change the number of neutrophils that transmigrated (**Figure 6D**). This suggests that increasing the number of FAs by RhoJ depletion did not affect neutrophil TEM efficiency.

TIAM-1 Increases FA Number and Blocks Basolateral Crawling of Neutrophils

We hypothesized that if the number of FAs at junction regions can be specifically increased, we may be able to steer neutrophil basolateral migration at the junction regions. By increasing the number of FA in one endothelial cell to the level that neutrophils cannot pass through, but not in the adjacent one, neutrophils would migrate underneath the endothelial cell that allow neutrophils to squeeze through FAs. Overexpression of an active mutant of the GEF Tiam1, Tiam1-C1199, induced massive numbers of FAs (**Figure 7A** and **Supplementary Figure 2D**) (29). Additionally, we found VE-cadherin to be more diffusely distributed over the cell surface. The total area that FAs covered was more than doubled (**Figure 7B**). Furthermore, the number of FAs was elevated (**Figure 7C**) and their size was increased (**Figure 7D**). By transiently expressing Tiam1-C1199, we obtained a monolayer of HUVECs with a mix of normal FA number, i.e., non-transfected endothelial cells and Tiam1-positive endothelial cells showing increased number of FAs, in particular at junction regions. We used this system to study whether neutrophils preferred either of the two cell types for basolateral crawling. The number of neutrophils that crossed the endothelium was unaltered. However, we observed that crawling neutrophils seem to avoid Tiam-1-expressing cells. Upon diapedesis, we found that neutrophils first started to penetrate underneath the Tiam1-C1199-expressing endothelial cell but after 2-3 μm underneath this cell, the neutrophil turned and migrated away from the Tiam1-positive endothelial cell and continued migrating underneath the control endothelial cell (**Figure 7E**, **Supplementary Figure 3A** and

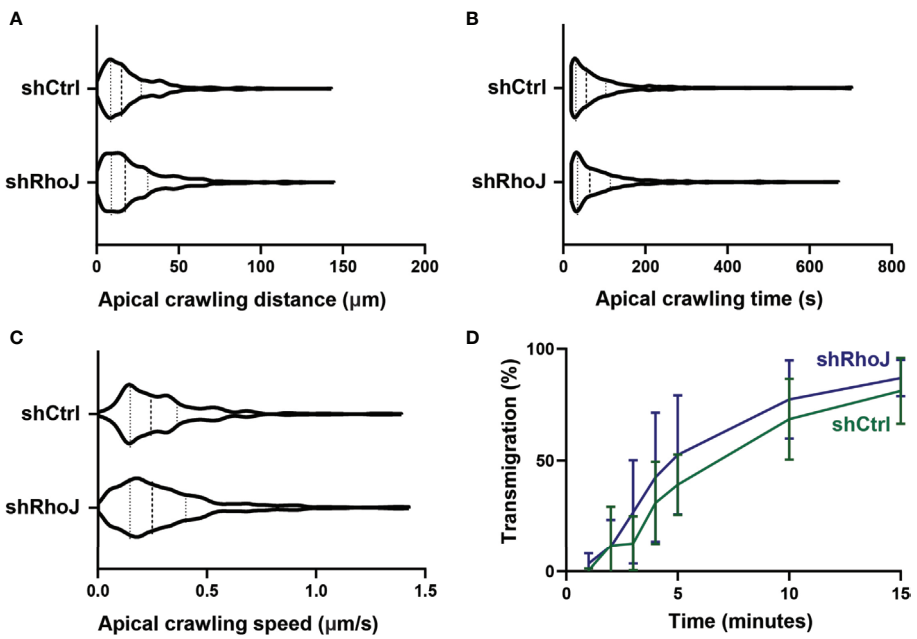

FIGURE 6 | Transendothelial migration upon RhoJ silencing in endothelial cells. **(A)** Quantification of the distance of apical neutrophils in the crawling stage on control (shCtrl) and RhoJ knockdown (shRhoJ) endothelial cells. Violin plot of three independent experiments including at least 100 neutrophils per experiment **(B)** Quantification of the apical crawling time of neutrophils on control (shCtrl) and RhoJ knockdown (shRhoJ) endothelial cells. Violin plot of three independent experiments including at least 100 neutrophils per experiment. **(C)** Quantification of the speed of apical neutrophils in the crawling stage on control (shCtrl) and RhoJ knockdown (shRhoJ) endothelial cells. Violin plot of three independent experiments including at least 100 neutrophils per experiment. **(D)** Quantification of the percentage of neutrophils that underwent diapedesis for control endothelial cells (shCtrl, green) and RhoJ silenced endothelial cells (shRhoJ, blue). Data from three independent experiments including at least 100 neutrophils per experiment. Error bars show standard deviation.

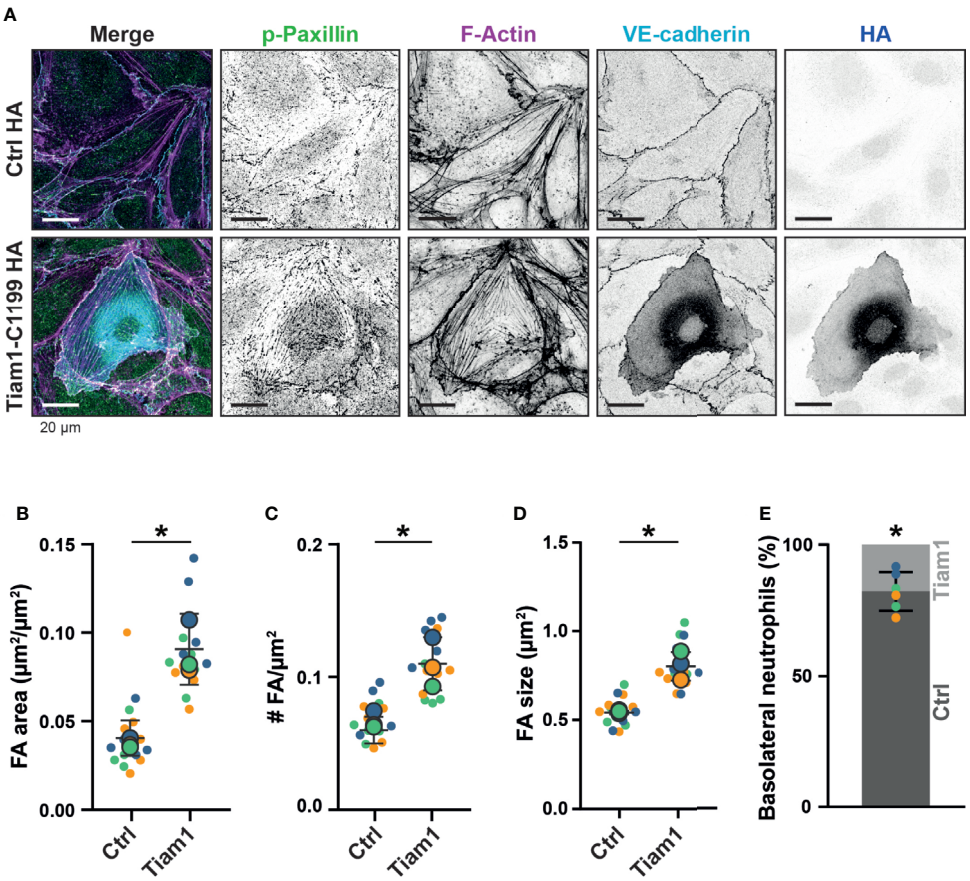

FIGURE 7 | Focal adhesions upon Tiam1-C1199 expression. **(A)** Immunofluorescent staining for phospho-paxillin (green), F-actin (magenta), VE-cadherin (Turquoise) and HA (blue) on HUVECs stimulated for 20h with TNFα. Images are inverted for clarification. Upper panel are control cells (Ctrl HA), lower panel are cells expressing Tiam1-C1199 (Tiam1-C1199). Scale bar, 20 µm. **(B)** Quantification of the area focal adhesions (FA) cover or control (Ctrl) and Tiam1-C1199-expressing cells (Tiam1-C1199). Superplot in which small dots are individual datapoints, large dots represent means from 3 independent experiments (three colors). Mean and standard deviation are indicated. Welch's T-test *p=0.02411431. **(C)** Quantification of the number of focal adhesions (FA) per field of view (FOV) for control (Ctrl) and Tiam1-C1199-expressing cells (Tiam1-C1199). Superplot in which small dots are individual datapoints, large dots represent means from 3 independent experiments (three colors). Mean and standard deviation are indicated. Welch's T-test *p=0.04694375. **(D)** Quantification of the size of focal adhesions (FA) in control (Ctrl) and Tiam1-C1199-expressing cells (Tiam1-C1199). Superplot in which small dots are individual datapoints, large dots represent means from 3 independent experiments (three colors). Mean and standard deviation are indicated. Welch's T-test *p=0.02819648 **(E)** Quantification of the percentage of TEM events in which a neutrophil migrates at a control-Tiam1-C1199 junction and migrates further underneath the Tiam1-C1199 cell (light bar) versus neutrophils that migrate further underneath the control cell (dark bar). Dots represent individual datapoints from three experiments (three colors). Error bar shows 95% confidence interval. One-sample Wilcoxon test: $p<0.05$.

Supplementary Movie 5). These results clearly demonstrated that neutrophils preferred endothelial cells with lower numbers of FAs for basolateral crawling. Moreover, we observed that neutrophils that transmigrated at cell-cell junctions, consisting of two Tiam1-expressing endothelial cells, were trapped at the junction (**Supplementary Figure 3B** and **Supplementary Movie 6**). This observation suggest that neutrophils can be hindered at the basolateral level by increasing the number of FAs that function as physical obstacles for neutrophils. To study if potential other mechanisms can drive preferential basolateral migration of neutrophils under neath control endothelial cells, like decreased adhesion molecule expression at the Tiam1-C1199 cells compared to the control endothelial cells, we performed immunofluorescent stainings. By using TIRF microscopy, we specifically imaged the basolateral side of the endothelium and found that the expression levels of ICAM-1 in Tiam1-C1199 cells were comparable to control cells (**Supplementary Figures 3C, D**). Moreover, also PECAM-1 stainings showed a similar pattern between control and Tai1-C1199 expressing endothelial cells (**Supplementary Figure 3E**). It should be noted that endothelial cells that express Tiam1-C1199 showed a larger morphology, most likely due to intrinsic rac1 activation, a well-known regulator of endothelial cell size (29). The percentage of neutrophils that underwent diapedesis across Tiam1-C1199-expressing HUVEC was similar to control situations.

Together, our data suggest that endothelial FAs can mark the basolateral migration path for neutrophils and may thereby regulate efficient entering of the underlying tissue.

DISCUSSION

Although many studies focus on the apical crawling of leukocytes that initiates the TEM process, little is known about leukocyte migration underneath the endothelium once they have crossed it. It is well recognized that neutrophils reside for about 20 minutes at the subendothelial space (4), indicating the importance of this phase. It is believed that they search for a spot to escape the basement membrane and the pericyte layer to enter the underlying tissue (30). However, it is unclear what factors contribute to the pause before the tissue is invaded. To increase our understanding of factors that regulate neutrophil migration at the basolateral level of the endothelium, we focused on this post-diapedesis step of the inflammatory response using TIRF microscopy.

Underneath the endothelium, neutrophils encounter focal, protein complexes that link the endothelial cell to the underlying substratum (31). Interestingly, when observing neutrophils migrating at this basolateral side of the endothelium, it appears that the endothelial cells themselves are not hampered in any way by the presence of these neutrophils. Endothelial cells remain firmly bound to the substratum. Using TIRF microcopy, our data show that neutrophils leave FAs intact and migrate around these static structures rather than breaking them down. Our observations contrast a previous study on T-cells in which FAs were studied with interference reflection microscopy, which is a label-free method. In that study, detachment was observed and it was proposed that transient weakening of FA attachment was required to widen subendothelial spaces (9). However, the signal of the T-cells interfered with that of the FAs and therefore unambiguous identification of FAs was not possible. Here, using dual color fluorescence imaging we were able to identify both FAs and neutrophils with high spatial and temporal resolution. Our observations support the idea that FAs at the basolateral side of the endothelium remain intact and act as physical obstacles.

Our data shows that the minimum gap between FAs through which neutrophils could squeeze themselves was 2 μm. During the migration through these gaps, neutrophils drastically deform their cell body. It was previously reported that using a system with artificial pores, neutrophils prefer pores sizes of at least 2 μm (32). This cut-off is strikingly similar to the size limit that we found for neutrophils, suggesting that the cellular deformation is triggered by physical cues rather than a chemical or signaling factor.

The largest organelle of the neutrophil, the nucleus, is multi-lobular, making it easier to deform. It is known that the nucleus is particularly important during migration of neutrophils. Renkawitz and colleagues showed that the nucleus can be used as a mechanical gauge that neutrophils use to migrate through a narrow pore (32). Similar to what we observed in our experiments, protrusions from the neutrophils poked into several pores, but once the nucleus fit through a certain narrow pore, the other protrusions are retracted, and the neutrophil migrated forward (32). This notion of the neutrophil trying several routes before choosing the path of least resistance and squeezing through two individual FAs was supported by our observations. These observations are also in line with the work by Barzilai and co-workers (33). They showed that the neutrophil used its nucleus as a "drill" to initiate the diapedesis step and penetrate the endothelium (33). Our data now add to the idea that the nucleus is not only used to penetrate the endothelial monolayer but is also used to find its way through the physical obstacles made by the basolateral FAs.

Our work indicates that FAs act as obstacles for neutrophils. It is important to note that FAs also include the basement membrane protein underneath the FA. Therefore, it is possible that the basement membrane itself may also function as an obstacle for migrating neutrophils. Interestingly, we noticed reduced presence of basement membrane proteins underneath the nucleus. This may explain why we see not so many neutrophils crawling underneath the nucleus. In particular under inflammatory conditions, the composition of the extracellular matrix can change, having an effect on how leukocytes may cross the vascular border (REF). In fact, different vascular beds display different basement membrane proteins (REF). And as the composition of the subendothelial space plays an important role in TEM, it is an important factor to consider when studying leukocyte transmigration. This consideration is often not included in *in vitro* studies. The matrix underneath the endothelium is far from homogenous. So-called low expression regions (LERs) have been identified by Wang and colleagues as sites with considerably lower expression of key vascular basement membrane constituents (34). Additional work by the Sorokin lab showed that basal membrane proteins such as laminin 511 can act as barriers for neutrophils to cross the endothelial cell junctions (35). They furthermore show in additional work that loss of endothelial laminin 511 results in enhanced experimental autoimmune encephalomyelitis due to increased T cell infiltration (36). These LERs are associated with gaps between pericytes and are preferentially used by transmigrating neutrophils (4). Neutrophils seem to prefer the path of least resistance, as supported by our experiments that showed that increased number of FAs prevents proper basolateral crawling of neutrophils. Interestingly, the gap size through which neutrophils crossed the pericyte layer and the basement membrane was entirely dependent on the presence of neutrophils and appeared to involve neutrophil-derived serine proteases (34). Wang and colleagues showed neutrophil-dependent degradation of basement membrane proteins, whereas our study among others (9) show that the size and number of FAs are not changed in the presence of neutrophils. This suggests that neutrophils have two ways of migrating through confined spaces: 1. By navigating around physical obstacles and 2. By taking the path of least resistance and degrade matrix proteins. In this way neutrophils could efficiently migrate into the tissue without causing unnecessary tissue damage.

In the present study, we did not take the role of pericytes into account. However, it is clear that pericytes play a particularly important role in the extravasation of neutrophils *in vivo* (4).

Neutrophils use their integrins to bind to ICAM-1 on pericytes and migrate towards gaps in the pericyte layer. These gaps are enlarged upon inflammation because of shape changes of pericytes, making space for neutrophils to exit the vessel wall (4). Neutrophils exhibit abluminal crawling for about 20 minutes before migrating further into the tissue. In this time, they migrated about 54 μm between the endothelial cells and pericytes (4). This underscores the importance of this post-diapedesis stage of TEM. Using our simplified setup without pericytes and with the use of the TIRF microscopy, we could specifically focus on FAs only.

Furthermore, substrate stiffness of the underlying tissue might also play an important role (37). We previously showed that substrate stiffness is translated by the endothelium *via* the protein DLC-1. This mechanism mainly affects the adhesion stage but not the diapedesis itself (37). Another study confirmed these findings and showed that neutrophil TEM increased with increasing substrate stiffness (38). However, extracellular matrix rigidity does induce FA formation in both arterial and venous endothelial cells (8). Therefore, it may also affect basolateral crawling, and this might result in altered inflammatory response.

In summary, we show that endothelial FAs act as physical obstacles for neutrophils that crawl at a basolateral side of the endothelium. FAs cause deformation of the neutrophil and slow down or even block basolateral crawling. This in the end may determine the efficiency for neutrophils entering the inflamed tissue and reaching the place of infection.

DATA AVAILABILITY STATEMENT

The raw data supporting the conclusions of this article will be made available by the authors, without undue reservation.

AUTHOR CONTRIBUTIONS

JA, EM, LS, MG, SN, BK, MF-B, JR, DG, and SH: Data collection, analysis, and interpretation. JB and JG: Project design. JA, JB, and JG: Drafting and writing the manuscript. All authors contributed to the article and approved the submitted version.

FUNDING

This work was supported by ZonMW NWO Vici grant # 91819632 (JB/MG) and NWO ALW-OPEN grant ALWOP.306 (EM).

SUPPLEMENTARY MATERIAL

The Supplementary Material for this article can be found online at: https://www.frontiersin.org/articles/10.3389/fimmu.2021.667213/full#supplementary-material

Supplementary Figure 1 | (A) Immunofluorescent staining for Laminin α4, Laminin 1/2, Collagen IV, or Fibronectin (green) and VE-cadherin (magenta). Right panel shows the merged image. Scale bar, 20 μm. **(B)** Stills from TIRF microcopy times lapse imaging showing 3 representative neutrophil shapes during crawling at the basolateral side of the endothelium. Bar, 10 μm. **(C)** Stills from widefield microscopy time lapse imaging showing 3 representative neutrophil shapes during crawling at the apical side of the endothelium. Bar, 10 μm. **(D)** 3D view stills from two ECs (green/turquoise) and a neutrophil (magenta) at three time points (apical crawling, mid-diapedesis, and basolateral crawling). Right panels show only the neutrophil. Bar, 5μm. **(E)** Immunofluorescent staining for phospho-paxillin (green) and VE-cadherin (magenta) of HUVECs grown on glass substrate. ROI is indicated in the merge. Images are inverted for clarification. Lower panel shows zoom from ROI. Scale bar, 50 μm. **(F)** Immunofluorescent staining for phospho-paxillin (green) and VE-cadherin (magenta) of HUVECs on an umbilical cord. ROI is indicated in the merge. Images are inverted for clarification. Lower panel shows zoom from ROI. Scale bar, 50 μm.

Supplementary Figure 2 | (A) Immunofluorescent staining of mesenteric artery for phospho-paxillin (green), F-actin (magenta) and VE-cadherin (cyan). Lower panels are zoom of the ROI indicated in upper panels. Scale bar, 20 μm. **(B)** Western blot analysis shows successful knock down of RhoJ. Actin is shown as loading control. **(C)** Quantification of Western blot in (A). Error bar median with 95% confidence interval. Mann-Whitney U-test: $p<0.05$. **(D)** Immunofluorescent staining for phospho-paxillin (green), F-actin (magenta), VE-cadherin (Turquoise) and HA (blue) on HUVECs stimulated for 20h with TNFα. ROI is indicated in the merge. Images are inverted for clarification. Upper panel are control cells (Ctrl HA), lower panel are cells expressing Tiam1-C1199 (Tiam1-C1199). Scale bar, 20 μm.

Supplementary Figure 3 | (A) DIC stills from time lapse image showing three Tiam1-C1199 cells (dotted white line) and neutrophils that transmigrate at a ctrl-Tiam1-C1199 junction. Basolateral crawling tracks of these neutrophils are indicated in blue. Stills from Supplemental Movie 5. Time indicated in seconds in upper right corner. Bar, 50 μm. **(B)** DIC stills from time lapse image showing three Tiam1-C1199 cells (dotted white line) and a neutrophil that transmigrates at a ctrl-Tiam1-C1199 junction (arrowhead). The neutrophil remains stuck between the two Tiam1-C1199 cells. Stills from Supplemental Movie 6. Time indicated in seconds in upper right corner. Bar, 50 μm. **(C)** Immunofluorescent staining for ICAM-1 (green) and HA (Tiam1-C1199 HA) (magenta) on HUVECs stimulated for 4h with TNFα. ROI is indicated in the merge. Images are acquired using TIRF microscopy. Scale bar, 20 μm. **(D)** Quantification of ICAM-1 expression levels using MFI (mean fluorescence intensity) in HUVEC expressing Tiam1-C1199 or control (ctrl), all stimulated for 4h with TNFα. Lines indicate medians. **(E)** Immunofluorescent staining for PECAM (green) and HA (Tiam1-C1199 HA) (magenta) on HUVECs stimulated for 4h with TNFα. ROI is indicated in the merge. Images are acquired using confocal microscopy, maximum intensity projection. Scale bar, 20 μm. **(F)** Table with statistical information of the superplots (**Figures 3D**, **5B**, **5C**, **7B**, **7C**, **7D**).

Supplementary Movie 1 | DIC time lapse imaging of TEM followed by basolateral crawling, showing extensive change of direction. Time is indicated in seconds in upper left corner. Bar, 20 μm.

Supplementary Movie 2 | Time lapse TIRF imaging of basolateral crawling of neutrophils, showing that focal adhesions act as physical barriers for neutrophils. mNeonGreen-Paxillin (grey) expressing endothelial cells and labelled neutrophils (magenta). Time is indicated in seconds in upper left corner. Bar, 20 μm.

Supplementary Movie 3 | Time lapse TIRF imaging of basolateral crawling of neutrophils, showing dynamic changes in cell shape. Endothelial cells (not shown) and labelled neutrophils (grey). Time is indicated in seconds in upper left corner. Bar, 20 μm.

Supplementary Movie 4 | Time lapse TIRF imaging of basolateral crawling of neutrophils, showing that focal adhesions act as physical barriers for neutrophils. mNeonGreen-Paxillin (grey) expressing endothelial cells and labelled neutrophils (magenta). Time is indicated in seconds in upper left corner. Bar, 20 μm.

Supplementary Movie 5 | DIC time lapse image of three Tiam1-C1199 cells (center) and neutrophils that avoid crawling underneath the Tiam1-C1199 cells. Stills are depicted in supplemental **Figure 2B**. Time is indicated in seconds in upper left corner. Bar, 50 μm.

Supplementary Movie 6 | DIC time lapse image of two Tiam1-C1199 cells (center) and a neutrophil that is trapped at the junction in between these two Tiam1-C1199 cells. Stills are depicted in supplemental **Figure 2C**. Time is indicated in seconds in upper left corner. Bar, 50 μm.

REFERENCES

1. Butcher EC. Leukocyte-Endothelial Cell Recognition: Three (or More) Steps to Specificity and Diversity. *Cell Elsevier* (1991) 1033–6.
2. Springer TA. Traffic Signals for Lymphocyte Recirculation and Leukocyte Emigration: The Multistep Paradigm. *Cell Elsevier* (1994) 301–14.
3. Hyun YM, Sumagin R, Sarangi PP, Lomakina E, Overstreet MG, Baker CM, et al. Uropod Elongation is a Common Final Step in Leukocyte Extravasation Through Inflamed Vessels. *J Exp Med* (2012) 209(7):1349–62.
4. Proebstl D, Voisin M-B, Woodfin A, Whiteford J, D'Acquisto F, Jones GE, et al. Pericytes Support Neutrophil Subendothelial Cell Crawling and Breaching of Venular Walls in Vivo. *J Exp Med* (2012) 209(6):1219–34.
5. Parsons SA, Sharma R, Roccamatisi DL, Zhang H, Petri B, Kubes P, et al. Endothelial Paxillin and Focal Adhesion Kinase (FAK) Play a Critical Role in Neutrophil Transmigration. *Eur J Immunol* (2012) 42(2):436–46.
6. Kuo J-C. Mechanotransduction At Focal Adhesions: Integrating Cytoskeletal Mechanics in Migrating Cells. *J Cell Mol Med* (2013) 17(6):704–12.
7. Zaidel-Bar R, Cohen M, Addadi L, Geiger B. Hierarchical Assembly of Cell-Matrix Adhesion Complexes. *Biochem Soc Trans* (2004) 32(Pt3):416–20. doi: 10.1042/BST0320416
8. van Geemen D, Smeets MWJ, van Stalborch A-MD, Woerdeman LAE, Daemen MJAP, Hordijk PL, et al. F-Actin-Anchored Focal Adhesions Distinguish Endothelial Phenotypes of Human Arteries and Veins. *Arterioscler Thromb Vasc Biol* (2014) 34(9):2059–67.
9. Lee J, Song KH, Kim T, Doh J. Endothelial Cell Focal Adhesion Regulates Transendothelial Migration and Subendothelial Crawling of T Cells. *Front Immunol* (2018) 9:48.
10. Vignal E, De Toledo M, Comunale F, Ladopoulou A, Gauthier-Rouvière C, Blangy A, et al. Characterization of TCL, a New Gtpase of the Rho Family Related to TC10 Andccdc42. *J Biol Chem* (2000) 275(46):36457–64.
11. Wilson E, Leszczynska K, Poulter NS, Edelmann F, Salisbury VA, Noy PJ, et al. RhoJ Interacts With the GIT-PIX Complex and Regulates Focal Adhesion Disassembly. *J Cell Sci* (2014) 127(Pt 14):3039–51.
12. Leszczynska K, Kaur S, Wilson E, Bicknell R, Heath VL. The Role of RhoJ in Endothelial Cell Biology and Angiogenesis. *Biochem Soc Trans* (2011) 39(6):1606–11.
13. Yuan L, Sacharidou A, Stratman AN, Le Bras A, Zwiers PJ, Spokes K, et al. RhoJ is an Endothelial Cell-Restricted Rho-GTPase That Mediates Vascular Morphogenesis and is Regulated by the Transcription Factor ERG. *Blood* (2011) 118(4):1145–53.
14. Heemskerk N, Van Rijssel J, Van Buul JD. Rho-GTPase Signaling in Leukocyte Extravasation: An Endothelial Point of View. *Cell Adhes Migr* (2014) 8(2):67–75.
15. van Buul JD, Allingham MJ, Samson T, Meller J, Boulter E, García-Mata R, et al. RhoG Regulates Endothelial Apical Cup Assembly Downstream From ICAM1 Engagement and is Involved in Leukocyte Trans-Endothelial Migration. *J Cell Biol* (2007) 178(7):1279–93.
16. Kroon J, Schaefer A, van Rijssel J, Hoogenboezem M, van Alphen F, Hordijk P, et al. Inflammation-Sensitive Myosin-X Functionally Supports Leukocyte Extravasation by Cdc42-Mediated ICAM-1-rich Endothelial Filopodia Formation. *J Immunol* (2018) 200(5):1790–801.
17. van Rijssel J, Kroon J, Hoogenboezem M, van Alphen FPJ, de Jong RJ, Kostadinova E, et al. The Rho-Guanine Nucleotide Exchange Factor Trio Controls Leukocyte Transendothelial Migration by Promoting Docking Structure Formation. *Mol Biol Cell* (2012) 23(15):2831–44.
18. Thompson PW, Randi AM, Ridley AJ. Intercellular Adhesion Molecule (ICAM)-1, But Not ICAM-2, Activates RhoA and Stimulates C-Fos and RhoA Transcription in Endothelial Cells. *J Immunol* (2002) 169(2):1007–13.
19. Schnoor M, Lai FPL, Zarbock A, Kläver R, Polaschegg C, Schulte D, et al. Cortactin Deficiency is Associated With Reduced Neutrophil Recruitment But Increased Vascular Permeability in Vivo. *J Exp Med* (2011) 208(8):1721–35.
20. Millán J, Hewlett L, Glyn M, Toomre D, Clark P, Ridley AJ. Lymphocyte Transcellular Migration Occurs Through Recruitment of Endothelial ICAM-1 to Caveola- and F-Actin-Rich Domains. *Nat Cell Biol* (2006) 8(2):113–23.
21. Martin-Ramirez J, Hofman M, van den Biggelaar M, Hebbel RP, Voorberg J. Establishment of Outgrowth Endothelial Cells From Peripheral Blood. *Nat Protoc* (2012) 7(9):1709–15.
22. Arts JJG, Mahlandt EK, Grönloh MLB, Schimmel L, Noordstra I, van Steen ACI, et al. Endothelial Junctional Membrane Protrusions Serve as Hotspots for Neutrophil Transmigration. *bioRxiv* (2021) 2021.01.18.427135.
23. Chertkova AO, Mastop M, Postma M, van Bommel N, van der Niet S, Batenburg KL, et al. Robust and Bright Genetically Encoded Fluorescent Markers for Highlighting Structures and Compartments in Mammalian Cells. *bioRxiv* (2020) 160374.
24. Goedhart J. Superplotsofdata - a Web App for the Transparent Display and Quantitative Comparison of Continuous Data From Different Conditions. *Mol Biol Cell* (2021) 32(6):470–74. doi: 10.1091/mbc.E20-09-0583
25. Yuan SY, Shen Q, Rigor RR, Wu MH. Neutrophil Transmigration, Focal Adhesion Kinase and Endothelial Barrier Function. *Microvasc Res* (2012) 83 (1):82–8.
26. Turner CE. Paxillin. *Int J Biochem Cell Biol* (1998) 30(9):955–9.
27. Hoffman BD. The Detection and Role of Molecular Tension in Focal Adhesion Dynamics. *Prog Mol Biol Transl Sci* (2014) 126:3–24.
28. Yun S, Budatha M, Dahlman JE, Coon BG, Cameron RT, Langer R, et al. Interaction Between Integrin Alpha 5 and PDE4D Regulates Endothelial Inflammatory Signalling. *Nat Cell Biol* (2016) 18(10):1043–53.
29. Klems A, van Rijssel J, Ramms AS, Wild R, Hammer J, Merkel M, et al. The GEF Trio Controls Endothelial Cell Size and Arterial Remodeling Downstream of Vegf Signaling in Both Zebrafish and Cell Models. *Nat Commun* (2020) 11(1):5319.
30. Voisin M-B, Nourshargh S. Neutrophil Trafficking to Lymphoid Tissues: Physiological and Pathological Implications. *J Pathol* (2019) 247(5):662–71.
31. Hallmann R, Zhang X, Di Russo J, Li L, Song J, Hannocks M-J, et al. The Regulation of Immune Cell Trafficking by the Extracellular Matrix. *Curr Opin Cell Biol* (2015) 36:54–61.
32. Renkawitz J, Kopf A, Stopp J, de Vries I, Driscoll MK, Merrin J, et al. Nuclear Positioning Facilitates Amoeboid Migration Along the Path of Least Resistance. *Nature* (2019) 568(7753):546–50.
33. Barzilai S, Yadav SK, Morrell S, Roncato F, Klein E, Stoler-Barak L, et al. Leukocytes Breach Endothelial Barriers by Insertion of Nuclear Lobes and Disassembly of Endothelial Actin Filaments. *Cell Rep* (2017) 18(3):685–99.
34. Wang S, Voisin M-B, Larbi KY, Dangerfield J, Scheiermann C, Tran M, et al. Venular Basement Membranes Contain Specific Matrix Protein Low Expression Regions That Act as Exit Points for Emigrating Neutrophils. *J Exp Med* (2006) 203(6):1519–32.
35. Song J, Zhang X, Buscher K, Wang Y, Wang H, Di Russo J, et al. Endothelial Basement Membrane Laminin 511 Contributes to Endothelial Junctional Tightness and Thereby Inhibits Leukocyte Transmigration. *Cell Rep* (2017) 18(5):1256–69.
36. Zhang X, Wang Y, Song J, Gerwien H, Chuquisana O, Chashchina A, et al. The Endothelial Basement Membrane Acts as a Checkpoint for Entry of Pathogenic T Cells Into the Brain. *J Exp Med* (2020) 217(7):e20191339. doi: 10.1084/jem.20191339
37. Schimmel L, van der Stoel M, Rianna C, van Stalborch A-MM, de Ligt A, Hoogenboezem M, et al. Stiffness-Induced Endothelial DLC-1 Expression Forces Leukocyte Spreading Through Stabilization of the ICAM-1 Adhesome. *Cell Rep* (2018) 24(12):3115–24.
38. Stroka KM, Aranda-Espinoza H. Endothelial Cell Substrate Stiffness Influences Neutrophil Transmigration Via Myosin Light Chain Kinase-Dependent Cell Contraction. *Blood* (2011) 118(6):1632–40.

Conflict of Interest: The authors declare that the research was conducted in the absence of any commercial or financial relationships that could be construed as a potential conflict of interest.

frontiers in Immunology

ORIGINAL RESEARCH
published: 31 May 2021
doi: 10.3389/fimmu.2021.678030

Defective Neutrophil Transendothelial Migration and Lateral Motility in ARPC1B Deficiency Under Flow Conditions

Lanette Kempers[1†], *Evelien G. G. Sprenkeler*[2,3*†], *Abraham C. I. van Steen*[1†], *Jaap D. van Buul*[1,4*‡] *and Taco W. Kuijpers*[2,3‡]

[1] *Molecular Cell Biology Laboratory, Department of Molecular and Cellular Haemostasis, Sanquin Research, Amsterdam University Medical Center (AUMC), Amsterdam, Netherlands,* [2] *Department of Blood Cell Research, Sanquin Research, AUMC, University of Amsterdam, Amsterdam, Netherlands,* [3] *Department of Pediatric Immunology, Rheumatology and Infectious Diseases, Emma Children's Hospital, AUMC, University of Amsterdam, Amsterdam, Netherlands,* [4] *Leeuwenhoek Centre for Advanced Microscopy, Section Molecular Cytology, Swammerdam Institute for Life Sciences, University of Amsterdam, Amsterdam, Netherlands*

OPEN ACCESS

Edited by:
Jörg Renkawitz, Ludwig Maximilian University of Munich, Germany

Reviewed by:
Christoph Andreas Reichel, Ludwig-Maximilians-Universität München, Germany
Craig T. Lefort, Rhode Island Hospital, United States

***Correspondence:**
Jaap D. van Buul
J.vanbuul@sanquin.nl
Evelien G. G. Sprenkeler
E.sprenkeler@sanquin.nl

[†]*These authors have contributed equally to this work and share first authorship*

[‡]*These authors have contributed equally to this work and share senior authorship*

Specialty section:
This article was submitted to Molecular Innate Immunity, a section of the journal Frontiers in Immunology

Received: *08 March 2021*
Accepted: *13 May 2021*
Published: *31 May 2021*

Citation:
Kempers L, Sprenkeler EGG, van Steen ACI, van Buul JD and Kuijpers TW (2021) Defective Neutrophil Transendothelial Migration and Lateral Motility in ARPC1B Deficiency Under Flow Conditions. Front. Immunol. 12:678030. doi: 10.3389/fimmu.2021.678030

The actin-related protein (ARP) 2/3 complex, essential for organizing and nucleating branched actin filaments, is required for several cellular immune processes, including cell migration and granule exocytosis. Recently, genetic defects in ARPC1B, a subunit of this complex, were reported. Mutations in *ARPC1B* result in defective ARP2/3-dependent actin filament branching, leading to a combined immunodeficiency with severe inflammation. *In vitro*, neutrophils of these patients showed defects in actin polymerization and chemotaxis, whereas adhesion was not altered under static conditions. Here we show that under physiological flow conditions human ARPC1B-deficient neutrophils were able to transmigrate through TNF-α-pre-activated endothelial cells with a decreased efficiency and, once transmigrated, showed definite impairment in subendothelial crawling. Furthermore, severe locomotion and migration defects were observed in a 3D collagen matrix and a perfusable vessel-on-a-chip model. These data illustrate that neutrophils employ ARP2/3-independent steps of adhesion strengthening for transmigration but rely on ARP2/3-dependent modes of migration in a more complex multidimensional environment.

Keywords: primary immunodeficiency, ARPC1B deficiency, ARP2/3 complex, neutrophil, neutrophil transmigration, inborn error of immunity, vessel-on-a-chip

INTRODUCTION

Neutrophils are the most abundant type of leukocytes in the human circulation and important effector cells in the innate immune system. They are the first cells recruited to sites of infection or inflammation, where they extravasate through the blood vessel into the tissue. This process, also known as transendothelial migration (TEM), can be divided into several steps, namely tethering, selectin-mediated rolling and slow rolling, selectin-mediated and chemokine-mediated integrin activation resulting in arrest, adhesion strengthening, spreading, intravascular crawling, and

transmigration (either paracellular or transcellular) (1). Once neutrophils cross the endothelial cell layer they encounter a second barrier, the vascular basement membrane (BM). This BM provides structural support for endothelial cells and is composed of a network of multiple extracellular matrix (ECM) proteins, including laminins and collagen type IV (2). After crossing these layers, neutrophils continue to migrate and enter the tissue to reach and fight infection.

By studying rare primary immunodeficiencies (PIDs), essential proteins in the different steps of TEM have been identified. Well-known PIDs resulting in defective TEM are leukocyte adhesion deficiencies (LADs), where patients have mutations in genes involved in leukocyte integrin signaling (LAD-I and LAD-III), resulting in an adhesion defect. In LAD-II, defective fucosylation of selectin ligands results in the inability of neutrophils to bind to endothelial selectins (E- and P-selectins), resulting in a rolling defect (3).

In 2017, a novel PID involving infections, bleeding episodes, allergy and auto-inflammation was identified caused by mutations in the *ARPC1B* gene (4). ARPC1B is one of 7 subunits of the actin-related protein (ARP) 2/3 complex, which is required for the formation of branched actin networks as it nucleates a daughter filament to the side of a pre-existing actin filament (5). These branched actin filaments are of vital importance for the formation of lamellipodia at the leading edge of migrating cells. Analysis of patient-derived neutrophils showed a defect in actin polymerization, resulting in a severe chemotaxis defect through 3-μm pore-size filters (4). Here we investigated ARPC1B-deficient neutrophil migration in more depth by using TEM flow and 3D vessel-on-a-chip models allowing us to monitor the full process of neutrophil migration from the vessel lumen into the tissue environment.

MATERIALS AND METHODS

Isolation of Human Primary Cells From Patient and Controls

Heparinized venous blood was drawn from healthy controls and an ARPC1B-deficient patient after informed consent had been obtained. A detailed description of the patient's history has been reported previously (4). Neutrophils were isolated as previously described (6). Subsequently, neutrophils ($5x10^6$/mL) were fluorescently labelled with Vybrant™ DiD Cell-Labeling Solution (dilution 1:1,000; Invitrogen, Carlsbad, CA, USA) or calcein-AM (33.3 ng/mL; Molecular Probes, Eugene, OR, USA) for 20 minutes at 37°C, washed twice in PBS, and resuspended to a concentration of $1x10^6$/mL in HEPES medium (containing 132 mM of NaCl, 20 mM of HEPES, 6.0 mM of KCl, 1.0 mM of $MgSO_4$, 1.0 mM of $CaCl_2$, 1.2 mM of potassium phosphate, 5.5 mM of glucose, and 0.5% (wt/vol) human serum albumin, pH 7.4). Labelling of neutrophils did not influence their TEM capacity as compared to unlabeled cells (data not shown).

All experiments involving human blood samples were conducted in accordance to the Declaration of Helsinki. The study was approved by the local ethical committees of the Amsterdam University Medical Center and Sanquin Blood Supply, Amsterdam, The Netherlands.

SDS-PAGE and Western Blot Analysis

Total cell lysates were prepared from freshly purified neutrophils. Samples were separated by SDS polyacrylamide gel electrophoresis and transferred onto a nitrocellulose membrane. Individual proteins were detected with antibodies against ARPC1B (rabbit polyclonal, Sigma-Aldrich, St Louis, MO, USA) and actin (mouse monoclonal, Sigma-Aldrich).

Secondary antibodies were donkey anti-mouse-IgG IRDye 800CW or donkey-anti–rabbit-IgG IRDye 680LT (LI-COR Biosciences, Lincoln, NB, USA). Visualization of bound antibodies was performed on an Odyssey Infrared Imaging system (LI-COR Biosciences).

Neutrophil Adhesion (Static Condition)

Neutrophils ($5x10^6$/mL) were labeled with calcein-AM (1 μM; Molecular Probes, Eugene, OR, USA) for 30 minutes at 37°C, washed twice in PBS, and resuspended to a concentration of $2x10^6$/mL in HEPES medium. Neutrophil adhesion was determined on an uncoated 96-well MaxiSorp plate (Nunc, Wiesbaden, Germany) in response to numerous stimuli as described previously (4).

Flow Cytometry

Flow cytometry was performed to assess the expression of various neutrophil surface markers. Fluorescein isothiocyanate (FITC)-, allophycocyanin (APC), phycoerythrin (PE), Brilliant Violet 510 (BV510)-, or Alexa Fluor 647 (AF647)-labelled monoclonal antibodies and isotype controls were used according to the instructions of the manufacturer. Antibodies were CD18-FITC (mouse IgG1 clone MEM48, Diaclone, Besançon cedex, France), CD11a-FITC (mouse IgG2a, Sanquin reagents, Amsterdam, The Netherlands), CD11b-FITC (mouse IgM clone CLB-mon-gran/1, B2, Sanquin reagents), CD11c-FITC (mouse IgG1 clone BU15, Bio-Rad, Kidlington, UK) CD66b-FITC (mouse IgG1 clone CLB-B13.9, Sanquin reagents), L-selectin-APC (mouse IgG clone DREG-56, BD Pharmingen, San Diego, CA, USA), CD177-FITC (mouse IgG1 clone MEM-166, Bio-Rad), FPR1-FITC (mouse IgG2a clone 350418, R&D Systems, Minneapolis, MN, USA), TNFRI-PE (mouse IgG1 clone 16803, R&D Sytems), TNFRII-APC (mouse IgG2A clone 22235, R&D Sytems), TLR4-APC (mouse IgG2A clone HTA125, Invitrogen), ICAM-1-AF647 (mouse IgG1 clone 15.2, Bio-Rad), PECAM-1-BV510 (mouse IgG1 clone WM59, BD Biosciences, San Jose, CA, USA), JAM-A (mouse IgG1 clone WK9, Thermo Fisher Scientific, Waltham, MA, USA).

Samples were analyzed on a FACSCanto-II flow cytometer using FACS-Diva software (BD Biosciences). Neutrophils were gated based on their forward- and side scatter. Per sample, 10,000 gated events were collected. Data were analyzed with FACS-Diva software.

Endothelial Cell Culture

Pooled human umbilical vein endothelial cells (HUVEC P1052; Lonza, Basel, Switzerland, cat C2519A) were cultured at 37°C with 5% CO_2 in fibronectin-coated 10 cm tissue culture plastic petri dishes

in Endothelial cell growth medium (EGM-2; PromoCell, Heidelberg, Germany, cat C22011) supplemented with supplementMix (Promocell, cat C39216). The HUVECs were passaged at 60-70% confluency and used for experiments at passage 3-4.

Transendothelial Migration Under Physiological Flow Conditions

Neutrophil transendothelial migration under flow conditions was assessed as described previously (7), with the exception of labeling of endothelial junctional VE-cadherin and PECAM-1. Neutrophils were flowed over the endothelium for a total of 45 minutes. To induce inflammation, HUVECs were stimulated with 10 ng/mL tumor necrosis factor-alpha (TNF-α; Peprotech, London, United Kingdom) overnight for 16 hours. Neutrophil migration was analyzed using IMARIS Bitplane software (Version 9.5/9.6). Tracking was done using assisted automatic tracking of the neutrophils using manual parameters to classify superendothelial and subendothelial neutrophils. Speed is calculated as the scalar equivalent of the object velocity. We used the track speed mean = average velocity of the spots over time according to the IMARIS reference manual 9.2.0. TEM time was analyzed using Fiji (ImageJ, version 1.52).

Collagen Gel Preparation

All following steps were carried out on ice to halt polymerization of the collagen. 50 µl of 10x PBS (Gibco, Thermo Fisher Scientific, cat 70011-044) was added to of 400 µl of bovine collagen type-1 (10 mg/mL FibriCol; Advanced BioMatrix, San Diego, CA, USA, cat 5133) and gently mixed. Subsequently, pH was set to 7.4 using 48.6 µl of 0.1M NaOH and checked. The collagen was then diluted 1:1 with medium to achieve a final collagen concentration of 4 mg/mL for vessel-on-a chip or 3D collagen experiments.

Migration in 3D Collagen Matrix

The 8 mg/mL neutralized collagen was mixed 1:1 with HEPES medium containing $8*10^6$ neutrophils and complement component 5a (C5a; 10 nM; Sino Biological, Wayne, PA, USA). An 8 µl drop of this mixture was placed in the middle of a well of an µ-Slide 8 Well (Ibidi, Gräfelfing, Germany, cat 80826) and flattened with a coverslip, creating a ±10 µm 3D matrix. The device was placed at 37°C for 30 minutes to allow collagen polymerization before adding 250 µL HEPES medium supplemented with 10 nM C5a (37°C). Neutrophil migration was then assessed using an LSM980 Airyscan2 (ZEISS, Oberkochen, Germany) using a 10x air objective (ZEISS, 420640-9900-000, Objective Plan-Apochromat 10x/0.45). Every 5 seconds an image was taken for 50 minutes in total. For integrin blocking experiments, neutrophils were pre-incubated with 10 µg/mL anti-CD11b monoclonal antibody (mAb) clone 44a and 10 µg/mL anti-CD18 mAb clone IB4 for 20 minutes. These antibodies were isolated from the supernatant of hybridoma clones obtained from the American Type Culture Collection (Rockville, MD, USA). Neutrophil migration through the collagen matrix was analyzed in IMARIS Bitplane software (Version 9.5/9.6). The tracking was performed automatically using the autoregressive motion algorithm and checked manually for accuracy. Speed is calculated as the scalar equivalent of the object velocity. We used the track speed mean = average velocity of the spots over time according to the IMARIS reference manual 9.2.0.

Perfusable Vessel-on-a-Chip

The vessels-on-a chip were made using the devices developed by the lab of Beebe, as previously described (8). Minor alterations to the protocol were made. Briefly, the devices were coated with 1% PEI (Polysciences Inc., Warrington, PA, USA, #23966) and incubated for 10 minutes at room temperature (RT). Sequentially chambers were coated with 0.1% glutaraldehyde (Merck, Darmstadt, Germany, #104239), washed 5x with water for injection (WFI; Gibco, #A12873-01) and air-dried. Collagen-1 was prepared according to the protocol above. 10 µl Collagen-1 was added to each chamber and polymerized for 30 minutes at 37°C, 5% CO_2. PBS-drenched cotton balls were added to the device to control humidity of the device. Rods were removed using tweezers and EGM-2 was added to the lumen. HUVECs were washed twice with PBS, trypsinized for 5 minutes, treated with trypsin neutralizing solution (TNS; Lonza, cat CC-5002) and centrifuged for 5 minutes at 200xg. HUVECs were then stained using CellTracker™ Green CMFDA Dye (1 µM; Molecular Probes, cat C7025) according to manufactures protocol, washed twice with PBS and pelleted. HUVECs were then resuspended to a concentration of $15*10^6$ cells/mL. 5µl of cell suspension was added to each lumen and placed in head-over-head at 37°C, 5% CO_2 for 2 hours at 1 RPM. Vessels were matured for 2 days with medium replacement twice daily.

Neutrophil Transendothelial Migration and Migration Through Collagen Matrix

To induce inflammation, the vessels were stimulated overnight with 10 ng/mL TNF-α. Before the experiment, excess medium was removed and 2 µl of HEPES medium containing $8*10^6$ DiD labelled neutrophils were added to each vessel. Vessels were incubated for 2.5 hours, washed twice and fixed for 15 minutes using 4% paraformaldehyde. Devices were then imaged using an LSM980 Airyscan2 (ZEISS) using a 10x air objective (ZEISS, 420640-9900-000, Objective Plan-Apochromat 10x/0.45). Analysis was done using IMARIS Bitplane software (Version 9.5/9.6).

Statistical Analysis

Experimental data were plotted and analyzed by GraphPad Prism V9.0.0 (GraphPad Software, San Diego, CA, USA). Results are shown as mean ± standard deviation. Normality was tested using the Shapiro-Wilk test. The paired or unpaired Student *t* test was used to test statistical significance (* = $p<0.05$; ** = $p<0.01$; *** = $p<0.001$; ns = non-significant).

RESULTS

ARPC1B-Deficient Neutrophils Display Impaired Subendothelial Motility Upon Transendothelial Migration

We investigated the capacity of neutrophils to transmigrate through an endothelial monolayer under physiological

flow conditions. HUVECs were grown on fibronectin, and stimulated with tumor necrosis factor-alpha (TNF-α) which leads to the upregulation of cell adhesion molecules such as ICAM-1 and VCAM-1, as well as the production of important chemoattractants for neutrophils like platelet-activating factor and interleukin-8 (9, 10). Inflamed endothelial cells also release and remodel ECM proteins, including different types of laminins, collagen-I and fibronectin (11).

Lack of ARPC1B expression in patient neutrophils was confirmed by Western blotting, which showed the complete absence of ARPC1B protein while actin levels were normal (**Supplementary Figure 1A**). Control and ARPC1B-deficient neutrophils were differently fluorescently labeled and simultaneously perfused over the inflamed endothelium. Control neutrophils rolled over the endothelium, whereupon they firmly adhered and transmigrated (**Figure 1A** and **Supplementary Video 1**). Patient neutrophils rolled and adhered on the endothelium in a similar fashion as control cells (**Figure 1B**), but once arrested, they hardly crawled away from their initial arrest site. Under normal inflammatory conditions, neutrophils crawl on endothelium in order to find suitable sites to transmigrate, mostly at endothelial junctions (12). The observed lack of crawling indicated that patient neutrophils crossed the endothelium at non-optimal locations. Furthermore, ARPC1B-deficient neutrophils remained mostly round-shaped and unable to polarize, which coincided with a significantly decrease in TEM speed as well as a reduced number of neutrophils that successfully crossed the endothelium (**Figures 1C, D**). Both control and ARPC1B-deficient neutrophils transmigrated solely *via* the paracellular pathway (**Supplementary Figure 1B**). The adherence of ARPC1B-deficient neutrophils to the endothelial monolayer under flow conditions is remarkable but well in accordance with our observations that ARPC1B-deficient neutrophils show

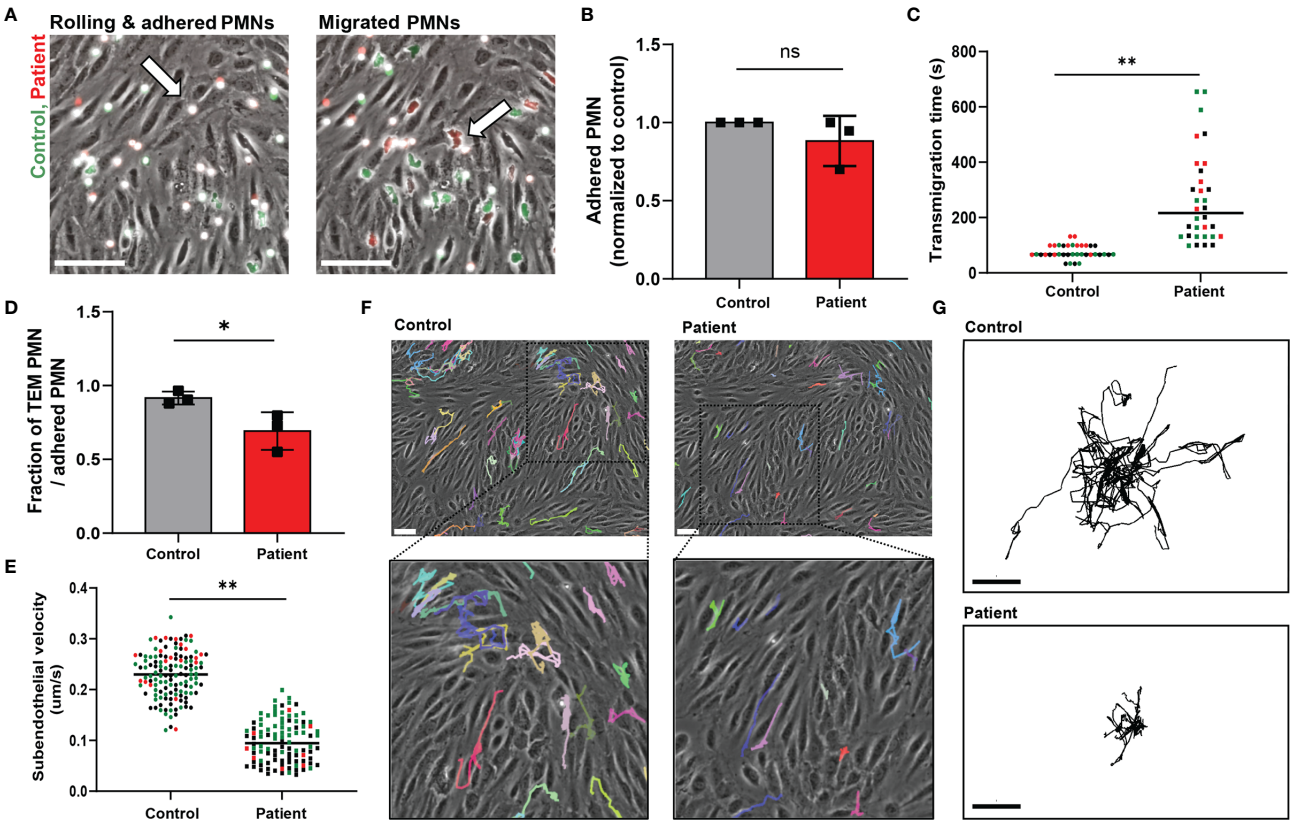

FIGURE 1 | ARPC1B-deficient neutrophils display impaired subendothelial motility upon transendothelial migration. **(A)** Neutrophil TEM through TNF-α inflamed HUVECs was investigated upon physiological flow conditions. Neutrophils (green = control; red = patient) rolled over the endothelium, whereupon they firmly adhered (left panel) and transmigrated (right panel). Neutrophils are circular above the endothelium (left panel, arrow) and become polarized (right panel, arrow) under the endothelium. Representative stills are displayed, see also **Supplementary Video 1**. Scale bar = 100 µm. **(B)** The number of firmly adhered ARPC1B-deficient neutrophils was quantified and normalized to control neutrophils (mean ± SD, n = 3). **(C)** Average time of neutrophils to complete transendothelial migration, starting from firm adherence. Individual cells are depicted. Colors (black, green and red) are corresponding to independent experiments. **(D)** Transendothelial migratory events were quantified and normalized to the number of firmly adhered neutrophils (mean ± SD, n = 3). **(E–G)** Subendothelial motility of transmigrated neutrophils, with **(E)** average velocity of neutrophils (n = 3, individual cells are depicted, colors are corresponding to independent experiments) and cell track analysis of subendothelial neutrophils with **(F)** representative cell trajectories of control and ARPC1B-deficient neutrophils as indicated lasting for 45 minutes (scale bar = 70 µm) and **(G)** showing trajectory plots displayed with their origins brought to a common point. Scale bar = 50 µm. Results are representative of 3 independent experiments. The Student *t* test was used to test statistical significance (*$p < 0.05$; **$p < 0.01$; ns, non-significant).

normal expression of adhesion and signaling receptors, including CD11a (integrin αL chain), CD11b (integrin αM chain), CD18 (integrin β2 chain), L-selectin, PECAM-1 and ICAM-1, as well as adherence under static conditions in response to a range of stimuli (**Supplementary Figure 1C, D**).

Once transmigrated, control neutrophils were actively migrating away from the initial TEM site underneath the endothelium. However, ARPC1B-deficient neutrophils that did cross the endothelium showed a prominent decrease in subendothelial motility (**Figure 1E**). Moreover, they failed to migrate away from their initial TEM site, in contrast to control neutrophils (**Figures 1F, G**). These results indicate that ARPC1B-deficient neutrophils have a minor defect in actual TEM, but a more pronounced defect in their ability to migrate underneath the endothelium.

Neutrophil Infiltration Into 3D Tissue Matrices Is Defective in ARPC1B Deficiency

The dimensions change for a neutrophil as soon as they enter the area underneath the endothelium, i.e. from a luminal 2D to an ECM 3D setting. It has been previously observed that several types of leukocytes, including granulocytes, are able to efficiently migrate in 3D matrices in an integrin-independent manner (13). We investigated neutrophil motility and migration in an artificial 3D gel of bovine collagen-I and visualized chemokinesis of neutrophils upon activation with the chemoattractant C5a. First, we confirmed the integrin-independency of (control) neutrophils for 3D migration in collagen by usage of blocking monoclonal antibodies directed against the common integrin β2 chain (clone IB4, CD18) or the αM chain (clone 44a, CD11b). Indeed, we did not observe an effect from integrin blockage on 3D migration in collagen I (**Supplementary Figure 2A**), indicating that this mode of migration is independent of the main integrins of neutrophils. Next, we investigated the requirement of ARPC1B in neutrophil migration in the collagen-I 3D gel by visualizing chemokinesis of differently fluorescently labeled control and ARPC1B-deficient neutrophils upon activation with C5a (**Supplementary Video 2** and **Figure 2A**) and TNF-α stimulation (**Supplementary Figure 2B**). Both C5a and TNF-α induced migration of control neutrophils in the collagen matrix. Quantification of migration paths upon C5a stimulation revealed that control neutrophils migrated successfully into the collagen matrix with average speeds of 0.085 um/s up to 0.31 um/s. However, ARPC1B-deficient neutrophils were practically non-motile (**Figure 2B**).

To study both processes, i.e. TEM and 3D matrix migration of neutrophils in one assay, we used a vessel-on-a-chip model (see *Methods*). Neutrophils were injected in the vessel, whereupon they were allowed to adhere and migrate for 2.5 hours before the vessels were washed and fixed. As the vessels were subsequently washed and fixed, non-adherent neutrophils were lost. Of note, no flow was applied on the vessel. Using the 3D vessel-on-a-chip model, we found that the number of ARPC1B-deficient neutrophils retrieved in the vessel was significantly lower than control neutrophils (**Supplementary Videos 3**, **4** and **Figures 2C, D**). Most ARPC1B-deficient neutrophils were found at the intraluminal site firmly adhered to the endothelium, as multiple washing steps did not remove them (**Figure 2E**). Around 45% of the retrieved control neutrophils transmigrated successfully, while only 15% of ARPC1B-deficient neutrophils completed their transendothelial migration route (**Figure 2F**). Neutrophils that did penetrate the matrix were found in closer proximity to the vessel compared to control neutrophils. ARPC1B-deficient neutrophils migrated on average 5 μm into the matrix, while this was almost 30 μm for control neutrophils (**Figure 2G**).

DISCUSSION

Overall, our results indicate that the ARP2/3 complex is particularly important for motility in a 3D environment subsequent to the endothelial cell layer itself. Yet, the initial steps of rolling and adhesion strengthening under flow conditions seems independent of ARPC1B, allowing transendothelial migration. Of interest, the number of ARPC1B-deficient neutrophils retrieved in the vessel was significantly lower than control neutrophils, though input was equal (**Figure 2D**). This indicates that these patient neutrophils were not firmly adhered to the endothelial cells and lost during washing. This might be explained by the fact that no physiological flow was applied to the vessel-on-a-chip system. Flow forces have been shown to induce forces between adhering cells and substrates that leads to integrin activation and adhesion strengthening (14, 15). This flow-enhanced integrin activity may explain the difference observed between firm adhesion under flow conditions and the static vessel-on-a-chip environment. Alternatively, it might also be that neutrophils which fail to transmigrate over a longer period of incubation in the vessel-on-a-chip approach (2.5 hours) are more prone to detach from the endothelium again compared to the shorter incubations under flow conditions (45 minutes) or static adhesion on plastic (30 minutes). The process of adhesion is energy-demanding and neutrophils which fail to transmigrate might be prone to detach from the endothelium again, perhaps as a result of being deprived from their energy reserves.

Recent attention was raised to the issue of leukocytes employing alternative migration mechanisms depending on 2- or 3 dimensionality (16). The impaired TEM observed when using the vessel-on-a-chip model may thus indicate that ARPC1B is of more importance for migration in 3D environments. Indeed, when neutrophils are flowed over inflamed endothelium, they migrate in a 2D-manner, while under the endothelium they are in a 'confined' 3D environment and clearly lack such capacity to move around. This implicates that ARPC1B-deficient neutrophils are able to extravasate, but cannot penetrate through the BM into the tissue. Interestingly, 69% of patients with APRC1B deficiency suffer from cutaneous vasculitis (17). Previous investigations showed that ARPC1B-deficient neutrophils release their azurophilic granules prematurely *in vitro* (4), both of which may contribute to the vascular damage as observed in these patients.

After neutrophils have crossed the endothelium, and before entering the tissue, there is a second layer of cells to cross: the

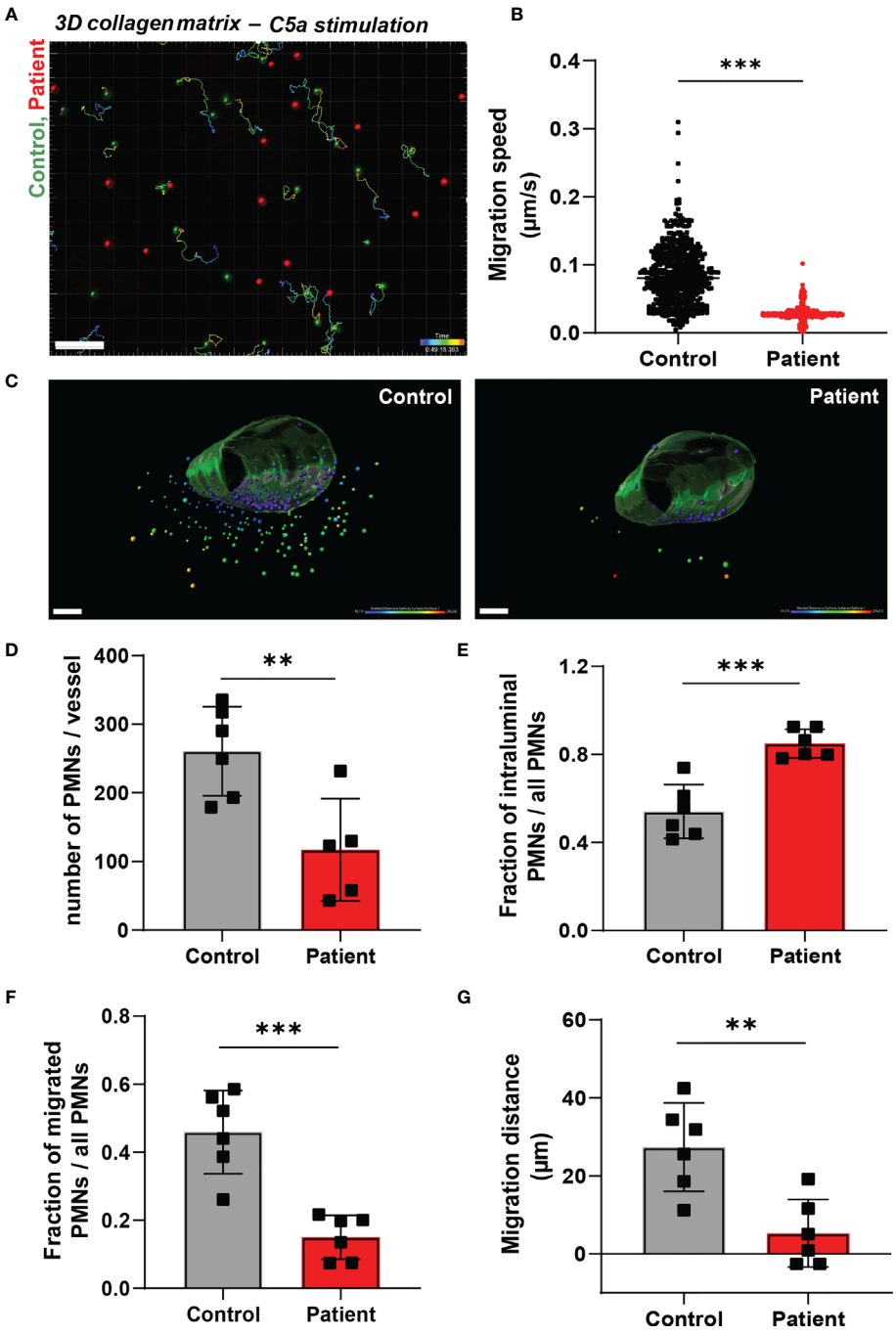

FIGURE 2 | Neutrophil infiltration into 3D tissue matrices is defective in ARPC1B deficiency. **(A)** Motility tracks of neutrophils (green = control; red = patient) in a collagen-I 3D matrix upon C5a stimulation, see also **Supplementary Video 2**. Only control neutrophils show motility tracks as ARPC1B-deficient neutrophils were found to be non-motile. Scale bar = 100 µm. Heat bar = time in minutes. Results are representative of 3 independent experiments. **(B)** Migration speed of neutrophils in collagen matrix (cells of 3 experiments pooled). **(C)** Representative images of neutrophil TEM in a perfusable vessel-on-a-chip, see also **Supplementary Videos 3**, **4**. Scale bar = 100 µm. Heat bar = distance starting from vessel surface. Results are representative of 6 vessels, 2 fields of view per vessel were analyzed. **(D–F)** Quantification of neutrophil TEM using vessel-on-a-chip model, with **(D)** number of neutrophils retrieved in the vessel, **(E)** number of intraluminal neutrophils (normalized to total number of neutrophils), **(F)** number of neutrophils infiltrated into subendothelial collagen matrix (normalized to total number of neutrophils), **(G)** and average migration distance of neutrophils into the vessel. Mean ± SD, results are representative of 6 vessels, 2 fields of view per vessel were analyzed. The Student *t* test was used to test statistical significance (**p < 0.01; ***p < 0.001; ns, non-significant).

pericytes (18). We were not able to include the role for pericytes in the current study as our vessel-on-a-chip has its limitations and does not allow culturing a second cell layer. However, this would be a future challenge.

Our results emphasize the importance of ARPC1B for neutrophil migration, thereby explaining the severe susceptibly of these rare patients to bacterial infections, while neutrophil killing mechanisms have been found to be intact (4).

DATA AVAILABILITY STATEMENT

The raw data supporting the conclusions of this article will be made available by the authors, without undue reservation.

ETHICS STATEMENT

The studies involving human participants were reviewed and approved by the local ethical committees of the Amsterdam University Medical Center and Sanquin Blood Supply, Amsterdam, The Netherlands. Written informed consent to participate in this study was provided by the participants' legal guardian/next of kin.

AUTHOR CONTRIBUTIONS

ES wrote the manuscript. all authors designed the experiments. LK, AS, and ES performed experiments. LK and AS analyzed the data. All authors contributed to the article and approved the submitted version.

FUNDING

ES and TK are supported by the European Union's Horizon 2020 research and innovation programme under Grant Agreement No 668303 and TK is supported by the E-Rare ZonMW grant #90030376506. AS is supported by LSBR grant #1649. LK is supported by LSBR grant #1820 JB is supported by ZonMW NWO Vici grant # 91819632.

ACKNOWLEDGMENTS

We are most grateful to the patient and parents for their collaboration.

SUPPLEMENTARY MATERIAL

The Supplementary Material for this article can be found online at: https://www.frontiersin.org/articles/10.3389/fimmu.2021.678030/full#supplementary-material

Supplementary Figure 1 | (A) Absence of ARPC1B protein and normal actin levels in patient neutrophils was found by Western blot. **(B)** Quantification of neutrophil migration *via* paracellular mode of control- and ARPC1B-deficient neutrophils. **(C)** Expression of adhesion and surface molecules on the neutrophil membrane was assessed by flow cytometry. Neutrophils are gated based on forward/side scatter. Mean fluorescence intensity (MFI) is corrected for the isotype control (mean ± SD, n = 1 – 5). **(D)** Adhesion of neutrophils to plastic (static condition) as percentage of total input upon stimulation with the indicated stimuli (mean + SD, n = 2 - 3).

Supplementary Figure 2 | (A) Migration speed of neutrophils in collagen matrix in response to C5a with or without blockage of integrin β2 chain (clone IB4, CD18) and the αM chain (clone 44a, CD11b). Individual cells are depicted. Colors (black, green and red) are corresponding to independent experiments. **(B)** Migration speed of control- and ARPC1B-deficient neutrophils in collagen matrix in response to PBS (negative control), C5a or TNF-α. Individual cells are depicted, n = 1.

Supplementary Video 1 | Neutrophil TEM through inflamed endothelium. Fluorescently labelled neutrophils (green = control; red = ARPC1B-deficient patient) were flowed over TNF-α inflamed HUVECs for 45 minutes, see also **Figure 1A**. Scale bar = 80 μm. Results are representative of 3 independent experiments.

Supplementary Video 2 | Neutrophil migration in a collagen-I 3D matrix. Migration of neutrophils (green = control; red = ARPC1B-deficient patient) in a collagen-I 3D matrix upon C5a stimulation, see also **Figure 2A**. Neutrophil motility was assessed for a total of 50 minutes. Only control neutrophils show motility tracks as ARPC1B-deficient neutrophils were found to be non-motile. Heat bar = time in minutes. Results are representative of 3 independent experiments.

Supplementary Video 3 | Control neutrophil TEM in a vessel-on-a-chip. Neutrophils were injected in the vessel, whereupon they were allowed to adhere and migrate for 2.5 hours before the vessels were washed and fixed, see also **Figure 2C**. Scale bar = 150 μm. Results are representative of 6 vessels.

Supplementary Video 4 | ARPC1B-deficient neutrophil TEM in a vessel-on-a-chip. Neutrophils were injected in the vessel, whereupon they were allowed to adhere and migrate for 2.5 hours before the vessels were washed and fixed, see also **Figure 2C**. Scale bar = 150 μm. Results are representative of 6 vessels.

REFERENCES

1. Ley K, Laudanna C, Cybulsky MI, Nourshargh S. Getting to the Site of Inflammation: The Leukocyte Adhesion Cascade Updated. *Nat Rev Immunol* (2007) 7(9):678–89. doi: 10.1038/nri2156
2. Wang S, Voisin MB, Larbi KY, Dangerfield J, Scheiermann C, Tran M, et al. Venular Basement Membranes Contain Specific Matrix Protein Low Expression Regions That Act as Exit Points for Emigrating Neutrophils. *J Exp Med* (2006) 203(6):1519–32. doi: 10.1084/jem.20051210
3. Etzioni A. Defects in the Leukocyte Adhesion Cascade. *Clin Rev Allergy Immunol* (2010) 38(1):54–60. doi: 10.1007/s12016-009-8132-3
4. Kuijpers TW, Tool ATJ, van der Bijl I, de Boer M, van Houdt M, de Cuyper IM, et al. Combined Immunodeficiency With Severe Inflammation and Allergy Caused by ARPC1B Deficiency. *J Allergy Clin Immunol* (2017) 140 (1):273–7 e10. doi: 10.1016/j.jaci.2016.09.061
5. Mullins RD, Heuser JA, Pollard TD. The Interaction of Arp2/3 Complex With Actin: Nucleation, High Affinity Pointed End Capping, and Formation of Branching Networks of Filaments. *Proc Natl Acad Sci USA* (1998) 95 (11):6181–6. doi: 10.1073/pnas.95.11.6181
6. Sprenkeler EGG, Henriet SSV, Tool ATJ, Kreft IC, van der Bijl I, Aarts CEM, et al. MKL1 Deficiency Results in a Severe Neutrophil Motility Defect Due to Impaired Actin Polymerization. *Blood* (2020) 135(24):2171–81. doi: 10.1182/blood.2019002633
7. Kroon J, Daniel AE, Hoogenboezem M, van Buul JD. Real-Time Imaging of Endothelial Cell-Cell Junctions During Neutrophil Transmigration Under Physiological Flow. *J Vis Exp* (2014) 90):e51766. doi: 10.3791/51766

8. Jimenez-Torres JA, Peery SL, Sung KE, Beebe DJ. LumeNEXT: A Practical Method to Pattern Luminal Structures in ECM Gels. *Adv Healthc Mater* (2016) 5(2):198–204. doi: 10.1002/adhm.201500608
9. Yang L, Froio RM, Sciuto TE, Dvorak AM, Alon R, Luscinskas FW. ICAM-1 Regulates Neutrophil Adhesion and Transcellular Migration of TNF-Alpha-Activated Vascular Endothelium Under Flow. *Blood* (2005) 106(2):584–92. doi: 10.1182/blood-2004-12-4942
10. Kuijpers TW, Hakkert BC, Hart MH, Roos D. Neutrophil Migration Across Monolayers of Cytokine-Prestimulated Endothelial Cells: A Role for Platelet-Activating Factor and IL-8. *J Cell Biol* (1992) 117(3):565–72. doi: 10.1083/jcb.117.3.565
11. Davis GE, Senger DR. Endothelial Extracellular Matrix: Biosynthesis, Remodeling, and Functions During Vascular Morphogenesis and Neovessel Stabilization. *Circ Res* (2005) 97(11):1093–107. doi: 10.1161/01.RES.0000191547.64391.e3
12. Schenkel AR, Mamdouh Z, Muller WA. Locomotion of Monocytes on Endothelium Is a Critical Step During Extravasation. *Nat Immunol* (2004) 5(4):393–400. doi: 10.1038/ni1051
13. Lammermann T, Bader BL, Monkley SJ, Worbs T, Wedlich-Soldner R, Hirsch K, et al. Rapid Leukocyte Migration by Integrin-Independent Flowing and Squeezing. *Nature* (2008) 453(7191):51–5. doi: 10.1038/nature06887
14. Polacheck WJ, German AE, Mammoto A, Ingber DE, Kamm RD. Mechanotransduction of Fluid Stresses Governs 3D Cell Migration. *Proc Natl Acad Sci USA* (2014) 111(7):2447–52. doi: 10.1073/pnas.1316848111
15. Sun Z, Costell M, Fassler R. Integrin Activation by Talin, Kindlin and Mechanical Forces. *Nat Cell Biol* (2019) 21(1):25–31. doi: 10.1038/s41556-018-0234-9
16. Kameritsch P, Renkawitz J. Principles of Leukocyte Migration Strategies. *Trends Cell Biol* (2020) 30(10):818–32. doi: 10.1016/j.tcb.2020.06.007
17. Volpi S, Cicalese MP, Tuijnenburg P, Tool ATJ, Cuadrado E, Abu-Halaweh M, et al. A Combined Immunodeficiency With Severe Infections, Inflammation, and Allergy Caused by ARPC1B Deficiency. *J Allergy Clin Immunol* (2019) 143(6):2296–9. doi: 10.1016/j.jaci.2019.02.003
18. Proebstl D, Voisin MB, Woodfin A, Whiteford J, D'Acquisto F, Jones GE, et al. Pericytes Support Neutrophil Subendothelial Cell Crawling and Breaching of Venular Walls In Vivo. *J Exp Med* (2012) 209(6):1219–34. doi: 10.1084/jem.20111622

Conflict of Interest: The authors declare that the research was conducted in the absence of any commercial or financial relationships that could be construed as a potential conflict of interest.

frontiers in Immunology

ORIGINAL RESEARCH
published: 03 June 2021
doi: 10.3389/fimmu.2021.666231

Optical Control of CD8$^+$ T Cell Metabolism and Effector Functions

*Andrea M. Amitrano[1,2], Brandon J. Berry[3], Kihong Lim[2], Kyun-Do Kim[4], Richard E. Waugh[5], Andrew P. Wojtovich[3,6] and Minsoo Kim[2]**

[1] Department of Pathology, University of Rochester Medical Center, Rochester, NY, United States, [2] Department of Microbiology and Immunology, David H. Smith Center for Vaccine Biology and Immunology, University of Rochester Medical Center, Rochester, NY, United States, [3] Department of Pharmacology and Physiology, University of Rochester Medical Center, Rochester, NY, United States, [4] Center for Convergent Research of Emerging Virus Infection, Korea Research Institute of Chemical Technology, Daejeon, South Korea, [5] Department of Biomedical Engineering, University of Rochester Medical Center, Rochester, NY, United States, [6] Department of Anesthesiology and Perioperative Medicine, University of Rochester Medical Center, Rochester, NY, United States

OPEN ACCESS

Edited by:
Emmanuel Donnadieu, Institut National de la Santé et de la Recherche Médicale (INSERM), France

Reviewed by:
Jens Volker Stein, Université de Fribourg, Switzerland
Panagiotis F. Christopoulos, Oslo University Hospital, Norway

***Correspondence:**
Minsoo Kim
minsoo_kim@urmc.rochester.edu

Specialty section:
This article was submitted to Molecular Innate Immunity, a section of the journal Frontiers in Immunology

Received: *09 February 2021*
Accepted: *12 May 2021*
Published: *03 June 2021*

Citation:
Amitrano AM, Berry BJ, Lim K, Kim K-D, Waugh RE, Wojtovich AP and Kim M (2021) Optical Control of CD8$^+$ T Cell Metabolism and Effector Functions. Front. Immunol. 12:666231. doi: 10.3389/fimmu.2021.666231

Although cancer immunotherapy is effective against hematological malignancies, it is less effective against solid tumors due in part to significant metabolic challenges present in the tumor microenvironment (TME), where infiltrated CD8$^+$ T cells face fierce competition with cancer cells for limited nutrients. Strong metabolic suppression in the TME is often associated with impaired T cell recruitment to the tumor site and hyporesponsive effector function *via* T cell exhaustion. Increasing evidence suggests that mitochondria play a key role in CD8$^+$ T cell activation, effector function, and persistence in tumors. In this study, we showed that there was an increase in overall mitochondrial function, including mitochondrial mass and membrane potential, during both mouse and human CD8$^+$ T cell activation. CD8$^+$ T cell mitochondrial membrane potential was closely correlated with granzyme B and IFN-γ production, demonstrating the significance of mitochondria in effector T cell function. Additionally, activated CD8$^+$ T cells that migrate on ICAM-1 and CXCL12 consumed significantly more oxygen than stationary CD8$^+$ T cells. Inhibition of mitochondrial respiration decreased the velocity of CD8$^+$ T cell migration, indicating the importance of mitochondrial metabolism in CD8$^+$ T cell migration. Remote optical stimulation of CD8$^+$ T cells that express our newly developed "OptoMito-On" successfully enhanced mitochondrial ATP production and improved overall CD8$^+$ T cell migration and effector function. Our study provides new insight into the effect of the mitochondrial membrane potential on CD8$^+$ T cell effector function and demonstrates the development of a novel optogenetic technique to remotely control T cell metabolism and effector function at the target tumor site with outstanding specificity and temporospatial resolution.

Keywords: optogenetics, metabolism, T cell migration, effector T cell, cancer immunotherapy

INTRODUCTION

Despite recent advances in the treatment of malignant tumors, cancer continues to be a widespread disease and a leading cause of death. $CD8^+$ T cell-based immunotherapy has emerged as a potential treatment for several types of cancer (1). For example, chimeric antigen receptor-transduced T cells (CAR-T cells) have been designed to augment $CD8^+$ T cell antitumor activity and are extremely successful in treating hematological malignancies (2, 3). However, this approach is ineffective against solid tumors due in part to the immunosuppressive tumor microenvironment (TME) which promotes T cell exhaustion (4–6).

The TME presents many metabolic challenges to $CD8^+$ T cell energy production by depleting oxygen, glucose, and other metabolites as well as limiting the uptake of key nutrients *via* the expression of inhibitory ligands (6–8). Tumor-infiltrating $CD8^+$ T cells (TILs) often show decreased mitochondrial mass and function and, thus, suppressed mitochondrial ATP production (5). Previous studies have shown that $CD8^+$ T cells are metabolically flexible and undergo metabolic reprogramming throughout each stage of T cell activation, which includes altering dependence on mitochondria for energy production (9–15). Here, we show an increase in both mitochondrial mass and membrane potential during $CD8^+$ T cell activation. In addition, $CD8^+$ T cells exhibit increased oxygen consumption and glycolysis during migration on intercellular adhesion molecule 1 (ICAM-1), suggesting that migrating $CD8^+$ T cells require elevated metabolism to fulfill the energy requirements of cell motility. Reprogramming effector $CD8^+$ T cell metabolism to increase mitochondrial mass and function has been shown to improve antitumor activity (5). In this study, we further characterized a novel tool, a photoactivatable proton pump called "OptoMito-On," to increase mitochondrial ATP production in $CD8^+$ T cells with the aim of improving T cell immunotherapies for solid malignancies.

RESULTS

Mitochondrial Function Increases During *In Vitro* $CD8^+$ T Cell Activation

The current therapeutic T cell manufacturing process (both for TILs and CARs) includes the activation and expansion of T cells from patient apheresis products using CD3/CD28 beads at a clinical scale with high concentrations of IL-2 (16). To investigate the mitochondrial dynamics throughout the *in vitro* T cell manufacturing process, we isolated all T cell types from the blood of healthy human donors and activated these T cells *in vitro* with anti-CD3 and anti-CD28 antibodies in the presence of IL-2. On days 0, 2, 5, and 7 of activation, the mitochondrial mass and membrane potential of the T cells was measured by flow cytometry analysis of MitoTracker Green FM and Tetramethylrhodamine (TMRM) signals, respectively (**Figures 1A, B**). During the activation of T cells, there was an increase in mitochondrial mass and mitochondrial membrane potential from Day 0 through Day 5, and both mitochondrial signals plateaued after Day 5 (**Figures 1A, B**). These results suggest the importance of mitochondrial function in order to support T cell activation. To determine if a similar trend in mitochondrial function is seen during the activation of mouse T cells, we isolated primary $CD8^+$ T cells from the spleen and lymph nodes of C57BL/6J mice. Again, the isolated $CD8^+$ T cells were activated with anti-CD3 and anti-CD28 antibodies in the presence of IL-2. On days 0, 2, 4, and 7 of activation, $CD8^+$ T cells were stained with MitoTracker Green FM or TMRM and analyzed by flow cytometry (**Figures 1C, D**). Similar to what was seen in human T cells, mouse $CD8^+$ T cells exhibit an increase in mitochondrial mass and mitochondrial membrane potential from Day 0 through Day 4, though a decrease or plateau was observed on Day 7 (**Figures 1C, D**), suggesting that increases in mitochondrial mass and function coincide with $CD8^+$ T cell proliferation and activation. In addition, activated mouse $CD8^+$ T cells exhibited a higher basal oxygen consumption rate (OCR) than naïve $CD8^+$ T cells, further demonstrating the requirement for increased mitochondrial function during $CD8^+$ T cell activation (**Figure 1E**). Glycolysis, as measured by the extracellular acidification rate (ECAR) was also elevated in activated $CD8^+$ T cells, supporting previous studies that showed the upregulation of aerobic glycolysis immediately after $CD8^+$ T cell activation with anti-CD3 and anti-CD28 **(Supplementary Figure 1A)** (14, 17, 18). In addition, activated $CD8^+$ T cells had a higher maximum OCR, without changes in the spare respiratory capacity of naïve and activated $CD8^+$ T cells (**Supplementary Figures 1B–D**). To ensure that the concentrations of the metabolic inhibitors used in the test are not harmful to T cells in these conditions, we performed flow cytometry on activated mouse $CD8^+$ T cells treated with the inhibitors and stained for Annexin-V. There was no increase in the percentage of T cell death following treatment with the inhibitors (**Supplementary Figure 1E**).

Mitochondrial Respiration Is Important for Cytokine Production and Migration of $CD8^+$ T Cells

To elicit an immune response against cancer, $CD8^+$ T cells need to release effector molecules, such as Granzyme B and IFN-γ. We found a positive correlation between TMRM signal with granzyme B and IFN-γ expression (**Figures 2A, B**), indicating that the increase in mitochondrial membrane potential may be important for supporting $CD8^+$ T cell effector functions. Efficient trafficking of T cells to the target tumor site is key in order to perform anticancer effector functions (19, 20). Therefore, in addition to effector functions, additional energy is likely required for $CD8^+$ T cell migration. To test this hypothesis, we next investigated whether mitochondrial metabolism is important for $CD8^+$ T cell migration. Activated $CD8^+$ T cells were plated on wells coated with poly-L-lysine (PLL), with or without the addition of CXCL12, to confine the $CD8^+$ T cells in place or on ICAM-1 + CXCL12 coated wells to facilitate cell migration mediated by lymphocyte function-associated antigen-1 (LFA-1) and ICAM-1 interactions (21). $CD8^+$ T cells on ICAM-1 + CXCL12-coated surfaces showed a significant

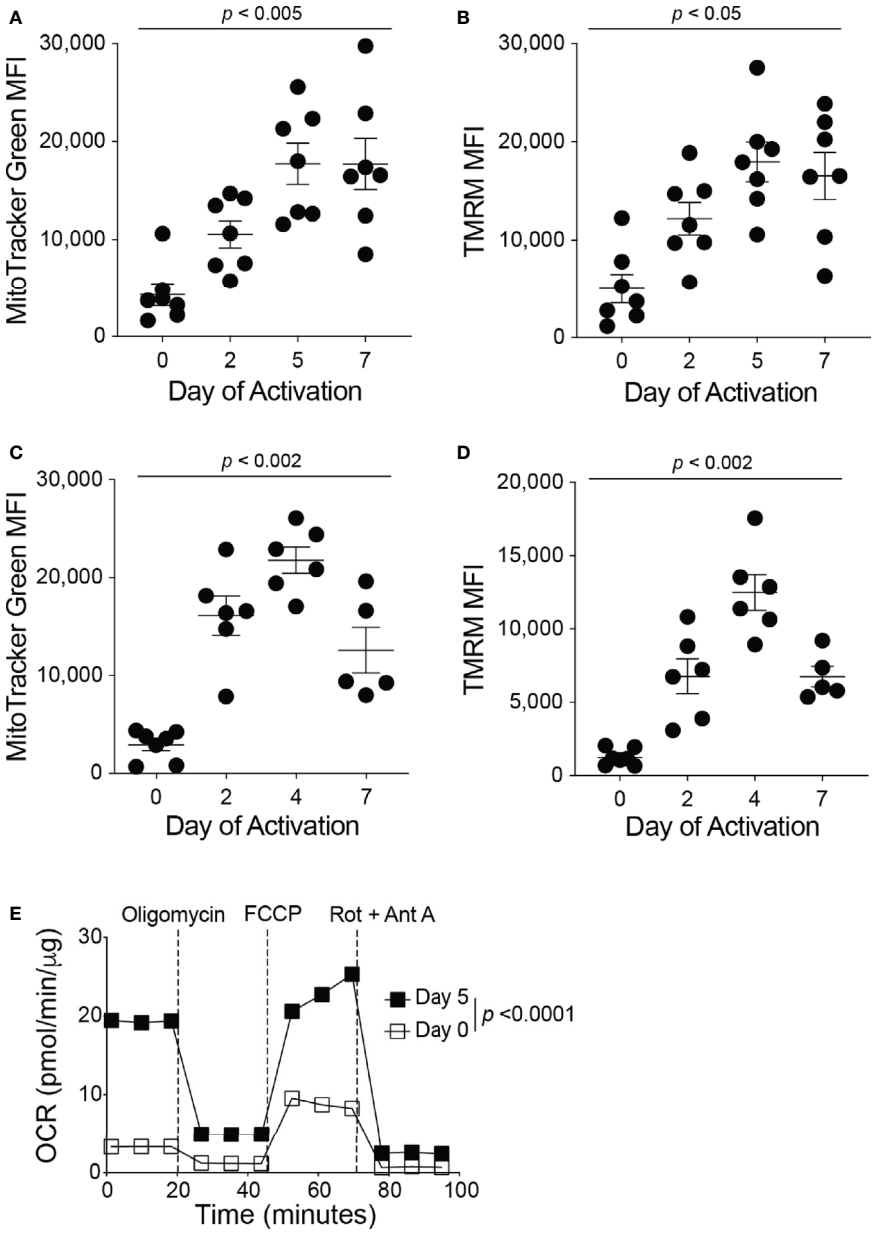

FIGURE 1 | Mitochondrial function increases during CD8$^+$ T cell activation. Flow cytometry analysis of **(A)** MitoTracker Green FM, reflecting mitochondrial mass, and **(B)** Tetramethylrhodamine (TMRM), reflecting mitochondrial membrane potential, displayed as mean fluorescence intensity (MFI) during human CD8$^+$ T cell activation (n = 7 donors). Flow cytometry analysis of **(C)** MitoTracker Green FM and **(D)** TMRM shown in MFI during mouse CD8$^+$ T cell activation (n = 5-7 mice). **(E)** The oxygen consumption rate (OCR), measured with the Seahorse MitoStress Test, of naïve (Day 0, PLL + CCL21 coated wells) and activated (Day 5, PLL + CXCL12 coated wells) CD8$^+$ T cells, normalized to protein content with a BCA assay; data shown as mean ± SEM (Representative of two independent experiments, n = 10 wells per group, error bars fall within symbols). All data shown as mean ± SEM. **(A, B)** Repeated measures one-way ANOVA with Bonferroni's post-test. **(C, D)** Ordinary one-way ANOVA with Bonferroni's post-test. **(E)** 2way ANOVA with Bonferroni's post-test.

increase in the basal and maximum OCR, as well as the basal ECAR, without changes in the spare respiratory capacity, compared to those on PLL-coated surfaces (**Figures 2C, D** and **Supplementary Figures 2A–D**). Our data suggest that CD8$^+$ T cells migrating on ICAM-1 increase ATP production through both mitochondrial respiration and glycolysis to supply the additional energy required for cell migration. In addition, when CD8$^+$ T cells were treated with mitochondrial respiration inhibitors, such as oligomycin, an ATP synthase inhibitor, or FCCP, a protonophore that uncouples OxPhos, there was a significant decrease in the velocity of CD8$^+$ T cells migrating on ICAM-1 + CXCL12, further demonstrating the importance of

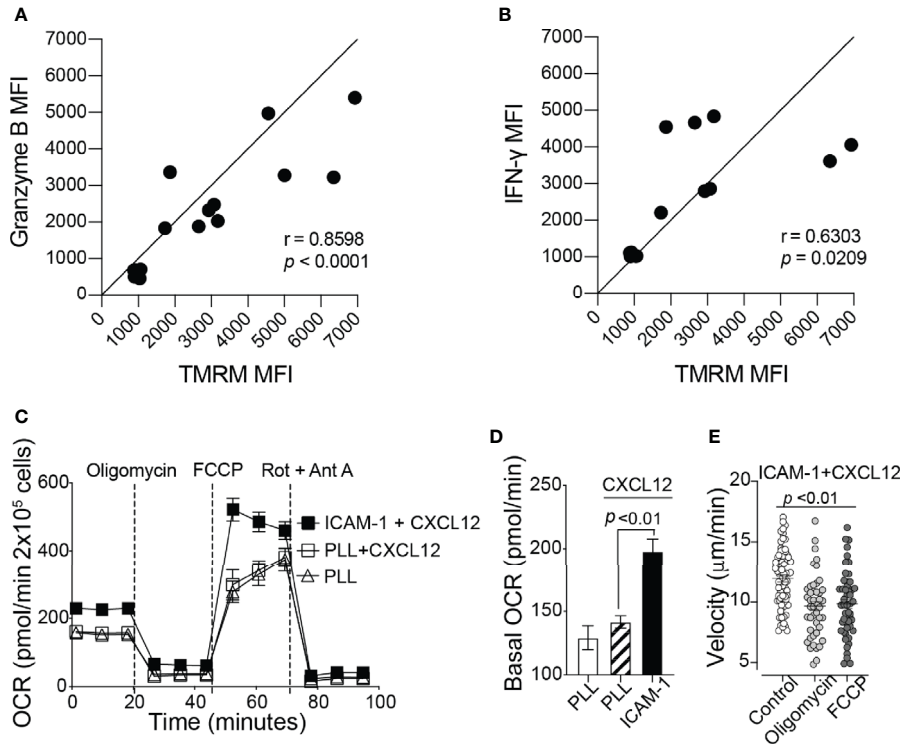

FIGURE 2 | Mitochondrial respiration is important for cytokine production and migration of $CD8^+$ T cells. Flow cytometry MFI of **(A)** Granzyme B and **(B)** IFN-γ production throughout mouse $CD8^+$ T cell activation, shown as a function of TMRM MFI (n = 6 mice). **(C)** The complete OCR trace and **(D)** the basal OCR measured with the Seahorse MitoStress Test, of activated $CD8^+$ T cells on Poly-L-lysine ± CXCL12, or migrating on ICAM-1 with CXCL12 (Representative of three independent experiments). **(E)** The velocity of activated $CD8^+$ T cells migrating on ICAM-1 + CXCL12. Treated cells (2 μM oligomycin or 2 μM FCCP) were incubated with the drug for 20 minutes before the start of the 20-minute movie (Representative of three experiments). Migration data analyzed with Volocity software. **(A, B)** Pearson's correlation. **(D, E)** Data shown as mean ± SEM and analyzed by one-way ANOVA with a Bonferroni post-test.

mitochondrial function in active $CD8^+$ T cell migration (**Figure 2E**).

$CD8^+$ T cells have increased levels of mitochondrial respiration to support the energetic demands of cell migration (**Figure 2**); thus, a hypoxic TME may suppress $CD8^+$ T cell migration at the tumor site by preventing sufficient ATP production to fuel migration. To test this hypothesis under TME-like hypoxic conditions, we used cobalt (II) chloride hexahydrate ($CoCl_2$) (22). Treatment of $CD8^+$ T cells with $CoCl_2$ reduced the basal and maximum OCR in a dose-dependent manner (**Supplementary Figures 3A, B**). In addition, $CoCl_2$ caused a reduction in the overall track velocity and the percentage of total migrating $CD8^+$ T cells on ICAM-1 + CXCL12-coated wells (**Supplementary Figures 3E–G**). It should be noted that $CoCl_2$ had no impact on $CD8^+$ T cell survival during the experiment, and there was no change in Annexin-V-positive cells treated with $CoCl_2$ (**Supplementary Figure 3H**). Although the effect was minimum, $CoCl_2$ also caused a decrease in the ECAR (**Supplementary Figures 3C, D**). Therefore, we cannot completely exclude the possibility that some of the outcomes of the cell migration assay may have resulted from the reduction in glycolysis with $CoCl_2$ treatment.

Optogenetic Regulation of Mitochondrial Membrane Potential

Although delivery of an immune-enhancing or a metabolism-promoting molecule to overcome local immunosuppression has been proposed, the full potential of this approach is limited by aberrant activation of the host immune system and nonspecific stimulation of tumor growth and metastasis. To overcome the metabolic challenges in the TME and to selectively enhance $CD8^+$ T cell functions, we developed a genetically encoded photoactivatable proton pump ("OptoMito-On") that is expressed in the inner mitochondrial membrane (**Figure 3A**) (23). The OptoMito-On construct consists of the light-driven proton pump, 'Mac,' that was derived from the fungus *Leptosphaeria maculans* (24) and is fused to the N-terminal mitochondrial targeting domain of the mitochondrial inner membrane protein Mitofilin (25), which delivers and orients Mac in the membrane (**Figure 3A**) (26, 27). During OxPhos, electrons from NADH and $FADH_2$, products of cellular metabolism, enter the mitochondrial electron transport chain (ETC), located in the inner mitochondrial membrane. As electrons are transferred through the ETC to oxygen, protons are pumped from the mitochondrial matrix to the

intermembrane space, thereby generating a protonmotive force that is composed of an electrical ($\Delta\psi_m$) and chemical (ΔpH) gradient across the inner membrane (**Figure 3A**) (28). Importantly, the establishment of this gradient requires both oxygen and reducing equivalents generated by cellular metabolism. ATP synthase (complex V) utilizes the protonmotive force to phosphorylate ADP to ATP. We predicted that OptoMito-On would mimic the function of the ETC by pumping protons to the intermembrane space upon stimulation with light and thus generate ATP *via* ATP synthase

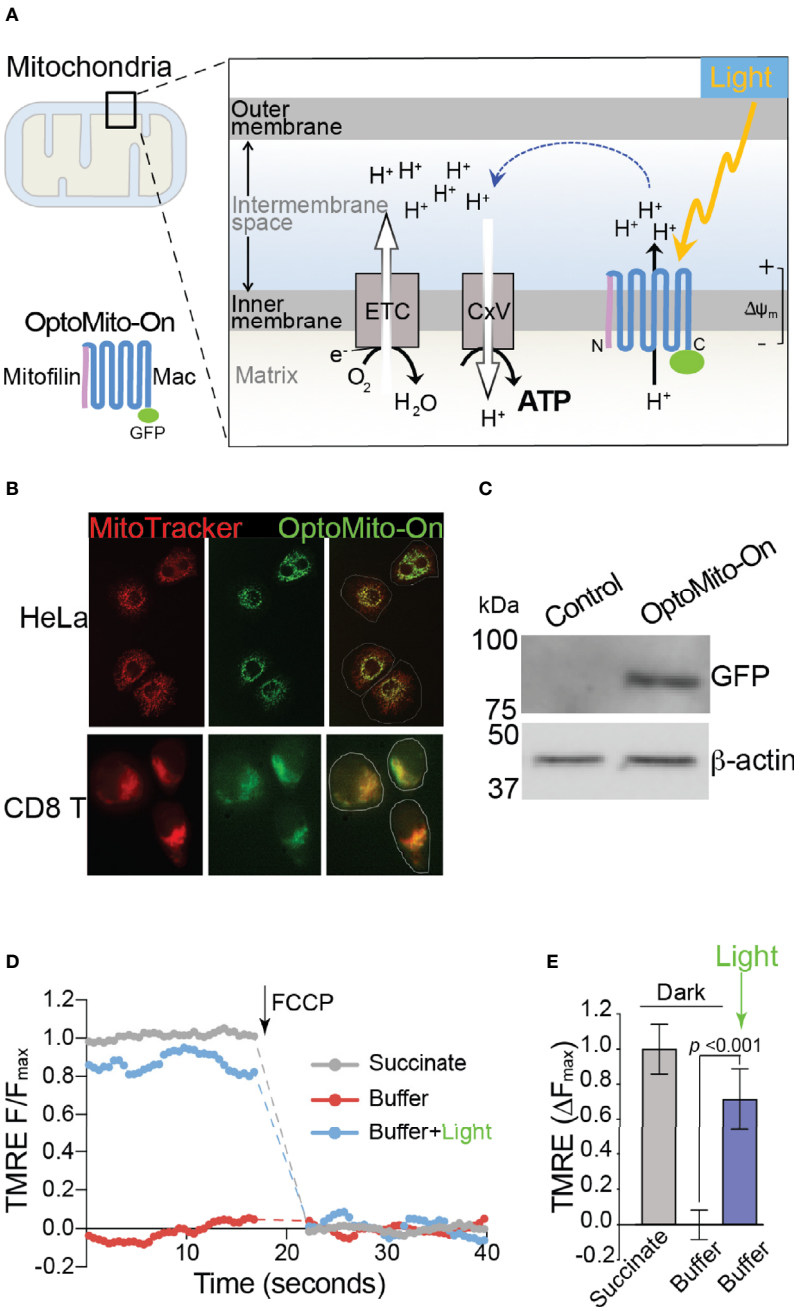

FIGURE 3 | Characterization of OptoMito-On. **(A)** Illustration of photoactivatable oxidative phosphorylation by OptoMito-On construct. **(B)** Images of HeLa cells and CD8$^+$ T cells expressing OptoMito-On and stained with MitoTracker Red CMXRos. **(C)** Immunoblot comparing control HEK293T cell lysate and HEK293T OptoMito-On cell lysate. The full-length OptoMito-On construct is 82 kDa and probed for with an anti-GFP antibody. β-actin is used as loading control. Both images are from the same lanes on one membrane. **(D)** Representative TMRE fluorescence trace of isolated mitochondria from OptoMito-On expressing HEK293T cells before and after addition of FCCP. Dashed lines indicate where FCCP was added. **(E)** Quantification of change in TMRE fluorescence. Data shown as mean ± SEM and analyzed by One-Way ANOVA with a Bonferroni post-test (n = 4).

in the absence of sufficient oxygen and substrates (common features in the TME).

We first transfected HeLa and mouse CD8$^+$ T cells with the OptoMito-On construct and labeled cells with MitoTracker to specifically stain the mitochondria. Confocal microscopy confirmed that there was a high degree of overlap between GFP signals (OptoMito-On) and red fluorescence signals (mitochondria), indicating that OptoMito-On was successfully expressed in the mitochondria (**Figure 3B** and **Supplementary Figure 4**). Expression of the full-length OptoMito-On construct was further confirmed by Western blot analysis of cell lysates prepared from HEK293T cells that expressed OptoMito-On (82 kDa) (**Figure 3C**).

Based on our model (**Figure 3A**), stimulation of OptoMito-On with light results in polarization of the mitochondrial inner membrane. To determine whether OptoMito-On reaches the inner mitochondrial membrane in the correct orientation and to confirm the functional responsiveness of OptoMito-On, we measured the mitochondrial membrane potential ($\Delta\psi_m$) using TMRE (29, 30). We first isolated mitochondria from HEK293T cells expressing OptoMito-On and treated them with succinate, a complex II ETC substrate, to generate a maximal mitochondrial membrane potential as a positive control (**Figure 3D**). In the absence of succinate (a negative control), the mitochondria did not generate a membrane potential. However, stimulation with 540-600 nm light was sufficient to rescue the mitochondrial membrane potential in the absence of succinate, indicating the expression and correct orientation of functional OptoMito-On in mitochondria (**Figures 3D, E**).

To test whether mitochondrial polarization driven by light-activated proton transport leads to enhanced ATP production (**Figure 3A**), we transfected HEK293T cells and mouse CD8$^+$ T cells with OptoMito-On, illuminated the cells (590 ± 10 nm, 0.32 mW/mm2 at 1 Hz), and immediately lysed them to detect ATP. 2-Deoxy-D-glucose (2-DG), a glucose analog, was used to inhibit glycolysis and thus mimic the glucose-deficient TME. Optical stimulation of OptoMito-On expressing HEK293T cells with or without 2-DG treatment yielded a significant increase in ATP compared with that of cells cultured in the dark (**Figures 4A, B**). Stimulation of GFP-expressing cells with light did not alter ATP levels, indicating that stimulation with light at 590 nm was not detrimental to cell viability. We observed a similar outcome in OptoMito-On expressing CD8$^+$ T cells (**Figure 4C**). However, unlike HEK293T cells, light stimulation of 2-DG treated OptoMito-On expressing T cells failed to increase ATP production (**Supplementary Figure 5A**). In earlier studies, 2-DG treatment of effector T cells showed a decrease in mitochondrial respiration as well as decreases in other effector functions, including cytokine production and cytolytic activity (13, 31). Therefore, we speculate that 2-DG treatment of OptoMito-On expressing CD8$^+$ T cells may have broader effects on overall metabolic functions than in HEK293T cells, preventing the light-induced increase in mitochondrial ATP production. In combination with the isolated mitochondria data, these results demonstrate that OptoMito-On can be expressed in cells and facilitates photoactivatable control of the mitochondrial membrane potential.

CD8$^+$ T cells are metabolically flexible and are able to adjust their reliance on metabolic pathways depending on the nutrient availability in their immediate environment (17). To determine whether boosting mitochondrial ATP production with OptoMito-On in activated CD8$^+$ T cells mediates changes in T cell glycolysis, we measured glucose consumption. Illumination of OT-I T cells with 530 nm light caused no change in the glucose consumption rate of both GFP and OptoMito-On expressing T cells (**Supplementary Figure 5B**). These results suggest that increasing mitochondrial ATP production with OptoMito-On does not impact the rate of glycolysis, at least during a one-hour light activation period.

OptoMito-On Enhances CD8$^+$ T Cell Functions

The roles of the mitochondrial membrane potential and cell metabolism in the regulation of T cell functions are not completely understood. To investigate the impact of mitochondrial ATP production induced by stimulation of OptoMito-On in CD8$^+$ T cell migration, CD8$^+$ T cells were transduced with either OptoMito-On or control GFP retrovirus, then allowed to migrate on an ICAM-1 + CXCL12 coated well in the presence (light) or absence (dark) of light stimulation

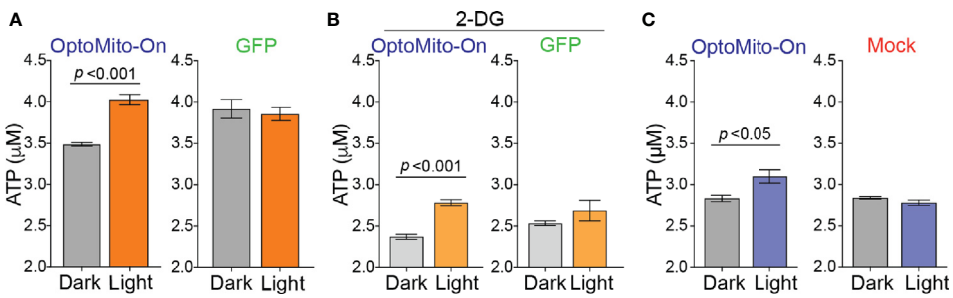

FIGURE 4 | Activation of OptoMito-On increases ATP production. **(A)** HEK293T cells expressing OptoMito-On or GFP were illuminated with 590 nm light for 2 hours, followed by a luciferase-based ATP assay. **(B)** Same set-up as in **(A)**, except HEK293T cells were treated with 10 mM 2-DG for 2 hours prior to illumination. **(C)** Activated CD8$^+$ T cells were sorted based on GFP expression. GFP negative cells were used as the mock control. CD8$^+$ T cells received 590 nm light for 30 minutes, followed by a luciferase-based ATP assay. All data shown as mean ± SEM and analyzed by an unpaired t-test (n = 4-7).

(**Movies 1** and **2**). CD8$^+$ T cells expressing OptoMito-On showed an increase in cell velocity, cell displacement, and track length compared to mock cells expressing GFP or that were negative for OptoMito-On, with no change in the meandering index (**Figures 5A–D**). Additionally, there was a large increase in the overall percentage of migrating CD8$^+$ T cells expressing OptoMito-On compared to those expressing GFP (**Figure 5E**). These results indicate that although stimulation of OptoMito-On with light may not improve the ability of T cells to become polarized towards chemoattractants, but increasing mitochondrial ATP production with OptoMito-On is able to enhance overall CD8$^+$ T cell migration, which we have shown requires increased mitochondrial metabolism.

In CD4$^+$ T cells, it has been shown that upon chemokine stimulation, an increase in cytosolic calcium stimulates mitochondrial ATP production and subsequent ATP release to activate autocrine signaling through P2X4 receptors to support cell migration (32). Additionally, mitochondria can localize to the uropod during T cell migration to supply ATP for cytoskeletal motor proteins (33). To further identify key cytoplasmic molecules that regulate OptoMito-On-mediated CD8$^+$ T cell migration, we performed an antibody array that specifically detects various cytoskeletal proteins.

Among the 141 antibody targets that were screened, the expression of 51 molecules were considerably increased or decreased after the activation of OptoMito-On by light in migrating CD8$^+$ T cells (**Figure 6A**). Cell migration is a complex process that involves the coordination of many signaling pathways. For example, dynamic regulation of the phosphorylation of focal adhesion kinase (FAK) and MEK1, as well as the expression of Src are involved in regulation of cell adhesion turnover at both the leading edge and in the rear of migrating cells (34).

Activation of FAK and Src promotes formation of a signaling complex that leads to further downstream signaling, such as the MAP kinase pathway which includes MEK1 (35). Consistently, the phosphorylation of FAK and MEK1 and the protein expression of Src were increased after stimulation of CD8$^+$ T cells that express OptoMito-On with light compared to cells in the dark (**Figure 6B**). Therefore, our data indicates that the increase in mitochondrial ATP production by light activation of OptoMito-On is sufficient to drive heightened levels of dynamic cytoskeleton rearrangements, such as increased cell adhesion turnover, leading to improved CD8$^+$ T cell migration. Importantly, there is still debate about whether activated CD8$^+$ T cells utilize focal adhesion independent or dependent motility (36, 37). Integrin activation is tightly regulated by interaction of cytoplasmic domains with signaling proteins. FAK has been shown to be a key inside-out signaling molecule that mediates LFA-1 ligation and TCR engagement in T cells (38–41)

In addition to cell migration, overnight illumination of OT-I CD8$^+$ T cells, isolated from OT-I T cell receptor transgenic mice, that express OptoMito-On significantly increased the percentage of granzyme B positive cells and the average mean fluorescence intensity of intracellular granzyme B (**Figures 7A, B**). These results indicate the feasibility of remote activation of T cell effector function by light stimulation of mitochondrial ATP production. Interestingly, light activation of OptoMito-On expressing T cells failed to increase IFN-γ production. It may be possible that IFN-γ production during T cell stimulation overrides light-induced cytokine production. In addition, while granzyme B and IFN-γ can be expressed simultaneously by T cells, their kinetics and relative levels of expression can vary during activation. Furthermore, the genes encoding granzyme B and IFN-γ may be differentially regulated in activated CD8$^+$ T cells by mitochondria OxPhos.

In order to further investigate the ability of OptoMito-On to improve CD8$^+$ T cell effector function, we performed a co-culture killing assay with OptoMito-On or GFP expressing OT-I T cells and OVA loaded murine lymphoma EL-4 cells. Light stimulation of OptoMito-On expressing OT-I T cells caused a significant increase in the expression of Annexin-V in

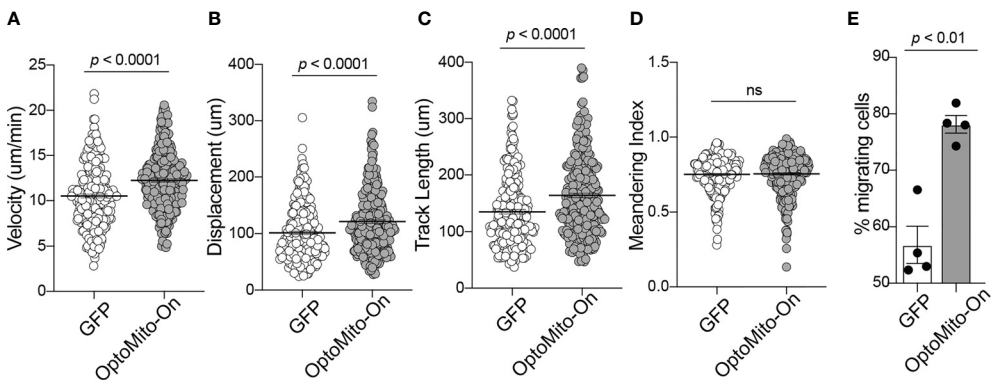

FIGURE 5 | Activation of OptoMito-On increases CD8$^+$ T cell migration. The velocity **(A)**, displacement **(B)**, track length **(C)**, meandering index **(D)**, and percent migrating cells **(E)** of Mock (or GFP) and OptoMito-On expressing Day 4 CD8$^+$ T cells migrating on ICAM-1 + CXCL12. The percentage of migrating cells was calculated as the number of cells migrating 5-20 μm/min divided by the total number of cells in the field of view during the 20-minute movie. All movies received 500 nm illumination and were analyzed with Volocity software. All data shown as mean ± SEM and analyzed by a two-tailed unpaired t-test with Welch's correction (**A–D**: includes four independent experiments, Mock: 271 cells, OptoMito-On: 312 cells; **E** : n = 4 movies on the same day). ns, not significant.

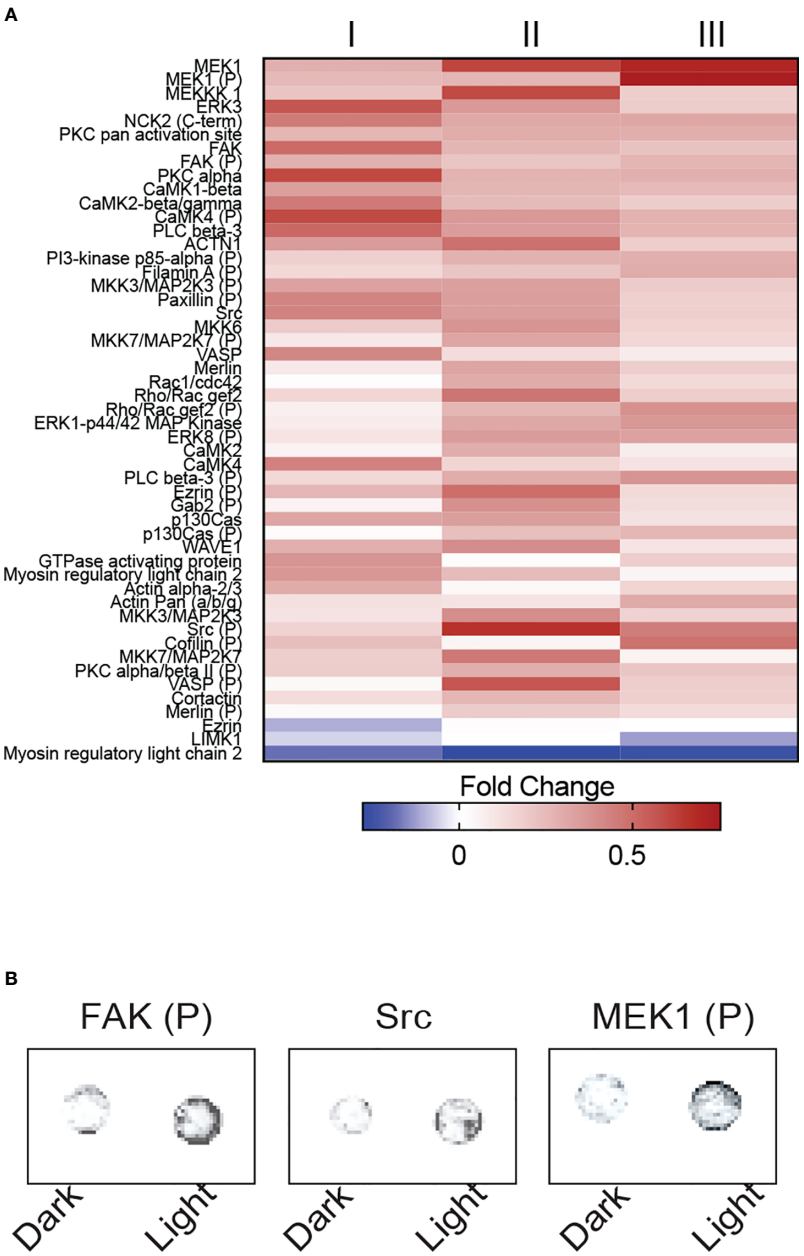

FIGURE 6 | OptoMito-On activation increases cytoskeletal rearrangements. **(A)** Heat map showing the fold change in protein expression from the dark to light conditions of the Full Moon BioSystems Cytoskeleton Phospho antibody array (n = 3). **(B)** Representative antibody array images of a few proteins of interest, FAK, Src, and MEK1.

EL-4 cells compared to GFP expressing T cells (**Figure 7C**). Our data suggest that illuminated OptoMito-On OT-I T cells are able to induce robust apoptosis of EL-4 cells, which correlates with the increased granzyme B production after light stimulation (**Figures 7A, B**). Therefore, OptoMito-On is capable of selectively improving the cytotoxic functions of effector $CD8^+$ T cells without augmenting the metabolism of target cells or other immunosuppressive cells at the tumor site.

DISCUSSION

Cellular metabolism involves a series of reactions that ultimately breakdown nutrients into usable energy. Under normal conditions, quiescent, resting T cells primarily utilize OxPhos to generate the energy source ATP. Cancer cells, however, reprogram their metabolic patterns from OxPhos to relying largely on aerobic glycolysis in order to support cell

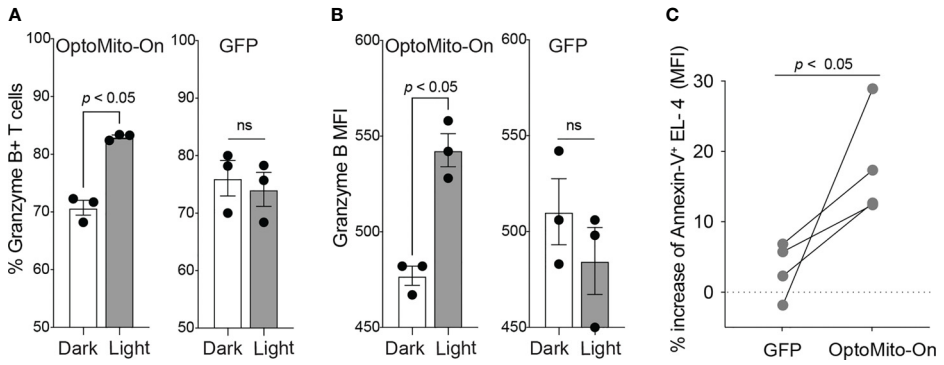

FIGURE 7 | OptoMito-On activation increases CD8$^+$ T cell effector functions. Flow cytometry results from an 18-hour light activation of GFP or OptoMito-On expressing CD8$^+$ T cells looking at the percentage of Granzyme B+ cells **(A)** and Granzyme B MFI **(B)** (n = 3). **(C)** Flow cytometry results of a 3-hour co-culture of OVA pulsed EL-4 cells with GFP or OptoMito-On expressing OT-I T cells. The graph shows the percent change of Annexin-V MFI of EL-4 cells from the dark to light condition. OT-I T cells were either kept in the dark or received 16-17 hours of 530 nm light before the addition of EL-4 cells. All data shown as mean ± SEM, A-B analyzed by One-Way ANOVA with a Bonferroni post-test, C analyzed by one-tailed paired t test (**A, B**: representative of two experiments, **C**: four independent experiments). ns, not significant.

proliferation. This aerobic form of glycolysis, known as the "Warburg effect," is useful for the rapid generation of ATP, the production of metabolic intermediates that are required for cell proliferation, and also for the survival of malignant cells in the hypoxic TME (42, 43). Similarly, while naïve T cells are relatively quiescent and rely primarily on OxPhos, CD8$^+$ T cells undergo metabolic reprogramming during activation by shifting their metabolic pathways to utilize both glycolysis and OxPhos to meet the demands of clonal expansion and effector functions following antigen stimulation (11, 15, 44). The fact that both cancer cells and CD8$^+$ T cells utilize overlapping forms of metabolism in the TME is an important obstacle to overcome for the development of effective immunotherapies because cancer cells will likely outcompete CD8$^+$ T cells for any available nutrients (6). We have shown that mitochondrial function is required for CD8$^+$ T cell activation, cytokine production, and migration, further supporting our rationale of targeting mitochondrial metabolism as a way to improve adoptive T cell therapy outcomes. Our study characterizes the use of a novel optogenetic tool, OptoMito-On, in mouse CD8$^+$ T cells to remotely control T cell mitochondrial metabolism, migration, and effector function with outstanding specificity and temporospatial resolution.

Metabolic reprogramming of cells is commonly studied through the global administration of drugs that lack target selectivity, and it has not been possible to specifically regulate metabolic pathways only in a selected cell type *in vivo*, in a reversible manner, and at a precise location and time. For the same reason, although there is increasing evidence that metabolism can affect the survival and antitumor function of T cells, the development of a cell-specific and clinically feasible method to generate T cells with favorable metabolic features has proven challenging. Here, we utilized OptoMito-On to circumvent this limitation by directly and selectively modulating T cell OxPhos and studied the effects of mitochondrial membrane potential on effector CD8$^+$ T cell function. Our results indicate that enhancing the overall mitochondrial membrane potential improves T cell functions by increasing CD8$^+$ T cell migration and effector molecule production. This new optogenetic approach highlights the development and application of optogenetic techniques to control T cell functions using light stimulation, thus providing a unique opportunity to understand the fundamental mechanisms of T cell metabolic function in many diseases.

Recent studies demonstrate important functions of OxPhos for cell migration (45–47). In naïve T cells, chemokine stimulation under a confined 3D condition induces actin retrograde flow and cellular elongation, suggesting the presence of force-generating cytoskeletal processes regulated by chemokine signaling (48). Our results on an ICAM-1 coated 2D surface showed that basal OCR of activated CD8$^+$ T cells is significantly increased compared to T cells on a PLL coated surface. During T cell migration on ICAM-1 substrate, force is exerted on the cytoplasmic domain of LFA-1, while the extracellular domain binds to ICAM-1 (49). These forces exerted on integrins are critical for LFA-1 mediated adhesion at the leading edge of migrating cells (50). Therefore, LFA-1 binding with ICAM-1 may prompt an increase in mitochondrial respiration to support the increased energy demands of migrating T cells. Activated CD8$^+$ T cells on PLL did not have an increase in OCR in the presence of CXCL12 treatment. PLL may prevent CD8$^+$ T cell polarization and elongation, thus impairing F-actin polymerization (33).

CD8$^+$ T cell metabolic pathways are tightly regulated to fuel their optimum effector function, but tumor-infiltrating T cells often show an overall phenotype of metabolic insufficiency in the strong immunosuppressive TME due to a persistent loss of mitochondrial function (5, 7, 51). Therefore, a better understanding of CD8$^+$ T cell mitochondrial function holds promise for the development of novel approaches to enhance T cell effector function, promote memory formation, and thus improve immunotherapy outcomes. This study further illustrates

the importance of mitochondrial metabolism in $CD8^+$ T cell effector functions and identifies the mitochondrial membrane potential as an ideal target to improve T cell therapy outcomes. T cells in the hypoxic TME have a decreased ATP/AMP ratio and display mitochondrial dysfunction, which correlates with a reduction in cytokine production. The treatment of chronically stimulated T cells with antioxidants to reduce mitochondrial oxidative stress was shown to reverse mitochondrial dysfunction and rescue effector T cell function, including IFN-γ, TNF, and Granzyme B production (52, 53). Therefore, the use of OptoMito-On to boost the mitochondrial membrane potential in chronically stimulated T cells can be beneficial in the TME to increase cytokine production in tumor-infiltrated T cells. We further predict that with different light intensities, gradual titration of metabolic activation to an appropriate therapeutic level may be possible, resulting in superior memory formation without T cell exhaustion or cell death due to overactivation of mitochondrial activity. The metabolic plasticity exhibited by $CD8^+$ T cells (OxPhos *vs.* glycolysis) is likely essential for their function. Therefore, it is also possible that long-term stimulation with OptoMito-On may eventually suppress $CD8^+$ T cell activity *in vivo* by circumventing this plasticity. We predict that the transition is required only for activation from quiescence and not for the ultimate effector functions of $CD8^+$ T cells. Adverse effects (e.g., increased cell death) from stimulation of the mitochondrial membrane potential for a long period of time *in vivo* could lead to the development of a potential control mechanism that can remove excess adoptively transferred $CD8^+$ T cells and ultimately decrease potential side effects.

METHODS

Antibodies and Reagents

The anti-mouse CD3ε (145-2C11) and anti-mouse CD45.2 (104) antibodies were purchased from BD Biosciences. The anti-human CD3 (UCHT1), anti-mouse CD28 (3751), and anti-mouse IFN-γ (XMG1.2) antibodies were purchased from BioLegend. Recombinant human IL-2 was purchased from PeproTech, anti-human CD3ε (OKT3) was purchased from Novus Biologicals, anti-mouse Granzyme B (NGZB) and Brefeldin A was purchased from eBioscience, Annexin-V and 10x Annexin V Binding Buffer was purchased from BD Pharmingen, tetramethylrhodamine ethyl ester (TMRE) and puromycin dihydrochloride were purchased from Thermo Fisher, and SIINFEKL peptide (OVA) was ordered from BioPeptide. Anti-human CD28 (37407), mouse CXCL12 (460-SD/CF), mouse ICAM-1 (796-IC), and mouse CCL21 (457-6C/CF) were purchased from R&D. Anti-human Fc receptor binding inhibitor (polyclonal), anti-mouse CD16/32 Fc block (93), Protein A (10-1100), tetramethylrhodamine (TMRM), Cell Trace Violet, MitoTracker Green FM, and MitoTracker Red CMXRos were purchased from Invitrogen. Carbonyl cyanide 4-(trifluoromethoxy) phenylhydrazone (FCCP), all trans-Retinal, 2-Deoxy-D-glucose, and cobalt (II) chloride hexahydrate were purchased from Sigma. The immunoblot antibody anti-ß-actin (C4) HRP was purchased from Santa Cruz Biotechnology, anti-GFP (ab290) was purchased from Abcam, and peroxidase-conjugated AffiniPure Goat Anti-Rabbit IgG (111-035-144) was purchased from Jackson ImmunoResearch.

Animals

Adult C57BL/6J and OT-I TCR transgenic (C57BL/6-Tg (TcraTcrb)1100Mjb/J) mice were purchased from the Jackson Laboratory and bred in our facility. Unless specified, it can be assumed that experiments were done with $CD8^+$ T cells isolated from C57BL/6J mice. All mice were maintained in a pathogen-free environment in the University of Rochester animal facility and the animal experiments were approved by the University Committee on Animal Resources at the University of Rochester.

Molecular Biology

The light-activated proton pump from *Leptosphaeria maculans* (Mac) fused to eGFP was amplified from the plasmid pFCK-Mac-GFP, a gift from Edward Boyden (Addgene plasmid #22223) (27) and fused to the N-terminal 187 amino acids of the *Immt* gene (mitofilin homologue) as previously described (23). The IMMT::Mac::GFP sequence was then cloned using restriction digestion into a pcDNA3.1 vector containing a CMV promoter (pBJB28 plasmid). Bionics cloned the Mitofilin::Mac::GFP sequence into a pMSCV vector, which was used to make retrovirus. The pcDNA3.1-GFP and pMigR1-GFP plasmids were used for negative control transfections in HEK293T cells and $CD8^+$ T cells, respectively.

Cell Culture

Isolated mouse $CD8^+$ T cells were cultured in RPMI 1640 supplemented with 80 U/mL IL-2, 10% FBS, 100 U/mL penicillin (Gibco), 100 µg/mL streptomycin (Gibco), 2 mM L-glutamine (Gibco), 20 mM HEPES buffer (Gibco), 1% MEM Non-Essential Amino Acids (Gibco), and 50 µM ß-mercaptoethanol (Sigma-Aldrich). Isolated human T cells were cultured in TexMACS medium supplemented with 200 U/mL IL-2, 3% human AB serum, 100 U/mL penicillin, and 100 µg/mL streptomycin. HeLa cells, HEK293T cells, and EL-4 cells were cultured in DMEM supplemented with 10% FBS, 100 U/mL penicillin, 100 µg/mL streptomycin, 2 mM L-glutamine, 20 mM HEPES buffer, 1% MEM Non-Essential Amino Acids, and 50 µM β-mercaptoethanol. Geneticin (Gibco) was added to complete DMEM media for stable HEK293T cell lines at 1 mg/mL and for stable HeLa cell lines at 500 µg/mL. All cell types that expressed OptoMito-On were cultured in media supplemented with 7 µM all-*trans*-retinal (ATR) for at least 48 hours prior to any experiments. ATR is a cofactor that is required for photosensory transduction by the proton pump 'Mac' (24).

T Cell Purification and Activation

Mouse $CD8^+$ T cells were purified from single-cell suspensions of the spleen and lymph nodes of C57BL/6J or OT-I TCR transgenic mice. Single-cell suspensions were prepared by mechanical disruption in a cell strainer. $CD8^+$ T cells were enriched by magnetic-bead depletion with rat anti-mouse MHC class II antibody (M5/114) and rat anti-mouse CD4 antibody (GK1.5), followed by sheep anti-rat IgG magnetic beads (Invitrogen 11035). Isolated $CD8^+$ T cells were cultured

up to 4 days in complete RPMI medium supplemented with 80 U/mL IL-2 following activation with plate-bound CD3ε Ab (6 μg/mL) and CD28 Ab (1.6 μg/mL) for 2 days. Human T cells were purified from healthy donor peripheral blood using the EasySep Direct Human T cell isolation kit (StemCell). Human T cell activation was achieved with plate-bound αCD3ε (1 μg/mL) and αCD28 (0.2 μg/mL) in complete TexMACS medium.

Immunoblotting

The membrane was blocked with 5% nonfat milk in PBS for at least 1 hour at room temperature after proteins were transferred from precast 4-20% gels (BioRad). Blots were incubated for 1 hour at room temperature with 1:1000 of anti-GFP (ab290, Abcam) or 1:5000 β-actin HRP (SantaCruz). The membrane was then incubated with 1:5000 horseradish peroxidase-conjugated anti-rabbit IgG heavy and light chains (Jackson ImmunoResearch) for 1 hour at room temperature. Protein was detected using SuperSignal West Pico PLUS chemiluminescent reagent (Thermo).

Metabolism Assays

The oxygen consumption rates (OCR) and extracellular acidification rates (ECAR) were measured in a Seahorse XFe 96 Analyzer with the Seahorse XF Cell MitoStress Test (Agilent). Measurements were made in L-15 medium supplemented with 2 mg/mL D-glucose under basal conditions and in response to 2 μM oligomycin, 2 μM FCCP, and 1 μM rotenone + 1 μM antimycin A. A BCA assay was used to normalize the Seahorse assay results in **Figure 1** and **Supplemental Figure 1** to total protein content. For all other Seahorse assays, the same number of cells was plated in each well. The Seahorse XFe96 Extracellular Flux Analyzer has been well characterized to determine the bioenergetics of T cells (54).

ATP Assay

ATP measurements were performed with the CellTiter-Glo Luminescent Cell Viability Assay following the manufacturer's instructions (Promega). The Lipofectamine 2000 DNA transfection protocol was used (Invitrogen). HEK293T cells expressing GFP were used as a negative control. Media was supplemented with 7 μM ATR. HEK293T cells were treated with 10 mM 2-DG 2 hours prior to light activation and 2-DG remained in the media during the 2-hour light activation. $CD8^+$ T cells were sorted based on GFP expression. GFP negative cells were used as the mock negative control and the light activation was for 30 minutes. The light sources and conditions are described below (590 nm at 0.32 mW/mm^2). The ATP assay in **Supplementary Figure 5B** was done with Day 6 OptoMito-On OT-I T cells enriched with 3 μg/mL puromycin. T cells were treated with 10 mM 2-DG for 30 minutes prior to a 30-minute light activation.

Mitochondrial Staining

To label mitochondria, 100-500 nM MitoTracker Red CMXRos for HeLa cells was used. Images of live cells in L-15 on poly-L-lysine coated ΔTs were acquired on an inverted microscope. Images of fixed OptoMito-On expressing HeLa cells were taken on a confocal microscope. During $CD8^+$ T cell activation, mitochondrial mass was determined with 200 nM MitoTracker Green FM and mitochondrial membrane potential with 20 nM TMRM. Background TMRM staining was subtracted by adding 10 μM FCCP while staining with TMRM. Cells were stained with MitoTracker Green FM or TMRM for 15 minutes at 37°C then stained with anti-mouse CD8 (Clone 53-6.7, BD Biosciences) or anti-human CD3 (UCHT1, Biolegend) followed by flow cytometry.

Mitochondria Isolation

OptoMito-On HEK293T cell mitochondria were isolated from cells trypsinized from 5 T75 flasks using differential centrifugation in sucrose-based media. Collected cells were washed in PBS and pelleted in a 15 mL tube. The pelleted cells were resuspended in 2 mL cold mitochondria isolation buffer (10 mM HEPES, 1 mM EDTA, 320 mM sucrose, pH 7.2), transferred to a Dounce homogenizer, and homogenized with a pestle for 60 passes. The cell lysate was then transferred to a 2 mL Eppendorf tube and spun down at 700 g for 8 minutes. The supernatant contained the crude mitochondria fraction and was carefully removed then stored on ice. The pellet was resuspended in 500 μL isolation buffer, spun down at 700 g for 5 minutes, and the supernatant was pooled with the crude mitochondria fraction. The crude mitochondria fraction was then spun at 17,000 g for 11 minutes. The resulting supernatant contained the cytosolic fraction and the pellet contained mitochondria. The mitochondrial pellet was then resuspended in 50 μL of isolation buffer and protein concentration was quantified using the Folin-phenol method.

Isolated Mitochondria TMRE Measurement

OptoMito-On isolated mitochondria (0.5 mg/mL) were stirred in mitochondrial respiration buffer (120 mM KCl, 25 mM sucrose, 5 mM $MgCl_2$, 5 mM KH_2PO_4, 1 mM EGTA, 10 mM HEPES, 1 mg/mL FF-BSA, pH 7.35) at 37°C in the presence of 2 μM rotenone and 5 mM succinate where indicated. 20 nM tetramethylrhodamine ethyl ester (TMRE) was added to observe mitochondrial membrane potential in non-quench mode, as previously described (23). TMRE signal was measured by Cary Eclipse Fluorescence Spectrophotometer (Agilent Technologies) using a 335-620 nm excitation filter and a 550-1,100 nm emission filter. Illumination was performed continuously (0.02 mW/mm^2, 540-600 nm GYX module, X-Cite LED1 by Excelitas, Waltham MA, USA) for 1 minute prior to fluorescence reading. After stable baseline measurements with or without succinate, 2 μM FCCP was added to completely depolarize mitochondrial proton motive force. Average fluorescence after FCCP addition was subtracted from the baseline to calculate the change in fluorescence (ΔF for conditions without succinate and ΔF_{max} for conditions with succinate). Data were then normalized to ΔF_{max} to show polarization of the $\Delta\psi_m$ by OptoMito-On relative to maximum endogenous polarization.

In Vitro T Cell Migration Imaging

Cell migration chambers (Millicell EZ slide eight-well glass, Millipore) were prepared by coating with Protein A (20 μg/mL), ICAM-1 (2.75 μg/mL), and CXCL12 (400 ng/mL) in PBS. Day 4 activated $CD8^+$ T cells were plated in L-15 medium (Invitrogen, Leibovitz's medium + 2 mg/mL D-glucose) in a 37°C chamber. Video microscopy was conducted using a TE2000-U microscope (Nikon) coupled to a CoolSNAP HQ CCD camera with a 10x objective and 0.45 numerical aperture. T cells were plated in L-15 medium at least 20 minutes at 37°C before imaging. Treatment of cells with inhibitors before imaging: $CoCl_2$ treatment was overnight (~16 hours) and maintained in L-15 media; FCCP and oligomycin were added to the cells 20 minutes before the movie started when cells are plated. OptoMito-On and Mock or GFP T cell migration movies all received 500 nm illumination with a Texas Red filter. Bright field or DIC images were acquired every 15 seconds for 20 minutes.

T Cell Migration Analysis

Migration analysis was performed in Volocity software (PerkinElmer). In order to select which T cell tracks to analyze in Volocity, we excluded cells that are smaller than 10 μm and greater than 200 μm. Additionally, static cells were ignored, broken tracks were automatically joined, and cell tracks less than 20 μm were excluded. We also omitted T cells that were migrating for less than 5 minutes of the 20-minute movie and removed cells that Volocity incorrectly tracked. The velocity (μm min^{-1}), displacement (net displacement, μm), track length (total path length, μm), and meandering index (net displacement/track length) of each cell track was measured (55). The percentage of migrating cells was calculated as the number of cells migrating 5-20 μm/min divided by the total number of cells in the field of view during a 20-minute movie.

OptoMito-On Expression in T Cells

Retroviruses were generated using the Phoenix-ecotropic packaging cell line (ATCC). For retroviral transductions, Phoenix cells were transfected to produce retrovirus using the calcium phosphate transfection method. Collected supernatant was concentrated with Retro-X Concentrator (Takara). Isolated mouse $CD8^+$ T cells were transduced one day after isolation in the presence of 8 μg/mL polybrene. Cells were then sorted on Day 3 or 4 based on GFP signal and used for experiments on Day 4-6. Typical transduction efficiency for OptoMito-On is 30%. Considerable time was spent optimizing the retrovirus transduction efficiency and the best efficiency was 45-50%. OptoMito-On or GFP transduced $CD8^+$ T cells were not sorted for the granzyme B assay; instead GFP+ cells were gated on during flow cytometry analysis. At least 30% of $CD8^+$ T cells were OptoMito-On+. For the ATP assay (**Supplementary Figure 5A**), OptoMito-On T cells were enriched with 3 μg/mL puromycin, resulting in at least 90% OptoMito-On+ T cells. All media for experiments using OptoMito-On expressing T cells or HEK293T cells was supplemented with 7 μM ATR at least two days before cells were used for experiments.

Antibody Array

Full Moon BioSystems Cytoskeleton Phospho Antibody Array (PCP141) was used following the manufacturer's instructions. OptoMito-On expressing $CD8^+$ T cells were sorted based on GFP expression and 150,000 cells were plated on ICAM-1 + CXCL12 coated 8-well dishes. T cells either received no light activation or received the same light activation as was done for *in vitro* T cell imaging (Texas Red filter at 630 nm). Immediately after the 20-minute movie +/- light activation, L-15 was aspirated to remove any unattached cells, followed by the addition of RIPA buffer, with phosphate & protease inhibitors added, to lyse the attached migrating cells. Cell lysate was pooled from multiple movies in order to have enough protein to complete three replicates of the antibody array and quantified with a BCA assay. The antibody array results were quantified using ImageJ, and the average fold change in protein expression from dark to light conditions was calculated to make a heat map.

Co-Culture Assay

Activated OT-I $CD8^+$ T cells transduced with OptoMito-On or GFP retrovirus were sorted on Day 3 or Day 4 of activation. 1 - 2 hours after cell sorting, 100,000 T cells were plated in each well of glass bottom 96-well plates in complete RPMI media. One plate remained in the dark, while the second plate was illuminated with 530 nm light at 0.0075 mW/mm^2 for 16-17 hours. EL-4 cells were pulsed with 1 μg/mL SIINFEKL (OVA) peptide and stained with 5 μM Cell Trace Violet for 20 minutes at 37°C, then washed in PBS before adding 100,000 EL-4 cells to the already plated $CD8^+$ T cells in complete RPMI media. The co-culture was done at a 1:1 ratio for 3 hours in duplicate for each experiment. The illuminated plate was only briefly removed from the LED array when EL-4 cells were added. At the completion of the co-culture, cells were collected, washed in cold PBS, then stained with Annexin-V APC in 1x Annexin V binding buffer for flow cytometry analysis. Cell Trace Violet positive cells were gated on to specifically look at the Annexin-V staining of EL-4 cells.

Glucose Consumption Assay

Activated OT-I $CD8^+$ T cells transduced with OptoMito-On or GFP retrovirus were sorted on Day 3 or Day 4 of activation. A couple hours after cell sorting, T cells were plated in each well of glass bottom 96-well plates in 100 μL Leibovitz's media, without any added glucose. One plate remained in the dark, while the second plate was illuminated with 530 nm light at about 0.013 mW/mm^2 for 1 hour. 1 mM 2-DG was added to each well before the 1-hour incubation in order to measure the glucose consumption rate with the Glucose Uptake-Glo Assay (Promega). After the 1-hour incubation, 50 μL of stop buffer was added to each well, then 75 μL of the cells were pipetted into a white 96-well plate. The remainder of the assay strictly followed the manufacturer's instructions. In order to subtract background signal, 2-DG wasn't added to control wells with the same number of cells.

Light Sources

A 540-600 nm GYX module, X-Cite LED1 by Excelitas, Waltham MA, USA was used at 0.02 mW/mm^2 to illuminate isolated mitochondria for the TMRE traces. An Amuza 590 nm LED array was used to illuminate HEK293T cells and CD8$^+$ T cells with light for the ATP assay. Each well of a glass-bottom 96-well plate (MatTek, P96G-1.5-5-F) received 590 nm light at 0.32 mW/mm^2 at 1 hertz, with a 500-ms light/500-ms dark cycle. An Amuza 530 nm LED array was used to illuminate OT-I CD8$^+$ T cells for the overnight Granzyme B experiment (0.0045 mW/mm^2), co-culture assay (0.0075 mW/mm^2), and glucose consumption assay (0.013 mW/mm^2). Each well of a glass-bottom 96-well plate received 530 nm light at 1 hertz with a 500-ms light/500-ms dark cycle. Light activation for *in vitro* T cell migration assays were performed on a TE2000-U microscope (Nikon, described above) using the Texas Red filter (630 nm) at approximately 0.75 mW/mm^2 with a 5-s light/5-s dark cycle using a Sola light engine (Nikon). The light intensities were determined with an energy meter console connected to a photodiode power sensor (PM100D, S130VC, ThorLabs).

Statistical Analyses

Assuming normal distribution, for comparison of non-paired experimental groups an unpaired t-test was utilized. Comparisons for more than two groups employed a One-way ANOVA or a Two-way ANOVA for more than 1 level of comparison. ANOVA tests were accompanied with Bonferroni's post-hoc test. Additionally, Pearson's correlation and a paired t-test was used when appropriate. Differences with a p-value < 0.05 were considered statistically significant. All statistical tests were performed with GraphPad Prism (v9). Means ± standard error of the mean (SEM) are shown.

Study Approval

All mouse procedures were approved by the University of Rochester Committee on Animal Resources under protocol UCAR-2008-096E and followed Institutional Animal Care and Use Committee guidelines. The Human Research Studies Review Board of the University of Rochester approved this study.

DATA AVAILABILITY STATEMENT

The raw data supporting the conclusions of this article will be made available by the authors, without undue reservation.

ETHICS STATEMENT

The animal study was reviewed and approved by University Committee on Animal Resources at the University of Rochester.

AUTHOR CONTRIBUTIONS

AA conducted the majority of the experiments with the help of BB who completed the cloning of the OptoMito-On construct into the pcDNA3.1 vector, isolated mitochondria, and collected TMRE traces. KL performed the antibody arrays. RW helped with human T cell assays. MK and AW conceived the idea of OptoMito-On and directed this study. K-DK helped design and optimize the light activation experiments and co-culture assay. AA and MK wrote the manuscript with suggestions from all the authors. All authors contributed to the article and approved the submitted version.

FUNDING

This project was financially supported through grants from the National Institute of Health (T32AI007285 (AA), P01AI102851 (MK), R01AI147362 (MK & RW), R01NS115906 (AW), and R21CA242843 (MK & AW). This project was financially supported by the National Research Council of Science and Technology (NST) grant through the Korean government (MSIP) (CRC-16-01-KRICT).

ACKNOWLEDGMENTS

We thank M. Youngman for drawing blood for experiments in this manuscript, as well as members of the Kim lab for useful suggestions and discussion.

SUPPLEMENTARY MATERIAL

The Supplementary Material for this article can be found online at: https://www.frontiersin.org/articles/10.3389/fimmu.2021.666231/full#supplementary-material

Supplementary Figure 1 | Overall CD8$^+$ T cell metabolism increases after activation. The complete ECAR trace **(A)**, the basal OCR **(B)**, the maximum OCR **(C)**, and the spare respiratory capacity **(D)** of naïve and activated CD8$^+$ T cells, measured with the Seahorse MitoStress Test and normalized to protein content with a BCA assay. **(A)**: data shown as mean ± SEM, error bars fall within symbols, analyzed by 2way ANOVA with a Bonferroni post-test; **(B–D)**: data shown as mean ± SEM and analyzed by Welch's t-test. **(E)** Increase in the percent of Annexin-V+ activated mouse CD8$^+$ T cells after treatment with 1 μM Rotenone + Antimycin A, 2 μM FCCP, or 2 μM Oligomycin for 1, 3, or 6 hours (n = 3).

Supplementary Figure 2 | Migrating CD8$^+$ T cells have increased glycolysis. The complete ECAR trace **(A)**, the basal ECAR **(B)**, the maximum OCR **(C)**, and the spare respiratory capacity **(D)** of activated CD8$^+$ T cells, measured with the Seahorse MitoStress Test. **(A)**: data shown as mean ± SEM, error bars fall within symbols; **(B–D)**: data shown as mean ± SEM and analyzed by One-Way ANOVA with a Bonferroni post-test.

Supplementary Figure 3 | CD8$^+$ T cell migration capacity is decreased in hypoxic conditions. **(A)** The complete OCR trace and **(B)** the basal OCR measured with the Seahorse MitoStress Test, of activated CD8$^+$ T cells treated with the hypoxia inducer, cobalt chloride hexahydrate ($CoCl_2$) overnight (n = 6 wells per group, error bars fall within symbols). **(C)** The complete ECAR trace and **(D)** the basal ECAR measured with the Seahorse MitoStress Test. **(E)** The overall track velocity of activated CD8$^+$ T cells treated with or without $CoCl_2$ and migrating on ICAM-1 + CXCL12 (includes all tracked cells migrating less than 15 μm/min). **(F)** The velocity of actively migrating CD8$^+$ T cells. **(G)** The percentage of migrating CD8$^+$ T cells (the number of cells migrating 5-20 μm/min divided by the total number of cells in the field of view during a 20-minute movie, n = 2 movies). **(H)** Flow cytometry results of activated CD8$^+$ T cells treated with $CoCl_2$ overnight and stained for Annexin-V. **(A–G)**: data shown as mean ± SEM and analyzed by One-Way ANOVA with a Bonferroni post-test.

Supplementary Figure 4 | OptoMito-On is expressed in mitochondria. $CD8^+$ T cells, HEK293T cells, and HeLa cells expressing OptoMito-On were stained with MitoTracker Red and images were taken on an inverted microscope. Then the Pearson's correlation coefficient was calculated in ImageJ software for the entire cell body of each cell. Data shown as mean ± SEM.

Supplementary Figure 5 | OptoMito-On does not impact glycolysis. **(A)** ATP assay with OptoMito-On OT-I T cells treated with or without 10 mM 2-DG. Same light activation setup as **Figure 4C**. Data shown as mean ± SEM (n = 3-4). **(B)** Sorted OT-I T cells expressing either OptoMito-On or GFP were plated in Leibovitz's media, illuminated with 530 nm for 1 hour or kept in the dark, and then the Glucose Uptake-Glo Assay protocol was followed. Data shown as mean ± SEM and analyzed by One-Way ANOVA with a Bonferroni post-test (representative of three experiments; RLU: relative luminescence units).

Movie 1 | Representative movie of $CD8^+$ T cells expressing GFP migrating on ICAM-1 + CXCL12 with 500 nm illumination.

Movie 2 | Representative movie of $CD8^+$ T cells expressing OptoMito-On migrating on ICAM-1 + CXCL12 with 500 nm illumination.

REFERENCES

1. Restifo NP, Dudley ME, Rosenberg SA. Adoptive Immunotherapy for Cancer: Harnessing the T Cell Response. *Nat Rev Immunol* (2012) 12:269. doi: 10.1038/nri3191
2. Eshhar Z, Waks T, Gross G, Schindler DG. Specific Activation and Targeting of Cytotoxic Lymphocytes Through Chimeric Single Chains Consisting of Antibody-Binding Domains and the Gamma or Zeta Subunits of the Immunoglobulin and T-cell Receptors. *Proc Natl Acad Sci* (1993) 90:720–4. doi: 10.1073/pnas.90.2.720
3. Brentjens RJ, Davila ML, Riviere I, Park J, Wang X, Cowell LG, et al. Cd19-Targeted T Cells Rapidly Induce Molecular Remissions in Adults With Chemotherapy-Refractory Acute Lymphoblastic Leukemia. *Sci Trans Med* (2013) 5:177ra138–177ra138. doi: 10.1126/scitranslmed.3005930
4. Srivastava S, Riddell SR. Chimeric Antigen Receptor T Cell Therapy: Challenges to Bench-to-Bedside Efficacy. *J Immunol* (2018) 200:459–68. doi: 10.4049/jimmunol.1701155
5. Scharping NE, Menk AV, Moreci RS, Whetstone RD, Dadey RE, Watkins SC, et al. The Tumor Microenvironment Represses T Cell Mitochondrial Biogenesis to Drive Intratumoral T Cell Metabolic Insufficiency and Dysfunction. *Immunity* (2016) 45:374–88. doi: 10.1016/j.immuni.2016.07.009
6. Chang C-H, Qiu J, O'Sullivan D, Buck, Michael D, Noguchi T, et al. Metabolic Competition in the Tumor Microenvironment Is a Driver of Cancer Progression. *Cell* (2015) 162:1229–41. doi: 10.1016/j.cell.2015.08.016
7. Siska PJ, Beckermann KE, Mason FM, Andrejeva G, Greenplate AR, Sendor AB, et al. Mitochondrial Dysregulation and Glycolytic Insufficiency Functionally Impair CD8 T Cells Infiltrating Human Renal Cell Carcinoma. *JCI Insight* (2017) 2:e93411. doi: 10.1172/jci.insight.93411
8. Parry RV, Chemnitz JM, Frauwirth KA, Lanfranco AR, Braunstein I, Kobayashi SV, et al. CTLA-4 and PD-1 Receptors Inhibit T-Cell Activation by Distinct Mechanisms. *Mol Cell Biol* (2005) 25:9543–53. doi: 10.1128/MCB.25.21.9543-9553.2005
9. Sena LA, Li S, Jairaman A, Prakriya M, Ezponda T, Hildeman DA, et al. Mitochondria Are Required for Antigen-Specific T Cell Activation Through Reactive Oxygen Species Signaling. *Immunity* (2013) 38:225–36. doi: 10.1016/j.immuni.2012.10.020
10. Frauwirth KA, Riley JL, Harris MH, Parry RV, Rathmell JC, Plas DR, et al. The CD28 Signaling Pathway Regulates Glucose Metabolism. *Immunity* (2002) 16:769–77. doi: 10.1016/S1074-7613(02)00323-0
11. Klein Geltink RI, O'Sullivan D, Corrado M, Bremser A, Buck MD, Buescher JM, et al. Mitochondrial Priming by CD28. *Cell* (2017) 171:385–97.e311. doi: 10.1016/j.cell.2017.08.018
12. Chang C-H, Curtis JD, Maggi LB, Faubert B, Villarino AV, O'Sullivan D, et al. Posttranscriptional Control of T Cell Effector Function by Aerobic Glycolysis. *Cell* (2013) 153:1239–51. doi: 10.1016/j.cell.2013.05.016
13. Cham Candace M, Driessens G, O'Keefe James P, Gajewski Thomas F. Glucose Deprivation Inhibits Multiple Key Gene Expression Events and Effector Functions in CD8+ T Cells. *Eur J Immunol* (2008) 38:2438–50. doi: 10.1002/eji.200838289
14. Sukumar M, Liu J, Ji Y, Subramanian M, Crompton JG, Yu Z, et al. Inhibiting Glycolytic Metabolism Enhances CD8+ T Cell Memory and Antitumor Function. *J Clin Invest* (2013) 123:4479–88. doi: 10.1172/JCI69589
15. Buck MD, O'Sullivan D, Klein Geltink RI, Curtis JD, Chang C-H, Sanin DE, et al. Mitochondrial Dynamics Controls T Cell Fate Through Metabolic Programming. *Cell* (2016) 166:63–76. doi: 10.1016/j.cell.2016.05.035
16. Gee AP. Gmp CAR-T Cell Production. *Best Pract Res Clin Haematol* (2018) 31:126–34. doi: 10.1016/j.beha.2018.01.002
17. Pearce EL, Poffenberger MC, Chang C-H, Jones RG. Fueling Immunity: Insights Into Metabolism and Lymphocyte Function. *Science* (2013) 342:1242454. doi: 10.1126/science.1242454
18. Menk AV, Scharping NE, Moreci RS, Zeng X, Guy C, Salvatore S, et al. Early TCR Signaling Induces Rapid Aerobic Glycolysis Enabling Distinct Acute T Cell Effector Functions. *Cell Rep* (2018) 22:1509–21. doi: 10.1016/j.celrep.2018.01.040
19. Binnewies M, Roberts EW, Kersten K, Chan V, Fearon DF, Merad M, et al. Understanding the Tumor Immune Microenvironment (TIME) for Effective Therapy. *Nat Med* (2018) 24:541–50. doi: 10.1038/s41591-018-0014-x
20. Bonaventura P, Shekarian T, Alcazer V, Valladeau-Guilemond J, Valsesia-Wittmann S, Amigorena S, et al. Cold Tumors: A Therapeutic Challenge for Immunotherapy. *Front Immunol* (2019) 10. doi: 10.3389/fimmu.2019.00168
21. Walling BL, Kim M. LFA-1 in T Cell Migration and Differentiation. *Front Immunol* (2018) 9. doi: 10.3389/fimmu.2018.00952
22. Weigent DA. Hypoxia and Cytoplasmic Alkalinization Upregulate Growth Hormone Expression in Lymphocytes. *Cell Immunol* (2013) 282:9–16. doi: 10.1016/j.cellimm.2013.03.007
23. Berry BJ, Trewin AJ, Milliken AS, Baldzizhar A, Amitrano AM, Lim Y, et al. Optogenetic Control of Mitochondrial Protonmotive Force to Impact Cellular Stress Resistance. *EMBO Rep* (2020) 21:e49113. doi: 10.15252/embr.201949113
24. Waschuk SA, Bezerra AG, Shi L, Brown LS. Leptosphaeria Rhodopsin: Bacteriorhodopsin-like Proton Pump From a Eukaryote. *Proc Natl Acad Sci U S A* (2005) 102:6879–83. doi: 10.1073/pnas.0409659102
25. Fischer LR, Igoudjil A, Magrane J, Li Y, Hansen JM, Manfredi G, et al. SOD1 Targeted to the Mitochondrial Intermembrane Space Prevents Motor Neuropathy in the Sod1 Knockout Mouse. *Brain* (2011) 134:196–209. doi: 10.1093/brain/awq314
26. John GB, Shang Y, Li L, Renken C, Mannella CA, Selker JML, et al. The Mitochondrial Inner Membrane Protein Mitofilin Controls Cristae Morphology. *Mol Biol Cell* (2005) 16:1543–54. doi: 10.1091/mbc.e04-08-0697
27. Chow BY, Han X, Dobry AS, Qian X, Chuong AS, Li M, et al. High-Performance Genetically Targetable Optical Neural Silencing by Light-Driven Proton Pumps. *Nature* (2010) 463:98–102. doi: 10.1038/nature08652
28. Berry BJ, Trewin AJ, Amitrano AM, Kim M, Wojtovich AP. Use the Protonmotive Force: Mitochondrial Uncoupling and Reactive Oxygen Species. *J Mol Biol* (2018) 430:3873–91. doi: 10.1016/j.jmb.2018.03.025
29. Sukumar M, Liu J, Mehta GU, Patel SJ, Roychoudhuri R, Crompton JG, et al. Mitochondrial Membrane Potential Identifies Cells With Enhanced Stemness for Cellular Therapy. *Cell Metab* (2016) 23:63–76. doi: 10.1016/j.cmet.2015.11.002
30. Perry SW, Norman JP, Barbieri J, Brown EB, Gelbard HA. Mitochondrial Membrane Potential Probes and the Proton Gradient: A Practical Usage Guide. *BioTechniques* (2011) 50:98–115. doi: 10.2144/000113610
31. Renner K, Geiselhöringer A-L, Fante M, Bruss C, Färber S, Schönhammer G, et al. Metabolic Plasticity of Human T Cells: Preserved Cytokine Production Under Glucose Deprivation or Mitochondrial Restriction, But 2-Deoxy-Glucose Affects Effector Functions. *Eur J Immunol* (2015) 45:2504–16. doi: 10.1002/eji.201545473
32. Ledderose C, Liu K, Kondo Y, Slubowski CJ, Dertnig T, Denicoló S, et al. Purinergic P2X4 Receptors and Mitochondrial ATP Production Regulate T Cell Migration. *J Clin Invest* (2018) 128:3583–94. doi: 10.1172/JCI120972

33. Campello S, Lacalle RA, Bettella M, Mañes S, Scorrano L, Viola A. Orchestration of Lymphocyte Chemotaxis by Mitochondrial Dynamics. *J Exp Med* (2006) 203:2879–86. doi: 10.1084/jem.20061877
34. Ridley AJ, Schwartz MA, Burridge K, Firtel RA, Ginsberg MH, Borisy G, et al. Cell Migration: Integrating Signals From Front to Back. *Science* (2003) 302:1704–9. doi: 10.1126/science.1092053
35. Cary LA, Guan JL. Focal Adhesion Kinase in Integrin-Mediated Signaling. *Front Biosci* (1999) 4:D102–113. doi: 10.2741/A414
36. Fowell DJ, Kim M. The Spatio-Temporal Control of Effector T Cell Migration. *Nat Rev Immunol* (2021) 1–15. doi: 10.1038/s41577-021-00507-0
37. Paluch EK, Aspalter IM, Sixt M. Focal Adhesion–Independent Cell Migration. *Annu Rev Cell Dev Biol* (2016) 32:469–90. doi: 10.1146/annurev-cellbio-111315-125341
38. Chapman NM, Houtman JC. Functions of the FAK Family Kinases in T Cells: Beyond Actin Cytoskeletal Rearrangement. *Immunol Res* (2014) 59:23–34. doi: 10.1007/s12026-014-8527-y
39. Rose DM, Liu S, Woodside DG, Han J, Schlaepfer DD, Ginsberg MH. Paxillin Binding to the α4 Integrin Subunit Stimulates Lfa-1 (Integrin αlβ2)-Dependent T Cell Migration by Augmenting the Activation of Focal Adhesion Kinase/Proline-Rich Tyrosine Kinase-2. *J Immunol* (2003) 170:5912–8. doi: 10.4049/jimmunol.170.12.5912
40. Eppler FJ, Quast T, Kolanus W. Dynamin2 Controls Rap1 Activation and Integrin Clustering in Human T Lymphocyte Adhesion. *PLoS One* (2017) 12: e0172443. doi: 10.1371/journal.pone.0172443
41. Raab M, Lu Y, Kohler K, Smith X, Strebhardt K, Rudd CE. LFA-1 Activates Focal Adhesion Kinases FAK1/PYK2 to Generate LAT-GRB2-SKAP1 Complexes That Terminate T-cell Conjugate Formation. *Nat Commun* (2017) 8:16001. doi: 10.1038/ncomms16001
42. Vander Heiden MG, Cantley LC, Thompson CB. Understanding the Warburg Effect: The Metabolic Requirements of Cell Proliferation. *Science* (2009) 324:1029–33. doi: 10.1126/science.1160809
43. Cascone T, McKenzie JA, Mbofung RM, Punt S, Wang Z, Xu C, et al. Increased Tumor Glycolysis Characterizes Immune Resistance to Adoptive T Cell Therapy. *Cell Metab* (2018) 27:977–87.e974. doi: 10.1016/j.cmet.2018.02.024
44. Wang R, Dillon CP, Shi LZ, Milasta S, Carter R, Finkelstein D, et al. The Transcription Factor Myc Controls Metabolic Reprogramming Upon T Lymphocyte Activation. *Immunity* (2011) 35:871–82. doi: 10.1016/j.immuni.2011.09.021
45. LeBleu VS, O'Connell JT, Gonzalez Herrera KN, Wikman H, Pantel K, Haigis MC, et al. Pgc-1α Mediates Mitochondrial Biogenesis and Oxidative Phosphorylation in Cancer Cells to Promote Metastasis. *Nat Cell Biol* (2014) 16:992–1003. doi: 10.1038/ncb3039
46. Porporato PE, Payen VL, Pérez-Escuredo J, De Saedeleer CJ, Danhier P, Copetti T, et al. A Mitochondrial Switch Promotes Tumor Metastasis. *Cell Rep* (2014) 8:754–66. doi: 10.1016/j.celrep.2014.06.043
47. Porporato PE, Filigheddu N, Pedro JMB-S, Kroemer G, Galluzzi L. Mitochondrial Metabolism and Cancer. *Cell Res* (2018) 28:265–80. doi: 10.1038/cr.2017.155
48. Hons M, Kopf A, Hauschild R, Leithner A, Gaertner F, Abe J, et al. Chemokines and Integrins Independently Tune Actin Flow and Substrate Friction During Intranodal Migration of T Cells. *Nat Immunol* (2018) 19:606–16. doi: 10.1038/s41590-018-0109-z
49. Nordenfelt P, Elliott HL, Springer TA. Coordinated Integrin Activation by Actin-Dependent Force During T-cell Migration. *Nat Commun* (2016) 7:13119. doi: 10.1038/ncomms13119
50. Nordenfelt P, Moore TI, Mehta SB, Kalappurakkal JM, Swaminathan V, Koga N, et al. Direction of Actin Flow Dictates Integrin LFA-1 Orientation During Leukocyte Migration. *Nat Commun* (2017) 8:2047. doi: 10.1038/s41467-017-01848-y
51. Buck MD, O'Sullivan D, Pearce EL. T Cell Metabolism Drives Immunity. *J Exp Med* (2015) 212:1345–60. doi: 10.1084/jem.20151159
52. Vardhana SA, Hwee MA, Berisa M, Wells DK, Yost KE, King B, et al. Impaired Mitochondrial Oxidative Phosphorylation Limits the Self-Renewal of T Cells Exposed to Persistent Antigen. *Nat Immunol* (2020) 21:1022–33. doi: 10.1038/s41590-020-0725-2
53. Scharping NE, Rivadeneira DB, Menk AV, Vignali PDA, Ford BR, Rittenhouse NL, et al. Mitochondrial Stress Induced by Continuous Stimulation Under Hypoxia Rapidly Drives T Cell Exhaustion. *Nat Immunol* (2021) 22:202–15. doi: 10.1038/s41590-020-00834-9
54. van der Windt GJW, Chang C-H, Pearce EL. Measuring Bioenergetics in T Cells Using a Seahorse Extracellular Flux Analyzer. *Curr Protoc Immunol* (2016) 113:3.16B.11–13.16B.14. doi: 10.1002/0471142735.im0316bs113
55. Beltman JB, Maree AF, de Boer RJ. Analysing Immune Cell Migration. *Nat Rev* (2009) 9:789–98. doi: 10.1038/nri2638

Conflict of Interest: The authors declare that the research was conducted in the absence of any commercial or financial relationships that could be construed as a potential conflict of interest.

frontiers in Immunology

ORIGINAL RESEARCH
published: 19 August 2021
doi: 10.3389/fimmu.2021.702345

Binding of Rap1 and Riam to Talin1 Fine-Tune β2 Integrin Activity During Leukocyte Trafficking

*Thomas Bromberger[1,2], Sarah Klapproth[1], Ina Rohwedder[3], Jasmin Weber[3], Robert Pick[4], Laura Mittmann[5,6], Soo Jin Min-Weißenhorn[7], Christoph A. Reichel[5,6], Christoph Scheiermann[3,4], Markus Sperandio[3] and Markus Moser[1,2]**

[1] Center for Translational Cancer Research (TranslaTUM), TUM School of Medicine, Technische Universität München, Munich, Germany, [2] Department of Molecular Medicine, Max Planck Institute of Biochemistry, Martinsried, Germany, [3] Walter Brendel Center of Experimental Medicine (WBex), Biomedical Center (BMC), Ludwig-Maximilians-Universität München, Martinsried, Germany, [4] Department of Pathology and Immunology, School of Medicine, University of Geneva, Geneva, Switzerland, [5] Walter Brendel Centre of Experimental Medicine (WBex), Klinikum der Universität München, Ludwig-Maximilians-Universität München, Munich, Germany, [6] Department of Otorhinolaryngology, Ludwig-Maximilians-Universität München, Munich, Germany, [7] Transgenic Core Facility, Max Planck Institute of Biochemistry, Martinsried, Germany

OPEN ACCESS

Edited by:
Emmanuel Donnadieu, Institut National de la Santé et de la Recherche Médicale (INSERM), France

Reviewed by:
Mark Philips, New York University, United States
Zhichao Fan, UCONN Health, United States

***Correspondence:**
Markus Moser
m.moser@tum.de

Specialty section:
This article was submitted to Molecular Innate Immunity, a section of the journal Frontiers in Immunology

Received: *29 April 2021*
Accepted: *04 August 2021*
Published: *19 August 2021*

Citation:
Bromberger T, Klapproth S, Rohwedder I, Weber J, Pick R, Mittmann L, Min-Weißenhorn SJ, Reichel CA, Scheiermann C, Sperandio M and Moser M (2021) Binding of Rap1 and Riam to Talin1 Fine-Tune β2 Integrin Activity During Leukocyte Trafficking. Front. Immunol. 12:702345. doi: 10.3389/fimmu.2021.702345

β2 integrins mediate key processes during leukocyte trafficking. Upon leukocyte activation, the structurally bent β2 integrins change their conformation towards an extended, intermediate and eventually high affinity conformation, which mediate slow leukocyte rolling and firm arrest, respectively. Translocation of talin1 to integrin adhesion sites by interactions with the small GTPase Rap1 and the Rap1 effector Riam precede these processes. Using Rap1 binding mutant talin1 and Riam deficient mice we show a strong Riam-dependent T cell homing process to lymph nodes in adoptive transfer experiments and by intravital microscopy. Moreover, neutrophils from compound mutant mice exhibit strongly increased rolling velocities to inflamed cremaster muscle venules compared to single mutants. Using Hoxb8 cell derived neutrophils generated from the mutant mouse strains, we show that both pathways regulate leukocyte rolling and adhesion synergistically by inducing conformational changes of the β2 integrin ectodomain. Importantly, a simultaneous loss of both pathways results in a rolling phenotype similar to talin1 deficient neutrophils suggesting that β2 integrin regulation primarily occurs *via* these two pathways.

Keywords: talin, Riam, Rap1, leukocyte adhesion, leukocyte rolling, integrin activation, leukocyte trafficking

INTRODUCTION

Trafficking of neutrophils to sites of inflammation as well as lymphocyte homing to various destinations are fundamental processes of the immune system to defend the host against invaders. In order to leave the blood system, leukocytes follow a defined series of steps, which allow them to transit from a flowing to an adherent state. The leukocyte adhesion cascade includes leukocyte rolling, arrest, crawling and transendothelial migration (1). Integrins, in particular members of the β2 integrin family, contribute to each of these processes upon activation, which may be triggered from surface proteins such as P-selectin glycoprotein ligand-1 (PSGL-1) or chemokine receptors (2–4). These signaling events induce a

conformational shift of the integrin´s ectodomain from a low towards an intermediate and eventually high ligand binding affinity, characterized by a bent and extended conformation with closed and open ligand binding pocket, respectively. While intermediate affinity integrin αLβ2 support slow leukocyte rolling, transition to the high affinity conformation is required for firm adhesion (3).

The thermodynamically unfavored extended β2 integrin conformations are stabilized by the binding of talin1 and kindlin-3 to the integrin´s cytoplasmic tail (5). Talin1 is a large cytoplasmic adapter protein, which consists of an N-terminal head domain comprising an atypical FERM domain and a long C-terminal rod domain. While the talin1 rod interacts with a variety of other adapter and signaling molecules as well as the actin cytoskeleton, talin head binding to the cytoplasmic tail of β integrin subunits is crucial for the induction of the active integrin conformations (6, 7). Cytoplasmic talin adopts an auto-inhibited conformation, which is stabilized by intra-molecular interactions between the talin head and rod domains. Therefore, membrane recruitment and release of auto-inhibition are prerequisites for talin1-mediated integrin activation (8–10).

The mechanism of talin recruitment has been in the focus of several recent studies, which led to the identification of different pathways. Interestingly, these pathways differ dependent on the cell type and integrin class. While a series of cell biological studies suggested that a ternary complex consisting of the small membrane-bound GTPase Rap1, its effector Riam and talin is necessary to recruit talin to the membrane (11–13), studies in Riam deficient mice revealed that this complex specifically regulates leukocyte β2 integrins but is not involved in the regulation of other integrin classes expressed in other cells such as platelets (14–16). More recently it has been shown that GTP-bound Rap1 directly binds to the talin head and this interaction is critical for platelet integrin activation (17–20). This pathway seems of general importance as it controls talin activity in the amoeba *Dictyostelium*, flies and mice (17, 21, 22). Mutation of the Rap1 binding site in the talin F0 domain impairs integrin-mediated functions of platelets and neutrophils both *in vitro* and *in vivo* (17, 19). Interestingly, recent studies showed that the F0 binding site synergizes with an additional Rap1 binding site in the structurally similar F1 domain and mutating both Rap1 binding domains causes an additive effect (23–25). It is also important to note that positively charged patches in the talin F2 and F3 domains together with a positively charged loop within the F1 domain interact with membrane lipids and contribute significantly to talin membrane targeting (23, 24, 26). While the Rap1/talin and talin/membrane interactions act synergistically on talin recruitment and integrin activation, mutations of the Riam binding sites in the talin R3 and R8 domains show no cooperative effect on integrin activity and function in fibroblasts (23). So far it has not been analyzed whether and how the more general Rap1/talin and the specific Rap1/Riam/talin pathways cooperate in regulating β2 integrin activity.

In this study, we aimed to decipher the roles of Rap1/talin and Rap1/Riam/talin recruitment pathways in hematopoietic cells by comparing integrin activity and function in Rap1 binding deficient talin knock-in ($Tln1^{3mut}$), Riam deficient ($Riam^{-/-}$) and double mutant (DM; $Tln1^{3mut}/Riam^{-/-}$) mice. Our data clearly demonstrate that both pathways synergize to regulate integrin-mediated leukocyte rolling and adhesion by inducing conformational changes of the β2 integrin ectodomain. A simultaneous, genetic block of both pathways results in a phenotype similar to talin1-deficient neutrophils.

MATERIAL AND METHODS

Mice

$Talin^{3mut}$ and $Riam^{-/-}$ single mutant mice were described earlier (14, 17). $Talin^{3mut}/Riam^{-/-}$ double mutant (DM) mice were generated by mating these single mutant animals. Mice were housed under specific pathogen free conditions. All animal experiments were performed with approval of the District Government of Bavaria (Regierung von Oberbayern, Munich).

Generation, Culture, and Differentiation of Hoxb8-FL Cells

Hoxb8-FL cells were generated and cultured from bone marrow of WT, $Tln1^{3mut}$, $Riam^{-/-}$ and DM mice as described previously (27, 28).

Hoxb8-FL cells were allowed to differentiate towards neutrophils by keeping them in RPMI1640 supplemented with 10% FBS, penicillin/streptomycin, 2% SCF-containing supernatant, 50 μM β-mercaptoethanol, and 20 ng/ml rmG-CSF (PeproTech) for 4 d.

CRISPR/Cas9-Mediated Gene Ablation and Expression of Human Integrin β2

CRISPR/Cas9 target sequences were identified with help of the CHOPCHOP (version 3) web tool (29). Guide RNAs to these sequences (Integrin β2: GCGCAAUGUCACGAGGCUGC, Talin1: GGAUCCGCUCACGAAUCAUG) were purchased from Integrated DNA technologies (IDT, Leuven, Belgium). RNA/protein complexes were allowed to form by incubating sgRNAs with TrueCut Cas9 Protein v2 (Thermo Fisher Scientific) for 10 min at room temperature. Subsequently, Hoxb8 cells were electroporated in the presence of the RNP complex using the NEON transfection system (Thermo Fisher Scientific).

To obtain talin1 deficient cells, single cell clones of electroporated cells were generated by limited dilution. Subsequently, knockout clones were identified by PCR and sequencing of the product (forward primer: TTAAATAGGAC GGACAGCTTACT, reverse: CTTCACTGTGGCCAAACAGC) and confirmed by Western blotting.

Integrin β2 CRISPR-targeted cells were infected with a pMIGR retroviral vector containing human integrin β2 cDNA by spinoculation. Cells expressing human but not mouse β2 integrin were sorted using a FACSAria™ III sorter (BD Biosciences, Heidelberg, Germany).

Antibodies

The following antibodies were used for Western blot diluted in 5% milk/TBS-T: mouse anti-Talin (Sigma-Aldrich, Munich, Germany 1:20000), rabbit anti-Riam (Abcam, Berlin, Germany, 1:1000), rabbit anti-Rap1 (Santa Cruz Biotechnology, Heidelberg, Germany, 1:500), rabbit anti-Kindlin-3 (homemade (30); 1:3000), rabbit anti-Lamellipodin (kindly provided by Prof. Gertler, MIT, Cambridge, MA), mouse anti-GAPDH (Merck Millipore, 1:20000), goat anti-mouse-HRP and goat anti-rabbit-HRP (Jackson ImmunoResearch Laboratories, Cambridge, UK 1:15000).

The following antibodies were used at a 1:200 dilution for FACS analysis to determine surface expression levels of relevant integrins and other receptors: hamster anti-mouse CD29-Alexa Fluor 647, rat anti-mouse CD18-APC, hamster anti-mouse CD61-Alexa Fluor 647, rat anti-mouse CD49d-Alexa Fluor 647, rat anti-mouse CD49e-Alexa Fluor 647, rat anti-mouse CD11a-APC, rat anti-mouse CD11b-APC, rat anti-mouse PSGL-1-BV421 (all BD Biosciences), hamster anti-mouse CD49b, rat anti-mouse CD41-PE, rat anti-mouse Gr-1-FITC (Thermo Fisher Scientific), rat anti-human CD18-APC (Biolegend, London, UK).

Isolation of Primary Neutrophils

Neutrophils were isolated from bone marrow using an EasySep Mouse Neutrophil Enrichment Kit (STEMCELL Technologies, Cologne, Germany) following the manufacturer's instructions.

Neutrophil Static Adhesion and Flow Chambers

Neutrophil static adhesion assays were performed with Hoxb8-derived neutrophils as previously described (17) after pre-incubating differentiated cells with 10 mM EDTA for 15 min.

Neutrophil adhesion under flow conditions was assessed in ibidi slides VI 0.1 (Ibidi, Martinsried, Germany) coated with rmP-Selectin (His-tag; R&D systems, Abingdon, UK) and Mouse soluble ICAM-1 (STEMCELL Technologies) with or without rmKC (R&D systems) in coating buffer (20 mM Tris-HCl pH 9.0, 150 mM NaCl, 2 mM $MgCl_2$) over night. Neutrophil suspensions of $0.75x10^6$ cells/ml density were perfused through flow chambers at a wall shear stress of 0.3 or 1 dyne/cm^2 for 10 min using a PHD ULTRA pump (Harvard Apparatus, Holliston, MA, USA). Movies of 10 s were recorded from five different fields of view within the last minute of perfusion using the Evos M7000 life cell imaging system (Thermo Fisher Scientific). ImageJ software was used to analyze velocities of rolling cells as well as the number of adherent cells.

β2 Integrin Activation Assay

Human β2 integrin expressing Hoxb8 cells were differentiated to neutrophils. Before addition of the reporter antibodies, cells were treated with 10 mM EDTA for 15 min. Stainings with conformation specific antibodies mAb24 and KIM127 were performed in RPMI adhesion medium (RPMI1640 containing 0.1% FBS, penicillin/streptomycin, 50 μM β-mercaptoethanol, 1 μM β-estradiol). Neutrophils were either left untreated or treated with 10 mM EDTA, 0.2 μg/ml TNFα, 10 μM fMLP, 1μg/ml CXCL1 or 1μg/ml PMA and stained with Alexa Fluor 647-labeled mouse anti-human extended conformation specific antibody KIM127 or BV421 conjugated mouse anti-human active conformation specific antibody mAb24 (Biolegend) for 30 min at 37°C. Staining intensities were acquired using a Cytoflex LX flow cytometer (Beckman Coulter, Krefeld, Germany). EDTA values were set to 0 and all data were normalized to total human integrin β2 intensities.

KIM127 antibody was labeled using the Alexa Fluor 647 antibody labeling kit (Thermo Fisher Scientific) following the manufacturer's instructions.

Platelet Integrin Activation, Aggregation, Spreading, and Microvascular Thrombosis

Platelet integrin activation, aggregation and spreading were assessed as previously described (17). The following agonists were used for these assays: Chrono-Par-Thrombin, Chrono-Par-ADP, Chrono-Par-Collagen (Probe & go Labordiagnostica GmbH, Lemgo, Germany), U46619 (Enzo Life Sciences GmbH, Lörrach, Germany) and Collagen-related peptide (CRP; kindly provided by Prof. Siess, LMU, Munich). Intravital microscopy of the cremaster to measure thrombus formation after photochemical injury *in vivo* was performed as described earlier (17, 31, 32).

Neutrophil Trafficking *In Vivo*

Neutrophil rolling, adhesion and extravasation *in vivo* was analyzed by intravital microscopy and subsequent histological analysis of TNF-α-stimulated cremaster muscle venules as previously described (17).

T Cell Homing FACS Assay and *In Vivo* Imaging

T cell homing was assessed by adoptive transfer experiments and subsequent FACS analysis as previously described (14).

For *in vivo* imaging of T cell trafficking to the lymph node $CD4^+$ T cells were enriched from spleens by negative selection. Briefly, spleens were incubated with biotinylated antibodies to Gr-1, B220, CD8, Ter-119 and F4/80 and subsequently with anti-biotin microbeads (Miltenyi Biotec, Bergisch Gladbach, Germany). Antibody bound cells were depleted using MS columns placed in a MidiMACS Separator (Miltenyi Biotec). Mice were injected intravenously with a 1:1 mixture of CFSE and Far Red labelled WT and $Tln1^{3mut}$, $Riam^{-/-}$ or DM cells. Preparation and imaging of the popliteal lymph node vasculature and data analysis were performed as described earlier (33).

Statistical Analysis

Data are presented as mean ± 95% confidence interval. ANOVA followed by Tukey's multiple comparison test was performed to determine statistical significance for comparison of data sets using Prism9 (GraphPad Software). Differences between groups were considered statistically significant if $p<0.05$.

RESULTS

To assess a potential cooperative function of the direct Rap1/talin and the Rap1/Riam/talin pathways on integrin regulation in

hematopoietic cells *in vivo*, we crossed Rap1 binding-deficient talin knock-in ($Tln1^{3mut}$) and Riam-deficient ($Riam^{-/-}$) mouse lines (14, 17) to generate $Tln1^{3mut}/Riam^{-/-}$ DM mice. These compound mutant mice are born at normal Mendelian ratio, are viable and exhibit no overt phenotype, similar to the single mutant mouse strains. An analysis of their peripheral blood revealed comparable cell counts between WT and $Tln1^{3mut}$ mice, whereas leukocyte numbers were strongly increased in $Riam^{-/-}$ mice and tended to be even higher in DM mice (**Table S1**).

Even though previous studies revealed that Riam is dispensable for platelet integrin activation and function (14, 15, 19), we wondered whether the mild integrin defect of $Tln1^{3mut}$ platelets is due to some functional rescue by the Riam pathway (17). Before we addressed this experimentally, we first showed comparable expression of talin, Rap1 and kindlin-3 in platelets from WT, $Tln1^{3mut}$, $Riam^{-/-}$ and DM mice by Western blot analyses, and confirmed lack of RIAM expression in $Riam^{-/-}$ and DM platelets (**Figure S1A**). In addition, flow cytometric analyses indicated similar integrin surface levels between wildtype and mutant platelets (**Figure S1B**). We then performed functional assays and analyzed αIIbβ3 integrin activity by conformation specific antibody (JON/A) and fibrinogen binding, agonist-induced platelet aggregation and platelet spreading on fibrinogen upon thrombin stimulation (**Figures S1C–F**). In sum, these experiments confirmed that Riam is not involved in the regulation of platelet integrins, which is also corroborated by the similar defects measured in DM and $Tln1^{3mut}$ platelets. Even *in vivo* microvascular thrombosis assays in cremaster venules and arterioles revealed a similar delay in thrombus formation in response to photochemical injury in $Tln1^{3mut}$ and DM mice, whereas no defect was measured in $Riam^{-/-}$ mice (**Figures S1G, H**). Altogether, our data corroborated the dispensable role of Riam and showed no synergistic action of the Rap1/talin and Rap1/Riam/talin pathways on talin-mediated platelet integrin regulation.

In contrast to the negligible role of Riam for platelet integrin regulation, the leukocyte specific β2 integrin family critically depends on Riam (14, 15). We have also shown previously that this integrin class is regulated *via* the direct Rap1/talin pathway (17). To investigate, whether the two talin recruitment pathways synergize to fine-tune leukocyte integrin activity, we used T cell homing into the lymph node as model, since this process, as we have previously reported, is β2 integrin and RIAM dependent (14). First, we determined lymph node cellularity of the different mouse lines under steady state conditions and found similar numbers in WT and $Tln1^{3mut}$ mice. In line with the crucial role of Riam for β2 integrin function we measured a reduced lymph node cellularity in $Riam^{-/-}$ mice, which was somewhat enhanced in DM mice. At the same time, we counted slightly increased numbers of splenocytes in Riam and DM mice, whereas thymus cellularity was unchanged in all four mouse lines (**Figure 1A**). To investigate, whether defective T cell homing contributes to the reduction in lymph node cellularity, we performed adoptive transfer experiments. Upon injection of a 1:1 mixture of CFSE-stained WT and FarRed-stained WT, $Tln1^{3mut}$, $Riam^{-/-}$ or DM splenocytes (dyes were switched between experiments) into WT recipient mice, we found a reduction in lymph node homing capacity for $Riam^{-/-}$ and DM $CD4^+$ T cells, which was most pronounced for DM cells (**Figures 1B, C**). Consistent with their reduced homing capacity, we detected an increased number of $Riam^{-/-}$ and DM $CD4^+$ T cells in the blood and spleen of the recipient animals, with highest numbers found in DM mice (**Figure 1C**). In a parallel experiment, we directly monitored lymphocyte homing into popliteal lymph nodes by intravital microscopy. Therefore, we isolated splenic $CD4^+$ T cells from WT and mutant mice, stained them with either CFSE or FarRed and injected a 1:1 mixture into WT recipient mice. The number of adherent cells in relation to the vascular surface area was then determined within the lymph node by intravital imaging (**Figure 1D**). This experiment revealed that less $Riam^{-/-}$ and DM T cells adhered to the lymph node vasculature compared to WT and $Tln1^{3mut}$ T cells (**Figures 1E, F**). In sum, these data suggest a dominant role of the Rap1/Riam/talin pathway in the regulation of T cell adhesion to the vasculature during lymph node homing. Even though no significant difference in T cell homing to the lymph nodes was measured between $Riam^{-/-}$ and DM T cells, the DM T cells consistently showed the strongest defects in both experiments.

We next chose another primarily β2 integrin dependent process to study the significance and relative impact of the Rap1/Talin and Rap1/RIAM/Talin pathways for leukocyte trafficking. Intravital microscopy of the inflamed mouse cremaster muscle represents an excellent method to investigate the different steps of the leukocyte adhesion cascade, such as leukocyte rolling, adhesion and extravasation. In accordance with our previous studies on $Tln1^{3mut}$ and $Riam^{-/-}$ mice (14, 17), $Tln1^{3mut}$ mice showed reduced numbers of adherent and perivascular cells, while their neutrophil rolling velocities were hardly affected (**Figures 2A–E**, **Videos S1–4**). $Riam^{-/-}$ neutrophils showed strongly reduced adhesion and extravasation (**Figures 2A–E**, **Videos S1–4**). This severe phenotype was not further aggravated in DM mice. As the extravasation efficiency is not significantly reduced between the groups, we conclude that the reduced number of extravasated cells is primarily caused by their defective adhesion (**Figure 2D**). However, the already strongly increased rolling velocity of $RIAM^{-/-}$ neutrophils was additionally markedly increased in DM animals (**Figure 2A**). Of note, talin1, kindlin-3 and Rap1 expression (**Figure 2F**) as well as surface levels of relevant integrins, L-selectin and PSGL-1 (**Figure 2G**) were comparable in neutrophils derived from mice of all four genotypes. These *in vivo* studies suggest that loss of either Rap1/talin or Rap1/Riam/talin pathway impaired leukocyte adhesion and extravasation and that a combined loss of both talin recruitment pathways drastically affects integrin-mediated leukocyte rolling.

In order to decipher the molecular roles of the two talin recruitment pathways in an *in vitro* cell culture system, we generated Hoxb8 cells from the four mouse strains. Hoxb8 cells are immortalized hematopoietic progenitor cells generated from murine bone marrow by expression of a retrovirally-delivered estrogen-regulated form of the transcription factor Hoxb8. Notably, in the presence of Flt3L these cells retain the

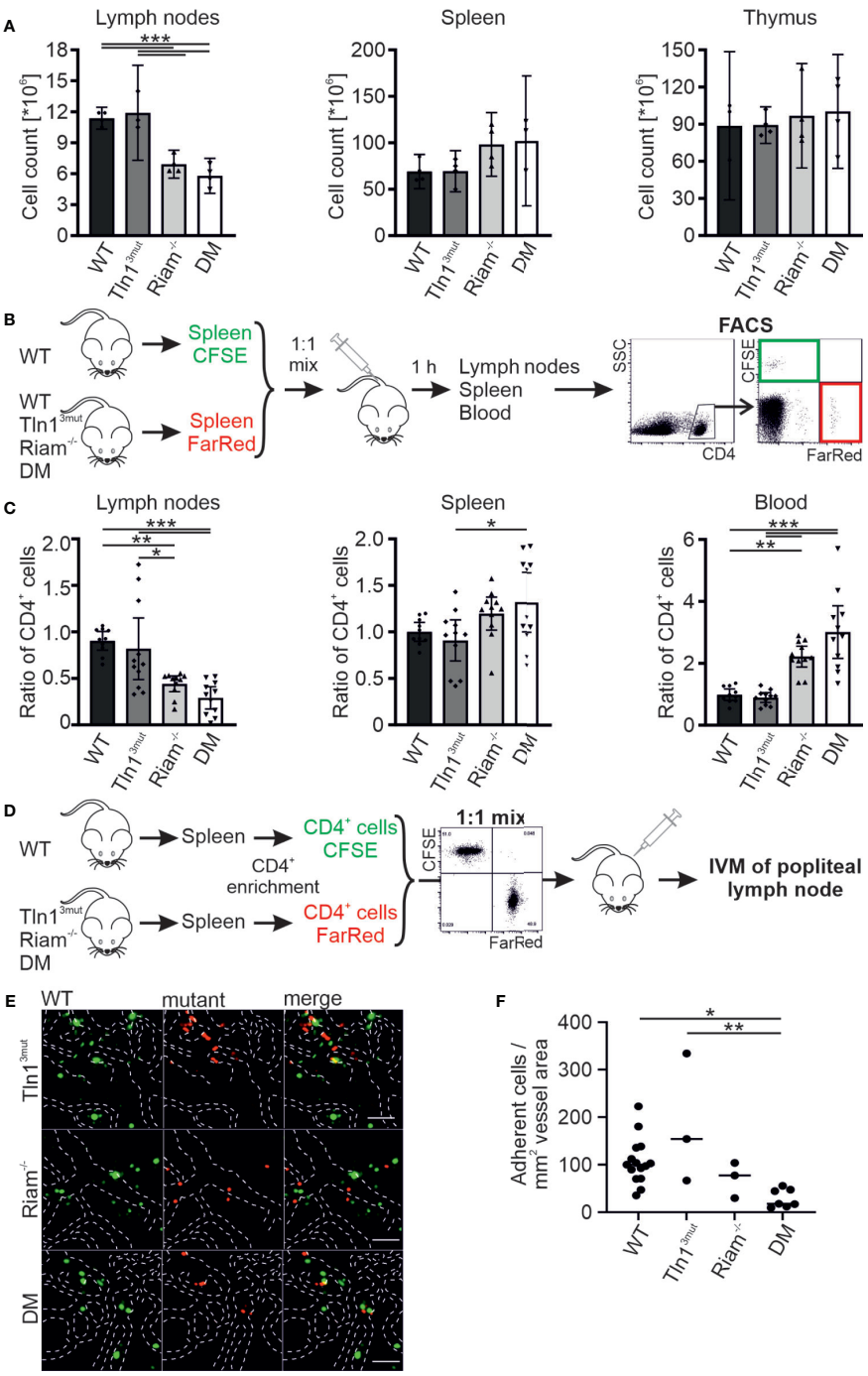

FIGURE 1 | The Rap1/talin and Rap1/Riam/talin pathways regulate T cell homing *in vivo*. **(A)** Cellularity of lymph nodes, spleens and thymi isolated from WT, Tln1^{3mut}, Riam$^{-/-}$ and DM mice (N = 4 mice). **(B, C)** T cell lymph node homing assessed in adoptive transfer experiments. A 1:1 mixture of CFSE-stained WT control and FarRed-stained WT, Tln1^{3mut}, Riam$^{-/-}$ or DM splenocytes (or swapped dyes) was injected into the tail vein of WT recipients. Ratios of CFSE and FarRed-stained CD4$^+$ cells in different organs were measured 1 h after injection by FACS analysis. **(C)** Ratios of transferred WT, Tln1^{3mut}, Riam$^{-/-}$ and DM to control cells obtained in lymph nodes, spleen and blood of recipient animals (N = 10/11/11/11). **(D–F)** Adhesion of CD4$^+$ T cells assessed *in vivo* by confocal intravital microscopy of the lymph node vasculature after adoptive transfer. **(D)** Schematic overview of the experiment. Recipient animals were injected with a 1:1 mix of CFSE stained WT and FarRed stained Tln1^{3mut}, Riam$^{-/-}$ or DM pre-enriched CD4$^+$ T cells (or swapped dyes) and subjected to intravital microscopy. **(E)** Exemplary confocal images of WT (green) and Tln1^{3mut}, Riam$^{-/-}$ or DM (red) cells in the popliteal lymph node vasculature. Blood vessel borders are highlighted by dashed white lines, scale bars: 50 µm. **(F)** Number of adherent cells normalized by the blood vessel surface area (N=12/3/3/6). All values are given as mean ± 95% confidence interval. Statistical significance was assessed using One-way ANOVA followed by Tukey's multiple comparison test. *p < 0.05, **p < 0.01, ***p < 0.001.

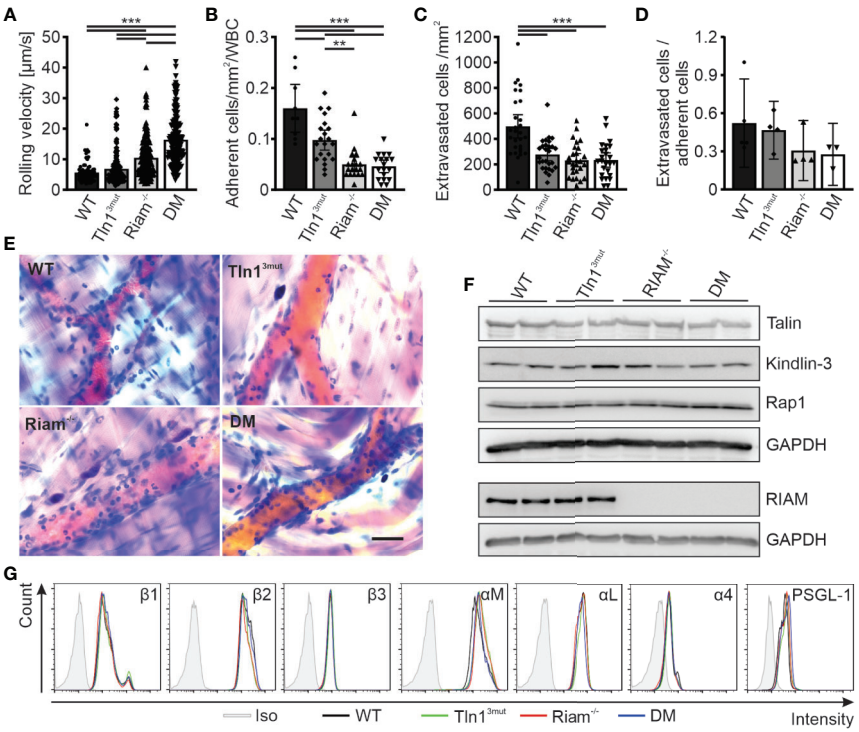

FIGURE 2 | Neutrophil rolling, adhesion and extravasation are impaired when the Rap1/talin and Rap1/Riam/talin pathways are blocked. **(A–E)** *In vivo* leukocyte rolling velocity **(A)**, adhesion efficiency **(B)**, extravasation **(C)** and extravasation efficiency **(D)** analyzed in cremaster muscle venules of WT, Tln1^{3mut}, Riam$^{-/-}$ and DM mice 2 h after intrascrotal TNFα injection. Rolling velocity and adhesion efficiency were assessed using intravital microscopy. Extravasation was analyzed by counting the number of perivascular cells in Giemsa stained cremaster muscle whole mounts (N = 3-6 vessels per mouse in 2/4/4/4 mice, 5/4/4/4 mice for **D**). **(E)** Representative images of Giemsa stained cremaster muscle whole mounts, scale bar: 30 µm. **(F)** Analysis of talin, kindlin-3, Rap1 and Riam expression in WT, Tln1^{3mut}, Riam$^{-/-}$ and DM neutrophils by western blot. GAPDH was used as loading control. **(G)** Integrin β1, β2, β3, αM, αL and α4 as well as PSGL-1 and L-Selectin surface levels on WT, Tln1^{3mut}, Riam$^{-/-}$ and DM neutrophils assessed by FACS analysis. Values represent mean ± 95% confidence interval. Statistical significance was assessed using One-way ANOVA followed by Tukey's multiple comparison test. **p < 0.01, ***p < 0.001.

capacity to differentiate into myeloid and lymphoid cells *in vitro*, which resemble phenotypically and functionally their primary counterparts (27). WT, Tln1^{3mut}, Riam$^{-/-}$ and DM Hoxb8 cells were differentiated into neutrophil-like cells by adding SCF and G-CSF to the culture medium and used for the ensuing assays. These neutrophil-like cells were comparable with regard to their talin1, kindlin-3, Riam and Rap1 protein levels as well as their surface levels of integrin subunits β2, αM, αL, and Gr-1 and PSGL-1 (**Figures 3A, B**). Moreover, the expression of the second mammalian MRL protein family member lamellipodin was not upregulated in response to Riam deficiency (**Figure 3C**). First, we performed static adhesion assays on the β2 integrin ligand ICAM-1, which showed significantly reduced adhesion of Tln1^{3mut} neutrophil-like cells in response to TNF-α and PMA, similar to the reported adhesion defect of primary Tln1^{3mut} neutrophils (17), and almost complete loss of adhesion of Riam$^{-/-}$ and DM cells (**Figure 3D**). Next, we studied cell adhesion under flow in P-selectin, ICAM-1 and CXCL1 coated flow chambers. Consistent with our previous experiments with primary Tln1^{3mut} and Riam$^{-/-}$ neutrophils (14, 17), we measured a mild adhesion defect of Tln1^{3mut} Hoxb8-derived neutrophils compared to an almost complete loss of adhesion of Riam$^{-/-}$ and DM neutrophils at a wall shear stress of 1 dyne/cm^2. Of note, adherent cells were hardly observed for all genotypes on surfaces coated with P-selectin and ICAM-1 only, which indicates that leukocyte adhesion is triggered by chemokine induced integrin inside-out activation (**Figure 3E**). To test, whether neutrophil adhesion can occur in the absence of the Rap1/Riam/talin pathway under low flow conditions, we compared WT, Tln1^{3mut}, Riam$^{-/-}$ and DM Hoxb8-derived neutrophils in flow chamber experiments at a shear rate of 0.3 dyne/cm^2. This experiment revealed indeed that in the absence of Riam some neutrophils adhered to the flow chambers, which became significantly less when the Rap1/talin pathway was additionally impaired (**Figure 3F**). In other words, the Rap1/talin pathway is sufficient to induce cell adhesion at least under low flow. This result further strengthened our *in vivo* findings that both pathways significantly contribute to talin-induced integrin-mediated leukocyte adhesion.

We then analyzed rolling of Hoxb8-derived neutrophils in P-selectin, ICAM1, CXCL1 coated flow chambers. While most leukocyte rolling is mediated *via* selectins, interactions of integrins with their ligands support leukocyte rolling and further decelerate their rolling velocity (integrin-mediated slow rolling) (2, 4, 34).

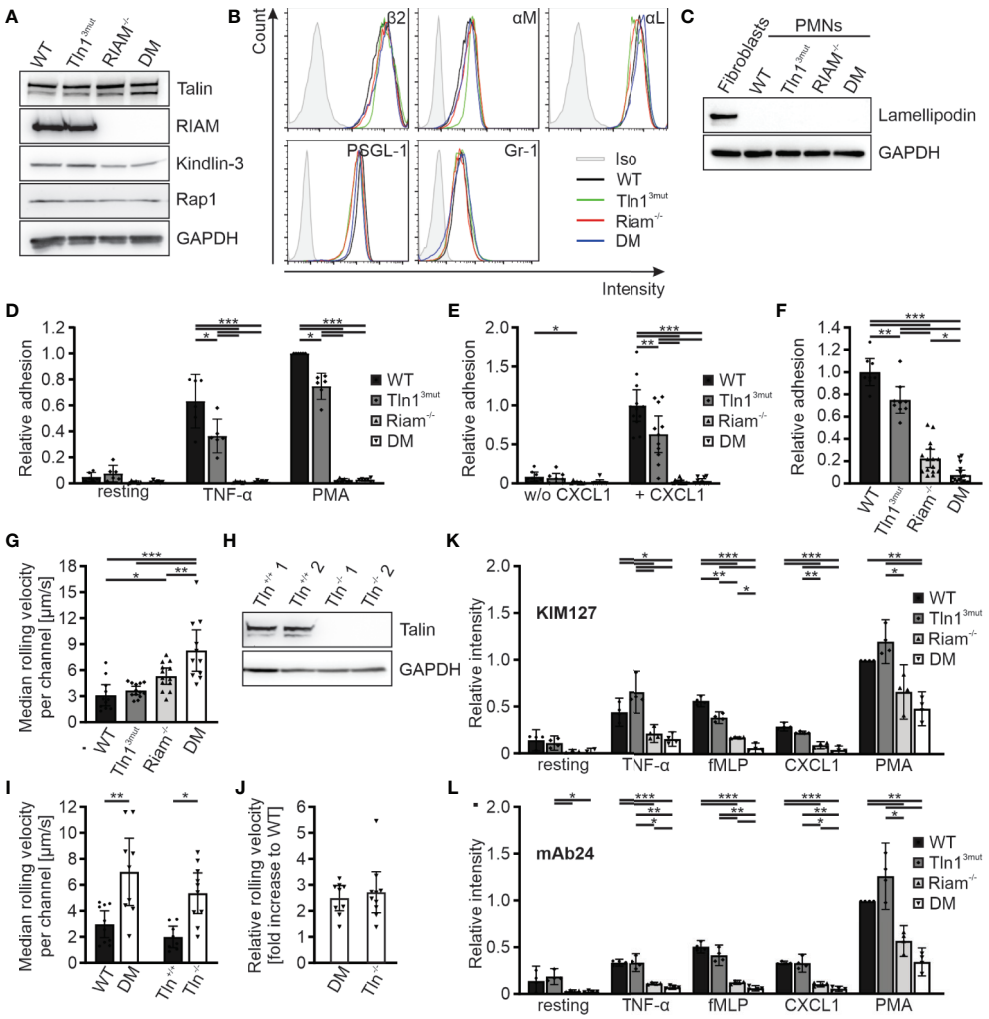

FIGURE 3 | Reduced integrin activity and function in Hoxb8 cell-derived Tln^{3mut}, Riam$^{-/-}$ and DM neutrophils. **(A)** Western blots showing Talin, Riam, kindlin-3 and Rap1 expression in Hoxb8 cells derived from WT, Tln1^{3mut}, Riam$^{-/-}$ and DM mice. GAPDH served as loading control. **(B)** FACS histograms showing surface levels of the integrin subunits β2, αM and αL as well as PSGL-1 and Gr-1 of WT (black), Tln1^{3mut} (green), Riam$^{-/-}$ (red) and DM (blue) Hoxb8-derived neutrophils. **(C)** Expression of lamellipodin in Hoxb8-derived neutrophils assessed by Western blot. Mouse embryonic fibroblast lysate served as positive control, GAPDH as loading control. **(D)** Relative adhesion of WT, Tln1^{3mut}, Riam$^{-/-}$ and DM Hoxb8-derived neutrophils on ICAM-1 either unstimulated (resting) or upon stimulation with TNFα or PMA under static conditions (N = 6). **(E–G)** Rolling and adhesion behavior of WT, Tln1^{3mut}, Riam$^{-/-}$ and DM Hoxb8-derived neutrophils assessed in flow chamber experiments. **(E)** Relative adhesion under flow at a wall shear rate of 1 dyne/cm^2 on P-selectin and ICAM-1 (N = 8 chambers in 4 experiments) or P-selectin, ICAM-1 and CXCL1 coated surfaces (N = 12/11/12/10 chambers in 4 experiments). **(F)** Relative adhesion under flow at a wall shear rate of 0.3 dyne/cm^2 on P-selectin, ICAM and CXCL1 coated surfaces: WT values are set to 1 (N = 8/9/15/16 chambers in 3 experiments). **(G)** Rolling velocities of Hoxb8-derived neutrophils at a shear rate of 1 dyne/cm^2 (N = 11/13/13/11 chambers in 4 experiments). **(H)** Western blot analysis of Talin and GAPDH expression in Tln1$^{+/+}$ and Tln1$^{-/-}$ Hoxb8 clones. **(I, J)** Median rolling velocities of WT and DM as well as Tln1$^{+/+}$ and Tln1$^{-/-}$ Hoxb8-derived neutrophils assessed in P-selectin, ICAM-1 and CXCL1 coated flow chambers under 1 dyne/cm^2 shear stress. Results are shown as absolute values **(I)** and fold rolling velocity increase of DM and Tln$^{-/-}$ cells to respective WT controls **(J)**. Two Tln1$^{+/+}$ and Tln1$^{-/-}$ clones were analyzed (N = 10/9/8/10 chambers in 2 experiments). **(K, L)** FACS analyses of integrin β2 activation by measuring staining intensities of conformation specific antibodies KIM127 **(K)** and mAb24 **(L)** normalized to total integrin β2 levels on Hoxb8-derived neutrophils expressing human β2 integrin either in resting state or in response to TNF-α, fMLP, CXCL1 or PMA. Values of PMA-stimulated WT cells were set to 1 (N = 4 experiments). All values represent mean ± 95% confidence interval. Statistical significance was assessed using ANOVA followed by Tukey's multiple comparison test. *p < 0.05, **p < 0.01, ***p < 0.001.

Consistent with the *in vivo* studies in the cremaster muscle (**Figure 2A**), rolling velocities were significantly increased in Riam$^{-/-}$ cells and considerably higher in DM neutrophils, which clearly indicate a synergistic effect of both talin recruitment pathways on integrin-mediated leukocyte rolling (**Figure 3G**). Since we have previously shown that talin-deficient neutrophils roll faster than Riam knockout neutrophils (14), we wondered whether a concurrent loss of both talin recruitment pathways will recapitulate a talin-knockout phenotype. Thus, we generated talin1 deficient Hoxb8 clones (Tln1$^{-/-}$) using the CRISPR/Cas9 technique and confirmed talin1 deficiency by Western blot analysis (**Figure 3H**). We then differentiated WT and DM Hoxb8 cells as

well as two Tln1$^{-/-}$ and two equally treated, but non-targeted WT clones (Tln$^{+/+}$) into neutrophils, and assessed their rolling velocities in flow chamber experiments. Strikingly, the median rolling velocities of DM and Tln1$^{-/-}$ neutrophils are similarly (~2.5-fold) increased compared to their respective control cells (**Figures 3I, J**). These experiments strongly suggest that the Rap1/talin and the Rap1/Riam/talin pathways are the key talin recruitment pathways involved in the induction of β2 integrin-mediated leukocyte rolling.

Integrin-mediated slow rolling and firm adhesion are conveyed by the intermediate-affinity extended-closed conformation and the high-affinity, extended-open conformation, respectively. We finally wanted to clarify, whether stimulation of the two talin recruitment pathways translates into conformational changes of the integrin ectodomain. However, as conformation specific antibodies exist only for human but not mouse β2 integrins, we induced a β2 integrin knock-out in WT, Tln1^{3mut}, Riam$^{-/-}$ and DM Hoxb8 cells using the CRISPR/Cas9 technology and reconstituted the cells with the human β2 integrin ortholog by retroviral transduction. These humanized Hoxb8 cells were then differentiated into neutrophils, stimulated with TNF-α, fMLP, CXCL1 and PMA and stained with the extended conformation specific antibody clone KIM127 (**Figure 3K**) or high-affinity conformation specific antibody clone mAb24 (**Figure 3L**). These experiments revealed a strong reduction in KIM127 and mAb24 binding to activated Riam$^{-/-}$ cells, which was further reduced in DM cells (**Figures 3K, L**). In sum, these data indicate that the two pathways converge in triggering conformational changes of the integrin towards an active conformation.

DISCUSSION

The recruitment of cytoplasmic talin to the plasma membrane represents an essential and complex process during integrin activation, which apparently proceeds in different ways dependent on cell type and integrin involved. For example, we recently showed that in fibroblasts the direct Rap1/talin pathway plays a central role in the regulation of integrin activation, whereas the talin/Riam interaction is irrelevant in these cells (23). Similarly, in platelets, the Rap1/talin pathway is dominant and regulates integrin activation through cooperative binding of Rap1 to the F0 and F1 domains of talin (24, 25). In this study, we corroborated a recent study showing that Riam is not involved in platelet integrin regulation. However, this work used a Rap1 binding mutant that still allowed weak binding of Rap1 to the talin F0 domain (17, 19).

In our current study, we mainly focused on leukocyte β2 integrins. Here we wanted to address the question whether talin recruitment to the plasma membrane during β2 integrin activation (inside-out signaling) can occur in the absence of Riam and whether the direct Rap1/talin pathway also contributes. This question arises, because β2 integrin function of Riam knockout mice is almost completely abolished similar as in the absence of talin. On the other hand, Rap1/talin binding mutants show a weak β2 integrin defect. Indeed, our studies show that Riam plays a dominant role in controlling β2 integrin function and loss of Riam results in a strong defect in leukocyte adhesion and extravasation and results in strongly impaired lymphocyte homing *in vivo*. Interestingly, this defect is further exacerbated by a loss of Rap1/talin interaction, which is reflected by a markedly increased leukocyte rolling velocity *in vivo* and further reduced leukocyte adhesion in *in vitro* flow chamber experiments of DM cells. This clearly indicates a synergy of both pathways in the regulation of β2 integrins. Why Riam primarily regulates the activity of β2 integrins and not, for example, integrins of fibroblasts or platelets, may be due only in part to the low expression of Riam in these cells, but more likely to the formation of a Riam-dependent β2 integrin-specific activation complex that is only formed in certain hematopoietic cells. This hypothesis is also supported by the fact that in the absence of Riam, β2 integrins on regulatory T cells can be activated by the Riam paralogue lamellipodin, which is highly expressed in these cells (35). In contrast, the Rap1/talin pathway appears to be a general mechanism for the regulation of all integrin classes, as reflected by studies in various model organisms and cell types such as *Dictyostelium*, fly, mouse, platelets, fibroblasts and leukocytes (17, 19, 21, 22). Apparently, two Rap1-mediated pathways with different direct effectors, Riam and Talin, have been established to control integrin activity: The Rap1/talin pathway that applies equally to all integrin classes independent of the cell type and the Rap1/Riam/talin pathway that is specific to β2 integrins. While the two pathways differ mechanistically in that the Riam N-terminus binds to the talin F3 and multiple sites of the talin rod and Rap1 binds directly to the talin F0 and F1 domains, ultimately both pathways lead to the recruitment of talin to the plasma membrane.

While the effect of the Rap1/talin pathway is relatively weak on β2 integrin-mediated adhesion, we found a strong impact on integrin-mediated rolling in DM cells, which requires integrin ectodomain extension adopting an intermediate ligand affinity conformation that transiently interacts with ligands on the vascular surface. That this process is possible when either pathway is blocked but results in a rolling defect similar to that seen in talin-null cells when both pathways are blocked, suggests that both pathways are used for the initial recruitment of talin to the membrane and induction of the extended conformation. Firm anchoring of the cells to the vascular wall or flow chamber surface, on the other hand, mainly relies on the Riam-dependent pathway, whereas the Rap1/talin pathway only allows adhesion at low shear forces. So, what distinguishes the two pathways and why does β2 integrin function strongly depend on the Rap1/Riam/talin pathway while other integrins do not? An explanation could be that the Rap1/talin pathway only contributes to talin activation by recruiting it to the plasma membrane, while the Rap1/Riam/talin pathway plays a dual role. Riam recruits talin to the membrane by interacting with the R3 domain and displaces autoinhibitory talin head-rod interactions by interacting with the F3 domain (36). Although talin recruitment to the plasma membrane through both pathways indirectly facilitates conformational activation of talin through attractive and repulsive interactions of the talin head and rod domains with negatively charged membrane lipids *via* a pull-push mechanism (37), the release of talin autoinhibition by Riam may be particularly important for efficient β2 integrin activation. Moreover, firm cell adhesion requires linkage of integrins to the actin cytoskeleton, which could either indirectly occur *via* subsequent exchange of Riam with vinculin upon talin

recruitment or directly *via* the C-terminal ENA/Vasp binding sites of Riam. The ability of this complex to promote the formation of cell protrusions and targeting of integrins to their tips might be a further explanation for the dominant role of Riam during leukocyte adhesion (11, 38–40).

It is important to note that the rather weak defects in rolling, adhesion and extravasation observed in Tln^{3mut} mice and Hoxb8-cells arise from an incomplete block of Rap1-binding, as only the Rap1-binding site within talin F0 domain was mutated here. Interaction with the Rap1-binding site in the subsequent talin F1 domain, which acts synergistically with the binding site within the F0 domain, is therefore still possible. The importance of both binding sites together is highlighted by the relatively mild phenotypes of mice in which only one of the two Rap1 binding sites was mutated, while double mutants are early embryonic lethal (17, 19, 24, 25). Therefore, we potentially underestimate the influence of the Rap1/talin pathway in our study due to compensation by the second Rap1 binding site.

Overall, our study shows for the first time that a concerted action of the Rap1/talin and the Rap1/Riam/talin pathways efficiently recruits talin from the cytoplasm to β2 integrin adhesions during the initial step of β2 integrin inside-out signaling.

DATA AVAILABILITY STATEMENT

The raw data supporting the conclusions of this article will be made available by the authors, without undue reservation.

ETHICS STATEMENT

The animal study was reviewed and approved by District government of Upper Bavaria, Munich, Germany.

AUTHOR CONTRIBUTIONS

TB and MM conceived the study, designed experiments, interpreted data, and wrote the manuscript with contributions from all other authors. TB, SK, IR, JW, RP, LM, and MM performed and analyzed experiments. SM-W, CR, CS, and MS provided vital reagents and critical expertise. All authors contributed to the article and approved the submitted version.

FUNDING

This work was supported by the Deutsche Forschungsgemeinschaft (SFB914 TP A01, B01, B03, B09 and Z03), eRARE/BMBF to MM (LADOMICs consortium) and the Max Planck Society.

SUPPLEMENTARY MATERIAL

The Supplementary Material for this article can be found online at: https://www.frontiersin.org/articles/10.3389/fimmu.2021.702345/full#supplementary-material

REFERENCES

1. Ley K, Laudanna C, Cybulsky MI, Nourshargh S. Getting to the Site of Inflammation: The Leukocyte Adhesion Cascade Updated. *Nat Rev Immunol* (2007) 7(9):678–89. doi: 10.1038/nri2156
2. Kuwano Y, Spelten O, Zhang H, Ley K, Zarbock A. Rolling on E- or P-Selectin Induces the Extended But Not High-Affinity Conformation of LFA-1 in Neutrophils. *Blood* (2010) 116(4):617–24. doi: 10.1182/blood-2010-01-266122
3. Lefort CT, Rossaint J, Moser M, Petrich BG, Zarbock A, Monkley SJ, et al. Distinct Roles for Talin-1 and Kindlin-3 in LFA-1 Extension and Affinity Regulation. *Blood* (2012) 119(18):4275–82. doi: 10.1182/blood-2011-08-373118
4. Zarbock A, Lowell CA, Ley K. Spleen Tyrosine Kinase Syk is Necessary for E-Selectin-Induced Alpha(L)Beta 2 Integrin-Mediated Rolling on Intercellular Adhesion Molecule-1. *Immunity* (2007) 26(6):773–83. doi: 10.1016/j.immuni.2007.04.011
5. Moser M, Legate KR, Zent R, Fassler R. The Tail of Integrins, Talin, and Kindlins. *Science* (2009) 324(5929):895–9. doi: 10.1126/science.1163865
6. Calderwood DA, Campbell ID, Critchley DR. Talins and Kindlins: Partners in Integrin-Mediated Adhesion. *Nat Rev Mol Cell Biol* (2013) 14(8):503–17. doi: 10.1038/nrm3624
7. Klapholz B, Brown NH. Talin - the Master of Integrin Adhesions. *J Cell Sci* (2017) 130(15):2435–46. doi: 10.1242/jcs.190991
8. Banno A, Goult BT, Lee H, Bate N, Critchley DR, Ginsberg MH. Subcellular Localization of Talin Is Regulated by Inter-Domain Interactions. *J Biol Chem* (2012) 287(17):13799–812. doi: 10.1074/jbc.M112.341214
9. Goult BT, Bate N, Anthis NJ, Wegener KL, Gingras AR, Patel B, et al. The Structure of an Interdomain Complex That Regulates Talin Activity. *J Biol Chem* (2009) 284(22):15097–106. doi: 10.1074/jbc.M900078200
10. Goult BT, Xu XP, Gingras AR, Swift M, Patel B, Bate N, et al. Structural Studies on Full-Length Talin1 Reveal a Compact Auto-Inhibited Dimer: Implications for Talin Activation. *J Struct Biol* (2013) 184(1):21–32. doi: 10.1016/j.jsb.2013.05.014
11. Lagarrigue F, Vikas Anekal P, Lee HS, Bachir AI, Ablack JN, Horwitz AF, et al. A RIAM/Lamellipodin-Talin-Integrin Complex Forms the Tip of Sticky Fingers That Guide Cell Migration. *Nat Commun* (2015) 6:8492. doi: 10.1038/ncomms9492
12. Han J, Lim CJ, Watanabe N, Soriani A, Ratnikov B, Calderwood DA, et al. Reconstructing and Deconstructing Agonist-Induced Activation of Integrin Alphaiibbeta3. *Curr Biol* (2006) 16(18):1796–806. doi: 10.1016/j.cub.2006.08.035
13. Lee HS, Lim CJ, Puzon-McLaughlin W, Shattil SJ, Ginsberg MH. RIAM Activates Integrins by Linking Talin to Ras Gtpase Membrane-Targeting Sequences. *J Biol Chem* (2009) 284(8):5119–27. doi: 10.1074/jbc.M807117200
14. Klapproth S, Sperandio M, Pinheiro EM, Prunster M, Soehnlein O, Gertler FB, et al. Loss of the Rap1 Effector RIAM Results in Leukocyte Adhesion Deficiency Due to Impaired Beta2 Integrin Function in Mice. *Blood* (2015) 126(25):2704–12. doi: 10.1182/blood-2015-05-647453
15. Stritt S, Wolf K, Lorenz V, Vogtle T, Gupta S, Bosl MR, et al. Rap1-GTP-Interacting Adaptor Molecule (RIAM) Is Dispensable for Platelet Integrin Activation and Function in Mice. *Blood* (2015) 125(2):219–22. doi: 10.1182/blood-2014-08-597542
16. Su W, Wynne J, Pinheiro EM, Strazza M, Mor A, Montenont E, et al. Rap1 and its Effector RIAM Are Required for Lymphocyte Trafficking. *Blood* (2015) 126(25):2695–703. doi: 10.1182/blood-2015-05-644104
17. Bromberger T, Klapproth S, Rohwedder I, Zhu L, Mittmann L, Reichel CA, et al. Direct Rap1/Talin1 Interaction Regulates Platelet and Neutrophil Integrin Activity in Mice. *Blood* (2018) 132(26):2754–62. doi: 10.1182/blood-2018-04-846766
18. Goult BT, Bouaouina M, Elliott PR, Bate N, Patel B, Gingras AR, et al. Structure of a Double Ubiquitin-Like Domain in the Talin Head: A Role in Integrin Activation. *EMBO J* (2010) 29(6):1069–80. doi: 10.1038/emboj.2010.4
19. Lagarrigue F, Gingras AR, Paul DS, Valadez AJ, Cuevas MN, Sun H, et al. Rap1 Binding to the Talin 1 F0 Domain Makes a Minimal Contribution to

Murine Platelet Gpiib-Iiia Activation. *Blood Adv* (2018) 2(18):2358–68. doi: 10.1182/bloodadvances.2018020487
20. Zhu L, Yang J, Bromberger T, Holly A, Lu F, Liu H, et al. Structure of Rap1b Bound to Talin Reveals a Pathway for Triggering Integrin Activation. *Nat Commun* (2017) 8(1):1744. doi: 10.1038/s41467-017-01822-8
21. Camp D, Haage A, Solianova V, Castle WM, Xu QA, Lostchuck E, et al. Direct Binding of Talin to Rap1 Is Required for Cell-ECM Adhesion in Drosophila. *J Cell Sci* (2018) 131(24):jcs225144. doi: 10.1242/jcs.225144
22. Plak K, Pots H, Van Haastert PJ, Kortholt A. Direct Interaction Between Talinb and Rap1 is Necessary for Adhesion of Dictyostelium Cells. *BMC Cell Biol* (2016) 17:1. doi: 10.1186/s12860-015-0078-0
23. Bromberger T, Zhu L, Klapproth S, Qin J, Moser M. Rap1 and Membrane Lipids Cooperatively Recruit Talin to Trigger Integrin Activation. *J Cell Sci* (2019) 132(21):jcs235531. doi: 10.1242/jcs.235531
24. Gingras AR, Lagarrigue F, Cuevas MN, Valadez AJ, Zorovich M, McLaughlin W, et al. Rap1 Binding and a Lipid-Dependent Helix in Talin F1 Domain Promote Integrin Activation in Tandem. *J Cell Biol* (2019) 218(6):1799–809. doi: 10.1083/jcb.201810061
25. Lagarrigue F, Paul DS, Gingras AR, Valadez AJ, Sun H, Lin J, et al. Talin-1 Is the Principal Platelet Rap1 Effector of Integrin Activation. *Blood* (2020) 136 (10):1180–90. doi: 10.1182/blood.2020005348
26. Chinthalapudi K, Rangarajan ES, Izard T. The Interaction of Talin With the Cell Membrane is Essential for Integrin Activation and Focal Adhesion Formation. *Proc Natl Acad Sci U S A* (2018) 115(41):10339–44. doi: 10.1073/pnas.1806275115
27. Redecke V, Wu RQ, Zhou JR, Finkelstein D, Chaturvedi V, High AA, et al. Hematopoietic Progenitor Cell Lines With Myeloid and Lymphoid Potential. *Nat Methods* (2013) 10(8):795–+. doi: 10.1038/nmeth.2510
28. Zehrer A, Pick R, Salvermoser M, Boda A, Miller M, Stark K, et al. A undamental Role of Myh9 for Neutrophil Migration in Innate Immunity. *J Immunol* (2018) 201(6):1748–64. doi: 10.4049/jimmunol.1701400
29. Labun K, Montague TG, Krause M, Cleuren YNT, Tjeldnes H, Valen E. CHOPCHOP V3: Expanding the CRISPR Web Toolbox Beyond Genome Editing. *Nucleic Acids Res* (2019) 47(W1):W171–4. doi: 10.1093/nar/gkz365
30. Ussar S, Wang HV, Linder S, Fassler R, Moser M. The Kindlins: Subcellular Localization and Expression During Murine Development. *Exp Cell Res* (2006) 312(16):3142–51. doi: 10.1016/j.yexcr.2006.06.030
31. Baez S. Open Cremaster Muscle Preparation for Study of Blood-Vessels by *In-Vivo* Microscopy. *Microvasc Res* (1973) 5(3):384–94. doi: 10.1016/0026-2862(73)90054-X
32. Rumbaut RE, Randhawa JK, Smith CW, Burns AR. Mouse Cremaster Venules are Predisposed to Light/Dye-Induced Thrombosis Independent of Wall Shear Rate, CD18, ICAM-1, or P-Selectin. *Microcirculation* (2004) 11 (3):239–47. doi: 10.1080/10739680490425949
33. Moretti FA, Klapproth S, Ruppert R, Margraf A, Weber J, Pick R, et al. Differential Requirement of Kindlin-3 for T Cell Progenitor Homing to the Non-Vascularized and Vascularized Thymus. *Elife* (2018) 7:e35816. doi: 10.7554/eLife.35816
34. Mueller H, Stadtmann A, Van Aken H, Hirsch E, Wang D, Ley K, et al. Tyrosine Kinase Btk Regulates E-Selectin-Mediated Integrin Activation and Neutrophil Recruitment by Controlling Phospholipase C (PLC) Gamma2 and PI3Kgamma Pathways. *Blood* (2010) 115(15):3118–27. doi: 10.1182/blood-2009-11-254185
35. Sun H, Lagarrigue F, Wang H, Fan ZC, Lopez-Ramirez MA, Chang JT, et al. Distinct Integrin Activation Pathways for Effector and Regulatory T Cell Trafficking and Function. *J Exp Med* (2021) 218(2):e20201524. doi: 10.1084/jem.20201524
36. Yang J, Zhu L, Zhang H, Hirbawi J, Fukuda K, Dwivedi P, et al. Conformational Activation of Talin by RIAM Triggers Integrin-Mediated Cell Adhesion. *Nat Commun* (2014) 5:5880. doi: 10.1038/ncomms6880
37. Song X, Yang J, Hirbawi J, Ye S, Perera HD, Goksoy E, et al. A Novel Membrane-Dependent on/Off Switch Mechanism of Talin FERM Domain at Sites of Cell Adhesion. *Cell Res* (2012) 22(11):1533–45. doi: 10.1038/cr.2012.97
38. Goult BT, Zacharchenko T, Bate N, Tsang R, Hey F, Gingras AR, et al. RIAM and Vinculin Binding to Talin are Mutually Exclusive and Regulate Adhesion Assembly and Turnover. *J Biol Chem* (2013) 288(12):8238–49. doi: 10.1074/jbc.M112.438119
39. Lee HS, Anekal P, Lim CJ, Liu CC, Ginsberg MH. Two Modes of Integrin Activation Form a Binary Molecular Switch in Adhesion Maturation. *Mol Biol Cell* (2013) 24(9):1354–62. doi: 10.1091/mbc.e12-09-0695
40. Lafuente EM, van Puijenbroek AA, Krause M, Carman CV, Freeman GJ, Berezovskaya A, et al. RIAM, an Ena/VASP and Profilin Ligand, Interacts With Rap1-GTP and Mediates Rap1-Induced Adhesion. *Dev Cell* (2004) 7 (4):585–95. doi: 10.1016/j.devcel.2004.07.021

Conflict of Interest: The authors declare that the research was conducted in the absence of any commercial or financial relationships that could be construed as a potential conflict of interest.

Publisher's Note: All claims expressed in this article are solely those of the authors and do not necessarily represent those of their affiliated organizations, or those of the publisher, the editors and the reviewers. Any product that may be evaluated in this article, or claim that may be made by its manufacturer, is not guaranteed or endorsed by the publisher.

frontiers in Immunology

MINI REVIEW
published: 10 September 2021
doi: 10.3389/fimmu.2021.734188

The Recruitment of Neutrophils to the Tumor Microenvironment Is Regulated by Multiple Mediators

Shuvasree SenGupta[1,2*], *Lauren E. Hein*[3,4] *and Carole A. Parent*[1,2,4,5]

[1] Life Sciences Institute, University of Michigan, Ann Arbor, MI, United States, [2] Department of Pharmacology, University of Michigan Medical School, Ann Arbor, MI, United States, [3] Cancer Biology Graduate Program, University of Michigan Medical School, Ann Arbor, MI, United States, [4] Rogel Cancer Center, University of Michigan Medical School, Ann Arbor, MI, United States, [5] Department of Cell and Developmental Biology, University of Michigan Medical School, Ann Arbor, MI, United States

Neutrophils sense and migrate towards chemotactic factors released at sites of infection/inflammation and contain the affected area using a variety of effector mechanisms. Aside from these established immune defense functions, neutrophils are emerging as one of the key tumor-infiltrating immune cells that influence cancer progression and metastasis. Neutrophil recruitment to the tumor microenvironment (TME) is mediated by multiple mediators including cytokines, chemokines, lipids, and growth factors that are secreted from cancer cells and cancer-associated stromal cells. However, the molecular mechanisms that underlie the expression and secretion of the different mediators from cancer cells and how neutrophils integrate these signals to reach and invade tumors remain unclear. Here, we discuss the possible role of the epithelial to mesenchymal transition (EMT) program, which is a well-established promoter of malignant potential in cancer, in regulating the expression and secretion of these key mediators. We also summarize and review our current understanding of the machineries that potentially control the secretion of the mediators from cancer cells, including the exocytic trafficking pathways, secretory autophagy, and extracellular vesicle-mediated secretion. We further reflect on possible mechanisms by which different mediators collaborate by integrating their signaling network, and particularly focus on TGF-β, a cytokine that is highly expressed in invasive tumors, and CXCR2 ligands, which are crucial neutrophil recruiting chemokines. Finally, we highlight gaps in the field and the need to expand current knowledge of the secretory machineries and cross-talks among mediators to develop novel neutrophil targeting strategies as effective therapeutic options in the treatment of cancer.

Keywords: neutrophils, tumor-associated neutrophils (TANs), chemokines, TGF-β, EMT, secretory pathways, secretory autophagy, EVs

OPEN ACCESS

Edited by:
Jörg Renkawitz, Ludwig Maximilian University of Munich, Germany

Reviewed by:
Leo Marc Carlin, University of Glasgow, United Kingdom
Geert Van Den Bogaart, University of Groningen, Netherlands

****Correspondence:***
Shuvasree SenGupta
sreesg@umich.edu

Specialty section:
This article was submitted to Molecular Innate Immunity, a section of the journal Frontiers in Immunology

Received: *30 June 2021*
Accepted: *26 August 2021*
Published: *10 September 2021*

Citation:
SenGupta S, Hein LE and Parent CA (2021) The Recruitment of Neutrophils to the Tumor Microenvironment Is Regulated by Multiple Mediators. Front. Immunol. 12:734188. doi: 10.3389/fimmu.2021.734188

INTRODUCTION

Neutrophils are the body's first responders to injury or infection. They have an unparalleled ability to migrate toward gradients of chemoattractants, which are released at sites of inflammation, and to clear pathogens or cell debris by using a plethora of functions including phagocytosis, the release of cytotoxic enzymes or reactive oxygen species (ROS), and the release of neutrophil extracellular traps

(NETs) (1). In addition, neutrophils have been reported in the tumor microenvironment (TME) (2), which has been described as a site of persistent inflammation similar to "*wounds that do not heal*" (3). The TME harbors a wide variety of diffusible mediators released from both tumor and stromal cells. These mediators induce neutrophil migration toward tumors and alter neutrophil function to promote or limit cancer progression. While studies have focused on understanding the tumor promoting or impairing properties of neutrophils, many questions remain unanswered about the identity of the mediators that control neutrophil recruitment to tumor sites and the function of tumor-associated neutrophils, referred to as TANs. In this perspective, we present an overview of the functions of TANs and the different classes of mediators that have been linked to neutrophil recruitment to tumors, discuss how cancer-associated changes such as the epithelial to mesenchymal transition (EMT) upregulate the expression of the mediators, and review the secretory mechanisms that potentially underlie the release of the mediators in the TME. Finally, we discuss our current understanding of the crosstalk between mediators, with a special focus on TGF-β and chemokines, to provide insights into the integrated mechanisms underlying neutrophil recruitment to the tumor niche and suggest gaps in knowledge that need to be filled for the development of anti-cancer therapeutic interventions.

PLASTICITY OF NEUTROPHILS IN CANCER

To phenotypically classify TANs and their wide range of functions that impact the outcomes of tumors, several categories have emerged: high-density/low-density, immature/mature, and anti-tumor/pro-tumor/pro-metastatic. Evidence is now suggesting that neutrophils exhibit phenotypic plasticity and can exist on a spectrum within any of these overlapping categories (4–7). For example, neutrophils are often described as "N1" (anti-tumor) or "N2" (pro-tumor) (8), but Zilionis et al. recently described a range of five neutrophil subsets in human lung cancer based on transcriptome analysis, with gene expression ranging from canonical neutrophil genes (N1 subset) to genes that were tumor-specific (N5 subset) (4). These seemingly different phenotypes are mostly generated due to exposure to specific mediator(s), either systemically in the bone marrow/blood or locally at the tumor sites. Studies using murine tumor models report that the immunosuppressive cytokine TGF-β is responsible for promoting the generation of neutrophils with a pro-tumoral "N2" phenotype (8), while the type I interferon IFN-β gives rise to an anti-tumoral "N1" phenotype (9). Further, the enzyme protease cathepsin c, secreted by breast cancer cells, has been reported to initiate a signaling cascade in mouse models that recruits neutrophils to the lung metastatic niche and promotes a pro-metastatic phenotype, and its secretion is correlated with shortened metastasis-free survival in humans (10).

Several neutrophil effector functions that support tumor progression have been identified, including immunosuppression, remodeling of the extracellular matrix (ECM), and promoting angiogenesis (11). For example, it has been demonstrated in mouse models that immunosuppressive neutrophils promote metastasis by releasing high levels of inducible nitric oxide synthase (iNOS), which inhibits proliferation of cytotoxic T cells (12). Additionally, the release of NETs from neutrophils, which are mesh-like structures of DNA fibers studded with granule proteins, is associated with metastatic progression (13–16). In particular, granule proteins such as neutrophil elastase (NE) and matrix metalloproteinase 9 (MMP9) released with NETs have been shown to awaken dormant cancer cells by remodeling the ECM and inducing cancer cell proliferation in mouse models (17).

Although most studies have reported a pro-tumor effect of neutrophils, some contexts exist where neutrophils exhibit anti-tumor effects, seemingly maintaining their canonical role to protect the body from harm. These anti-tumor actions of neutrophils in mouse models include the direct killing of cancer cells through the release of cytotoxic ROS (including hydrogen peroxide) and the restriction of tumor growth by stimulating cancer cell detachment from the basement membrane by the release of MMP9 (18–20). Additionally, the neutrophil-dependent stimulation of T cell responses can indirectly contribute to anti-tumor activity, shown both in mouse models and in cells isolated from human tissue samples (11, 21). While it has been reported that specific mediators contribute to the pro- or anti-tumoral actions of neutrophils, the mechanisms underlying how the mediators are expressed and secreted by cancer cells and the interplay among the different mediators in regulating neutrophil function remain unknown.

DIFFUSIBLE MEDIATORS IN THE TUMOR NICHE

Cancer cells and stromal cells, including cancer-associated fibroblasts (CAFs), T cells, monocytes, tumor-associated macrophages, and TANs, can secrete diverse mediators that diffuse through tissues, potentially signaling to circulating or tissue-patrolling neutrophils to recruit them to the tumor niche. **Table 1** provides a list of recently identified neutrophil mediators released in various mouse and human tissue or cell line models of cancer and their sources. These mediators primarily consist of chemokines, growth factors, and cytokines. The chemokines CXCL1, 2, 5, 6 and 8, which induce neutrophil chemotaxis through CXCR2/1 chemokine receptors, have been reported to be important for neutrophil recruitment in many cancer types (22, 25–28, 30–38). Chemokines are critical to recruit neutrophils not only to primary tumor sites but also to pre-metastatic niches and metastatic sites. For example, CXCL1, 2, and 5 released from tumor-associated mesenchymal stromal cells in a mouse model of breast cancer resulted in increased neutrophil recruitment to primary tumor sites (22). Additionally, CXCL5 and 7 released from tumor-activated platelets were reported to be crucial for neutrophil recruitment to the pre-metastatic niche and subsequent tumor cell seeding in the mouse lung (26). G-CSF and GM-CSF are important growth factors commonly upregulated in cancer, and their primary functions are to regulate the release of mature neutrophils from the bone marrow into the blood and to

TABLE 1 | List of diffusible mediators along with their cellular origin, potential impact on neutrophils and tumor progression, and the study models.

Cancer Type	Source of diffusible mediators in the TME	Diffusible Mediators	Potential impact on neutrophils	Model	Ref
breast cancer	tumor-associated mesenchymal stromal cells	CXCL1, CXCL2, CXCL5	increased migration to tumor site	mouse	(22)
	γδ T cells at tumor site	IL-17	increased migration to tumor site, change to pro-tumor phenotype, increased metastasis	mouse	(12)
	origin unclear	G-CSF (induced by IL-17)			
	cancer cells	G-CSF	recruitment to metastatic sites	mouse	(23)
	cancer cells	chemokines active *via* CXCR2, TGF-β	increased migration	human (C)	(24)
	cancer cells	IL-6, CCL3 (induced by cathepsin c)	increased migration to tumor site, NET formation, ROS production; pro-metastasis (cathepsin c works *via* the PR3-IL-1β-NF-κB axis of neutrophils to upregulate secretion of IL-6 and CCL3)	mouse	(10)
colorectal cancer	γδ T cells at tumor site	CXCL8 (IL-8), GM-CSF	increased migration	human (T)	(25)
		IL-17A, GM-CSF	expansion of the PMN-MDSC population		
		CXCL8 (IL-8), IL-17A, TNFα	extended survival		
	platelets interacting with tumor cells in pre-metastatic niche	CXCL5, CXCL7	increased recruitment to early pre-metastatic niche	mouse	(26)
	cancer cells	CXCL1	increased recruitment to tumor site and tumor progression	mouse	(27)
	cancer cells	CXCL5	increased recruitment to tumor site and increased metastasis	mouse	(28)
	origin unclear	TGF-β	increased recruitment to metastatic site		
	Th17 cells	CXCL8 (IL-8)	increased migration	human (T)	(29)
hepato-cellular carcinoma	tumor-associated monocytes	CXCL2, CXCL8	increased migration and extended survival	human (T)	(30)
	cancer cells	CXCL5	increased migration	mouse; human (C)	(31, 32)
lung cancer	tumor-associated monocytes, macrophages, neutrophils, and DCs	CXCL1	these migration-inducing chemokines are shown to have elevated levels of mRNA	mouse	(33)
	TANs	CXCL2			
	cancer cells	CXCL5			
melanoma	TANs	CXCL1, CXCL2	increased migration to tumor site and angiogenesis	mouse	(34)
ovarian cancer	tumor cells	CXCL8 (most impact) and other chemokines active *via* CXCR2	increased migration	human (T)	(35)
pancreatic cancer	cancer cells	CXCL5	increased migration to tumor site *via* CXCR2	mouse	(36)
	stromal cells	CXCL2			
	PDAC tumors	GM-CSF, G-CSF	these migration-inducing chemokines are shown to have elevated levels of mRNA	human (T)	(37)
	neoplastic ductal cells	CXCL1, CXCL2, CXCL5, CXCL8		human (T)	
	tumor cells	GM-CSF, G-CSF, CXCL1, CXCL2, CXCL5	increased migration to tumor site *via* CXCR2	mouse	
thyroid cancer	cancer cells	chemokines active *via* CXCR1/2	increased migration	human (C)	(38)
		GM-CSF	increased survival		

The model type is specific for the experiments that detailed the impact on neutrophils. C, cell line; T, tissue.

extend the survival of neutrophils (38, 39). In addition, cytokines, including interleukins (IL-17A, IL-6) (10, 12, 25, 40), interferons (IFN-β) (9), TNF-α (25), and TGF-β (5, 8, 24, 28), have been linked to neutrophil recruitment and extended neutrophil survival, as well as regulating neutrophil function. While a growing number of studies report the effect of individual mediators on neutrophil recruitment and function, it is likely that antagonistic, additive, or synergistic effects of different classes of mediators are crucial for neutrophil recruitment and function in the context of cancer.

MECHANISMS REGULATING THE SECRETION OF DIFFUSIBLE MEDIATORS FROM CANCER CELLS

Cancer cells are known to upregulate the transcription of many diffusible mediators due to the constitutive activation or overexpression of oncoproteins (41). In many cases, the higher expression of the mediators correlates with poor clinical progression (42, 43). However, little is known about the

secretory mechanisms that regulate the release of the mediators from cancer cells into the tumor niche and how the process of secretion may be altered due to cancer-associated changes compared to the mechanisms observed in non/early malignant cells. Here, we suggest that EMT induction is a key process that alters the tumor secretome and highlight the mechanisms and molecular players known to regulate the secretion of the mediators. We envision that similar mechanisms underlie the secretion of neutrophil recruiting mediators from cancer cells (**Figure 1**).

Epithelial to Mesenchymal Transition

EMT is classified into three subtypes based on the biological context. Type I EMT is associated with embryonic development and multiple organ formation. Type 2 EMT is involved in wound healing through tissue repair and regeneration, which if unrestrained, could lead to tissue fibrosis, and organ damage. Type 3 EMT is exclusively associated with malignancy and metastatic spread, where cancer cells acquire the ability to invade locally and disseminate systemically (44). Epithelial cells undergoing all three types of EMT tend to lose their epithelial characteristics and acquire migratory mesenchymal cell-like properties. However, EMT is emerging as a dynamic process where cells adopt partial EMT or intermediate/hybrid states featuring a combination of phenotypes of both cell types (45–47). Type 3 EMT (subsequently referred to as EMT) triggers cytoskeletal remodeling, loss of cell-cell adhesion and cell polarity, and gain of migratory and invasive properties, which are proposed to be required for metastasis. A wide range of diffusible mediators released from transformed or non-transformed cells in the tumor niche are known to induce EMT, including growth factors (EGF), cytokines (TGF-β, TNF-α), chemokines (CXCL8, CXCL6), and lipid mediators (leukotriene B_4 (LTB_4)) (48, 49). Interestingly, EMT has been associated with altered secretory profiles of cancer cells (50–54). For instance, secreted factors from EMT-positive breast cancer

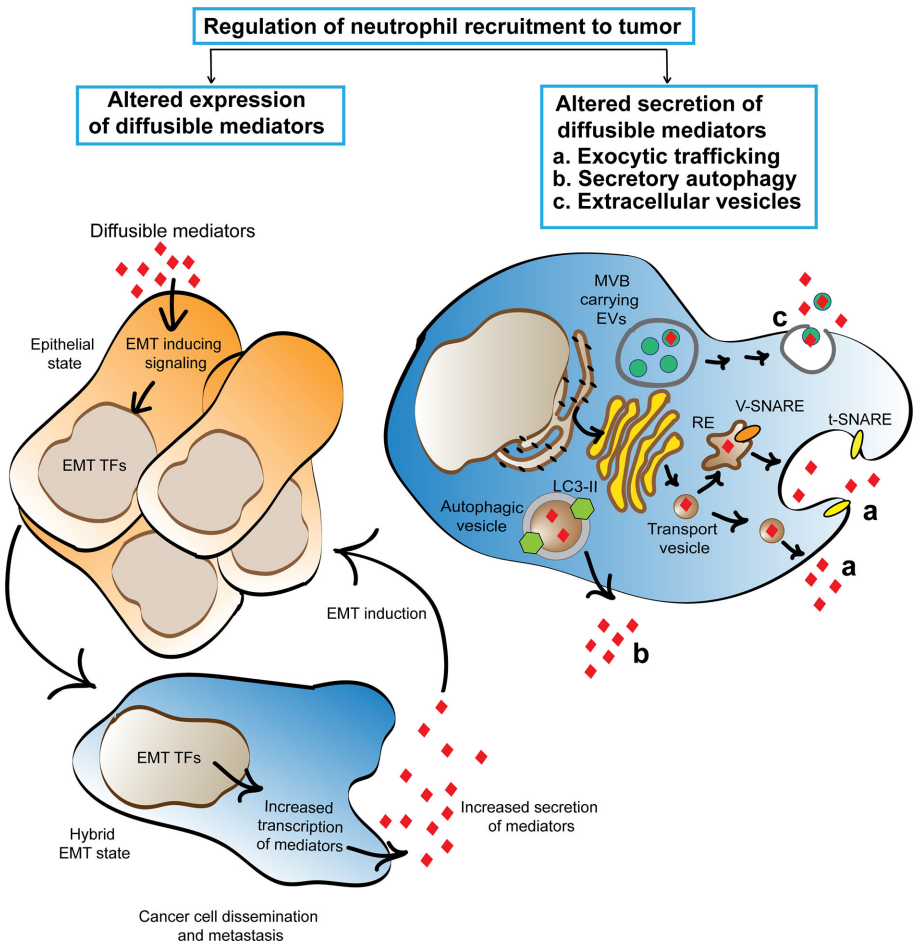

FIGURE 1 | Cartoon depicting the proposed mechanisms that regulate the cancer secretome and favor neutrophil trafficking to tumors. Cancer associated EMT program activation alters cancer cell secretome by inducing the expression of neutrophil recruiting mediators. Three machineries, namely exocytic trafficking, secretory autophagy, and extracellular vesicles are proposed to enhance the release of neutrophil recruiting mediators from cancer cells. The secreted mediators promote EMT using a feed forward mechanism and initiate a chronic cycle of inflammation that supports cancer cell dissemination. TFs, transcription factors; RE, recycling endosome.

cell lines have been reported to induce the *in vivo* recruitment of granulocytic myeloid derived suppressor cells (G-MDSC), which phenotypically resemble murine neutrophils and share immunosuppressive functions with "N2" neutrophils (50, 55). EMT-induced altered secretome of breast cancer cell lines also favors a tumor-permissive niche by activating tumor-associated macrophages, which further support EMT induction of cancer cells (54).

EMT inducing signals mediate their effects by stimulating a transcription program *via* the activation or enhanced expression of key EMT transcription factors: SNAIL, Twist and Zeb family proteins, and the T-box transcription factor Brachyury (56, 57). The role of these transcription factors in suppressing epithelial cell-cell adhesion proteins and inducing mesenchymal adhesion molecules has been widely studied (58, 59). Interestingly, the same transcription factors are also emerging as key regulators for the expression of mediators such as cytokines (TNF-α), chemokines (CCL2, CXCL6, GRO, CXCL8, CXCL11), and growth factors (GM-CSF) in cancer cells (50, 52, 53, 60–63). For example, chemokines, including CXCL6 and CXCL8, are one of the many secreted mediators that are upregulated in a Snail-dependent manner when EMT pathways are activated in cancer cells by EGF or TGF-β treatment (50). As many of the secreted mediators from EMT-activated tumors are established chemoattractants of neutrophils (GRO, CXCL8, GM-CSF) and monocytes (CCL2), the release of these mediators upon EMT induction is poised to regulate the immune landscape of the tumor niche.

Exocytic Trafficking Pathways

Conventional mechanisms that underlie the secretion of diffusible mediators, such as cytokines and chemokines, involve constitutive and regulated exocytosis pathways, depending on the cellular and inflammatory context (64–66). Much of our current knowledge comes from characterization in immune cells, particularly macrophages and dendritic cells (DCs) for constitutive secretion, and granulocytes for regulated secretion. In general, cytokines and chemokines carry a leader peptide sequence for secretion that facilitates their trafficking through the ER-Golgi network. Newly synthesized proteins are continuously exocytosed through trafficking from the Golgi network to the plasma membrane *via* small transport vesicles or tubules, which transport the cargo to the plasma membrane either directly or by merging with recycling endosomes (67). In contrast, pre-formed proteins after transiting through the Golgi network are stockpiled in vesicles or granules, which undergo regulated exocytosis in response to external inputs through receptor-ligand interactions (65). Key molecular players of the trafficking machinery include the evolutionary conserved membrane fusion proteins of the soluble N-ethylmaleimide-sensitive factor (NSF) attachment protein receptor (SNARE) protein family (67). Fusion of the vesicle and target membrane to form the core-SNARE complex is mediated by V (vesicle-associated)-SNARE and t (target membrane)-SNARE members for both constitutive and regulated exocytosis. For instance, the V-SNARE member vesicle-associated membrane protein 3 (VAMP3) localized in recycling endosomes mediates the membrane fusion of CXCL6- and TNF-α-carrying vesicles with the plasma membrane that leads to their constitutive secretion from macrophages and DCs (68–70). In granulocytes, such as eosinophils, however, CXCL6 is released through receptor mediated degranulation or regulated exocytosis, where the function of late endosomal V-SNARE members such as VAMP2 and VAMP7 have been implicated (71–74). VAMP7 is also reported to control the release of CXCL12 from VAMP7-positive late endosomal compartments in DCs, suggesting that the trafficking machinery varies greatly depending on cell types and mediators. Further, both V-SNAREs and t-SNAREs may play a rate-limiting role as their upregulation has been noted in stimulated macrophages and DCs with concomitant increase in mediator secretion (70, 75, 76). In addition, other molecular players such as Rho GTPases, including Rac1 and Cdc42, play important roles in TNF secretion in macrophage by delivering TNF-carrying recycling endosomes to the cell surface (77).

While cytokine trafficking in epithelial cells most likely utilizes the constitutive pathway (64), the mechanisms underlying mediator secretion are not well established in malignant cells even though cancer cells are known to abundantly secrete diverse mediators. An upregulation of signature genes associated with ER to Golgi trafficking pathways has been linked to the increased secretion of mediators, including CCL20, from murine breast cancer cell lines with high metastatic potential (78). Moreover, it has been shown that the secretion of CCL5 depends on the exocytosis of CCL5-carrying pre-made vesicles in the hormone receptor positive breast cancer cell line MCF-7 (79). Whether specific VAMP proteins mediate CCL5 trafficking and vesicle fusion with the plasma membrane and if/how the machinery differs in early- and late-stage malignant cells compared to non-malignant epithelial cells have yet to be determined. Of note, VAMP3 has been reported to be involved in CXCL6 and TNF-α release from the synovial sarcoma cell line SW982, indicating an active role of VAMP proteins in diffusible mediator secretion from cancer cells (80). Furthermore, studies have reported enhanced expression of V-SNARE and t-SNARE members in cancer cells along the course of tumor progression, which may further promote the exocytic release of the mediators in the TME (81).

Autophagy

An unconventional mechanism for diffusible mediator secretion is autophagy. Autophagy is traditionally known for intracellular degradation and recycling of cargos, including damaged organelles or protein aggregates, to maintain cellular homeostasis. The fusion of autophagic vacuole carrying cargos with lysosomes results in cargo degradation by acid hydrolysis and proteolysis (82). Our understanding of the machinery involved in autophagy-dependent secretion, also known as secretory autophagy (SA) (83), is however less clear. Under nutrient deprived conditions in yeast, SA is known to mediate the release of leader peptide-less proteins (84). However, there is emerging evidence that SA is involved in the secretion of mediators that are both leader-less, such as IL-1β and IL18, and leader-positive, such as CXCL6, CXCL8, and TGF-β (85, 86). Attempts to define the sequence of events leading to SA of IL-1β

from macrophages in response to lysosomal damage identified several molecular players key to the process (87). For example, TRIM16 serves as the SA cargo receptor that together with VAMP member Sec22b sequesters IL-1β in LC3-II-positive vesicles, where LC3-II is a canonical autophagosome marker. Further, the fusion of cargo vesicles with the plasma membrane as well as the release of cargos are achieved by the coordinated action of dedicated SNARE proteins including syntaxin 3, syntaxin 4, SNAP-23, and SNAP-29.

SA in both cancer cells and CAFs has recently been implicated in shaping the tumor secretome and promoting cancer progression (88, 89). For instance, secretion of CXCL8, IL-1β, LIF (leukemia inhibitory factor), and Fam3 (family with sequence similarity 3 member C) were found elevated or impaired in a murine melanoma cell line when stimulated with an autophagy-inducing peptide or subjected to autophagy related gene knockdown approaches, respectively (90). More strikingly, a correlation between the elevated presence of the same mediators in the serum of patients with high-autophagy melanoma, compared to patients with low-autophagy melanoma, was reported in the same study. Autophagy is also recognized to contribute to oncogenic RAS driven cancer cell migration and invasion by inducing the secretion of the migration promoting CXCL6 chemokine and the transcription of pro-invasive molecules, including MMP2 and WNT5A (91). In addition, CXCL6 secretion was mediated by autophagy in the triple-negative breast cancer cell line MDA-MB-468, which depends on autophagy for survival (92). In contrast, autophagy inhibition promoted CXCL6 secretion from MCF-7 cells, which otherwise does not depend on autophagy for survival. The apparent contrasting effect of autophagy on CXCL6 secretion reflects context dependent regulation of cytokine secretion by autophagy and highlights the need to explore more comprehensively the role of autophagy in mediator secretion in different cancer types and subtypes.

Extracellular Vesicles

Extracellular vesicles (EVs) are heterogeneous in size (93). Exosomes are smaller EVs with a diameter less than 150 nm that originate as intraluminal vesicles (ILVs) by the inward budding of late endosomal vesicles that form multivesicular bodies (MVBs). Upon fusion of MVBs with the plasma membrane, ILVs are released as exosomes in the extracellular milieu. By contrast, other larger EVs (diameter up to 1000 nm) are generated through the outward budding of the plasma membrane (93) and come in different flavors, including microvesicles or ectosomes, migrasomes (secreted along retraction fibers of migrating cells), and oncosomes (secreted by cancer cells) (93–96). EVs are well established as vehicles for diverse cargos, including proteins, lipids, and nucleic acids that mediate intercellular communication. EVs released from cancer cells, CAFs, and immune cells have been shown to induce directional migration of the same or other cell types through autocrine and paracrine communication (93, 97). Interestingly, cancer cell-secreted exosomes were shown to mediate the systemic mobilization of neutrophils to the spleen in an *in vivo* model of breast cancer (98). However, the role of exosomes as the vehicle for tumor-secreted mediators that directly induce neutrophil migration remains to be determined. A diverse group of cytokines, chemokines and growth factors were found to be associated at the surface of EVs or encapsulated inside EVs that were isolated from cultured immune cells, tissue explants, and different types of biological fluids (99). The availability of the mediators in a free or EV-associated form was reported to depend on the activating stimuli and the cellular system studied. Furthermore, CCL chemokines were found to be enriched in exosomes when tumor cells were exposed to heat stress (100). The degree of exosomal chemokine release may therefore be tunable as tumor cells are exposed to changing physicochemical factors in the dynamic TME. EVs are also emerging as a vital means of tumor-stromal cell communication that further promote tumor progression and metastasis. For instance, osteosarcoma cells release EVs carrying membrane-associated TGF-β1, which was shown to educate mesenchymal stromal cells to release CXCL6, and promote further tumor growth and metastasis (101). In addition, osteosarcoma-derived EVs were shown to induce lung fibroblast differentiation in a TGF-β1 dependent manner, indicating a potential role of EV-associated immune mediators to endorse distant metastasis (102).

INTERPLAY BETWEEN TGF-β AND CHEMOKINES TO MAXIMIZE NEUTROPHIL RECRUITMENT

As mentioned, given the presence of diverse cell types in the tumor niche, the TME harbors multiple diffusible mediators. Neutrophil navigation to the tumor niche could therefore be orchestrated by the interplay of different mediators. We recently reported that CXCR2 ligands, potentially growth-related oncogene (GRO) members (CXCL1/2/3), and TGF-β1, which are abundantly secreted by triple-negative breast cancer cells, concertedly induce robust neutrophil migration (24). TGF-β ligands belong to the TGF-β subfamily, with three known mammalian isoforms: TGF-β1, TGF-β2 and TGF-β3, of which TGF-β1 is the most commonly expressed. Cells secrete all isoforms as a latent complex that is activated by the presence of integrins, ECM proteins, and proteolytic enzymes (103). Once released in an active form, all isoforms interact and activate the type II/type I TGF-β receptor complex and propagate signals through SMAD-dependent and -independent pathways (104, 105). TGF-β target genes are involved in regulating fundamental cellular functions such as proliferation, differentiation, migration, senescence, apoptosis, along with maintaining immune homeostasis. The signaling outcome of TGF-β is highly context dependent in cancer. During early stages of cancer, it can prevent tumorigenesis by inhibiting cell proliferation, regulating cell cycle progression, and promoting apoptosis. However, cancer-associated disruption of TGF-β receptor/signaling components and/or the activation of EMT inducing signaling of TGF-β may promote the dissemination of cancer cells (105, 106). The mechanistic basis for the complexity of TGF-β signaling outcome has achieved significant clarity over the years. However, the mechanism and outcome of the crosstalk of TGF-β with other diffusible mediators on tumor progression are only beginning to be understood.

Both cancer and immune cells express TGF-β receptors. Receptor expression on immune cells is further modulated by the mediators present in the tumor niche. For instance, mediators secreted from metastatic prostate cancer cells upregulate the gene expression of the type I TGF-β receptor (TGF-β RI) in neutrophils (107), suggesting that the effect of TGF-β on neutrophil function is tunable. In an *in vivo* murine model of lung cancer and mesothelioma, TGF-β has been reported to promote the tumor supporting functions of neutrophils and treatment with a systemic inhibitor of TGF-β RI led to increased neutrophil recruitment to tumors indicating a negative regulation of neutrophil migration by TGF-β signaling (8). Conversely, TGF-β signaling was reported to promote neutrophil recruitment to metastatic sites in a genetically engineered *in vivo* mouse model of metastatic colorectal cancer (28). Additionally, *in vitro* studies documented various ways by which TGF-β can foster or hinder other neutrophil responses, such as prolonging neutrophil survival, promoting phagocytosis and respiratory burst (108), and impairing granule exocytosis (109).

The role of TGF-β in directional migration of neutrophils is, surprisingly, not clear. Studies have reported strong to no direct effect of TGF-β on neutrophil chemotaxis (110, 111). Given its pleiotropic role, TGF-β may indirectly regulate neutrophil chemotaxis. Indeed, TGF-β1 was reported to promote chemotaxis of immature DCs to CC and CXC chemokines by upregulating chemokine receptor expression (112). Whether TGF-β1 uses a similar mechanism to regulate CXCR1/2 expression and mediate its effect on neutrophil chemotaxis remains unknown. TGF-β1 has also been reported to promote the secretion of CXCL5 from hepatocellular carcinoma cell lines, which in turn induces neutrophil migration (32). Furthermore, TGF-β1 is known to enhance the secretion of leukotrienes from monocyte-derived macrophages and DCs, of which LTB_4 is a potent neutrophil recruiting lipid mediator (113, 114). Finally, chemokines may also synergize with TGF-β to optimize cellular responses by triggering the activation of downstream signaling components, such as SMAD3, which was reported to be phosphorylated by chemokines like CCL2 (115).

TARGETING STRATEGIES/PERSPECTIVE

Our knowledge of the multifaceted functions of neutrophils in cancer is rapidly expanding. Yet, a precise understanding of the diffusible mediators that are secreted in the TME and induce neutrophil trafficking to the tumor niche is lacking. Many cancer therapeutic strategies, such as chemotherapy, radiotherapy, and immune-checkpoint inhibitors, have the potential to affect the level of circulating neutrophils or modulate the recruitment or function of TANs, which may in turn impact patient prognosis (116). More effort should therefore be placed on directly targeting the diffusible mediators themselves or the pathways that underlie neutrophil recruitment to the TME. Integrating such neutrophil-focused approaches with routinely applied therapeutic strategies may lead to a synergistic protection against cancer progression. However, the fact that neutrophils are quintessential soldiers of the immune system requires careful consideration in developing neutrophil targeting strategies for cancer therapy. From a mechanistic standpoint, it is therefore crucial to address several questions in the context of neutrophil recruitment to specifically target the process without compromising the overall protective role of neutrophils. For example, (i) which trafficking molecules regulate the secretion of neutrophil recruiting mediators in cancer cells? (ii) Does EMT induction change the expression of these regulators and enhance the release of the mediators? (iii) Does the exocytic pathway/SA/EV-dependent release of mediators further promote EMT by triggering an autocrine-paracrine loop? and (iv) How do mediators from distinct classes such as chemokines and cytokines/growth factors/lipid mediators collaborate to optimize neutrophil recruitment to tumors and reprogram TAN function? Addressing these basic questions will provide a deeper understanding of the molecular players and signaling components that dictate neutrophil trafficking to tumors, which will assist in the design of effective therapeutic strategies.

AUTHOR CONTRIBUTIONS

SS, LEH, and CAP equally contributed to conceptualizing, writing, and editing the manuscript. All authors contributed to the article and approved the submitted version.

FUNDING

This work was supported by funding from the University of Michigan School of Medicine.

REFERENCES

1. Kolaczkowska E, Kubes P. Neutrophil Recruitment and Function in Health and Inflammation. *Nat Rev Immunol* (2013) 13(3):159–75. doi: 10.1038/nri3399
2. SenGupta S, Subramanian BC, Parent CA. Getting TANned: How the Tumor Microenvironment Drives Neutrophil Recruitment. *J Leukocyte Biol* (2019) 105(3):449–62. doi: 10.1002/JLB.3RI0718-282R
3. Dvorak HF. Tumors: Wounds That do Not Heal. Similarities Between Tumor Stroma Generation and Wound Healing. *N Engl J Med* (1986) 315 (26):1650–9. doi: 10.1056/NEJM198612253152606
4. Zilionis R, Engblom C, Pfirschke C, Savova V, Zemmour D, Saatcioglu HD, et al. Single-Cell Transcriptomics of Human and Mouse Lung Cancers Reveals Conserved Myeloid Populations Across Individuals and Species. *Immunity* (2019) 50(5):1317–34.e10. doi: 10.1016/j.immuni.2019.03.009
5. Sagiv JY, Michaeli J, Assi S, Mishalian I, Kisos H, Levy L, et al. Phenotypic Diversity and Plasticity in Circulating Neutrophil Subpopulations in Cancer. *Cell Rep* (2015) 10(4):562–73. doi: 10.1016/j.celrep.2014.12.039
6. Hsu BE, Tabariès S, Johnson RM, Andrzejewski S, Senecal J, Lehuédé C, et al. Immature Low-Density Neutrophils Exhibit Metabolic Flexibility That Facilitates Breast Cancer Liver Metastasis. *Cell Rep* (2019) 27(13):3902–15.e6. doi: 10.1016/j.celrep.2019.05.091
7. Coffelt SB, Wellenstein MD, de Visser KE. Neutrophils in Cancer: Neutral No More. *Nat Rev Cancer* (2016) 16(7):431–46. doi: 10.1038/nrc.2016.52

8. Fridlender ZG, Sun J, Kim S, Kapoor V, Cheng G, Ling L, et al. Polarization of Tumor-Associated Neutrophil Phenotype by TGF-Beta: "N1" Versus "N2" TAN. *Cancer Cell* (2009) 16(3):183–94. doi: 10.1016/j.ccr.2009.06.017
9. Andzinski L, Kasnitz N, Stahnke S, Wu CF, Gereke M, von Köckritz-Blickwede M, et al. Type I IFNs Induce Anti-Tumor Polarization of Tumor Associated Neutrophils in Mice and Human. *Int J Cancer* (2016) 138 (8):1982–93. doi: 10.1002/ijc.29945
10. Xiao Y, Cong M, Li J, He D, Wu Q, Tian P, et al. Cathepsin C Promotes Breast Cancer Lung Metastasis by Modulating Neutrophil Infiltration and Neutrophil Extracellular Trap Formation. *Cancer Cell* (2021) 39(3):423–37.e7. doi: 10.1016/j.ccell.2020.12.012
11. Jaillon S, Ponzetta A, Di Mitri D, Santoni A, Bonecchi R, Mantovani A. Neutrophil Diversity and Plasticity in Tumour Progression and Therapy. *Nat Rev Cancer* (2020) 20(9):485–503. doi: 10.1038/s41568-020-0281-y
12. Coffelt SB, Kersten K, Doornebal CW, Weiden J, Vrijland K, Hau CS, et al. IL-17-Producing γδ T Cells and Neutrophils Conspire to Promote Breast Cancer Metastasis. *Nature* (2015) 522(7556):345–8. doi: 10.1038/nature14282
13. Tohme S, Yazdani HO, Al-Khafaji AB, Chidi AP, Loughran P, Mowen K, et al. Neutrophil Extracellular Traps Promote the Development and Progression of Liver Metastases After Surgical Stress. *Cancer Res* (2016) 76 (6):1367–80. doi: 10.1158/0008-5472.CAN-15-1591
14. Park J, Wysocki RW, Amoozgar Z, Maiorino L, Fein MR, Jorns J, et al. Cancer Cells Induce Metastasis-Supporting Neutrophil Extracellular DNA Traps. *Sci Trans Med* (2016) 8(361):361ra138. doi: 10.1126/scitranslmed.aag1711
15. Cools-Lartigue J, Spicer J, McDonald B, Gowing S, Chow S, Giannias B, et al. Neutrophil Extracellular Traps Sequester Circulating Tumor Cells and Promote Metastasis. *J Clin Invest* (2013) 123(8):3446–58. doi: 10.1172/JCI67484
16. Rayes RF, Mouhanna JG, Nicolau I, Bourdeau F, Giannias B, Rousseau S, et al. Primary Tumors Induce Neutrophil Extracellular Traps With Targetable Metastasis Promoting Effects. *JCI Insight* (2019) 5(16):e128008. doi: 10.1172/jci.insight.128008
17. Albrengues J, Shields MA, Ng D, Park CG, Ambrico A, Poindexter ME, et al. Neutrophil Extracellular Traps Produced During Inflammation Awaken Dormant Cancer Cells in Mice. *Sci (New York NY)* (2018) 361(6409): eaao4227. doi: 10.1126/science.aao4227
18. Mahiddine K, Blaisdell A, Ma S, Créquer-Grandhomme A, Lowell CA, Erlebacher A. Relief of Tumor Hypoxia Unleashes the Tumoricidal Potential of Neutrophils. *J Clin Invest* (2020) 130(1):389–403. doi: 10.1172/JCI130952
19. Blaisdell A, Crequer A, Columbus D, Daikoku T, Mittal K, Dey SK, et al. Neutrophils Oppose Uterine Epithelial Carcinogenesis via Debridement of Hypoxic Tumor Cells. *Cancer Cell* (2015) 28(6):785–99. doi: 10.1016/j.ccell.2015.11.005
20. Granot Z, Henke E, Comen EA, King TA, Norton L, Benezra R. Tumor Entrained Neutrophils Inhibit Seeding in the Premetastatic Lung. *Cancer Cell* (2011) 20(3):300–14. doi: 10.1016/j.ccr.2011.08.012
21. Eruslanov EB, Bhojnagarwala PS, Quatromoni JG, Stephen TL, Ranganathan A, Deshpande C, et al. Tumor-Associated Neutrophils Stimulate T Cell Responses in Early-Stage Human Lung Cancer. *J Clin Invest* (2014) 124 (12):5466–80. doi: 10.1172/JCI77053
22. Yu PF, Huang Y, Han YY, Lin LY, Sun WH, Rabson AB, et al. Tnfα-Activated Mesenchymal Stromal Cells Promote Breast Cancer Metastasis by Recruiting CXCR2(+) Neutrophils. *Oncogene* (2017) 36(4):482–90. doi: 10.1038/onc.2016.217
23. Zhang L, Yao J, Wei Y, Zhou Z, Li P, Qu J, et al. Blocking Immunosuppressive Neutrophils Deters Py696-EZH2-Driven Brain Metastases. *Sci Trans Med* (2020) 12(545):eaaz5387. doi: 10.1126/scitranslmed.aaz5387
24. SenGupta S, Hein LE, Xu Y, Zhang J, Konwerski JR, Li Y, et al. Triple-Negative Breast Cancer Cells Recruit Neutrophils by Secreting TGF-β and CXCR2 Ligands. *Front Immunol* (2021) 12:659996. doi: 10.3389/fimmu.2021.659996
25. Wu P, Wu D, Ni C, Ye J, Chen W, Hu G, et al. γδt17 Cells Promote the Accumulation and Expansion of Myeloid-Derived Suppressor Cells in Human Colorectal Cancer. *Immunity* (2014) 40(5):785–800. doi: 10.1016/j.immuni.2014.03.013
26. Labelle M, Begum S, Hynes RO. Platelets Guide the Formation of Early Metastatic Niches. *Proc Natl Acad Sci USA* (2014) 111(30):E3053–61. doi: 10.1073/pnas.1411082111
27. Triner D, Xue X, Schwartz AJ, Jung I, Colacino JA, Shah YM. Epithelial Hypoxia-Inducible Factor 2α Facilitates the Progression of Colon Tumors Through Recruiting Neutrophils. *Mol Cell Biol* (2017) 37(5). doi: 10.1128/MCB.00481-16
28. Jackstadt R, van Hooff SR, Leach JD, Cortes-Lavaud X, Lohuis JO, Ridgway RA, et al. Epithelial NOTCH Signaling Rewires the Tumor Microenvironment of Colorectal Cancer to Drive Poor-Prognosis Subtypes and Metastasis. *Cancer Cell* (2019) 36(3):319–36.e7. doi: 10.1016/j.ccell.2019.08.003
29. Amicarella F, Muraro MG, Hirt C, Cremonesi E, Padovan E, Mele V, et al. Dual Role of Tumour-Infiltrating T Helper 17 Cells in Human Colorectal Cancer. *Gut* (2017) 66(4):692–704. doi: 10.1136/gutjnl-2015-310016
30. Peng ZP, Jiang ZZ, Guo HF, Zhou MM, Huang YF, Ning WR, et al. Glycolytic Activation of Monocytes Regulates the Accumulation and Function of Neutrophils in Human Hepatocellular Carcinoma. *J Hepatol* (2020) 73(4):906–17. doi: 10.1016/j.jhep.2020.05.004
31. Zhou SL, Dai Z, Zhou ZJ, Wang XY, Yang GH, Wang Z, et al. Overexpression of CXCL5 Mediates Neutrophil Infiltration and Indicates Poor Prognosis for Hepatocellular Carcinoma. *Hepatol (Baltimore Md)* (2012) 56(6):2242–54. doi: 10.1002/hep.25907
32. Haider C, Hnat J, Wagner R, Huber H, Timelthaler G, Grubinger M, et al. Transforming Growth Factor-β and Axl Induce CXCL5 and Neutrophil Recruitment in Hepatocellular Carcinoma. *Hepatol (Baltimore Md)* (2019) 69(1):222–36. doi: 10.1002/hep.30166
33. Faget J, Groeneveld S, Boivin G, Sankar M, Zangger N, Garcia M, et al. Neutrophils and Snail Orchestrate the Establishment of a Pro-Tumor Microenvironment in Lung Cancer. *Cell Rep* (2017) 21(11):3190–204. doi: 10.1016/j.celrep.2017.11.052
34. Jablonska J, Wu CF, Andzinski L, Leschner S, Weiss S. CXCR2-Mediated Tumor-Associated Neutrophil Recruitment Is Regulated by IFN-β. *Int J Cancer* (2014) 134(6):1346–58. doi: 10.1002/ijc.28551
35. Yang M, Zhang G, Wang Y, He M, Xu Q, Lu J, et al. Tumour-Associated Neutrophils Orchestrate Intratumoural IL-8-Driven Immune Evasion Through Jagged2 Activation in Ovarian Cancer. *Br J Cancer* (2020) 123 (9):1404–16. doi: 10.1038/s41416-020-1026-0
36. Chao T, Furth EE, Vonderheide RH. CXCR2-Dependent Accumulation of Tumor-Associated Neutrophils Regulates T-Cell Immunity in Pancreatic Ductal Adenocarcinoma. *Cancer Immunol Res* (2016) 4(11):968–82. doi: 10.1158/2326-6066.CIR-16-0188
37. Nywening TM, Belt BA, Cullinan DR, Panni RZ, Han BJ, Sanford DE, et al. Targeting Both Tumour-Associated CXCR2(+) Neutrophils and CCR2(+) Macrophages Disrupts Myeloid Recruitment and Improves Chemotherapeutic Responses in Pancreatic Ductal Adenocarcinoma. *Gut* (2018) 67(6):1112–23. doi: 10.1136/gutjnl-2017-313738
38. Galdiero MR, Varricchi G, Loffredo S, Bellevicine C, Lansione T, Ferrara AL, et al. Potential Involvement of Neutrophils in Human Thyroid Cancer. *PloS One* (2018) 13(6):e0199740. doi: 10.1371/journal.pone.0199740
39. SenGupta S, Rane MJ, Uriarte SM, Woolley C, Mitchell TC. Human Neutrophils Depend on Extrinsic Factors Produced by Monocytes for Their Survival Response to TLR4 Stimulation. *Innate Immun* (2019) 25 (8):473–86. doi: 10.1177/1753425919871994
40. Wu L, Awaji M, Saxena S, Varney ML, Sharma B, Singh RK. IL-17-CXC Chemokine Receptor 2 Axis Facilitates Breast Cancer Progression by Up-Regulating Neutrophil Recruitment. *Am J Pathol* (2020) 190(1):222–33. doi: 10.1016/j.ajpath.2019.09.016
41. Gorbachev AV, Fairchild RL. Regulation of Chemokine Expression in the Tumor Microenvironment. *Crit Rev Immunol* (2014) 34(2):103–20. doi: 10.1615/CritRevImmunol.2014010062
42. Khanna S, Graef S, Mussai F, Thomas A, Wali N, Yenidunya BG, et al. Tumor-Derived GM-CSF Promotes Granulocyte Immunosuppression in Mesothelioma Patients. *Clin Cancer Res An Off J Am Assoc Cancer Res* (2018) 24(12):2859–72. doi: 10.1158/1078-0432.CCR-17-3757
43. Yu S, Yi M, Xu L, Qin S, Li A, Wu K. CXCL1 as an Unfavorable Prognosis Factor Negatively Regulated by DACH1 in Non-Small Cell Lung Cancer. *Front Oncol* (2020) 9:1515–. doi: 10.3389/fonc.2019.01515
44. Kalluri R. EMT: When Epithelial Cells Decide to Become Mesenchymal-Like Cells. *J Clin Invest* (2009) 119(6):1417–9. doi: 10.1172/JCI39675
45. Aiello NM, Kang Y. Context-Dependent EMT Programs in Cancer Metastasis. *J Exp Med* (2019) 216(5):1016–26. doi: 10.1084/jem.20181827

46. Pastushenko I, Blanpain C. EMT Transition States During Tumor Progression and Metastasis. *Trends Cell Biol* (2019) 29(3):212–26. doi: 10.1016/j.tcb.2018.12.001
47. Nieto MA, Huang RY, Jackson RA, Thiery JP. EMT: 2016. *Cell* (2016) 166 (1):21–45. doi: 10.1016/j.cell.2016.06.028
48. Suarez-Carmona M, Lesage J, Cataldo D, Gilles C. EMT and Inflammation: Inseparable Actors of Cancer Progression. *Mol Oncol* (2017) 11(7):805–23. doi: 10.1002/1878-0261.12095
49. Zhao J, Ou B, Han D, Wang P, Zong Y, Zhu C, et al. Tumor-Derived CXCL5 Promotes Human Colorectal Cancer Metastasis Through Activation of the ERK/Elk-1/Snail and AKT/Gsk3β/β-Catenin Pathways. *Mol Cancer* (2017) 16(1):70. doi: 10.1186/s12943-017-0629-4
50. Suarez-Carmona M, Bourcy M, Lesage J, Leroi N, Syne L, Blacher S, et al. Soluble Factors Regulated by Epithelial-Mesenchymal Transition Mediate Tumour Angiogenesis and Myeloid Cell Recruitment. *J Pathol* (2015) 236 (4):491–504. doi: 10.1002/path.4546
51. Dominguez C, David JM, Palena C. Epithelial-Mesenchymal Transition and Inflammation at the Site of the Primary Tumor. *Semin Cancer Biol* (2017) 47:177–84. doi: 10.1016/j.semcancer.2017.08.002
52. Koo YJ, Kim TJ, Min KJ, So KA, Jung US, Hong JH. CXCL11 Mediates TWIST1-Induced Angiogenesis in Epithelial Ovarian Cancer. *Tumour Biol J Int Soc Oncodevelopmental Biol Med* (2017) 39(5):1010428317706226. doi: 10.1177/1010428317706226
53. Brenot A, Knolhoff BL, DeNardo DG, Longmore GD. SNAIL1 Action in Tumor Cells Influences Macrophage Polarization and Metastasis in Breast Cancer Through Altered GM-CSF Secretion. *Oncogenesis* (2018) 7(3):32. doi: 10.1038/s41389-018-0042-x
54. Su S, Liu Q, Chen J, Chen J, Chen F, He C, et al. A Positive Feedback Loop Between Mesenchymal-Like Cancer Cells and Macrophages Is Essential to Breast Cancer Metastasis. *Cancer Cell* (2014) 25(5):605–20. doi: 10.1016/j.ccr.2014.03.021
55. Fleming V, Hu X, Weber R, Nagibin V, Groth C, Altevogt P, et al. Targeting Myeloid-Derived Suppressor Cells to Bypass Tumor-Induced Immunosuppression. *Front Immunol* (2018) 9:398. doi: 10.3389/fimmu.2018.00398
56. Roselli M, Fernando RI, Guadagni F, Spila A, Alessandroni J, Palmirotta R, et al. Brachyury, a Driver of the Epithelial-Mesenchymal Transition, Is Overexpressed in Human Lung Tumors: An Opportunity for Novel Interventions Against Lung Cancer. *Clin Cancer Res An Off J Am Assoc Cancer Res* (2012) 18(14):3868–79. doi: 10.1158/1078-0432.CCR-11-3211
57. Tsai JH, Yang J. Epithelial-Mesenchymal Plasticity in Carcinoma Metastasis. *Genes Dev* (2013) 27(20):2192–206. doi: 10.1101/gad.225334.113
58. Yang J, Mani SA, Donaher JL, Ramaswamy S, Itzykson RA, Come C, et al. Twist, a Master Regulator of Morphogenesis, Plays an Essential Role in Tumor Metastasis. *Cell* (2004) 117(7):927–39. doi: 10.1016/j.cell.2004.06.006
59. Chen M, Wu Y, Zhang H, Li S, Zhou J, Shen J. The Roles of Embryonic Transcription Factor BRACHYURY in Tumorigenesis and Progression. *Front Oncol* (2020) 10:961. doi: 10.3389/fonc.2020.00961
60. Low-Marchelli JM, Ardi VC, Vizcarra EA, van Rooijen N, Quigley JP, Yang J. Twist1 Induces CCL2 and Recruits Macrophages to Promote Angiogenesis. *Cancer Res* (2013) 73(2):662–71. doi: 10.1158/0008-5472.CAN-12-0653
61. Hwang WL, Yang MH, Tsai ML, Lan HY, Su SH, Chang SC, et al. SNAIL Regulates Interleukin-8 Expression, Stem Cell-Like Activity, and Tumorigenicity of Human Colorectal Carcinoma Cells. *Gastroenterology* (2011) 141(1):279–91, 91.e1-5. doi: 10.1053/j.gastro.2011.04.008
62. Hsu DS, Wang HJ, Tai SK, Chou CH, Hsieh CH, Chiu PH, et al. Acetylation of Snail Modulates the Cytokinome of Cancer Cells to Enhance the Recruitment of Macrophages. *Cancer Cell* (2014) 26(4):534–48. doi: 10.1016/j.ccell.2014.09.002
63. Fernando RI, Castillo MD, Litzinger M, Hamilton DH, Palena C. IL-8 Signaling Plays a Critical Role in the Epithelial-Mesenchymal Transition of Human Carcinoma Cells. *Cancer Res* (2011) 71(15):5296–306. doi: 10.1158/0008-5472.CAN-11-0156
64. Stanley AC, Lacy P. Pathways for Cytokine Secretion. *Physiol (Bethesda Md)* (2010) 25(4):218–29. doi: 10.1152/physiol.00017.2010
65. Stow JL, Murray RZ. Intracellular Trafficking and Secretion of Inflammatory Cytokines. *Cytokine Growth Factor Rev* (2013) 24(3):227–39. doi: 10.1016/j.cytogfr.2013.04.001
66. Lacy P, Stow JL. Cytokine Release From Innate Immune Cells: Association With Diverse Membrane Trafficking Pathways. *Blood* (2011) 118(1):9–18. doi: 10.1182/blood-2010-08-265892
67. Murray RZ, Stow JL. Cytokine Secretion in Macrophages: SNAREs, Rabs, and Membrane Trafficking. *Front Immunol* (2014) 5:538. doi: 10.3389/fimmu.2014.00538
68. Manderson AP, Kay JG, Hammond LA, Brown DL, Stow JL. Subcompartments of the Macrophage Recycling Endosome Direct the Differential Secretion of IL-6 and TNFalpha. *J Cell Biol* (2007) 178(1):57–69. doi: 10.1083/jcb.200612131
69. Verboogen DRJ, Revelo NH, Ter Beest M, van den Bogaart G. Interleukin-6 Secretion Is Limited by Self-Signaling in Endosomes. *J Mol Cell Biol* (2019) 11(2):144–57. doi: 10.1093/jmcb/mjy038
70. Murray RZ, Kay JG, Sangermani DG, Stow JL. A Role for the Phagosome in Cytokine Secretion. *Sci (New York NY)* (2005) 310(5753):1492–5. doi: 10.1126/science.1120225
71. Lacy P, Logan MR, Bablitz B, Moqbel R. Fusion Protein Vesicle-Associated Membrane Protein 2 Is Implicated in IFN-Gamma-Induced Piecemeal Degranulation in Human Eosinophils From Atopic Individuals. *J Allergy Clin Immunol* (2001) 107(4):671–8. doi: 10.1067/mai.2001.113562
72. Logan MR, Lacy P, Bablitz B, Moqbel R. Expression of Eosinophil Target SNAREs as Potential Cognate Receptors for Vesicle-Associated Membrane Protein-2 in Exocytosis. *J Allergy Clin Immunol* (2002) 109(2):299–306. doi: 10.1067/mai.2002.121453
73. Willetts L, Felix LC, Jacobsen EA, Puttagunta L, Condjella RM, Zellner KR, et al. Vesicle-Associated Membrane Protein 7-Mediated Eosinophil Degranulation Promotes Allergic Airway Inflammation in Mice. *Commun Biol* (2018) 1:83. doi: 10.1038/s42003-018-0081-z
74. Davoine F, Lacy P. Eosinophil Cytokines, Chemokines, and Growth Factors: Emerging Roles in Immunity. *Front Immunol* (2014) 5:570–. doi: 10.3389/fimmu.2014.00570
75. Chiaruttini G, Piperno GM, Jouve M, De Nardi F, Larghi P, Peden AA, et al. The SNARE VAMP7 Regulates Exocytic Trafficking of Interleukin-12 in Dendritic Cells. *Cell Rep* (2016) 14(11):2624–36. doi: 10.1016/j.celrep.2016.02.055
76. Pagan JK, Wylie FG, Joseph S, Widberg C, Bryant NJ, James DE, et al. The T-SNARE Syntaxin 4 Is Regulated During Macrophage Activation to Function in Membrane Traffic and Cytokine Secretion. *Curr Biol CB* (2003) 13 (2):156–60. doi: 10.1016/S0960-9822(03)00006-X
77. Stanley AC, Wong CX, Micaroni M, Venturato J, Khromykh T, Stow JL, et al. The Rho GTPase Rac1 Is Required for Recycling Endosome-Mediated Secretion of TNF in Macrophages. *Immunol Cell Biol* (2014) 92(3):275–86. doi: 10.1038/icb.2013.90
78. Howley BV, Link LA, Grelet S, El-Sabban M, Howe PH. A CREB3-Regulated ER-Golgi Trafficking Signature Promotes Metastatic Progression in Breast Cancer. *Oncogene* (2018) 37(10):1308–25. doi: 10.1038/s41388-017-0023-0
79. Soria G, Lebel-Haziv Y, Ehrlich M, Meshel T, Suez A, Avezov E, et al. Mechanisms Regulating the Secretion of the Promalignancy Chemokine CCL5 by Breast Tumor Cells: CCL5's 40s Loop and Intracellular Glycosaminoglycans. *Neoplasia* (2012) 14(1):1–IN3. doi: 10.1593/neo.111122
80. Boddul SV, Meng J, Dolly JO, Wang J. SNAP-23 and VAMP-3 Contribute to the Release of IL-6 and Tnfα From a Human Synovial Sarcoma Cell Line. *FEBS J* (2014) 281(3):750–65. doi: 10.1111/febs.12620
81. Raja SA, Abbas S, Shah STA, Tariq A, Bibi N, Yousuf A, et al. Increased Expression Levels of Syntaxin 1A and Synaptobrevin 2/Vesicle-Associated Membrane Protein-2 Are Associated With the Progression of Bladder Cancer. *Genet Mol Biol* (2019) 42(1):40–7. doi: 10.1590/1678-4685-gmb-2017-0339
82. Dikic I, Elazar Z. Mechanism and Medical Implications of Mammalian Autophagy. *Nat Rev Mol Cell Biol* (2018) 19(6):349–64. doi: 10.1038/s41580-018-0003-4
83. Gonzalez CD, Resnik R, Vaccaro MI. Secretory Autophagy and Its Relevance in Metabolic and Degenerative Disease. *Front Endocrinol (Lausanne)* (2020) 11:266. doi: 10.3389/fendo.2020.00266
84. Manjithaya R, Anjard C, Loomis WF, Subramani S. Unconventional Secretion of Pichia Pastoris Acb1 Is Dependent on GRASP Protein, Peroxisomal Functions, and Autophagosome Formation. *J Cell Biol* (2010) 188(4):537–46. doi: 10.1083/jcb.200911149

85. New J, Thomas SM. Autophagy-Dependent Secretion: Mechanism, Factors Secreted, and Disease Implications. *Autophagy* (2019) 15(10):1682–93. doi: 10.1080/15548627.2019.1596479
86. Nüchel J, Ghatak S, Zuk AV, Illerhaus A, Mörgelin M, Schönborn K, et al. TGFB1 Is Secreted Through an Unconventional Pathway Dependent on the Autophagic Machinery and Cytoskeletal Regulators. *Autophagy* (2018) 14 (3):465–86. doi: 10.1080/15548627.2017.1422850
87. Kimura T, Jia J, Kumar S, Choi SW, Gu Y, Mudd M, et al. Dedicated SNAREs and Specialized TRIM Cargo Receptors Mediate Secretory Autophagy. *EMBO J* (2017) 36(1):42–60. doi: 10.15252/embj.201695081
88. Bustos SO, Antunes F, Rangel MC, Chammas R. Emerging Autophagy Functions Shape the Tumor Microenvironment and Play a Role in Cancer Progression - Implications for Cancer Therapy. *Front Oncol* (2020) 10:606436. doi: 10.3389/fonc.2020.606436
89. New J, Arnold L, Ananth M, Alvi S, Thornton M, Werner L, et al. Secretory Autophagy in Cancer-Associated Fibroblasts Promotes Head and Neck Cancer Progression and Offers a Novel Therapeutic Target. *Cancer Res* (2017) 77(23):6679–91. doi: 10.1158/0008-5472.CAN-17-1077
90. Kraya AA, Piao S, Xu X, Zhang G, Herlyn M, Gimotty P, et al. Identification of Secreted Proteins That Reflect Autophagy Dynamics Within Tumor Cells. *Autophagy* (2015) 11(1):60–74. doi: 10.4161/15548627.2014.984273
91. Lock R, Kenific CM, Leidal AM, Salas E, Debnath J. Autophagy-Dependent Production of Secreted Factors Facilitates Oncogenic RAS-Driven Invasion. *Cancer Discovery* (2014) 4(4):466–79. doi: 10.1158/2159-8290.CD-13-0841
92. Maycotte P, Jones KL, Goodall ML, Thorburn J, Thorburn A. Autophagy Supports Breast Cancer Stem Cell Maintenance by Regulating IL6 Secretion. *Mol Cancer Res MCR* (2015) 13(4):651–8. doi: 10.1158/1541-7786.MCR-14-0487
93. Sung BH, Parent CA, Weaver AM. Extracellular Vesicles: Critical Players During Cell Migration. *Dev Cell* (2021) 56(13):1861–74. doi: 10.1016/j.devcel.2021.03.020
94. Al-Nedawi K, Meehan B, Micallef J, Lhotak V, May L, Guha A, et al. Intercellular Transfer of the Oncogenic Receptor EGFRvIII by Microvesicles Derived From Tumour Cells. *Nat Cell Biol* (2008) 10(5):619–24. doi: 10.1038/ncb1725
95. Cocucci E, Meldolesi J. Ectosomes and Exosomes: Shedding the Confusion Between Extracellular Vesicles. *Trends Cell Biol* (2015) 25(6):364–72. doi: 10.1016/j.tcb.2015.01.004
96. Ma L, Li Y, Peng J, Wu D, Zhao X, Cui Y, et al. Discovery of the Migrasome, an Organelle Mediating Release of Cytoplasmic Contents During Cell Migration. *Cell Res* (2015) 25(1):24–38. doi: 10.1038/cr.2014.135
97. Harris DA, Patel SH, Gucek M, Hendrix A, Westbroek W, Taraska JW. Exosomes Released From Breast Cancer Carcinomas Stimulate Cell Movement. *PloS One* (2015) 10(3):e0117495. doi: 10.1371/journal.pone.0117495
98. Bobrie A, Krumeich S, Reyal F, Recchi C, Moita LF, Seabra MC, et al. Rab27a Supports Exosome-Dependent and -Independent Mechanisms That Modify the Tumor Microenvironment and can Promote Tumor Progression. *Cancer Res* (2012) 72(19):4920–30. doi: 10.1158/0008-5472.CAN-12-0925
99. Fitzgerald W, Freeman ML, Lederman MM, Vasilieva E, Romero R, Margolis L. A System of Cytokines Encapsulated in ExtraCellular Vesicles. *Sci Rep* (2018) 8(1):8973. doi: 10.1038/s41598-018-27190-x
100. Chen T, Guo J, Yang M, Zhu X, Cao X. Chemokine-Containing Exosomes Are Released From Heat-Stressed Tumor Cells via Lipid Raft-Dependent Pathway and Act as Efficient Tumor Vaccine. *J Immunol (Baltimore Md 1950)* (2011) 186(4):2219–28. doi: 10.4049/jimmunol.1002991
101. Baglio SR, Lagerweij T, Pérez-Lanzón M, Ho XD, Léveillé N, Melo SA, et al. Blocking Tumor-Educated MSC Paracrine Activity Halts Osteosarcoma Progression. *Clin Cancer Res An Off J Am Assoc Cancer Res* (2017) 23 (14):3721–33. doi: 10.1158/1078-0432.CCR-16-2726
102. Mazumdar A, Urdinez J, Boro A, Migliavacca J, Arlt MJE, Muff R, et al. Osteosarcoma-Derived Extracell Vesicles Induce Lung Fibroblast Reprogramming. *Int J Mol Sci* (2020) 21(15):5451. doi: 10.3390/ijms21155451
103. Munger JS, Sheppard D. Cross Talk Among TGF-β Signaling Pathways, Integrins, and the Extracellular Matrix. *Cold Spring Harbor Perspect Biol* (2011) 3(11):a005017. doi: 10.1101/cshperspect.a005017
104. Bierie B, Moses HL. Tumour Microenvironment: TGFbeta: The Molecular Jekyll and Hyde of Cancer. *Nat Rev Cancer* (2006) 6(7):506–20. doi: 10.1038/nrc1926
105. Massagué J. TGFbeta in Cancer. *Cell* (2008) 134(2):215–30. doi: 10.1016/j.cell.2008.07.001
106. Gu S, Feng X-H. TGF-β Signaling in Cancer. *Acta Biochim Biophys Sin* (2018) 50(10):941–9. doi: 10.1093/abbs/gmy092
107. Costanzo-Garvey DL, Keeley T, Case AJ, Watson GF, Alsamraae M, Yu Y, et al. Neutrophils Are Mediators of Metastatic Prostate Cancer Progression in Bone. *Cancer Immunol Immunother CII* (2020) 69(6):1113–30. doi: 10.1007/s00262-020-02527-6
108. Lagraoui M, Gagnon L. Enhancement of Human Neutrophil Survival and Activation by TGF-Beta 1. *Cell Mol Biol (Noisy-le-Grand France)* (1997) 43 (3):313–8.
109. Shen L, Smith JM, Shen Z, Eriksson M, Sentman C, Wira CR. Inhibition of Human Neutrophil Degranulation by Transforming Growth Factor-Beta1. *Clin Exp Immunol* (2007) 149(1):155–61. doi: 10.1111/j.1365-2249.2007.03376.x
110. Brandes ME, Mai UE, Ohura K, Wahl SM. Type I Transforming Growth Factor-Beta Receptors on Neutrophils Mediate Chemotaxis to Transforming Growth Factor-Beta. *J Immunol (Baltimore Md 1950)* (1991) 147(5):1600–6.
111. Parekh T, Saxena B, Reibman J, Cronstein BN, Gold LI. Neutrophil Chemotaxis in Response to TGF-Beta Isoforms (TGF-Beta 1, TGF-Beta 2, TGF-Beta 3) Is Mediated by Fibronectin. *J Immunol (Baltimore Md 1950)* (1994) 152(5):2456–66.
112. Sato K, Kawasaki H, Nagayama H, Enomoto M, Morimoto C, Tadokoro K, et al. TGF-Beta 1 Reciprocally Controls Chemotaxis of Human Peripheral Blood Monocyte-Derived Dendritic Cells via Chemokine Receptors. *J Immunol (Baltimore Md 1950)* (2000) 164(5):2285–95. doi: 10.4049/jimmunol.164.5.2285
113. Esser J, Gehrmann U, D'Alexandri FL, Hidalgo-Estévez AM, Wheelock CE, Scheynius A, et al. Exosomes From Human Macrophages and Dendritic Cells Contain Enzymes for Leukotriene Biosynthesis and Promote Granulocyte Migration. *J Allergy Clin Immunol* (2010) 126(5):1032–40, 40.e1-4. doi: 10.1016/j.jaci.2010.06.039
114. Subramanian BC, Majumdar R, Parent CA. The Role of the LTB(4)-BLT1 Axis in Chemotactic Gradient Sensing and Directed Leukocyte Migration. *Semin Immunol* (2017) 33:16–29. doi: 10.1016/j.smim.2017.07.002
115. Fang WB, Jokar I, Zou A, Lambert D, Dendukuri P, Cheng N. CCL2/CCR2 Chemokine Signaling Coordinates Survival and Motility of Breast Cancer Cells Through Smad3 Protein- and P42/44 Mitogen-Activated Protein Kinase (MAPK)-Dependent Mechanisms. *J Biol Chem* (2012) 287 (43):36593–608. doi: 10.1074/jbc.M112.365999
116. Shaul ME, Fridlender ZG. Tumour-Associated Neutrophils in Patients With Cancer. *Nat Rev Clin Oncol* (2019) 16(10):601–20. doi: 10.1038/s41571-019-0222-4

Conflict of Interest: The authors declare that the research was conducted in the absence of any commercial or financial relationships that could be construed as a potential conflict of interest.

Publisher's Note: All claims expressed in this article are solely those of the authors and do not necessarily represent those of their affiliated organizations, or those of the publisher, the editors and the reviewers. Any product that may be evaluated in this article, or claim that may be made by its manufacturer, is not guaranteed or endorsed by the publisher.

frontiers in Immunology

ORIGINAL RESEARCH
published: 16 September 2021
doi: 10.3389/fimmu.2021.702453

CAL-1 as Cellular Model System to Study CCR7-Guided Human Dendritic Cell Migration

*Edith Uetz-von Allmen[1], Guerric P. B. Samson[1,2], Vladimir Purvanov[1], Takahiro Maeda[3] and Daniel F. Legler[1,4,5]**

[1] Biotechnology Institute Thurgau (BITg) at the University of Konstanz, Kreuzlingen, Switzerland, [2] Graduate School for Cellular and Biomedical Sciences (GCB), University of Bern, Bern, Switzerland, [3] Department of Laboratory Medicine, Nagasaki University Graduate School of Biomedical Sciences, Nagasaki, Japan, [4] Theodor Kocher Institute, University of Bern, Bern, Switzerland, [5] Department of Biology, University of Konstanz, Konstanz, Germany

Dendritic cells (DCs) are potent and versatile professional antigen-presenting cells and central for the induction of adaptive immunity. The ability to migrate and transport peripherally acquired antigens to draining lymph nodes for subsequent cognate T cell priming is a key feature of DCs. Consequently, DC-based immunotherapies are used to elicit tumor-antigen specific T cell responses in cancer patients. Understanding chemokine-guided DC migration is critical to explore DCs as cellular vaccines for immunotherapeutic approaches. Currently, research is hampered by the lack of appropriate human cellular model systems to effectively study spatio-temporal signaling and CCR7-driven migration of human DCs. Here, we report that the previously established human neoplastic cell line CAL-1 expresses the human DC surface antigens CD11c and HLA-DR together with co-stimulatory molecules. Importantly, if exposed for three days to GM-CSF, CAL-1 cells induce the endogenous expression of the chemokine receptor CCR7 upon encountering the clinically approved TLR7/8 agonist Resiquimod R848 and readily migrate along chemokine gradients. Further, we demonstrate that CAL-1 cells can be genetically modified to express fluorescent (GFP)-tagged reporter proteins to study and visualize signaling or can be gene-edited using CRISPR/Cas9. Hence, we herein present the human CAL-1 cell line as versatile and valuable cellular model system to effectively study human DC migration and signaling.

Keywords: human dendritic cell line, cell migration, chemokine receptor CCR7, CCL19, CCL21, chemotaxis, expression of fluorescent reporter proteins, CRISPR/Cas9 mediated CCR7 knockout

OPEN ACCESS

Edited by:
Jörg Renkawitz, Ludwig Maximilian University of Munich, Germany

Reviewed by:
Kari Vaahtomeri, University of Helsinki, Finland
Pablo José Sáez, University Medical Center Hamburg-Eppendorf, Germany

***Correspondence:**
Daniel F. Legler
daniel.legler@bitg.ch

Specialty section:
This article was submitted to Molecular Innate Immunity, a section of the journal Frontiers in Immunology

Received: *29 April 2021*
Accepted: *31 August 2021*
Published: *16 September 2021*

Citation:
Uetz-von Allmen E, Samson GPB, Purvanov V, Maeda T and Legler DF (2021) CAL-1 as Cellular Model System to Study CCR7-Guided Human Dendritic Cell Migration. Front. Immunol. 12:702453. doi: 10.3389/fimmu.2021.702453

INTRODUCTION

Dendritic cells (DCs) are sentinels of the innate and adaptive immune system and play essential roles in initiating, coordinating and regulating adaptive immune responses (1). They reside in peripheral tissues where they are poised to capture and process antigens derived from invading pathogens. Upon pathogen encounter, DCs undergo a complex process of maturation, induce the expression of co-stimulatory molecules and migrate *via* the lymph system to the next draining lymph node (2, 3). In lymph nodes, DCs present pathogen-derived antigens to cognate T cells to

trigger an adaptive immune response (4). Due to the unique ability of DCs to prime and activate naïve T cells, DC-based vaccination strategies are exploited as cancer therapies in which DCs are loaded with tumor antigens to mount tumor antigen specific immune responses (5–7). Notably, DCs comprise a heterogeneous population of cells (8–10). Human peripheral blood includes two main DC populations, namely myeloid and plasmacytoid DCs, with different functional properties (11). Nonetheless, one key feature for their use as an effective cellular vaccine is that the tumor antigen loaded DCs must efficiently migrate to lymphoid organs to encounter and prime tumor antigen specific T cells (7). Leukocyte migration is controlled by the expression of specialized chemokine receptors and integrins (12). Importantly, expression of the chemokine receptor CCR7 is essential to all DC subtypes for their homing to lymphoid organs (3). In fact, DCs up-regulate the expression of CCR7 upon encounter of a danger signal and acquire a migratory phenotype (13, 14). CCR7-expressing DCs migrate along CCL19 and CCL21 chemokine gradients and *via* the lymph system to reach the T cell zone of the next draining lymph node (15, 16). Besides controlling DC homing, CCR7 also coordinates the recruitment of circulating T cells from the blood to the lymph nodes and acts as co-stimulatory molecule to efficiently prime T cells (17). Notably, besides common expression by interstitial lymphatic endothelial cells and lymphoid tissue stroma cells (18), disparate lymphoid chemokine expression has been noted between men and mice. CCL21 is not produced, but trapped and presented by human high endothelial venules (HEVs), whereas in mice this chemokine is synthesized directly by HEVs (19).

CCR7-dependent DC migration has extensively been studied using *in vitro* differentiated bone-marrow derived precursor cells, so called BMDCs, obtained from wild-type or gene targeted mice as cellular model systems. Recent technical advances, although not trivial, enabled the transient immortalization of murine hematopoietic precursor cells by a retrovirally delivered and induced expression of the transcription factor Hoxb8 (20). Upon relieve from the induced Hoxb8 expression, such precursor cells can be differentiated in the presence of GM-CSF to immature DCs that resemble immature BMDCs (21, 22). However, the usefulness of murine BMDC cultures in the study of DC biology has been debated (23, 24). Moreover, the technical achievement of using Hoxb8-DCs are currently restricted to mouse DC models. Human DC subsets can be isolated in very limited numbers from peripheral blood (11) and hence are not exploited as cellular model systems to study molecular mechanisms of DC migration. The most widely used human DC model system is monocyte-derived DCs (MoDCs), which comprises the isolation of peripheral blood monocytes and their *in vitro* differentiation to MoDCs in the presence of GM-CSF and IL-4 for several days (7, 25–28). A drawback of these MoDCs is that they show substantial donor to donor variation, are refractory to genetic manipulation and hence not suitable as effective cellular model to study CCR7-driven DC migration. Attempts to use human leukemia cell lines with monocyte-like properties under DC differentiating culture conditions were of limited success (29). Own attempts to induce endogenous CCR7 expression in any of these human cell lines failed. A DC-like cell line of human origin that upon exposure to a danger signal induces CCR7 expression and migration combined with the ability to be genetically edited is lacking but highly desired to study human DC migration.

A human plasmacytoid DC line, termed CAL-1, has been established from a patient with blastic natural killer cell lymphoma (30), also referred to as blastic plasmacytoid DC neoplasm (31). CAL-1 cells were shown to express transcripts for TLR2, TLR4, TLR7 and TLR9 and are sensitive to single-stranded RNA (a ligand for TLR7), to Resiquimod R848 (R848; a ligand for TLR7/8) and to unmethylated CpG oligodeoxynucleotides (ODNs; ligands for TLR9) (30, 32, 33). Moreover, upon TLR ligation, CAL-1 cells are reported to secrete the cytokines TNFα, IFNγ, and IL-6, and to express the co-stimulatory molecules CD40, CD80 and CD86 (30, 32). However, unlike plasmacytoid DCs, CAL-1 cells respond to IL-3 and GM-CSF to form dendrites, a characteristic feature of MoDCs, and up-regulate MHC class II (30, 34). Here, we demonstrate that CAL-1 cells exposed to GM-CSF up-regulate the expression of CCR7 in response to a danger signal. Moreover, we show that these cells are well suited to study CCR7 signaling and cell migration. Finally, we provide evidence that CAL-1 cells can be genetically modified – e.g. to express a fluorescent reporter protein – while retaining their migratory capacity in response to the chemokines CCL19 and CCL21 in 2D and 3D environments.

MATERIALS AND METHODS

Cell Culture

CAL-1 cells, obtained under a material transfer agreement, were cultured in complete growth medium RPMI 1640 containing 2mM L-alanyl-L-glutamine (Pan Biotech Ref. P04-18500, Chemie Brunschwig, Basel, Switzerland), supplemented with 10% FCS (Gibco Ref. 10270-106; LuBioScience, Luzern, Switzerland) and 1% penicillin/streptomycin (BioWhittaker Lonza; VWR Scientific, Nyon, Switzerland) in suspension tissue culture flasks or plates (Greiner Bio-One; Huberlab, Aesch, Switzerland). Floating cells were passaged to new culture flasks for cell maintenance. Where indicated, CAL-1 cells (2x 10^5 cells/ml) were exposed to 10ng/ml human GM-CSF (Peprotech, LuBioScience; catalog #300-03) for 3 days, referred to as GM/CAL-1 cells, washed, resuspended at a density of 1x 10^6 cells/ml in complete growth medium without GM-CSF and then left untreated or matured for another 18-19h with either the TLR7/8 agonist Resiquimod R848 (10μg/ml; Sigma–Aldrich, Buchs, Switzerland; #SML0196) or the TLR9 ligand CpG-B ODN 2006 (1μM; InvivoGen; LabForce, Muttenz, Switzerland; #tlrl-2006-1).

Flow Cytometry

Cultured cells were collected, washed and resuspended in complete growth medium at 1x 10^6 cells/ml and stained for

20min at 4°C using the following anti-human antibodies (1:20): APC-labeled CCR7 and the matched isotype control antibody (R&D Systems; Bio-Techne, Zug, Switzerland), CD123 (clone 6H6, Abeomics; LucernaChem, Luzern, Switzerland), CD11c (clone 3.9), HLA-DR (BioLegend through LucernaChem), and FITC-labeled anti-CD40 (Serotec; Bio-Rad, Cressier, Switzerland) or anti-CD86 (BD Biosciences, Allschwil, Switzerland). Unbound antibodies were removed by washing with 1x PBS and cell pellets were resuspended in FACS buffer (1x PBS supplemented with 0.5% FCS). Samples were filtered (50µM Cup Filcons from BD), measured with a BD LSRII or a LSRFortessa flow cytometer using the BD FACSDiva™ 6 software and analyzed with the FlowJo software (BD). SYTOX® Blue or TO-PRO™-3 iodide (Invitrogen; Thermo Fisher Scientific, Allschwil, Switzerland) was added as a dead cell indicator.

Generation of CAL-1 Cell (sub) Lines Stably Expressing the PH-Akt-GFP Reporter

CAL-1 cells were transfected with 5µg of the plasmid DNA pcDNA3-PH-Akt-EGFP (35) using the Neon™ Transfection System 100µl Kit with buffer E2 (Invitrogen; Thermo Fisher). Cells (1x 10^6) were electroporated using a single pulse of 1600V and 20ms after resuspension in Opti-MEM® I reduced serum medium (Gibco; Thermo Fisher). The transfected cells (24h) were grown under a selective pressure of 0.3mg/ml G418 for two weeks and then bulk sorted for medium to high GFP expression on a BD Aria IIu cell sorter (BD Biosciences). Aliquots of this CAL-1 PH-Akt-GFP^{line} were frozen. Experiments with the CAL-1 PH-Akt-GFP^{line} were performed 19-26 days after bulk sorting (that is 34-41 days after transfection) with one freeze-thaw cycle in between. A frozen sample of the CAL-1 PH-Akt-GFP^{line} was thawed, cultured for 11 days under continuous G418 selection and used to establish two sub-lines (CAL-1 PH-Akt-GFP$^{subline\ 1}$ and CAL-1 PH-Akt-GFP$^{subline\ 2}$) by cell sorting. Aliquots of the sublines were frozen 6 days after sorting. Experiments with CAL-1 PH-Akt-GFP$^{subline\ 1}$ or CAL-1 PH-Akt-GFP$^{subline\ 2}$ were performed 7-10 days, respectively 8-15 days, after thawing.

Generation of CCR7 Knockout and Parental CAL-1 Cell Clones

CRISPR/Cas9–based gene knockout (KO) CAL-1 clones lacking the CCR7 gene were established using the U6-gRNA : CMV-Cas9-2a-tGFP transfection (p01) plasmid from Sigma and the Neon transfection system (5µg DNA per 1x 10^6 cells; one pulse of 1600V and 20ms). The single-guide RNA (sgRNA)–targeting sequence in the CCR7 gene was 5′-CGCAACTTTGAGC GCAACA (CRISPRD HSPD0000007879). Single cell clones were FACS-sorted into 96-well tissue culture plates 48h after transfection based on GFP expression (0.5% of the cell population) using a BD Aria IIu cell sorter and cultured under standard maintenance conditions. Colony formation was observed under a microscope. Due to the lack of a specific antibody to CCR7 that would work in Western blotting, site-specific genome editing was verified using PCR or PCR combined with blunt end cloning followed by Sanger sequencing. Additional cell clones of the parental CAL-1 cell line were established by single cell sorting using a BD Aria IIu cell sorter. Three individual clones were randomly selected, expanded and subsequently differentiated and matured. Chemokine binding and cell migration experiments of these three cell clones were performed 27-29 days after single cell sorting.

FITC-Dextran Uptake Assay

CAL-1 or GM/CAL-1 cells (2x 10^6) were stimulated with 1µg/ml Resiquimod R848 for 30min before incubating with 1mg/ml FITC-dextran (FD40, Sigma-Aldrich) for the indicated time points at 37°C. Alternatively, CAL-1 or GM/CAL-1 cells were matured with 1µg/ml Resiquimod R848 or 1µM CpG-B ODN 2006 for 24h before cells were incubated with FITC-dextran for 30min. The reaction was stopped by adding ice-cold RPMI medium. Then, cells were extensively washed with ice-cold medium and once with PBS before being resuspended in FACS buffer (1x PBS, 2% FCS). FITC-dextran uptake kinetics was quantified by flow cytometry.

Intracellular Cytokine Staining (ICS)

CAL-1 or GM/CAL-1 cells (2x 10^5 in 180µl medium) were incubated in the presence or absence of TLR ligands (1µM CpG-B or 1µg/ml R848) in a 96 well round bottom plate for 6h at 37°C, 5% CO_2. Brefeldin A (10µg/ml) was added for the last 4h of stimulation. Cells were centrifuged for 5min at 300x g, fixed for 20min on ice using 4% PFA and then washed twice with 200µl permeabilization buffer (2mM EDTA, 2% FCS, 0.1% saponin, 0.02% NaN_3 in 1x PBS). Intracellular cytokine production was measured by flow cytometry using the following staining: cells were incubated with APC conjugated anti-human TNFα (clone Mab11, BioLegend, 1:20) for 90min on ice in the presence of permeabilization buffer, then washed with permeabilization buffer and resuspended with ice-cold FACS buffer.

Cytosolic Free Ca^{2+} Mobilization

R848-matured GM/CAL-1 cells (1x 10^6/ml) were loaded with 4µM fluo-3-AM (Molecular Probes/Invitrogen; Thermo Fisher) in loading-buffer (145mM NaCl, 5mM KCl, 1mM Na_2HPO_4, 1mM $MgCl_2$, 5mM glucose, 1mM $CaCl_2$, and 10mM HEPES, pH 7.5) for 20min at 37°C and then washed twice with loading-buffer. Where indicated, R848-matured GM/CAL-1 cells were pre-treated with 200ng/ml of *Bordetella pertussis* toxin (PTx; BML-G100, Enzo Life Sciences, Lausen, Switzerland) for 3h prior to fluo-3 loading. Human chemokine-induced cytosolic free calcium mobilization-related fluorescence intensity changes were recorded over time by flow cytometry as described (36). Data were corrected for mean basal fluorescence intensity before stimulation and normalized to the mean intensity in the presence of ionomycin (1µg/ml). Flow cytometry analysis was performed in parallel to ensure CCR7 surface expression.

Cell Stimulation and Western Blot Analysis

R848-matured GM/CAL-1 cells were washed with RPMI 1640 medium without additives (RPMI) and incubated at a density of

1x 10^6 cells/ml in serum-free RPMI for 2h at 37°C, 5% CO_2. Serum starved cells were scraped and washed once with RPMI. Aliquots of 1.5x 10^6 cells in 50µl RPMI were incubated for 5min at 37°C and then stimulated with 50µl of pre-warmed RPMI or medium containing a 2-fold chemokine concentration (final concentration: 100nM of human CCL19 or CCL21, which is known to induce maximal responses (37, 38); Peprotech #300-29B and #300-35) for indicated time points. Cell stimulation was terminated by the addition of 25µl of 5x Laemmli sodium dodecyl sulphate (SDS) loading buffer containing 4% β-mercaptoethanol. DNA was immediately sheared by vortexing or rapidly passing the sample up and down through a 200µl tip several times. Samples were boiled and proteins (15µl whole cell lysates) were separated under reducing conditions on 10% SDS-polyacrylamide gel electrophoresis (SDS-PAGE) and analyzed by Western blot (39, 40) using the respective antibodies from Cell Signaling (BioConcept, Allschwil, Switzerland), diluted 1:1'000 in staining buffer (1x PBS, 3% BSA, 0.05% Tween 20, 0.02% NaN_3) and rolling overnight at 4°C: rabbit anti-p44/42 MAPK (t-Erk1/2), mouse anti-phospho-p44/42 MAPK (Thr202/Tyr204; p-Erk1/2) and rabbit anti-phospho-Akt (Ser473; p-Akt) after blocking the membranes for 1h at RT with 1x Roti®-Block (Carl Roth, Arlesheim, Switzerland). A mAb against β-actin was used as loading control (Abcam; LucernaChem). After washing with PBS-T buffer (1x PBS, 0.02% Tween 20), HRP-conjugated secondary antibodies diluted 1:5'000 in PBS-T buffer containing 5% low-fat dry milk were bound and detected using Clarity™ Western ECL Substrate (Bio-Rad). Thereafter, membranes were stripped with Restore™ Western Blot Stripping Buffer (Thermo Fisher) for 15min at RT and then washed and re-probed with β-actin control antibody. Band volume intensities for p-Erk1/2 or p-Akt were quantified using the Image Lab Software Version 4.1 (Bio-Rad) and normalized to t-Erk. A portion of R848-matured GM/CAL-1 cells was analyzed for CCR7 surface expression by flow cytometry for each experiment.

Chemokine Binding Assay

Individual GM/CAL-1 CCR7-KO clones, GM/CAL-1 control cells and cell clones were matured with Resiquimod R848 and assessed for fluorescent CCL19-S6^{649P1} (41) binding at 7°C. A 96 well V-plate containing 90µl per well of a 2x 10^6 per ml cell suspension (in RPMI) was equilibrated at 7°C for 15min. Ten µl of a 200nM chemokine solution (final chemokine concentration: 20nM) or RPMI medium alone were added and incubated with the cells for 30min. The plate was centrifuged for 3min at 10°C, the supernatant discarded and the cells washed once with 150µl ice cold RPMI followed by a washing step with FACS buffer. CCL19-S6^{649P1} fluorescence was measured on a BD LSRFortessa flow cytometer.

2D-Transwell Migration Assay

R848-matured GM/CAL-1 cells, stable transfected (sub)lines, or gene edited GM/CAL-1 cell clones (1×10^5 in complete growth medium) were seeded into the top chambers on a polycarbonate filter with a pore size of 5µm in a 24-well Transwell plate (Corning Costar; Vitaris, Baar, Switzerland) and allowed to migrate towards the lower chamber wells containing 600µl of complete growth medium without chemokine (random migration) or supplied with 30nM human CCL19 or CCL21, an optimal concentration for DCs in this assay (37, 38), for 3h at 37°C, 5% CO_2. A 500µl aliquot of migrated cells was collected and acquired for 60sec at high flow rate on a BD LSRII or for 90sec at medium flow rate on a BD LSRFortessa flow cytometer (39). Values are given as percentage of migrated cells relative to the input of cells.

3D Migration Assay and Imaging

Migration through a three-dimensional collagen type I gel matrix was performed in tissue culture-treated ibiTreat µ-slide chemotaxis chambers (ibidi, Vitaris, Baar, Switzerland) as described (42, 43). Briefly, dead cells were removed using a dead cell removal kit, and the remaining viable R848-matured GM/CAL-1 cells, cell clones or stable transfected (sub)lines were resuspended at 10^7 cells/ml in RPMI supplemented with 10% heat inactivated FCS. Twenty µl 10x DMEM, 10µl 7.5% $NaHCO_3$, and 150µl PureCol collagen I (Advanced Biomatrix; CellSystems, Troisdorf, Germany) were premixed, carefully mixed with 90µl cell suspension, applied to µ-slide chemotaxis chambers, and then allowed to polymerize. Chemokines were added to the right reservoir (100nM) and allowed to establish a stable gradient as described (42). Cell migration was recorded using the Zeiss ZEN pro 2012 software by time-lapse video microscopy at 2-min intervals using a 10x objective and a MRm camera on a Zeiss Axiovert 200M equipped with an automated stage and a 37°C environmental Tokai Hit INU (Shizuoka Japan) incubation system for 2.5h (75 frames). Cell tracking was performed using the ImageJ/Fiji (NIH, National Institutes of Health, USA) plugin 'Manual Tracking' and migration parameters were quantified using the 'Chemotaxis and Migration Tool' from ibidi. Analysis was restricted to motile cells by eliminating objects that displaced less than twice the cell body size during the 2.5h imaging process. For live cell imaging, migrating R848-matured GM/CAL-1 cells stably expressing PH-Akt-GFP were imaged on a Zeiss Axiovert 200M (5min intervals) and on a laser scanning microscope (Leica TCS SP5; Leica, Heerbrugg, Switzerland using the HCX PL APO CS 63.0×1.40 OIL UV objective) at 1min intervals using a microscope stage fitted with a Tokai Hit Thermoplate at 37°C.

Statistical Data Analysis

Data are presented in the figures as means ± SEM or SD, as indicated in the corresponding figure legends. For multiple group comparisons, a one-way ANOVA test was performed, followed by Dunnett's or Tukey's multiple comparisons tests using GraphPad Prism 6.07 (GraphPad Software, San Diego, CA, USA). Asterisks in graphs indicate statistical significance (****$p < 0.0001$; ***$p < 0.001$; **$p < 0.01$; *$p < 0.05$).

RESULTS

Phenotypic Characterization of Human CAL-1 Cells

The human dendritic cell line CAL-1 originates from a patient with blastic natural killer cell lymphoma (30), a disease also

known as blastic plasmacytoid dendritic cell neoplasma (31). Accordingly, CAL-1 cells were reported to express the human pDC marker CD123 (IL-3Rα), together with the MHC class II molecule HLA-DR and low levels of the α_x integrin CD11c (30). Using flow cytometric analysis, we confirm that CAL-1 cells expressed CD11c and high levels of CD123 and HLA-DR (**Figure 1A**). Moreover, CAL-1 cells also expressed the co-stimulatory molecule CD86, but barely expressed the co-stimulatory molecule CD40 (**Figure 1A**). The chemokine receptor CCR7, required for lymph node homing of DCs, was not detected on the surface of CAL-1 cells (**Figure 1A**). Exposing CAL-1 cells to the danger signal and DC maturation stimulus CpG-B (a ligand for TLR9) for 18h did not substantially alter CD123, CD11c, CD86 or HLA-DR expression and failed to effectively induce surface expression of CD40 and CCR7 (**Figure 1A**). Similarly, maturing CAL-1 cells with the TLR7/8 ligand R848, although inducing CD40, only marginally induced CCR7 on some of the cells (**Figure 1A**).

CCR7 Induction in CAL-1 Cells Upon Exposure to GM-CSF and Maturation by R848

CAL-1 cells were reported to enhance CD11c surface expression (30) and to up-regulate MHC class II RNA expression (34) upon cultivation in the presence of GM-CSF for 3 days. Hence, we exposed CAL-1 cells for 3 days to GM-CSF and subsequently

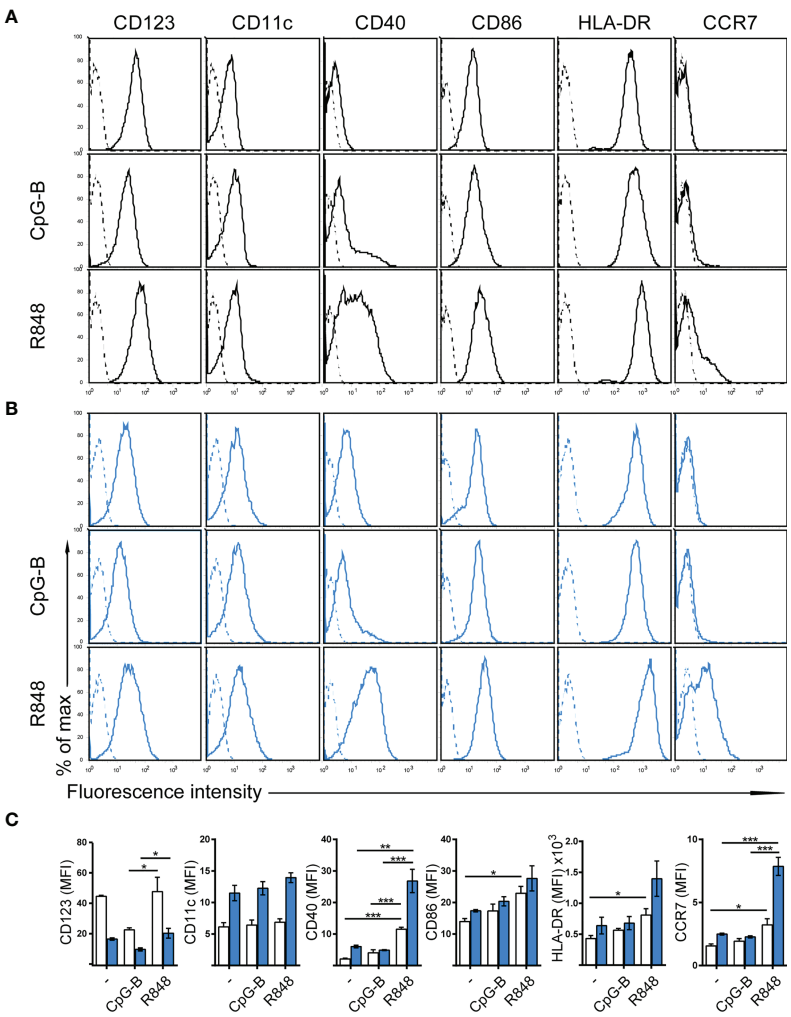

FIGURE 1 | Phenotypic characterization of human CAL-1 cells and CCR7 induction upon exposure to GM-CSF and maturation by R848. **(A)** Surface expression of CD123, CD11c, CD40, CD86, HLA-DR and CCR7 (solid lines) on CAL-1 cells that were stimulated or not for 18-19h with the TLR9 ligand CpG-B ODN 2006 (1μM) or the TLR7/8 ligand Resiquimod R848 (10μg/ml). Representative flow cytometry histograms derived from one out of three independent experiments are depicted. Unstained cells or isotype-matched controls for CCR7 stainings are shown as dashed lines. **(B)** Surface expression of CD123, CD11c, CD40, CD86, HLA-DR and CCR7 on CAL-1 cells cultured for 3 days in the presence of 10ng/ml GM-CSF. Where indicated, these GM/CAL-1 cells were in addition matured by either CpG-B or R848 as in **(A)**. Representative flow cytometry histograms derived from one out of three independent experiments are depicted. **(C)** Quantitative analysis of surface markers on CAL-1 (white bars) and GM/CAL-1 (blue bars) cells. Mean values ± SEM of the 3 independent experiments **(A, B)** are shown.

induced maturation by either CpG-B or R848 for 18 to 19h. Notably, CAL-1 cells cultured for 3 days in GM-CSF, subsequently termed GM/CAL-1 cells, expressed lower levels of CD123 (**Figures 1B, C** blue bars) compared to CAL-1 cells cultured in the absence of GM-CSF (**Figures 1A, C** white bars), irrespectively whether cells were in addition matured by CpG-B or R848 (**Figure 1**). By contrast, GM/CAL-1 cells expressed slightly higher surface levels of CD11c than CAL-1 cells cultured under traditional conditions, and CD11c expression levels remained unaltered upon maturation (**Figures 1B, C**). The expression of the co-stimulatory molecules CD40 and CD86, as well as HLA-DR, were highest in GM/CAL-1 cells matured with R848 (**Figures 1B, C**). Importantly, GM/CAL-1 cells matured by R848, but not by CpG-B, profoundly induced surface expression of CCR7 (**Figures 1B, C**), a prerequisite for the homing of antigen-bearing DCs to draining lymph nodes. Collectively these results indicate that the human dendritic cell line CAL-1 acquires a more myeloid-like phenotype if exposed to GM-CSF, and most importantly up-regulates the expression of the chemokine receptor CCR7 upon maturation by the TLR7/8 ligand R848.

FITC-Dextran Uptake and TNFα Production by CAL-1 and GM/CAL-1 Cells

Next, we determined FITC-dextran uptake as a surrogate for antigen uptake by these human cells. For this, we pre-stimulated CAL-1 cells with R848 for 30min and determined FITC-dextran uptake over time by flow cytometry. As shown in **Figure 2A**, CAL-1 cells readily and continuously took up FITC-dextran. Similarly, R848 pre-stimulated GM/CAL-1 cells retained their capacity to take-up FITC-dextran (**Figure 2A**). Maturing CAL-1 and GM/CAL-1 cells with either CpG-B or R848 for 24h before adding FITC-dextran for 30min barely affected the cell's capacity to take-up FITC-dextran (**Figure 2B**). As expected (32, 33), stimulating CAL-1 cells with either CpG-B or R848 strongly induced the production of TNFα as determined by a flow cytometric intracellular cytokine staining assay (**Figure 2C**). GM/CAL-1 cells also produced TNFα upon TLR stimulation (**Figure 2C**), however, the percentage of cytokine producing cells was reduced compared to CAL-1 cells cultured in the absence of GM-CSF.

Mature GM/CAL-1 Cells Elicit CCR7 Signaling Pathways

To assess whether R848-driven GM/CAL-1 cell maturation induces functional CCR7 expression, we determined if chemokine stimulation elicits signal transduction. Activation of chemokine receptors by cognate ligands typically mobilize intracellular calcium (44), which is required for human MoDC migration (45). Stimulating R848-matured GM/CAL-1 cells with 30nM of either CCL19 or CCL21 induced a rapid and transient increase in the cytosolic free Ca^{2+} ($[Ca^{2+}]_i$) (**Figure 3A**). Chemokine-mediated $[Ca^{2+}]_i$ mobilization was abrogated by *Bordetella pertussis* toxin (PTx) treatment (**Figure 3A**), which manifests G_i-protein dependent CCR7 signaling. Furthermore, we determined additional signaling pathways downstream of CCR7. Both ligands induced the phosphorylation of ERK1/2 of the MAP-kinase signaling cascade in R848-matured GM/CAL-1 cells (**Figure 3B**). Chemokine-mediated ERK1/2 phosphorylation peaked at 2min after CCR7 triggering and remained detectable for up to at least 10min. Similarly, CCL19 and CCL21 stimulation resulted in transient phosphorylation of protein kinase B (PKB)/Akt (**Figure 3B**).

Mature GM/CAL-1 Cells Readily Migrate Towards CCR7 Ligands

Next, we assessed the migratory capacity of R848-matured GM/CAL-1 cells in two-dimensional Transwell chemotaxis assays where cells migrate across a semipermeable filter into the lower compartment containing the chemokine. Mature GM/CAL-1 cells essentially did not migrate towards medium, but effectively migrated in response to 30nM of either CCL19 or CCL21 (**Figure 4A**). Subsequently, we monitored cell migration by time-lapse video microscopy where we embedded mature GM/CAL-1 cells in a collagen I three-dimensional gel matrix within ibiTreat μ-slide chemotaxis chambers. R848-matured GM/CAL-1 cells exposed to CCL19 or CCL21 gradients established within this 3D-device showed a polarized phenotype typical for migrating cells (**Figure 4B**). Notably, about 30% of the R848-matured GM/CAL-1 cells exposed to either CCR7 ligand were motile; i.e. displaced more than twice the cell diameter within the 2.5h period of measurement (**Figure 4B**). In the absence of chemokines, less than 4% of the R848-matured GM/CAL-1 cells were motile (**Figure 4B**). For comparison, as little as 2.4 ± 0.5% of R848-matured CAL-1 cells (i.e. that were not exposed to GM-CSF) were motile and only marginally more cells, namely 3.3 ± 1.7%, were motile if stimulated with CCL19 (**Figure 4B**). By contrast, R848-matured GM/CAL-1 cells efficiently and readily migrated along CCL19 and CCL21 gradients in a 3D collagen environment (**Figure 4C**). Tracking the paths of migrating cells revealed a directionality of R848-matured GM/CAL-1 cells of 0.82 ± 0.03 for CCL19, 0.77 ± 0.03 for CCL21, and 0.46 ± 0.08 for medium, respectively (**Figure 4D**). The forward migration indices on the x-axis along the chemokine gradient (xFMI) were 0.77 ± 0.03 for cells migrating towards CCL19 and 0.73 ± 0.03 for cell migration in response to CCL21, whereas the xFMI of cells migrating in response to medium was -0.00 ± 0.03 (**Figure 4D**). Migrating R848-matured GM/CAL-1 cells reached a velocity of 1.77 ± 0.17 μm/min in the direction of CCL19 and 1.85 ± 0.16 μm/min towards CCL21, but only 0.45 ± 0.13 μm/min in response to medium (**Figure 4D**). Hence, we demonstrated that GM/CAL-1 cells matured by R848 express functional CCR7, elicit early chemokine-mediated G_i-dependent signaling pathways and readily migrate in response to chemokines in 2D and 3D environments.

Mature GM/CAL-1 Cells Serve as a Versatile Model System to Study Human DC Migration

Importantly, we set out to probe the tractability of expressing fluorescent reporter proteins in this human DC line. As a proof-of-concept, we established a CAL-1 cell line stably expressing the

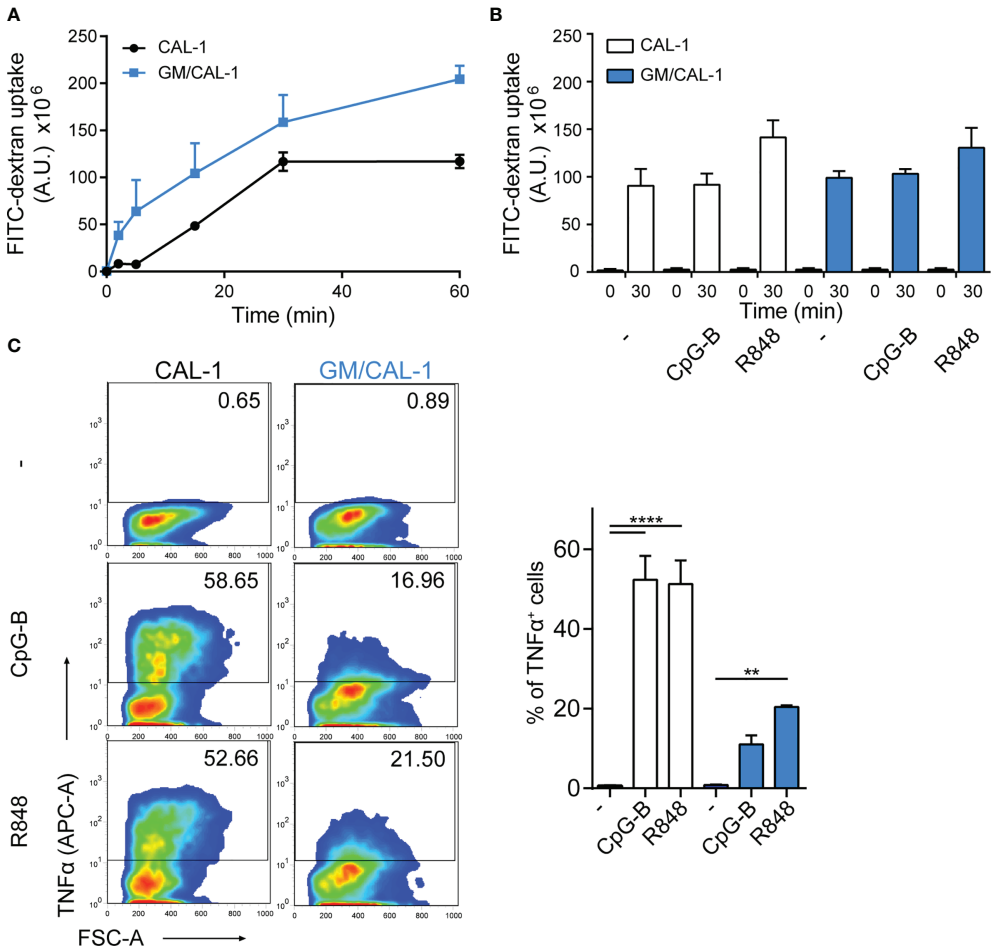

FIGURE 2 | FITC-dextran uptake and TNFα production by CAL-1 and GM/CAL-1 cells **(A)** Time-dependent FITC-dextran uptake by CAL-1 and GM/CAL-1 cells. CAL-1 cells were cultured in the absence (CAL-1; back line) or presence of GM-CSF (GM/CAL-1; blue line) for 3 days, pre-stimulated with R848 for 30min and subsequently incubated with 1mg/ml of FITC-dextran for indicated time periods at 37°C. Cells were extensively washed and FITC-dextran uptake was quantified by flow cytometry. The area under the curve [A.U.] was calculated by multiplying the mean fluorescence intensity (MFI) values and the event count of live, FITC-positive cells. Mean values ± SEM of 3 independent experiments are shown. **(B)** FITC-dextran uptake by mature CAL-1 and GM/CAL-1 cells. CAL-1 (white bars) and GM/CAL-1 (blue bars) were left untreated (–) or matured with either CpG-B or R848 for 24h. FITC-dextran uptake at t=0 or t=30min of incubation with 1mg/ml of FITC-dextran was determined and quantified by flow cytometry as in **(A)**. Mean values ± SEM of 3 independent experiments are shown. **(C)** TNFα production by CAL-1 and GM/CAL-1 cells. CAL-1 or GM/CAL-1 cells were stimulated or not with CpG-B or R848 for 6h. For the last 4h of incubation 10µg/ml Brefeldin A was added to prevent cytokine secretion. Cells were fixed, permeabilized, and the percentage of cells with intracellularly accumulated TNFα was determined by ICS and flow cytometry. One representative pseudocolor dot plot (left panels) and quantification of three (bar graphs on the right panel; CAL-1: white bars, GM/CAL-1: blue bars) independent experiments are shown as mean values ± SEM.

PH-domain of Akt fused to EGFP (PH-Akt-GFP), a biosensor for the major second messenger lipid phosphatidylinositol-3,4,5-trisphosphate (35), that is produced down-stream of G-protein activation upon chemokine stimulation (44, 46). To achieve this, we nucleofected CAL-1 cells with the fluorescent reporter plasmid and let the cells grow under selective antibiotic pressure. After two weeks, GFP-positive cells were bulk sorted to establish a stable PH-Akt-GFP expressing CAL-1 cell line (**Figure 5A**). R848-matured GM/CAL-1 PH-Akt-GFP^{line} cells expressed endogenously induced CCR7 on the cell surface together with transfected PH-Akt-GFP (**Figure 5C**). These cells were subsequently subjected to ibiTreat µ-slide chemotaxis chambers and allowed to migrate along a CCL19 gradient within a 3D collagen environment. PH-Akt-GFP was expressed in the cytosol of R848-matured GM/CAL-1 cells and accumulated at the leading edge while cells migrated in 3D collagen towards CCL19 (**Figure 5C** and **Supplementary Video 1**). To substantiate these findings, we established two additional CAL-1 sublines with different PH-Akt-GFP expression levels, referred to as subline 1 and subline 2 (**Figure 5A**). R848-matured GM/CAL-1 PH-Akt-GFP$^{subline\ 2}$ cells were allowed to migrate towards CCL19 in 3D collagen. Drawing a line alongside the cell axis and plotting the intensity of GFP along this line clearly revealed accumulation of PH-Akt-

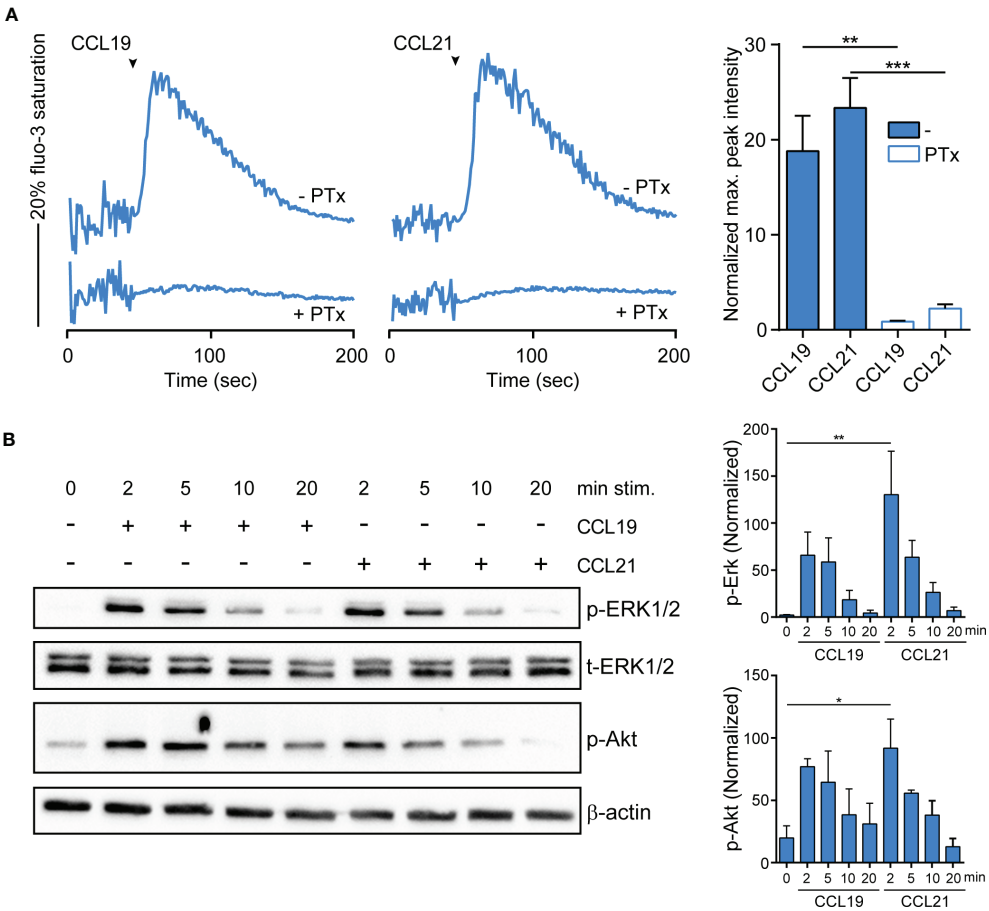

FIGURE 3 | CCR7-mediated calcium mobilization and phosphorylation of ERK1/2 and Akt in R848-matured GM/CAL-1 cells. **(A)** CCL19/CCL21-induced calcium mobilization in mature GM/CAL-1 cells. R848-matured GM/CAL-1 cells were treated or not with 200ng/ml PTx for 3h, loaded with fluo-3-AM and stimulated with 30nM of either CCL19 or CCL21. Changes in intracellular calcium levels were recorded by flow cytometry over time. Chemokine addition is indicated by arrowheads. One representative (left panels) and mean values ± SEM of 3 independent experiments (right panel) are shown. Maximal peak intensity of chemokine-induced fluo-3 fluorescence was baseline corrected and normalized to ionomycin treatment by calculating the mean of ten maximal fluo-3 fluorescence values derived from each stimulation condition, respectively. **(B)** CCR7 triggering results in transient ERK1/2 and Akt phosphorylation. R848-matured GM/CAL-1 cells were stimulated with 100nM of either CCL19 or CCL21 for the indicated time periods. Chemokine-mediated activation of ERK1/2 and Akt was determined by Western blotting. Phosphorylation was determined using antibodies recognizing the phosphorylated forms of Thr202/Tyr204 of ERK1/2 (p-ERK1/2), and the phosphorylated form of S473 of Akt (p-Akt). Antibodies recognizing total ERK1/2 (t-ERK) and β-actin served as control for equal protein loading. One representative (left panel) and mean values ± SEM of 3 independent experiments (right panel) are shown.

GFP at the front of the migrating cells (**Figure 5B**). Side-by-side comparison of parental CAL-1 with the CAL-1 PH-Akt-GFP line and the two CAL-1 PH-Akt-GFP sublines revealed similar CCR7 induction upon sequential exposure to GM-CSF and R848-induced maturation (**Figure 5D**). Importantly, the GM/CAL-1 PH-Akt-GFP line and the two sublines robustly migrated in response to CCL19 and CCL21 as assessed in Transwell migration assays (**Figure 5E**).

Finally, we targeted CCR7 by CRISPR/Cas9 gene editing to generate two CCR7-knockout CAL-1 cell clones, named CCR7-KO #1 and CCR7-KO #10. In addition, we established three CAL-1 clones (#2, #3, #11) from parental CAL-1 cells by single cell sorting. Parental CAL-1 cells, the two CCR7-KO clones and the three single cell clones were exposed to GM/CSF followed by R848-driven maturation. Parental GM/CAL-1 cells, as well as the three parental cell clones effectively bound fluorescently labelled CCL19-S6^{649P1} (41) although with some clonal variation (**Figure 6A**). By contrast, the CCR7-KO cell clones failed to bind the fluorescent CCR7 ligand (**Figure 6A**). Moreover, GM-CSF exposed and R848-matured CCR7-KO clones failed to migrate in response to CCL19 and CCL21, whereas the parental R848-matured GM/CAL-1 cell line and the individual cell clones efficiently migrated towards the chemokines (**Figure 6B**).

In summary, we demonstrated that CAL-1 cells induced CCR7 expression if exposed to GM-CSF and matured by the TLR7/8 ligand Resiquimod R848. To the best of our knowledge, this is the first report of a human DC-like cell line with endogenous CCR7 expression permitting to study CCR7

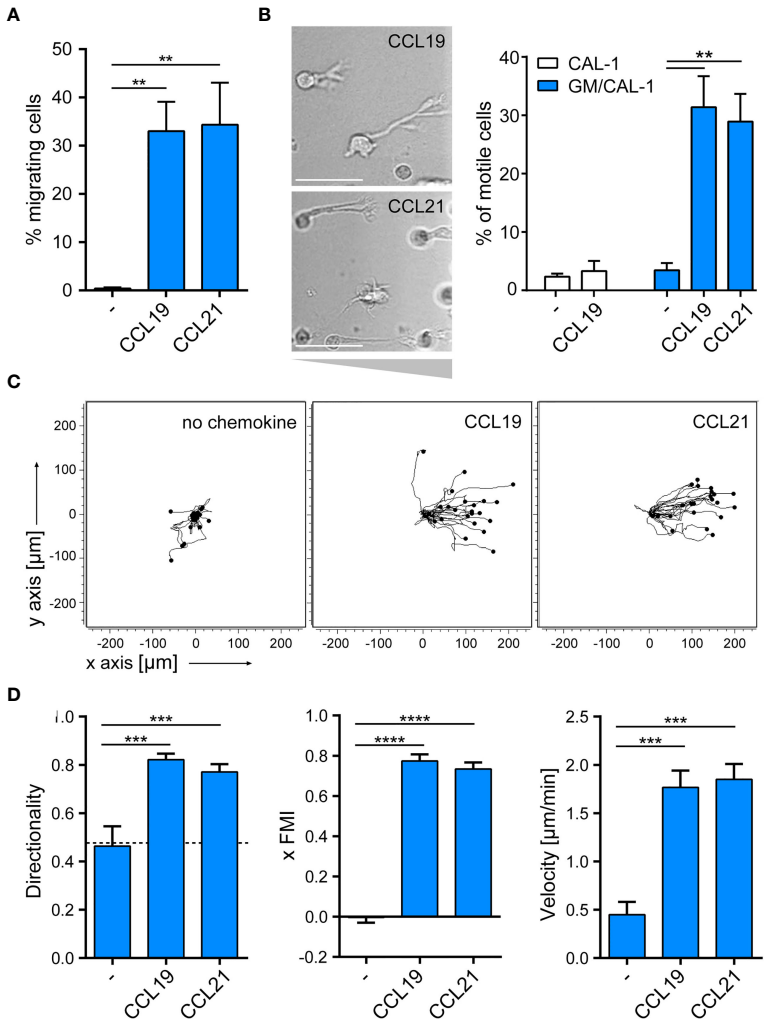

FIGURE 4 | R848-matured GM/CAL-1 cells readily migrate towards CCR7 ligands in 2D and 3D environments. **(A)** Mature GM/CAL-1 cells specifically migrate in response to CCL19 and CCL21 in 2D Transwell migration assays. CAL-1 cells were cultured for 3 days in 10ng/ml GM-CSF followed by maturation with 10µg/ml R848 for another 18.5h. R848-matured GM/CAL-1 cells were allowed to migrate towards medium (–), or 30nM of either CCL19 or CCL21 in Transwell chemotaxis chambers for 3h. Percent migrated cells was determined by flow cytometry. Mean values ± SD derived from n = 3 independent experiments are shown. **(B–D)** Mature GM/CAL-1 cells migrate directionally along chemokine gradients in 3D. R848-matured GM/CAL-1 cells were embedded into a three-dimensional collagen type I gel matrix in Ibidi µ-slide chemotaxis chambers and allowed to migrate along CCL19 or CCL21 gradients. Cell migration was monitored by time-lapse video microscopy (time lag τ = 2 min). **(B)** Representative DIC images of migrating mature GM/CAL-1 cells are shown on the left panel. Scale bar: 50µm. Percentage of motile CAL-1 (not treated with GM-CSF; white bars) or GM/CAL-1 (blue bars) cells in a 3D environment in the presence or absence of chemokine derived from all cells located in the entire matrix area is depicted on the right. Mean values ± SEM of at least 3 independent experiments are shown. **(C)** Single R848-matured GM/CAL-1 cells randomly moving in the absence (left panel), or migrating towards CCL19 (middle panel) or CCL21 (right panel panel) from a representative experiment were tracked using an ImageJ/Fiji plug-in and individual tracks are shown in a spider plot. **(D)** Directionality, xFMI and velocity of individually migrating cells derived from three independent experiments were quantified. Mean values ± SEM of 3-6 independent experiments are shown. At least 10 cells per condition for every experiment, and a total of 65, 112 or 92 cells were analyzed for steady state (in the absence of chemokine), CCL19- or CCL21- directed migration, respectively.

signaling and migration. As a proof-of-concept using PH-Akt-GFP, we further show that CAL-1 cells can be genetically modified to express fluorescent reporter proteins to study spatio-temporal signaling. The established CAL-1 PH-Akt-GFP cell lines and sublines remain stable and possess comparable migration capacities as the parental cell line. Moreover, we demonstrate that knockout cell clones can be generated. Hence, we here provide evidence that GM/CAL-1 cells serve a unique, valuable cellular model system to study human DC migration.

DISCUSSION

DCs are used as cellular vaccines to transport and deliver tumor antigens to cognate T cells to augment tumor antigen-specific T cell

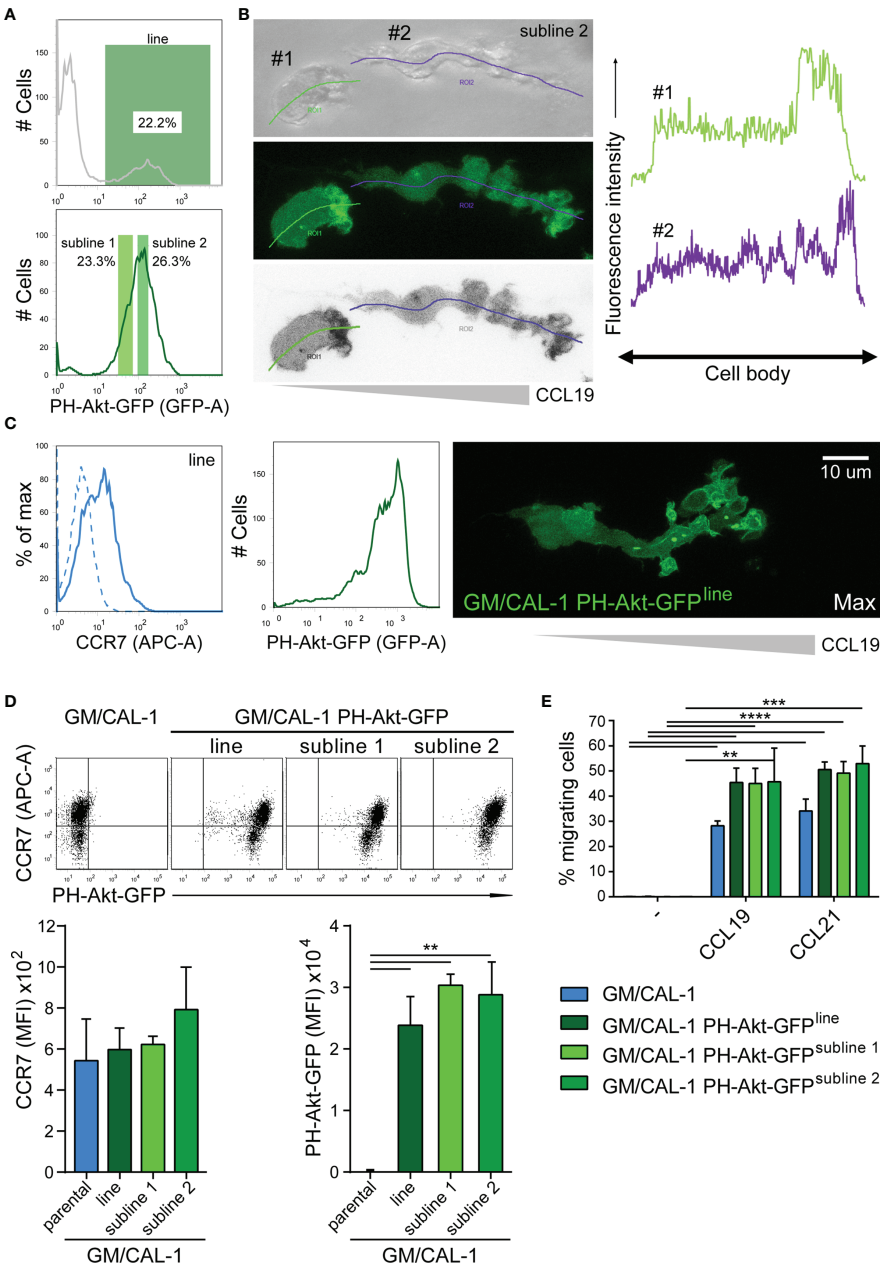

FIGURE 5 | Establishing stable cell lines to monitor PH-Akt-GFP, a biosensor for PIP_3, in migrating R848-matured GM/CAL-1 cells. **(A)** Generation of a stable CAL-1 PH-Akt-GFP line and two sublines. CAL-1 cells were nucleofected with a plasmid coding for PH-Akt-GFP. After two weeks of selection, 22.2% of the cell population stably expressed PH-Akt-GFP and was bulk sorted (upper panel), revealing a stable line termed CAL-1 PH-Akt-GFP^{line}. After 21 days in culture under G418 selection, two sub-lines were generated according to the gating strategy shown in the lower panel. **(B)** PH-Akt-GFP accumulates at the leading edge of migrating cells. R848-matured GM/CAL-1 PH-Akt-GFP$^{subline\ 2}$ cells were embedded in 3D collagen and allowed to migrate towards CCL19. Bright field (upper left panel), GFP-fluorescent confocal (middle left panel), and inverted gray scale confocal (lower left panel) image of two individual migrating cells are shown. Line scan plots for PH-Akt-GFP along the cell axis of the two cells are depicted in the right panels. **(C)** Surface expression of CCR7 (left flow cytometry panel; blue solid line; isotype control: dashed line) and PH-Akt-GFP fluorescence (right flow cytometry panel) in R848-matured GM/CAL-1 PH-Akt-GFP^{line} cells was determined by flow cytometry. Maximal PH-Akt-GFP projection of a cell migrating through a 3D collagen I matrix along a CCL19 gradient is shown on the right. The corresponding time-lapse confocal microscopy video 1 can be found in the supplement. **(D)** CAL-1 PH-Akt-GFP (sub)lines retain their transgene and comparably induce CCR7 upon exposure to GM/CSF and maturation by R848. Representative CCR7/PH-Akt-GFP dot plots (upper panel) and quantification of all three independent experiments performed with parental GM/CAL-1 cells or GM/CAL-1 PH-Akt-GFP line and sublines, respectively, for CCR7 surface expression (lower left bar graph) and PH-Akt-GFP expression (lower right bar graph) are depicted as mean values ± SEM of median fluorescence intensities. **(E)** R848-matured GM/CAL-1, GM/CAL-1 PH-Akt-GFP^{line}, GM/CAL-1 PH-Akt-GFP$^{subline\ 1}$, or GM/CAL-1 PH-Akt-GFP$^{subline\ 2}$ migrate in response to 30nM CCL19 or 30nM CCL21 in a 2D Transwell chemotaxis assay. Percentage of migrated cells was determined by flow cytometry after 3h of migration. Mean values ± SD of 3 independent experiments are shown.

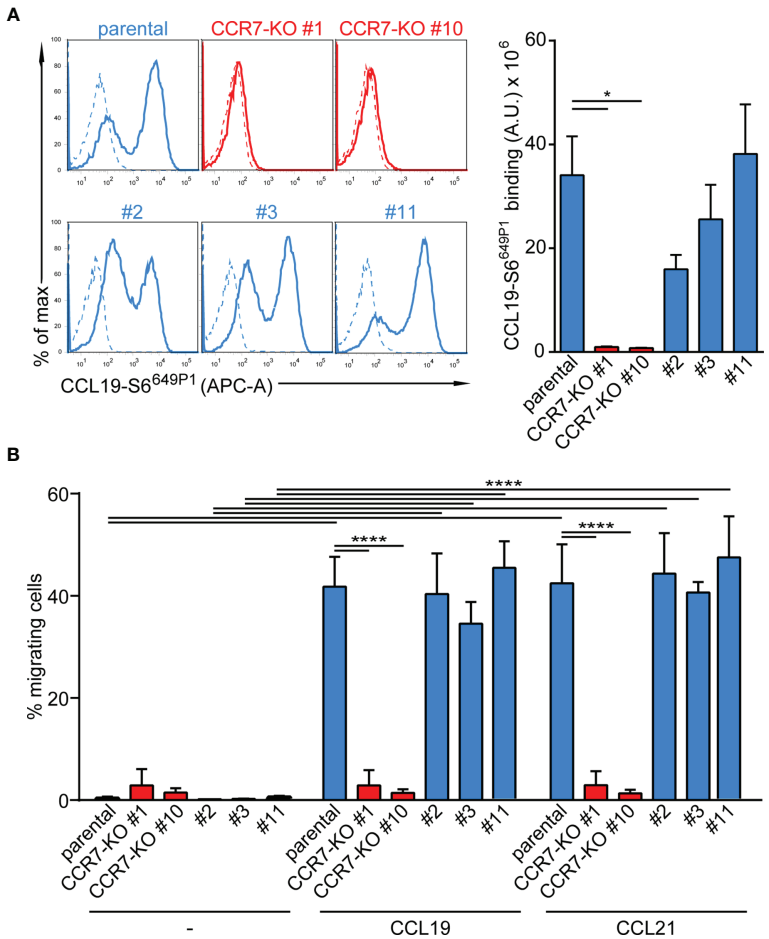

FIGURE 6 | Functional characterization of CCR7-KO and parental CAL-1 single cell clones. **(A)** R848-matured GM/CAL-1 CCR7-KO single cell clones fail to bind fluorescent CCL19-S6^{649P1}, while R848-matured parental GM/CAL-1 cells or individual parental single cell clones bind the fluorescent chemokine. Cells (1.8x 10^5) were incubated for 30min with 20nM of fluorescent chemokine at 7°C. Chemokine binding was measured by flow cytometry. Representative histograms (solid lines: with chemokine, dashed lines: without chemokine) and quantification of CCL19-S6^{649P1} binding to R848-matured GM/CAL-1 cells (parental), GM/CAL-1 CCR7-KO clone #1 and #10, as well as three single clones (#2, #3, #11) established from parental CAL-1 cells. A representative histogram plot and mean values ± SEM of 3 independent experiments are shown. For quantification, the area under the curve [A.U.] was calculated by multiplying the mean CCL19-S6^{649P1} fluorescence intensity (MFI) values by the event count of live cells. **(B)** R848-matured GM/CAL-1 single cell clones retain their migratory capacity while CCR7-KO clones do not. R848-matured parental GM/CAL-1 and individual single cell clones were assessed by 2D Transwell migration assays in response to medium (–), 30nM CCL19 or CCL21 for 3h. Percentage of migrating cells was determined by flow cytometry. Mean values ± SD of 3 independent experiments are shown.

responses in cancer patients. Importantly, to be successful as cellular immunotherapy, DCs must migrate to lymph nodes to encounter antigen-specific T cells and to launch an adaptive immune response against the tumor (7). Hence, understanding how chemokines guide DC migration and homing to lymph nodes is pivotal, and cellular model systems to study human DC migration are highly desired. The chemokine receptor CCR7 is responsible for controlling DC migration from peripheral tissues to draining lymph nodes. Whereas most blood circulating T cells express CCR7, peripheral DCs induce this chemokine receptor only upon encounter of danger signals (13, 14, 26). CCR7 induction has been shown to predominantly involve the transcription factors NF-κB and AP-1 (47, 48). Interestingly, among all chemokine receptors, CCR7 possesses a unique signal sequence that facilitates its package into COPII vesicles for efficient ER to Golgi trafficking, and thus surface expression (36). Whereas bacterial-derived LPS, a ligand for TLR4, is the most used and effective danger signal to induce CCR7 expression on mouse BMDCs (49), human MoDCs only poorly respond to LPS, but instead readily respond to pro-inflammatory cytokines and synthetic TLR ligands, such as CpG or Resiquimod (13, 14, 26). MoDCs are likely to be the most commonly used model system to study human DCs. However, human MoDCs show substantial donor to donor variations and need to be differentiated from freshly isolated blood monocytes. A human cell line with DC characteristics and features that can be genetically manipulated would be a valuable tool to investigate molecular mechanisms controlling CCR7-depedent cell migration. Human leukemia cells of myeloid origin, such as conventional, as well as differentiated and

matured HL60 and THP1 cells, or MUTZ cells were tested (29), but none of these attempts succeeded in cells that expressed CCR7 and migrated towards its chemokine ligands.

In the present study, we explored the human CAL-1 cell line that has been established from a patient with blastic plasmacytoid DC neoplasm (30). Although Karrich and colleagues previously reported a homogeneous CCR7 expression on CAL-1 cells in the absence of a maturation stimulus without assessing receptor functions (32), we did not detect CCR7 under these conditions. Moreover, in our hands, exposing CAL-1 cells to CpG-B failed to induce CCR7 expression. However, we observed that CAL-1 cells stimulated with Resiquimod slightly induced CCR7. Spurred by this observation, combined with previous reports that CAL-1 cells (in contrast to plasmacytoid DCs) are sensitive to GM-CSF (30, 34), we exposed CAL-1 cells to GM-CSF for 3 days and subsequently triggered them by synthetic TLR ligands. Exposure to GM-CSF resulted in the down-regulation of CD123, while enhancing the expression of CD11c and MHC class II. Moreover, GM/CAL-1 cells were able to take-up FITC-dextran, suggesting that they are able to take-up antigens, and to secrete cytokines like TNFα. Importantly, such GM/CAL-1 cells triggered with Resiquimod induced expression of endogenous CCR7. Hence, GM/CAL-1 cells share critical characteristics and features of human MoDCs. We further demonstrated that Resiquimod-matured GM/CAL-1 cells readily migrate in response to both CCR7 ligands, CCL19 and CCL21, in two-dimensional and 3-dimentional collagen environments. Moreover, CCR7 activation triggered, in a G_i-protein dependent manner, a transient Ca^{2+} response in Resiquimod-matured GM/CAL-1 cells, which is a key component of the migration machinery (45, 50). Notably, in our hands, Resiquimod-stimulated CAL-1 cells that were not previously exposed to GM-CSF remained rather immobile and essentially failed to migrate towards CCR7 ligands in 3D environments.

Finally, the ability to genetically modify human DC-like cells is highly desired. As a proof-of-concept, we established a CAL-1 cell line and two sublines stably expressing the fluorescent biosensor PH-Akt-GFP, which upon exposure to GM-CSF and maturation with Resiquimod, accumulated at the leading edge of cells migrating towards CCR7 ligands. Interestingly, we also noted vesicular structures at the front of migrating cells that stained for PH-Akt-GPF. This observation is in line with our previous study showing endomembrane CCR7 signaling (43). Hence, CAL-1 cells expressing fluorescent biosensors can be exploited in future studies to shed light in spatial signaling during cell migration. Moreover, CAL-1 cells can be modified by introducing siRNA as successfully reported by Miura and colleagues (34). Here, we provide evidence that CAL-1 cells can also be gene edited using the CRISPR/Cas9 technology, thereby extending the palette of technologies to genetically modify and exploit this cell line. Taken together, in the present study, we demonstrated that human CAL-1 cells serve as versatile cellular model system to study CCR7-guided human DC migration.

DATA AVAILABILITY STATEMENT

The original contributions presented in the study are publicly available. This data can be found here: https://zenodo.org/record/4719596#.YUC2-J0zaUm and https://zenodo.org/record/5507215#.YUDCMp0zaUk.

AUTHOR CONTRIBUTIONS

EU-vA and DFL designed the study, analyzed data and wrote the manuscript. EU-vA, GS, and VP performed all experiments. TM provided essential reagents. All authors reviewed the manuscript. DFL supervised the overall study and acquired funding. All authors contributed to the article and approved the submitted version.

FUNDING

This study was supported in parts by research funding from the Swiss National Science Foundation (grant number 310030_189144), the Thurgauische Stiftung für Wissenschaft und Forschung, and the State Secretariat for Education, Research and Innovation to DFL.

ACKNOWLEDGMENTS

We thank Ilona Kindinger and Cecilia Kramp for technical support.

SUPPLEMENTARY MATERIAL

The Supplementary Material for this article can be found online at: https://www.frontiersin.org/articles/10.3389/fimmu.2021.702453/full#supplementary-material

Supplementary Video 1 | Representative time-lapse confocal microscopy video (Maximal projections; duration: 32min; scale bar: 10μm) of a R848-matured GM/CAL-1 PH-Akt-GFP^{line} cell migrating along a CCL19 gradient formed in a three-dimensional collagen I matrix using ibiTreat μ-slide chemotaxis chambers. The image depicted in **Figure 5C** is taken from this movie at t= 11min.

REFERENCES

1. Banchereau J, Steinman RM. Dendritic Cells and the Control of Immunity. *Nature* (1998) 392(6673):245–52. doi: 10.1038/32588
2. Mellman I, Steinman RM. Dendritic Cells: Specialized and Regulated Antigen Processing Machines. *Cell* (2001) 106(3):255–8. doi: 10.1016/s0092-8674(01)00449-4
3. Worbs T, Hammerschmidt SI, Forster R. Dendritic Cell Migration in Health and Disease. *Nat Rev Immunol* (2017) 17(1):30–48. doi: 10.1038/nri.2016.116
4. Guermonprez P, Valladeau J, Zitvogel L, Thery C, Amigorena S. Antigen Presentation and T Cell Stimulation by Dendritic Cells. *Annu Rev Immunol* (2002) 20:621–67. doi: 10.1146/annurev.immunol.20.100301.064828
5. Palucka K, Banchereau J. Dendritic-Cell-Based Therapeutic Cancer Vaccines. *Immunity* (2013) 39(1):38–48. doi: 10.1016/j.immuni.2013.07.004

6. Bol KF, Schreibelt G, Gerritsen WR, de Vries IJ, Figdor CG. Dendritic Cell-Based Immunotherapy: State of the Art and Beyond. *Clin Cancer Res* (2016) 22(8):1897–906. doi: 10.1158/1078-0432.CCR-15-1399
7. Bryant CE, Sutherland S, Kong B, Papadimitrious MS, Fromm PD, Hart DNJ. Dendritic Cells as Cancer Therapeutics. *Semin Cell Dev Biol* (2019) 86:77–88. doi: 10.1016/j.semcdb.2018.02.015
8. Merad M, Sathe P, Helft J, Miller J, Mortha A. The Dendritic Cell Lineage: Ontogeny and Function of Dendritic Cells and Their Subsets in the Steady State and the Inflamed Setting. *Annu Rev Immunol* (2013) 31:563–604. doi: 10.1146/annurev-immunol-020711-074950
9. Murphy TL, Grajales-Reyes GE, Wu X, Tussiwand R, Briseno CG, Iwata A, et al. Transcriptional Control of Dendritic Cell Development. *Annu Rev Immunol* (2016) 34:93–119. doi: 10.1146/annurev-immunol-032713-120204
10. Cabeza-Cabrerizo M, Cardoso A, Minutti CM, Pereira da Costa M, Reis ESC. Dendritic Cells Revisited. *Annu Rev Immunol* (2021) 26(39):1311–66. doi: 10.1146/annurev-immunol-061020-053707
11. MacDonald KP, Munster DJ, Clark GJ, Dzionek A, Schmitz J, Hart DN. Characterization of Human Blood Dendritic Cell Subsets. *Blood* (2002) 100 (13):4512–20. doi: 10.1182/blood-2001-11-0097
12. Griffith JW, Sokol CL, Luster AD. Chemokines and Chemokine Receptors: Positioning Cells for Host Defense and Immunity. *Annu Rev Immunol* (2014) 32:659–702. doi: 10.1146/annurev-immunol-032713-120145
13. Sallusto F, Schaerli P, Loetscher P, Schaniel C, Lenig D, Mackay CR, et al. Rapid and Coordinated Switch in Chemokine Receptor Expression During Dendritic Cell Maturation. *Eur J Immunol* (1998) 28(9):2760–9. doi: 10.1002/(SICI)1521-4141(199809)28:09<2760::AID-IMMU2760>3.0.CO;2-N
14. Hauser MA, Schaeuble K, Kindinger I, Impellizzieri D, Krueger WA, Hauck CR, et al. Inflammation-Induced CCR7 Oligomers Form Scaffolds to Integrate Distinct Signaling Pathways for Efficient Cell Migration. *Immunity* (2016) 44 (1):59–72. doi: 10.1016/j.immuni.2015.12.010
15. Weber M, Hauschild R, Schwarz J, Moussion C, de Vries I, Legler DF, et al. Interstitial Dendritic Cell Guidance by Haptotactic Chemokine Gradients. *Science* (2013) 339(6117):328–32. doi: 10.1126/science.1228456
16. Ulvmar MH, Werth K, Braun A, Kelay P, Hub E, Eller K, et al. The Atypical Chemokine Receptor CCRL1 Shapes Functional CCL21 Gradients in Lymph Nodes. *Nat Immunol* (2014) 15(7):623–30. doi: 10.1038/ni.2889
17. Laufer JM, Kindinger I, Artinger M, Pauli A, Legler DF. CCR7 Is Recruited to the Immunological Synapse, Acts as Co-Stimulatory Molecule and Drives LFA-1 Clustering for Efficient T Cell Adhesion Through Zap70. *Front Immunol* (2019) 9:3115. doi: 10.3389/fimmu.2018.03115
18. Hauser MA, Legler DF. Common and Biased Signaling Pathways of the Chemokine Receptor CCR7 Elicited by Its Ligands CCL19 and CCL21 in Leukocytes. *J Leukoc Biol* (2016) 99(6):869–82. doi: 10.1189/jlb.2MR0815-380R
19. Carlsen HS, Haraldsen G, Brandtzaeg P, Baekkevold ES. Disparate Lymphoid Chemokine Expression in Mice and Men: No Evidence of CCL21 Synthesis by Human High Endothelial Venules. *Blood* (2005) 106(2):444–6. doi: 10.1182/blood-2004-11-4353
20. Redecke V, Wu R, Zhou J, Finkelstein D, Chaturvedi V, High AA, et al. Hematopoietic Progenitor Cell Lines With Myeloid and Lymphoid Potential. *Nat Methods* (2013) 10(8):795–803. doi: 10.1038/nmeth.2510
21. Leithner A, Renkawitz J, De Vries I, Hauschild R, Hacker H, Sixt M. Fast and Efficient Genetic Engineering of Hematopoietic Precursor Cells for the Study of Dendritic Cell Migration. *Eur J Immunol* (2018) 48(6):1074–7. doi: 10.1002/eji.201747358
22. Hammerschmidt SI, Werth K, Rothe M, Galla M, Permanyer M, Patzer GE, et al. CRISPR/Cas9 Immunoengineering of Hoxb8-Immortalized Progenitor Cells for Revealing CCR7-Mediated Dendritic Cell Signaling and Migration Mechanisms *In Vivo*. *Front Immunol* (2018) 9:1949. doi: 10.3389/fimmu.2018.01949
23. Helft J, Bottcher J, Chakravarty P, Zelenay S, Huotari J, Schraml BU, et al. GM-CSF Mouse Bone Marrow Cultures Comprise a Heterogeneous Population of CD11c(+)MHCII(+) Macrophages and Dendritic Cells. *Immunity* (2015) 42(6):1197–211. doi: 10.1016/j.immuni.2015.05.018
24. Lutz MB, Inaba K, Schuler G, Romani N. Still Alive and Kicking: *In-Vitro*-Generated GM-CSF Dendritic Cells! *Immun* (2016) 44(1):1–2. doi: 10.1016/j.immuni.2015.12.013
25. Sallusto F, Lanzavecchia A. Efficient Presentation of Soluble Antigen by Cultured Human Dendritic Cells Is Maintained by Granulocyte/Macrophage Colony-Stimulating Factor Plus Interleukin 4 and Downregulated by Tumor Necrosis Factor Alpha. *J Exp Med* (1994) 179 (4):1109–18. doi: 10.1084/jem.179.4.1109
26. Legler DF, Krause P, Scandella E, Singer E, Groettrup M. Prostaglandin E2 Is Generally Required for Human Dendritic Cell Migration and Exerts Its Effect *via* EP2 and EP4 Receptors. *J Immunol* (2006) 176(2):966–73. doi: 10.4049/jimmunol.176.2.966
27. Krause P, Singer E, Darley PI, Klebensberger J, Groettrup M, Legler DF. Prostaglandin E2 Is a Key Factor for Monocyte-Derived Dendritic Cell Maturation: Enhanced T Cell-Stimulatory Capacity Despite IDO. *J leukocyte Biol* (2007) 82(5):1106–14. doi: 10.1189/jlb.0905519
28. Krause P, Bruckner M, Uermosi C, Singer E, Groettrup M, Legler DF. Prostaglandin E2 Enhances T Cell Proliferation by Inducing the Co-Stimulatory Molecules OX40L, CD70 and 4-1BBL on Dendritic Cells. *Blood* (2009) 113(11):2451–60. doi: 10.1182/blood-2008-05-157123
29. van Helden SF, van Leeuwen FN, Figdor CG. Human and Murine Model Cell Lines for Dendritic Cell Biology Evaluated. *Immunol Lett* (2008) 117(2):191–7. doi: 10.1016/j.imlet.2008.02.003
30. Maeda T, Murata K, Fukushima T, Sugahara K, Tsuruda K, Anami M, et al. A Novel Plasmacytoid Dendritic Cell Line, CAL-1, Established From a Patient With Blastic Natural Killer Cell Lymphoma. *Int J Hematol* (2005) 81(2):148–54. doi: 10.1532/ijh97.04116
31. Sapienza MR, Pileri A, Derenzini E, Melle F, Motta G, Fiori S, et al. Blastic Plasmacytoid Dendritic Cell Neoplasm: State of the Art and Prospects. *Cancers* (2019) 11(5):595. doi: 10.3390/cancers11050595
32. Karrich JJ, Balzarolo M, Schmidlin H, Libouban M, Nagasawa M, Gentek R, et al. The Transcription Factor Spi-B Regulates Human Plasmacytoid Dendritic Cell Survival Through Direct Induction of the Antiapoptotic Gene BCL2-A1. *Blood* (2012) 119(22):5191–200. doi: 10.1182/blood-2011-07-370239
33. Dallari S, Macal M, Loureiro ME, Jo Y, Swanson L, Hesser C, et al. Src Family Kinases Fyn and Lyn Are Constitutively Activated and Mediate Plasmacytoid Dendritic Cell Responses. *Nat Commun* (2017) 8:14830. doi: 10.1038/ncomms14830
34. Miura R, Kasakura K, Nakano N, Hara M, Maeda K, Okumura K, et al. Role of PU.1 in MHC Class II Expression *via* CIITA Transcription in Plasmacytoid Dendritic Cells. *PloS One* (2016) 11(4):e0154094. doi: 10.1371/journal.pone.0154094
35. Varnai P, Balla T. Visualization of Phosphoinositides That Bind Pleckstrin Homology Domains: Calcium- and Agonist-Induced Dynamic Changes and Relationship to Myo-[3H]Inositol-Labeled Phosphoinositide Pools. *J Cell Biol* (1998) 143(2):501–10. doi: 10.1083/jcb.143.2.501
36. Uetz-von Allmen E, Rippl AV, Farhan H, Legler DF. A Unique Signal Sequence of the Chemokine Receptor CCR7 Promotes Package Into COPII Vesicles for Efficient Receptor Trafficking. *J Leukoc Biol* (2018) 104(2):375–89. doi: 10.1002/JLB.2VMA1217-492R
37. Hauser MA, Kindinger I, Laufer JM, Spate AK, Bucher D, Vanes SL, et al. Distinct CCR7 Glycosylation Pattern Shapes Receptor Signaling and Endocytosis to Modulate Chemotactic Responses. *J Leukoc Biol* (2016) 99 (6):993–1007. doi: 10.1189/jlb.2VMA0915-432RR
38. Jorgensen AS, Adogamhe PE, Laufer JM, Legler DF, Veldkamp CT, Rosenkilde MM, et al. CCL19 With CCL21-Tail Displays Enhanced Glycosaminoglycan Binding With Retained Chemotactic Potency in Dendritic Cells. *J Leukoc Biol* (2018) 104(2):401–11. doi: 10.1002/JLB.2VMA0118-008R
39. Schaeuble K, Hauser MA, Singer E, Groettrup M, Legler DF. Cross-Talk Between TCR and CCR7 Signaling Sets a Temporal Threshold for Enhanced T Lymphocyte Migration. *J Immunol* (2011) 187(11):5645–52. doi: 10.4049/jimmunol.1101850
40. Matti C, Salnikov A, Artinger M, D'Agostino G, Kindinger I, Uguccioni M, et al. ACKR4 Recruits GRK3 Prior to β-Arrestins But Can Scavenge Chemokines in the Absence of β-Arrestins. *Front Immunol* (2020) 11:720. doi: 10.3389/fimmu.2020.00720
41. Artinger M, Matti C, Gerken OJ, Veldkamp CT. Legler DF. A Versatile Toolkit for Semi-Automated Production of Fluorescent Chemokines to Study CCR7 Expression and Functions. *Int J Mol Sci* (2021) 22(8):4158. doi: 10.3390/ijms22084158

42. Purvanov V, Matti C, Samson GPB, Kindinger I, Legler DF. Fluorescently Tagged CCL19 and CCL21 to Monitor CCR7 and ACKR4 Functions. *Int J Mol Sci* (2018) 19(12):E3876. doi: 10.3390/ijms19123876
43. Laufer JM, Hauser MA, Kindinger I, Purvanov V, Pauli A, Legler DF. Chemokine Receptor CCR7 Triggers an Endomembrane Signaling Complex for Spatial Rac Activation. *Cell Rep* (2019) 29(4):995–1009.e6. doi: 10.1016/j.celrep.2019.09.031
44. Legler DF, Thelen M. New Insights in Chemokine Signaling. *F1000Research* (2018) 7:95. doi: 10.12688/f1000research.13130.1
45. Scandella E, Men Y, Legler DF, Gillessen S, Prikler L, Ludewig B, et al. CCL19/CCL21-Triggered Signal Transduction and Migration of Dendritic Cells Requires Prostaglandin E2. *Blood* (2004) 103(5):1595–601. doi: 10.1182/blood-2003-05-1643
46. Ogilvie P, Thelen S, Moepps B, Gierschik P, da Silva Campos AC, Baggiolini M, et al. Unusual Chemokine Receptor Antagonism Involving a Mitogen-Activated Protein Kinase Pathway. *J Immunol* (2004) 172(11):6715–22. doi: 10.4049/jimmunol.172.11.6715
47. Mathas S, Hinz M, Anagnostopoulos I, Krappmann D, Lietz A, Jundt F, et al. Aberrantly Expressed C-Jun and JunB Are a Hallmark of Hodgkin Lymphoma Cells, Stimulate Proliferation and Synergize With NF-Kappa B. *EMBO J* (2002) 21(15):4104–13. doi: 10.1093/emboj/cdf389
48. Cuesta-Mateos C, Brown JR, Terron F, Munoz-Calleja C. Of Lymph Nodes and CLL Cells: Deciphering the Role of CCR7 in the Pathogenesis of CLL and Understanding Its Potential as Therapeutic Target. *Front Immunol* (2021) 12:662866. doi: 10.3389/fimmu.2021.662866
49. Lutz MB, Schuler G. Immature, Semi-Mature and Fully Mature Dendritic Cells: Which Signals Induce Tolerance or Immunity? *Trends Immunol* (2002) 23(9):445–9. doi: 10.1016/s1471-4906(02)02281-0
50. Saez PJ, Saez JC, Lennon-Dumenil AM, Vargas P. Role of Calcium Permeable Channels in Dendritic Cell Migration. *Curr Opin Immunol* (2018) 52:74–80. doi: 10.1016/j.coi.2018.04.005

Conflict of Interest: The authors declare that the research was conducted in the absence of any commercial or financial relationships that could be construed as a potential conflict of interest.

Publisher's Note: All claims expressed in this article are solely those of the authors and do not necessarily represent those of their affiliated organizations, or those of the publisher, the editors and the reviewers. Any product that may be evaluated in this article, or claim that may be made by its manufacturer, is not guaranteed or endorsed by the publisher.

frontiers in Immunology

MINI REVIEW
published: 17 September 2021
doi: 10.3389/fimmu.2021.730835

Intravascular Crawling of Patrolling Monocytes: A Lèvy-Like Motility for Unique Search Functions?

Rocío Moreno-Cañadas[†], *Laura Luque-Martín*[†] *and Alicia G. Arroyo*[*]

Molecular Biomedicine Department, Centro de Investigaciones Biológicas Margarita Salas (CIB-CSIC), Madrid, Spain

Patrolling monocytes (PMo) are the organism's preeminent intravascular guardians by their continuous search of damaged endothelial cells and harmful microparticles for their removal and to restore homeostasis. This surveillance is accomplished by PMo crawling on the apical side of the endothelium through regulated interactions of integrins and chemokine receptors with their endothelial ligands. We propose that the search mode governs the intravascular motility of PMo *in vivo* in a similar way to T cells looking for antigen in tissues. Signs of damage to the luminal side of the endothelium (local death, oxidized LDL, amyloid deposits, tumor cells, pathogens, abnormal red cells, etc.) will change the diffusive random towards a Lèvy-like crawling enhancing their recognition and clearance by PMo damage receptors as the integrin αMβ2 and CD36. This new perspective can help identify new actors to promote unique PMo intravascular actions aimed at maintaining endothelial fitness and combating harmful microparticles involved in diseases as lung metastasis, Alzheimer's angiopathy, vaso-occlusive disorders, and sepsis.

Keywords: patrolling monocytes, crawling, search theory, Lèvy-like walk, intravascular surveillance, microparticle deposits, αMβ2 integrin, CD36

OPEN ACCESS

Edited by:
Jörg Renkawitz,
Ludwig Maximilian University of Munich, Germany

Reviewed by:
Florian Gaertner,
Institute of Science and Technology Austria (IST Austria), Austria
Catherine Hedrick,
La Jolla Institute for Immunology (LJI), United States

***Correspondence:**
Alicia G. Arroyo
agarroyo@cib.csic.es

[†]*These authors have contributed equally to this work*

Specialty section:
This article was submitted to Molecular Innate Immunity, a section of the journal Frontiers in Immunology

Received: *25 June 2021*
Accepted: *30 August 2021*
Published: *17 September 2021*

Citation:
Moreno-Cañadas R, Luque-Martín L and Arroyo AG (2021) Intravascular Crawling of Patrolling Monocytes: A Lèvy-Like Motility for Unique Search Functions? Front. Immunol. 12:730835. doi: 10.3389/fimmu.2021.730835

INTRODUCTION

Among the two main subsets of circulating monocytes, non-classical monocytes ($CCR2^-$ $CX3CR1^{high}Ly6C^{low}$ in mouse, $CCR2^-$ $CX3CR1^{high}CD14^{dim}CD16^+$ in humans) are also called patrolling monocytes (PMo) by their ability to actively patrol the vascular endothelium to search for harmful microparticles (pathogens, circulating tumor cells, amyloid deposits, abnormal red blood cells, etc.) or dying endothelial cells and promote their removal to restore homeostasis (1–5). Therefore, PMo are considered protective in pathological contexts such as lung metastasis, Alzheimer's disease angiopathy, atherosclerosis, sepsis, and vaso-occlusive disorders (1–3, 6–9). Once PMo extravasate, although they do it rarely, their actions can be beneficial or detrimental depending on the context and the environmental cues that drive their differentiation into distinctive types of macrophages (10–13).

Since pioneering studies by Geissmann's group (1), PMo have been observed patrolling in the microvasculature of dermis, mesentery, brain, lung, kidney and muscle, and in carotid and femoral arteries under homeostatic and inflammatory conditions [reviewed in (4)]. PMo differentiate from classical monocytes in defined vascular niches of the bone marrow and spleen through an

intermediate subpopulation (5, 14). PMo numbers in the circulation are also regulated by β-adrenergic stimulation during exercise and stress (15, 16), pattern recognition receptors as NOD2 (17), soluble factors as tumor exosome-derived PEDF (18), and chemokines as CX3CL1 (17, 19, 20) indicating that their abundance is exquisitely sensitive to signals triggered by damage, stress or inflammation as a protective response.

PMo perform their surveillance function by crawling on the endothelium (1, 19), but the influence of their primary PMo search function into their motility has been overlooked. Recent reports suggest, however, that particle encounter and patrolling activity can be related (21, 22). Following the "search theory," we propose to consider PMo crawling as a movement guided by the "exploration-exploitation trade off" (23), which comprises, but is not limited to, non-informed explorative search without much guidance cues and informed exploitative search with input from the environment. We will describe intravascular PMo crawling from this perspective taking as a reference walks described for T cells in search of an antigen in the lymph node and other tissues (23, 24).

PATROLLING MONOCYTE CRAWLING: A SEARCH MODE MOTILITY

Intravascular PMo crawling is defined as the scanning movement of the apical surface of endothelial cells, which in the microvasculature does not depend on the direction of blood flow, travels long distances without greater directionality, performs looped trajectories and without immediate extravasation (1, 4, 25). In large vessels, PMo crawling displays an overall with-the-flow direction with no typical hairpin and loop patterns (26). Unlike rolling leukocytes, PMo adhere firmly while crawling and are slower by a factor of 100 to 1,000 (1).

As an exploration movement, intravascular PMo crawling must transition among random motility modes balancing migration speed with sufficient dwell time and meandering for a thorough survey of the endothelial surface. Diffusive random crawling involves walks with little or no directional persistence (Brownian-type tracks) with the intention of surveying the largest surface in the shortest possible time to find local alarm signals. Tracks of PMo crawling consistent with this mode are observed in steady-state and inflammatory conditions (1, 2, 25–28). However, PMo modify their crawling pattern in the presence of local endothelial damage (19, 29) or microparticles (8, 21, 26). Tracks in these cases resemble superdiffusive random walks, particularly the Lèvy-like walk, which consists of an alternation of long, quick, and directed trajectories (flights) with short and slow random turning directions. In this situation, PMo no longer perform only exploration, but signal-informed movement to find their final target. Both diffusive random and Lèvy-like crawling can coexist in the microvasculature [see Movie S2 in (1)]. Additionally, a high density of local damage will disrupt PMo Lèvy-like walk and promote confined crawling by the frequent encounter of PMo with their target. Intravascular crawling often ends with PMo detachment and continuation of patrol. PMo rarely perform a truly directional crawling leading to transendothelial migration, in contrast to classical and intermediate monocytes that arrest and transmigrate more frequently (13, 27), so we will not consider it further as it is not related to intravascular surveillance.

Kinetic parameters of the different types of intravascular PMo search crawling are summarized in **Table 1**. In general, diffusive random PMo crawling is faster and longer to scan large surfaces efficiently. In contrast, Lèvy-like PMo walks comprise slower and shorter tracks connected by fast-speed steps (although information on individual tracks of this type is not available). These parameters are further reduced during confined crawling. Speed better captures the different modes, while straightness seems less informative in describing PMo crawling, as both random and confined walks can show similar values, however reflecting different search and find behaviors (**Table 1**). Analogous motilities are found in NKT cells randomly searching for antigens in liver sinusoids (31) or T cells performing Lèvy-like and confined walks to look for antigen in tissues (30, 32, 33, 35) (**Table 1**).

The morpho-dynamics and the locomotion mode of PMo are not well defined. PMo appear round and seem to crawl *in vivo* in a millipodia-like manner (36) during diffusive random crawling (2, 28). In this mode, cells do not polarize, probably allowing them to move faster. During Lèvy-like crawling, PMo alternate between elongating, while crawling in a more meticulous manner by an amoeboid movement, and being round during flights to the next location (3, 8, 21, 29) (**Figure 1A**). The possible mechanisms underlying the amoeboid locomotion of PMo (actin polymerization, blebbing, etc.) remain unexplored (37).

REGULATORS OF DIFFUSIVE RANDOM *VERSUS* LÈVY-LIKE PMo CRAWLING

We will review recognized intrinsic and extrinsic players in PMo crawling from the search theory perspective and suggest how they can determine diffusive random and Lèvy-type crawling modes. Particularly, we will highlight the relevance of local endothelial damage signals in PMo locomotion.

Diffusive Random Crawling

PMo perform diffusive random crawling in most steady-state and inflammatory contexts to explore large endothelial areas without expecting much damage. These kinds of tracks are observed in PMo crawling in mesentery vessels and in arteries but also in dermis, lung, and kidney capillaries (1–3, 21, 25–29). For this type of crawling, PMo need to be sufficiently attached to resist shear stress but with dynamic adhesions to allow fast movement. In the microvasculature, PMo adherence depends on β2 integrins, mostly on αLβ2 integrin (LFA-1, CD11a/CD18) in steady-state conditions by its interaction with ICAM-1 and with additional contribution of αMβ2 integrin (Mac-1, CD11b/CD18) in inflamed conditions (1, 2, 27, 38) (**Figure 1A**). Indeed, αMβ2 integrin seems to determine the fast velocity of diffusive random crawling in steady-state conditions since its inhibition does not affect the abundance of PMo crawlers, but it reduces their speed in mesenteric vessels (29). Diffusive random crawling is also favored in the microvasculature by the interaction of CX3CR1 in PMo with CX3CL1 (**Figure 1A**), a transmembrane ligand abundantly produced by endothelial cells in lung and

TABLE 1 | Cellular kinetic parameters of the proposed crawling modes in various territories and conditions: mean speed (μm/min), length (μm), duration (min), and straightness (distance traveled/length of the trajectory).

Diffusive random crawling		Lèvy-like walk		Confined crawling		References
PMo	**NKT cells**	**PMo**	**LT**	**PMo**	**LT**	
Lung (capillaries)						
Healthy		*Tumor cells (4 h)*	*LPS lung*	*Tumor cells (24 h)*	*LPS lung*	(3, 30)
≈10 μm/min		6.7 μm/min	2.3 μm/min	1.5 μm/min	0–1 μm/min	
Other organs						
Healthy	*Healthy*	*TLR7/8 agonist*	*Tumor skin*		*Tumor skin*	(2, 31–33)
Kidney	Liver sinusoids	Kidney	4.3 μm/min		1.4 μm/min	
≈9 μm/min	16.5 μm/min	≈7.5 μm/min	0.4		0.5	
≈80 μm		≈150 μm				
≈9 min		≈22 min	*Infected brain*			
≈0.6	0.4	≈0.3	6.4 μm/min			
Arteries						
Healthy		*Hyperlipidemia*		*Atheroma plaque*		(21, 26)
Carotid		Carotid		Carotid		
36 μm/min		30 μm/min		20 μm/min		
134 μm		140 μm		167 μm		
4.7 min		6.1 min		7.7 min		
0.2		0.22		0.05		
Femoral		Femoral				
12 μm/min		5 μm/min				
nd		≈200 μm				
≈0.6		≈0.6				
		TLR7/8 agonist				
		Carotid				
		19 μm/min				
		124 μm				
		5.7 min				
		0.1				
Venules						
Healthy		*TLR7/8 agonist*				(1, 27, 29, 34)
Mesentery		Mesentery				
≈9 μm/min		≈5-6 μm/min				
≈200 μm		≈180 μm				
≈20 min		≈23 min				
≈0.6		≈0.4				
Dermis						
17 μm/min						
249 μm						
14 min						
0.6						
Cremaster						
≈10 μm/min						
147.3 μm						
≈0.7						

Most of the values given are approximate; for accurate values, please refer to the original articles. The parameters for PMo and NKT are intravascular, while for LT they are in the tissue. Note that the parameters do not correspond to individual tracks but to the average of all observed tracks.
PMo, patrolling monocytes; NKT cells, natural killer T cells; LT, T lymphocytes.

kidney (1, 3, 29, 38). Moreover, in vascular territories with high shear stress like arteries and the glomerulus, resistance to detachment to support diffusive random crawling is provided by the interaction of α4β1 integrin with its endothelial ligand VCAM-1, with minor or no role of CX3CR1 (26, 38), probably related to CX3CL1 downregulation by shear stress (39).

So far millipede-like crawling has been described in T cells in which it relied on the rapid turnover of traction points formed by high-affinity αLβ2 integrin interactions with endothelial ICAM-1 (36). However, since this type of T cell motility leads to extravasation and not to intraluminal surveillance as in PMo, further research will be required to explore if a similar β2 integrin-mediated mechanism accounts for PMo millipodia-based crawling (40). Nevertheless, the drastic reduction of this type of crawling in arteries in steady state in the absence of kindlin-3, an inside-out regulator of β2 integrins, points to the requirement of high-affinity β2 integrin interactions (22). Accordingly, CX3CR1 favors diffuse random crawling of PMo, probably by its outside-in upregulation of β2 integrin affinity (41) as also supported by reduced PMo crawling in inflammatory conditions under GPCR signaling inhibition (2, 29). Of note, endothelial ligands involved in diffusive random PMo crawling are not distributed homogeneously on the luminal side of the endothelial cells increasing the possibility that they serve as

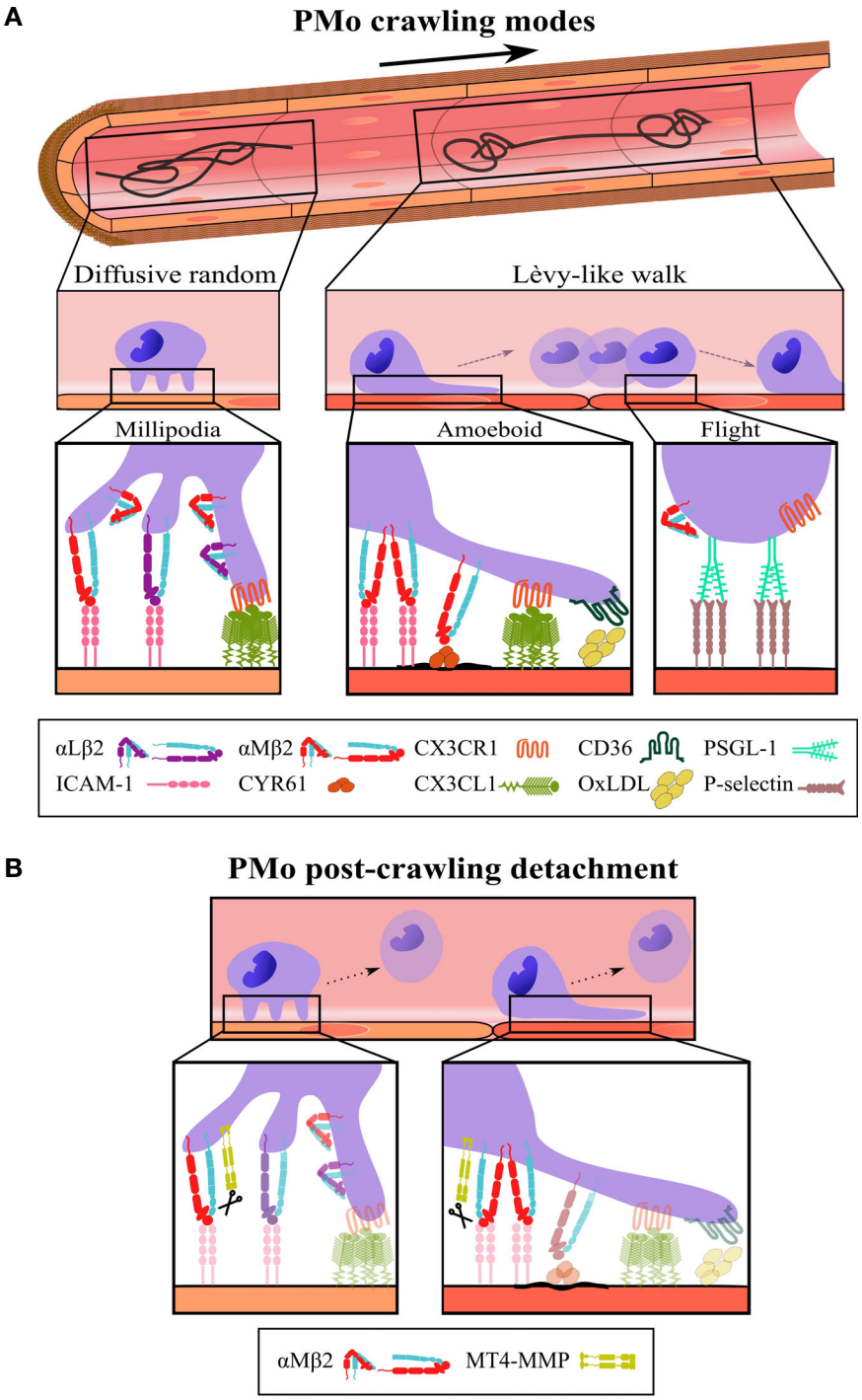

FIGURE 1 | Schematic representation of the different modes, steps, and players in intravascular PMo crawling. (**A**, Top) Representative tracks performed by PMo crawling on the vascular endothelium according to the search theory: diffusive random crawling (left) and Lèvy-like walk (right); the bold arrow indicates blood flow direction. Middle, side views of PMo morphology (round and elongated) and the corresponding locomotion modes (millipodia and amoeboid) during diffusive random crawling and Lèvy-like walks; in the last, the flight phase is also indicated. Bottom, magnifications display the molecular players and interactions relevant to each type and step of crawling as described in the text; molecular interactions depicted for the flight phase are speculative. **(B)** The cleavage of αM integrin by the protease MT4-MMP is proposed as a possible mechanism for PMo post-crawling detachment (12), an important step to maintain PMo intravascular surveillance; scissors indicate cleavage. The β2 integrins are represented in the folded (inactive) and extended (active) conformations.

footholds for the millipodia. Thus, apical microdomains organized by tetraspanins or the actin cytoskeleton contain pre-formed clusters of about 2.5 ICAM-1 (42) and 3-to-7 CX3CL1 (43, 44) molecules (**Figure 1A**) and the matricellular protein CYR61/CCN1, another αMβ2 integrin ligand, also forms hotspots in the mesenteric vessels (29). Interestingly, the nanoarchitecture of the apical endothelial membrane is sensitive to factors such as shear stress or the cytokine TNFα, able to promote upward protrusions of about 160 nm, that increase the abundance and/or accessibility of ICAM-1 nanoclusters (45, 46). These effects could influence PMo intravascular crawling.

Lèvy-Like Crawling

How do PMo perceive that they have to increase the frequency of Lèvy-like walks for a more efficient search, especially for small targets, and how do they re-adapt their arsenal of adhesion and chemokine receptors to this type of movement?

PMo show an amoeboid morphology when crawling in the slow phase of Lèvy-like walk suggestive of signals driven by β2 integrin interactions as shown in neutrophils (47, 48). This is supported by the presence of a few Lèvy-like tracks in steady-state in the lung and kidney capillaries, territories with abundant endothelial CX3CL1, upregulator of β2 integrin affinity (3, 19). Indeed, PMo surface expression of β2 integrins, particularly αMβ2, is higher in the lung than in the blood, pointing to its tissue-dependent regulation (22, 49). Hyperlipidemia does not change the kinetic parameters of PMo except for the reduced speed, which correlates with a higher proportion of Lèvy-type tracks (21, 26) (**Table 1**). Lèvy-like walks are also visible in carotid arteries stimulated with a TLR7/8 agonist that induces endothelial cell damage (26). In this context, α4β1 integrin is required to resist shear stress (26), but since inhibition of the αLβ2 integrin reduces the number of PMo crawlers but not the frequency of Lèvy-type walks, αMβ2 integrin seems the main actor for this type of locomotion (26) (**Figure 1A**). Likewise, αMβ2 is necessary for longer interactions and above a shear stress threshold in contrast to αLβ2 integrin in neutrophils (50).

Nevertheless, the highest frequency of tracks resembling intermittent Lèvy-like motility is found in mouse vascular territories with deposits of harmful microparticles or aggregates including oxidized LDL (oxLDL) in the carotid artery of atheroprone mice fed a high-fat diet (21); β-amyloid aggregates in the lumen of brain veins in Alzheimer's angiopathy (8, 51); apoptotic endothelial cells upon TLR7/8 stimulation in kidney glomerulus (2); circulating tumor metastasizing cells in lung capillaries (3); CYR61 secreted by platelets in mesenteric vessels after TLR7/8 addition (29); and sickle red blood cells (9, 52, 53), among others (**Figure 1A**). Notably, many of these particles can be recognized by αMβ2 integrin itself or in cooperation with other scavenger receptors such as CD36 and TLR (54, 55); in fact, CD36 or TLR7 deficiency decreased Lèvy-like PMo crawling on the vasculature of mice fed a high-fat diet or stimulated with a TLR7/8 agonist, respectively (2, 21). αMβ2 integrin is a promiscuous receptor that can bind more than 50 ligands including β-amyloid, iC3b, and CYR61 (56, 57). Although αMβ2 integrin binds ICAM-1 with lower affinity than αLβ2 integrin, it binds other ligands such as fibrinogen with 25-fold more affinity, which, together with their counter-regulated expression by inflammatory cytokines as TNFα (27), may confer αMβ2 integrin an advantage for endothelial interaction in the presence of deposits or damage. Indeed, blockade of αMβ2 integrin eradicates Lèvy-like tracks in for example steady-state mesenteric veins similarly to blockade of its ligand CYR61 after TLR7/8 stimulation (29). We propose to consider αMβ2 integrin as the essential damage receptor in PMo (beyond its function as an adhesion receptor) that seems to govern the Lèvy-like walk, acting as a decision-making receptor to integrate intravascular search and motility in homeostasis and pathology.

Outside-in signals by multivalence interaction may favor microparticle-induced clustering of αMβ2 integrin and thus its higher avidity (40) (**Figure 1A**). It will be interesting to explore whether αMβ2 integrin can reside in preformed nanoclusters in GPI domains as shown for αLβ2 integrin in monocytes and serve for its dynamic recruitment at adhesion sites for amoeboid locomotion (58). Indeed, PMo engulfing oxLDL *via* CD36 increased their levels of F-actin and upregulated genes related to Rab GTPases, integrin recycling, and lamellipodia formation (21), suggesting that this machinery may contribute to actin-driven amoeboid PMo motility during Lèvy-like walks in line with the role of actin flows in coupling speed and directional persistence (59). Intrinsic factors identified for intermittent (Lèvy-like) tissue motility in T cells include the unconventional myosin MYO1G that acts as a turning motor (35) and the Rho-associated protein kinase (ROCK) required for high-speed and directionality (30). Whether similar intrinsic regulators of speed fluctuations and turning patterns exist in PMo remains unknown.

αMβ2 integrin activity can also be regulated in circulating PMo by its crosstalk with other scavenger receptors as CD36 (**Figure 1A**), able of recognizing a variety of damage signals ranging from apoptotic cells to modified lipids (55). In a mouse model of atherosclerosis, CD36 uptake of oxLDL in PMo induces DAP12/Src family kinase (SFK) signaling and leads to increased F-actin polymerization (and probably higher β2 integrin avidity) and enhanced PMo Lèvy-like crawling (21), and a similar boosting of PMo particle engulfment is observed in sickle red blood cell clearance (9, 52, 53). This intravascular educational program constitutes an interesting feedforward mechanism for more efficient search and removal of particles by PMo, thus helping to prevent spread of inflammatory damage to the tissues.

Extrinsic factors as shear stress may regulate β2 integrin affinity (60) and ICAM-1 clustering (46), alter endothelial glycocalyx (61), and favor endothelial cell damage (26) or deposition of oxLDL (62) in areas of disturbed blood flow. The deposited microparticles can themselves promote local changes in the apical endothelial membrane that can augment the frequency of PMo Lèvy-like walks, such as increased membrane stiffness by the uptake of oxLDL by endothelial CD36 (62) and the pathogen-induced protrusion of microvilli (63), by altering specific lipid domains in both cases.

After meticulous amoeboid crawling on the endothelium during the slow phase of Lèvy-like walk, PMo become rounder and move quickly and directionally (flight) to the next area for another meticulous search (8) using mechanisms yet to be

clarified. Several factors can underlie speed fluctuations (23), but although αLβ2 integrin/ICAM-1 interactions support high-speed and straight migration of T cells in the lymph node (64), movies of PMo Lèvy-like crawling show that this acceleration step seems to relate to PMo decreased adhesiveness (**Figure 1A**). Similar flights are perceived during PMo crawling in mice deficient in kindlin-3 or treated with SFK inhibitors pointing to reduced β2 integrin affinity as permissive for PMo high-speed step (2, 21, 22). PMo sliding behavior is also visible in CX3CR1-deficient mice (3, 22). Thus, although CX3CR1-CX3CL1 axis modulates Lèvy-like walks by regulating β2 integrin affinity (2, 3), it seems dispensable for the acceleration phase, and its absence does not seem to decrease the frequency of these tracks (1, 26, 29). The low-adhesive contact of PMo with the endothelium points to the involvement of low affinity and reversible receptor-ligand pairs resembling selectin interactions during rolling (4), although in the movies PMo seem to jump or slide rather than roll (8, 26). Since PMo do not express selectins, PSGL1 is a candidate to underlie PMo flights by its interaction with P-selectin expressed by the endothelium under certain stimulation and regulated by preformed membrane microdomains (65) (**Figure 1A**). The carbohydrate modification of PSGL-1 Slan is a marker for a subset of PMo and modulates innate and adaptive immune responses, but its possible contribution to PMo crawling has not been investigated (66, 67).

Therefore, the local presence of microparticles or damage on endothelial cells are the key factors to promote environmental-guided Lèvy-like PMo migration. This fact may explain the lack of Lèvy-like tracks *in vitro* since although inflammatory cytokines and flow were incorporated, no aggregates were present (25). Moreover, if there is massive endothelial damage or larger deposits, Lèvy-like walk will change into confined meticulous crawling (23) as observed in the lung 1 day after injection of tumor cells (3) and near arterial atheroma plaques (26) (**Table 1**), allowing enough time for PMo interaction to increase the likelihood of engulfment. Increased retention during Lèvy-like or confined crawling due to the geometric constraints of certain vascular territories could also induce the production of chemokines and cytokines by PMo and/or the endothelial cells with which they interact. These soluble factors will serve to recruit cooperating circulating leukocytes such as neutrophils to cope with dying endothelial cells in response to TLR7/8 stimulation in the glomerulus (2) and natural killer cells to help eliminate circulating tumor cells in the lung microvasculature (3).

Post-Crawling Detachment

After crawling PMo usually undergo detachment, a key step to maintain PMo surveying the vasculature by avoiding their extravasation. This allows several rounds of endothelial scanning by PMo and prevents spreading of damaging microparticles to the tissues. Our group recently identified that the GPI-anchored protease MT4-MMP could cleave the αM integrin chain at $N^{977}L$ position (not conserved in αL integrin) serving as a possible mechanism for PMo post-crawling detachment (12) (**Figure 1B**). Accordingly, in MT4-MMP absence there were increased numbers of PMo crawling on the activated endothelium of the cremaster muscle in an αMβ2 integrin-dependent manner and also transmigrating into the inflamed aorta (12). These data support that PMo detachment post-crawling prevents β2 integrin-dependent transendothelial migration (27). These findings also indicate that a pool of αMβ2 integrin molecules reside at GPI microdomains of the PMo plasma membrane what could account for fine-tuned contribution of αMβ2 integrin to diffusive random or Lèvy-like walk crawling, and in particular to PMo post-crawling detachment. Of interest, shear stress can induce αM integrin cleavage by cathepsin B in neutrophils (68). Whether this cleavage, β2 integrin processing by other proteases (69, 70), or proteolysis-independent mechanisms play additional roles in PMo detachment post-crawling remains unknown.

CONCLUSIONS AND PERSPECTIVES

Leaving aside the discussion about true Lèvy-like walks in biological systems (24), we consider interesting to complement the current perspective of intravascular PMo crawling with the point of view that the search mode influences PMo motility as proposed for tissue T cells (23). Although PMo motility patterns are far more complex than the simplification herein proposed, this change of paradigm may help understand PMo crawling better and identify novel regulators to boost PMo protective intravascular actions and prevent disease. Open questions remain about the dynamic regulation of integrins and other intrinsic actors (actin, GTPases), endothelial players, and extrinsic factors (shear stress) during these distinct modes of PMo crawling. It would also be necessary to determine instantaneous and individual track PMo kinetic parameters in future work.

These questions undoubtedly raise the need to implement innovative techniques and tools to fully understand these events at the single-cell scale and *in vivo*. For example: (i) novel *in vitro* settings for live time-lapse to recapitulate *in vivo* complexity using immobilized ligands in lipid bilayers and under flow (46); (ii) advanced microscopy techniques for visualization and 3D reconstruction of intravascular PMo (71) together with novel PMo markers as PD-L1 (34) to avoid the limitation of CX3CR1 heterozygous mice; and (iii) innovative techniques for *in vivo* single-molecule tracking to characterize receptor and ligand clustering at PMo and endothelial plasma membrane (29, 72, 73).

AUTHOR CONTRIBUTIONS

RM-C and LL-M prepared the Table and Figure, respectively. RM-C, LL-M, and AGA wrote the text. All authors contributed to the article and approved the submitted version.

FUNDING

The work in this manuscript has been funded by the Spanish Ministry of Science and Innovation (grants SAF2017-83229-R and PID2020-112981RB-I00 to AGA and fellowship PRE2018-085163 to LL-M). RM-C has a contract with the Community of Madrid co-financed by the European Social Fund for Youth Employment. We acknowledge support of the publication fee by the CSIC Open Access Publication Support Initiative through its Unit of Information Resources for Research (URICI).

REFERENCES

1. Auffray C, Fogg D, Garfa M, Elain G, Join-Lambert O, Kayal S, et al. Monitoring of Blood Vessels and Tissues by a Population of Monocytes With Patrolling Behavior. *Science* (2007) 317(5838):666–70. doi: 10.1126/science.1142883
2. Carlin LM, Stamatiades EG, Auffray C, Hanna RN, Glover L, Vizcay-Barrena G, et al. Nr4a1-Dependent Ly6C(low) Monocytes Monitor Endothelial Cells and Orchestrate Their Disposal. *Cell* (2013) 153(2):362–75. doi: 10.1016/j.cell.2013.03.010
3. Hanna RN, Cekic C, Sag D, Tacke R, Thomas GD, Nowyhed H, et al. Patrolling Monocytes Control Tumor Metastasis to the Lung. *Science* (2015) 350(6263):985–90. doi: 10.1126/science.aac9407
4. Buscher K, Marcovecchio P, Hedrick CC, Ley K. Patrolling Mechanics of Non-Classical Monocytes in Vascular Inflammation. *Front Cardiovasc Med* (2017) 4:80. doi: 10.3389/fcvm.2017.00080
5. Tahir S, Steffens S. Nonclassical Monocytes in Cardiovascular Physiology and Disease. *Am J Physiol Cell Physiol* (2021) 320(5):C761–70. doi: 10.1152/ajpcell.00326.2020
6. Cassetta L, Pollard JW. Cancer Immunosurveillance: Role of Patrolling Monocytes. *Cell Res* (2016) 26(1):3–4. doi: 10.1038/cr.2015.144
7. Cros J, Cagnard N, Woollard K, Patey N, Zhang SY, Senechal B, et al. Human CD14dim Monocytes Patrol and Sense Nucleic Acids and Viruses *via* TLR7 and TLR8 Receptors. *Immunity* (2010) 33(3):375–86. doi: 10.1016/j.immuni.2010.08.012
8. Michaud JP, Bellavance MA, Prefontaine P, Rivest S. Real-Time *In Vivo* Imaging Reveals the Ability of Monocytes to Clear Vascular Amyloid Beta. *Cell Rep* (2013) 5(3):646–53. doi: 10.1016/j.celrep.2013.10.010
9. Allali S, Maciel TT, Hermine O, de Montalembert M. Innate Immune Cells, Major Protagonists of Sickle Cell Disease Pathophysiology. *Haematologica* (2020) 105(2):273–83. doi: 10.3324/haematol.2019.229989
10. Narasimhan PB, Eggert T, Zhu YP, Marcovecchio P, Meyer MA, Wu R, et al. Patrolling Monocytes Control NK Cell Expression of Activating and Stimulatory Receptors to Curtail Lung Metastases. *J Immunol* (2020) 204(1):192–8. doi: 10.4049/jimmunol.1900998
11. Thomas G, Tacke R, Hedrick CC, Hanna RN. Nonclassical Patrolling Monocyte Function in the Vasculature. *Arterioscler Thromb Vasc Biol* (2015) 35(6):1306–16. doi: 10.1161/ATVBAHA.114.304650
12. Clemente C, Rius C, Alonso-Herranz L, Martin-Alonso M, Pollan A, Camafeita E, et al. MT4-MMP Deficiency Increases Patrolling Monocyte Recruitment to Early Lesions and Accelerates Atherosclerosis. *Nat Commun* (2018) 9(1):910. doi: 10.1038/s41467-018-03351-4
13. Sidibe A, Ropraz P, Jemelin S, Emre Y, Poittevin M, Pocard M, et al. Angiogenic Factor-Driven Inflammation Promotes Extravasation of Human Proangiogenic Monocytes to Tumours. *Nat Commun* (2018) 9(1):355. doi: 10.1038/s41467-017-02610-0
14. Gamrekelashvili J, Giagnorio R, Jussofie J, Soehnlein O, Duchene J, Briseno CG, et al. Regulation of Monocyte Cell Fate by Blood Vessels Mediated by Notch Signalling. *Nat Commun* (2016) 7:12597. doi: 10.1038/ncomms12597
15. Graff RM, Kunz HE, Agha NH, Baker FL, Laughlin M, Bigley AB, et al. Beta2-Adrenergic Receptor Signaling Mediates the Preferential Mobilization of Differentiated Subsets of CD8+ T-Cells, NK-Cells and Non-Classical Monocytes in Response to Acute Exercise in Humans. *Brain Behav Immun* (2018) 74:143–53. doi: 10.1016/j.bbi.2018.08.017
16. Steppich B, Dayyani F, Gruber R, Lorenz R, Mack M, Ziegler-Heitbrock HW. Selective Mobilization of CD14(+)CD16(+) Monocytes by Exercise. *Am J Physiol Cell Physiol* (2000) 279(3):C578–86. doi: 10.1152/ajpcell.2000.279.3.C578
17. Lessard AJ, LeBel M, Egarnes B, Prefontaine P, Theriault P, Droit A, et al. Triggering of NOD2 Receptor Converts Inflammatory Ly6C(high) Into Ly6C(low) Monocytes With Patrolling Properties. *Cell Rep* (2017) 20(8):1830–43. doi: 10.1016/j.celrep.2017.08.009
18. Plebanek MP, Angeloni NL, Vinokour E, Li J, Henkin A, Martinez-Marin D, et al. Pre-Metastatic Cancer Exosomes Induce Immune Surveillance by Patrolling Monocytes at the Metastatic Niche. *Nat Commun* (2017) 8(1):1319. doi: 10.1038/s41467-017-01433-3
19. Carlin LM, Auffray C, Geissmann F. Measuring Intravascular Migration of Mouse Ly6C(low) Monocytes *In Vivo* Using Intravital Microscopy. *Curr Protoc Immunol* (2013) Chapter 14:Unit 14 33 1–16. doi: 10.1002/0471142735.im1433s101
20. White GE, McNeill E, Channon KM, Greaves DR. Fractalkine Promotes Human Monocyte Survival *via* a Reduction in Oxidative Stress. *Arterioscler Thromb Vasc Biol* (2014) 34(12):2554–62. doi: 10.1161/ATVBAHA.114.304717
21. Marcovecchio PM, Thomas GD, Mikulski Z, Ehinger E, Mueller KAL, Blatchley A, et al. Scavenger Receptor CD36 Directs Nonclassical Monocyte Patrolling Along the Endothelium During Early Atherogenesis. *Arterioscler Thromb Vasc Biol* (2017) 37(11):2043–52. doi: 10.1161/ATVBAHA.117.309123
22. Marcovecchio PM, Zhu YP, Hanna RN, Dinh HQ, Tacke R, Wu R, et al. Frontline Science: Kindlin-3 Is Essential for Patrolling and Phagocytosis Functions of Nonclassical Monocytes During Metastatic Cancer Surveillance. *J Leukoc Biol* (2020) 107(6):883–92. doi: 10.1002/JLB.4HI0420-098R
23. Krummel MF, Bartumeus F, Gerard A. T Cell Migration, Search Strategies and Mechanisms. *Nat Rev Immunol* (2016) 16(3):193–201. doi: 10.1038/nri.2015.16
24. Reynolds AM. Current Status and Future Directions of Levy Walk Research. *Biol Open* (2018) 7(1):bio030106. doi: 10.1242/bio.030106
25. Collison JL, Carlin LM, Eichmann M, Geissmann F, Peakman M. Heterogeneity in the Locomotory Behavior of Human Monocyte Subsets Over Human Vascular Endothelium *In Vitro*. *J Immunol* (2015) 195(3):1162–70. doi: 10.4049/jimmunol.1401806
26. Quintar A, McArdle S, Wolf D, Marki A, Ehinger E, Vassallo M, et al. Endothelial Protective Monocyte Patrolling in Large Arteries Intensified by Western Diet and Atherosclerosis. *Circ Res* (2017) 120(11):1789–99. doi: 10.1161/CIRCRESAHA.117.310739
27. Sumagin R, Prizant H, Lomakina E, Waugh RE, Sarelius IH. LFA-1 and Mac-1 Define Characteristically Different Intralumenal Crawling and Emigration Patterns for Monocytes and Neutrophils *In Situ*. *J Immunol* (2010) 185(11):7057–66. doi: 10.4049/jimmunol.1001638
28. Westhorpe CLV, Norman MU, Hall P, Snelgrove SL, Finsterbusch M, Li A, et al. Effector CD4(+) T Cells Recognize Intravascular Antigen Presented by Patrolling Monocytes. *Nat Commun* (2018) 9(1):747. doi: 10.1038/s41467-018-03181-4
29. Imhof BA, Jemelin S, Ballet R, Vesin C, Schapira M, Karaca M, et al. CCN1/CYR61-Mediated Meticulous Patrolling by Ly6Clow Monocytes Fuels Vascular Inflammation. *Proc Natl Acad Sci USA* (2016) 113(33):E4847–56. doi: 10.1073/pnas.1607710113
30. Mrass P, Oruganti SR, Fricke GM, Tafoya J, Byrum JR, Yang L, et al. ROCK Regulates the Intermittent Mode of Interstitial T Cell Migration in Inflamed Lungs. *Nat Commun* (2017) 8(1):1010. doi: 10.1038/s41467-017-01032-2
31. Geissmann F, Cameron TO, Sidobre S, Manlongat N, Kronenberg M, Briskin MJ, et al. Intravascular Immune Surveillance by CXCR6+ NKT Cells Patrolling Liver Sinusoids. *PloS Biol* (2005) 3(4):e113. doi: 10.1371/journal.pbio.0030113
32. Harris TH, Banigan EJ, Christian DA, Konradt C, Tait Wojno ED, Norose K, et al. Generalized Levy Walks and the Role of Chemokines in Migration of Effector CD8+ T Cells. *Nature* (2012) 486(7404):545–8. doi: 10.1038/nature11098
33. Lau D, Garcon F, Chandra A, Lechermann LM, Aloj L, Chilvers ER, et al. Intravital Imaging of Adoptive T-Cell Morphology, Mobility and Trafficking Following Immune Checkpoint Inhibition in a Mouse Melanoma Model. *Front Immunol* (2020) 11:1514. doi: 10.3389/fimmu.2020.01514
34. Bianchini M, Duchene J, Santovito D, Schloss MJ, Evrard M, Winkels H, et al. PD-L1 Expression on Nonclassical Monocytes Reveals Their Origin and Immunoregulatory Function. *Sci Immunol* (2019) 4(36):eaar3054. doi: 10.1126/sciimmunol.aar3054
35. Gerard A, Patino-Lopez G, Beemiller P, Nambiar R, Ben-Aissa K, Liu Y, et al. Detection of Rare Antigen-Presenting Cells Through T Cell-Intrinsic Meandering Motility, Mediated by Myo1g. *Cell* (2014) 158(3):492–505. doi: 10.1016/j.cell.2014.05.044
36. Shulman Z, Shinder V, Klein E, Grabovsky V, Yeger O, Geron E, et al. Lymphocyte Crawling and Transendothelial Migration Require Chemokine Triggering of High-Affinity LFA-1 Integrin. *Immunity* (2009) 30(3):384–96. doi: 10.1016/j.immuni.2008.12.020
37. Lammermann T, Sixt M. Mechanical Modes of 'Amoeboid' Cell Migration. *Curr Opin Cell Biol* (2009) 21(5):636–44. doi: 10.1016/j.ceb.2009.05.003
38. Finsterbusch M, Hall P, Li A, Devi S, Westhorpe CL, Kitching AR, et al. Patrolling Monocytes Promote Intravascular Neutrophil Activation and Glomerular Injury in the Acutely Inflamed Glomerulus. *Proc Natl Acad Sci USA* (2016) 113(35):E5172–81. doi: 10.1073/pnas.1606253113

39. Babendreyer A, Molls L, Dreymueller D, Uhlig S, Ludwig A. Shear Stress Counteracts Endothelial CX3CL1 Induction and Monocytic Cell Adhesion. *Mediators Inflammation* (2017) 2017:1515389. doi: 10.1155/2017/1515389
40. Herter J, Zarbock A. Integrin Regulation During Leukocyte Recruitment. *J Immunol* (2013) 190(9):4451–7. doi: 10.4049/jimmunol.1203179
41. Goda S, Imai T, Yoshie O, Yoneda O, Inoue H, Nagano Y, et al. CX3C-Chemokine, Fractalkine-Enhanced Adhesion of THP-1 Cells to Endothelial Cells Through Integrin-Dependent and -Independent Mechanisms. *J Immunol* (2000) 164(8):4313–20. doi: 10.4049/jimmunol.164.8.4313
42. Barreiro O, Yanez-Mo M, Serrador JM, Montoya MC, Vicente-Manzanares M, Tejedor R, et al. Dynamic Interaction of VCAM-1 and ICAM-1 With Moesin and Ezrin in a Novel Endothelial Docking Structure for Adherent Leukocytes. *J Cell Biol* (2002) 157(7):1233–45. doi: 10.1083/jcb.200112126
43. Hermand P, Pincet F, Carvalho S, Ansanay H, Trinquet E, Daoudi M, et al. Functional Adhesiveness of the CX3CL1 Chemokine Requires Its Aggregation. Role of the Transmembrane Domain. *J Biol Chem* (2008) 283 (44):30225–34. doi: 10.1074/jbc.M802638200
44. Ostuni MA, Hermand P, Saindoy E, Guillou N, Guellec J, Coens A, et al. CX3CL1 Homo-Oligomerization Drives Cell-to-Cell Adherence. *Sci Rep* (2020) 10(1):9069. doi: 10.1038/s41598-020-65988-w
45. Franz J, Brinkmann BF, Konig M, Huve J, Stock C, Ebnet K, et al. Nanoscale Imaging Reveals a Tetraspanin-CD9 Coordinated Elevation of Endothelial ICAM-1 Clusters. *PloS One* (2016) 11(1):e0146598. doi: 10.1371/journal.pone.0146598
46. Piechocka IK, Keary S, Sosa-Costa A, Lau L, Mohan N, Stanisavljevic J, et al. Shear Forces Induce ICAM-1 Nanoclustering on Endothelial Cells That Impact on T Cell Migration. *Biophys J* (2021) 120(13):2644–56. doi: 10.1101/2020.06.29.177816
47. Bouti P, Webbers SDS, Fagerholm SC, Alon R, Moser M, Matlung HL, et al. Beta2 Integrin Signaling Cascade in Neutrophils: More Than a Single Function. *Front Immunol* (2020) 11:619925. doi: 10.3389/fimmu.2020.619925
48. Zhang H, Schaff UY, Green CE, Chen H, Sarantos MR, Hu Y, et al. Impaired Integrin-Dependent Function in Wiskott-Aldrich Syndrome Protein-Deficient Murine and Human Neutrophils. *Immunity* (2006) 25(2):285–95. doi: 10.1016/j.immuni.2006.06.014
49. Rodero MP, Poupel L, Loyher PL, Hamon P, Licata F, Pessel C, et al. Immune Surveillance of the Lung by Migrating Tissue Monocytes. *Elife* (2015) 4: e07847. doi: 10.7554/eLife.07847
50. Neelamegham S, Taylor AD, Burns AR, Smith CW, Simon SI. Hydrodynamic Shear Shows Distinct Roles for LFA-1 and Mac-1 in Neutrophil Adhesion to Intercellular Adhesion Molecule-1. *Blood* (1998) 92(5):1626–38. doi: 10.1182/blood.V92.5.1626
51. Cheng Y, Tian DY, Wang YJ. Peripheral Clearance of Brain-Derived Abeta in Alzheimer's Disease: Pathophysiology and Therapeutic Perspectives. *Transl Neurodegener* (2020) 9(1):16. doi: 10.1186/s40035-020-00195-1
52. Liu Y, Jing F, Yi W, Mendelson A, Shi P, Walsh R, et al. HO-1(Hi) Patrolling Monocytes Protect Against Vaso-Occlusion in Sickle Cell Disease. *Blood* (2018) 131(14):1600–10. doi: 10.1182/blood-2017-12-819870
53. Liu Y, Zhong H, Bao W, Mendelson A, An X, Shi P, et al. Patrolling Monocytes Scavenge Endothelial-Adherent Sickle RBCs: A Novel Mechanism of Inhibition of Vaso-Occlusion in SCD. *Blood* (2019) 134 (7):579–90. doi: 10.1182/blood.2019000172
54. Bednarczyk M, Stege H, Grabbe S, Bros M. Beta2 Integrins-Multi-Functional Leukocyte Receptors in Health and Disease. *Int J Mol Sci* (2020) 21(4):1402. doi: 10.3390/ijms21041402
55. Silverstein RL, Febbraio M. CD36, a Scavenger Receptor Involved in Immunity, Metabolism, Angiogenesis, and Behavior. *Sci Signal* (2009) 2 (72):re3. doi: 10.1126/scisignal.272re3
56. Brust M, Aouane O, Thiebaud M, Flormann D, Verdier C, Kaestner L, et al. The Plasma Protein Fibrinogen Stabilizes Clusters of Red Blood Cells in Microcapillary Flows. *Sci Rep* (2014) 4:4348. doi: 10.1038/srep04348
57. Yakubenko VP, Lishko VK, Lam SC, Ugarova TP. A Molecular Basis for Integrin Alphambeta 2 Ligand Binding Promiscuity. *J Biol Chem* (2002) 277 (50):48635–42. doi: 10.1074/jbc.M208877200
58. van Zanten TS, Cambi A, Koopman M, Joosten B, Figdor CG, Garcia-Parajo MF. Hotspots of GPI-Anchored Proteins and Integrin Nanoclusters Function as Nucleation Sites for Cell Adhesion. *Proc Natl Acad Sci USA* (2009) 106 (44):18557–62. doi: 10.1073/pnas.0905217106
59. Maiuri P, Rupprecht JF, Wieser S, Ruprecht V, Benichou O, Carpi N, et al. Actin Flows Mediate a Universal Coupling Between Cell Speed and Cell Persistence. *Cell* (2015) 161(2):374–86. doi: 10.1016/j.cell.2015.01.056
60. Li N, Yang H, Wang M, Lu S, Zhang Y, Long M. Ligand-Specific Binding Forces of LFA-1 and Mac-1 in Neutrophil Adhesion and Crawling. *Mol Biol Cell* (2018) 29(4):408–18. doi: 10.1091/mbc.E16-12-0827
61. Li W, Wang W. Structural Alteration of the Endothelial Glycocalyx: Contribution of the Actin Cytoskeleton. *Biomech Model Mechanobiol* (2018) 17(1):147–58. doi: 10.1007/s10237-017-0950-2
62. Le Master E, Huang RT, Zhang C, Bogachkov Y, Coles C, Shentu TP, et al. Proatherogenic Flow Increases Endothelial Stiffness *via* Enhanced CD36-Mediated Uptake of Oxidized Low-Density Lipoproteins. *Arterioscler Thromb Vasc Biol* (2018) 38(1):64–75. doi: 10.1161/ATVBAHA.117.309907
63. Mikaty G, Soyer M, Mairey E, Henry N, Dyer D, Forest KT, et al. Extracellular Bacterial Pathogen Induces Host Cell Surface Reorganization to Resist Shear Stress. *PloS Pathog* (2009) 5(2):e1000314. doi: 10.1371/journal.ppat.1000314
64. Katakai T, Habiro K, Kinashi T. Dendritic Cells Regulate High-Speed Interstitial T Cell Migration in the Lymph Node *via* LFA-1/ICAM-1. *J Immunol* (2013) 191(3):1188–99. doi: 10.4049/jimmunol.1300739
65. Mylvaganam S, Riedl M, Vega A, Collins RF, Jaqaman K, Grinstein S, et al. Stabilization of Endothelial Receptor Arrays by a Polarized Spectrin Cytoskeleton Facilitates Rolling and Adhesion of Leukocytes. *Cell Rep* (2020) 31(12):107798. doi: 10.1016/j.celrep.2020.107798
66. Ahmad F, Dobel T, Schmitz M, Schakel K. Current Concepts on 6-Sulfo LacNAc Expressing Monocytes (slanMo). *Front Immunol* (2019) 10:948. doi: 10.3389/fimmu.2019.00948
67. Hofer TP, van de Loosdrecht AA, Stahl-Hennig C, Cassatella MA, Ziegler-Heitbrock L. 6-Sulfo LacNAc (Slan) as a Marker for Non-Classical Monocytes. *Front Immunol* (2019) 10:2052. doi: 10.3389/fimmu.2019.02052
68. Akenhead ML, Fukuda S, Schmid-Schonbein GW, Shin HY. Fluid Shear-Induced Cathepsin B Release in the Control of Mac1-Dependent Neutrophil Adhesion. *J Leukoc Biol* (2017) 102(1):117–26. doi: 10.1189/jlb.3A0716-317RR
69. Vaisar T, Kassim SY, Gomez IG, Green PS, Hargarten S, Gough PJ, et al. MMP-9 Sheds the Beta2 Integrin Subunit (CD18) From Macrophages. *Mol Cell Proteomics* (2009) 8(5):1044–60. doi: 10.1074/mcp.M800449-MCP200
70. Zen K, Guo YL, Li LM, Bian Z, Zhang CY, Liu Y. Cleavage of the CD11b Extracellular Domain by the Leukocyte Serprocidins is Critical for Neutrophil Detachment During Chemotaxis. *Blood* (2011) 117(18):4885–94. doi: 10.1182/blood-2010-05-287722
71. Amich J, Mokhtari Z, Strobel M, Vialetto E, Sheta D, Yu Y, et al. Three-Dimensional Light Sheet Fluorescence Microscopy of Lungs To Dissect Local Host Immune-Aspergillus Fumigatus Interactions. *mBio* (2020) 11(1): e02752–19. doi: 10.1128/mBio.02752-19
72. Miller H, Cosgrove J, Wollman AJM, Taylor E, Zhou Z, O'Toole PJ, et al. High-Speed Single-Molecule Tracking of CXCL13 in the B-Follicle. *Front Immunol* (2018) 9:1073. doi: 10.3389/fimmu.2018.01073
73. Orndorff RL, Hong N, Yu K, Feinstein SI, Zern BJ, Fisher AB, et al. NOX2 in Lung Inflammation: Quantum Dot Based in Situ Imaging of NOX2-Mediated Expression of Vascular Cell Adhesion Molecule-1. *Am J Physiol Lung Cell Mol Physiol* (2014) 306(3):L260–8. doi: 10.1152/ajplung.00278.2013

Conflict of Interest: The authors declare that the research was conducted in the absence of any commercial or financial relationships that could be construed as a potential conflict of interest.

frontiers in Immunology

REVIEW
published: 25 October 2021
doi: 10.3389/fimmu.2021.718432

Trafficking of Mononuclear Phagocytes in Healthy Arteries and Atherosclerosis

Lukas Tomas[1,2*†], *Filip Prica*[1,2†] *and Christian Schulz*[1,2]

[1] Department of Medicine I, University Hospital, Ludwig Maximilian University, Munich, Germany, [2] DZHK (German Centre for Cardiovascular Research), Partner Site Munich Heart Alliance, Munich, Germany

Monocytes and macrophages play essential roles in all stages of atherosclerosis – from early precursor lesions to advanced stages of the disease. Intima-resident macrophages are among the first cells to be confronted with the influx and retention of apolipoprotein B-containing lipoproteins at the onset of hypercholesterolemia and atherosclerosis development. In this review, we outline the trafficking of monocytes and macrophages in and out of the healthy aorta, as well as the adaptation of their migratory behaviour during hypercholesterolemia. Furthermore, we discuss the functional and ontogenetic composition of the aortic pool of mononuclear phagocytes and its link to the atherosclerotic disease process. The development of mouse models of atherosclerosis regression in recent years, has enabled scientists to investigate the behaviour of monocytes and macrophages during the resolution of atherosclerosis. Herein, we describe the dynamics of these mononuclear phagocytes upon cessation of hypercholesterolemia and how they contribute to the restoration of tissue homeostasis. The aim of this review is to provide an insight into the trafficking, fate and disease-relevant dynamics of monocytes and macrophages during atherosclerosis, and to highlight remaining questions. We focus on the results of rodent studies, as analysis of cellular fates requires experimental manipulations that cannot be performed in humans but point out findings that could be replicated in human tissues. Understanding of the biology of macrophages in atherosclerosis provides an important basis for the development of therapeutic strategies to limit lesion formation and promote plaque regression.

Keywords: atherosclerosis, macrophage, monocyte, regression, trafficking

OPEN ACCESS

Edited by:
Emmanuel Donnadieu, Institut National de la Santé et de la Recherche Médicale (INSERM), France

Reviewed by:
Ishak Ozel Tekin, Bülent Ecevit University, Turkey
Gordon A. Francis, University of British Columbia, Canada

***Correspondence:**
Lukas Tomas
lukas.tomas@med.uni-muenchen.de

†These authors have contributed equally to this work and share first authorship

Specialty section:
This article was submitted to Molecular Innate Immunity, a section of the journal Frontiers in Immunology

Received: *31 May 2021*
Accepted: *30 September 2021*
Published: *25 October 2021*

Citation:
Tomas L, Prica F and Schulz C (2021) Trafficking of Mononuclear Phagocytes in Healthy Arteries and Atherosclerosis. Front. Immunol. 12:718432. doi: 10.3389/fimmu.2021.718432

INTRODUCTION

Atherosclerosis is characterised by a chronic, low-grade inflammation in the arterial wall. As the underlying pathology for myocardial infarction and stroke, it is the leading cause of death worldwide (1). The inflammatory response in the arterial wall is initiated by the hypercholesterolemia-induced subendothelial retention of apolipoprotein (apo)B-containing lipoproteins, mainly low-density lipoprotein (LDL), at sites of non-laminar and low shear stress blood flow. These sites are characterised by a higher abundance of macrophages (2–4),

inflammation-primed endothelial cells (5) and particularly in humans a pro-retentive thickened intima rich in smooth muscle cells and altered extracellular matrix (6–8). The subendothelial retention makes the lipoproteins susceptible to enzymatic and non-enzymatic modification. In particular, oxidation of LDL triggers a sterile inflammatory reaction by activating the endothelial cells to upregulate adhesion molecules and secrete chemokines which attract monocytes and other leukocytes. Modification of lipoproteins also promotes their uptake by macrophages and vascular smooth muscle cells (VSMC) leading to the appearance of foam cells. Additionally, oxidized LDL contains several bioactive molecules, including oxidized phospholipids, which act as damage-associated molecular patterns (DAMPs), and together with early cholesterol crystal formation cause an activation of surrounding innate immune cells (9, 10). The continuous influx, retention and modification of apoB-containing lipoproteins, together with the defective resolution of inflammation and dysfunctional clearance of dead cells (efferocytosis) fuel the chronic inflammation (11). The persistent inflammatory activity also leads to the generation of autoantigens and involvement of the adaptive immune system at later stages of the disease (12, 13).

Resident arterial macrophages play a crucial role in tissue homeostasis and serve as immune sentinels within the tissue. Adventitial macrophages, for instance, are important regulators of collagen production and the arterial tone (14). At areas of low blood velocity and shear stress, macrophages beneath the endothelium survey the environment to detect pathogens or potentially hazardous deposits (15). As such, aortic intima-resident macrophages are among the first cells to encounter trapped apoB-containing lipoproteins at the initiation of hypercholesterolemia (2–4). Mainly based on their expression of CD11c, these subendothelial phagocytes were initially described as dendritic cells, but recent results have challenged this view and have identified macrophages as the main cell type to first encounter the trapped lipids (16). Furthermore, in mice with a deficiency of monocytes and macrophages, a delayed and almost abolished development of atherosclerotic plaques can be seen (17–21). This further underlines the importance of the monocyte-macrophage axis in the initiation of atherosclerotic disease. With the development of mouse models for atherosclerotic regression, it has become clear that macrophages are not only important drivers of the disease, but their plasticity and diverse repertoire of homeostatic functions also makes them important effectors in atherosclerotic regression (22).

Since the description of the Mononuclear Phagocyte System, the prevailing paradigm was that tissue resident macrophages are continuously seeded from circulating monocytes. In recent years, however, it has become obvious that under homeostasis the tissue macrophage pool is mainly maintained through local proliferation and does not solely depend on monocyte influx (23–25). Monocyte-independent seeding of resident tissue macrophages starts early in embryonic development. Macrophages originating from the extra-embryonic yolk sac (YS) populate tissues during embryonal development as erythro-myeloid progenitor (EMP)-derived macrophages and persist into adulthood (26, 27). Microglia in the central nervous system are for instance exclusively derived from YS progenitors, without input from blood monocytes (28, 29). However, in most organs, a second wave of monocyte-derived macrophages, originating from definitive haematopoietic stem cells within the fetal liver and bone marrow (BM), co-colonize the tissues (30, 31). The question of tissue macrophage ontogeny has critical implications. EMP-derived macrophages migrate to tissues at the time of organogenesis and seem indispensable in various developmental processes (32–36). This developmental and homeostatic function might prevail in adult life, generating an important link between macrophage ontogeny and function. Indeed, we and others have found that macrophages of different ontogeny perform distinct tissue-specific functions and maintain a specific phenotype (37–41). Delineating monocyte-macrophage ontogeny and trafficking might improve our understanding of the maladaptive chronic inflammatory response in atherosclerosis development, as well as their role in atherosclerosis regression. Ultimately, this could lead to targeted approaches tackling the high rates of global cardiovascular mortality and morbidity resulting from atherosclerosis.

In this Review we address the knowns and unknowns of the trafficking, dynamics and fates of vascular monocytes and macrophages in the healthy and atherosclerotic aorta. Analysing these properties in human tissues is complicated by the availability of human material and models. Therefore, we will focus primarily on results from the mouse as a model organism but put these results into human context where possible at the end of this Review.

MONOCYTES AND MACROPHAGES IN THE HEALTHY AORTA

The development and broad accessibility of novel high-dimensional analysis techniques, such as multi-parameter flow cytometry, single-cell RNA sequencing (scRNA-seq) and cytometry by time of flight, has enabled scientists to obtain a clearer picture of leukocyte diversity in the healthy mouse aorta. These studies revealed that myeloid cells, and in particular macrophages, are the dominant immune cell type in the healthy arterial wall (16, 37, 42, 43). Arterial macrophages are primarily located in the fibrous outer arterial layer, the adventitia. Only a small number of macrophages can be found in the innermost layer, the intima, just below the endothelial cells. Based on histological and scRNA-seq data, it's estimated that up to 10% of the arterial macrophages are located in the intima, whereas 90% are positioned within the adventitial layer (16, 37, 44).

The aorta is populated with macrophages early on during embryonic development. Macrophages can be observed in the fetal aorta at embryonic day 16.5 and most likely start inhabiting the niche from embryonic day 9.5 onwards (27, 32, 44). This prenatal wave of macrophages colonising the aorta is dominated by YS EMP-derived macrophages which travel to the aorta without a monocyte intermediate. After birth, the brief influx

of blood monocytes, which consequently differentiate into tissue resident macrophages, contributes to the aortic macrophage pool (37, 44). Despite the monocytic influx, YS EMP-derived macrophages are not replaced by BM-derived macrophages, as has been suggested previously. Rather, the entire adventitial macrophage pool of EMP- and BM-derived macrophages continues to expand in numbers until 45 weeks of age, with YS EMP-derived macrophages being the dominant tissue-resident macrophage population (**Figure 1**). In aged mice, at around 90 weeks, a general drop of adventitial macrophage numbers mainly affecting EMP-derived macrophages can be observed (37). In contrast to adventitial macrophages, macrophages residing in the intima have recently been reported to seed almost exclusively after birth (16). Using various mouse models, including CD115, CX3CR1 and Flt3 reporter mice, Williams et al. showed that the macrophages inhabiting the intimal layer originate exclusively from definitive haematopoiesis. Interestingly, intimal macrophages are primarily found in locations of increased hemodynamic stress, which are predilection sites for atherosclerosis development (2, 3). Although we did not specifically investigate this aspect, our results show no site-specific tropism of adventitial macrophages throughout the aortic segments, in contrast to intimal macrophages (37). This puts further emphasis on understanding the origin, dynamics, and function of intima-resident macrophages. Given the critical role of intimal macrophages in atherosclerosis development, it will be interesting to see the results by Williams et al. confirmed with more efficient fate-mapping models, such as the recently generated $Rank^{Cre}$ (45) and $Ms4a3^{Cre}$ mice (30), in a quantitative approach.

Of note, one group has identified an unconventional Sca-$1^{+}CD45^{+}$ cellular subset in the adult murine aorta, proposed to be adventitial macrophage-committed progenitor cells (46, 47). A recent scRNA-seq study also identified an interferon-poised subset of Sca-1^{+} aortic macrophages, whereas the macrophage progenitor potential of aortic cells has been questioned by others (48, 49). Whether these Sca-$1^{+}CD45^{+}$ cells are indeed a macrophage progenitor population or potentially are provided by Sca-1^{+} mesenchymal stem cells remains to be elucidated (43, 50–54).

Under homeostasis, the adult arterial macrophage pool experiences little dynamic. Adventitial EMP- and BM-derived

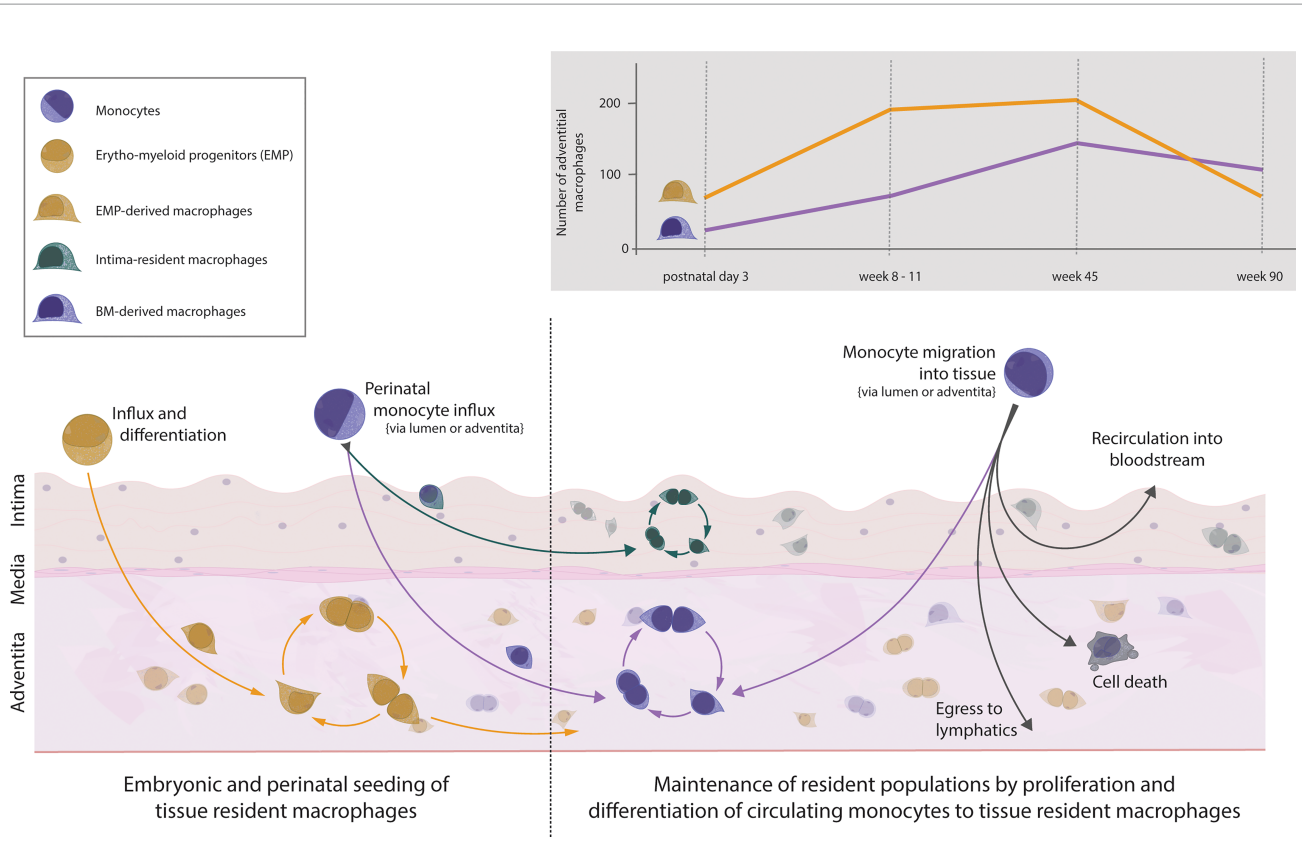

FIGURE 1 | Vascular macrophages and monocytes in the healthy mouse aorta. Influx of EMP-derived macrophages into the tissue during embryogenesis starts around embryonic day 9.5. Macrophages settle within the aortic adventitia and sustain solely through local proliferation. Around embryonic day 18.5, monocytes from the bone marrow seed the aorta and differentiate within the adventitia (forming a population of BM-derived tissue resident macrophages) as well as within the intima (forming a separate population of intima-resident macrophages). This recently defined population of intimal macrophages is heavily seeded perinatally but maintains solely through local proliferation. Thus, the adventitia is colonised with macrophages of dual origin which self-sustain numbers through proliferation, and in the case of adventitial BM-derived cells, replenishment from circulating monocytes. The number of cells of different ontogeny varies throughout life, with numbers changing in age adopted from (37). The fate of monocytes migrating into the steady-state aorta follows several possible fates: differentiation into BM-derived macrophages, further migration towards lymphatics, apoptosis, or migration back into circulation.

macrophages self-maintain with minimal input from monocytes entering the arterial wall. Using irradiation-free chimeras and parabionts, we and others have found that over a period of 9 months, only 20% of the arterial macrophages are replenished by monocytes (37, 44). In addition, this number seems to be a constant, as we observed a similar 20% monocyte input after a 3-month observation period (37). Contrary to the macrophages residing in the adventitia, the intimal macrophages appear to not be replaced by monocytes under homeostasis (16).

Besides the quantitatively limited replenishment of the macrophage pool in the adventitia, monocytes have important homeostatic functions in the vasculature. Non-classical $Ly6C^{low}CCR2^{-}$ monocytes, which derive from $Ly6C^{high}CCR2^{+}$ in mice, crawl along the endothelium to survey the cellular integrity and sense dangers, as well as to remove cellular debris (55–57). $Ly6C^{low}$ monocytes are, however, thought to rarely cross the endothelial barrier into the tissue (57, 58). In contrast, classical $Ly6C^{high}$ monocytes are highly mobile and extravasate, mainly guided by their CCR2 expression. A population of transiently sessile monocytes has been found in the lungs and skin of mice in their steady-state (59). These 'tissue monocytes' have previously also been identified in the spleen, which acts as a reservoir to quickly mobilize immune cells upon inflammation (60). Contrary to splenic monocytes, the $Ly6C^{high}$ monocytes in lung and skin can survey the tissue environment and transport antigens to lymph nodes (59). Although the question of sessile monocyte existence has not been addressed for the arterial wall, monocytes are readily identified in the healthy arterial wall (3, 42, 43, 61). Their homeostatic turnover and ability to recirculate into the blood or leave *via* afferent lymphatics into adjacent lymph nodes, similarly to the surveying monocytes in lung and skin, remains to be determined.

The high motility of $Ly6C^{high}$ monocytes comes with the price of potentially spreading infectious agents (62, 63). This might in part explain the presence of infectious agents within atherosclerotic plaques (64). A remaining question is the location of vessel wall entry of $Ly6C^{high}$ monocytes. It has not yet been clarified if and to what extent classical $Ly6C^{high}$ monocytes enter the healthy vascular wall *via* vasa vasorum in the adventitia or from the luminal side. This is of particular interest in advanced plaques, where intra-plaque sprouting of leaky vessels occurs and could drive the chronic inflammation through the constant supply of monocytes (65).

Analogous to the heterogenous homeostatic functions of monocytes, we and others have found that resident adventitial macrophages have a diverse functional outfit. Traditionally, macrophages have been divided in classically activated M1 and alternatively activated M2 macrophages (66). These two states are, however, *in vitro*-based extremes on opposite poles of a continuum of macrophage functionality. Novel multiparametric analysis methods have established the high plasticity and different nuances in the macrophage functional outfit (67–69), also in the aortic wall. Recent integrated analyses of scRNA-seq datasets from healthy and atherosclerotic mouse aortas revealed the presence of 5 major macrophage subsets (70, 71). As described in more detail below, these subsets are (I) inflammatory, (II) triggering receptor expressed on myeloid cells 2 $(TREM2)^{+}$, (III) interferon inducible, (IV) resident-like and (V) cavity macrophages. These five subsets can be found both in the atherosclerotic and healthy aorta, although the complexity of macrophage phenotypes increases in atherosclerotic aortas (70, 71). Strikingly, by employing scRNA-seq in $Rank^{Cre}Rosa26^{eYFP}$ mice we were able to map the transcriptional heterogeneity in adventitial macrophages to their origin. The healthy mouse adventitia harbours a macrophage subset with a homeostatic and anti-inflammatory transcriptional profile that derives almost exclusively from YS EMPs. These macrophages were characterised by a high expression of the hyaluronan receptor encoding gene Lyve-1, a known marker for resident macrophages, which maps them to the macrophage subset responsible for the regulation of aortic collagen production (14), and to the resident-like macrophages described above. Furthermore, EMP-derived macrophages expressed high levels of stabilin 1 (Stab1) and growth arrest specific 6 (Gas6), both of which are important for efferocytosis, a process crucial for the inhibition of atherosclerosis (37, 72–74). In contrast, a cluster that lacked *eYFP* transcript expression and was comprised of monocyte-derived macrophages expressed gene sets that were associated with pro-inflammatory properties, including *Il1β* (37), similar to the subset of inflammatory macrophages. Thus, there seems to be a division of labour in arterial macrophage subsets of different ontogeny, where EMP-derived macrophages are responsible for homeostatic processes like collagen production and efferocytosis. BM-derived macrophages in turn are in a poised state for defending the arterial integrity against pathogens. Thus, it would not be surprising if macrophages of diverse origins play different roles during atherosclerosis progression and regression, given their distinct set of functions.

ENHANCED MONOCYTE INFLUX AND MACROPHAGE PROLIFERATION DURING ATHEROSCLEROSIS DEVELOPMENT AND PROGRESSION

The intima-resident macrophages are among the first cells exposed to the increased influx of apoB-containing lipoproteins during hypercholesterolemia. These cells are critical in atherosclerosis initiation. The aorta of mice engineered to lack aortic intima-resident macrophages displays decreased lipid deposition in the early stages of atherosclerosis (4, 16). Within days of sustained hypercholesterolemia, the capacity of macrophages to metabolize the accumulating lipids and cholesterol is overwhelmed. This leads to the deposition of lipid droplets within the macrophage cytoplasm, resulting in the typical foam cell appearance, and even macrophage death. Macrophage death and defective clearance are known to be major drivers of the atherosclerotic process (16, 75, 76).

Initially, foam cells appear to be exclusively derived from resident intimal macrophages in the mouse (16). Of note, in humans, VSMCs also play a role in the early development of foam cells (77). Continuous inflammatory triggering by the

persistent influx of apoB-containing lipoproteins causes a substantial monocyte recruitment within the first 1-2 weeks of hypercholesterolemia (16, 78, 79). The subendothelial inflammatory foci lead to the expression of adhesion molecules on activated endothelial cells and the secretion of chemokines, most importantly of CCL2/MCP-1, CX3CL1 and CCL5 (80) These factors are essential for the infiltration of primarily Ly6C^{high} monocytes into the developing atherosclerotic plaque (81, 82). Combined absence of all three chemokine-chemokine receptor pairs results in an almost complete inhibition of lesion development (82–84). Intravital imaging studies suggest that the luminal ('inside-out') recruitment is important in the early phases of plaque development, whereas ('outside-in') recruitment *via* adventitial vasa vasorum is the main route for myeloid cells to enter advanced plaques (78, 85). More quantitative approaches with adoptive transfer of monocytes and bead labelling found that both the influx and luminal recruitment routes are important already in early atherosclerotic development, and persist in advanced plaques (86, 87). The route of plaque-invading monocytes is an important avenue of research, as these cells have been recognized to fuel the inflammatory reaction in developing plaques and blocking their entry might represent a promising therapeutic target.

In addition to causing a local inflammatory responses and recruitment of Ly6C^{high} monocytes into the vessel wall, hypercholesterolemia induces a Ly6C^{high} dominated monocytosis (81, 82). Elevated levels of cholesterol in haematopoietic stem cells foster the formation of lipid rafts and stabilisation of growth factor receptors, which promote their myelopoietic activity and monocytosis (88–90). Supplementing the enhanced myelopoiesis in the bone marrow, extramedullary haematopoiesis in the spleen contributes to increased production of monocytes and marked recruitment into the developing atherosclerotic lesion (60, 91). Other lifestyle-related factors such as hyperglycaemia or stress also have the potential to enhance myelopoiesis and fuel the cycle of monocyte production and entry into the plaque (92–94). Importantly, the circulating monocytes are poised for pro-inflammatory reactions with increased levels of surface receptors such as CD86 and TLR4, as well as increased levels of reactive oxygen species, among other features (44, 95–97). Thus, hypercholesterolemia leads to augmented recruitment and an increased number of circulating monocytes with a heightened inflammatory potential. A topic that warrants further investigation is the role of recently identified monocyte subsets that appear during inflammatory conditions, such as segregated-nucleus-containing atypical monocytes (98), in atherosclerosis development.

The recruited Ly6C^{high} monocytes are thought to primarily differentiate into intimal macrophages (75). Data from developing atherosclerotic plaques is lacking, but it is conceivable that Ly6C^{high} monocytes have alternative fates within the lesion (**Figure 2**). As has been shown for sterile liver injury, Ly6C^{high} monocytes can exhibit distinct monocyte-specific functions, including the uptake of trapped apoB-containing lipoproteins (99–101). In this way, monocytes participate in the vicious cycle of cellular apoptosis and necrosis following the metabolic stress of intracellular cholesterol accumulation. Some Ly6C^{high} monocytes might also recirculate into the blood and lymph and present antigens, including *de novo* generated autoantigens to the cells of the adaptive immune system (12, 13, 59). Ly6C^{low} monocytes, on the other hand, show an intensified patrolling behaviour at atheroprone sites, which display increased endothelial damage during hypercholesterolemia (58, 102). Despite their main task as patrolling intravascular cells, Ly6C^{low} monocytes can also be found in the atherosclerotic plaque, highlighting their potential to extravasate – although to a lesser extent than classical Ly6C^{high} monocytes (70, 82). These cells display an anti-inflammatory transcriptional signature with elevated transcripts for cholesterol efflux and vascular repair, thereby promoting the inflammation resolution (58). It is still debated whether the extravasation of Ly6C^{low} monocytes is of importance in the atherosclerotic disease process (58). If so, the anti-atherosclerotic phenotype of Ly6C^{low} monocytes presumably ameliorates the disease process and enhancing Ly6C^{low} monocyte extravasation might be a potential therapeutic target.

Akin to other chronic inflammatory diseases, the initial, mainly CCR2-dependent, recruitment of monocyte-derived macrophages is a crucial pathomechanism in the development of atherosclerosis (82–84, 103–106). However, as the atherosclerotic lesion progresses, monocyte recruitment becomes less important, as evidenced by studies with CCR2- or monocyte-depletion models (21, 107–109). The limited impact of blocking monocyte recruitment on progression of advanced plaques might be due to a failure of monocytes to penetrate the lesion. A recent report suggests that monocytes cannot migrate deeply into the lesion and only accumulate superficially, similar to tree ring formation (87). This is, however, contradicted by results showing migrating CD11c^{+}, which appear to be similar to foamy monocytes or macrophages, within atherosclerotic plaques (100, 101, 110). Consequently, there might be other reasons for the non-reliance on monocyte entry in progressing plaques, such as local macrophage proliferation, as discussed below.

Hypercholesterolemia leads to a substantial influx of monocytes. It has recently been suggested that the perinatally seeded intima-resident macrophages are completely replaced by invading monocyte-derived macrophages within weeks of hypercholesterolemia (16). Although similar results have been observed for liver Kupffer cells during Listeria infection (111), this contrasts with the fate of adventitial macrophages in other models of sterile and non-sterile aortic inflammation. We and others found that, after a transient recruitment of monocyte-derived macrophages in the acute phase, the resident macrophage population prevails even in chronic inflammatory models (37, 44). Our results focused on adventitial macrophages, but the different response of intimal macrophages in atherosclerosis is an intriguing characteristic that might be contributing to the defective inflammation resolution in atherosclerosis (61, 81). Given that in mice the entire adventitial macrophage pool requires approximately one year for a complete cell turnover (44), it is likely that the turnover of intimal macrophages during hypercholesterolemia is accelerated by mechanisms like emigration or cell death, which in turn could

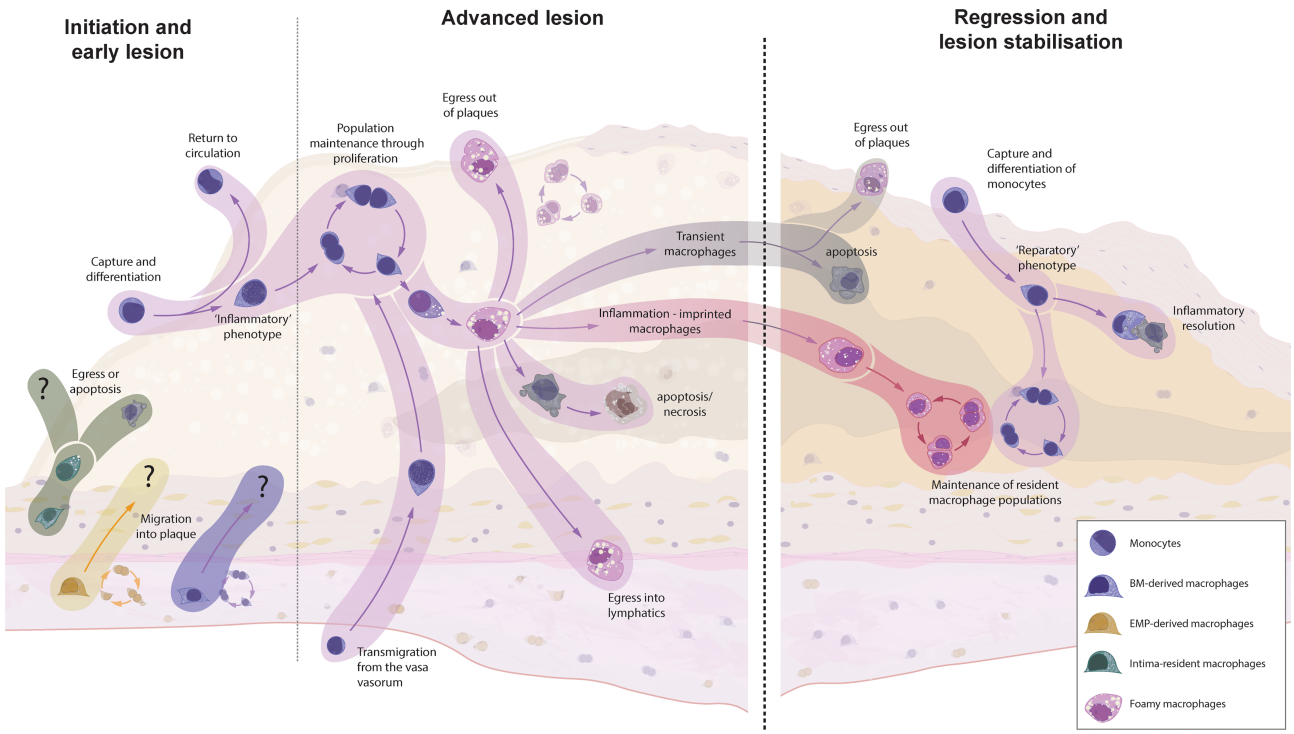

FIGURE 2 | The origin and fate of macrophages in murine models of atherosclerotic plaque formation and regression. Intima-resident macrophages are the first to encounter accumulating apoB-containing lipoproteins but are replaced by recruited macrophages within weeks. It is unknown whether resident adventitial (EMP- and BM-derived) macrophages can invade the intima at any point of atherosclerosis progression or regression. Monocyte recruitment is the dominant source for plaque macrophages during early atherosclerosis, whereas local macrophage proliferation takes over at later stages. In other inflammatory disorders, macrophages can migrate either transendothelially or *via* lymphatics to clear the inflammatory triggers and present them to the adaptive immune system. However, hypercholesterolemia supresses emigration, leading to a continuous accumulation of cells, resulting in increased apoptosis and secondary necrosis. Upon the cessation of hypercholesterolemia, the fate of localised macrophages is yet unknown. Research from other inflammatory disorders has shown that, upon removal of the inflammatory stimuli, a number of macrophages will clear through apoptosis (transient macrophages), but inflammatory imprinting can define a population of surviving macrophages which have an acquired epigenetic memory - which might have detrimental effect on disease resolution and recurrence of inflammation. Additionally, a novel wave of monocyte recruitment defines a fresh population of reparatory macrophages, which aid in tissue clearance and tissue repair.

fuel atherosclerotic development. Nonetheless, it is possible that intima-resident macrophage numbers also rebound after the cessation of hypercholesterolemia, but this remains to be elucidated.

The fate of the intima-resident macrophages is of particular interest in the context of atherosclerosis, as we know from other inflammatory conditions that most monocytes recruited under inflammatory conditions do not stably engraft as resident macrophages. These transient macrophages disappear upon the resolution of inflammation (25, 39, 112, 113), which has also been shown in the aorta (44). Future studies will have to elucidate the macrophage composition and origin within the intimal niche after the cessation of hypercholesterolemia. Studies focussing on the lung and other tissues have also found that some *de novo* recruited macrophages are not transiently resident but persist even after inflammation resolution. Importantly, these macrophages were shown to acquire an epigenetic memory of the inflammatory situation (inflammation-imprinted resident macrophages), which might have detrimental effects on tissue repair or repetitive insults (113). Whether the newly recruited atherosclerotic macrophages share fates with inflammatory macrophages in other tissues and vanish after removal of the inflammatory stimulus is the topic of ongoing research.

Despite the increased macrophage apoptosis and necrosis in atherosclerotic plaques, macrophage numbers are stable throughout disease progression (49). It has been estimated that in early atherosclerosis monocyte recruitment accounts for approximately 70% of the macrophage replenishment, while more than 85% of the macrophages in advanced plaques stem from *in situ* proliferation (49). Interestingly, whereas proliferation of intimal macrophages increases as the atherosclerotic lesions progresses, adventitial macrophages do not proliferate more, as if they were not affected by the ongoing inflammatory process (49). Macrophage loss in atherosclerotic plaques is mainly a result of cell death. In infectious settings, macrophages emigrate from the site of infection either *via* reverse transendothelial migration or *via* lymphatics to clear the inflammatory triggers and present them to the adaptive immune system (62, 114). Hypercholesterolemia, however, suppresses emigration signals *via* CCR7 and macrophage

migratory capacity, leading to a continuous accumulation of macrophages and increased local cell death with the development of a necrotic core (62, 115–118). In general, the migration behaviour of plaque macrophages has been characterised as 'dancing on the spot', i.e. macrophages do not migrate within the plaque but only extend and retract their dendrites (87, 110, 119). This inability to migrate begs the question whether resident adventitial macrophages are capable of crossing the muscular media and migrate into the developing plaque.

Phenotype and functions of macrophages are governed by transcriptional regulation. It has been suggested that the transcriptional programs of intima-resident macrophages and recruited monocyte-derived macrophages converge on a similar foamy macrophage profile early in hypercholesterolemia (16, 71). But developing atherosclerotic plaques harbour many heterogenous subsets of macrophages. As described above, efforts to integrate the various scRNA-seq studies of the murine atherosclerotic plaque have defined 5 distinct macrophage subsets: (I) inflammatory, (II) TREM2$^+$, (III) interferon inducible, (IV) resident-like and (V) cavity macrophages (70, 71). Inflammatory macrophages show elevated expression levels of pro-inflammatory cytokines like interleukin 1β and tumor necrosis factor. The strong pro-inflammatory gene profile and the importance of interleukin 1β in atherosclerotic disease points towards a major role of this macrophage subset in aggravating the chronic atherogenic inflammation. These cells were furthermore characterized by high CCR2 expression and presumably are transient inflammatory macrophage descendants from invading Ly6C^{high} monocytes. Macrophages expressing TREM2 have been identified as the foam cell population in atherosclerotic plaques (120–122). TREM2 is a transmembrane glycoprotein that can interact with apolipoprotein E and TREM2$^+$ macrophages show a transcriptomic signature enriched for lipid metabolism pathways, pinpointing their role in lipid and cholesterol handling (38, 123). TREM2$^+$ macrophages have previously been shown to possess anti-inflammatory functions (124). The TREM2$^+$ macrophage subset in atherosclerotic plaques is also characterized by dramatically decreased expression levels of pro-inflammatory molecules like interleukin 1β, tumor necrosis factor or NLR family pyrin containing domain 3 (Nlrp3) (120, 121). Furthermore, TREM2$^+$ macrophages have been found to express increased levels of CD11c (110), similar to foamy monocytes (100, 101). Interestingly, TREM2 expression is found in a variety of disease-associated macrophages, including microglia during neurodegenerative disease and lipid-associated macrophages in obesity (38, 125). Even in our dataset of adventitial macrophages during angiotensin II-induced arterial inflammation, we were able to identify TREM2$^+$ macrophages (71). Consequently, TREM2$^+$ macrophages might represent a phenotype that is associated with tissues exhibiting increased lipid deposition and apoptosis. In both scenarios, macrophages capable of handling lipid depositions are required for tissue homeostasis. Additionally, apoptotic cell death, which leads to increased lipid and cholesterol deposition, is associated with anti-inflammatory cell functions (76). It is interesting to note that TREM2$^+$ macrophages do not seem to be related to only one ontogeny but can derive from both YS and BM (38, 71, 125). The interferon-inducible macrophages are a rather small subset in the atherosclerotic plaque (70). These macrophages are characterised by expression of several interferon-inducible genes, including *Isg15* and *Irf7*. Future studies will have to investigate this so far unknown subset but given the pro-atherosclerotic role of type I interferon signalling, interferon-inducible macrophages might be detrimental in the course of the disease (126). The identified resident-like macrophage subset is characterised by high expression of *Lyve-1*, a gene that is important in resident adventitial macrophages for regulation of collagen production in the arterial wall (14). Similar to our dataset of Lyve-1 expressing macrophages in the healthy aorta (37), resident-like macrophages in the atherosclerotic plaque showed increased gene expression of Gas6 (48, 70, 121). Consequently, resident-like macrophages might be important in the efferocytotic clearance of apoptotic plaque cells and thus be major influencer of the balance between progressing and regressing atherosclerotic plaques. A drawback of the scRNA-seq studies is that we cannot distinguish between intimal and adventitial macrophages. Thus, the presence of resident-like macrophages in atherosclerotic aortas does not provide evidence for a role of Lyve-1$^+$ resident macrophage in the intima-focussed atherosclerotic disease process. The discovery of a macrophage subset expressing a gene signature reminiscent of 'cavity macrophages' is an interesting aspect, in light of recent reports. Mature macrophages from serous cavities like the peritoneum or pericardium have been shown to invade surrounding tissue during sterile inflammation where they play important roles during tissue repair (127–129). The presence of cavity macrophages in atherosclerotic aortas indicates that adjacent macrophages, from serous cavities or potentially even the adventitia, can invade the atherosclerotic aorta and intima.

Even though resident adventitial macrophages constitute 90% of the aortic macrophages and are the only arterial subset originating from EMPs, their involvement in the atherosclerotic disease process is unclear. The role of adventitial macrophage subsets, including the YS EMP-derived adventitial macrophages, warrants further investigation. As described above, EMP-derived adventitial macrophages show a distinct transcriptional signature of anti-inflammatory and efferocytic functions, that is preserved during chronic arterial inflammation (37). Failing efferocytosis, in particular, has been shown to be a major pathogenic factor in atherosclerotic development (76). Adventitial EMP-derived macrophages seem to be predestined to counteract this failure and inhibit the inflammatory cycle within atherosclerotic plaques – if they invade the growing lesion. As outlined herein, plaque macrophages show diminished migratory behaviour, and adventitial macrophages are not thought to invade the growing plaques. On the other hand, the presence of cavity macrophages suggests that certain macrophage subsets might still be able to invade the developing lesions. Also, a CD11c$^+$ cell subset, which resemble foamy macrophages, has been shown to be actively migrating within the plaque. These results warrant further

investigation on the trafficking of adventitial macrophages and macrophages of different ontogenies during the various stages of atherosclerosis development.

MACROPHAGE EGRESS AND MONOCYTE MIGRATION IN REGRESSING ATHEROSCLEROTIC PLAQUES

Atherosclerosis is characterised by a failure to resolve the inflammatory response. The continuous influx and retention of apoB-containing lipoproteins represents a persistent inflammatory stimulus. The lowering of blood lipid levels, in particular cholesterol levels (130), allows the resolution phase to commence. The resolution or regression of atherosclerotic plaques can lead to a reduction of plaque size, but most importantly results in the scarring and stabilisation of advanced lesions, lowering the risk of myocardial infarction and stroke (22). The reduction of plaque leukocyte abundance and a phenotypic switch in plaque cells are important hallmarks during atherosclerosis regression (131). Macrophages are highly plastic cells, and as such are fundamental players in the tissue repair processes seen in atherosclerosis regression.

Traditional mouse models of atherosclerosis, like the LDL receptor and apolipoprotein E knockout mouse, have greatly contributed to our understanding of the atherosclerotic disease process. These models, however, lack the ability to normalise hypercholesterolemia and induce regression. Fortunately, in recent years several mouse models of atherosclerosis regression were developed (132–138). The common denominator of these models is the normalisation of cholesterol levels after a phase of hypercholesterolemia to induce advanced atherosclerotic plaques. Examples include the transplantation of atherosclerotic aortic segments into normocholesterolemic mice or the inducible deficiency of the microsomal triglyceride transfer protein, as in the Reversa mouse (132, 133). The variety of regression models, as well as their individual limitations, such as surgical inflammation and a lack of lymphatic anastomosis in the transplantation model might be the reason for the heterogeneous results regarding the fate of macrophages in atherosclerosis regression. A novel approach uses antisense oligonucleotides, targeting the LDL receptor to transiently cause hypercholesterolemia and induce atherosclerotic plaques. In this model, regression can be induced either by discontinuing the antisense oligonucleotides or through treatment with sense oligonucleotides for the LDL receptor (136). The LDL receptor antisense method offers a promising approach, as it allows scientists to omit time- and labour-intensive cross-breedings when using transgenic animals in regression. Furthermore, due to its limited off-target effects, antisense treatment is even used in human hyperlipidaemic disease (139, 140).

A hallmark of atherosclerosis regression is the reduction of the plaque macrophage content (87, 117, 141–146). Macrophage emigration from arteries *via* afferent lymphatics or reverse transendothelial migration aids the host defence by presenting antigens to the adaptive immune system (62, 114). As described above, hypercholesterolemia blunts the CCR7-guided emigration *via* the expression of neuroimmune guidance cues, including netrin 1 and semaphoring 3E, and by increasing plasma membrane cholesterol content which affects intracellular signalling as well as other mechanisms (62, 115–118, 147). Not surprisingly, the reversal of hypercholesterolemia has been shown to induce CCR7 expression in plaque macrophages and with it their efflux *via* afferent lymphatics (117, 142–144, 148–150). Whether lesional macrophages leave the regressing plaque *via* reverse transendothelial migration, as well as the quantitative relevance of macrophage emigration to the overall loss of plaque macrophages has not yet been clarified. Increased macrophage emigration has been observed in several different models of atherosclerosis regression, including the aortic transplantation, the Reversa mouse and apoB-targeted antisense oligonucleotide treatment (117, 142–144, 148–150), whereas other reports have found no difference in macrophage emigration behaviour during regression (87, 145, 146). Importantly, emigration of plaque macrophages to lymph nodes might aid the development of the recently described post-resolution phase, although it is unknown whether this establishment of adaptive immunity takes place in atherosclerosis regression (151).

Another common mechanism of leukocyte removal during tissue repair is programmed cell death *via* apoptosis (152). Effective clearance of apoptotic cells by macrophages avoids secondary necrosis and suppresses inflammation. Additionally, efferocytosis aids tissue repair by inducing a pro-resolving phenotype in phagocytosing macrophages (76). Whereas a recent report identified increased macrophage apoptosis as part of the regression mechanism (149), other studies did not find elevated numbers of apoptotic macrophages in regressing plaques (145, 146, 150). In order for apoptosis to act as a pro-resolving stimulus, efferocytosis needs to be functional. In atherosclerosis progression, however, defective efferocytosis is an essential pathogenic mechanism (11). The role of macrophage apoptosis in atherosclerosis regression remains elusive, and further studies investigating the presence and functionality of efferocytosis in atherosclerosis regression are warranted.

As macrophage numbers in advanced atherosclerotic plaques are primarily maintained through local proliferation, another means of reducing the plaque macrophage burden is through the suspension of proliferation. Indeed, a decrease in proliferating macrophages can be observed within 3 weeks of regression (145, 149). An inhibition of macrophage proliferation upon cessation of hypercholesterolemia is not an unexpected finding, as the retained and modified apoB-containing lipoproteins are potent inducers of M-CSF, contributing to an increase in local macrophage proliferation in advanced plaques (49, 153, 154).

In addition to macrophage survival and proliferation, monocyte recruitment is another factor influencing plaque macrophage numbers. The reversal of hypercholesterolemia presumably blunts the heightened monocytopoiesis and normalises circulating Ly6C^{high} monocyte levels. However, so far, no difference could be detected in studies evaluating the monocyte frequency even after 4 weeks of regression (145, 146). These intriguing results warrant

further studies focusing on the timing and return to a steady-state haematopoiesis following the onset of normocholesterolemia. Nonetheless, monocyte extravasation is not only dependent on the number of circulating monocytes, but also on their potential to invade the regressing plaque. Similarly to mechanisms halting proliferation of plaque macrophages, decreased *de novo* generation of macrophages from immigrating monocytes would result in a reduction of plaque macrophage abundance. Experimentally, several groups have detected a suppressed migration of Ly6C^{high} as well as Ly6C^{low} monocytes into the regressing plaque by using the adoptive transfer of labelled monocytes, as well as by monocyte tracking with fluorescent beads (145, 146, 155). The quantitative relevance of this effect might, however, be limited. Härdtner et al. estimated that the limited monocyte recruitment accounts for only about 25% of plaque macrophage reduction (145), whereas another report found no suppression of monocyte influx in regressing plaques, despite using similar methods (149). In summary, there are various mechanisms at play reducing the abundance of inflammatory macrophages in regressing atherosclerotic plaques. Presumably, all four mechanisms mentioned herein are relevant for ameliorating the inflammatory burden, likely occurring at various stages of regression. Longitudinal studies of macrophage trafficking, in combination with fate-mapping models and other methodologies capable of tracing the fates of lesional macrophages will hopefully advance our understanding of the cellular dynamics in regression.

The diminished monocyte influx during atherosclerosis regression is an interesting avenue for further research. The resolution and repair phase after myocardial infarction, as well as following sterile injuries in other organs, depends on the continuous influx of monocytes, which consequently differentiate into reparatory and pro-resolving macrophages (156–160). The importance of monocyte migration into the arterial wall to facilitate inflammation resolution and tissue repair has recently also been established for atherosclerosis regression. Applying the aortic transplantation models in numerous chemokine receptor knockout and reporter mice, Rahman et al. found that inhibiting the entry of Ly6C^{high}, but not Ly6C^{low} monocytes, into the atherosclerotic plaque during normocholesterolemia abrogates atherosclerosis regression (161). Analogous to their phenotype in the steady-state, Ly6C^{high} monocytes might not necessarily differentiate into macrophages, but instead participate in tissue repair with their monocyte-specific functions. In a model of sterile liver injury, as well as during the resolution phase after myocardial infarction, recruited classical Ly6C^{high} monocytes performed a phenotypic switch to non-classical Ly6C^{low} monocytes, which was crucial for optimal tissue repair (99, 157). The precise functions of circulating Ly6C^{low} monocytes during atherosclerosis regression have not yet been clarified. Given their role in the integrity of the endothelium, it is conceivable that intravascular Ly6C^{low} monocytes participate in the reorganisation of the endothelial layer during the plaque size reduction. It will be interesting to see first results of studies focussing on the role Ly6C^{low} monocytes during atherosclerosis regression, for instance in a mouse model with a Ly6C^{low} monocyte-specific deficiency (162).

Akin to the inflammation-poised phenotype of monocytes circulating during hypercholesterolemia and atherosclerosis development described above, resolution-dedicated monocyte subsets have been found to be present in the inflammatory resolution of sepsis and colitis (163). However, as to whether the reparatory Ym1 (chitinase-like protein 3)$^{+}$Ly6C^{high} monocyte subset described is also present during atherosclerosis resolution has not been investigated. Nevertheless, Ly6C^{high} monocytes have been found to exhibit an altered surface expression of various proteins during the regression of atherosclerosis (146). This underlines the importance of the quality over the quantity of the monocyte response and offers an explanation as to why atherosclerosis regression continues undisturbed in studies with suppressed monocyte recruitment.

Emerging scRNA-seq studies of atherosclerosis regression have been providing us with an insight regarding the heterogeneity of the remaining and recruited macrophages in regressing plaques (48, 149). Interestingly, the same, previously mentioned, five main macrophage clusters present during atherosclerosis have also been observed in regressing plaques (48, 70, 149). This might be less surprising for the subsets of cavity-like and TREM2^{+} macrophages. As mentioned above, cavity macrophages have been found to be essential mediators of tissue repair (127–129). The scRNA-seq studies of atherosclerosis regression, however, are unable to inform us about the location of the analysed macrophages, and thus it is unclear as to whether these cavity macrophages have invaded the intima, or if they participate in the resolution of the intimal inflammation However, TREM2^{+} macrophages are known to be equipped for lipid handling, and the accumulation of extracellular lipids is part of the tissue repair when dead and apoptotic cells need to be cleared by efferocytosis, a process that is increased in regressing plaques (149).

Although these studies identified the same major macrophage clusters in regressing plaques as in atherosclerosis development, there were subtle differences in expression levels representing a spectrum of activation states (48, 149). The subset of inflammatory macrophages, for instance, showed decreased expression levels of *Il1β* and *Nlrp3*, compared to atherosclerotic macrophages before the induction of atherosclerosis regression (149). Interestingly, the described interferon-inducible macrophages had increased transcription levels of *signal transducer and activator of transcription 6* (*Stat6)*, which is known to induce type 2 or reparatory immune responses (149). Notably, when atherosclerotic aortic segments were transplanted in normocholesterolemic Stat6-deficient mice, atherosclerosis regression was abrogated, which was associated with a pro-inflammatory phenotype of plaque macrophages (161). A question that has not been finally resolved is if the already present plaque macrophages can be repolarized by the regressing conditions to adjust their functional program towards a reparatory phenotype or if an influx of *de novo* reparatory macrophages is required. The study by Rahman et al. found that Ly6C^{high} monocyte influx is an absolute requirement for plaque regression and differentiation of reparatory macrophages (161). This is in line with evidence that

inflammatory macrophages cannot be repolarized to reparatory macrophages (164) undefined. In other reports inflammatory macrophages could be repolarized to a reparatory phenotype, although only a limited number of phenotypic markers were assessed (165, 166). Furthermore, an elegant *in vivo* tracking approach found a phenotypic adjustment of individual macrophages from inflammatory inducible nitric oxide synthase-expressing to arginase-expressing macrophages in a model of chronic central nervous inflammation (167). If and to what extent a local phenotypic switch of macrophages occurs in the regressing atherosclerotic plaque remains elusive and warrants further studies.

Interestingly, when Lin et al. broke down the transcriptional differences in macrophages during progression and regression in more detail, they identified one substantial macrophage subset and 42 distinctly regulated genes that were predominantly present during regression. The macrophage subset was characterised by high expression of *Stab1*, which is important for efferocytosis. In addition to *Stab1*, *Gas6* represents another upregulated molecule important for efferocytosis (48). Intriguingly, we have previously found that adventitial EMP-derived macrophages are characterised by high expression levels of both Stab1 and Gas6 (37). The presence of a regression-specific macrophage subset expressing a similar signature might indicate a role for EMP-derived macrophages in the tissue repair during atherosclerosis regression, and even hint towards the migration of these prenatally seeded adventitial macrophages into the intima. Relatedly, EMP-derived macrophages are known to be important regulators of tissue repair in the heart (168, 169). So far, it was assumed that adventitial macrophages do not cross the media and immigrate into the intima, but future studies will have to re-evaluate the fate of adventitial EMP-derived macrophages during atherosclerotic disease.

HUMAN TRANSLATABILITY

The wide array of available methods, including genetic fate-mapping models, intravital imaging or tracking of adoptively transferred cells, makes the mouse an ideal model system for studying the trafficking behaviour and dynamics of monocytes and macrophages. Although these models allow us to study the trafficking of mononuclear phagocytes in the mouse vasculature, ultimately the goal is to advance our understanding of these features in the human-being. Since similar scientific manipulations are unfeasible in the human, descriptive studies are used to determine the translatability of results in the mouse to the human situation.

In mice YS EMP-derived macrophages seed the aorta during early embryonic development. Haematopoiesis is a conserved process between men and mice, with an initial haematopoietic wave originating in the extra-embryonic YS, followed by a transition to intra-embryonic definitive haematopoiesis (170, 171). We and others have previously identified primitive macrophages in the human YS that show a phenotype similar to mouse EMP-derived macrophages in the mouse (27, 172, 173). A recent study employing scRNA-seq on human embryonic tissue at different time points of organogenesis found tissue-resident macrophages originating from the YS as well as the fetal liver (174), thus providing evidence for an initial seeding of vascular macrophage during early human embryogenesis and corroborating rodent studies. A second wave of monocyte-derived macrophage presumably follows the initial seeding with YS-derived macrophages in the human. Direct evidence for this in the arterial wall is lacking but studies in other human tissues were able to translate the results of mouse studies to humans. Langerhans cells in the skin have been shown to be YS-derived resident epidermal macrophages seeding the tissue in the first wave, whereas dermal macrophages are of monocytic origin in mice (31, 175). In humans with an inherited severe monocytopenia, a dramatically reduced frequency of $CD14^+$ dermal macrophages but sustained numbers of Langerhans cells could be observed (176, 177). The skin is an easily accessible organ with different macrophage ontogenies that enables investigation of macrophage trafficking in humans. Other future options might include the study of conserved epigenetic marks between the murine and human system also in the cardiovascular system and especially the arterial wall.

Like in the mouse, macrophages are a major subset or even the dominant immune subset in the non-atherosclerotic arterial wall of humans, although the human arteries also contain significant numbers of T lymphocytes (16, 37, 42, 43, 178–180). Arterial phagocytes can be found in the intima, directly beneath the endothelial layer, mirroring their function as immune sentinels, as well as in the adventitia (2, 180–185). Arterial resident macrophages are more prevalent in the adventitial layer than in the intima, although the difference is less pronounced compared to the mouse (186, 187). As would be expected for immune sentinels, intima-resident macrophages can be found more frequently at atheroprone sites, which show non-laminar and low shear stress blood flow (2, 180, 183). Studies in other human organs have provided evidence that tissue-resident macrophages self-sustain mainly through local proliferation without monocyte input, although there might be differences depending on the macrophage subset. In studies of sex-mismatched hand allografts, YS-derived Langerhans cells were not replaced by recipient cells but remained of donor origin up to 10 years post-transplantation (188, 189). This is in line with results of sex-mismatched heart transplants, where only 31% of presumably BM-derived $CCR2^+$ macrophages were of recipient origin compared to less than 1% $CCR2^-$, potentially YS-derived, resident macrophages, after a mean period of 8.8 years post-transplantation (190). The arterial wall of the vessels in the transplanted organs has not been examined separately, but a recent scRNA-seq study of human healthy arterial tissue identified a proliferative macrophage subset (178), hinting towards a self-sustaining arterial resident macrophage population.

Although the human intima harbours subendothelial macrophages and $CD11c^+$ phagocytes that mirror the recently identified aortic intima-resident macrophage of the mouse (16, 181, 191), there are important differences in the intimal composition between mouse models and humans that need to

be considered. The human intima is thickened and comprises abundant VSMCs and extracellular matrix at sites prone to atherosclerotic development. Additionally, VSMCs are very plastic cells and in addition to being producers of extracellular matrix components can be phagocytic and develop into foam cells. The discrimination of VSMC and macrophage foam cells is complicated by the fact that, VSMCs can express macrophage markers like CD68, whereas macrophages have also been found to express VSMC lineage markers (51, 192–195). Lineage-tracing studies in mice have shown a varying degree of foam cells originating from VSMCs, ranging from 16% to 70% (53, 195–197). In humans, it has been estimated through the analysis of histone marks that 18% of $CD68^+$ plaque cells originate from the VSMC lineage (51). Future studies will have to determine to what extent VSMCs and macrophages contribute to the foam cell pool at different phases of the atherosclerotic process.

The inflammatory reaction following the influx, retention and modification leads to a continuous recruitment of human monocytes into the growing atherosclerotic lesion (198, 199). Evidence for an important role of monocyte recruitment in the development of human atherosclerosis derives from studies showing an association of monocyte counts with atherosclerotic plaque development during several years of follow-up (200–202). Human monocytes can be distinguished into three different subsets: (I) classical $CD14^+CD16^-$, analogous to the $Ly6C^{high}$ mouse population, (II) non-classical $CD14^{dim}CD16^+$, aligning with the murine $Ly6C^{low}$ subset, and (III) intermediate $CD14^+CD16^+$ monocytes (203). Emerging results from multiparametric analyses identified further subsets and it will be interesting to determine their functional relevance in atherosclerosis (204–206). The non-classical $CD14^{dim}CD16^+$ monocytes fulfil similar endothelial surveillance functions as in the mouse, whereas the role of intermediate monocytes is not yet clear in the atherosclerotic progress (55–57, 203). The classical $CD14^+CD16^-$ are thought to mainly enter the growing atherosclerotic lesion (207), as this subsets preferentially migrates into tissues and differentiates to macrophages (208–211). Consequently, it has been shown that higher numbers of circulating $CD14^+CD16^-$ monocytes predict cardiovascular events (212, 213). Interestingly though, classical $CD14^+CD16^-$ monocytes do not associate with a more high-risk plaque phenotype in patients with advanced atherosclerosis (214). This might be owed to a more important role of local macrophage proliferation than monocyte recruitment in advanced atherosclerosis, similar to what has been observed in mice. In line with this, advanced atherosclerotic plaques contain a significant fraction of proliferating macrophages (71, 215–219). Another striking similarity between the human and mouse plaque macrophages relates to their phenotype. An integrated analysis of scRNA-seq subsets of the mouse and human revealed a conserved phenotype between the two species, with detection of (I) inflammatory, (II) foamy $TREM2^+$, (III) resident-like and (IV) interferon-inducible macrophages (71).

In summary, there are important differences between human and mouse atherosclerosis, as exemplified by the presence of a thickened VSMC-rich intima in the human arterial wall. Nonetheless, studies in rodent models have been instructive in examining basic principles of the trafficking of mononuclear phagocytes and will continue to provide valuable insight. Novel techniques, such as spatial transcriptomics (220), hold a great promise in translating murine results to the human situation.

CONCLUSION AND OUTSTANDING QUESTIONS

Monocytes and macrophages are key effector cells during all phases of atherosclerotic disease. Their trafficking in and out of the arterial wall directly influences the disease process. Although we have gained substantial insight into these processes during atherosclerosis development, there are still major gaps in our knowledge. For instance, it is currently unknown if invading monocytes persist in a non-differentiated state within the plaque or if their only fate is the differentiation to plaque macrophages. Answering this question is complicated by the phenotypic similarities of monocytes and macrophages. The combination of newly developed fate-mapping models with novel methodologies, like spatial transcriptomics, display a promising avenue for future investigations of cellular fates within the plaque. Along these lines, the recently identified subset of intima-resident macrophages illustrates the potential of such methodologies to deciphering macrophage dynamics within the arterial wall by using novel methodologies.

Nonetheless it is unclear if intima-resident macrophages vanish entirely upon onset of hypercholesterolemia or can rebound once cholesterol levels are normalised. Another remaining question relates to the dynamics of replacing intima-resident macrophages by recruited macrophages. Does the resident subset die, emigrate or just stop its proliferation?

Another major remaining question is the role of adventitia-resident macrophages in atherosclerosis. During atherosclerosis development, perinatally seeded intima-resident macrophages are quickly replaced by recruited inflammatory macrophages. The replacing cells are presumably transient macrophages, which do not engraft after inflammation resolution. As mentioned earlier, it is currently unclear whether a small subset of intima-resident prevails during atherosclerosis progression, and whether these cells are capable of rebounding following the cessation of hypercholesterolemia. Consequently, adventitial macrophages might be the only long-term resident macrophages in the aorta during atherosclerosis development. In contrast to the recruited inflammatory macrophages in the intima, adventitial macrophages do not show increased proliferation during atherosclerosis development, resulting in largely stable macrophage numbers despite the continuous inflammation in the local environment (49). This, and the low migratory capacity of plaque macrophages could argue for a limited role of adventitia-resident macrophages in the atherosclerotic process. On the other hand, regressing atherosclerotic plaques contain a subset of macrophages possessing a transcriptional signature that is reminiscent of homeostatic and pro-resolving EMP-derived adventitial macrophages. Future studies will have to evaluate the

role of adventitial macrophages in atherosclerosis and investigate if these cells are capable of migration into the intima. Given their pro-resolving phenotype, adventitial EMP-derived macrophage and their migration into the atherosclerosis-affected intima also display a potential therapeutic target.

In general, we are lacking studies that quantitatively examine the recruitment and different fates of monocytes and macrophages during the different phases of atherosclerosis progression, and in particular during atherosclerosis regression. Novel fate mapping and conditional gene deletion models, such as the Ms4a3^{cre} (30), CCR2^{cre} (221–223) and Rank^{cre} (45) mice, together with high-dimensional analysis approaches will aid in deepening our understanding of these processes.

In this Review, we have mainly focused on results from mouse models but summarized evidence for similarities as well as differences between the rodent and human arterial wall. Many aspects pertaining the trafficking of monocytes and macrophages are difficult to corroborate in humans, given the unfeasibility of fate-mapping techniques. Nonetheless, the development of novel methods, including scRNA-seq and spatial omics-technologies will continue to expand the possibilities of analysing monocyte and macrophage dynamics in humans. Although several findings in the mouse can be translated to the human, there are differences in the pathological mechanisms, which call for an increased effort in performing human studies.

AUTHOR CONTRIBUTIONS

LT and CS conceived the idea and article structure. FP and LT wrote and edited the manuscript. FP created the illustrations and CS revised the manuscript and provided oversight. All authors have made a substantial, direct and intellectual contribution to the article and approved the submitted version.

FUNDING

LT is supported by a Walter Benjamin fellowship of the German Research Foundation (DFG). This study was supported by the DFG, SFB 1123 project A07 to CS.

REFERENCES

1. Roth GA, Abate D, Abate KH, Abay SM, Abbafati C, Abbasi N, et al. Global, Regional, and National Age-Sex-Specific Mortality for 282 Causes of Death in 195 Countries and Territories, 1980–2017: A Systematic Analysis for the Global Burden of Disease Study 2017. *Lancet* (2018) 392:1736–88. doi: 10.1016/s0140-6736(18)32203-7
2. Millonig G, Niederegger H, Rabl W, Hochleitner BW, Hoefer D, Romani N, et al. Network of Vascular-Associated Dendritic Cells in Intima of Healthy Young Individuals. *Arterioscler Thromb Vasc Biol* (2001) 21:503–8. doi: 10.1161/01.atv.21.4.503
3. Jongstra-Bilen J, Haidari M, Zhu S-N, Chen M, Guha D, Cybulsky MI. Low-Grade Chronic Inflammation in Regions of the Normal Mouse Arterial Intima Predisposed to Atherosclerosis. *J Exp Med* (2006) 203:2073–83. doi: 10.1084/jem.20060245
4. Paulson KE, Zhu S-N, Chen M, Nurmohamed S, Jongstra-Bilen J, Cybulsky MI. Resident Intimal Dendritic Cells Accumulate Lipid and Contribute to the Initiation of Atherosclerosis. *Circ Res* (2010) 106:383–90. doi: 10.1161/circresaha.109.210781
5. Hajra L, Evans AI, Chen M, Hyduk SJ, Collins T, Cybulsky MI. The NF-Kappa B Signal Transduction Pathway in Aortic Endothelial Cells Is Primed for Activation in Regions Predisposed to Atherosclerotic Lesion Formation. *Proc Natl Acad Sci USA* (2000) 97:9052–7. doi: 10.1073/pnas.97.16.9052
6. Yahagi K, Kolodgie FD, Otsuka F, Finn AV, Davis HR, Joner M, et al. Pathophysiology of Native Coronary, Vein Graft, and in-Stent Atherosclerosis. *Nat Rev Cardiol* (2016) 13:79–98. doi: 10.1038/nrcardio.2015.164
7. Kwon GP, Schroeder JL, Amar MJ, Remaley AT, Balaban RS. Contribution of Macromolecular Structure to the Retention of Low-Density Lipoprotein at Arterial Branch Points. *Circulation* (2008) 117:2919–27. doi: 10.1161/circulationaha.107.754614
8. Steffensen LB, Mortensen MB, Kjolby M, Hagensen MK, Oxvig C, Bentzon JF. Disturbed Laminar Blood Flow Vastly Augments Lipoprotein Retention in the Artery Wall: A Key Mechanism Distinguishing Susceptible From Resistant Sites. *Arterioscler Thromb Vasc Biol* (2015) 35:1928–35. doi: 10.1161/atvbaha.115.305874
9. Moore KJ, Tabas I. Macrophages in the Pathogenesis of Atherosclerosis. *Cell* (2011) 145:341–55. doi: 10.1016/j.cell.2011.04.005
10. Borén J, Chapman MJ, Krauss RM, Packard CJ, Bentzon JF, Binder CJ, et al. Low-Density Lipoproteins Cause Atherosclerotic Cardiovascular Disease: Pathophysiological, Genetic, and Therapeutic Insights: A Consensus Statement From the European Atherosclerosis Society Consensus Panel. *Eur Heart J* (2020) 41:2313–30. doi: 10.1093/eurheartj/ehz962
11. Tabas I. Macrophage Death and Defective Inflammation Resolution in Atherosclerosis. *Nat Rev Immunol* (2010) 10:36–46. doi: 10.1038/nri2675
12. Lorenzo C, Delgado P, Busse CE, Sanz-Bravo A, Martos-Folgado I, Bonzon-Kulichenko E, et al. ALDH4A1 Is an Atherosclerosis Auto-Antigen Targeted by Protective Antibodies. *Nature* (2020) 589:1–6. doi: 10.1038/s41586-020-2993-2
13. Gisterå A, Hansson GK. The Immunology of Atherosclerosis. *Nat Rev Nephrol* (2017) 13:368–80. doi: 10.1038/nrneph.2017.51
14. Lim HY, Lim SY, Tan CK, Thiam CH, Goh CC, Carbajo D, et al. Hyaluronan Receptor LYVE-1-Expressing Macrophages Maintain Arterial Tone Through Hyaluronan-Mediated Regulation of Smooth Muscle Cell Collagen. *Immunity* (2018) 49:326–41.e7. doi: 10.1016/j.immuni.2018.06.008
15. Choi J-H, Do Y, Cheong C, Koh H, Boscardin SB, Oh Y-S, et al. Identification of Antigen-Presenting Dendritic Cells in Mouse Aorta and Cardiac Valves. *J Exp Med* (2009) 206:497–505. doi: 10.1084/jem.20082129
16. Williams JW, Zaitsev K, Kim K-W, Ivanov S, Saunders BT, Schrank PR, et al. Limited Proliferation Capacity of Aortic Intima Resident Macrophages Requires Monocyte Recruitment for Atherosclerotic Plaque Progression. *Nat Immunol* (2020) 21:1–11. doi: 10.1038/s41590-020-0768-4
17. Smith JD, Trogan E, Ginsberg M, Grigaux C, Tian J, Miyata M. Decreased Atherosclerosis in Mice Deficient in Both Macrophage Colony-Stimulating Factor (Op) and Apolipoprotein E. *Proc Natl Acad Sci USA* (1995) 92:8264–8. doi: 10.1073/pnas.92.18.8264
18. Qiao JH, Tripathi J, Mishra NK, Cai Y, Tripathi S, Wang XP, et al. Role of Macrophage Colony-Stimulating Factor in Atherosclerosis: Studies of Osteopetrotic Mice. *Am J Pathol* (1997) 150:1687–99.
19. Rajavashisth T, Qiao JH, Tripathi S, Tripathi J, Mishra N, Hua M, et al. Heterozygous Osteopetrotic (Op) Mutation Reduces Atherosclerosis in LDL Receptor- Deficient Mice. *J Clin Invest* (1998) 101:2702–10. doi: 10.1172/jci119891
20. Villiers WJS de, Smith JD, Miyata M, Dansky HM, Darley E, Gordon S. Macrophage Phenotype in Mice Deficient in Both Macrophage-Colony–Stimulating Factor (Op) and Apolipoprotein E. *Arterioscler Thromb Vasc Biol* (1998) 18:631–40. doi: 10.1161/01.atv.18.4.631
21. Stoneman V, Braganza D, Figg N, Mercer J, Lang R, Goddard M, et al. Monocyte/Macrophage Suppression in CD11b Diphtheria Toxin Receptor Transgenic Mice Differentially Affects Atherogenesis and Established Plaques. *Circ Res* (2007) 100:884–93. doi: 10.1161/01.res.0000260802.75766.00
22. Goldberg IJ, Sharma G, Fisher EA. Atherosclerosis: Making a U Turn. *Annu Rev Med* (2020) 71:191–201. doi: 10.1146/annurev-med-042418-011108

23. Ajami B, Bennett JL, Krieger C, Tetzlaff W, Rossi FMV. Local Self-Renewal can Sustain CNS Microglia Maintenance and Function Throughout Adult Life. *Nat Neurosci* (2007) 10:1538–43. doi: 10.1038/nn2014
24. Yona S, Kim K-W, Wolf Y, Mildner A, Varol D, Breker M, et al. Fate Mapping Reveals Origins and Dynamics of Monocytes and Tissue Macrophages Under Homeostasis. *Immunity* (2012) 38:79–91. doi: 10.1016/j.immuni.2012.12.001
25. Hashimoto D, Chow A, Noizat C, Teo P, Beasley MB, Leboeuf M, et al. Tissue-Resident Macrophages Self-Maintain Locally Throughout Adult Life With Minimal Contribution From Circulating Monocytes. *Immunity* (2013) 38:792–804. doi: 10.1016/j.immuni.2013.04.004
26. Perdiguero EG, Klapproth K, Schulz C, Busch K, Azzoni E, Crozet L, et al. Tissue-Resident Macrophages Originate From Yolk-Sac-Derived Erythro-Myeloid Progenitors. *Nature* (2014) 518:547–51. doi: 10.1038/nature13989
27. Stremmel C, Schuchert R, Wagner F, Thaler R, Weinberger T, Pick R, et al. Yolk Sac Macrophage Progenitors Traffic to the Embryo During Defined Stages of Development. *Nat Commun* (2018) 9:75. doi: 10.1038/s41467-017-02492-2
28. Alliot F, Godin I, Pessac B. Microglia Derive From Progenitors, Originating From the Yolk Sac, and Which Proliferate in the Brain. *Brain Res Dev Brain Res* (1999) 117:145–52. doi: 10.1016/s0165-3806(99)00113-3
29. Ginhoux F, Greter M, Leboeuf M, Nandi S, See P, Gokhan S, et al. Fate Mapping Analysis Reveals That Adult Microglia Derive From Primitive Macrophages. *Science* (2010) 330:841–5. doi: 10.1126/science.1194637
30. Liu Z, Gu Y, Chakarov S, Bleriot C, Kwok I, Chen X, et al. Fate Mapping via Ms4a3-Expression History Traces Monocyte-Derived Cells. *Cell* (2019) 178:1509–25.e19. doi: 10.1016/j.cell.2019.08.009
31. Mass E. Delineating the Origins, Developmental Programs and Homeostatic Functions of Tissue-Resident Macrophages. *Int Immunol* (2018) 30:493–501. doi: 10.1093/intimm/dxy044
32. Mass E, Ballesteros I, Farlik M, Halbritter F, Gunther P, Crozet L, et al. Specification of Tissue-Resident Macrophages During Organogenesis. *Science* (2016) 353:aaf4238–aaf4238. doi: 10.1126/science.aaf4238
33. Jacome-Galarza CE, Percin GI, Muller JT, Mass E, Lazarov T, Eitler J, et al. Developmental Origin, Functional Maintenance and Genetic Rescue of Osteoclasts. *Nature* (2019) 568:541–5. doi: 10.1038/s41586-019-1105-7
34. Fantin A, Vieira JM, Gestri G, Denti L, Schwarz Q, Prykhozhij S, et al. Tissue Macrophages Act as Cellular Chaperones for Vascular Anastomosis Downstream of VEGF-Mediated Endothelial Tip Cell Induction. *Blood* (2010) 116:829–40. doi: 10.1182/blood-2009-12-257832
35. DeFalco T, Bhattacharya I, Williams AV, Sams DM, Capel B. Yolk-Sac–Derived Macrophages Regulate Fetal Testis Vascularization and Morphogenesis. *Proc Natl Acad Sci USA* (2014) 111:E2384–93. doi: 10.1073/pnas.1400057111
36. Leid J, Carrelha J, Boukarabila H, Epelman S, Jacobsen SEW, Lavine KJ. Primitive Embryonic Macrophages Are Required for Coronary Development and Maturation. *Circ Res* (2016) 118:1498–511. doi: 10.1161/circresaha.115.308270
37. Weinberger T, Esfandyari D, Messerer D, Percin G, Schleifer C, Thaler R, et al. Ontogeny of Arterial Macrophages Defines Their Functions in Homeostasis and Inflammation. *Nat Commun* (2020) 11:4549. doi: 10.1038/s41467-020-18287-x
38. Jaitin DA, Adlung L, Thaiss CA, Weiner A, Li B, Descamps H, et al. Lipid-Associated Macrophages Control Metabolic Homeostasis in a Trem2-Dependent Manner. *Cell* (2019) 178:686–98.e14. doi: 10.1016/j.cell.2019.05.054
39. Werner Y, Mass E, Kumar PA, Ulas T, Händler K, Horne A, et al. Cxcr4 Distinguishes HSC-Derived Monocytes From Microglia and Reveals Monocyte Immune Responses to Experimental Stroke. *Nat Neurosci* (2020) 23:351–62. doi: 10.1038/s41593-020-0585-y
40. Mould KJ, Barthel L, Mohning MP, Thomas SM, McCubbrey AL, Danhorn T, et al. Cell Origin Dictates Programming of Resident Versus Recruited Macrophages During Acute Lung Injury. *Am J Resp Cell Mol Biol* (2017) 57:294–306. doi: 10.1165/rcmb.2017-0061oc
41. Cronk JC, Filiano AJ, Louveau A, Marin I, Marsh R, Ji E, et al. Peripherally Derived Macrophages can Engraft the Brain Independent of Irradiation and Maintain an Identity Distinct From Microglia. *J Exp Med* (2018) 215:1627–47. doi: 10.1084/jem.20180247
42. Kalluri AS, Vellarikkal SK, Edelman ER, Nguyen L, Subramanian A, Ellinor PT, et al. Single-Cell Analysis of the Normal Mouse Aorta Reveals Functionally Distinct Endothelial Cell Populations. *Circulation* (2019) 140:147–63. doi: 10.1161/circulationaha.118.038362
43. Gu W, Ni Z, Tan Y-Q, Deng J, Zhang S-J, Lv Z-C, et al. Adventitial Cell Atlas of Wt (Wild Type) and ApoE (Apolipoprotein E)-Deficient Mice Defined by Single-Cell RNA Sequencing. *Arterioscler Thromb Vasc Biol* (2019) 39:1055–71. doi: 10.1161/atvbaha.119.312399
44. Ensan S, Li A, Besla R, Degousee N, Cosme J, Roufaiel M, et al. Self-Renewing Resident Arterial Macrophages Arise From Embryonic CX3CR1(+) Precursors and Circulating Monocytes Immediately After Birth. *Nat Immunol* (2016) 17:159–68. doi: 10.1038/ni.3343
45. Percin GI, Eitler J, Kranz A, Fu J, Pollard JW, Naumann R, et al. CSF1R Regulates the Dendritic Cell Pool Size in Adult Mice via Embryo-Derived Tissue-Resident Macrophages. *Nat Commun* (2018) 9:5279. doi: 10.1038/s41467-018-07685-x
46. Psaltis PJ, Harbuzariu A, Delacroix S, Witt TA, Holroyd EW, Spoon DB, et al. Identification of a Monocyte-Predisposed Hierarchy of Hematopoietic Progenitor Cells in the Adventitia of Postnatal Murine Aorta. *Circulation* (2012) 125:592–603. doi: 10.1161/circulationaha.111.059360
47. Psaltis PJ, Puranik AS, Spoon DB, Chue CD, Hoffman SJ, Witt TA, et al. Characterization of a Resident Population of Adventitial Macrophage Progenitor Cells in Postnatal Vasculature. *Circ Res* (2014) 115:364–75. doi: 10.1161/circresaha.115.303299
48. Lin J-D, Nishi H, Poles J, Niu X, Mccauley C, Rahman K, et al. Single-Cell Analysis of Fate-Mapped Macrophages Reveals Heterogeneity, Including Stem-Like Properties, During Atherosclerosis Progression and Regression. *JCI Insight* (2019) 4:e124574. doi: 10.1172/jci.insight.124574
49. Robbins CS, Hilgendorf I, Weber GF, Theurl I, Iwamoto Y, Figueiredo J-L, et al. Local Proliferation Dominates Lesional Macrophage Accumulation in Atherosclerosis. *Nat Med* (2013) 19:1166–72. doi: 10.1038/nm.3258
50. Dobnikar L, Taylor AL, Chappell J, Oldach P, Harman JL, Oerton E, et al. Disease-Relevant Transcriptional Signatures Identified in Individual Smooth Muscle Cells From Healthy Mouse Vessels. *Nat Commun* (2018) 9:4567. doi: 10.1038/s41467-018-06891-x
51. Shankman LS, Gomez D, Cherepanova OA, Salmon M, Alencar GF, Haskins RM, et al. KLF4-Dependent Phenotypic Modulation of Smooth Muscle Cells has a Key Role in Atherosclerotic Plaque Pathogenesis. *Nat Med* (2015) 21:628–37. doi: 10.1038/nm.3866
52. Pan H, Xue C, Auerbach BJ, Fan J, Bashore AC, Cui J, et al. Single-Cell Genomics Reveals a Novel Cell State During Smooth Muscle Cell Phenotypic Switching and Potential Therapeutic Targets for Atherosclerosis in Mouse and Human. *Circulation* (2020) 142:2060–75. doi: 10.1161/circulationaha.120.048378
53. Alencar GF, Owsiany KM KS, Sukhavasi K, Mocci G, Nguyen A, Williams CM, et al. The Stem Cell Pluripotency Genes Klf4 and Oct4 Regulate Complex SMC Phenotypic Changes Critical in Late-Stage Atherosclerotic Lesion Pathogenesis. *Circulation* (2020) 142:2045–59. doi: 10.1161/circulationaha.120.046672
54. Kudernatsch RF, Letsch A, Stachelscheid H, Volk H, Scheibenbogen C. Doublets Pretending to be CD34+ T Cells Despite Doublet Exclusion. *Cytometry A* (2013) 83A:173–6. doi: 10.1002/cyto.a.22247
55. Auffray C, Fogg D, Garfa M, Elain G, Join-Lambert O, Kayal S, et al. Monitoring of Blood Vessels and Tissues by a Population of Monocytes With Patrolling Behavior. *Science* (2007) 317:666–70. doi: 10.1126/science.1142883
56. Cros J, Cagnard N, Woollard K, Patey N, Zhang S-Y, Senechal B, et al. Human CD14dim Monocytes Patrol and Sense Nucleic Acids and Viruses via TLR7 and TLR8 Receptors. *Immunity* (2010) 33:375–86. doi: 10.1016/j.immuni.2010.08.012
57. Carlin LM, Stamatiades EG, Auffray C, Hanna RN, Glover L, Vizcay-Barrena G, et al. Nr4a1-Dependent Ly6Clow Monocytes Monitor Endothelial Cells and Orchestrate Their Disposal. *Cell* (2013) 153:362–75. doi: 10.1016/j.cell.2013.03.010
58. Marcovecchio PM, Thomas GD, Mikulski Z, Ehinger E, Mueller KAL, Blatchley A, et al. Scavenger Receptor CD36 Directs Nonclassical Monocyte Patrolling Along the Endothelium During Early Atherogenesis. *Arterioscler Thromb Vasc Biol* (2017) 37:2043–52. doi: 10.1161/atvbaha.117.309123
59. Jakubzick C, Gautier EL, Gibbings SL, Sojka DK, Schlitzer A, Johnson TE, et al. Minimal Differentiation of Classical Monocytes as They Survey Steady-

State Tissues and Transport Antigen to Lymph Nodes. *Immunity* (2013) 39:599–610. doi: 10.1016/j.immuni.2013.08.007
60. Swirski FK, Nahrendorf M, Etzrodt M, Wildgruber M, Cortez-Retamozo V, Panizzi P, et al. Identification of Splenic Reservoir Monocytes and Their Deployment to Inflammatory Sites. *Science* (2009) 325:612–6. doi: 10.1126/science.1175202
61. Swirski FK, Pittet MJ, Kircher MF, Aikawa E, Jaffer FA, Libby P, et al. Monocyte Accumulation in Mouse Atherogenesis Is Progressive and Proportional to Extent of Disease. *Proc Natl Acad Sci USA* (2006) 103:10340–5. doi: 10.1073/pnas.0604260103
62. Roufaiel M, Gracey E, Siu A, Zhu S-N, Lau A, Ibrahim H, et al. CCL19-CCR7-Dependent Reverse Transendothelial Migration of Myeloid Cells Clears Chlamydia Muridarum From the Arterial Intima. *Nat Immunol* (2016) 17:1263–72. doi: 10.1038/ni.3564
63. Drevets DA, Dillon MJ, Schawang JS, Rooijen Nv, Ehrchen J, Sunderkötter C, et al. The Ly-6chigh Monocyte Subpopulation Transports Listeria Monocytogenes Into the Brain During Systemic Infection of Mice. *J Immunol* (2004) 172:4418–24. doi: 10.4049/jimmunol.172.7.4418
64. Libby P, Egan D, Skarlatos S. Roles of Infectious Agents in Atherosclerosis and Restenosis: An Assessment of the Evidence and Need for Future Research. *Circulation* (1997) 96:4095–103. doi: 10.1161/01.cir.96.11.4095
65. Mulligan-Kehoe MJ, Simons M. Vasa Vasorum in Normal and Diseased Arteries. *Circulation* (2014) 129:2557–66. doi: 10.1161/circulationaha.113.007189
66. Mills CD, Kincaid K, Alt JM, Heilman MJ, Hill AM. M-1/M-2 Macrophages and the Th1/Th2 Paradigm. *J Immunol* (2000) 164:6166–73. doi: 10.4049/jimmunol.164.12.6166
67. Murray PJ, Allen JE, Biswas SK, Fisher EA, Gilroy DW, Goerdt S, et al. Macrophage Activation and Polarization: Nomenclature and Experimental Guidelines. *Immunity* (2014) 41:14–20. doi: 10.1016/j.immuni.2014.06.008
68. Nahrendorf M, Swirski FK. Abandoning M1/M2 for a Network Model of Macrophage Function. *Circ Res* (2016) 119:414–7. doi: 10.1161/circresaha.116.309194
69. Mantovani A. Reflections on Immunological Nomenclature: In Praise of Imperfection. *Nat Immunol* (2016) 17:215–6. doi: 10.1038/ni.3354
70. Zernecke A, Winkels H, Cochain C, Williams JW, Wolf D, Soehnlein O, et al. Meta-Analysis of Leukocyte Diversity in Atherosclerotic Mouse Aortas. *Circ Res* (2020) 127:402–26. doi: 10.1161/circresaha.120.316903
71. Zernecke A, Erhard F, Weinberger T, Schulz C, Ley K, Saliba A-E, et al. Integrated scRNA-Seq Analysis Identifies Conserved Transcriptomic Features of Mononuclear Phagocytes in Mouse and Human Atherosclerosis. *Biorxiv* (2020). doi: 10.1101/2020.12.09.417535
72. Rantakari P, Patten DA, Valtonen J, Karikoski M, Gerke H, Dawes H, et al. Stabilin-1 Expression Defines a Subset of Macrophages That Mediate Tissue Homeostasis and Prevent Fibrosis in Chronic Liver Injury. *Proc Natl Acad Sci USA* (2016) 113:9298–303. doi: 10.1073/pnas.1604780113
73. Nepal S, Tiruppathi C, Tsukasaki Y, Farahany J, Mittal M, Rehman J, et al. STAT6 Induces Expression of Gas6 in Macrophages to Clear Apoptotic Neutrophils and Resolve Inflammation. *Proc Natl Acad Sci USA* (2019) 116:16513–8. doi: 10.1073/pnas.1821601116
74. Kojima Y, Volkmer J-P, McKenna K, Civelek M, Lusis AJ, Miller CL, et al. CD47-Blocking Antibodies Restore Phagocytosis and Prevent Atherosclerosis. *Nature* (2016) 536:86–90. doi: 10.1038/nature18935
75. Moore KJ, Sheedy FJ, Fisher EA. Macrophages in Atherosclerosis: A Dynamic Balance. *Nat Rev Immunol* (2013) 13:709–21. doi: 10.1038/nri3520
76. Doran AC, Yurdagul A, Tabas I. Efferocytosis in Health and Disease. *Nat Rev Immunol* (2020) 20:254–67. doi: 10.1038/s41577-019-0240-6
77. Allahverdian S, Chehroudi AC, McManus BM, Abraham T, Francis GA. Contribution of Intimal Smooth Muscle Cells to Cholesterol Accumulation and Macrophage-Like Cells in Human Atherosclerosis. *Circulation* (2014) 129:1551–9. doi: 10.1161/circulationaha.113.005015
78. Chèvre R, González-Granado JM, Megens RTA, Sreeramkumar V, Silvestre-Roig C, Molina-Sánchez P, et al. High-Resolution Imaging of Intravascular Atherogenic Inflammation in Live Mice. *Circ Res* (2014) 114:770–9. doi: 10.1161/circresaha.114.302590
79. Zhu S-N, Chen M, Jongstra-Bilen J, Cybulsky MI. GM-CSF Regulates Intimal Cell Proliferation in Nascent Atherosclerotic Lesions. *J Exp Med* (2009) 206:2141–9. doi: 10.1084/jem.20090866
80. Marchini T, Mitre LS, Wolf D. Inflammatory Cell Recruitment in Cardiovascular Disease. *Front Cell Dev Biol* (2021) 9:635527. doi: 10.3389/fcell.2021.635527
81. Swirski FK, Libby P, Aikawa E, Alcaide P, Luscinskas FW, Weissleder R, et al. Ly-6Chi Monocytes Dominate Hypercholesterolemia-Associated Monocytosis and Give Rise to Macrophages in Atheromata. *J Clin Invest* (2007) 117:195–205. doi: 10.1172/jci29950
82. Tacke F, Alvarez D, Kaplan TJ, Jakubzick C, Spanbroek R, Llodra J, et al. Monocyte Subsets Differentially Employ CCR2, CCR5, and CX3CR1 to Accumulate Within Atherosclerotic Plaques. *J Clin Invest* (2007) 117:185–94. doi: 10.1172/jci28549
83. Combadiere C, Potteaux S, Rodero M, Simon T, Pezard A, Esposito B, et al. Combined Inhibition of CCL2, CX3CR1, and CCR5 Abrogates Ly6Chi and Ly6Clo Monocytosis and Almost Abolishes Atherosclerosis in Hypercholesterolemic Mice. *Circulation* (2008) 117:1649–57. doi: 10.1161/circulationaha.107.745091
84. Saederup N, Chan L, Lira SA, Charo IF. Fractalkine Deficiency Markedly Reduces Macrophage Accumulation and Atherosclerotic Lesion Formation in CCR2-/- Mice: Evidence for Independent Chemokine Functions in Atherogenesis. *Circulation* (2008) 117:1642–8. doi: 10.1161/circulationaha.107.743872
85. Eriksson EE. Intravital Microscopy on Atherosclerosis in Apolipoprotein E–Deficient Mice Establishes Microvessels as Major Entry Pathways for Leukocytes to Advanced Lesions. *Circulation* (2011) 124:2129–38. doi: 10.1161/circulationaha.111.030627
86. McNeill E, Iqbal AJ, Jones D, Patel J, Coutinho P, Taylor L, et al. Tracking Monocyte Recruitment and Macrophage Accumulation in Atherosclerotic Plaque Progression Using a Novel Hcd68gfp/ApoE-/- Reporter Mouse-Brief Report. *Arterioscler Thromb Vasc Biol* (2017) 37:258–63. doi: 10.1161/atvbaha.116.308367
87. Williams JW, Martel C, Potteaux S, Esaulova E, Ingersoll MA, Elvington A, et al. Limited Macrophage Positional Dynamics in Progressing or Regressing Murine Atherosclerotic Plaques. *Arterioscler Thromb Vasc Biol* (2018) 38:1702–10. doi: 10.1161/atvbaha.118.311319
88. Yvan-Charvet L, Pagler T, Gautier EL, Avagyan S, Siry RL, Han S, et al. ATP-Binding Cassette Transporters and HDL Suppress Hematopoietic Stem Cell Proliferation. *Science* (2010) 328:1689–93. doi: 10.1126/science.1189731
89. Murphy AJ, Akhtari M, Tolani S, Pagler T, Bijl N, Kuo C-L, et al. ApoE Regulates Hematopoietic Stem Cell Proliferation, Monocytosis, and Monocyte Accumulation in Atherosclerotic Lesions in Mice. *J Clin Invest* (2011) 121:4138–49. doi: 10.1172/jci57559
90. Hermetet F, Buffière A, Aznague A, Barros J-PP de, Bastie J-N, Delva L, et al. High-Fat Diet Disturbs Lipid Raft/TGF-β Signaling-Mediated Maintenance of Hematopoietic Stem Cells in Mouse Bone Marrow. *Nat Commun* (2019) 10:523. doi: 10.1038/s41467-018-08228-0
91. Robbins CS, Chudnovskiy A, Rauch PJ, Figueiredo J-L, Iwamoto Y, Gorbatov R, et al. Extramedullary Hematopoiesis Generates Ly-6chigh Monocytes That Infiltrate Atherosclerotic Lesions. *Circulation* (2012) 125:364–74. doi: 10.1161/circulationaha.111.061986
92. Nagareddy PR, Murphy AJ, Stirzaker RA, Hu Y, Yu S, Miller RG, et al. Hyperglycemia Promotes Myelopoiesis and Impairs the Resolution of Atherosclerosis. *Cell Metab* (2013) 17:695–708. doi: 10.1016/j.cmet.2013.04.001
93. McAlpine CS, Kiss MG, Rattik S, He S, Vassalli A, Valet C, et al. Sleep Modulates Haematopoiesis and Protects Against Atherosclerosis. *Nature* (2019) 566:383–7. doi: 10.1038/s41586-019-0948-2
94. Heidt T, Sager HB, Courties G, Dutta P, Iwamoto Y, Zaltsman A, et al. Chronic Variable Stress Activates Hematopoietic Stem Cells. *Nat Med* (2014) 20:754–8. doi: 10.1038/nm.3589
95. Shirai T, Nazarewicz RR, Wallis BB, Yanes RE, Watanabe R, Hilhorst M, et al. The Glycolytic Enzyme PKM2 Bridges Metabolic and Inflammatory Dysfunction in Coronary Artery Disease. *J Exp Med* (2016) 213:337–54. doi: 10.1084/jem.20150900
96. Devêvre EF, Renovato-Martins M, Clément K, Sautès-Fridman C, Cremer I, Poitou C. Profiling of the Three Circulating Monocyte Subpopulations in Human Obesity. *J Immunol* (2015) 194:3917–23. doi: 10.4049/jimmunol.1402655
97. Lian Z, Perrard XD, Peng X, Raya JL, Hernandez AA, Johnson CG, et al. Replacing Saturated Fat With Unsaturated Fat in Western Diet Reduces

Foamy Monocytes and Atherosclerosis in Male Ldlr–/– Mice. *Arterioscler Thromb Vasc Biol* (2018) 40:72–85. doi: 10.1161/atvbaha.119.313078
98. Wolf AA, Yáñez A, Barman PK, Goodridge HS. The Ontogeny of Monocyte Subsets. *Front Immunol* (2019) 10:1642. doi: 10.3389/fimmu.2019.01642
99. Dal-Secco D, Wang J, Zeng Z, Kolaczkowska E, Wong CHY, Petri B, et al. A Dynamic Spectrum of Monocytes Arising From the in Situ Reprogramming of CCR2+ Monocytes at a Site of Sterile injury In Situ Monocyte Conversion in Sterile Injury. *J Exp Med* (2015) 212:447–56. doi: 10.1084/jem.20141539
100. Wu H, Gower RM, Wang H, Perrard X-YD, Ma R, Bullard DC, et al. Functional Role of CD11c+ Monocytes in Atherogenesis Associated With Hypercholesterolemia. *Circulation* (2009) 119:2708–17. doi: 10.1161/circulationaha.108.823740
101. Xu L, Perrard XD, Perrard JL, Yang D, Xiao X, Teng B-B, et al. Foamy Monocytes Form Early and Contribute to Nascent Atherosclerosis in Mice With Hypercholesterolemia. *Arterioscler Thromb Vasc Biol* (2018) 35:1787–97. doi: 10.1161/atvbaha.115.305609
102. Quintar A, McArdle S, Wolf D, Marki A, Ehinger E, Vassallo M, et al. Endothelial Protective Monocyte Patrolling in Large Arteries Intensified by Western Diet and Atherosclerosis. *Circ Res* (2017) 120:1789–99. doi: 10.1161/circresaha.117.310739
103. Platt AM, Bain CC, Bordon Y, Sester DP. Mowat AMcI. An Independent Subset of TLR Expressing CCR2-Dependent Macrophages Promotes Colonic Inflammation. *J Immunol* (2010) 184:6843–54. doi: 10.4049/jimmunol.0903987
104. Zigmond E, Varol C, Farache J, Elmaliah E, Satpathy AT, Friedlander G, et al. Ly6Chi Monocytes in the Inflamed Colon Give Rise to Proinflammatory Effector Cells and Migratory Antigen-Presenting Cells. *Immunity* (2012) 37:1076–90. doi: 10.1016/j.immuni.2012.08.026
105. Fife BT, Huffnagle GB, Kuziel WA, Karpus WJ. Cc Chemokine Receptor 2 Is Critical for Induction of Experimental Autoimmune Encephalomyelitis. *J Exp Med* (2000) 192:899–906. doi: 10.1084/jem.192.6.899
106. Yamasaki R, Lu H, Butovsky O, Ohno N, Rietsch AM, Cialic R, et al. Differential Roles of Microglia and Monocytes in the Inflamed Central Nervous System. *J Exp Med* (2014) 211:1533–49. doi: 10.1084/jem.20132477
107. Guo J, Waard V, Eck MV, Hildebrand RB, Wanrooij EJAv, Kuiper J, et al. Repopulation of Apolipoprotein E Knockout Mice With CCR2-Deficient Bone Marrow Progenitor Cells Does Not Inhibit Ongoing Atherosclerotic Lesion Development. *Arterioscler Thromb Vasc Biol* (2005) 25:1014–9. doi: 10.1161/01.atv.0000163181.40896.42
108. Aiello RJ, Perry BD, Bourassa P-A, Robertson A, Weng W, Knight DR, et al. CCR2 Receptor Blockade Alters Blood Monocyte Subpopulations But Does Not Affect Atherosclerotic Lesions in Apoe–/– Mice. *Atherosclerosis* (2010) 208:370–5. doi: 10.1016/j.atherosclerosis.2009.08.017
109. Ye D, Zhao Y, Hildebrand RB, Singaraja RR, Hayden MR, Berkel TJCV, et al. The Dynamics of Macrophage Infiltration Into the Arterial Wall During Atherosclerotic Lesion Development in Low-Density Lipoprotein Receptor Knockout Mice. *Am J Pathol* (2011) 178:413–22. doi: 10.1016/j.ajpath.2010.11.007
110. McArdle S, Buscher K, Ghosheh Y, Pramod AB, Miller J, Winkels H, et al. Migratory and Dancing Macrophage Subsets in Atherosclerotic Lesions. *Circ Res* (2019) 125:1038–51. doi: 10.1161/circresaha.119.315175
111. Blériot C, Dupuis T, Jouvion G, Eberl G, Disson O, Lecuit M. Liver-Resident Macrophage Necroptosis Orchestrates Type 1 Microbicidal Inflammation and Type-2-Mediated Tissue Repair During Bacterial Infection. *Immunity* (2015) 42:145–58. doi: 10.1016/j.immuni.2014.12.020
112. Ajami B, Bennett JL, Krieger C, McNagny KM, Rossi FMV. Infiltrating Monocytes Trigger EAE Progression, But do Not Contribute to the Resident Microglia Pool. *Nat Neurosci* (2011) 14:1142–9. doi: 10.1038/nn.2887
113. Guilliams M, Svedberg FR. Does Tissue Imprinting Restrict Macrophage Plasticity? *Nat Immunol* (2021) 22:1–10. doi: 10.1038/s41590-020-00849-2
114. Bellingan GJ, Caldwell H, Howie SE, Dransfield I, Haslett C. In Vivo Fate of the Inflammatory Macrophage During the Resolution of Inflammation: Inflammatory Macrophages Do Not Die Locally, But Emigrate to the Draining Lymph Nodes. *J Immunol* (1996) 157:2577–85.
115. Gils JMv, Derby MC, Fernandes LR, Ramkhelawon B, Ray TD, Rayner KJ, et al. The Neuroimmune Guidance Cue Netrin-1 Promotes Atherosclerosis by Inhibiting the Emigration of Macrophages From Plaques. *Nat Immunol* (2012) 13:136–43. doi: 10.1038/ni.2205
116. Wanschel A, Seibert T, Hewing B, Ramkhelawon B, Ray TD, Gils JMv, et al. Neuroimmune Guidance Cue Semaphorin 3e Is Expressed in Atherosclerotic Plaques and Regulates Macrophage Retention. *Arterioscler Thromb Vasc Biol* (2018) 33:886–93. doi: 10.1161/atvbaha.112.300941
117. Llodrá J, Angeli V, Liu J, Trogan E, Fisher EA, Randolph GJ. Emigration of Monocyte-Derived Cells From Atherosclerotic Lesions Characterizes Regressive, But Not Progressive, Plaques. *Proc Natl Acad Sci USA* (2004) 101:11779–84. doi: 10.1073/pnas.0403259101
118. Nagao T, Qin C, Grosheva I, Maxfield FR, Pierini LM. Elevated Cholesterol Levels in the Plasma Membranes of Macrophages Inhibit Migration by Disrupting RhoA Regulation. *Arterioscler Thromb Vasc Biol* (2007) 27:1596–602. doi: 10.1161/atvbaha.107.145086
119. McArdle S, Chodaczek G, Ray N, Ley K. Intravital Live Cell Triggered Imaging System Reveals Monocyte Patrolling and Macrophage Migration in Atherosclerotic Arteries. *J BioMed Opt* (2015) 20:026005–5. doi: 10.1117/1.jbo.20.2.026005
120. Kim K, Shim D, Lee JS, Zaitsev K, Williams JW, Kim K-W, et al. Transcriptome Analysis Reveals Nonfoamy Rather Than Foamy Plaque Macrophages Are Proinflammatory in Atherosclerotic Murine Models. *Circ Res* (2018) 123:1127–42. doi: 10.1161/circresaha.118.312804
121. Cochain C, Vafadarnejad E, Arampatzi P, Pelisek J, Winkels H, Ley K, et al. Single-Cell RNA-Seq Reveals the Transcriptional Landscape and Heterogeneity of Aortic Macrophages in Murine Atherosclerosis. *Circ Res* (2018) 122:1661–74. doi: 10.1161/circresaha.117.312509
122. Cochain C, Saliba A-E, Zernecke A. Letter by Cochain et al. Regarding Article, "Transcriptome Analysis Reveals Nonfoamy Rather Than Foamy Plaque Macrophages Are Proinflammatory in Atherosclerotic Murine Models." *Circ Res* (2018) 123:e48–9. doi: 10.1161/circresaha.118.314120
123. Bailey CC, DeVaux LB, Farzan M. The Triggering Receptor Expressed on Myeloid Cells 2 Binds Apolipoprotein E. *J Biol Chem* (2015) 290:26033–42. doi: 10.1074/jbc.m115.677286
124. Turnbull IR, Gilfillan S, Cella M, Aoshi T, Miller M, Piccio L, et al. Cutting Edge: TREM-2 Attenuates Macrophage Activation. *J Immunol* (2006) 177:3520–4. doi: 10.4049/jimmunol.177.6.3520
125. Keren-Shaul H, Spinrad A, Weiner A, Matcovitch-Natan O, Dvir-Szternfeld R, Ulland TK, et al. A Unique Microglia Type Associated With Restricting Development of Alzheimer's Disease. *Cell* (2017) 169:1276–90.e17. doi: 10.1016/j.cell.2017.05.018
126. Chen H-J, Tas SW, de Winther MPJ. Type-I Interferons in Atherosclerosis. *J Exp Med* (2019) 217:e20190459. doi: 10.1084/jem.20190459
127. Wang J, Kubes P. A Reservoir of Mature Cavity Macrophages That Can Rapidly Invade Visceral Organs to Affect Tissue Repair. *Cell* (2016) 165:668–78. doi: 10.1016/j.cell.2016.03.009
128. Deniset JF, Belke D, Lee W-Y, Jorch SK, Deppermann C, Hassanabad AF, et al. Gata6+ Pericardial Cavity Macrophages Relocate to the Injured Heart and Prevent Cardiac Fibrosis. *Immunity* (2019) 51:131–40.e5. doi: 10.1016/j.immuni.2019.06.010
129. Zindel J, Peiseler M, Hossain M, Deppermann C, Lee WY, Haenni B, et al. Primordial GATA6 Macrophages Function as Extravascular Platelets in Sterile Injury. *Science* (2021) 371:eabe0595. doi: 10.1126/science.abe0595
130. Josefs T, Basu D, Vaisar T, Arets B, Kanter JE, Huggins L-A, et al. Atherosclerosis Regression and Cholesterol Efflux in Hypertriglyceridemic Mice. *Circ Res* (2021) 128:690–705. doi: 10.1161/circresaha.120.317458
131. Burke AC, Huff MW. Regression of Atherosclerosis. *Curr Opin Lipidol* (2018) 29:87–94. doi: 10.1097/mol.0000000000000493
132. Lieu HD, Withycombe SK, Walker Q, Rong JX, Walzem RL, Wong JS, et al. Eliminating Atherogenesis in Mice by Switching Off Hepatic Lipoprotein Secretion. *Circulation* (2003) 107:1315–21. doi: 10.1161/01.cir.0000054781.50889.0c
133. Reis ED, Li J, Fayad ZA, Rong JX, Hansoty D, Aguinaldo J-G, et al. Dramatic Remodeling of Advanced Atherosclerotic Plaques of the Apolipoprotein E–deficient Mouse in a Novel Transplantation Model. *J Vasc Surg* (2001) 34:541–2A. doi: 10.1067/mva.2001.115963
134. Craeyveld EV, Gordts SC, Nefyodova E, Jacobs F, Geest BD. Regression and Stabilization of Advanced Murine Atherosclerotic Lesions: A Comparison of LDL Lowering and HDL Raising Gene Transfer Strategies. *J Mol Med Berl* (2011) 89:555–67. doi: 10.1007/s00109-011-0722-x
135. Peled M, Nishi H, Weinstock A, Barrett TJ, Zhou F, Quezada A. Fisher EA. A Wild-Type Mouse-Based Model for the Regression of Inflammation in

Atherosclerosis. *PLoS One* (2017) 12:e0173975. doi: 10.1371/journal.pone.0173975
136. Basu D, Hu Y, Huggins L-A, Mullick AE, Graham MJ, Wietecha T, et al. Novel Reversible Model of Atherosclerosis and Regression Using Oligonucleotide Regulation of the LDL Receptor. *Circ Res* (2018) 122:560–7. doi: 10.1161/circresaha.117.311361
137. Zadelaar S, Kleemann R, Verschuren L, Weij J deV-Vd, Hoorn Jvd, Princen HM, et al. Mouse Models for Atherosclerosis and Pharmaceutical Modifiers. *Arterioscler Thromb Vasc Biol* (2007) 27:1706–21. doi: 10.1161/atvbaha.107.142570
138. Tsukamoto K, Tangirala R, Chun SH, Puré E, Rader DJ. Rapid Regression of Atherosclerosis Induced by Liver-Directed Gene Transfer of ApoE in ApoE-Deficient Mice. *Arterioscler Thromb Vasc Biol* (1999) 19:2162–70. doi: 10.1161/01.atv.19.9.2162
139. Graham MJ, Lee RG, Brandt TA, Tai L-J, Fu W, Peralta R, et al. Cardiovascular and Metabolic Effects of ANGPTL3Antisense Oligonucleotides. *N Engl J Med* (2017) 377:222–32. doi: 10.1056/nejmoa1701329
140. Witztum JL, Gaudet D, Freedman SD, Alexander VJ, Digenio A, Williams KR, et al. Volanesorsen and Triglyceride Levels in Familial Chylomicronemia Syndrome. *N Engl J Med* (2019) 381:531–42. doi: 10.1056/nejmoa1715944
141. Trogan E, Fayad ZA, Itskovich VV, Aguinaldo J-GS, Mani V, Fallon JT, et al. Serial Studies of Mouse Atherosclerosis by In Vivo Magnetic Resonance Imaging Detect Lesion Regression After Correction of Dyslipidemia. *Arterioscler Thromb Vasc Biol* (2004) 24:1714–9. doi: 10.1161/01.atv.0000139313.69015.1c
142. Feig JE, Pineda-Torra I, Sanson M, Bradley MN, Vengrenyuk Y, Bogunovic D, et al. LXR Promotes the Maximal Egress of Monocyte-Derived Cells From Mouse Aortic Plaques During Atherosclerosis Regression. *J Clin Invest* (2010) 120:4415–24. doi: 10.1172/jci38911
143. Feig JE, Parathath S, Rong JX, Mick SL, Vengrenyuk Y, Grauer L, et al. Reversal of Hyperlipidemia With a Genetic Switch Favorably Affects the Content and Inflammatory State of Macrophages in Atherosclerotic Plaques. *Circulation* (2011) 123:989–98. doi: 10.1161/circulationaha.110.984146
144. Trogan E, Feig JE, Dogan S, Rothblat GH, Angeli V, Tacke F, et al. Gene Expression Changes in Foam Cells and the Role of Chemokine Receptor CCR7 During Atherosclerosis Regression in ApoE-Deficient Mice. *Proc Natl Acad Sci USA* (2006) 103:3781–6. doi: 10.1073/pnas.0511043103
145. Härdtner C, Kornemann J, Krebs K, Ehlert CA, Jander A, Zou J, et al. Inhibition of Macrophage Proliferation Dominates Plaque Regression in Response to Cholesterol Lowering. *Basic Res Cardiol* (2020) 115:78. doi: 10.1007/s00395-020-00838-4
146. Potteaux S, Gautier EL, Hutchison SB, Rooijen Nv, Rader DJ, Thomas MJ, et al. Suppressed Monocyte Recruitment Drives Macrophage Removal From Atherosclerotic Plaques of Apoe-/- Mice During Disease Regression. *J Clin Invest* (2011) 121:2025–36. doi: 10.1172/jci43802
147. Pagler TA, Wang M, Mondal M, Murphy AJ, Westerterp M, Moore KJ, et al. Deletion of ABCA1 and ABCG1 Impairs Macrophage Migration Because of Increased Rac1 Signaling. *Circ Res* (2011) 108:194–200. doi: 10.1161/circresaha.110.228619
148. Feig JE, Shang Y, Rotllan N, Vengrenyuk Y, Wu C, Shamir R, et al. Statins Promote the Regression of Atherosclerosis via Activation of the CCR7-Dependent Emigration Pathway in Macrophages. *PLoS One* (2011) 6:e28534. doi: 10.1371/journal.pone.0028534
149. Sharma M, Schlegel MP, Afonso MS, Brown EJ, Rahman K, Weinstock A, et al. Regulatory T Cells License Macrophage Pro-Resolving Functions During Atherosclerosis Regression. *Circ Res* (2020) 127:335–53. doi: 10.1161/circresaha.119.316461
150. Mueller PA, Zhu L, Tavori H, Huynh K, Giunzioni I, Stafford JM, et al. Deletion of Macrophage Low-Density Lipoprotein Receptor-Related Protein 1 (LRP1) Accelerates Atherosclerosis Regression and Increases CCR7 Expression in Plaque Macrophages. *Circulation* (2018) 138:1850–63. doi: 10.1161/circulationaha.117.031702
151. Fullerton JN, Gilroy DW. Resolution of Inflammation: A New Therapeutic Frontier. *Nat Rev Drug Discov* (2016) 15:551–67. doi: 10.1038/nrd.2016.39
152. Gautier EL, Ivanov S, Lesnik P, Randolph GJ. Local Apoptosis Mediates Clearance of Macrophages From Resolving Inflammation in Mice. *Blood* (2013) 122:2714–22. doi: 10.1182/blood-2013-01-478206
153. Rajavashisth TB, Andalibi A, Territo MC, Berliner JA, Navab M, Fogelman AM, et al. Induction of Endothelial Cell Expression of Granulocyte and Macrophage Colony-Stimulating Factors by Modified Low-Density Lipoproteins. *Nature* (1990) 344:254–7. doi: 10.1038/344254a0
154. Sinha SK, Miikeda A, Fouladian Z, Mehrabian M, Edillor C, Shih D, et al. Local M-CSF (Macrophage Colony-Stimulating Factor) Expression Regulates Macrophage Proliferation and Apoptosis in Atherosclerosis. *Arterioscler Thromb Vasc Biol* (2020) 41:220–33. doi: 10.1161/atvbaha.120.315255
155. Baba O, Huang L-H, Elvington A, Szpakowska M, Sultan D, Heo GS, et al. CXCR4-Binding Positron Emission Tomography Tracers Link Monocyte Recruitment and Endothelial Injury in Murine Atherosclerosis. *Arterioscler Thromb Vasc Biol* (2021) 41:822–36. doi: 10.1161/atvbaha.120.315053
156. Nahrendorf M, Swirski FK, Aikawa E, Stangenberg L, Wurdinger T, Figueiredo J-L, et al. The Healing Myocardium Sequentially Mobilizes Two Monocyte Subsets With Divergent and Complementary Functions. *J Exp Med* (2007) 204:3037–47. doi: 10.1084/jem.20070885
157. Hilgendorf I, Gerhardt L, Tan TC, Winter C, Holderried TAW, Chousterman BG, et al. Ly-6chigh Monocytes Depend on Nr4a1 to Balance Both Inflammatory and Reparative Phases in the Infarcted Myocardium. *Circ Res* (2014) 114:1611–22. doi: 10.1161/circresaha.114.303204
158. Duffield JS, Forbes SJ, Constandinou CM, Clay S, Partolina M, Vuthoori S, et al. Selective Depletion of Macrophages Reveals Distinct, Opposing Roles During Liver Injury and Repair. *J Clin Invest* (2005) 115:56–65. doi: 10.1172/jci200522675
159. Goren I, Allmann N, Yogev N, Schürmann C, Linke A, Holdener M, et al. A Transgenic Mouse Model of Inducible Macrophage Depletion: Effects of Diphtheria Toxin-Driven Lysozyme M-Specific Cell Lineage Ablation on Wound Inflammatory, Angiogenic, and Contractive Processes. *Am J Pathol* (2009) 175:132–47. doi: 10.2353/ajpath.2009.081002
160. Lucas T, Waisman A, Ranjan R, Roes J, Krieg T, Müller W, et al. Differential Roles of Macrophages in Diverse Phases of Skin Repair. *J Immunol* (2010) 184:3964–77. doi: 10.4049/jimmunol.0903356
161. Rahman K, Vengrenyuk Y, Ramsey SA, Vila NR, Girgis NM, Liu J, et al. Inflammatory Ly6Chi Monocytes and Their Conversion to M2 Macrophages Drive Atherosclerosis Regression. *J Clin Invest* (2017) 127:2904–15. doi: 10.1172/jci75005
162. Thomas GD, Hanna RN, Vasudevan NT, Hamers AA, Romanoski CE, McArdle S, et al. Deleting an Nr4a1 Super-Enhancer Subdomain Ablates Ly6C(low) Monocytes While Preserving Macrophage Gene Function. *Immunity* (2016) 45:975–87. doi: 10.1016/j.immuni.2016.10.011
163. Ikeda N, Asano K, Kikuchi K, Uchida Y, Ikegami H, Takagi R, et al. Emergence of Immunoregulatory Ym1+Ly6Chi Monocytes During Recovery Phase of Tissue Injury. *Sci Immunol* (2018) 3:eaat0207. doi: 10.1126/sciimmunol.aat0207
164. Van den Bossche J, Baardman J, Otto NA, van der Velden S, Neele AE, van den Berg SM, et al. Mitochondrial Dysfunction Prevents Repolarization of Inflammatory Macrophages. *Cell Rep* (2016) 17:684–96. doi: 10.1016/j.celrep.2016.09.008
165. Khallou-Laschet J, Varthaman A, Fornasa G, Compain C, Gaston A-T, Clement M, et al. Macrophage Plasticity in Experimental Atherosclerosis. *PLoS One* (2010) 5:e8852. doi: 10.1371/journal.pone.0008852
166. Arnold L, Henry A, Poron F, Baba-Amer Y, Rooijen Nv, Plonquet A, et al. Inflammatory Monocytes Recruited After Skeletal Muscle Injury Switch Into Antiinflammatory Macrophages to Support Myogenesis. *J Exp Med* (2007) 204:1057–69. doi: 10.1084/jem.20070075
167. Locatelli G, Theodorou D, Kendirli A, Jordão MJC, Staszewski O, Phulphagar K, et al. Mononuclear Phagocytes Locally Specify and Adapt Their Phenotype in a Multiple Sclerosis Model. *Nat Neurosci* (2018) 21:1196–208. doi: 10.1038/s41593-018-0212-3
168. Lavine KJ, Epelman S, Uchida K, Weber KJ, Nichols CG, Schilling JD, et al. Distinct Macrophage Lineages Contribute to Disparate Patterns of Cardiac Recovery and Remodeling in the Neonatal and Adult Heart. *Proc Natl Acad Sci USA* (2014) 111:16029–34. doi: 10.1073/pnas.1406508111
169. Epelman S, Lavine KJ, Beaudin AE, Sojka DK, Carrero JA, Calderon B, et al. Embryonic and Adult-Derived Resident Cardiac Macrophages Are Maintained Through Distinct Mechanisms at Steady State and During Inflammation. *Immunity* (2014) 40:91–104. doi: 10.1016/j.immuni.2013.11.019

170. Tavian M, Peault B. Embryonic Development of the Human Hematopoietic System. *Int J Dev Biol* (2003) 49:243–50. doi: 10.1387/ijdb.041957mt
171. Godin I, Cumano A. The Hare and the Tortoise: An Embryonic Haematopoietic Race. *Nat Rev Immunol* (2002) 2:593–604. doi: 10.1038/nri857
172. Enzan H. Electron Microscopic Studies of Macrophages in Early Human Yolk Sacs. *Acta Pathol Jpn* (1986) 36:49–64. doi: 10.1111/j.1440-1827.1986.tb01460.x
173. Migliaccio G, Migliaccio AR, Petti S, Mavilio F, Russo G, Lazzaro D, et al. Human Embryonic Hemopoiesis. Kinetics of Progenitors and Precursors Underlying the Yolk Sac—-Liver Transition. *J Clin Invest* (1986) 78:51–60. doi: 10.1172/jci112572
174. Bian Z, Gong Y, Huang T, Lee CZW, Bian L, Bai Z, et al. Deciphering Human Macrophage Development at Single-Cell Resolution. *Nature* (2020) 582:571–6. doi: 10.1038/s41586-020-2316-7
175. Doebel T, Voisin B, Nagao K. Langerhans Cells – The Macrophage in Dendritic Cell Clothing. *Trends Immunol* (2017) 38:817–28. doi: 10.1016/j.it.2017.06.008
176. Bigley V, Haniffa M, Doulatov S, Wang X-N, Dickinson R, McGovern N, et al. The Human Syndrome of Dendritic Cell, Monocyte, B and NK Lymphoid Deficiency. *J Exp Med* (2011) 208:227–34. doi: 10.1084/jem.20101459
177. McGovern N, Schlitzer A, Gunawan M, Jardine L, Shin A, Poyner E, et al. Human Dermal CD14+ Cells Are a Transient Population of Monocyte-Derived Macrophages. *Immunity* (2014) 41:465–77. doi: 10.1016/j.immuni.2014.08.006
178. Hu Z, Liu W, Hua X, Chen X, Chang Y, Hu Y, et al. Single-Cell Transcriptomic Atlas of Different Human Cardiac Arteries Identifies Cell Types Associated With Vascular Physiology. *Arterioscler Thromb Vasc Biol* (2021) 41:1408–27. doi: 10.1161/atvbaha.120.315373
179. Li Y, Ren P, Dawson A, Vasquez HG, Ageedi W, Zhang C, et al. Single-Cell Transcriptome Analysis Reveals Dynamic Cell Populations and Differential Gene Expression Patterns in Control and Aneurysmal Human Aortic Tissue. *Circulation* (2020) 142:1374–88. doi: 10.1161/circulationaha.120.046528
180. Waltner-Romen M, Falkensammer G, Rabl W, Wick G. A Previously Unrecognized Site of Local Accumulation of Mononuclear Cells. *J Histochem Cytochem* (1998) 46:1347–50. doi: 10.1177/002215549804601202
181. Stary HC, Blankenhorn DH, Chandler AB, Glagov S, Insull W, Richardson M, et al. A Definition of the Intima of Human Arteries and of Its Atherosclerosis-Prone Regions. A Report From the Committee on Vascular Lesions of the Council on Arteriosclerosis, American Heart Association. *Circulation* (1992) 85:391–405. doi: 10.1161/01.cir.85.1.391
182. Wick G, Romen M, Amberger A, Metzler B, Mayr M, Falkensammer G, et al. Atherosclerosis, Autoimmunity, and Vascular-Associated Lymphoid Tissue. *FASEB J* (1997) 11:1199–207. doi: 10.1096/fasebj.11.13.9367355
183. Bobryshev YV, Lord RS. Ultrastructural Recognition of Cells With Dendritic Cell Morphology in Human Aortic Intima. Contacting Interactions of Vascular Dendritic Cells in Athero-Resistant and Athero-Prone Areas of the Normal Aorta. *Arch Histol Cytol* (1995) 58:307–22. doi: 10.1679/aohc.58.307
184. Millonig G, Malcom GT, Wick G. Early Inflammatory-Immunological Lesions in Juvenile Atherosclerosis From the Pathobiological Determinants of Atherosclerosis in Youth (PDAY)-Study. *Atherosclerosis* (2002) 160:441–8. doi: 10.1016/s0021-9150(01)00596-2
185. Dutertre C-A, Clement M, Morvan M, Schäkel K, Castier Y, Alsac J-M, et al. Deciphering the Stromal and Hematopoietic Cell Network of the Adventitia From Non-Aneurysmal and Aneurysmal Human Aorta. *PLoS One* (2014) 9:e89983. doi: 10.1371/journal.pone.0089983
186. Kortelainen M-L, Porvari K. Adventitial Macrophage and Lymphocyte Accumulation Accompanying Early Stages of Human Coronary Atherogenesis. *Cardiovasc Pathol* (2014) 23:193–7. doi: 10.1016/j.carpath.2014.03.001
187. Watanabe M, Sangawa A, Sasaki Y, Yamashita M, Tanaka-Shintani M, Shintaku M, et al. Distribution of Inflammatory Cells in Adventitia Changed With Advancing Atherosclerosis of Human Coronary Artery. *J Atheroscler Thromb* (2007) 14:325–31. doi: 10.5551/jat.e489
188. Kanitakis J, Petruzzo P, Dubernard J-M. Turnover of Epidermal Langerhans' Cells. *N Engl J Med* (2004) 351:2661–2. doi: 10.1056/nejm200412163512523
189. Kanitakis J, Morelon E, Petruzzo P, Badet L, Dubernard J. Self-Renewal Capacity of Human Epidermal Langerhans Cells: Observations Made on a Composite Tissue Allograft. *Exp Dermatol* (2011) 20:145–6. doi: 10.1111/j.1600-0625.2010.01146.x
190. Bajpai G, Schneider C, Wong N, Bredemeyer A, Hulsmans M, Nahrendorf M, et al. The Human Heart Contains Distinct Macrophage Subsets With Divergent Origins and Functions. *Nat Med* (2018) 24:1234–45. doi: 10.1038/s41591-018-0059-x
191. Pryshchep O, Ma-Krupa W, Younge BR, Goronzy JJ, Weyand CM. Vessel-Specific Toll-Like Receptor Profiles in Human Medium and Large Arteries. *Circulation* (2008) 118:1276–84. doi: 10.1161/circulationaha.108.789172
192. Iwata H, Manabe I, Fujiu K, Yamamoto T, Takeda N, Eguchi K, et al. Bone Marrow–Derived Cells Contribute to Vascular Inflammation But Do Not Differentiate Into Smooth Muscle Cell Lineages. *Circulation* (2010) 122:2048–57. doi: 10.1161/circulationaha.110.965202
193. Caplice NM, Bunch TJ, Stalboerger PG, Wang S, Simper D, Miller DV, et al. Smooth Muscle Cells in Human Coronary Atherosclerosis can Originate From Cells Administered at Marrow Transplantation. *Proc Natl Acad Sci USA* (2003) 100:4754–9. doi: 10.1073/pnas.0730743100
194. Martin K, Weiss S, Metharom P, Schmeckpeper J, Hynes B, O'Sullivan J, et al. Thrombin Stimulates Smooth Muscle Cell Differentiation From Peripheral Blood Mononuclear Cells via Protease-Activated Receptor-1, RhoA, and Myocardin. *Circ Res* (2009) 105:214–8. doi: 10.1161/circresaha.109.199984
195. Albarrán-Juárez J, Kaur H, Grimm M, Offermanns S, Wettschureck N. Lineage Tracing of Cells Involved in Atherosclerosis. *Atherosclerosis* (2016) 251:445–53. doi: 10.1016/j.atherosclerosis.2016.06.012
196. Misra A, Feng Z, Chandran RR, Kabir I, Rotllan N, Aryal B, et al. Integrin Beta3 Regulates Clonality and Fate of Smooth Muscle-Derived Atherosclerotic Plaque Cells. *Nat Commun* (2018) 9:2073. doi: 10.1038/s41467-018-04447-7
197. Wang Y, Dubland JA, Allahverdian S, Asonye E, Sahin B, Jaw JE, et al. Smooth Muscle Cells Contribute the Majority of Foam Cells in ApoE (Apolipoprotein E)-Deficient Mouse Atherosclerosis. *Arterioscler Thromb Vasc Biol* (2019) 39:876–87. doi: 10.1161/atvbaha.119.312434
198. Bobryshev YV. Monocyte Recruitment and Foam Cell Formation in Atherosclerosis. *Micron* (2006) 37:208–22. doi: 10.1016/j.micron.2005.10.007
199. Valk FMvd, Kroon J, Potters WV, Thurlings RM, Bennink RJ, Verberne HJ, et al. In Vivo Imaging of Enhanced Leukocyte Accumulation in Atherosclerotic Lesions in Humans. *J Am Coll Cardiol* (2014) 64:1019–29. doi: 10.1016/j.jacc.2014.06.1171
200. Johnsen SH, Fosse E, Joakimsen O, Mathiesen EB, Stensland-Bugge E, Njølstad I, et al. Monocyte Count Is a Predictor of Novel Plaque Formation. *Stroke* (2005) 36:715–9. doi: 10.1161/01.str.0000158909.07634.83
201. Chapman CML, Beilby JP, McQuillan BM, Thompson PL, Hung J. Monocyte Count, But Not C-Reactive Protein or Interleukin-6, Is an Independent Risk Marker for Subclinical Carotid Atherosclerosis. *Stroke* (2004) 35:1619–24. doi: 10.1161/01.str.0000130857.19423.ad
202. Nasir K, Guallar E, Navas-Acien A, Criqui MH, Lima JAC. Relationship of Monocyte Count and Peripheral Arterial Disease. *Arterioscler Thromb Vasc Biol* (2005) 25:1966–71. doi: 10.1161/01.atv.0000175296.02550.e4
203. Kapellos TS, Bonaguro L, Gemünd I, Reusch N, Saglam A, Hinkley ER, et al. Human Monocyte Subsets and Phenotypes in Major Chronic Inflammatory Diseases. *Front Immunol* (2019) 10:2035. doi: 10.3389/fimmu.2019.02035
204. Villani A-C, Satija R, Reynolds G, Sarkizova S, Shekhar K, Fletcher J, et al. Single-Cell RNA-Seq Reveals New Types of Human Blood Dendritic Cells, Monocytes, and Progenitors. *Science* (2017) 356:eaah4573. doi: 10.1126/science.aah4573
205. Hamers AAJ, Dinh HQ, Thomas GD, Marcovecchio P, Blatchley A, Nakao CS, et al. Human Monocyte Heterogeneity as Revealed by High-Dimensional Mass Cytometry. *Arterioscler Thromb Vasc Biol* (2019) 39:25–36. doi: 10.1161/atvbaha.118.311022
206. Roussel M, Ferrell PB, Greenplate AR, Lhomme F, Gallou SL, Diggins KE, et al. Mass Cytometry Deep Phenotyping of Human Mononuclear Phagocytes and Myeloid-Derived Suppressor Cells From Human Blood and Bone Marrow. *J Leukoc Biol* (2017) 102:437–47. doi: 10.1189/jlb.5ma1116-457r

207. Fernandez DM, Rahman AH, Fernandez NF, Chudnovskiy A, Amir E-AD, Amadori L, et al. Single-Cell Immune Landscape of Human Atherosclerotic Plaques. *Nat Med* (2019) 25:1576–88. doi: 10.1038/s41591-019-0590-4
208. Weber C, Belge K, Hundelshausen P, Draude G, Steppich B, Mack M, et al. Differential Chemokine Receptor Expression and Function in Human Monocyte Subpopulations. *J Leukoc Biol* (2000) 67:699–704. doi: 10.1002/jlb.67.5.699
209. Ancuta P, Rao R, Moses A, Mehle A, Shaw SK, Luscinskas FW, et al. Fractalkine Preferentially Mediates Arrest and Migration of CD16+ Monocytes. *J Exp Med* (2003) 197:1701–7. doi: 10.1084/jem.20022156
210. Wong KL, Tai JJ-Y, Wong W-C, Han H, Sem X, Yeap W-H, et al. Gene Expression Profiling Reveals the Defining Features of the Classical, Intermediate, and Nonclassical Human Monocyte Subsets. *Blood* (2011) 118:e16–31. doi: 10.1182/blood-2010-12-326355
211. Sander J, Schmidt SV, Cirovic B, McGovern N, Papantonopoulou O, Hardt A-L, et al. Cellular Differentiation of Human Monocytes Is Regulated by Time-Dependent Interleukin-4 Signaling and the Transcriptional Regulator Ncor2. *Immunity* (2017) 47:1051–66.e12. doi: 10.1016/j.immuni.2017.11.024
212. Berg KE, Ljungcrantz I, Andersson L, Bryngelsson C, Hedblad B, Fredrikson GN, et al. Elevated CD14++CD16−Monocytes Predict Cardiovascular Events. *Circ Cardiovasc Genet* (2012) 5:122–31. doi: 10.1161/circgenetics.111.960385
213. Rogacev KS, Cremers B, Zawada AM, Seiler S, Binder N, Ege P, et al. CD14++CD16+ Monocytes Independently Predict Cardiovascular Events. *J Am Coll Cardiol* (2012) 60:1512–20. doi: 10.1016/j.jacc.2012.07.019
214. Meeuwsen JAL, Vries JJ de, Duijvenvoorde Av, Velden Svd, Laan SWvd, Koeverden IDv, et al. Circulating CD14+CD16− Classical Monocytes do Not Associate With a Vulnerable Plaque Phenotype, and Do Not Predict Secondary Events in Severe Atherosclerotic Patients. *J Mol Cell Cardiol* (2019) 127:260–9. doi: 10.1016/j.yjmcc.2019.01.002
215. Rekhter MD, Gordon D. Active Proliferation of Different Cell Types, Including Lymphocytes, in Human Atherosclerotic Plaques. *Am J Pathol* (1995) 147:668–77.
216. Katsuda S, Boyd HC, Fligner C, Ross R, Gown AM. Human Atherosclerosis. III. Immunocytochemical Analysis of the Cell Composition of Lesions of Young Adults. *Am J Pathol* (1992) 140:907–14.
217. Gordon D, Reidy MA, Benditt EP, Schwartz SM. Cell Proliferation in Human Coronary Arteries. *Proc Natl Acad Sci USA* (1990) 87:4600–4. doi: 10.1073/pnas.87.12.4600
218. Lutgens E, Muinck ED de, Kitslaar PJEHM, Tordoir JHM, Wellens HJJ, Daemen MJAP. Biphasic Pattern of Cell Turnover Characterizes the Progression From Fatty Streaks to Ruptured Human Atherosclerotic Plaques. *Cardiovasc Res* (1999) 41:473–9. doi: 10.1016/s0008-6363(98)00311-3
219. Chai JT, Ruparelia N, Goel A, Kyriakou T, Biasiolli L, Edgar L, et al. Differential Gene Expression in Macrophages From Human Atherosclerotic Plaques Shows Convergence on Pathways Implicated by Genome-Wide Association Study Risk Variants. *Arterioscler Thromb Vasc Biol* (2018) 38:1. doi: 10.1161/atvbaha.118.311209
220. Vickovic S, Eraslan G, Salmén F, Klughammer J, Stenbeck L, Schapiro D, et al. High-Definition Spatial Transcriptomics for in Situ Tissue Profiling. *Nat Methods* (2019) 16:987–90. doi: 10.1038/s41592-019-0548-y
221. Chen H-R, Sun Y-Y, Chen C-W, Kuo Y-M, Kuan IS, Li Z-RT, et al. Fate Mapping via CCR2-CreER Mice Reveals Monocyte-to-Microglia Transition in Development and Neonatal Stroke. *Sci Adv* (2020) 6:eabb2119. doi: 10.1126/sciadv.abb2119
222. Heung LJ, Hohl TM. Inflammatory Monocytes Are Detrimental to the Host Immune Response During Acute Infection With Cryptococcus Neoformans. *PLoS Pathog* (2019) 15:e1007627. doi: 10.1371/journal.ppat.1007627
223. Xu Z, Rao Y, Huang Y, Zhou T, Feng R, Xiong S, et al. Efficient Strategies for Microglia Replacement in the Central Nervous System. *Cell Rep* (2020) 32:108041. doi: 10.1016/j.celrep.2020.108041

Conflict of Interest: The authors declare that the research was conducted in the absence of any commercial or financial relationships that could be construed as a potential conflict of interest.

frontiers in Immunology

REVIEW
published: 15 November 2021
doi: 10.3389/fimmu.2021.750537

Molecular Tuning of Actin Dynamics in Leukocyte Migration as Revealed by Immune-Related Actinopathies

Anton Kamnev[1,2], *Claire Lacouture*[3,4], *Mathieu Fusaro*[3] *and Loïc Dupré*[1,2,3]*

[1] Ludwig Boltzmann Institute for Rare and Undiagnosed Diseases, Vienna, Austria, [2] Department of Dermatology, Medical University of Vienna, Vienna, Austria, [3] Toulouse Institute for Infectious and Inflammatory Diseases (INFINITy), INSERM, CNRS, Toulouse III Paul Sabatier University, Toulouse, France, [4] Laboratoire De Physique Théorique, IRSAMC, Université De Toulouse (UPS), CNRS, Toulouse, France

Motility is a crucial activity of immune cells allowing them to patrol tissues as they differentiate, sample or exchange information, and execute their effector functions. Although all immune cells are highly migratory, each subset is endowed with very distinct motility patterns in accordance with functional specification. Furthermore individual immune cell subsets adapt their motility behaviour to the surrounding tissue environment. This review focuses on how the generation and adaptation of diversified motility patterns in immune cells is sustained by actin cytoskeleton dynamics. In particular, we review the knowledge gained through the study of inborn errors of immunity (IEI) related to actin defects. Such pathologies are unique models that help us to uncover the contribution of individual actin regulators to the migration of immune cells in the context of their development and function.

Keywords: leukocytes, cell migration, chemotaxis, actin, cytoskeleton, actin regulators, inborn errors of immunity, IEI

OPEN ACCESS

Edited by:
Hélène D. Moreau, INSERM U932 Immunité et Cancer, France

Reviewed by:
Hassan Abolhassani, Karolinska University Hospital, Sweden
Erin Janssen, Boston Children's Hospital and Harvard Medical School, United States

***Correspondence:**
Loïc Dupré
loic.dupre@rud.lbg.ac.at

Specialty section:
This article was submitted to Molecular Innate Immunity, a section of the journal Frontiers in Immunology

Received: *30 July 2021*
Accepted: *12 October 2021*
Published: *15 November 2021*

Citation:
Kamnev A, Lacouture C, Fusaro M and Dupré L (2021) Molecular Tuning of Actin Dynamics in Leukocyte Migration as Revealed by Immune-Related Actinopathies. Front. Immunol. 12:750537. doi: 10.3389/fimmu.2021.750537

INTRODUCTION

Understanding how the diverse motility strategies of immune cells are controlled at the molecular level is of paramount importance when investigating immune cell responses in the context of health and disease and when designing cell-based immunotherapies. Motility is inherent to leukocyte development and differentiation for proper positioning in specific regions of lymphoid organs (1, 2). Moreover, motility is essential for mature immune cells to travel across organs and ensure their immuno-surveillance function (3, 4). Given the diversity of tissue environments and barriers crossed by any given leukocyte along its life cycle, motility needs to be regulated as a highly adaptable function (5). The intrinsic regulation of leukocyte motility relies on the integration of motility signals into adapted cell shape remodelling. This process is governed by the actin cytoskeleton that promotes the protrusive and contractile activities necessary for cell movement (6). Furthermore actin remodelling sustains other motility-related activities, such as organelle recycling, mitochondria positioning and nuclear envelope deformation (7). The molecular machinery responsible for actin remodelling comprises actin-binding proteins as well as upstream regulators accounting for a few hundreds of proteins (8, 9). In the context of leukocyte migration, the knowledge we have today about the specific roles of actin regulators stems in part from the study of rare inborn errors of immunity (IEI) caused by mutations in corresponding genes.

The elucidation of molecular mechanisms underlying IEIs has revealed that more than 20 are either directly caused by, or associated with, defective actin cytoskeleton remodelling (10–14). These disease entities might therefore be considered as actinopathies specific to the immune system (from here onwards referred to as actinopathies). In this review, we present updated knowledge on actinopathies with a focus on leukocyte motility defects. In the first part of the review, we assemble knowledge on leukocyte circulation through the organism affected by actinopathies. In the second part, we turn to the cellular scale and present some of the motility challenges leukocytes face while executing their function. Finally, in the third part of the review, we zoom in on the subcellular scale and examine how actin remodelling shapes diverse cellular protrusions and ultrastructures to propel cell through dense environments following migration stimuli.

SUMMARY OF IDENTIFIED MOTILITY DEFECTS ACROSS ACTINOPATHIES

Table 1 presents an updated list of 23 actinopathies with a focus on the leukocyte motility defects characterized so far in each of these pathologies. In addition, we sorted identified defects in motility by the experimental model used in the study: primary material from patient *versus* cellular and animal models of the specific gene defect. The molecular mechanisms affected in actinopathies span multiple facets of the molecular machinery responsible for actin remodelling, as detailed in (14). Since multiple molecular layers operate upstream of actin remodelling, it is not obvious to define a threshold for the inclusion of gene defects falling under the umbrella of actinopathies. We here focus on actin itself (β-actin), actin-binding proteins or subunits of actin-binding protein complexes (ARPC1B, CORO1A, DIAPH1, HEM1, MKL1, MSN, MYH9, WASP, WDR1 and WIP), direct regulators of actin-binding proteins (CARMIL2, PSTPIP1 and STK4/MST1), RHO GTPases (CDC42, RAC2, RHOG and RHOH) and GTPase regulators (ARHGEF1, DOCK2, DOCK8, RASGRP1 and TTC7A). **Table 1** highlights crucial contribution of actinopathy discovery to our understanding of the role of individual molecular regulators in the motility and specific functions of immune cells.

MOTILITY DEFECTS IN ACTINOPATHIES AT THE ORGANISM LEVEL

The life journey of leukocytes is indissociable from their trafficking across the organism. From their differentiation in primary lymphoid organs to their homing and recirculation in secondary lymphoid organs and peripheral tissues, immune cells navigate through various tissues (**Figure 1**). They use both blood and lymphatic systems to commute between the organs they visit or colonise. To date, most actinopathies have been found to be associated with impaired migration of immune cells within and between organs (**Figure 1**). This section will review data collected on actinopathies and complementary animal models that have provided fundamental knowledge about leukocyte trafficking at the organism scale.

Bone Marrow Colonisation and Positioning During Hematopoiesis

The foetal liver is the initial site of hematopoiesis. After the development of bones, hematopoietic stem cells migrate to the bone marrow (BM), which then becomes the major site of maturation of most immune cells (106). The precise positioning within BM niches of developing hematopoietic cell subsets (**Figure 1A**) is important for the tuning of differentiation (107). This is controlled, at least in part, by chemokine receptors, adhesion molecules and local concentrations of Ca^{2+} and oxygen (108).

The earliest motility defect in immune cell ontogeny reported in the context of actinopathies applies to the Wiskott-Aldrich syndrome (WAS). Indeed, hematopoietic progenitors from *Was*-KO mice displayed reduced migration from foetal liver to BM (93). Impaired colonisation of BM by WASP-deficient cells could explain biased X-inactivation observed in WAS female carriers. Although the complex orchestration of hematopoietic cell positioning within the BM is expected to require motility steps and acquisition of specific motility properties as cells differentiate, little is known about the function of actin regulators in these processes. In the context of actinopathies, reported bias in peripheral blood cell counts and immunophenotype in patients may reflect defects in BM migration and positioning. Indeed, in the context of WASP deficiency, the proportion of immature B cells in the BM is decreased, while that of transitional B cells in the periphery is increased (77). Such bias in B cell development has been proposed to result from the defective ability of B cells from WAS patients to respond to CXCL12, which plays a major role in immature B cell retention in the BM.

Differently, deficiency in MSN appears to be associated with a defective egress of B cells from the BM, at least in the murine KO model (39). Interestingly, in the context of B cell development, MSN expression peaks in immature B cells. Analysis of B cell subpopulations in BM and peripheral blood point to a defective egress of immature B cells from the BM parenchyma into the sinusoids.

Deficiency in WDR1, a key actin severing protein, causes an even more severe defect in B cell differentiation (99). Indeed, patient BM displayed very low frequency of $CD20^+$ B cell precursors, which was accompanied by a marked peripheral B cell lymphopenia. However, in contrast to WASP deficiency, WDR1 deficiency did not appear to affect the ability of B cells to respond to CXCL12. Rather, defective activation and regulation of apoptosis upon BCR engagement might explain the early B cell development defect in this actinopathy.

As highlighted by the Wiskott-Aldrich syndrome, proper positioning of megakaryocytes in the BM is a key step in the control of platelet production. Megakaryocytes from WASP-deficient mice displayed impaired CXCL12-evoked migration upon interaction with fibrillar collagen I (95). This combined

TABLE 1 | Actin-related inborn errors of immunity and associated leukocyte motility defects.

Actin-related inborn errors of immunity			Leukocyte motility defects	
Gene (Protein)*	**Protein function**	**Clinical symptoms**	**Patient cells**	**Cellular and animal models**
ACTB (β-actin)	Non-muscle actin isoform; polymerises to F-actin	Mental retardation, recurrent bacterial and viral infections	**Neutrophils**: impaired chemotaxis in response to fMLP and zymosan-activated serum (15)	**Mice CD4+ T cells**: defective chemotaxis towards CCL21 (16)
ARHGEF1	GEF; regulates RhoA activity	Airway infections, defective antibody production	**B cells/T cells**: ↓ CXCL12-evoked migration (17) **T cells:** ↓ RhoA/ROCK mediated actin polymerisation upon LPA/S1P stimulation, ↓ de-adhesion on fibronectin, increased uropod length (17)	**Mice germinal centre B cells**: aberrant dissemination associated with inability to transduce S1P-evoked inhibition of migration (18)
ARPC1B	ARP2/3 complex subunit; polymerises F-actin branches	Failure to thrive, platelet abnormalities, eczema, infections, vasculitis, hepatosplenomegaly, thrombocytopenia	**Macrophages**: defective podosome assembly (19) **T cells**: ↓ spontaneous motility, weak IS (20), defective lamellipodium during migration and aberrant emission of filopodia-like protrusions (21) **Platelets**: defective spreading and lamellipodia assembly (22)	**THP1 cells**: defective podosome assembly (19)
CARMIL2	Regulates F-actin polymerisation at the barbed end	Malignancy (EBV+), IBD, recurrent skin and upper airway infections, failure to thrive	**T cells**: dispersed polarity and increased spontaneous migratory speed but ↓ directness; defective CXCL12 chemotaxis (23)	not reported**
CDC42	GTPase; regulates cell motility and polarity	Autoinflammation, HLH, malignant lymphoproliferation	**PBMC, BM CD34+ cells**: ↓chemotaxis toward CXCL12, abnormal filopodial pattern and cell polarization (24)	**Mice neutrophils:** ↓ neutrophil infiltration into interstitial tissues (25), loss of polarity during migration and aberrant filopodia emission instead of lamellipodium (26)
CORO1A	Inhibits the Arp2/3 complex; enhances F-actin disassembly *via* cofilin	Bacterial and viral infections, aggressive EBV-associated B cell lymphoproliferation, T cell lymphopenia, T-B+ SCID	**T cells**: SCID condition with visible thymus (27); severely impaired thymic output (28)	**Mice thymocytes/T cells**: impaired egress of mature thymocytes, patch-like talin-rich and abnormally distributed clusters instead of uropod (29, 30); cell-intrinsic migration defect toward SIP1, CCL21, CXCL12, defect in lymph nodes entry/egress (28) **Mice neutrophils**: defective LFA-1-dependent adhesion under flow; defective extravasation (31)
DIAPH1	Nucleates and elongates F-actin	Seizures, cortical blindness, microcephaly syndrome (SCBMS), mitochondrial dysfunction and immunodeficiency	**T cells**: impaired adhesion and inefficient microtubule-organizing centre repositioning to the immunologic synapse (32)	**Mice thymocytes**: ↓ chemotaxis to CCL21 and CXCL12, impaired egress from thymus (33) **Mice T cells:** impaired trafficking to secondary lymphoid organ, reduced chemotaxis (CCL21, CXCL12), ↓ production of F-actin, impaired polarity in response to chemotactic stimuli (33)
DOCK2	GEF; activates RAC1 and RAC2	Severe invasive bacterial and viral infections	**T, B and NK cells**: defective chemotaxis in response to CCL21 and CXCL12, ↓ actin polymerisation (34), low density of B cells, plasma cells and T cells in the lamina propria of the colon (34)	**Mice T and B cells**: ↓ motility inside T cell area and B cell follicle, ↓ S1P-induced cell migration, delayed lymphocyte egress from LN, ↓ cell motility of T cells in close proximity to efferent lymphatic vessels (35, 36)
DOCK8	GEF; activates CDC42	Upper airway infections, susceptibility to viral infection	**T and NK cells**: abnormally elongated shape leading to cytothripsis in confined spaces (37)	**Mice DCs:** ↓ traffic to the draining LN (38) **Mice CD4 thymocytes:** defective thymic egress and ↑ migration to CXCL12 (39) **Mice T cells:** defective transmigration and homing in LN (40) **Mice Tfh:** impaired migration to germinal centre (41) **Mice microglia**: ↓ filopodia formation (42)
NCKAP1L (HEM1)	WAVE2 complex subunit; activates the ARP2/3 complex to promote branched F-actin networks	Fever, recurrent bacterial and viral skin infections, severe respiratory tract infections, poor antibody responses, autoimmune manifestations	**T cells**: defective membrane ruffling, loss of lamellipodia, reduced F-actin density at the leading edge with abnormal puncta, spikes, and blebs, ↓ migratory velocity (43, 44), lack of polarization (45) **B cells**: aberrant morphology, defective directional migration when exposed to CCL19 gradient (44) **Neutrophils:** ↓ velocity, ↓ directional persistence, misdirected competing leading edges (43), abnormal distribution of F-actinat at the leading edge instead of the lamellipodium (45)	**Mice neutrophils and macrophages**: defective migration (46, 47), spiky shape (47) and defect in actin polymerisation (46), accumulation within and near blood vessels and defective migration in 3D chemokine gradient (47) **Mice DC**: lack of lamellipodia, ↑ speed, ↑ directional persistance and migration speed paths in 3D collagen gels (48) **Zebrafish neutrophils**: defective migration (45)

(Continued)

TABLE 1 | Continued

Actin-related inborn errors of immunity			Leukocyte motility defects	
Gene (Protein)*	**Protein function**	**Clinical symptoms**	**Patient cells**	**Cellular and animal models**
MKL1	Regulates transcription of actin and actin cytoskeleton related genes	Severe bacterial infections, skin abscesses	**Neutrophils**: actin polymerisation defect, ↓ motility and chemotactic response, failure in firm adherence and transendothelial migration under shear flow conditions (49) **DCs**: unable to spread normally or to form podosomes (50)	**Neutrophil-like HL-60 cells**: failure of uropod retraction (50)
MSN (moesin)	Links membrane proteins to actin filaments	Eczema, episodic bacterial and VZV infections, lymphopenia	**T cells**: impaired chemotaxis in response to CCL21 and CXCL12 (51)	**Mice thymocytes**: defective thymic egress (39) **Mice B cells:** defective egress from the BM (39) **Mice T cells:** defective egress from the LN, ↓ of microvilli density failed internalization of S1PR1 (52), impaired ability to exit the bloodstream (53) **Mice neutrophils:** ↑ rolling velocity in inflamed blood vessels (54)
MYH9	F-actin dependent motor protein	May-Hegglin anomaly, Sebastian syndrome, Fechtner syndrome, Epstein syndrome, mild macrothrombocytopenia	not reported**	**Mice neutrophils**: ↓ in migration velocity and euclidean distance during mechanotactic migration, transmigration and migration in confined 3D environments (55) **Mice T cells**: ↑ adhesion, impaired interstitial migration (56) **Human primary T cells (siRNA, blebbistatin)**: aberrant uropod elongation (57)
PSTPIP1	Adaptor protein; interacts with WASP	Oligoarticular pyogenic arthritis, acne, pyoderma gangrenosum-like lesions	**Macrophages**: impaired chemotaxis to M-CSF, impaired invasion into gel, defect in podosome formation (replaced by filopodia-like protrusions) (58, 59) **CD4+ T cells**: faster motility in collagen matrix, ↑ F-actin content (60)	not reported**
RAC2	GTPase; regulates cell migration and polarisation	Lymphopenia, recurrent respiratory infections, poor wound healing, leukocytosis	**Neutrophils:** ↓ actin polymerisation and chemotaxis, failure to assemble lamellipodium (43, 61), defective migration to fMLP (62)	**Zebrafish T lymphoid progenitors**: inability in homing to the thymus because of defective cell-autonomous motility (63) **Zebrafish neutrophils**: impaired migration to infection site (64) **Mice T cells:** reduced chemotaxis (65) **Mice neutrophils:** decreased infiltration into interstitial tissue (66)
RASGRP1	GEF; activates RAS	Severe pneumonia, failure to thrive, EBV susceptibility	**CD8 T cells**: ↓ migration speed in response to CXCL12 (67)	not reported**
RHOG	GTPase; activates RAC1	HLH features, fever, cytopenia, low haemoglobin	**not reported****	**NK-92 cells**: migration defect in response to CXCL12, CXCL13, CCL21 (68)
RHOH	GTPase; inhibits RAC1, RHOA & CDC42	Persistent EV-HPV infections, skin lesions	**T cells**: defect in skin-homing, ↓ percentages of T cells expressing tissue-homing markers (CLA, CCR4, CCR6, CCR10, $\alpha4\beta7$) (69)	**HPC cells:** ↑CXCL12-induced chemotaxis and chemokinesis (70)
STK4/ MST1	Serine-threonine protein kinase; Regulates the actin-bundling protein L-plastin	Recurrent infections, EBV infections, skin lesions and infections	**PBMCs and B cells**: defect in LFA-1-mediated adhesion and chemotaxis in response to CXCL11 (71) **T cells**: defective chemotaxis in response to CCL19 and CCL21 (72), ↓ expression of the homing receptors CCR7, CD62L (72)	**Mice thymocytes**: defect in thymic egress (73, 74), defect in response to CCL21 and CCL19 (73), and to CXCL12 and CCL25 (74) **Mice T and B cells:** impaired homing to peripheral lymph nodes and emigration from LN to blood, impaired arrest on HEV, problem in cell polarization, defective interstitial migration (73, 74) **Mice DCs:** impaired retention and/or homing of DCs in the spleen, ↓skin DC migration into draining LN (73)
TTC7A	Regulates the RHOA pathway	Early-onset IBD, lymphocytopenia and alopecia	**T cells**: ↑ spreading and adhesion, impaired chemotaxis toward CCL21 and CXCL12 (but ↓ receptor expression) (75)	not reported**
WAS (WASP)	Activates the ARP2/3	Thrombocytopenia, eczema, recurrent	**B cells**: thinner and shorter protrusions, ↓ chemotactic migration to CXCL13 (76), CXCL12 (77). reduction of area in	**Mice B cells:** ↓ chemotactic migration to CXCL13, CCL19, CXCL12, abnormal spleen

(Continued)

TABLE 1 | Continued

Actin-related inborn errors of immunity			Leukocyte motility defects	
Gene (Protein)*	**Protein function**	**Clinical symptoms**	**Patient cells**	**Cellular and animal models**
	complex to promote branched F-actin networks	infections, increased incidence of autoimmunity and lymphomas	LN (78) **DCs:** defective migration (79), unstable lamellipodia (79), fail to maintain polarization at the leading edge, inability to form podosomes, extreme elongation of uropod (80) **Monocytes:** defect in cell polarization, reduced migration to fMLP, MCP-1 and MIP-1α (81) **NK cells:** ↓ chemotactic migration and transendothelial migration toward CXCL12 and CX3CL1 (82) **Neutrophils:** impairment in integrin clustering, normal rolling but defect in arrest and firm adhesion under shear flow (83) **Macrophages:** ↓ of podosomes and abnormal polarization, ↓ number and abnormal distribution of filopodia, defective assembly of podosomes (84) **T cells:** ↓ migration in response to CXCL12 (85), depletion of lymphocytes from LN paracortical regions (78), normal localization of revertant T cells in secondary lymphoid organs (86), aberrant actin cytoskeleton dynamics at the IS (87), defective stop behaviour upon antigen encounter (88), inability to form invasive podosome, defect in trans-endothelial migration (89), disrupted lamellipodium irradiating in different directions (87, 90)	architecture, delayed GC reaction, deficient homing to spleen and LN, aberrant microvilli formation upon anti-CD40+IL-4 stimulation (76) **Mice DCs:** no dominant leading edge, inability to detach appropriately, ↓ migration toward CCL21, delayed migration from skin to draining LN, DC abnormally retained in the MZ (91), reduced migration toward CCL3 (92) **Mice BM precursors**: impaired migration in response to CXCL12 and deficient homing (93) **Mice neutrophils:** impaired firm arrest under shear stress, ↓ migratory capacity under shear stress, delay in migration into an inflamed site *in vivo* (83) **RAW/RL5 macrophages:** ↓ of podosomes and impaired chemotactic migration to CSF1 (94) **Mice megakaryocytes:** defect in migration on CXCL12 (95) **Mice T cells**: impaired migration in response to CCL19, compromised adhesion under shear flow (96)
		X-linked neutropenia (activating mutations in WASP)	**Neutrophils,** increased migration into tissues, ↑ adhesion under shearing flow, increased in adhesion footprint and spreading area (97)	**Mice DC**: abnormal speed fluctuations and ↓ global displacement, impaired entry into the draining LN (98)
WDR1	Promotes severing of F-actin together with cofilin	Autoinflammation, skin and airway infections	**B cells:** defect in differentiation, no defect in CXCL12 (99) **Neutrophils**: nuclear hernations, failure to polarize in response to fMLP; impaired random and fMLP-directed migration, increased F-actin (99–101) **DCs** and **monocytes:** enlarged actin-rich podosomes, high number of podosome-like structures (99, 100)	**Mice neutrophils**: impaired chemotaxis toward MIP-2 (102)
WIPF1 (WIP)	Stabilizes WASP	Eczema, T cell lymphopenia and thrombocytopenia	**T cells**: impaired migration toward CCL19 and CXCL12, filamentous appearance and abnormal lamellipodium (103) **B cells:** impaired migration toward CCL19, ↓ cell speed and directional migration; emission of multipolar filopodia (103) **DCs**: defective polarization, ruffles in place of leading edge (104)	**B cell line:** unstable lamellipodium and defective directional migration in CCL19 gradient (103) **THP1 cells**: defective podosome formation and impaired transendothelial migration (105) **Mice DCs:** defective podosome formation with abnormal structure, failed to develop a major leading front and instead formed multiple simultaneous and unstable lateral lamellae and ruffles (104)

**protein name specified only when distinct from gene name.*

***no data on defects in motility of immune cells in primary or animal model has been reported.*

3D, three-dimensions; BM, bone marrow; CCL, Chemokine (C-C motif) ligand; CLA, cutaneous lymphocyte antigen; CSF1, colony stimulating factor 1; CXCL, C-X-C motif chemokine ligand 10; DC, dendritic cell; EBV, Epstein-Barr virus; EV-HPV, Epidermodysplasia verruciformis-human papillomavirus; fMLP, n-formyl-méthionyl-leucyl-phénylalanine; GEF, guanine exchange factor; GTPase, guanosine triphosphate hydrolysing enzyme; HL-60, human neutrophilic cell line; HLH, hemophagocytic lymphohistiocytosis; IBD, inflammatory bowel disease; IS, immune synapse; LFA-1, lymphocyte function-associated antigen 1; LN, lymph node; LPA, lysophosphatidic acid; MCP1, monocyte chemoattractant protein 1; M-CSF, Macrophage colony-stimulating factor; MIP1-α, macrophage inflammatory protein-1 alpha; MZ, marginal zone; RL-5, macrophage cell line; S1P, sphingosine 1-phosphate; S1PR1, sphingosine 1-phosphate receptor 1; SCID, severe combined immunodeficiency; THP-1, Tohoku Hospital Pediatrics-1 (human monocytic cell line); VZV, varicella zoster virus.

adhesion and motility defect was shown to be associated with an inability of these cells to assemble actin-rich podosomes (see chapter 4 for detailed description). As a result of these defects, WASP-deficient megakaryocytes appeared to shed platelets ectopically within the BM space, which might explain the severe thrombocytopenia characteristic of WAS.

Beyond the few reports cited above, we currently lack insight in the relevance of actinopathy-related proteins in the multiplicity of motility steps occurring in the context of hematopoietic development in the BM. Certainly, the application of intravital imaging (109) to relevant murine models is expected to help filling this knowledge gap.

Leukocyte Migration During Thymopoiesis

Thymopoiesis is initiated upon the migration of progenitor T cells from the BM to the thymus. Then, the negative and positive selection steps of T cell differentiation occurring in the

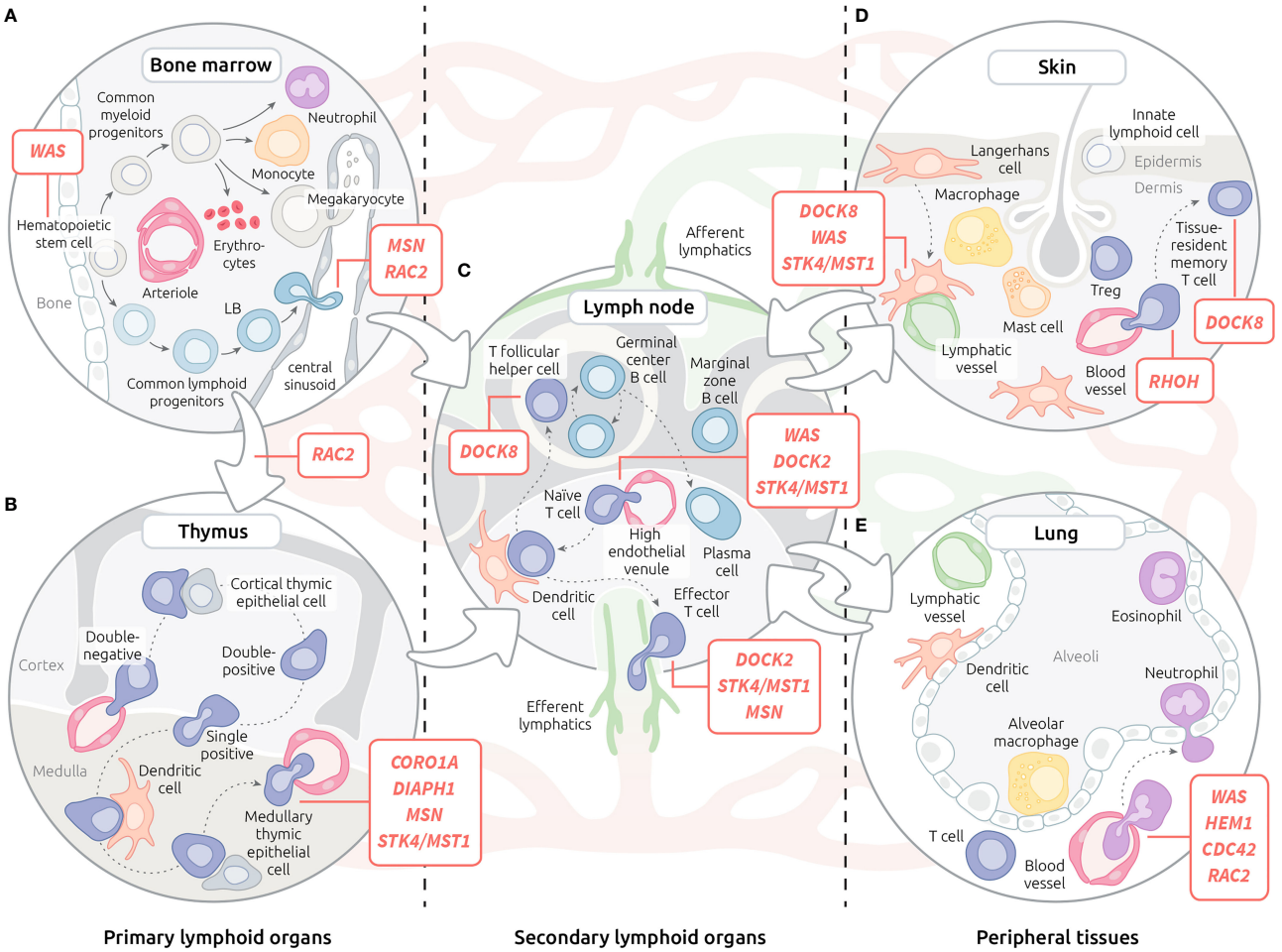

FIGURE 1 | Motility defects in actinopathies at the organism level. **(A)** Leukocyte trafficking in the bone marrow. **(B)** T lymphocyte trafficking in the thymus. **(C)** Recirculation of leukocytes through blood, lymphatic system and lymph nodes. **(D)** Migration of leukocytes within the skin. **(E)** Migration of leukocytes within the lungs. Red lines indicate steps of leukocyte trafficking affected by actinopathies with affected genes displayed in corresponding bubble. Lymphatic vessels are depicted in green, while red vessels are depicted in red.

thymus are intimately associated with regulated trafficking from cortico-medullary junction to the cortex, followed by migration to the medulla (**Figure 1B**). This trafficking is governed by several chemokine gradients and parallel up-regulation of chemokine receptors throughout the differentiation process (2). Once T cells reach the single positive stage, they initiate expression of S1PR1, the receptor of sphingosine-1 phosphate, a molecule crucial for egress from the thymus (110).

To date, only one actinopathy, RAC2 deficiency, has been suggested to be associated with a defect of migration of T cell precursors to the thymus. Depending on the effect of the mutation, RAC2-deficient patients present with severe T cell lymphopenia, suggestive of a defective thymic function (111). Interestingly, the use of a Rac2-deficient zebrafish model has revealed defective migration of T cell progenitors from the caudal hematopoietic tissue to the thymus (63), pointing to an early migration defect as the reason for T cell lymphopenia.

The migration within the thymus, in particular from the thymic cortex to the medulla area (promoted by CCL21), has been studied in CD4+ T cells from *Actb* knock-out mice. An *in vitro* transwell migration assay revealed a lack of response of these cells to CCL21, suggesting that β-actin would be necessary for this aspect of T cell motility (16).

Defect of T cell egress from thymus has been documented for CORO1A deficiency (27). CORO1A deficiency was first described in a child with a T-B^{+}NK^{+} severe combined immunodeficiency (SCID) phenotype. However, unlike many SCID patients with absent or undetectable thymus, the patient had a thymic image on CT-scan, suggesting defective thymic egress rather than developmental impairment. This finding agrees with previous research of CORO1A deficiency in murine models which documented defective thymic egress as well (29, 30). This defect has been shown to be related to impaired migration of T cells toward S1P, although low

survival of the CORO1A-deficient T cells might contribute to the severity of the defective thymic output (27).

In addition to CORO1A deficiency, defects in T cell egress from the thymus have been documented in murine models defective in a number of actinopathy-related molecules: DOCK8 (112), DIAPH1 (33), STK4/MST1 (73, 74) and MSN (39, 52). T cells from DOCK2-deficient mice failed to migrate toward S1P, which resulted in defective thymic egress and peripheral lymphopenia (35). The T cell lymphopenia observed in DOCK8-deficient mice was associated with accumulation of mature single positive T cells in the thymus, as a result of increased chemotaxis in response to CXCL12 (112). Knock-out of *Diaph1* in mice caused impaired chemotaxis toward CCL21 and CXCL12, associated with reduced T cell numbers in spleen and lymph node (LN), but normal cellularity and cell distribution in the thymus (33). A defective egress of *Diaph1*-/- thymocytes in response to CCL21 was identified using an organ culture of the thymus. Patients with STK4/MST1 deficiency have a profound CD4 lymphopenia with very low circulating naive CD4 and CD8 T cells. In addition, patient CD4 T cells displayed a defective migration toward CCL19 and CCL21 (72). STK4/MST1-deficient mice were shown to accumulate mature thymocytes in the thymus, which was associated with peripheral T cell lymphopenia. A transwell assay with thymic lobes was used to show that *Mst1*-/- T cells have impaired emigration from the thymus in response to CCL19 (73). In a complementary study, STK4/MST1-deficient thymocytes exhibited defective migration in response to CCL19, CCL21, CXCL12 and CCL25 but not S1P (74). Thus, STK4/MST1 could act as a signalling hub for several chemokines. Finally, *Msn*-/- mice exhibited an accumulation of mature single positive thymocytes with peripheral lymphopenia (39), in line with the finding that MSN expression is induced at the single positive stage at which it regulates the response to S1P *via* the downregulation of S1PR1 (52).

In conclusion, a number of actinopathies associated with T cell lymphopenia are associated with perturbations in the egress of mature T cells from the thymus. Whether some of the considered actinopathies might also be associated with more subtle alterations in the precise positioning of developing T cells in the different regions of the thymus remains to be investigated.

Leukocyte Homing and Positioning in Secondary Lymphoid Organs

The architecture of secondary lymphoid organs is defined by specialized areas, the organization of which highly depends on the selective migration programs of immune cell subsets interacting in these areas (**Figure 1C**). Therefore, histological analysis of lymphoid organ biopsies in actinopathies, when available, can be informative to reveal leukocyte migration defects. This is the case for WAS patients in whom examination of LNs and spleen pointed out a reduction in T and B cell areas (78). This abnormal architecture was partly recapitulated in *Was*-KO mice that harbour reduced B cell areas and slower germinal centre reaction after immunization (76). This defect was found to be B cell intrinsic since homing capacity was impaired when WASP-deficient B cells were transferred into wild-type recipients.

Histological examination of the *lamina propria* of the colon of a child with DOCK2 deficiency suffering from colitis showed low density of B cells, plasma cells, and T cells (34). This was suggestive of a defective homing of lymphocytes to local lymphoid tissues in the context of inflammation. In agreement, data on isolated B and T cells from DOCK2-deficient patients have revealed defects in RAC1 activation, actin polymerization and migration towards chemokines. The major role of DOCK2 in driving leukocyte trafficking to the LN had previously been established in *Dock2*-/- mice (36). Indeed, the accumulation of *Dock2*-/- cells in LNs was reduced upon adoptive transfer. Multiphoton intravital microscopy has been successfully used to investigate the intra-nodal migratory behaviour of *Dock2*-/- T and B cells (35). Although these cells localized properly, they featured reduced motility with erratic oscillations in contrast to the random walk pattern observed in control cells. DOCK2-deficient T and B cells also exhibited a two-fold increase in dwelling time caused by a defect in LN egress with impaired response to S1P signalling.

DOCK8 deficiency is also associated with combined defects of lymphocyte subsets in the context of secondary lymphoid organs. Defective homing of *Dock8*-KO T cells to LNs was suggested to be attributable to the role of DOCK8 in activating WASP *via* CDC42 (40). A genetic screen revealed that DOCK8 is required for the formation of marginal zone B cells, the persistence of B cells in germinal centres and their affinity maturation. However, these B cell intrinsic defects were associated neither with homing nor with chemokine-induced motility, but rather with a defect in LFA-1 polarization at the immunological synapse (IS) (113). T cell defects in the *Dock8*-KO mice were also shown to contribute to the poor antibody responses to T cell dependent antigens. In particular the migration of T follicular helper cells to B cell follicles was severely reduced (41). The role of DOCK8 in T and B cell function is further highlighted by cases of somatic reversion showing clinical improvement as a consequence of partial functional restoration of the T and B cell memory compartments (114).

Patients with MSN deficiency typically have very low T cell count in their peripheral blood but do not experience as many severe infections as SCID patients (51). A possible explanation for this discrepancy might be an abnormal retention of MSN-deficient lymphocytes in LNs. In support of this possibility, lymphocyte entry into the spleen and LNs was documented to be only minimally impacted in the *Msn*-/- model, while lymphocytes egress from LNs was reduced (39). Such differential defect in LN entry as opposed to egress might be due to a preponderant role of MSN in regulating S1P-dependent egress, as suggested by the recent finding that ezrin-radixin-moesin (ERM) proteins are particularly important to spatially control a bleb-based motility mechanism, specifically triggered by S1P (53).

STK4/MST1 deficiency in humans is associated with reduced expression of the homing receptors CCR7 and CD62L on lymphocytes and impaired migration towards CCL19 and

CCL21 (72). These defects are expected to severely impact lymphocyte homing to secondary lymphoid organs, in agreement with the reduced cellularity found in the secondary lymphoid organs of STK4/MST1-deficient mice at steady state and upon adoptive transfer of B and T cells (73). Furthermore, evidences suggest that STK4/MST1 contributes to LN and non-lymphoid tissue egress (74). In addition to its role as a transcriptional regulator, STK4/MST1 has been shown to exert a direct function on actin cytoskeleton remodelling in T cells through phosphorylation of L-plastin (115). It is therefore possible that the extended role of STK4/MST1 in regulating lymphocyte trafficking might result from its combined function as a regulator of both actin cytoskeleton and transcription.

Dendritic cells (DCs) are of critical importance for mounting an adaptive immune response. After antigen uptake in the peripheral tissue, these antigen-presenting cells migrate to the draining LNs through the lymph to activate specific T cells. It was shown in mice that WASP-deficient DCs exhibit a delayed migration from the skin to the draining LNs. In WASP-deficient animals, LNs do not increase in size and cellularity, reflecting the absence of lymphocyte traffic modification (91). Bone marrow-derived DCs were also studied in a mouse model of X-linked neutropenia (XLN), caused by gain-of-function mutations in the WAS gene (L272P). Unlike WAS-KO DC, WAS L272P DC show abnormal speed fluctuations and reduced global displacement. When tested *in vivo*, both seem to impair skin DC entry into the draining LN (98). In addition to WASP, a correct expression of DOCK8 in DCs seems to be a prerequisite for efficient T cell priming *in vivo*. Indeed, DOCK8 deficiency does not impact antigen uptake nor its presentation, but decreases DC trafficking to the draining LNs (38). A defect of skin DC migration to the draining LNs was also observed in STK4/MST1-deficient mice (73). Of note, STK4/MST1- and DOCK8-deficient patients share a common susceptibility to cutaneous warts, which could be explained by impairment of skin DC homing to the LNs.

In conclusion, a number of actinopathies are associated with alterations in the homing of lymphocytes and DCs to LNs (WASP, DOCK2, STK4/MST1) and/or in the egress of antigen-experienced lymphocytes from LNs (DOCK2, MSN, STK4/MST1). Interestingly, each examined deficiency appears to impact non-redundant mechanisms and steps accounting for LN homing and egress.

Leukocyte Migration in Peripheral Organs

Because of their contact with the environment, the skin and the lungs represent the main sites of pathogen entry (**Figures 1D, E**). It is therefore not surprising that most IEIs are associated with increased susceptibility to skin and lung infections (116). In the context of actinopathies, defective recruitment to these sites of both innate immune cells and primed lymphocytes may account for reduced ability to fight local infections.

During the primary phase of an infection, innate cells (e.g., neutrophils and monocytes) migrate to the site of inflammation. The infection spectrum observed in WAS patients may be suggestive of a neutrophil defect. This was confirmed in WASP-deficient mice where impaired integrin-dependent function in neutrophils was linked to a delay in migration into an inflamed site (83). On the contrary, despite a severe neutropenia, XLN patients are not at high risk of infections (117). This could be explained by normal numbers of neutrophils in peripheral sites, as exemplified in XLN patients saliva (97). Interestingly, neutrophils from XLN mice exhibit an increased infiltrating capacity with a competitive advantage over WT neutrophils in mixed bone marrow chimeras. The study of HEM1-null macrophages and neutrophils suggested an impaired migration *in vitro* (46, 47). More precisely, the knock-down of *nckap1l*, the gene encoding for HEM1, in zebrafish was responsible for a defective neutrophil migration after tail injury along with a decrease in circulating neutrophils (45). In a model of lipopolysaccharide (LPS)-induced lung inflammation, a prominent role of CDC42 was discovered in neutrophil emigration. Murine marrow cells with inducible KO of *Cdc42* were infused in irradiated mice. After LPS challenge, neutrophil counts in the lungs were significantly lower for *Cdc42*-/- reconstituted mice, revealing a defect in neutrophil infiltration (25). RAC2-deficient mice presented a decrease in cellular inflammatory exudate despite a persistent neutrophilic leukocytosis. This phenotype was reminiscent of leukocyte adhesion deficiency and thus suggested a defect in migration to the site of inflammation (66). To recapitulate the phenotype observed in humans, Deng and colleagues engineered a zebrafish model harbouring the inhibitory D57N mutation in Rac2 (64). This model allowed the observation of an impaired neutrophil migration to the site of infection with high neutrophil counts in peripheral blood. Interestingly, researchers discovered the role of RAC2 signalling in neutrophil retention in the bone marrow as Rac2 D57N mutation was able to partially rescue a zebrafish model of WHIM with constitutive CXCR4 signalling.

Once activated, effector T cells have to move to the site of infection (e.g., lung or skin) to exert their helper or cytolytic function. For this purpose, they express tissue homing chemokines receptors or specific integrin. Some of these T cells will acquire a tissue residency program to respond rapidly to a second antigen encounter (118). Interestingly, DOCK8-deficient patients suffer from numerous skin infections (119, 120). This peculiar infectious phenotype motivated studies on the role of DOCK8 in migration into the skin constrained environment, as we will detail in part 3. In DOCK8 deficiency, non-DC mononuclear phagocytes are prone to migration-induced cell death. This drives the skewing of the $CD4^+$ T cell response to a Th2 profile in the context of respiratory tract infection with *Cryptococcus neoformans* (121). RHOH-deficient patients also display susceptibility for skin infections with persistent Epidermodysplasia verruciformis linked to human papillomavirus infections (EV-HPV), that could be explained by a defect in lymphocyte skin-homing (69). The study of RHOH-deficient patients evidenced several differences in tissue-homing markers compared to healthy donors. In particular, a defect in $b7^+$ T cells was documented and confirmed in *RhoH*-/- mice.

In conclusion, the study of actinopathies has uncovered a number of key molecules driving effective trafficking and localization of immune cells within the organism. In these pathologies, defective recruitment of effector cells to tissues particularly exposed to infectious agents, such as the lungs and the skin, is at least in part accounting for the susceptibility of patients to infections.

MOTILITY DEFECTS IN ACTINOPATHIES AT THE TISSUE LEVEL

To gain insight into the actual leukocyte motility defects underlying actinopathies, it is important to consider the precise steps accounting for the translocation of leukocytes to tissues and their navigation within those tissues [as reviewed in (122)]. As described in chapter 2 (organism scale), among the trafficking defects associated with actinopathies are navigation of naïve lymphocytes to secondary lymphoid organs and migration of activated lymphocytes to infection sites. Although each subset of immune cells tends to migrate along a specific route, four migration steps are shared as depicted in **Figure 2**: 1) adhesion to the blood vessel at the site of priming or infection, 2) trans-endothelial migration (TEM), 3) navigation through the interstitial space and 4) interaction with a target (e.g., pathogens, antigen presenting cell or other cells of the immune system).

Adhesion to the Endothelium

The mechanism of exit from blood circulation used by immune cells is well-studied and has been reviewed in detail elsewhere (123). In case of infection, tissue-resident sentinel cells (e.g., macrophages, dendritic and mast cells) release cytokines (including TNF-α, IL-1β or histamine), which, in turn, activate endothelial cells in proximal blood vessels. Activated endothelium increases expression of key adhesion molecules, such as selectins and integrin ligands, at its surface. Selectins are responsible for initial low-affinity adhesion of immune cells leading to rolling of immune cells along the activated endothelium (**Figure 2-1**). Rolling helps immune cells to sample chemokines bound at the surface of endothelium and eventually leads to activation of integrin receptors (e.g., LFA-1) in immune cells. Activated integrin receptors bind to endothelium with much higher affinity and allow immune cells to resist the blood flow following initial adhesion at the exit site (**Figure 2-2**).

Studies in a murine model of WAS has revealed compromised ability of WASP-deficient T cells to adhere under shear flow (**Figure 2-6**) (96). Further study of XLN found that neutrophils in both XLN patients and XLN mouse models displayed dramatic increase in adhesion under shearing flow and increased migration into tissue (97). These studies suggest WASP to be important for proper adhesion of immune cells at the exit site of blood vessels. DOCK8 deficiency was also documented to result in defective attachment of T cells to ICAM-1 under flow, resulting in LN homing defects (40). In that study, DOCK8, WIP and WASP were reported to form a molecular complex positioning DOCK8 as a major guanine nucleotide-exchange factor to activate WASP.

MKL1 is a myocardin-related transcription factor, which regulates transcription of actin and multiple cytoskeleton-related genes (124, 125). Recent study of MKL1-deficient neutrophils demonstrated role of MKL1 in leukocyte adhesion under shear flow (49). Specifically, neutrophils lacking MKL1 displayed lower amount of F-actin following stimulation by an adhesive substrate.

Trans-Endothelial Migration

Following arrest at the exit site, immune cells exit the blood vessel *via* the complex process of TEM. This can occur by two major mechanisms: para-cellular transmigration (**Figure 2-3A**) and trans-cellular transmigration (**Figure 2-3B**). During para-cellular TEM immune cells leave the blood vessel between endothelial cells using transient disruption of adherens junctions. In contrast, cells using trans-cellular TEM leave the blood vessel by pushing directly though endothelial cells using invasive podosomes (89). By probing the physical properties of the endothelium, leukocytes may opt for the path of least resistance, as shown by manipulating junctional integrity (126). Breaching of endothelial cell junctions or foraging through endothelial cells require protrusive activities and high deformability, both coordinated by actin remodelling (127).

Seminal study of trans-cellular TEM mechanism revealed a key role of WASP in T cell migration (89). Researchers demonstrated that invasive podosomes (reviewed in detail in chapter 4) are crucial for trans-cellular TEM of T cells. Furthermore, results showed that WASP-deficient lymphocytes were unable to form invasive podosomes and failed to migrate through endothelial cells by trans-cellular TEM. These findings suggest that immune cells lacking WASP are restricted to para-cellular TEM to exit blood vessel. It is, however, unclear if compromised adhesion of WASP-deficient immune cells under shear flow discussed in chapter 3.1 is linked to inability of these cells to form podosomes.

In addition to WASP deficiency, studies of immune cells from patients deficient in proline-serine-threonine phosphatase interacting protein 1 (PSTPIP1), a scaffolding protein involved in the regulation of WASP activity (128, 129), showed defective podosome formation as well (58). Further experiments would be required to clarify whether PSTPIP1 deficiency compromises TEM *in vivo*.

Recently, 3 additional actin-related deficiencies have been added to the list of actinopathies affecting TEM of immune cells: MKL1 (49), HEM1 (47) and ERM (53) deficiencies. MKL1 deficiency led to poor adhesion and TEM of patient neutrophils (49). Studies of HEM1 deficiency in murine models showed drastic accumulation of HEM1-deficient myeloid cells both within and near the blood vessels (47). It is unclear, however, which step of immune cell migration (trans-endothelial or interstitial) might be affected in HEM1-deficient cells. Finally, recent study of ERM-deficient mice revealed crucial

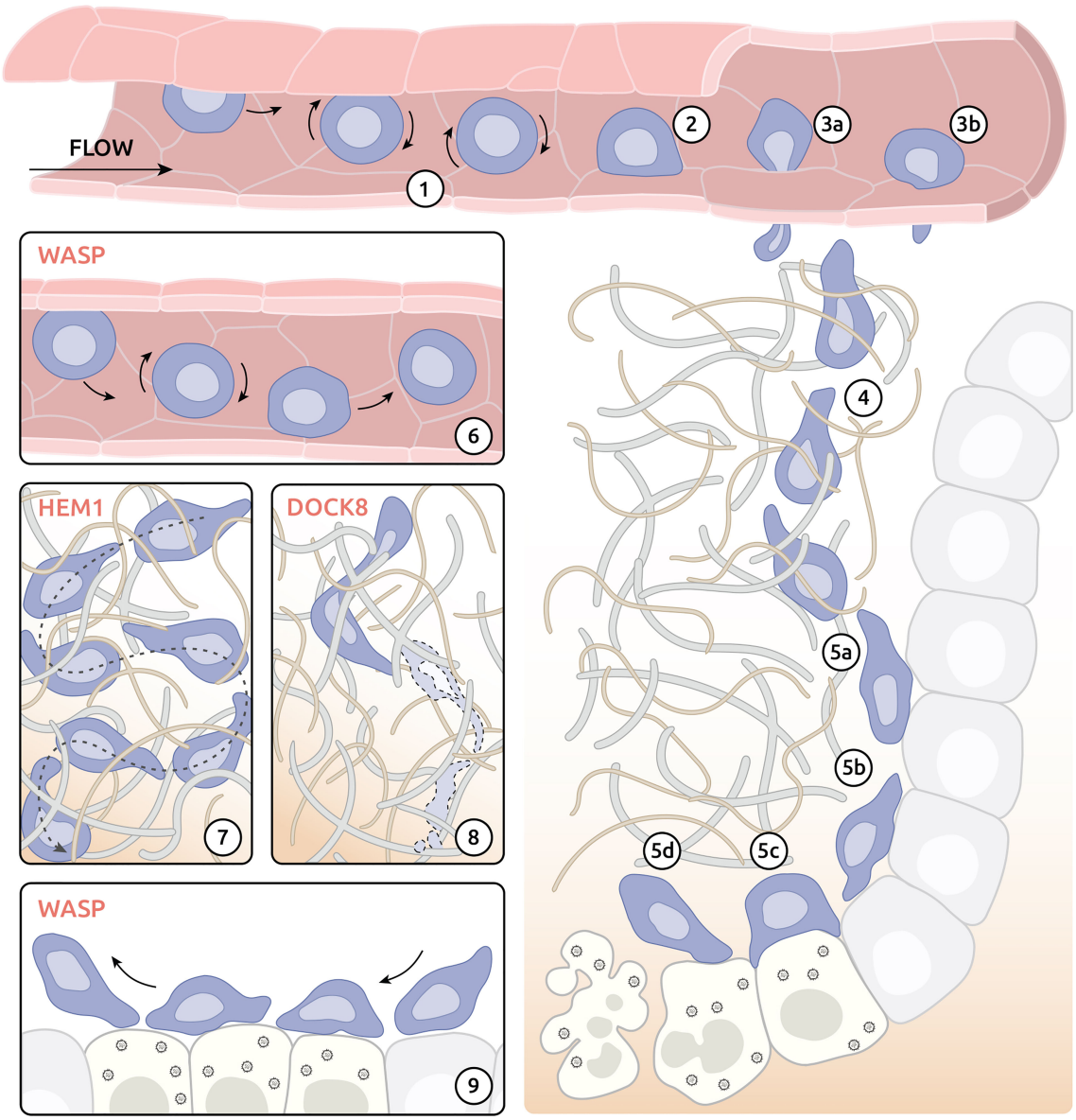

FIGURE 2 | Migratory challenges and actinopathy-associated defects of effector $CD8^+$ T cells on the tissue level. **(1)** Weak adhesion (rolling) of effector T cells after interaction with activated endothelium. **(2)** Adhesion at the site of exit. **(3)** Exit of the blood vessel by migration between **(3a)** or through **(3b)** endothelium cells. **(4)** Interstitial navigation following chemokine gradient. **(5)** Execution of cytolytic activity at the site of infection. **(5a)** Interaction with target cells. **(5b)** Kynapse-based scanning of target cells. **(5c)** Development of IS with infected cells and delivery of cytotoxic compounds. **(5d)** Destabilization of immune synapse (IS) and detachment from targeted cell. **(6)** Compromised attachment of WASP-deficient T cells to the endothelium at the exit site. **(7)** Reduced capacity of directional migration in tissue environment of HEM1-deficient T cells. **(8)** Cytothripsis of DOCK8-deficient T cells during migration through confined environment. **(9)** Impaired formation of IS by WASP-deficient T cells.

role of proper coupling between actin cytoskeleton and plasma membrane in TEM of murine T cells (53). Specifically authors showed impaired ability of T cells from MSN and moesin/ezrin-deficient mice to exit the blood stream.

Interstitial Migration

After crossing the endothelial barrier, leukocytes migrate to their targets through interstitium and tissue environments (**Figure 2-4**). Immune cells may employ two major modes of migration: adhesion-dependent and adhesion-independent [reviewed in (122)]. Both modes of migration are extremely dependent on active and precise remodelling of actin cytoskeleton but differ in mechanism of action. Adhesion-dependent migration involves attachment of plasma membrane receptors at the leading edge (such as integrins) to the extracellular substrate followed by crosslinking of membrane receptors and actin cytoskeleton.

Resulting link of extracellular matrix to actin cytoskeleton allows cells to use a molecular clutch mechanism for propulsion of the cell body forward (130, 131). In contrast, adhesion-independent migration uses combination of reward actin flow and contractility of actomyosin cortex to match the topology of surrounding 3D environment. Such mechanism allows for a "chimneying" type of directional motion that applies to lymphocytes, neutrophils and DCs (132). Although adhesion-dependent and adhesion-independent migration modalities have classically been opposed, leukocytes appear to be able to use a continuum of strategies, as shown by the use of channels with variable geometries (132).

To date, studies of virtually all actin-related IEIs revealed defects in immune cell migration *in vitro* (**Table 1**). In contrast, data on ability of immune cells to migrate *in vivo* is available for a handful of gene defects: *DOCK8* (37), *DOCK2* (35), *NCKAP1L* (47) and *MYH9* (55). Deficiency of DOCK8, an atypical immune system specific guanine nucleotide-exchange factor, is probably one of the best described actin-related IEIs affecting interstitial migration of immune cells. *Ex vivo* studies of DOCK8-deficient T cells migrating in the skin revealed dramatic stretching of the cell leading to cell death by stretching-induced rupture termed cytothripsis (37) (**Figure 2-8**). The exact mechanism of DOCK8 deficiency induced cell rupture remains to be clarified. Interestingly, studies of other DOCK deficiencies (e.g., DOCK2) found normal interstitial migration of immune cells (35). Specifically, lymphocytes from DOCK2-null mice successfully navigated through complex 3D environment albeit with decreased velocity.

Recent studies of HEM1 (47)- and MYH9 (55)- deficient cells expanded the number of actin-related IEIs affecting interstitial migration of immune cells. Mouse models of both HEM1 and MYH9 deficiencies demonstrated compromised ability of leukocytes to migrate in a 3D chemokine gradient (**Figure 2-7**). Directionality of immune cell migration, however, was preserved in both deficiencies.

Dynamic Assembly of the Immunological Synapse

The immunological synapse (IS) describes a tight junction formed by a T cell with either an antigen-presenting cell or an infected cell. At the tissue level formation of IS consists of 4 major phases (**Figures 2-5 A~D**): a) initial contact, b) spreading, c) mature synapse and d) destabilisation and termination [reviewed in (14)]. All phases of IS formation are controlled by a complex network of activatory and inhibitory stimuli and require sophisticated orchestration of actin-cytoskeleton [reviewed in (133)]. In accordance, numerous actin-related IEIs have been associated with defects in morphology and functions of IS, such as T cell activation, cytokine secretion and cytolytic activity (reviewed in (14); summarized in **Table 1**). In addition to T cells, the other subsets of lymphocytes including B cells, NK cells and innate lymphoid cells (ILCs) also assemble IS with partner cells or target cells. Although the molecular composition of the IS might vary among those lymphocyte subsets, its dependence on actin remodelling is a shared property. Exemplified by WASP

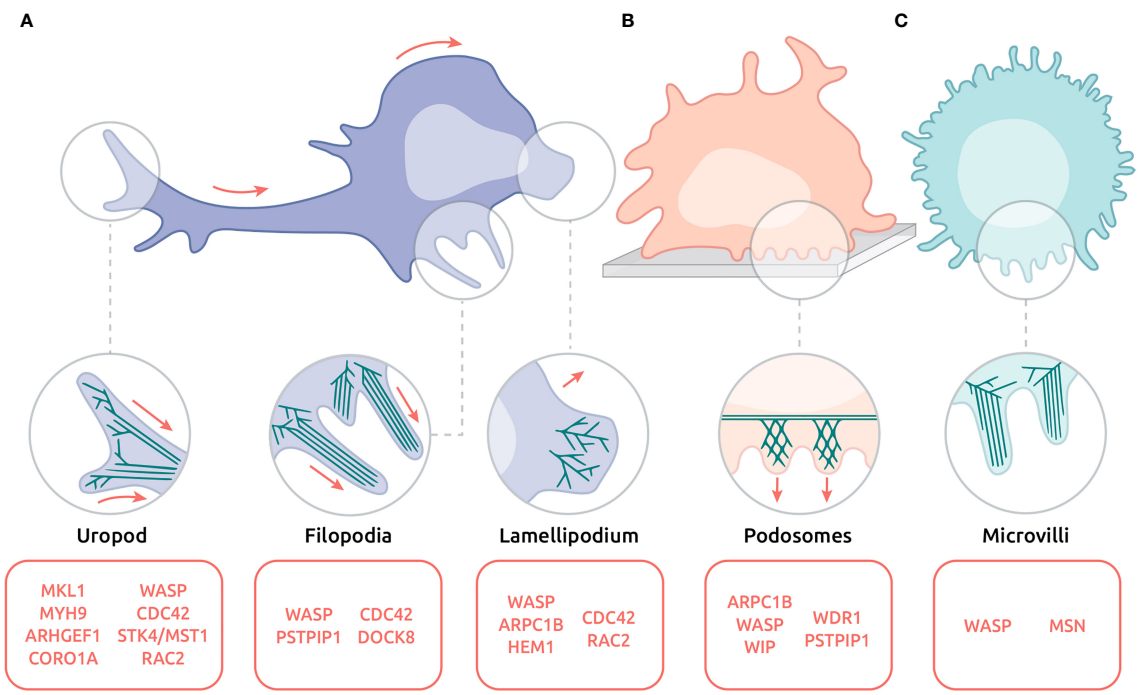

FIGURE 3 | Actin-based protrusions affected in actinopathies on the ultrastructural level. **(A)** Migrating lymphocyte with uropod, filopodia and lamellipodium. **(B)** Adhering DC emitting an array of podosomes. **(C)** Circulating neutrophil decorated with microvilli. Red arrows indicate direction of movement. Protein names listed in red indicate their involvement in the corresponding protrusions.

deficiency, it is therefore expected that IS defects across numerous lymphocyte subsets are associated with numerous actinopathies.

To date, little is known about the impact of actin-related IEIs on interaction dynamics between lymphocytes and their targets in the context of tissue environments. One may speculate that deficiencies in WASP and DOCK2 for example might alter lymphocyte scanning activity. Indeed the roles of WASP in the stabilization and termination of the IS (88, 134–136) are expected to translate into biased interaction of lymphocytes with antigen-presenting cells or target cells in peripheral organs (**Figure 2-9**). The over-stabilization of the IS observed between $CD4^+$ T cells and DCs in the DOCK2-deficient mice (137) is also expected to alter the serial scanning behaviour of the $CD4^+$ T cells. More *in vivo* studies however, would be needed to clarify the impact of the actinopathy-related proteins to the motility behaviour of various lymphocyte subsets in the context of antigen search and IS dynamics.

MOTILITY DEFECTS IN ACTINOPATHIES AT THE ULTRASTRUCTURAL LEVEL

The highly adaptable motility property of leukocytes is supported by their ability to emit a variety of highly dynamic actin-rich protrusions (**Figure 3**). Protrusions such as leading-edge lamellipodia and filopodia may exert an exploratory function. Others like podosomes and microvilli may rather promote and regulate adhesion. The uropod at the trailing edge is the site of contractile activities that regulates cell detachment in the context of motility. In addition, the actin cytoskeleton is involved in controlling the squeezing of the nucleus in the context of migration through confined spaces. Section below summarizes cellular protrusions affected in actinopathies. These natural deficiencies thereby highlight the key function of actin regulators in controlling leukocyte motility at the ultrastructural level.

Lamellipodium

Located at the leading edge, the lamellipodium is a large expansion of the plasma membrane, generated by actin polymerization and branching **(Figure 3A-Lamellipodium)** [see (138) for review]. In lymphocytes it supports not only the exploratory behaviour during migration but also IS assembly during APC encounter (139). In accordance with the major role of actin cytoskeleton remodelling in lamellipodium formation, defects in its development and organization have been reported in deficiencies affecting the ARP2/3 complex-dependent process of actin branching. ARPC1B is an essential subunit of the ARP2/3 complex that is critical for its assembly and maintenance (140). Upon interaction with a surface coated with ICAM-1 and α-CD3 antibodies to mimic APC encounter, ARPC1B-deficient T cells fail to assemble a circular lamellipodium and instead emit aberrant thin filopodia (20, 21, 90). ARPC1B deficiency in human T cells is also associated with defective migration in response to chemokines (20), presumably because of a defective lamellipodium. Indeed, ARP3 subunit knock-down, which also leads to a destabilization of the ARP2/3 complex, results in a reduced exploratory behaviour of murine T cells in both 3D collagen matrices and zebrafish embryos (141). Interestingly, reduced motility of ARP3-deficient T cells is associated with reduced cortical tension and a switch from the leading-edge lamellipodia to blebs.

Although WASP operates as an ARP2/3 activator, its involvement in the regulation of lamellipodial protrusion is not as prominent as it is for ARP2/3 (142, 143). Indeed, WASP is not essential for lamellipodium emergence, but rather controls its stability and dynamics, as shown in T cells in the context of IS assembly (134, 135). Instead of emitting a radially distributed lamellipodium, WASP-deficient $CD8^+$ T cells display a disrupted lamellipodium that irradiates in different directions (87, 90). Alternation of arrest phases at the contact with APC and motility phases to search for new APC is key to the tuning of lymphocyte activation and function. In this context WASP appears to play a particularly central role since its ubiquitination-dependent degradation activated upon TCR ligation sets the turnover of the IS (136). In line with the role of WASP in stabilizing the lamellipodia of T cells and DCs isolated from WAS patients emitted unstable lamellipodia (79) and failed to maintain polarization at the leading edge (80). On the other hand, a study of neutrophils carrying a gain-of-function mutation in WASP (L270P) showed an increase of the spreading area of the lamellipodia compared with normal neutrophils, which was correlated with an increase in the adhesion footprint (97).

In agreement with its function as a chaperone of WASP (144), WIP plays a prominent role in lamellipodial assembly as well. Upon interaction with surfaces coated with ICAM-1 and α-CD3 antibodies or fibronectin and chemokines, T cells derived from a WIP-deficient patient failed to assemble lamellipodia (103). Furthermore, upon exposure to a CCL19 gradient, WIP-depleted B cells emitted multipolar filopodia and pseudopodia, which were associated with reduced speed and directional migration (103). Comparably, WIP-deficient DCs displayed defective polarization due to unstable lamellae and ruffles in place of the leading edge (104).

The pentameric WAVE complex is a key ARP2/3 activator in addition to WASP, albeit sustaining distinct cellular activities (61, 145, 146). HEM1 is a hematopoietic-specific subunit of the WAVE complex. Recent studies found deficiency in HEM1 to be a novel form of immune-related actinopathy (43–45). In the absence of HEM1 the other subunits of the WAVE complex are unstable and degraded. Deficiency of the WAVE complex severely affects actin branching and consequently lamellipodial dynamics. HEM1-deficient T cells struggle to spread and lack lamellipodial protrusions. In addition, HEM1 deficiency leads to a decrease in F-actin density at the leading edge (43, 44). Upon stimulation with ICAM-1, HEM1-deficient T cells isolated from patients, present lack of a leading edge or an abnormal distribution of F-actin at the leading edge instead of the lamellipodium (45). HEM1-deficient B cells also displayed an aberrant morphology associated with defective directional migration when exposed to a CCL19 gradient (44). As

reported above for ARP3 knock-down, HEM1-deficient B cells adopted a bleb-driven type of motility. Before the discovery of HEM1 deficiency in humans, its role had been studied in the context of murine DC migration (48). Interestingly, the lack of lamellipodia in *Nckap1l*-/- immature DCs was associated with increased speed and unusually straight migration paths in 3D collagen gels. Preserved motility of HEM1-deficient cells suggests that the lamellipodium of leukocytes acts as an exploratory device allowing change in direction rather than as a force generating structure (48). This notion is sustained by TIRF analysis of the actin cytoskeleton in migratory DCs, neutrophils, T and B cells which showed that the lamellipodium undulates at the front of the cells and makes only transient and limited contacts with the substrate (48, 147). A recent study widened the role of HEM1 in supporting lamellipodia assembly in macrophages and platelets. In particular, HEM1-deficient macrophages adopted a spiky shape with filopodia emitted instead of lamellipodia, which was associated with reduced motility in collagen gels (47). Taken together, studies on HEM1 deficiency indicate that the WAVE complex is a crucial driver of ARP2/3-dependent lamellipodia assembly in hematopoietic cells.

The RHO GTPases RAC1 and RAC2 act as upstream regulators of lamellipodia assembly by activating the WAVE complex. Studies of patients suffering from severe disease associated predominantly with neutrophil dysfunction identified dominant negative mutations in RAC2, altering the activity of both RAC2 and RAC1 (148, 149). Upon stimulation with fMLP, patient-derived neutrophils failed to assemble a lamellipodium and to polarize. Similarly, neutrophils with mutated RAC2 failed to migrate in response to zymosan-activated serum. Study of a loss-of-function mutation in RAC2 in patients suffering from common variable immunodeficiency revealed impaired chemotaxis of RAC2-deficient neutrophils (150). Preserved activity of RAC1 in these patients could result in residual neutrophil function and, thus, explain the distinct clinical phenotype of RAC2 deficiency. Furthermore, recent study of 3 patients with a gain-of-function mutation in RAC2 showed defective migration of neutrophils to fMLP as well (62).

Filopodia

Filopodia are usually described as thin protrusions, composed of bundles of parallel actin filaments, that emerge from the tip of the lamellipodia of migrating cells **(Figure 3A-Filopodia)** [see (151) for review]. Lamellipodia-associated filopodia are considered as sensors. In leukocytes, filopodia are more often dissociated from the lamellipodia and may emerge as micrometre-long protrusions from different parts of the cell body. In addition to their role as environment sensors, filopodia play a role in phagocytosis in macrophages (152).

CDC42 is considered the main RHO GTPase involved in filopodia assembly (153). Recent study of the distinct immunological syndrome with immune dysregulation and inflammation identified mutation in CDC42 (R186C) leading to impaired ability of the protein to interact with its binding partners: IQGAP1 and, to a lesser extent, WASP (24). In the affected patients, both fibroblasts and immune cells displayed lack of cell polarization associated with aberrant density and distribution of filopodia. In addition, hematopoietic stem cells, peripheral blood mononuclear cells (PBMCs) and NK cells from affected patients displayed reduced migratory capacity towards CXCL12.

An early study on the CDC42 activator DOCK8 (42), showed that disruption of actin polymerisation induced by Cytochalasin D treatment of mice microglia led to accumulation of DOCK8 at the sites of filopodia formation. However, similar treatment of cells from DOCK8-deficient mice led to a 30% reduction in number of cells with filopodia compared to cells from WT mice.

As a further support of the role of the CDC42 axis in regulating filopodia assembly and dynamics, WASP deficiency was reported to result in a decrease in the number of filopodia in macrophages. The remaining filopodia occupied a large distribution around the cell instead of being concentrated in one specific edge (84). Moreover, a reduction of the length of filopodia-type protrusions in B cells has been observed in the context of WASP deficiency (76).

Uropod

The uropod is a highly contractile structure at the rear of migrating cells, and plays a decisive role in cellular migration [see (154) for review] **(Figure 3A-Uropod).** The cell propulsion relies on myosin-based contractions at the uropod that allow detachment from the substrate and rearward squeezing (155).

A number of studies in cell lines and murine models have assessed the role of MYH9 in leukocyte motility. A study on human lymphocytes observed that the uropod of migrating T cells is enriched in MYH9 (57). Chemical inhibition of MYH9 activity with blebbistatin and genetic inhibition with siRNA resulted in aberrant elongation of the uropod, suggesting that the de-adhesion process was impaired upon the loss of MYH9 activity. Other studies showed that T lymphocytes can rapidly switch between an adhesion-dependent sliding motility and an amoeboid walking motility that depends on MyoIIA (156). *Myh9* conditional knockout in T cells impaired the turnover of adhesion sites, resulting in increased adhesion and impaired interstitial migration *in vivo* (56). Interestingly, a downregulation of MYH9 in mice neutrophils showed no defect in term of cellular shape (with a rear comparable to a normal uropod), but caused decrease in migration (55). *MYH9* mutations in humans have been found to be the cause of heterogeneous group of diseases, mostly characterized by macrothrombocytopenia, hearing loss and renal disease (157). Whether defects in the motility of leukocytes and in particular uropod dynamics might contribute to yet uncharacterized immune cell defects in individuals with *MYH9* mutations remains to be investigated.

Although CDC42 is mainly localized at the cell leading edge, it is also involved in the modulation of the myosin light-chain pathway at the uropod (26). *Via* its control over WASP activation, CDC42 has also been reported to regulate CD11b reorganization at the uropod (25). In line with a role of the CDC42-WASP axis in uropod dynamics, WASP-deficient leukocytes displayed extreme elongation of uropods (80).

Abnormally elongated uropods in T cells have also been described in the context of deficiency in ARHGEF1, a regulator of RHOA GTPase. This defect was associated with a decrease in the mean square displacement of migrating T cells (17). A failure of uropod retraction was also reported in MKL1-deficient neutrophil-like HL-60 cells, presumably because of a reduced expression of myosin light chain 9 (MYL9), a component of the myosin II complex (50). Deficiency in CORO1A in mice has also been reported to impair uropod assembly in T cells. Instead of this structure, CORO1A-deficient T cells formed several patch-like talin-rich clusters, abnormally distributed around the cell cortex (30). The uropod has also been reported to be affected in RAC2 deficiency (148) and STK4/MST1 deficiency (73), highlighting the complexity of the molecular control of actin dynamics in the context of this cellular structure.

Podosomes

Podosomes are actin-driven micron-scale cellular adhesive protrusions and are crucial for adhesion, migration and degradation of the extracellular matrix. The actin cytoskeleton within podosomes is mostly composed of branched actin filaments. Moreover, podosomes are linked together by a network of unbranched actin filaments [see (158) for review] (**Figure 3B-Podosomes**).

In this context, the WASP-ARP2/3 pathway appears crucial in the assembly of podosomes, while the WAVE complex is dispensable. Indeed both WASP and ARPC1B deficiencies are associated with the defective assembly of podosomes by monocyte-derived macrophages (19, 84). In contrast, macrophages from *Nckap1l*-KO mice have a preserved ability to assemble podosomes although they display multiple defects in lamellipodia, focal adhesions and endocytosis (47). The specificity of WASP in activating ARP2/3 towards podosome assembly might be related to its specific location in podosome priming areas and its ability to recruit ARP2/3 at such sites (84). Reconstitution experiments in WAS patient-derived macrophages using micro-injections of full-length human WASP sequence suggested that the chemotactic response to the cytokine colony stimulating factor-1 is dependent on WASP-driven assembly of podosomes (159). To date, studies of WASP revealed its key role in podosome assembly in multiple cellular systems beyond macrophages: immature DCs (80), THP-1 (19) and T cells (89). Moreover, experiments using RNA interference to induce partial down-regulation of the intracellular WASP level in DCs led to compromised podosome formation (160), indicating that a precise regulation of WASP expression might be crucial for assembly of podosomes.

As an essential partner of WASP, WIP has been reported to be essential for podosome assembly as well. In WIP-deficient mice, DCs formed few podosomes associated with loss of podosomal structure, including the actin core and the vinculin rings (104). Moreover, the authors found that lack of podosome formation in WIP-deficient DCs is compensated by assembly of large vinculin-rich focal adhesion contacts. In human macrophages, WIP localizes to the core of podosomes, where it co-localizes with F-actin (105). To date, however, defects in podosome formation have not been examined in WIP-deficient patient cells.

Studies of patients with mutations in *PSTPIP1* found decreased numbers of macrophages emitting podosomes as well (58). Similar to WASP-deficient cells, deficiency in PSTPIP1 led to increase in the number and the size of vinculin-containing focal complexes compared to normal cells. A follow-up study proposed that defect of migration of PSTPIP1-deficient macrophages resulted in a switch from formation of podosomes to filopodia (59).

MKL1 deficiency is associated with a severe defect in podosome formation resulting in impaired adhesion (50). Indeed, a complete absence of podosomes has been reported in MKL1-deficient DCs on fibronectin. Conjointly, the spreading of MKL1-deficient cells was reduced, and the F-actin staining was severely decreased compare to normal DCs.

As opposed to deficiencies in ARPC1B, WASP, WIP, PSTPIP1, and MKL1, deficiency in WDR1 is associated with a reinforcement of podosomes in myeloid cells (100). WDR1, together with cofilin, promotes actin severing and is important for actin filament turnover. Its impact on leukocyte podosomes has been initially described on monocyte-derived DCs (100). In these cells, the number of podosomes was close to that of normal cells, but their volume and F-actin content were increased. A complementary study on WDR1-deficient monocytes on fibronectin found an abnormally high number of actin-rich podosome-like structures compared to normal monocytes (99). These findings support the notion that WDR1-mediated actin filament turnover is particularly important for podosome formation.

Microvilli

Microvilli are very thin finger-like protrusions that tend to decorate most of the cell surface **(Figure 3C-Microvilli).** In leukocytes, they have initially been described by scanning electron microscopy in B and T cells (161), macrophages (162) and DCs (163). Their function in leukocytes is to help migration and assist antigen sensing [see (164) for review]. In particular, in T cells most of the TCR molecules are localized at the surface of the microvilli, increasing the probability to detect antigen (165).

Initial studies have reported WASP as a key regulator of microvilli. Lymphocytes from WAS patients were shown to harbour reduced density of what appeared as blunted microvilli (166, 167). However, in a more recent study microvilli density was found to be unaltered in fresh WASP-deficient human lymphocytes (168). Furthermore, *Was*-KO B cells were observed to have aberrant microvilli formation upon anti-CD40 plus IL-4 stimulation, but not upon LPS stimulation (76). These studies suggest that the WASP-dependent assembly of microvilli in lymphocytes is dependent on the activation status of these cells. In addition to WASP, MSN appear to also regulate microvilli assembly. Indeed, experiments using scanning electron microscopy on murine MSN-deficient lymphocytes revealed a decrease of microvilli density, as well as defective development of these structures (39).

Nucleus and Organelles

Deformability is an essential property of leukocytes that allows probing narrow interstices and migrating through very constrained environments. Whereas the plasma membrane is extremely deformable, the nucleus is more rigid, thereby imposing a physical checkpoint for leukocyte motility. The squeezing of the nucleus is well described in multiple cell types [see (169–171) for reviews]. In leukocytes, this process is associated with an active mechanism of pore-size discrimination facilitated by frontward positioning of the nucleus (172). Indeed, to facilitate crossing of the endothelial barrier, T cells use MyoIIA-driven contractility to squeeze the nucleus through the endothelial junctions (173). In addition, a formin-dependent actin polymerization mechanism was shown to push the nucleus at the back of effector T cells migrating in constrained inflamed tissues (174). In particular, FMNL1 was shown to promote actin polymerization at the back of the cell to enable translation of the rigid nucleus through restrictive barriers of extracellular matrix. DIAPH1, a formin highly expressed in leukocytes, has recently been shown to be associated to immune cell defects in humans when mutated (32). Whether DIAPH1 also contributes to nucleus squeezing has not yet been investigated. A further striking evidence for the role of actin remodelling in the integrity of the nucleus in the context of leukocyte migration stems from the DOCK8 deficiency. As described in chapter 3, DOCK8-deficient T cells migrating in dense environments display abnormally elongated shapes leading to cytothripsis. Interestingly, pieces of deformed nuclei were observed in the cellular fragments resulting from this atypical cell death process. This suggests that DOCK8 plays a key role in nucleus integrity by regulating the mechanical forces imposed on migrating T cells (37).

Multiple aspects of intracellular vesicle trafficking are sustaining cell polarity and motility (175). These mechanisms, such as endo- and exocytic pathways, are increasingly recognized as being dependent on vesicle-associated actin remodelling activities (176).

In the context of actin-related IEI, we currently lack direct evidence that the involved molecules might control immune cell motility *via* the regulation of vesicle trafficking.

However, given the fact that proteins such as WASP regulate endosome trafficking (177), it would be interesting to further investigate the possible contribution of vesicle trafficking to the actinopathy-associated cell motility defects.

OUTLOOK

The generalization of exome sequencing as an approach to identify the genetic aetiology of rare IEIs has led to the recent characterization of multiple actinopathies. This review highlights 23 gene defects related to actin cytoskeleton remodelling in immune cells and highlighted the motility impairments associated with these defects. Although alteration of leukocyte motility is not the sole explanation for the complex immune dysfunction associated with actinopathies, it certainly plays a major role. Leukocyte motility, when viewed through the prism of actinopathies highlights gaps in our knowledge of molecules and pathways crucial for the integrity of the immune system. Many actinopathies share defects in leukocyte motility (e.g., T cell egress from the thymus, homing of lymphocytes to secondary lymphoid organs, migration towards chemokines, assembly of the uropod of migrating lymphocytes) while others display unique defects specific to certain molecules (e.g., cytothripsis in DOCK8-deficient T cells during interstitial migration). Partial overlap of defects in immune cell motility among different actinopathies suggests that multiple leukocyte motility steps require the combination of multiple actin remodelling activities.

Research on actinopathies provided unique insight into the regulation of leukocyte motility. However, our current picture of the role of individual disease-related molecules remains very fragmented. Lack of detailed understanding is related to both novelty of many of the deficiencies and the amount of work it takes to apprehend the multiplicity of motility steps that immune cells undergo. Moreover, studies of immune cell motility are further complicated by the diversification of motility strategies adopted by the different immune cell subsets and restricted amount of patient material available. In an effort to address some of those limitations we have recently introduced morphological profiling of leukocytes *via* high-content cell imaging (90). Such approach can be applied to restricted sample sizes, can be used in standardizing the comparison of morphological defects in primary leukocytes from patients and has proven to be efficient at discriminating defects in closely related deficiencies such as ARPC1B and WASP deficiencies. Beyond high-content cell imaging, recent advances in super-resolution microscopy and design of probes and micro-patterned surfaces for live imaging are expected to probe cell migration more precisely and identify novel actinopathy-related leukocyte defects. Furthermore, a more systematic application of live tissue imaging in murine or zebrafish models is expected to complement *in vitro* studies with patient cells and fill the gap in our understanding of leukocyte motility across the different cellular and tissue scales.

AUTHOR CONTRIBUTIONS

AK, MF, CL, and LD conceptualized the review and the figures. All authors contributed substantially to the text of the manuscript. All authors approved the submitted version.

FUNDING

This work received support from WWTF (PrecisePID project LS16-060 to LD) and CNRS (International Research Project SysTact to LD). MF is supported by the Fondation pour la recherche médicale (FDM202006011216).

ACKNOWLEDGMENTS

We wish to thank Tatjana Hirschmugl (Scillustration, Graz and Vienna, Austria) for design and production of the artwork.

REFERENCES

1. Mazo IB, Massberg S, von Andrian UH. Hematopoietic Stem and Progenitor Cell Trafficking. *Trends Immunol* (2011) 32:493–503. doi: 10.1016/j.it.2011.06.011
2. Takahama Y. Journey Through the Thymus: Stromal Guides for T-Cell Development and Selection. *Nat Rev Immunol* (2006) 6:127–35. doi: 10.1038/nri1781
3. Nourshargh S, Hordijk PL, Sixt M. Breaching Multiple Barriers: Leukocyte Motility Through Venular Walls and the Interstitium. *Nat Rev Mol Cell Biol* (2010) 11:366–78. doi: 10.1038/nrm2889
4. Krummel MF, Bartumeus F, Gérard A. T Cell Migration, Search Strategies and Mechanisms. *Nat Rev Immunol* (2016) 16:193–201. doi: 10.1038/nri.2015.16
5. Friedl P, Wolf K. Plasticity of Cell Migration: A Multiscale Tuning Model. *J Cell Biol* (2010) 188:11–9. doi: 10.1083/jcb.200909003
6. Vicente-Manzanares M, Sánchez-Madrid F. Role of the Cytoskeleton During Leukocyte Responses. *Nat Rev Immunol* (2004) 4:110–22. doi: 10.1038/nri1268
7. Mastrogiovanni M, Juzans M, Alcover A, Di Bartolo V. Coordinating Cytoskeleton and Molecular Traffic in T Cell Migration, Activation, and Effector Functions. *Front Cell Dev Biol* (2020) 8:591348. doi: 10.3389/fcell.2020.591348
8. Rottner K, Faix J, Bogdan S, Linder S, Kerkhoff E. Actin Assembly Mechanisms at a Glance. *J Cell Sci* (2017) 3427–35. doi: 10.1242/jcs.206433
9. Svitkina T. The Actin Cytoskeleton and Actin-Based Motility. *Cold Spring Harb Perspect Biol* (2018) 10:1–21. doi: 10.1101/cshperspect.a018267
10. Burns SO, Zarafov A, Thrasher AJ. Primary Immunodeficiencies Due to Abnormalities of the Actin Cytoskeleton. *Curr Opin Hematol* (2017) 24:16–22. doi: 10.1097/MOH.0000000000000296
11. Janssen E, Geha RS. Primary Immunodeficiencies Caused by Mutations in Actin Regulatory Proteins. *Immunol Rev* (2019) 287:121–34. doi: 10.1111/imr.12716
12. Tangye SG, Bucciol G, Casas-Martin J, Pillay B, Ma CS, Moens L, et al. Human Inborn Errors of the Actin Cytoskeleton Affecting Immunity: Way Beyond WAS and WIP. *Immunol Cell Biol* (2019) 97:389–402. doi: 10.1111/imcb.12243
13. Papa R, Penco F, Volpi S, Gattorno M. Actin Remodeling Defects Leading to Autoinflammation and Immune Dysregulation. *Front Immunol* (2021) 11:604206. doi: 10.3389/fimmu.2020.604206
14. Dupré L, Boztug K, Pfajfer L. Actin Dynamics at the T Cell Synapse as Revealed by Immune-Related Actinopathies. *Front Cell Dev Biol* (2021) 9:665519. doi: 10.3389/fcell.2021.665519
15. Nunoi H, Yamazaki T, Tsuchiya H, Kato S, Malech HL, Matsuda I, et al. A Heterozygous Mutation of -Actin Associated With Neutrophil Dysfunction and Recurrent Infection. *Proc Natl Acad Sci* (1999) 96:8693–8. doi: 10.1073/pnas.96.15.8693
16. Bunnell TM, Burbach BJ, Shimizu Y, Ervasti JM. β-Actin Specifically Controls Cell Growth, Migration, and the G-Actin Pool. *Mol Biol Cell* (2011) 22:4047–58. doi: 10.1091/mbc.E11-06-0582
17. Bouafia A, Lofek S, Bruneau J, Chentout L, Lamrini H, Trinquand A, et al. Loss of ARHGEF1 Causes a Human Primary Antibody Deficiency. *J Clin Invest* (2019) 129:1047–60. doi: 10.1172/JCI120572
18. Muppidi JR, Schmitz R, Green JA, Xiao W, Larsen AB, Braun SE, et al. Loss of Signalling *via* G α 13 in Germinal Centre B-Cell-Derived Lymphoma. *Nature* (2014) 516:254–8. doi: 10.1038/nature13765
19. Rivers E, Rai R, Lötscher J, Hollinshead M, Markelj G, Thaventhiran J, et al. Wiskott Aldrich Syndrome Protein Regulates Non-Selective Autophagy and Mitochondrial Homeostasis in Human Myeloid Cells. *Elife* (2020) 9:1–23. doi: 10.7554/eLife.55547
20. Brigida I, Zoccolillo M, Cicalese MP, Pfajfer L, Barzaghi F, Scala S, et al. T-Cell Defects in Patients With ARPC1B Germline Mutations Account for Combined Immunodeficiency. *Blood* (2018) 132:2362–74. doi: 10.1182/blood-2018-07-863431
21. Randzavola LO, Kuijpers TW, Gillian M, Randzavola LO, Strege K, Juzans M, et al. Loss of ARPC1B Impairs Cytotoxic T Lymphocyte Maintenance and Cytolytic Activity. *J Clin Invest* (2019) 129:1–15. doi: 10.1172/JCI129388
22. Kahr WHA, Pluthero FG, Elkadri A, Warner N, Drobac M, Chen CH, et al. Loss of the Arp2/3 Complex Component ARPC1B Causes Platelet Abnormalities and Predisposes to Inflammatory Disease. *Nat Commun* (2017) 8:1–14. doi: 10.1038/ncomms14816
23. Schober T, Magg T, Laschinger M, Rohlfs M, Linhares ND, Puchalka J, et al. A Human Immunodeficiency Syndrome Caused by Mutations in CARMIL2. *Nat Commun* (2017) 8:1–13. doi: 10.1038/ncomms14209
24. Lam MT, Coppola S, Krumbach OHF, Prencipe G, Insalaco A, Cifaldi C, et al. A Novel Disorder Involving Dyshematopoiesis, Inflammation, and HLH Due to Aberrant CDC42 Function. *J Exp Med0* (2019). p. 2778–99. doi: 10.1084/jem.20190147
25. Kumar S, Xu J, Perkins C, Guo F, Snapper S, Finkelman FD, et al. Cdc42 Regulates Neutrophil Migration *via* Crosstalk Between WASp, CD11b, and Microtubules. *Blood* (2012) 120:3563–74. doi: 10.1182/blood-2012-04-426981
26. Szczur K, Zheng Y, Filippi MD. The Small Rho GTPase Cdc42 Regulates Neutrophil Polarity *via* CD11b Integrin Signaling. *Blood* (2009) 114:4527–37. doi: 10.1182/blood-2008-12-195164
27. Shiow L, Roadcap D, Paris K, Watson S, Cyster J. The Actin Regulator Coronin-1A Is Mutated in a Thymic Egress Deficient Mouse Strain and in a T–B+ NK+ SCID Patient. *Nature* (2008) 9:1307–15. doi: 10.1038/ni.1662.The
28. Yee CS, Massaad MJ, Bainter W, Ohsumi TK, Föger N, Chan AC, et al. Recurrent Viral Infections Associated With a Homozygous CORO1A Mutation That Disrupts Oligomerization and Cytoskeletal Association. *J Allergy Clin Immunol* (2016) 137:879–88.e2. doi: 10.1016/j.jaci.2015.08.020
29. Yagi H, Matsumoto M, Nakamura M, Makino S, Suzuki R, Harada M, et al. Defect of Thymocyte Emigration in a T Cell Deficiency Strain (CTS) of the Mouse. *J Immunol* (1996) 157:3412–9.
30. Foger N, Rangell L, Danilenko D, Chan A. Requirement for Coronin 1 in T Lymphocyte Trafficking and Cellular Homeostasis. *Sci (80-)* (2006) 313:839–42. doi: 10.1016/b978-1-4832-3292-8.50018-7
31. Pick R, Begandt D, Stocker TJ, Salvermoser M, Thome S, Böttcher RT, et al. Coronin 1A, a Novel Player in Integrin Biology, Controls Neutrophil Trafficking in Innate Immunity. *Blood* (2017) 130:847–58. doi: 10.1182/blood-2016-11-749622
32. Kaustio M, Nayebzadeh N, Hinttala R, Tapiainen T, Åström P, Mamia K, et al. Loss of DIAPH1 Causes SCBMS, Combined Immunodeficiency, and Mitochondrial Dysfunction. *J Allergy Clin Immunol* (2021) 148:599–611. doi: 10.1016/j.jaci.2020.12.656
33. Sakata D, Taniguchi H, Yasuda S, Adachi-Morishima A, Hamazaki Y, Nakayama R, et al. Impaired T Lymphocyte Trafficking in Mice Deficient in an Actin-Nucleating Protein, Mdia1. *J Exp Med* (2007) 204:2031–8. doi: 10.1084/jem.20062647
34. Dobbs K, Domínguez Conde C, Zhang S-Y, Parolini S, Audry M, Chou J, et al. Inherited DOCK2 Deficiency in Patients With Early-Onset Invasive Infections. *N Engl J Med* (2015) 372:2409–22. doi: 10.1056/nejmoa1413462
35. Nombela-Arrieta C, Mempel TR, Soriano SF, Mazo I, Wymann MP, Hirsch E, et al. A Central Role for DOCK2 During Interstitial Lymphocyte Motility and Sphingosine-1-Phosphate-Mediated Egress. *J Exp Med* (2007) 204:497–510. doi: 10.1084/jem.20061780
36. Nombela-Arrieta C, Lacalle RA, Montoya MC, Kunisaki Y, Megías D, Marqués M, et al. Differential Requirements for DOCK2 and Phosphoinositide-3-Kinase γ During T and B Lymphocyte Homing. *Immunity* (2004) 21:429–41. doi: 10.1016/j.immuni.2004.07.012
37. Zhang Q, Dove CG, Hor JL, Murdock HM, Strauss-Albee DM, Garcia JA, et al. DOCK8 Regulates Lymphocyte Shape Integrity for Skin Antiviral Immunity. *J Exp Med* (2014) 211:2549–66. doi: 10.1084/jem.20141307
38. Harada Y, Tanaka Y, Terasawa M, Pieczyk M, Habiro K, Katakai T, et al. DOCK8 Is a Cdc42 Activator Critical for Interstitial Dendritic Cell Migration During Immune Responses. *Blood* (2012) 119:4451–61. doi: 10.1182/blood-2012-01-407098
39. Hirata T, Nomachi A, Tohya K, Miyasaka M, Tsukita S, Watanabe T, et al. Moesin-Deficient Mice Reveal a Non-Redundant Role for Moesin in Lymphocyte Homeostasis. *Int Immunol* (2012) 24:705–17. doi: 10.1093/intimm/dxs077
40. Janssen E, Tohme M, Hedayat M, Leick M, Kumari S, Ramesh N, et al. A DOCK8-WIP-WASp Complex Links T Cell Receptors to the Actin Cytoskeleton. *J Clin Invest* (2016) 126:3837–51. doi: 10.1172/JCI85774

41. Janssen E, Tohme M, Butts J, Giguere S, Sage PT, Velázquez FE, et al. DOCK8 Is Essential for LFA-1–Dependent Positioning of T Follicular Helper Cells in Germinal Centers. *JCI Insight* (2020) 5:1–13. doi: 10.1172/jci.insight.134508
42. Ruusala A, Aspenström P. Isolation and Characterisation of DOCK8, a Member of the DOCK180-Related Regulators of Cell Morphology. *FEBS Lett* (2004) 572:159–66. doi: 10.1016/j.febslet.2004.06.095
43. Cook SA, Comrie WA, Poli MC, Similuk M, Oler AJ, Faruqi AJ, et al. HEM1 Deficiency Disrupts Mtorc2 and F-Actin Control in Inherited Immunodysregulatory Disease. *Sci (80-)* (2020) 369:202–7. doi: 10.1126/science.aay5663
44. Salzer E, Zoghi S, Kiss MG, Kage F, Rashkova C, Stahnke S, et al. The Cytoskeletal Regulator HEM1 Governs B Cell Development and Prevents Autoimmunity. *Sci Immunol* (2020) 5:1–16. doi: 10.1126/sciimmunol.abc3979
45. Castro CN, Rosenzwajg M, Carapito R, Shahrooei M, Konantz M, Khan A, et al. NCKAP1L Defects Lead to a Novel Syndrome Combining Immunodeficiency, Lymphoproliferation, and Hyperinflammation. *J Exp Med* (2020) 217:1–18. doi: 10.1084/JEM.20192275
46. Park H, Staehling-Hampton K, Appleby MW, Brunkow ME, Habib T, Zhang Y, et al. A Point Mutation in the Murine Heml Gene Reveals an Essential Role for Hematopoietic Protein 1 in Lymphopoiesis and Innate Immunity. *J Exp Med* (2008) 205:2899–913. doi: 10.1084/jem.20080340
47. Stahnke S, Doering H, Kusch C, Nieswandt B, Rottner K, Stradal TEB. Loss of Hem1 Disrupts Macrophage Function and Impacts Migration, Phagocytosis, and Integrin- Mediated Adhesion. *Curr Biol* (2021) 31:1–14. doi: 10.1016/j.cub.2021.02.043
48. Leithner A, Eichner A, Müller J, Reversat A, Brown M, Schwarz J, et al. Diversified Actin Protrusions Promote Environmental Exploration But Are Dispensable for Locomotion of Leukocytes. *Nat Cell Biol* (2016) 18:1253–9. doi: 10.1038/ncb3426
49. Sprenkeler EGG, Henriet SSV, Tool ATJ, Kreft IC, van der Bijl I, Aarts CEM, et al. MKL1 Deficiency Results in a Severe Neutrophil Motility Defect Due to Impaired Actin Polymerization. *Blood* (2020) 135:2171–81. doi: 10.1182/blood.2019002633
50. Record J, Malinova D, Zenner HL, Plagnol V, Nowak K, Syed F, et al. Immunodeficiency and Severe Susceptibility to Bacterial Infection Associated With a Loss-of-Function Homozygous Mutation of MKL1. *Blood* (2015) 126:1527–35. doi: 10.1182/blood-2014-12-611012
51. Lagresle-Peyrou C, Luce S, Ouchani F, Soheili TS, Sadek H, Chouteau M, et al. X-Linked Primary Immunodeficiency Associated With Hemizygous Mutations in the Moesin (MSN) Gene. *J Allergy Clin Immunol* (2016) 138:1681–1689.e8. doi: 10.1016/j.jaci.2016.04.032
52. Nomachi A, Yoshinaga M, Liu J, Kanchanawong P, Tohyama K, Thumkeo D, et al. Moesin Controls Clathrin-Mediated S1PR1 Internalization in T Cells. *PloS One* (2013) 8:1–13. doi: 10.1371/journal.pone.0082590
53. Robertson TF, Chengappa P, Gomez Atria D, Wu CF, Avery L, Roy NH, et al. Lymphocyte Egress Signal Sphingosine-1-Phosphate Promotes ERM-Guided, Bleb-Based Migration. *J Cell Biol* (2021) 220:1–17. doi: 10.1083/jcb.202007182
54. Matsumoto M, Hirata T. Moesin Regulates Neutrophil Rolling Velocity *In Vivo*. *Cell Immunol* (2016) 304–305:59–62. doi: 10.1016/j.cellimm.2016.04.007
55. Zehrer A, Pick R, Salvermoser M, Boda A, Miller M, Stark K, et al. Begandt D. A Fundamental Role of Myh9 for Neutrophil Migration in Innate Immunity. *J Immunol* (2018) 201:1748–64. doi: 10.4049/jimmunol.1701400
56. Jacobelli J, Friedman RS, Conti MA, Lennon-Dumenil AM, Piel M, Sorensen CM, et al. Confinement-Optimized Three-Dimensional T Cell Amoeboid Motility Is Modulated *via* Myosin IIA-Regulated Adhesions. *Nat Immunol* (2010) 11:953–61. doi: 10.1038/ni.1936
57. Morin NA, Oakes PW, Hyun YM, Lee D, Chin EY, King MR, et al. Nonmuscle Myosin Heavy Chain IIA Mediates Integrin LFA-1 De-Adhesion During T Lymphocyte Migration. *J Exp Med* (2008) 205:195–205. doi: 10.1084/jem.20071543
58. Cortesio CL, Wernimont SA, Kastner DL, Cooper KM, Huttenlocher A. Impaired Podosome Formation and Invasive Migration of Macrophages From Patients With a PSTPIP1 Mutation and PAPA Syndrome. *Arthritis Rheum* (2010) 62:2556–8. doi: 10.1002/art.27521.Impaired
59. Starnes TW, Bennin DA, Bing X, Eickhoff JC, Grahf DC, Bellak JM, et al. The F-BAR Protein PSTPIP1 Controls Extracellular Matrix Degradation and Filopodia Formation in Macrophages. *Blood* (2014) 123:2703–14. doi: 10.1182/blood-2013-07-516948
60. Janssen WJM, Grobarova V, Leleux J, Jongeneel L, van Gijn M, van Montfrans JM, et al. Proline-Serine-Threonine Phosphatase Interacting Protein 1 (PSTPIP1) Controls Immune Synapse Stability in Human T Cells. *J Allergy Clin Immunol* (2018) 142:1947–55. doi: 10.1016/j.jaci.2018.01.030
61. Takenawa T, Suetsugu S. The WASP-WAVE Protein Network: Connecting the Membrane to the Cytoskeleton. *Nat Rev Mol Cell Biol* (2007) 8:37–48. doi: 10.1038/nrm2069
62. Hsu AP, Donkó A, Arrington ME, Swamydas M, Fink D, Das A, et al. Dominant Activating RAC2 Mutation With Lymphopenia, Immunodeficiency, and Cytoskeletal Defects. *Blood* (2019) 133:1977–88. doi: 10.1182/blood-2018-11-886028
63. Lu X, Zhang Y, Liu F, Wang L. Rac2 Regulates the Migration of T Lymphoid Progenitors to the Thymus During Zebrafish Embryogenesis. *J Immunol* (2020) 204:2447–54. doi: 10.4049/jimmunol.1901494
64. Deng Q, Yoo SK, Cavnar PJ, Green JM, Huttenlocher A. Dual Roles for Rac2 in Neutrophil Motility and Active Retention in Zebrafish Hematopoietic Tissue. *Dev Cell* (2011) 21:735–45. doi: 10.1016/j.devcel.2011.07.013
65. Croker BA, Handman E, Hayball JD, Baldwin TM, Voigt V, Cluse LA, et al. Rac2-Deficient Mice Display Perturbed T-Cell Distribution and Chemotaxis, But Only Minor Abnormalities in TH1 Responses. *Immunol Cell Biol* (2002) 80:231–40. doi: 10.1046/j.1440-1711.2002.01077.x
66. Roberts AW, Chaekyun K, Zhen L, Lowe JB, Kapur R, Petryniak B, et al. Deficiency of the Hematopoietic Cell-Specific Rho Family GTPase Rac2 Is Characterized by Abnormalities in Neutrophil Function and Host Defense. *Immunity* (1999) 10:183–96. doi: 10.1016/S1074-7613(00)80019-9
67. Salzer E, Cagdas D, Hons M, Mace EM, Garncarz W, Petronczki ÖY, et al. RASGRP1 Deficiency Causes Immunodeficiency With Impaired Cytoskeletal Dynamics. *Nat Immunol* (2016) 17:1352–60. doi: 10.1038/ni.3575
68. Kalinichenko A, Perinetti Casoni G, Dupré L, Trotta L, Huemer J, Galgano D, et al. RhoG Deficiency Abrogates Cytotoxicity of Human Lymphocytes and Causes Hemophagocytic Lymphohistiocytosis. *Blood* (2021) 137:2033–45. doi: 10.1182/blood.2020008738
69. Crequer A, Troeger A, Patin E, Ma CS, Picard C, Pedergnana V, et al. Human RHOH Deficiency Causes T Cell Defects and Susceptibility to EV-HPV Infections. *J Clin Invest* (2012) 122:3239–47. doi: 10.1172/JCI62949
70. Chae HD, Lee KE, Williams DA, Gu Y. Cross-Talk Between RhoH and Rac1 in Regulation of Actin Cytoskeleton and Chemotaxis of Hematopoietic Progenitor Cells. *Blood* (2008) 111:2597–605. doi: 10.1182/blood-2007-06-093237
71. Dang TS, Willet JDP, Griffin HR, Morgan NV, O'Boyle G, Arkwright PD, et al. Defective Leukocyte Adhesion and Chemotaxis Contributes to Combined Immunodeficiency in Humans With Autosomal Recessive MST1 Deficiency. *J Clin Immunol* (2016) 36:117–22. doi: 10.1007/s10875-016-0232-2
72. Nehme NT, Schmid JP, Debeurme F, André-Schmutz I, Lim A, Nitschke P, et al. MST1 Mutations in Autosomal Recessive Primary Immunodeficiency Characterized by Defective Naive T-Cell Survival. *Blood* (2012) 119:3458–68. doi: 10.1182/blood-2011-09-378364
73. Katagiri K, Katakai T, Ebisuno Y, Ueda Y, Okada T, Kinashi T. Mst1 Controls Lymphocyte Trafficking and Interstitial Motility Within Lymph Nodes. *EMBO J* (2009) 28:1319–31. doi: 10.1038/emboj.2009.82
74. Dong Y, Du X, Ye J, Han M, Xu T, Zhuang Y. Tao W. A Cell-Intrinsic Role for Mst1 in Regulating Thymocyte Egress. *J Immunol* (2009) 183:3865–72. doi: 10.4049/jimmunol.0900678
75. Lemoine R, Pachlopnik-Schmid J, Farin HF, Bigorgne A, Debré M, Sepulveda F, et al. Immune Deficiency-Related Enteropathy-Lymphocytopenia-Alopecia Syndrome Results From Tetratricopeptide Repeat Domain 7A Deficiency. *J Allergy Clin Immunol* (2014) 134:1354–64.e6. doi: 10.1016/j.jaci.2014.07.019
76. Westerberg L, Larsson M, Hardy SJ, Fernández C, Thrasher AJ, Severinson E. Wiskott-Aldrich Syndrome Protein Deficiency Leads to Reduced B-Cell Adhesion, Migration, and Homing, and a Delayed Humoral Immune Response. *Blood* (2005) 105:1144–52. doi: 10.1182/blood-2004-03-1003

77. Castiello MC, Bosticardo M, Pala F, Catucci M, Chamberlain N, Van Zelm MC, et al. Wiskott-Aldrich Syndrome Protein Deficiency Perturbs the Homeostasis of B-Cell Compartment in Humans. *J Autoimmun* (2014) 50:42–50. doi: 10.1016/j.jaut.2013.10.006
78. Snover DC, Frizzera G, Spector BD, Perry GS, Kersey JH. Wiskott-Aldrich Syndrome: Histopathologic Findings in the Lymph Nodes and Spleens of 15 Patients. *Hum Pathol* (1981) 12:821–31. doi: 10.1016/S0046-8177(81)80085-8
79. Binks M, Jones GE, Brickell PM, Kinnon C, Katz DR, Thrasher AJ. Intrinsic Dendritic Cell Abnormalities in Wiskott-Aldrich Syndrome. *Eur J Immunol* (1998) 28:3259–67. doi: 10.1002/(SICI)1521-4141(199810)28:10<3259::AID-IMMU3259>3.0.CO;2-B
80. Burns S, Thrasher AJ, Blundell MP, Machesky L, Jones GE. Configuration of Human Dendritic Cell Cytoskeleton by Rho GTPases, the WAS Protein, and Differentiation. *Blood* (2001) 98:1142–9. doi: 10.1182/blood.V98.4.1142
81. Badolato R, Sozzani S, Malacarne F, Bresciani S, Fiorini M, Borsatti A, et al. Monocytes From Wiskott-Aldrich Patients Display Reduced Chemotaxis and Lack of Cell Polarization in Response to Monocyte Chemoattractant Protein-1 and Formyl-Methionyl-Leucyl-Phenylalanine. *J Immunol* (1998) 161:1026–33.
82. Stabile H, Carlino C, Mazza C, Giliani S, Morrone S, Notarangelo LD, et al. Impaired NK-Cell Migration in WAS/XLT Patients: Role of Cdc42/WASp Pathway in the Control of Chemokine-Induced β2 Integrin High-Affinity State. *Blood* (2010) 115:2818–26. doi: 10.1182/blood-2009-07-235804
83. Zhang H, Schaff UY, Green CE, Chen H, Sarantos MR, Hu Y, et al. Impaired Integrin-Dependent Function in Wiskott-Aldrich Syndrome Protein-Deficient Murine and Human Neutrophils. *Immunity* (2006) 25:285–95. doi: 10.1016/j.immuni.2006.06.014
84. Linder S, Nelson D, Weiss M, Aepfelbacher M. Wiskott-Aldrich Syndrome Protein Regulates Podosomes in Primary Human Macrophages. *Proc Natl Acad Sci USA* (1999) 96:9648–53. doi: 10.1073/pnas.96.17.9648
85. Haddad E, Zugaza JL, Louache F, Debili N, Crouin C, Schwarz K, et al. The Interaction Between Cdc42 and WASP Is Required for SDF-1-Induced T-Lymphocyte Chemotaxis. *Blood* (2001) 97:33–8. doi: 10.1182/blood.V97.1.33
86. Trifari S, Scaramuzza S, Catucci M, Ponzoni M, Mollica L, Chiesa R, et al. Revertant T Lymphocytes in a Patient With Wiskott-Aldrich Syndrome: Analysis of Function and Distribution in Lymphoid Organs. *J Allergy Clin Immunol* (2010) 125:439–48.e8. doi: 10.1016/j.jaci.2009.11.034
87. Houmadi R, Guipouy D, Rey-Barroso J, Vasconcelos Z, Cornet J, Manghi M, et al. The Wiskott-Aldrich Syndrome Protein Contributes to the Assembly of the LFA-1 Nanocluster Belt at the Lytic Synapse. *Cell Rep* (2018) 22:979–91. doi: 10.1016/j.celrep.2017.12.088
88. Lafouresse F, Cotta-de-Almeida V, Malet-Engra G, Galy A, Valitutti S, Dupré L. Wiskott-Aldrich Syndrome Protein Controls Antigen-Presenting Cell-Driven CD4 + T-Cell Motility by Regulating Adhesion to Intercellular Adhesion Molecule-1. *Immunology* (2012) 137:183–96. doi: 10.1111/j.1365-2567.2012.03620.x
89. Carman CV, Sage PT, Sciuto TE, de la Fuente MA, Geha RS, Ochs HDD, et al. Transcellular Diapedesis Is Initiated by Invasive Podosomes. *Immunity* (2007) 26:784–97. doi: 10.1016/j.immuni.2007.04.015
90. German Y, Vulliard L, Kamnev A, Pfajfer L, Huemer J, Mautner A-K, et al. Morphological Profiling of Human T and NK Lymphocytes by High-Content Cell Imaging. *Cell Rep* (2021) 36:1–14. doi: 10.1016/j.celrep.2021.109318
91. De Noronha S, Hardy S, Sinclair J, Blundell MP, Strid J, Schulz O, et al. Impaired Dendritic-Cell Homing *In Vivo* in the Absence of Wiskott-Aldrich Syndrome Protein. *Blood* (2005) 105:1590–7. doi: 10.1182/blood-2004-06-2332
92. Bouma G, Burns S, Thrasher AJ. Impaired T-Cell Priming *In Vivo* Resulting From Dysfunction of WASp-Deficient Dendritic Cells. *Blood* (2007) 110:4278–84. doi: 10.1182/blood-2007-06-096875
93. Lacout C, Haddad E, Sabri S, Svinarchouk F, Garçon L, Capron C, et al. A Defect in Hematopoietic Stem Cell Migration Explains the Nonrandom X-Chromosome Inactivation in Carriers of Wiskott-Aldrich Syndrome. *Blood* (2003) 102:1282–9. doi: 10.1182/blood-2002-07-2099
94. Dovas A, Gevrey JC, Grossi A, Park H, Abou-Kheir W, Cox D. Regulation of Podosome Dynamics by WASp Phosphorylation: Implication in Matrix Degradation and Chemotaxis in Macrophages. *J Cell Sci* (2009) 122:3873–82. doi: 10.1242/jcs.051755
95. Sabri S, Foudi A, Boukour S, Franc B, Charrier S, Jandrot-Perrus M, et al. Deficiency in the Wiskott-Aldrich Protein Induces Premature Proplatelet Formation and Platelet Production in the Bone Marrow Compartment. *Blood* (2006) 108:134–40. doi: 10.1182/blood-2005-03-1219
96. Snapper SB, Meelu P, Nguyen D, Stockton BM, Bozza P, Alt FW, et al. WASP Deficiency Leads to Global Defects of Directed Leukocyte Migration *In Vitro* and *In Vivo*. *J Leukoc Biol* (2005) 77:993–8. doi: 10.1189/jlb.0804444
97. Keszei M, Record J, Kritikou JS, Wurzer H, Geyer C, Thiemann M, et al. Constitutive Activation of WASp in X-Linked Neutropenia Renders Neutrophils Hyperactive. *J Clin Invest* (2018) 128:4115–31. doi: 10.1172/JCI64772
98. Oliveira MMS, Kung S, Moreau HD, Maurin M, Record J, Sanséau D, et al. The WASp L272P Gain-of-Function Mutation Alters Dendritic Cell Coordination of Actin Dynamics for Migration and Adhesion. *J Leukoc Biol* (2021), 1–11. doi: 10.1002/jlb.1ab0821-013rr
99. Pfajfer L, Mair NK, Gulez N, Rey-barroso J, Ijspeert H, Tangye SG, et al. Mutations Affecting the Actin Regulator WD Repeat – Containing Protein 1 Lead to Aberrant Lymphoid Immunity. *J Allergy Clin Immunol* (2018) 142:1589–604.e11. doi: 10.1016/j.jaci.2018.04.023
100. Standing ASI, Malinova D, Hong Y, Record J, Moulding D, Blundell MP, et al. Autoinflammatory Periodic Fever, Immunodeficiency, and Thrombocytopenia (PFIT) Caused by Mutation in Actinregulatory Gene WDR1. *J Exp Med* (2017) 214:59–71. doi: 10.1084/jem.20161228
101. Kuhns DB, Fink DL, Choi U, Sweeney C, Lau K, Priel DL, et al. Cytoskeletal Abnormalities and Neutrophil Dysfunction in WDR1 Deficiency. *Blood* (2016) 128:2135–43. doi: 10.1182/blood-2016-03-706028
102. Kile BT, Panopoulos AD, Stirzaker RA, Hacking DF, Tahtamouni LH, Willson TA, et al. Mutations in the Cofilin Partner Aip1/Wdr1 Cause Autoinflammatory Disease and Macrothrombocytopenia. *Blood* (2007) 110:2371–80. doi: 10.1182/blood-2006-10-055087
103. Pfajfer L, Seidel MG, Houmadi R, Boztug K, Dupré L. WIP Deficiency Severely Affects Human Lymphocyte Architecture During Migration and Synapse Assembly. *Blood* (2018) 130:1949–54. doi: 10.1182/blood-2017-04-777383
104. Chou HC, Antón IM, Holt MR, Curcio C, Lanzardo S, Worth A, et al. WIP Regulates the Stability and Localization of WASP to Podosomes in Migrating Dendritic Cells. *Curr Biol* (2006) 16:2337–44. doi: 10.1016/j.cub.2006.10.037
105. Tsuboi S. Requirement for a Complex of Wiskott-Aldrich Syndrome Protein (WASP) With WASP Interacting Protein in Podosome Formation in Macrophages. *J Immunol* (2007) 178:2987–95. doi: 10.4049/jimmunol.178.5.2987
106. Ciriza J, Thompson H, Petrosian R, Manilay JO, García-Ojeda ME. The Migration of Hematopoietic Progenitors From the Fetal Liver to the Fetal Bone Marrow: Lessons Learned and Possible Clinical Applications. *Exp Hematol* (2013) 41:411–23. doi: 10.1016/j.exphem.2013.01.009
107. Bonaud A, Lemos JP, Espéli M, Balabanian K. Hematopoietic Multipotent Progenitors and Plasma Cells: Neighbors or Roommates in the Mouse Bone Marrow Ecosystem? *Front Immunol* (2021) 12:658535. doi: 10.3389/fimmu.2021.658535
108. Lévesque JP, Helwani FM, Winkler IG. The Endosteal Osteoblastic Niche and Its Role in Hematopoietic Stem Cell Homing and Mobilization. *Leukemia* (2010) 24:1979–92. doi: 10.1038/leu.2010.214
109. Upadhaya S, Krichevsky O, Akhmetzyanova I, Sawai CM, Fooksman DR, Reizis B. Intravital Imaging Reveals Motility of Adult Hematopoietic Stem Cells in the Bone Marrow Niche. *J Clean Prod* (2020) 27:336–345.e4. doi: 10.1016/j.stem.2020.06.003
110. James KD, Jenkinson WE. Anderson G. T-Cell Egress From the Thymus: Should I Stay or Should I Go? *J Leukoc Biol* (2018) 104:275–84. doi: 10.1002/JLB.1MR1217-496R
111. Lougaris V, Baronio M, Gazzurelli L, Benvenuto A, Plebani A. RAC2 and Primary Human Immune Deficiencies. *J Leukoc Biol* (2020) 108:687–96. doi: 10.1002/JLB.5MR0520-194RR
112. Lambe T, Crawford G, Johnson AL, Crockford TL, Bouriez-Jones T, Smyth AM, et al. DOCK8 Is Essential for T-Cell Survival and the Maintenance of CD8 + T-Cell Memory. *Eur J Immunol* (2011) 41:3423–35. doi: 10.1002/eji.201141759

113. Randall KL, Lambe T, Johnson A, Treanor B, Kucharska E, Domaschenz H, et al. Dock8 Mutations Cripple B Cell Immunological Synapses, Germinal Centers and Long-Lived Antibody Production. *Nat Immunol* (2009) 10:1283–91. doi: 10.1038/ni.1820
114. Pillay BA, Fusaro M, Gray PE, Statham AL, Burnett L, Bezrodnik L, et al. Somatic Reversion of Pathogenic DOCK8 Variants Alters Lymphocyte Differentiation and Function to Effectively Cure DOCK8 Deficiency. *J Clin Invest* (2021) 131:1-17. doi: 10.1172/JCI142434
115. Xu X, Wang X, Todd EM, Jaeger ER, Vella JL, Mooren OL, et al. Mst1 Kinase Regulates the Actin-Bundling Protein L-Plastin To Promote T Cell Migration. *J Immunol* (2016) 197:1683–91. doi: 10.4049/jimmunol.1600874
116. Notarangelo LD. Primary Immunodeficiencies. *J Allergy Clin Immunol* (2010) 125:S182–94. doi: 10.1016/j.jaci.2009.07.053
117. Beel K, Cotter MM, Blatny J, Bond J, Lucas G, Green F, et al. A Large Kindred With X-Linked Neutropenia With an I294T Mutation of the Wiskott-Aldrich Syndrome Gene. *Br J Haematol* (2009) 144:120–6. doi: 10.1111/j.1365-2141.2008.07416.x
118. Fowell DJ, Kim M. The Spatio-Temporal Control of Effector T Cell Migration. *Nat Rev Immunol* (2021) 21:582–96. doi: 10.1038/s41577-021-00507-0
119. Aydin SE, Kilic SS, Aytekin C, Kumar A, Porras O, Kainulainen L, et al. DOCK8 Deficiency: Clinical and Immunological Phenotype and Treatment Options - a Review of 136 Patients. *J Clin Immunol* (2015) 35:189–98. doi: 10.1007/s10875-014-0126-0
120. Su HC, Jing H, Angelus P, Freeman AF. Insights Into Immunity From Clinical and Basic Science Studies of DOCK8 Immunodeficiency Syndrome. *Immunol Rev* (2019) 287:9–19. doi: 10.1111/imr.12723
121. Schneider C, Shen C, Gopal AA, Douglas T, Forestell B, Kauffman KD, et al. Migration-Induced Cell Shattering Due to DOCK8 Deficiency Causes a Type 2–Biased Helper T Cell Response. *Nat Immunol* (2020) 21:1528–39. doi: 10.1038/s41590-020-0795-1
122. Weninger W, Biro M, Jain R. Leukocyte Migration in the Interstitial Space of Non-Lymphoid Organs. *Nat Rev Immunol* (2014) 14:232–46. doi: 10.1038/nri3641
123. Ley K, Laudanna C, Cybulsky MI, Nourshargh S. Getting to the Site of Inflammation: The Leukocyte Adhesion Cascade Updated. *Nat Rev Immunol* (2007) 7:678–89. doi: 10.1038/nri2156
124. Miralles F, Posern G, Zaromytidou AI, Treisman R. Actin Dynamics Control SRF Activity by Regulation of Its Coactivator MAL. *Cell* (2003) 113:329–42. doi: 10.1016/S0092-8674(03)00278-2
125. Vartiainen MK, Guettler S, Larijani B, Treisman R. Nuclear Actin Regulates Dynamic Subcellular Localization and Activity of the SRF Cofactor MAL. *Sci (80-)* (2007) 316:1749–52. doi: 10.1126/science.1141084
126. Martinelli R, Zeiger AS, Whitfield M, Sciuto TE, Dvorak A, van Vliet KJ, et al. Probing the Biomechanical Contribution of the Endothelium to Lymphocyte Migration: Diapedesis by the Path of Least Resistance. *J Cell Sci* (2014) 127:3720–34. doi: 10.1242/jcs.148619
127. Alon R, van Buul JD. Leukocyte Breaching of Endothelial Barriers: The Actin Link. *Trends Immunol* (2017) 38:606–15. doi: 10.1016/j.it.2017.05.002
128. Côté JF, Chung PL, Théberge JF, Hallé M, Spencer S, Lasky LA, et al. PSTPIP Is a Substrate of PTP-PEST and Serves as a Scaffold Guiding PTP-PEST Toward a Specific Dephosphorylation of WASP. *J Biol Chem* (2002) 277:2973–86. doi: 10.1074/jbc.M106428200
129. Badour K, Zhang J, Shi F, Leng Y, Collins M, Siminovitch KA. Fyn and PTP-PEST-Mediated Regulation of Wiskott-Aldrich Syndrome Protein (WASp) Tyrosine Phosphorylation Is Required for Coupling T Cell Antigen Receptor Engagement to WASp Effector Function and T Cell Activation. *J Exp Med* (2004) 199:99–111. doi: 10.1084/jem.20030976
130. Gardel ML, Schneider IC, Aratyn-schaus Y, Waterman CM, Engineering B, Biology C, et al. Mechanical Integration of Actin and Adhesion Dynamics in Cell Migration. *Annu Rev Cell Dev Biol* (2010) 26:315–33. doi: 10.1146/annurev.cellbio.011209.122036.Mechanical
131. Plotnikov SV, Waterman CM. Guiding Cell Migration by Tugging. *Curr Opin Cell Biol* (2013) 25:619–26. doi: 10.1016/j.ceb.2013.06.003
132. Reversat A, Gaertner F, Merrin J, Stopp J, Tasciyan S, Aguilera J, et al. Cellular Locomotion Using Environmental Topography. *Nature* (2020) 582:582–5. doi: 10.1038/s41586-020-2283-z
133. Blumenthal D, Burkhardt JK. Multiple Actin Networks Coordinate Mechanotransduction at the Immunological Synapse. *J Cell Biol* (2020) 219:1–12. doi: 10.1083/jcb.201911058
134. Sims TN, Soos TJ, Xenias HS, Dubin-Thaler B, Hofman JM, Waite JC, et al. Opposing Effects of Pkcθ and WASp on Symmetry Breaking and Relocation of the Immunological Synapse. *Cell* (2007) 129:773–85. doi: 10.1016/j.cell.2007.03.037
135. Calvez R, Lafouresse F, de Meester J, Galy A, Valitutti S, Dupré L. The Wiskott-Aldrich Syndrome Protein Permits Assembly of a Focused Immunological Synapse Enabling Sustained T-Cell Receptor Signaling. *Haematologica* (2011) 96:1415–23. doi: 10.3324/haematol.2011.040204
136. Kumari S, Mak M, Poh Y, Tohme M, Watson N, Melo M, et al. Cytoskeletal Tension Actively Sustains the Migratory T-Cell Synaptic Contact. *EMBO J* (2020) 39:1–18. doi: 10.15252/embj.2019102783
137. Ackerknecht M, Gollmer K, Germann P, Ficht X, Abe J, Fukui Y, et al. Antigen Availability and DOCK2-Driven Motility Govern CD4 + T Cell Interactions With Dendritic Cells *In Vivo*. *J Immunol* (2017) 199:520–30. doi: 10.4049/jimmunol.1601148
138. Krause M, Gautreau A. Steering Cell Migration: Lamellipodium Dynamics and the Regulation of Directional Persistence. *Nat Rev Mol Cell Biol* (2014) 15:577–90. doi: 10.1038/nrm3861
139. Dustin ML, Long EO. Cytotoxic Immunological Synapses. *Immunol Rev* (2010) 235:24–34. doi: 10.1111/j.0105-2896.2010.00904.x
140. Welch MD, DePace AH, Verma S, Iwamatsu A, Mitchison TJ. The Human Arp2/3 Complex Is Composed of Evolutionarily Conserved Subunits and Is Localized to Cellular Regions of Dynamic Actin Filament Assembly. *J Cell Biol* (1997) 138:375–84. doi: 10.1083/jcb.138.2.375
141. Obeidy P, Ju LA, Oehlers SH, Zulkhernain NS, Lee Q, Ni JLG, et al. Partial Loss of Actin Nucleator Actin Related Protein 2/3 Activity Triggers Blebbing in Primary T Lymphocytes. *Immunol Cell Biol* (2020) 98:93–113. doi: 10.1111/imcb.12304
142. Machesky LM, Insall RH. Scar1 and the Related Wiskott-Aldrich Syndrome Protein, WASP, Regulate the Actin Cytoskeleton Through the Arp2/3 Complex. *Curr Biol* (1998) 8:1347–56. doi: 10.1016/S0960-9822(98)00015-3
143. Padrick SB, Doolittle LK, Brautigam CA, King DS, Rosen MK. Arp2/3 Complex Is Bound and Activated by Two WASP Proteins. *Proc Natl Acad Sci USA* (2011) 108:E472-9. doi: 10.1073/pnas.1100236108
144. De La Fuente MA, Sasahara Y, Calamito M, Antón IM, Elkhal A, Gallego MD, et al. WIP Is a Chaperone for Wiskott-Aldrich Syndrome Protein (WASP). *Proc Natl Acad Sci USA* (2007) 104:926–31. doi: 10.1073/pnas.0610275104
145. Higgs HN, Pollard TD. Regulation of Actin Filament Network Formation Through Arp2/3 Complex: Activation by a Diverse Array of Proteins. *Annu Rev Biochem* (2001) 70:649–76. doi: 10.1146/annurev.biochem.70.1.649
146. Pollitt AY, Insall RH. WASP and SCAR/WAVE Proteins: The Drivers of Actin Assembly. *J Cell Sci* (2009) 122:2575–8. doi: 10.1242/jcs.023879
147. Rey-Barroso J, Calovi DS, Combe M, German Y, Moreau M, Canivet A, et al. Switching Between Individual and Collective Motility in B Lymphocytes Is Controlled by Cell-Matrix Adhesion and Inter-Cellular Interactions. *Sci Rep* (2018) 8:1–16. doi: 10.1038/s41598-018-24222-4
148. Ambruso DR, Knall C, Abell AN, Panepinto J, Kurkchubasche A, Thurman G, et al. Human Neutrophil Immunodeficiency Syndrome Is Associated With an Inhibitory Rac2 Mutation. *Proc Natl Acad Sci USA* (2000) 97:4654–9. doi: 10.1073/pnas.080074897
149. Accetta D, Syverson G, Bonacci B, Reddy S, Bengtson C, Surfus J, et al. Human Phagocyte Defect Caused by a Rac2 Mutation Detected by Means of Neonatal Screening for T-Cell Lymphopenia. *J Allergy Clin Immunol* (2011) 127:535–38.e2. doi: 10.1016/j.jaci.2010.10.013
150. Alkhairy OK, Rezaei N, Graham RR, Abolhassani H, Borte S, Hultenby K, et al. RAC2 Loss-of-Function Mutation in 2 Siblings With Characteristics of Common Variable Immunodeficiency. *J Allergy Clin Immunol* (2015) 135:1380–4.e5. doi: 10.1016/j.jaci.2014.10.039
151. Mattila PK, Lappalainen P. Filopodia: Molecular Architecture and Cellular Functions. *Nat Rev Mol Cell Biol* (2008) 9:446–54. doi: 10.1038/nrm2406
152. Kress H, Stelzer EHK, Holzer D, Buss F, Griffiths G, Rohrbach A. Filopodia Act as Phagocytic Tentacles and Pull With Discrete Steps and a Load-Dependent Velocity. *Proc Natl Acad Sci USA* (2007) 104:11633–8. doi: 10.1073/pnas.0702449104
153. Krugmann S, Jordens I, Gevaert K, Driessens M, Vandekerckhove J, Hall A. Cdc42 Induces Filopodia by Promoting the Formation of an IRSp53:Mena Complex. *Curr Biol* (2001) 11:1645–55. doi: 10.1016/S0960-9822(01)00506-1

154. Sánchez-Madrid F, Serrador JM. Bringing Up the Rear: Defining the Roles of the Uropod. *Nat Rev Mol Cell Biol* (2009) 10:353–9. doi: 10.1038/nrm2680
155. Smith LA, Aranda-Espinoza H, Haun JB, Dembo M, Hammer DA. Neutrophil Traction Stresses Are Concentrated in the Uropod During Migration. *Biophys J* (2007) 92:L58–60. doi: 10.1529/biophysj.106.102822
156. Jacobelli J, Bennett FC, Pandurangi P, Tooley AJ, Krummel MF. Myosin-IIA and ICAM-1 Regulate the Interchange Between Two Distinct Modes of T Cell Migration. *J Immunol* (2009) 182:2041–50. doi: 10.4049/jimmunol.0803267
157. Syndrome Consortium T. Mutations in MYH9result in the May-Hegglin Anomaly, and Fechtner and Sebastian Syndromes. *Nat Genet* (2000) 26:103–5. doi: 10.1038/79063
158. Murphy DA, Courtneidge SA. The "Ins" and "Outs" of Podosomes and Invadopodia: Characteristics, Formation and Function. *Nat Rev Mol Cell Biol* (2011) 12:413–26. doi: 10.1038/nrm3141
159. Jones GE, Zicha D, Dunn GA, Blundell M, Thrasher A. Restoration of Podosomes and Chemotaxis in Wiskott-Aldrich Syndrome Macrophages Following Induced Expression of WASp. *Int J Biochem Cell Biol* (2002) 34:806–15. doi: 10.1016/S1357-2725(01)00162-5
160. Olivier A, Jeanson-Leh L, Bouma G, Compagno D, Blondeau J, Seye K, et al. A Partial Down-Regulation of WASP Is Sufficient to Inhibit Podosome Formation in Dendritic Cells. *Mol Ther* (2006) 13:729–37. doi: 10.1016/j.ymthe.2005.11.003
161. Alexander E, Sanders S, Braylan R. Purported Difference Between Human T- and B-Cell Surface Morphology Is an Artefact. *Nature* (1976) 261:239–41. doi: 10.1038/261239a0
162. Parakkal P, Pinto J, Hanifin JM. Surface Morphology of Human Mononuclear Phagocytes During Maturation and Phagocytosis. *J Ultrasructure Res* (1974) 48:216–26. doi: 10.1016/S0022-5320(74)80078-X
163. Fisher PJ, Bulur PA, Vuk-Pavlovic S, Prendergast FG, Dietz AB. Dendritic Cell Microvilli: A Novel Membrane Structure Associated With the Multifocal Synapse and T-Cell Clustering. *Blood* (2008) 112:5037–45. doi: 10.1182/blood-2008-04-149526
164. Orbach R, Su X. Surfing on Membrane Waves: Microvilli, Curved Membranes, and Immune Signaling. *Front Immunol* (2020) 11:2187. doi: 10.3389/fimmu.2020.02187
165. Ghosh S, Di Bartolo V, Tubul L, Shimoni E, Kartvelishvily E, Dadosh T, et al. ERM-Dependent Assembly of T Cell Receptor Signaling and Co-Stimulatory Molecules on Microvilli Prior to Activation. *Cell Rep* (2020) 30:3434–3447.e6. doi: 10.1016/j.celrep.2020.02.069
166. Kenney DM, Cairns L, Remold-O'donnell E, Peterson J, Rosen FS, Parkman R. Morphological Abnormalities in the Lympcytes of Patients the Wiskott-Aldrich Syndrome. *Blood* (1986) 68:1329–32. doi: 10.1182/blood.V68.6.1329.1329
167. Molina IJ, Kenney DM, Rosen FS, Remold-O'donnell E. T Cell Lines Characterize Events in the Pathogenesis of the Wiskott-Aldrich Syndrome. *J Exp Med* (1992) 176:867–74. doi: 10.1084/jem.176.3.867
168. Majstoravich S, Zhang J, Nicholson-Dykstra S, Linder S, Friedrich W, Siminovitch KA, et al. Lymphocyte Microvilli Are Dynamic, Actin-Dependent Structures That do Not Require Wiskott-Aldrich Syndrome Protein (WASp) for Their Morphology. *Blood* (2004) 104:1396–403. doi: 10.1182/blood-2004-02-0437
169. McGregor AL, Hsia CR, Lammerding J. Squish and Squeeze - the Nucleus as a Physical Barrier During Migration in Confined Environments. *Curr Opin Cell Biol* (2016) 40:32–40. doi: 10.1016/j.ceb.2016.01.011
170. Sneider A, Hah J, Wirtz D, Kim DH. Recapitulation of Molecular Regulators of Nuclear Motion During Cell Migration. *Cell Adhes Migr* (2019) 13:50–62. doi: 10.1080/19336918.2018.1506654
171. Yamada KM, Sixt M. Mechanisms of 3D Cell Migration. *Nat Rev Mol Cell Biol* (2019) 20:738–52. doi: 10.1038/s41580-019-0172-9
172. Renkawitz J, Kopf A, Stopp J, de Vries I, Driscoll MK, Merrin J, et al. Nuclear Positioning Facilitates Amoeboid Migration Along the Path of Least Resistance. *Nature* (2019) 568:546–50. doi: 10.1038/s41586-019-1087-5
173. Jacobelli J, Estin Matthews M, Chen S, Krummel MF. Activated T Cell Trans-Endothelial Migration Relies on Myosin-IIA Contractility for Squeezing the Cell Nucleus Through Endothelial Cell Barriers. *PloS One* (2013) 8:1–13. doi: 10.1371/journal.pone.0075151
174. Thompson SB, Sandor AM, Lui V, Chung JW, Waldman MM, Long RA, et al. Formin-Like 1 Mediates Effector T Cell Trafficking to Inflammatory Sites to Enable T Cell-Mediated Autoimmunity. *Elife* (2020) 9:1–27. doi: 10.7554/eLife.58046
175. Maritzen T, Schachtner H, Legler DF. On the Move: Endocytic Trafficking in Cell Migration. *Cell Mol Life Sci* (2015) 72:2119–34. doi: 10.1007/s00018-015-1855-9
176. Zech T, Calaminus SDJ, Machesky LM. Actin on Trafficking: Could Actin Guide Directed Receptor Transport? *Cell Adhes Migr* (2012) 6:476–81. doi: 10.4161/cam.21373
177. Piperno GM, Naseem A, Silvestrelli G, Amadio R, Caronni N, Cervantes-Luevano KE, et al. Wiskott-Aldrich Syndrome Protein Restricts cGAS/STING Activation by dsDNA Immune Complexes. *JCI Insight* (2020) 5:e132857. doi: 10.1172/jci.insight.132857

Conflict of Interest: The authors declare that the research was conducted in the absence of any commercial or financial relationships that could be construed as a potential conflict of interest.

Publisher's Note: All claims expressed in this article are solely those of the authors and do not necessarily represent those of their affiliated organizations, or those of the publisher, the editors and the reviewers. Any product that may be evaluated in this article, or claim that may be made by its manufacturer, is not guaranteed or endorsed by the publisher.

frontiers in Immunology

REVIEW
published: 16 December 2021
doi: 10.3389/fimmu.2021.750480

Pannexin Channel Regulation of Cell Migration: Focus on Immune Cells

*Paloma A. Harcha[1], Tamara López-López[2], Adrián G. Palacios[1] and Pablo J. Sáez[2]**

[1] Centro Interdisciplinario de Neurociencia de Valparaíso, Instituto de Neurociencia, Facultad de Ciencias, Universidad de Valparaíso, Valparaíso, Chile, [2] Cell Communication and Migration Laboratory, Institute of Biochemistry and Molecular Cell Biology, Center for Experimental Medicine, University Medical Center Hamburg-Eppendorf, Hamburg, Germany

The role of Pannexin (PANX) channels during collective and single cell migration is increasingly recognized. Amongst many functions that are relevant to cell migration, here we focus on the role of PANX-mediated adenine nucleotide release and associated autocrine and paracrine signaling. We also summarize the contribution of PANXs with the cytoskeleton, which is also key regulator of cell migration. PANXs, as mechanosensitive ATP releasing channels, provide a unique link between cell migration and purinergic communication. The functional association with several purinergic receptors, together with a plethora of signals that modulate their opening, allows PANX channels to integrate physical and chemical cues during inflammation. Ubiquitously expressed in almost all immune cells, PANX1 opening has been reported in different immunological contexts. Immune activation is the epitome coordination between cell communication and migration, as leukocytes (i.e., T cells, dendritic cells) exchange information while migrating towards the injury site. In the current review, we summarized the contribution of PANX channels during immune cell migration and recruitment; although we also compile the available evidence for non-immune cells (including fibroblasts, keratinocytes, astrocytes, and cancer cells). Finally, we discuss the current evidence of PANX1 and PANX3 channels as a both positive and/or negative regulator in different inflammatory conditions, proposing a general mechanism of these channels contribution during cell migration.

Keywords: cell communication, leukocytes, cancer, inflammation, Ca^{2+} signaling, amoeboid migration, mesenchymal migration, mechanotransduction

OPEN ACCESS

Edited by:
Emmanuel Donnadieu, Institut National de la Santé et de la Recherche Médicale (INSERM), France

Reviewed by:
Eliseo A. Eugenin, University of Texas Medical Branch at Galveston, United States
Leigh Anne Swayne, University of Victoria, Canada

***Correspondence:**
Pablo J. Sáez
p.saez@uke.de

Specialty section:
This article was submitted to Molecular Innate Immunity, a section of the journal Frontiers in Immunology

Received: *30 July 2021*
Accepted: *15 November 2021*
Published: *16 December 2021*

Citation:
Harcha PA, López-López T, Palacios AG and Sáez PJ (2021) Pannexin Channel Regulation of Cell Migration: Focus on Immune Cells. Front. Immunol. 12:750480. doi: 10.3389/fimmu.2021.750480

1 INTRODUCTION

Cell communication and cell migration are key phenomena for development, tissue repair, and immune response; thus coordination of these responses are key for sustaining life (1–4). Indeed, a fine coordination of leukocyte communication is required for migration to clear an infection, or recruit other migrating cells towards an injury site. Interestingly, immune cells use different migratory strategies associated with their immune function and location (5–7). For example, under resting conditions immune cells would randomly patrol the tissue, but upon activation undergo directional migration to reach the secondary lymphoid organs (8). Despite presenting unique features, immune cell migration follows the general rules of cell migration, and depends on

cytoskeletal dynamics (actin, non-muscular myosin II [MyoII]), and microtubules, as described in detail in the following reviews (6, 9–11). The study of immune cell migration is directly linked to development of new techniques to monitor the behavior of these cells in their native microenvironment (5, 12, 13), although this is still very challenging. However, researchers have developed *ex vivo* (i.e., tissue slices), and *in vitro* systems that mimic some tissue properties (i.e., confinement, properties of the extracellular matrix, etc). Thus, motility has been studied in models with different levels of microenvironment complexity (i.e., 1D, 2D, and 3D), topographies (that do or do not impose cellular deformation), or that mimic their transmigration through tissue layers (6, 13, 14).

1.1 Danger Signals and the Role of Purinergic Signaling

Immune cell migration is also controlled by microenvironmental chemical cues, such as chemokines and danger signals, affecting cell positioning along the tissue (15–17). Danger signals are molecules that trigger the immune system, and are classified due to their origin: damage-associated molecular patterns (DAMPs) [such as extracellular adenosine-5′-triphosphate (ATP)], and pathogen-associated molecular patterns (PAMPs) [such as lipopolysaccharide (LPS) (16). Both DAMPs and PAMPs trigger immune cell maturation, and expression of receptors (i.e. chemokine receptors) promoting directional migration towards the injury site. Interestingly, extracellular ATP acts both as a DAMP when released from damaged cells, or as signaling molecule when released from healthy cells. In both cases, ATP activates purinergic receptors (P2) triggering subsequent downstream signaling that depends on the activated receptor.

P2 receptors are classified into ionotropic (P2X) receptors that allow calcium ions (Ca^{2+}) influx, and metabotropic (P2Y) receptors that trigger Ca^{2+} release from intracellular stores (18). Both families of P2 are widely expressed on immune cells, controlling a plethora of functions (18), including cell communication. The activation of specific P2X and P2Y receptors family members depends on the exposure time and agonist concentration, which allows the spatiotemporal regulation of the signaling (19). In addition to the differential activation of P2 receptors the concentration of adenine nucleotides, such as ATP, is integrated by immune cells and decoded as low or high inflammatory state (18). Immune cells use different cell communication mechanisms dependent or independent on cell contacts, which amplify signals according to that inflammatory state (2, 6, 7, 20). The release of small molecules *via* plasma membrane channels, such as connexins (CXs) and pannexins (PANXs), and its coupling to purinergic signaling represents a widely used mechanism for cell communication, which plays a role in paracrine (between cells) and autocrine (cell autonomous) signaling (2, 18, 21).

1.2 Cell Polarity and PANX-Dependent Signaling

CXs and PANXs are membrane proteins that allow the exchange of small molecules (i.e., glucose, ATP) and ions between the cytoplasm and the extracellular milieu (22). Upon docking, CX channels of adjacent cells form intercellular channels that connect their cytoplasm, namely gap junction channels, although PANX channels until now are shown to form only hemichannels at the plasma membrane. The latter puts PANX channels and purinergic signaling in the center stage of both cell-autonomous signaling and contact-independent cell communication (23), which are required for efficient motility. Migrating cells use cellular polarity, the asymmetric organization of intracellular components, as the navigation system that determines the direction of migration (6, 10, 11). Cell polarity is dynamically set by changing the position of organelles, cytoskeleton, and signaling proteins (10, 24). Thus, polarization of the actin cytoskeleton allows the establishment of a front-rear migration axis, which subsequently polarizes other proteins (10). Interestingly, F-actin and its regulator Arp3 directly interact with PANX1 (25–27), suggesting that F-actin polarization and nucleation of new microfilaments might directly control PANX1 localization. Indeed, actin flow and polarization permits the concomitant polarization of PANX1 to the leading edge in migrating immune cells (28–30). Similarly, PANX3 stability at the plasma membrane requires intact actin cytoskeleton (25), suggesting that a similar mechanism might take place during cell migration.

Altogether, the co-polarization of PANXs with the actin cytoskeleton, and their indirect functional impact on microtubules, *via* protein-protein interaction with a microtubule stabilizer (31), could imply a polarization of the PANX-dependent signaling. Therefore, ATP and other molecules that permeate through PANX-channels will be released in a polarized manner that might sustain the cell polarity and direction of migration (28, 30, 32).

In this review, we summarize the contribution of PANX1 channels during cell migration. The first part of this review is focused on different immune cells, as example of PANX1 channel contribution to leukocyte migration and recruitment. Then, we describe PANX1 and PANX3 contribution to migration of non-immune cells, such as astrocytes, skin cells, and cancer cells, as well as the few available evidence for the PANX2 and its putative role during cell migration. Afterwards, we dedicate a final section of PANX1 contribution to cell migration during neuroinflammatory conditions, and aging.

2 IMMUNE CELL MIGRATION

Most leukocytes use amoeboid migration to move within tissues. This migration mode is characterized by limited adhesion to the extracellular matrix with little (or non-) proteolytic activity, preventing extracellular matrix modification (5). Therefore, in order to undergo fast migration after damage, immune cells must deform their cellular body while facing microenvironment obstacles (6, 9). Leukocytes highly rely on acto-myosin cytoskeleton contractility, and mechanosensitive channels, including PANXs channels (6, 9, 30). Interestingly, PANX1 is required for homing of bone-marrow derived immune cell precursors (33), suggesting that these channels are required

from early stages of development. Moreover, since leukocytes reside in different tissues and are exposed to different mechanical and chemical signals, these cells exhibit different migration strategies. Despite this cell-specific migratory behavior, the contribution of PANX1 channels to purinergic and Ca^{2+} signaling, and to cytoskeleton regulation is well established. In general PANX1 channels are positive regulators of immune cell migration as summarized in this section (**Table 1**).

2.1 Neutrophils

Neutrophils, key components of the innate immune system, are polymorphonuclear phagocytic cells found in the bloodstream. Upon danger signal (i.e. chemokine/cytokine detection after infection or injury) neutrophils leave the bloodstream to invade vascular tissues (52). In the tissue, neutrophils have phagocytic activity, producing reactive oxygen species, forming neutrophil extracellular traps (NETs), and releasing cytokines,

TABLE 1 | Summary of CXs and PANX channels contribution to immune cell migration.

Cell type	Channel	Channel blockers//receptor inhibitors	P2R, AR	Migratory stimuli	Migration techniques	Ref.
DCs						
BMDCs (m)	CX43	αGA, CX43 KO	n.e.	CCL21	3D chemotaxis in collagen	(34)
DEC205$^+$ DCs (m)	CX43, CX45	n.e.	n.e.	BaCl muscle damage	*In vivo* homing to LNs	(35)
BMDCs (m)	PANX1	PANX1 KO// A-740003, Apyrase, BAPTA, KN-62, oATP	$P2X_7$	Extracellular ATP	microchannels, 3D collagen, *in vivo* homing to LNs	(32)
Macrophage						
Peritoneal macrophages (m)	PANX1-indep.	PANX1 KO//P2Y2 KO, P2Y12 KO, AR-C69931 MX, 8-SPT, MRS-2179, NF449	$P2Y_2$, $P2Y_{12}$	2D chemotaxis	2D chemotaxis	(36)
Cortical CX3CR1$^+$ microglia (m)	und.	Cbx, FFA//Apyrase, RB2, PPADS, Suramin	P2Y	Laser ablation, extracellular ATP	*In vivo* recruitment to injury site 2PEF	(37)
Retinal CX3CR1$^+$ microglia (m)	PANX1	Pbc//Apyrase, Suramin	P2	AMPA	*Ex vivo* retinal explants process dynamics	(38)
Cortical CD68$^+$ microglia (m)	PANX1	Trovafloxacin	n.e.	Controlled cortical impact	*In vivo* recruitment to injury site	(39)
BV-2 microglia cell line	PANX1	Trovafloxacin, BBFCF, ^{10}PANX1	P2	C5a	Transmigration in transwells	(39)
Monocytes						
PBMCs (m)	CX43	αGA, octanol	n.e.	MCP-1	Transmigration through endothelial layer	(40)
PBMCs (h), THP-1 cell line	PANX1?	$P2Y_6$ siRNA, BMSCCR222, PTX, U73122, BAPTA, Apyrase, MRS2578	$P2Y_6$	CCL2, fMLP	Transmigration in transwells	(41)
Neutrophils						
PMNs (m)	PANX1	Cbx, ^{10}PANX1, P2Y2 KO, DIDS, Suramin	$P2Y_2$	fMLP	Chemotaxis in 2D release from a pipette	(42)
PMNs (h), HL-60 cell line	PANX1	Cbx, ^{10}PANX1//CSC, CGS21680, H89	A2a	fMLP	Chemotaxis in 2D release from a pipette	(43)
Lung neutrophils (m)	CX43	CX43+/-, Gap26	n.e.	LPS	Counting of *in vivo* homing to the lungs	(44)
HL-60 cell line	CX43 (as neg. reg.)	Gap19, ^{10}PANX1//P2Y1 KO, SB 203580	$P2Y_1$	LPS	Chemotaxis in 2D confined under agarose	(45)
Neutrophils (z.f.)	CX43	Cbx, CX43 morphans, lyz:cx43DN-T2A-mCherry	n.e.	Laser ablation	*In vivo* recruitment to injury site 2PEF	(46)
T cells						
Innate lymphoid cells (ILCs)	PANX1	PANX1 KO	n.e.	House dust mite	No direct effect	(47)
CD4$^+$ T cells (m)	PANX1	PANX1 KO	n.e	House dust mite	*In vivo* recruitment to lung	(47)
CD4$^+$ PMBCs (h)	PANX1	Cbx, PANX1 KD, ^{10}PANX1//Apyrase, suramin, CCCP	$P2X_4$	CXCL12	Chemotaxis in 2D, transmigration in transwells	(29, 48)
CD4$^+$ splenocytes (m)	PANX1	PANX1 KO	n.e.	Tissue CXCL12	Counting of *in vivo* spinal cord recruitment	(29)
CD4$^+$ T cells (m)	PANX1	Cbx	$P2Y_{10}$	CCL19	Transmigration in transwells	(49)
CD3$^+$ cells (m)	PANX1	Pbc	n.e.	und.	Counting of *in vivo* spinal cord recruitment	(50)
Other						
Brain mast cells (m)	CX43, PANX1	n.e.	n.e.	Amyloid β-Peptide	Cortical recruitment in APPswe/PS1dE9 Alzheimer's model.	(51)
HSPCs (m)	PANX1	^{10}PANX1	und.	G-CSF, AMD3100	*In vivo* homing to tissue	(33)

2PEF, 2-photon excitation microscopy; aGA, a-glycyrrhetinic acid; AMPA, a-amino-3-hydroxy-5-methyl-4-isoxazole propionic acid; BMDCs, Bone-marrow derived DCs; Cbx, Carbenoxolone; HSPCs, hematopoietic stem/progenitor cells; FFA, flufenamic acid; G-CSF, granulocyte colony-stimulating factor; h, human; fMLP, N-formyl-Met-Leu-Phe peptide; KD, knock-down; KO, knock-out; LPS, lipopolysaccharide; LN, lymph node; m, mouse; N.E., not evaluated; oATP, oxidized ATP; PBMCs, peripheral blood mononuclear cells; PTX, Pertussis toxin; PMNs, Polymorphonuclear cells; Pbc, Probenecid; und., undetermined; z.f., zebra fish.

chemokines and bactericidal peptides (17, 53). PANX1 channels are highly expressed in neutrophils and contribute to their activation (42, 43, 54, 55). For instance, after exposure to non-esterified fatty acids (i.e., oleic and linoleic acid), NET formation requires activation of $P2X_1$ receptors by extracellular ATP, released *via* PANX1 channels (55).

Indeed, adenine nucleotide release and purinergic signaling cascade activation are key for neutrophil migration, particularly when the release of ATP is used as a navigational cue (43, 54). Accordingly, several purinergic receptors regulate neutrophil migration, including P2X1 (45), $P2Y_2$ (42, 54, 56), $P2Y_6$ (57), $P2Y_{11}$ (58), $P2Y_{14}$ (59), A1 (60), and A2a (61). Interestingly, components of the purinergic signaling that contribute to migratory response are polarized (**Figure 1**), and therefore provide a spatio-temporal dimension to this phenomenon (43, 54).

Neutrophils migration towards a N-formyl-Met-Leu-Phe (FMLP) gradient, which mimics a bacterial-induced chemotactic response, also depends on extracellular ATP sensing. During FMLP-induced migration ATP is released in a polarized manner, as PANX1 is polarized to the leading edge together with F-actin (42). This polarization towards the leading edge relies on the direct interaction between F-actin and the C-terminus of PANX1 previously described (25, 27). ATP released *via* PANX1 leads to the subsequent activation of $P2Y_2$ and A3 receptors, which are also localized at the leading edge generating an autocrine feedback loop required to maintain the polarization of the cell and to amplify the gradient sensing (42, 54). Interestingly, PANX1 channels also contribute to the inhibitory signals at the rear of the cell (43). The continuous degradation of ATP by ectonucleotidases produces adenosine, which activates adenosine A2a receptors at the cell rear, leading to intracellular cAMP/PKA signaling, and inhibiting excitatory signals from the leading edge (43). Since adenosine activates both A3 and A2a, PANX1 indirectly contributes to excitatory and inhibitory signals required for cell migration, as

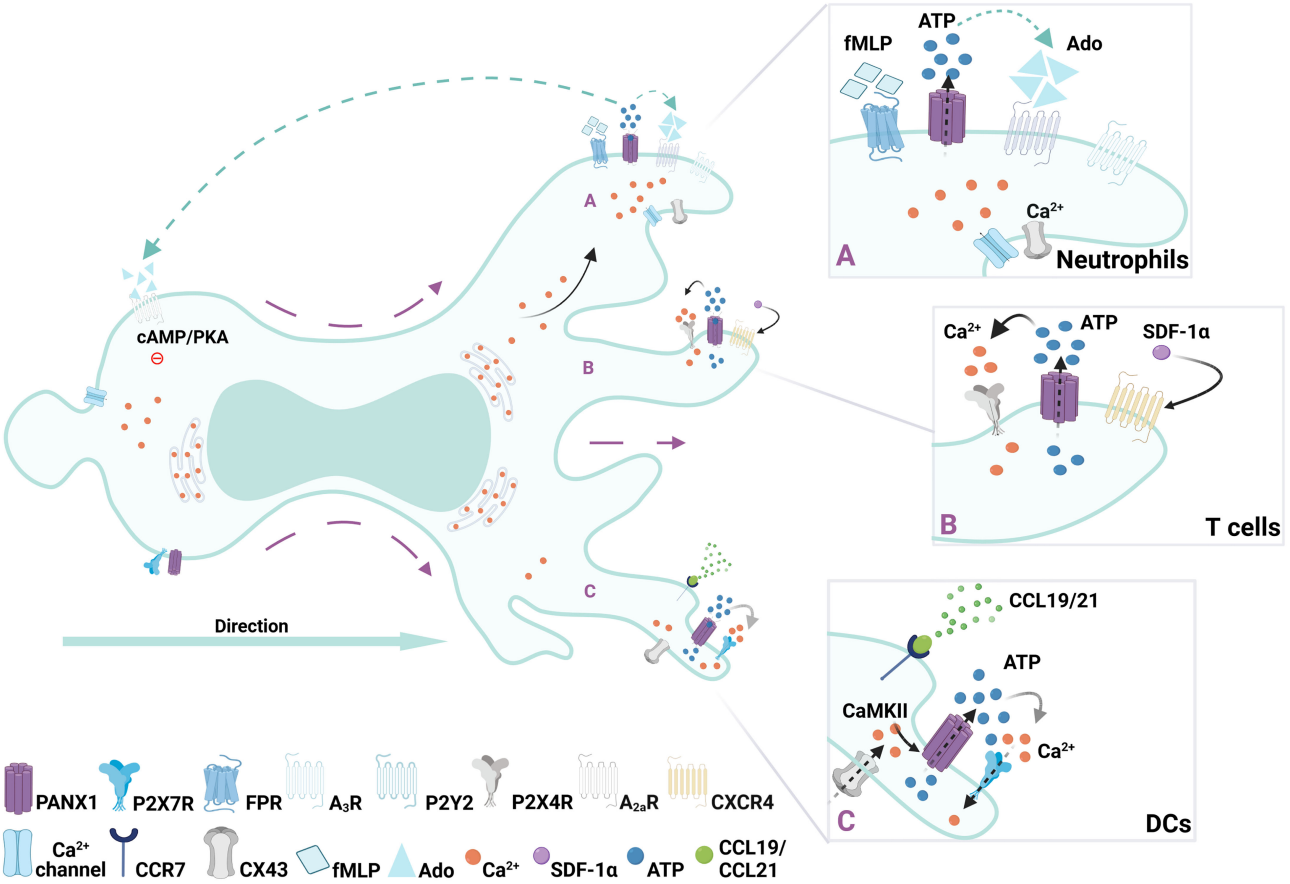

FIGURE 1 | Regulation of immune cell migration by PANX1 channels. Redistribution of surface PANX1channels have been described during migration of immune cells. **(A)** In neutrophils after FMLP gradient sensing, opening of PANX1 channels polarize towards the leading edge (right side of the cell) allowing ATP release, subsequently activating local purinergic $P2Y_2$ and -upon ATP degradation- adenosine A3 receptors. Then, at the rear of the migrating cell, activation of the adenosine A2a receptors by adenosine (Ado) promotes inhibitory cascades mediated by cAMP/PKA, leading to an orchestrated cytoskeleton rearrangement required for migration. **(B)** In T cells activation of CXCR4 receptor with SDF-1 triggers controlled burst of ATP after PANX1 channels opening, which is accompanied by mitochondria and $P2X_4$ translocation to the leading edge where Ca^{2+} influx occurs. **(C)** In DCs, ATP-induced fast migration requires an autocrine feedback loop between PANX1 channels and $P2X_7$ receptor, which triggers Ca^{2+} influx and subsequent activation of CaMKII, which maintains PANX1 channels opened.

shown in **Figure 1**. So far, polarization of positive and negative signals regulated by PANX1 has only been reported on neutrophils, although is tempting to assume it as a general mechanism for immune cell migration.

Moreover, neutrophils present additional pathways to release ATP, such as CXs and tweety family member 3 (TTYH3) maxi anion channels (2, 42), but it seems that different channels and purinergic receptors are recruited depending on the stimuli of the immune response. For example, in a mouse model CX43 hemichannels contribute to LPS-induced neutrophil recruitment in the lungs (44). Similarly, CX43 hemichannels provide a path for ATP release that promotes neutrophil swarming during laser wound tissue damage in zebrafish (46). However, when CX43-mediated ATP release is coupled to activation of $P2X_1$ receptors, this reduces the migration of human neutrophils and HL-60 neutrophil-like in an under agarose assay, and then acts as a stop signal (45).

Overall, PANX1 contributes to neutrophil cell migration by establishing a polarity axis, which is supported by re-localization of the actin cytoskeleton, and the purinergic signaling-related proteins involved in the migratory response. However, the putative role of PANX2 and PANX3, and in pathological conditions remains largely unexplored.

2.2 T Cells

T cell migration is a key step during the adaptive immune response, and its pattern varies with the activation state and the microenvironmental context. Before antigen exposure, and during antigen-presenting cells (APC) search in the lymph nodes, T cells have a diffusive and random migration (Brownian type), whereas less diffusive chemotactic movements (Lévy type) is exhibited by recently activated T cell to migrate into secondary lymphoid organs for priming; or highly directional migration (ballistic) induced by haptotaxis cues and chemotaxis gradient caused by cognate APC at the peripheral tissues (8). Adaptive immune response progression requires purinergic signaling to modulate T cell functions (28). For example, $P2X_7$ receptor modulates the balance between the number of differentiated Th_{17} and T_{reg} lymphocytes (62). Accordingly, PANX1 and purinergic receptors are essential for T cell activation and cell death (63–65). In both cases, ATP is released through PANX1 channels activating purinergic receptors, triggering intracellular cascades, and inducing the corresponding T cell response.

Acute chemokine stromal-derived factor 1α (SDF-1α, also known as CXCL12) stimulation induces PANX1 channel opening, cell polarization, and migration of $CD4^+$ immature T cells (29, 48), as shown in **Figure 1**. Particularly SDF-1a recognition leads to a well-controlled PANX1 channel opening by a G protein-coupled receptor mechanism, leading to a rapid burst of ATP release, and subsequent focal adhesion kinase (FAK) phosphorylation (29). In this context, SDF-1α promotes translocation of $P2X_4$ and mitochondria to the leading edge, increasing Ca^{2+} influx and pseudopod protrusion needed for cell polarization and migration (48). Polarized at the back of the cells, $P2Y_{11}$ receptors are also activated, triggering inhibitory signaling *via* cAMP/PKA activation (**Figure 1**), and preventing mitochondria activity at the cell rear (66). Thus, polarized migratory T cells might present mitochondria at both leading edge (48), and/or at the cell rear (67), suggesting that specific chemical (i.e. chemokine treatments) and physical (i.e. adhesion of the surface) cues of the microenvironment differentially shape intracellular organelle location and migratory function. In fact, supporting the role of PANX-mediated signaling in T cell polarity, protein-protein interaction of PANX1 and collapsin response mediator protein 2 (CRMP2), indirectly controls microtubule stability (31). Interestingly, CRMP2 polarization towards the cell rear is required for T cell chemotaxis (68).

In freshly isolated naïve T cells subsets, $CD4^+$ and $CD8^+$ cells, PANX1 is abundantly present at the plasma membrane, whereas PANX2 abundance is much lower (65). Therefore, it is conceivable that upon stimulation the abundance of PANX2, and/or PANX3, could increase under specific conditions. Accordingly, *in vivo* data in murine model of experimental autoimmune encephalomyelitis disease suggests that stimulated T cells require functional PANX channels to transmigrate into the spinal cord (29, 50). PANX contribution during cell migration of specific T cell subsets remains largely unknown, but there is evidence that regulatory T cells required PANX1 to downregulate the response of effector T cells *in vivo* in a model of allergic airway inflammation (47). The latter data is very provocative, because it suggests that when PANX1 acts as a cell communication effector protein, it contributes to limit immune cell recruitment (47). Alternatively, PANX1 could promote T cell infiltration when is acting as a migration effector protein, likely by sustaining local signaling, which subsequently permits the polarization of the actin cytoskeleton or microtubule stability. Whether this migratory *versus* cell communication role of PANX1 is affected by the expression of other PANXs, or whether this is a mechanism present in other cell types is yet to be explored.

2.3 Dendritic Cells

Immature dendritic cells (DCs) normally reside in peripheral tissues where they scan the microenvironment in search of danger signals (69, 70). After antigen uptake, DCs migrate to secondary lymphoid organs, to initiate adaptive immune responses (69, 70). Resident DCs constantly internalize extracellular material, by phagocytosis or micropinocytosis, but upon danger signal detection these processes are downregulated and the migratory strategy changes from slow/random to fast/persistent (6, 30). Purinergic signaling is key for DCs response, as several P2X and P2Y receptors are expressed. In particular, $P2X_7$ receptor together with PANX1, are required to sustain fast migratory phases (30, 32, 71). Transient exposure to high extracellular ATP concentrations activates $P2X_7$ receptor, opening PANX1 channels to release ATP establishing an autocrine loop (32). This autocrine loop triggers Ca^{2+} influx *via* $P2X_7$, calmodulin kinase II (CaMKII) activation and F-actin cytoskeleton to the cell rear (**Figure 1**), and is necessary to sustain DC fast migration (32). Interestingly, CaMKII directly controls the opening of PANX1 channels providing a direct link between purinergic and Ca^{2+} signaling that might be responsible for maintaining DCs migration (72). PANX1 appears to be

equally distributed in migrating DCs, suggesting that this protein does not need to polarized to control DC speed. Since CaMKII regulates actin dynamics (73), its activity directly impacts on acto-myosin contractility, which is required for DC migration (30, 74). Thus, PANX1 contributes to DC migration by sustaining Ca^{2+} signaling *via* $P2X_7$, which activates CaMKII maintaining actin polarization at the cell rear and subsequent contractility.

Activating signals trigger a maturation program in which several phenotypic changes, including the decrease of macropinocytosis, are required for the fast migration of DCs (6, 69). Interestingly, in other cells (i.e. neuroblastoma) ATP induces the internalization of PANX1 into macropinosomes (75), but it is not known whether the exact mechanism takes place during DC maturation and migration. Upon maturation, DCs increase the expression of cell surface molecules related to antigen presentation and directional migration, such as CCR7 chemokine receptor (6, 69). Directional migration in DCs largely depends on CCL19/CCL21 activation of CCR7 with the concomitant activation of CX43 channels (34). In the same line, migratory DCs increase the expression of CX43 and CX45 during homing to lymph nodes (35). Conversely, PANX1 channels were dispensable for this response as shown by the lack of effect observed with PANX blockers (34).

These data suggest that PANX1 channels might contribute to the early stages of DC migration upon danger signal detection, and that later stages including CCR7-dependent chemotaxis relies in the activity of CXs. This putative functional distinction between CXs and PANXs during DC migration might rely in different protein turnover at the plasma membrane, and/or the non-channel signaling function, as is shown for CX43 (76).

2.4 Monocytes and Macrophages

Although monocytes and macrophage originate from a common myeloid precursor and share several markers, they differ in their location, as monocytes are generally found in the bloodstream, while macrophages are tissue-resident cells. However, circulating monocytes differentiate into monocyte-derived macrophages (MMs) or monocyte-derived DCs (Mo-DCs) upon sensing of danger signals at the injury site (77). During CCL2-induced chemotaxis, monocytes release ATP, thus generating an autocrine loop with subsequent activation of P2Y6 receptors that is required for efficient migration (41), similar to other cells (see section *Dendritic Cells*, DCs). However, the molecular mechanism for ATP release was not elucidated. Monocytes, and macrophages, express both CXs and PANXs, but only CXs role has been shown during extravasation and migration. Particularly, CXs contribute by forming gap junction channels between monocytes and the endothelium (2, 40, 78). However, the functional role of PANXs expressed in monocytes (22), remains unaddressed.

Resident macrophages are named according to the different tissues in which they reside, although in general these cells share their primary functions: cellular detritus clearance, phagocytosis of pathogen particles, and in a lesser extent, antigen presentation (79). Resident brain macrophages, named microglia, quickly reacting to danger signals to prevent neuronal damage (80). ATP released during tissue damage acts as a chemoattractant of microglia *in vivo*, which extend their processes towards the injury site, a response that might require PANX1 channel activation (37). However, this need to be confirmed as only general blockers were used. Similarly, retinal microglia process extension induced by α-amino-3-hydroxy-5-methyl-4-isoxazole propionic acid (AMPA) receptor activation is prevented with Probenecid, a general PANX channel blocker (38). In addition, trovafloxacin another proposed PANX1 blocker (81), reduces microglia recruitment after traumatic brain injury (39). In a similar model PANX1 is required to induced the recruitment of microglia and other myeloid cells, and the lack of PANX1 improved the posttraumatic recovery of the mice (82). In addition, C5a-induced transmigration of microglia depends on PANX1-dependent ATP release, likely *via* an autocrine loop (39), such as the one shown in DCs (see section *Dendritic Cells*, DCs). However, this response might be specific different macrophage subsets, as PANX1 channels have only a mild contribution to C5a-induced chemotaxis in peritoneal macrophages, which was dependent on $P2Y_2$ and $P2Y_{12}$ receptors (36). Conversely, CX43 contributes to LPS-induced migration of peritoneal macrophages (83), suggesting that different channels might be required under other conditions.

Depending on the chemical cues of the microenvironment (i.e. cytokines), macrophages polarize to M1 or M2 macrophages, which exhibited different migratory properties (84). Interestingly, macrophage M1 polarization reduces PANX1 expression, whereas M2 polarization induces its upregulation (85). However, whether PANX channels play a role during the migration of these cells is still unknown.

3 ROLE OF TISSUE PANXs ON LEUKOCYTE RECRUITMENT

Immune cell migration is not only induced by activation of PANX expressed in the migrating cell, but also can be indirectly promoted by PANX channels activated in the tissue. Initial observations by Chekeni et al, revealed that PANX1 channels were required for the release of "find me" signals (i.e., ATP and UTP) during T cell apoptosis, which triggered monocyte recruitment (86).

In liver, recruitment of monocytes is a hallmark of hepatic inflammation, involving apoptosis of hepatocytes induced by saturated free fatty acids (lipoapoptosis). Exposure to lipoapoptotic supernants elicits monocyte recruitment in an ATP-dependent chemokine-independent manner (87). PANX1 channels release ATP during lipoaptosis leading to c-Jun NH2-terminal kinase (JNK) activation in liver cells, revealing that hepatocytic PANX1 is key regulator of immune recruitment during nonalcoholic steatohepatitis (NASH) progression. In the same line, during obesity progression there is also accumulation of unsaturated fatty acids, which induce skeletal muscle inflammation and recruitment of immune cells. Thus, *in vitro* experiments with a muscle cell line that form myotubes show that treatment with palmitate induces ATP release from

myotubes, which triggers monocyte recruitment (88). Interestingly, the release of ATP from the myotubes was independent of PANX1, but dependent on PANX3 channels (88). Consequently, myotubes that lack of PANX3 are unable to release ATP upon palmitate treatment, and do not trigger monocyte migration (88). A similar mechanism could occur during wound healing in a dorsal skin mouse model (89). PANX3 KO mice presented a delayed healing and inflammation resolution at the injury site. Indeed, the number of $CD4^+$ T cells, neutrophils and macrophages was reduced in PANX3 KO mice, suggesting that tissue PANX3 was required for immune cell recruitment (89).

In the central nervous system the choroid plexus, located in the brain ventricle, is a key immune barrier between the cerebrospinal fluid and the blood. Epiplexus cells, resident innate immune cells of the choroid plexus, share markers and function with macrophages, DCs and other phagocytic cells (90). Under resting conditions epiplexus cells are sessile, but upon detection of extracellular ATP these cells increase their motility (91). This response depends on the ATP release *via* PANX1 channels from the epithelium of the choroid plexus, although epiplexus do not express PANX1 (91). Whether if during chronic inflammation or infection PANX expression is induced remains unknown.

Moreover, adipocyte-derived ATP release during adrenergic stimulation triggers macrophages recruitment (92). In addition, PANX1 opening is required for insulin-stimulated glucose uptake in adipocytes (93). Since insulin activates PANX1 channels causing the release of ATP, which in turn results in a signaling cascade indirectly allowing the transport of glucose into adipocytes, PANX1 might play a role in sustaining the inflammation observed during insulin resistance.

4 ROLE OF PANXs ON MIGRATION OF NON-IMMUNE CELLS

Unlike most immune cells that alter and deform little/transiently the extracellular matrix, mesenchymal cells require proteolytic enzymes to modify the microenvironment to undergo migration (5). Moreover, mesenchymal migratory cells use their actin cytoskeleton, form focal adhesion, and align with the extracellular matrix, with which and form focal adhesion (5, 10). However, despite these differences with amoeboid cell migration, mesenchymal cell migration also depends on acto-myosin contractility to move, although the motility of these cells is significantly slower (10). Another key protein for migration is the extracellular-signal-regulated protein kinase (ERK), a mitogen-activated protein kinase (MAPK), is a serine/threonine kinase, which modulates migration through phosphorylation of myosin light chain kinase (MLCK), calpain protease, paxillin, and focal adhesion kinase (FAK) (94). ERK activation can be triggered by cell matrix proteins (fibronectin, vitronectin, and collagen), growth factors (VEGF, FGF, EGF, insulin) and also indirectly by mechanical stress (94, 95). Indeed, mechanical stretch activates ERK through EGF receptor activation, triggering cell contraction (95). PANX1 channel opening is also affected by mechanical stress, although some evidence suggests that this occurs in an indirect fashion (96). However, regardless of the pathways activated PANX channel activity is affected by mechanotransduction and therefore these channels might contribute during cell migration and deformation of extracellular matrix, as it occurs during mesenchymal migration.

During the past years, increasing interest have grown on study PANX1 role during mesenchymal migration, particularly in the context of cancer progression (**Table 2**). For this reason, we decided to include in the following section, the latest publications associating PANX1 with non-immune cell migration.

4.1 Fibroblasts and Keratinocytes, Role of PANXs During Skin Cell Migration

The skin forms an active barrier and provides the first layer of defense by preventing the entry of foreign agents. This organ is a complex multilayer organization of cells with different but complementary functions, such as keratinocytes, melanocytes, fibroblasts, and immune cells (106, 107). During tissue damage skin resident cells communicate by using contact-dependent and independent mechanisms to quickly heal the wound (108). Consequently, ATP release and associated purinergic signaling play a key role during skin inflammation and wound healing (108). In particular, PANX1 is expressed in keratinocytes and fibroblasts from human and mice skin, as discussed below (98, 105, 109–111).

PANX1 levels decrease during adulthood, but increase after tissue damage (98). PANX1 is required for skin wound healing, as shown in a murine model of skin punch biopsies with a lack of PANX1 reduced tissue repair, but simultaneously increased fibrosis (98). Surprisingly, *in vitro* experiments revealed that the lack of PANX1 in keratinocytes increases their migratory potential. In contrast isolated skin fibroblasts from PANX1 knockout mice were more proliferative but showed decreased contractile properties in comparison to control conditions (98), suggesting that PANX1 expression is cell type specific, and that tissue interaction controls the overall migratory response in a cell-type specific and tissue specific manner. In the same line, PANX1 negatively regulates human dermal fibroblast migration when kept in monocultures. Indeed, fibroblasts lacking PANX1 or those treated with PANX1 channel blockers increase their speed of collective migration in wound healing assays, a similar but smaller response occurs when cells lack PANX3 (105). The decrease in cell migration during wound healing in fibroblasts is linked to decreased ATP release and activation of purinergic receptors. Consequently, $P2X_7$ receptors blockade increases the speed of migration in human dermal fibroblasts (105). However, this last data should be considered carefully depending on the working model to be compared with, as the authors also report no effect over migration with $P2X_7$ blockade in murine dermal fibroblasts (105). Additionally, *in vivo* experiments in a mice model reveal that PANX3 was required for proper wound healing (89). This suggests that different models of study might

TABLE 2 | Summary of PANX1 contribution to non-immune cell migration.

Cell type	PANX1 effect on migration	Channel blockers//receptor inhibitors	P2R	Migratory stimuli	Migration techniques	Ref.
Astrocyte DITNC1 cell line	Increase	BBG, Apyrase	n.e.	Thy-1	2D wound healing	(97)
Cortical astrocytes (m)	Increase	n.e.	n.e.	Thy-1	2D wound healing	(97)
Dermal fibroblasts	No effect	PANX1 KO	n.e.	Wound	*In vivo* wound healing	(98)
I-10 Leydig tumor cell line	Increase	Cbx, Pbc, PANX1 siRNA, U0126	n.e.	None	2D wound healing, transmigration in transwells	(99)
MDA-LM2 and CN-LM1A breast cancer cells (h)	Increase	^{10}PANX1, Cbx, Panx1 siRNA	n.e.	None	Counting of *in vivo* metastatic foci	(100)
BICR-M1Rk breast cancer cells (rt)	Increase	Cytochalasin B	n.e.	None	2D random migration	(25)
hTCEpi corneal epithelial cells (h)	Increase	^{10}PANX1, BBG, NF157, Suramin, Apyrase, PPADS	P2X, P2Y	Electric field	2D galvanotaxis	(101)
N2a cells, neuroblastoma (m)	Increase	PANX1 siRNA	n.e.	Wound	2D wound healing	(26)
Rh18 eRMS, Rh30 aRMS cell line	Overexp. decrease migration	PANX1 loss of function mutants, AHNAK siRNA	n.e.	Wound	2D wound healing, 3D spheroid growth, *in vivo* tumor growth	(102, 103)
C6 glioma cells (rt)	Overexp. decrease migration	n.e.	n.e.	None	Transmigration in transwells, 3D spheroid growth	(104)
Keratinocytes from neonatal skin (m)	decrease	PANX1 KO	n.e.	Wound	*In vivo* wound healing	(98)
HDF (h), MDF (m)	decrease PANX3 effect on migration	Pbc, ^{10}PANX1, PANX1 siRNA, A-740003,	$P2X_7$	Wound	2D wound healing	(105)
HDF (h)	decrease	PANX3 siRNA	$P2X_7$	Wound	2D wound healing	(105)
	Increase		n.e.	Wound	*In vivo* wound healing	(89)
HaCaT keratinocyte (h)	Increase	PANX3 siRNA	n.e.	TFG-ß1	Transmigration in transwells	(89)

aRMS, Alveolar rhabdomyosarcoma; BBG, Brilliant blue G; eRMS, embryonal rhabdomyosarcoma; h, human; HDFs, human dermal fibroblasts; m, mouse; MDFs, murine dermal fibroblasts; Overexp, Overexpression; rt, rat.

require different purinergic receptors. In any case, PANX1- and PANX3-dependent ATP release was consistently associated with a decrease in the collective and single migration of dermal fibroblasts, a response that relies in reorganization of the actin cytoskeleton (105).

These data reveal that PANX1 channels contribute to cell migration as a positive or negative regulators depending on the cell type and components of the microenvironment, including the available adenine nucleotides (**Figure 3**). However, the analysis of specific downstream signaling, and how the chemical cues of the microenvironment affect the role of PANX1 during migration remains largely unexplored.

4.2 PANXs Role During Astrocytic Migration Under Inflammation

Astrocytes are the more numerous glial cell in the brain, where these cells protect and feed the neurons (112). Astrocytes are crucial for tissue repairing during brain injury, and avoid spreading of neuronal damage by glial scar formation (112). During inflammation reactive astrocytes exhibit functional and morphological changes, as well as an increase in the expression of DAMPs receptors (112). Neuronal interaction with astrocytes controls cell migration *via* direct interaction of membrane proteins, such asThy-1 (CD90) (113, 114). Thy-1 is a membrane glycophosphatidylinositol (GPI) anchored protein that binds to αVβ3-containing integrin and syndecan-4 to stimulate FAK and actin reorganization (i.e. stress fibers formation), leading to morphological changes and migration in DITNC1 cell line. This astrocyte like cell line express high levels of αVβ3 Integrin and Syndecan-4, which resemble those observed in reactive astrocytes after tissue damage (115, 116). In DITNC1 cells Thy-1 stimulation triggers activation of intracellular signaling (PI3K and PLCγ) leading to Ca^{2+} release from intracellular stores opening CX43 and PANX1 channels. The ATP released *via* these channels activates $P2X_7$ receptors and subsequent Ca^{2+} influx (117, 118), revealing that Thy-1 induction of DITNC1 cell migration depends on PANX1 channels.

Under resting conditions primary astrocytes express very low levels of αVβ3 Integrin and Syndecan-4, but their expression is induced during neuroinflammation (97). TNF is a cytokine associated with neuroinflammation and accordingly triggers expression of αVβ3 Integrin and Syndecan-4 in astrocytes, accompanied by PANX1, CX43, $P2X_7$ receptors allowing the establishment of molecular toolkit required for Thy-1 signaling (97). Indeed, TNF-stimulated astrocytes respond to Thy-1, which leads to astrocyte cell migration by triggering PANX1 and CX43 ATP release and subsequent $P2X_7$ receptor activation (**Figure 2**) (97), supporting the data obtained in DITNC1 cells.

In another pro-inflammatory context, reactive astrocytes derived from Amyotrophic Lateral Sclerosis (ALS) model hSOD1G93A transgenic mice present an increased abundance of several migration-related molecules, including αvβ3 Integrin, syndecan-4 proteoglycan, $P2X_7$ receptor, PANX1, and CX43 (97). Thy-1 recognition induced both adhesion and migration of hSOD1G93A astrocytes (97). Intriguingly, TNF stimulation, and in ALS models triggers Thy-1 associated signaling expression, which pre-set a migratory phenotype in astrocytes, to which it is possible to speculate that, in general, pro-

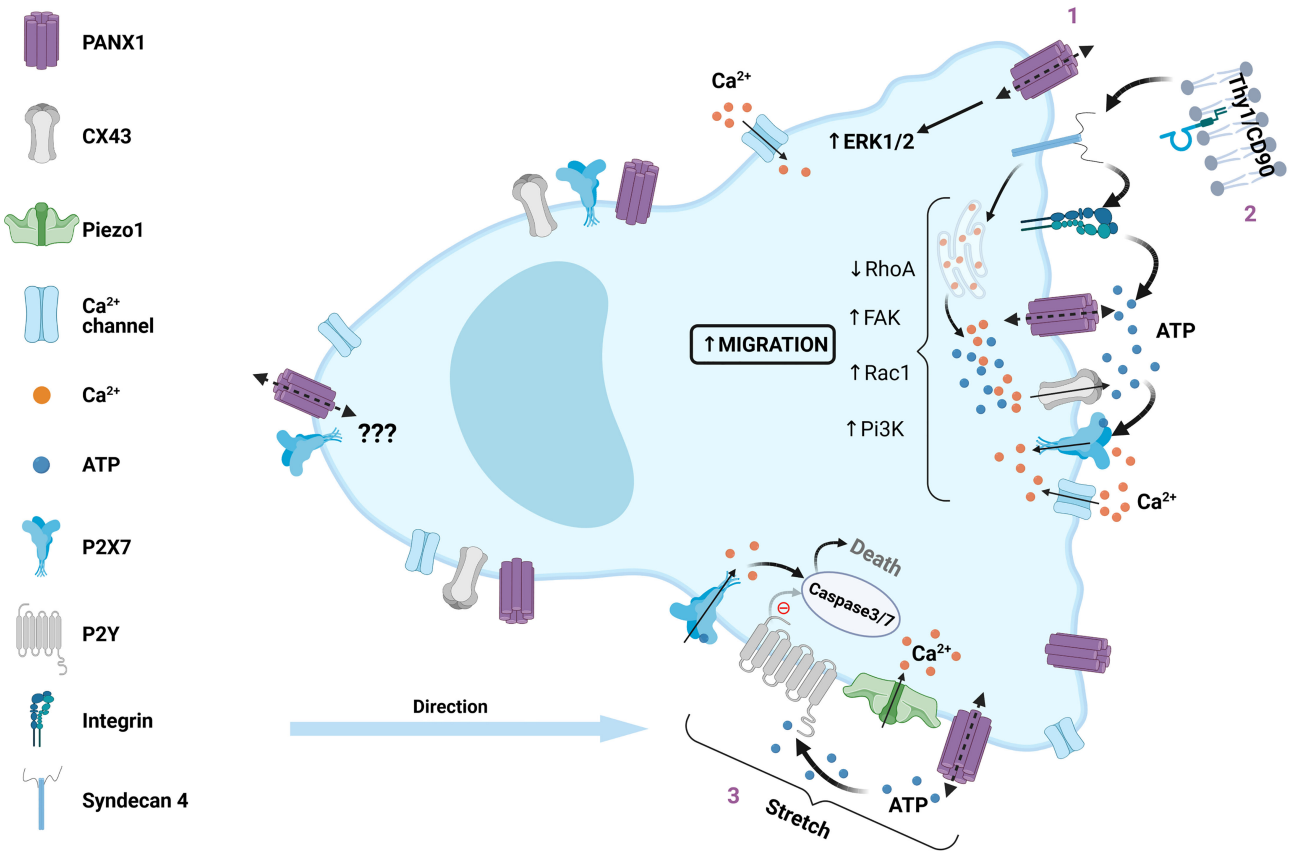

FIGURE 2 | Role of PANX1 channels in mesenchymal cell migration. Intracellular regulation of PANX1 channels during migration of mesenchymal non-immune cells is described as a positive or negative regulation, here we summarize the positive regulation. (1) Increased cell migration is correlated with PANX1 overexpression *via* activation of ERK1/2 pathway, which could also play a major role during collective cell migration (not included in this figure). (2) Thy1/CD90, a surface protein expressed in normal cells, but overexpressed in certain pathologies, interacts with αVβ3-containing integrin and Syndecan 4, which promotes cell migration. The downstream signaling involves focal adhesion kinase (FAK) activation, PI3K, PLCγ and IP3 production, leading to Ca^{2+} release from intracellular stores, and opening of both CX43 and PANX1 channels. The latter promotes extracellular ATP release and subsequent $P2X_7$ activation, Ca^{2+} influx and PKCα activation leading to Rac1 activation and RhoA inhibition. (3) Mechanical deformation during transepithelial migration lead to PANX1 channel activation, releasing ATP and activation of $P2X_7$ receptors, leading to cell death by caspase 3/7 activation. Alternatively, PANX1 mutations that change its function lead to P2Y activation, preventing caspase activation and cell death.

inflammatory conditions will induce a similar response preparing reactive astrocytes to migrate if needed, but whether PANX channels play a role during astrocyte migration in all pro-inflammatory conditions will require further studies.

4.3 Cancer Cells, Differential Contribution of PANXs to Tumor Progression

Tumor progression involves a series of sequential steps, which lead to tumor growth and metastasis. Cancer cell migration is the key step that allows invasion and colonization of new tissues. The stimulation of this response occurs during the epithelial to mesenchymal transition (EMT) (119, 120). Interestingly, dichotomic contribution of PANX1 on cancer cell migration has been reported (summarized in **Table 2**). Particularly, PANX1 can acts as a negative regulator for C6 cells motility, which are derived from rat glia. Indeed, overexpression of PANX1 reduces C6 glioma cell migration in different levels of complexity models of study (i.e. 2D, 3D spheroids, and *in vivo*) (104). In the same line a similar response is observed in rhabdomyosarcoma cells, in which inducible expression of PANX1 prevents cell migration (102). However, in this model PANX1 seems to play a role independent of its channel function, because it requires PANX1 physical interaction with AHNAK, a large scaffold protein (102, 103). Thus, at least in this rhabdomyosarcoma model it seems that PANX1 contribution might be related either to cytoskeleton re-organization and signaling, as shown for CX43 C-terminus (76). Interestingly, PANX1 expression induces gene and protein level upregulation of CX43, which has a tumor suppressive role in rhabdomyosarcoma (121). Altogether, these data supports the notion that PANX1 is a negative regulator tumor suppressor factor in cancer cells. However, in other cancer cell lines, PANX1 acts as a pro-migration factor as we discuss below (**Figure 3**).

Pioneer studies that revealed PANX1 interaction with the actin cytoskeleton, suggested its pro-migratory phenotype in

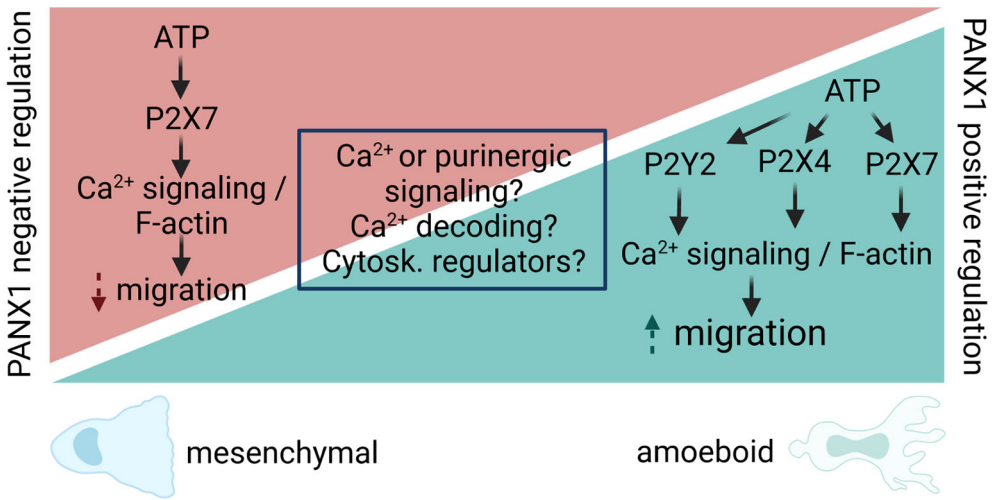

FIGURE 3 | Proposed model for PANX1 channel regulation of cell migration. PANX1 channels act as positive or negative regulators of cell migration, despite the fact that some pathways and proteins are shared by those opposite responses. We propose that different outcomes are likely to occur due difference in Ca^{2+} and/or purinergic signaling (i.e. agonists, concentrations, etc). In particular, for Ca^{2+} signaling, the local (microdomain, nanodomain) regulation of it might activate different signaling cascades leading to increase or decrease of cell migration. In addition, the decoding of Ca^{2+} signals by Ca^{2+}-sensitive enzymes (i.e. CaMKII) could directly modify the opening of PANX1, leading to changes in cytoskeleton dynamics directly or indirectly (i.e. cytoskeleton -Cytosk.- regulators) will result in signaling cascades that promote or inhibit cell migration. Therefore, the main contribution of PANX1 channels would be to amplify the initial response, and this would be downstream of the intrinsic cell-type specific Ca^{2+} response that ultimately determines the migratory outcome.

breast cancer (25). Indeed, PANX1 promotes motility, transmigration, and *in vivo* invasion in melanoma, breast and testicular cancer cells: B16-BL6, B16-F10; CN34, CN-LM1A, MDA-MB-231 MDA-MB-468, MDA-LM2, and I-10 cells, respectively (99, 100, 122, 123). In some cases, such as testicular cancer PANX1 activity was required for ERK1/2 activity, E-cadherin and metalloproteinase 9 (MMP-9) revealing that these channels contribute with different aspects of cell migration (99).

Like normal fibroblasts (see section above), MDA-MB-231 cells are sensitive to Thy-1 that increases cell migration by releasing ATP *via* PANX1 channels with subsequent activation of $P2X_7$ receptors in a positive feedback loop (123). Consequently, a mutation that increases the permeability of PANX1 channels leading to an exacerbated ATP release, also promotes cell motility, but not trans-endothelial migration (100), suggesting that PANX1 contributes to specific steps during tumor progression.

Which are the signals that lead to a positive or negative modulation of PANX1 on migration? As reviewed in this section, we hypothesize that it might depend on the cell type (**Table 2**), but the exact molecular mechanisms and signaling pathways that determine the outcome of the response remain unknown (**Figure 3**). The involvement of the other membrane channels that share functional and structural similarities with PANXs, such as the Leucine-rich repeat-containing 8 (LRRC8) proteins (124), is largely unexplored. Indeed, LRRC8A acts as a positive regulator of cancer cell migration (125), but how the activity of these channels affect the opening of PANXs, and how LRRC8 protein expression changes during cancer progression is not yet shown.

4.4 PANXs and Cell Migration During Aging, Senescence, and Neurodegeneration

Cellular changes progressively alter immune function during chronic inflammation and natural ageing, increasing susceptibility to infections and tumors (126). Associated with a chronic low-grade inflammatory state, is well accepted that cell motility decreases over time, which on immune cells might be due to accumulation of DNA damage after nuclear breakage (127). However, studies of cell migration in aging models are still scattered. Impaired phagocytosis and migration of DCs have been reported in aged humans (128). Not only cell decline (129), but also naive $CD8^+$ and $CD4^+$ T cell from old mice present lower migration and microtubules gene expression (130). Migration of aged marginal zone B cells at the spleen has also been reported to be impaired, consequently affecting immunoglobulin production (131). Human monocytes form elder volunteers showed altered gene profile of cellular motility (132), while bone marrow mesenchymal stem cells from aged human donors also present lower proliferation and migration abilities (133).

In the central nervous system, with smaller branches and slower motility process, microglia from aged mice exhibit reduced protrusion activity and cell migration after acute injury (134). During chronic neuroinflammation, aged mice of an Alzheimer's disease model present increased mast cell infiltration in the brain parenchyma (51). Conversely, aged neutrophils migrate faster to the injury (135, 136), despite having impaired phagocytic and degranulation activity (137, 138). Similarly, myoblast have augmented migratory features (speed and directionality) during wound healing (139). Aging is likely to exert a cell-specific effect, and therefore it is hard to anticipate whether PANX1, and other

PANXs, will contribute as a positive or a negative regulator as this will depend on the spatiotemporal regulation and accumulation of different ligands in the microenvironment.

5 CONCLUDING REMARKS

In the present review, we summarize the contribution of PANX channels during cell migration, emphasizing PANX1, that has been more widely studied. We have focused on immune cells as the integration of cell communication and cell migration is key for their function, despite mainly migrating as single cells. An interesting aspect of PANX-dependent purinergic signaling is the possibility that single migrating cells would have an impact on their neighbors. Using a mathematical model, Agliari et al. explored the hypothesis that ATP release and autocrine signaling during immune cell migration might impact neighboring cells while migrating as a group of single cells (140). The statistical inference approach revealed that migrating DCs have no instantaneous cell communication *via* release of small soluble molecules, such as ATP (140). However, the model only predicts immediate interactions and the release of adenine nucleotides or other small molecules will act with a delay considering the diffusion time and other parameters. The latter shows the need for the simultaneous study of cell communication and cell migration in a coordinated manner by using computational methods and theoretical frameworks, as it has been done for chemotaxis, or collective cell migration (141–143).

Another key aspect to link PANX1 and cell migration is the direct association between PANX channels and cytoskeletal components (actin, MyoII, microtubules), which are master regulators of cell migration. There is evidence of direct and indirect modulation of PANX channels by the cytoskeleton, which modifies membrane dynamics (144). In addition, PANX1 channels are somehow mechanosensitive, although in a lesser extent in comparison to other channels such as Piezo1 and Piezo2 (145). Still PANX1 could quickly react to changes in the membrane tension (96, 100, 146), providing a fast feedback mechanism in which the opening of the channel can be controlled by the mechanical cues of the microenvironment that surrounds the migrating cell. This could be sustained in time by the activation of enzymes that directly modify the opening of the channel, such as Ca^{2+}-sensitive CaMKII (72), or by a positive feedback with P2 receptors (147, 148) (**Figures 2**, **3**). In addition, some evidence suggests a non-channel contribution of PANX1 during migration of rhabdomyosarcoma (102, 103), which has been observed in other channels that can act as signaling proteins such as CX43 (76), or as enzymes and therefore receive the name of 'chanzymes', such as TRPM7 (149).

PANX channels interplay with purinergic signaling and indirectly with Ca^{2+} signaling is well established (2, 30), but its direct contribution with Ca^{2+} influx seems to be cell specific (32, 51, 65, 150). Then, local Ca^{2+} signaling regulation could lead to different migratory outcome (**Figure 3**). Moreover, whether other ions, such as K^+, could be relevant for the migratory is not yet demonstrated, although PANX1 channels directly contribute to migration induced by changes in the electric field, process named galvanotaxis (101). On the other hand, whether the opening of PANX channels contribute to ion flux and membrane voltage of the migrating cell is yet unexplored.

It is tempting to speculate about the necessity of PANX polarization during migration of leukocytes, but this should be carefully verified for each cell and stimuli. In neutrophils there is PANX1 polarization during migration (43, 86), but the same is not clear in T cells (29), and polarization seems to be not required for fast DC migration (32) (**Figure 2**). Therefore, the use of recently developed techniques, such as super resolution, optogenetics, and the development of new tools for live cell imaging monitoring of PANXs, will greatly improve our understanding of their role during cell migration.

Lastly, most of the studies have focused on PANX1, which seems to be a leading player during cell migration, but it is unclear the role of the other PANXs. Do PANXs have redundant functions? Are these cell-type specific? For example glioma cell migration is unaffected when changing the expression of PANX2, although cell growth was directly impacted (151). These data suggests that PANX2 and PANX3 might have other roles unrelated to cell migration and might be associated to cell growth and volume as recently reviewed (152). In the case of PANX3, which seems to act as a negative regulator of collective cell migration, it will be interesting to explore whether also prevent single cell migration. Finally, the role of PANXs has not yet been elucidated during chronic inflammation (i.e. obesity) or during aging (23, 152), conditions that change the responsiveness of immune cells (153). We propose that both conditions, chronic inflammation and aging, might induce the expression of different PANX isoforms in immune cells, leading to an increased migratory potential. However, how different PANXs isoforms orchestrate single and collective cell migration is still an unexplored field.

AUTHOR CONTRIBUTIONS

PH wrote large parts of the manuscript and provided advice for the figures. TL-L wrote some sections of the manuscript, and drafted the figures. AP contributed to drafting the manuscript. PS conceived the review, wrote and edited the manuscript, and revised the text and the figures. All authors contributed to the article and approved the submitted version.

FUNDING

This project has received funding from the European Union's Horizon 2020 research and innovation programme under the Marie Skłodowska-Curie grant agreement No 953489, ITN EndoConnect (PS), MINECO Spain PID2020-116086RB-I00 (PS), Forschungszentrum Medizintechnik Hamburg (FMTHH) 04fmthh2021 (PS), ANID Postdoctoral Project N° 3200342 (PH), MILENIO ICM-ANID P09-022-F (AP and PH).

ACKNOWLEDGMENTS

The authors would like to acknowledge David McGrath and Nabil Al Dam for reading the review and providing feedback. The figures of this review were created with BioRender.com, to which BioRender's Academic License Terms apply.

REFERENCES

1. Mayor R, Carmona-Fontaine C. Keeping in Touch With Contact Inhibition of Locomotion. *Trends Cell Biol* (2010) 20:319–28. doi: 10.1016/j.tcb.2010.03.005
2. Sáez PJ, Shoji KF, Aguirre A, Sáez JC. Regulation of Hemichannels and Gap Junction Channels by Cytokines in Antigen-Presenting Cells. *Mediators Inflamm* (2014) 2014:742734. doi: 10.1155/2014/742734
3. Ma L, Li Y, Peng J, Wu D, Zhao X, Cui Y, et al. Discovery of the Migrasome, an Organelle Mediating Release of Cytoplasmic Contents During Cell Migration. *Cell Res* (2015) 25:24–38. doi: 10.1038/cr.2014.135
4. Kriebel PW, Majumdar R, Jenkins LM, Senoo H, Wang W, Ammu S, et al. Extracellular Vesicles Direct Migration by Synthesizing and Releasing Chemotactic Signals. *J Cell Biol* (2018) 217:2891–910. doi: 10.1083/jcb.201710170
5. Yamada KM, Sixt M. Mechanisms of 3D Cell Migration. *Nat Rev Mol Cell Biol* (2019) 20:738–52. doi: 10.1038/s41580-019-0172-9
6. Kameritsch P, Renkawitz J. Principles of Leukocyte Migration Strategies. *Trends Cell Biol* (2020) 30:818–32. doi: 10.1016/j.tcb.2020.06.007
7. Miskolci V, Klemm LC, Huttenlocher A. Cell Migration Guided by Cell-Cell Contacts in Innate Immunity. *Trends Cell Biol* (2021) 31:86–94. doi: 10.1016/j.tcb.2020.11.002
8. Krummel MF, Bartumeus F, Gerard A. T Cell Migration, Search Strategies and Mechanisms. *Nat Rev Immunol* (2016) 16:193–201. doi: 10.1038/nri.2015.16
9. Vargas P, Barbier L, Saez PJ, Piel M. Mechanisms for Fast Cell Migration in Complex Environments. *Curr Opin Cell Biol* (2017) 48:72–8. doi: 10.1016/j.ceb.2017.04.007
10. Seetharaman S, Etienne-Manneville S. Cytoskeletal Crosstalk in Cell Migration. *Trends Cell Biol* (2020) 30:720–35. doi: 10.1016/j.tcb.2020.06.004
11. Kopf A, Kiermaier E. Dynamic Microtubule Arrays in Leukocytes and Their Role in Cell Migration and Immune Synapse Formation. *Front Cell Dev Biol* (2021) 9:635511. doi: 10.3389/fcell.2021.635511
12. Germain RN, Robey EA, Cahalan MD. A Decade of Imaging Cellular Motility and Interaction Dynamics in the Immune System. *Science* (2012) 336:1676–81. doi: 10.1126/science.1221063
13. Garcia-Arcos JM, Chabrier R, Deygas M, Nader G, Barbier L, Saez PJ, et al. Reconstitution of Cell Migration at a Glance. *J Cell Sci* (2019) 132. doi: 10.1242/jcs.225565
14. Sáez PJ, Barbier L, Attia R, Thiam HR, Piel M, Vargas P. Leukocyte Migration and Deformation in Collagen Gels and Microfabricated Constrictions. *Methods Mol Biol* (2018) 1749:361–73. doi: 10.1007/978-1-4939-7701-7_26
15. Matzinger P. Tolerance, Danger, and the Extended Family. *Annu Rev Immunol* (1994) 12:991–1045. doi: 10.1146/annurev.iy.12.040194.005015
16. Kono H, Rock KL. How Dying Cells Alert the Immune System to Danger. *Nat Rev Immunol* (2008) 8:279–89. doi: 10.1038/nri2215
17. David BA, Kubes P. Exploring the Complex Role of Chemokines and Chemoattractants *In Vivo* on Leukocyte Dynamics. *Immunol Rev* (2019) 289:9–30. doi: 10.1111/imr.12757
18. Di Virgilio F, Sarti AC, Coutinho-Silva R. Purinergic Signaling, DAMPs, and Inflammation. *Am J Physiol Cell Physiol* (2020) 318:C832–5. doi: 10.1152/ajpcell.00053.2020
19. Bours MJ, Swennen EL, Di Virgilio F, Cronstein BN, Dagnelie PC. Adenosine 5'-Triphosphate and Adenosine as Endogenous Signaling Molecules in Immunity and Inflammation. *Pharmacol Ther* (2006) 112:358–404. doi: 10.1016/j.pharmthera.2005.04.013
20. Kienle K, Lammermann T. Neutrophil Swarming: An Essential Process of the Neutrophil Tissue Response. *Immunol Rev* (2016) 273:76–93. doi: 10.1111/imr.12458
21. Kepp O, Bezu L, Yamazaki T, Di Virgilio F, Smyth MJ, Kroemer G, et al. ATP and Cancer Immunosurveillance. *EMBO J* (2021) 40:e108130. doi: 10.15252/embj.2021108130
22. Seo JH, Dalal MS, Contreras JE. Pannexin-1 Channels as Mediators of Neuroinflammation. *Int J Mol Sci* (2021) 22. doi: 10.3390/ijms22105189
23. Giaume C, Naus CC, Saez JC, Leybaert L. Glial Connexins and Pannexins in the Healthy and Diseased Brain. *Physiol Rev* (2021) 101:93–145. doi: 10.1152/physrev.00043.2018
24. Vaidziulyte K, Coppey M, Schauer K. Intracellular Organization in Cell Polarity - Placing Organelles Into the Polarity Loop. *J Cell Sci* (2019) 132. doi: 10.1242/jcs.230995
25. Bhalla-Gehi R, Penuela S, Churko JM, Shao Q, Laird DW. Pannexin1 and Pannexin3 Delivery, Cell Surface Dynamics, and Cytoskeletal Interactions. *J Biol Chem* (2010) 285:9147–60. doi: 10.1074/jbc.M109.082008
26. Wicki-Stordeur LE, Swayne LA. Panx1 Regulates Neural Stem and Progenitor Cell Behaviours Associated With Cytoskeletal Dynamics and Interacts With Multiple Cytoskeletal Elements. *Cell Commun Signal* (2013) 11:62. doi: 10.1186/1478-811X-11-62
27. Boyce AK, Wicki-Stordeur LE, Swayne LA. Powerful Partnership: Crosstalk Between Pannexin 1 and the Cytoskeleton. *Front Physiol* (2014) 5:27. doi: 10.3389/fphys.2014.00027
28. Junger WG. Immune Cell Regulation by Autocrine Purinergic Signalling. *Nat Rev Immunol* (2011) 11:201–12. doi: 10.1038/nri2938
29. Velasquez S, Malik S, Lutz SE, Scemes E, Eugenin EA. Pannexin1 Channels Are Required for Chemokine-Mediated Migration of CD4+ T Lymphocytes: Role in Inflammation and Experimental Autoimmune Encephalomyelitis. *J Immunol* (2016) 196:4338–47. doi: 10.4049/jimmunol.1502440
30. Sáez PJ, Sáez JC, Lennon-Duménil AM, Vargas P. Role of Calcium Permeable Channels in Dendritic Cell Migration. *Curr Opin Immunol* (2018) 52:74–80. doi: 10.1016/j.coi.2018.04.005
31. Xu X, Wicki-Stordeur LE, Sanchez-Arias JC, Liu M, Weaver MS, Choi CSW, et al. Probenecid Disrupts a Novel Pannexin 1-Collapsin Response Mediator Protein 2 Interaction and Increases Microtubule Stability. *Front Cell Neurosci* (2018) 12:124. doi: 10.3389/fncel.2018.00124
32. Sáez PJ, Vargas P, Shoji KF, Harcha PA, Lennon-Duménil AM, Sáez JC. ATP Promotes the Fast Migration of Dendritic Cells Through the Activity of Pannexin 1 Channels and P2X7 Receptors. *Sci Signal* (2017) 10. doi: 10.1126/scisignal.aah7107
33. Cymer M, Brzezniakiewicz-Janus K, Bujko K, Thapa A, Ratajczak J, Anusz K, et al. Pannexin-1 Channel "Fuels" by Releasing ATP From Bone Marrow Cells a State of Sterile Inflammation Required for Optimal Mobilization and Homing of Hematopoietic Stem Cells. *Purinergic Signal* (2020) 16:313–25. doi: 10.1007/s11302-020-09706-1
34. Ruez R, Dubrot J, Zoso A, Bacchetta M, Molica F, Hugues S, et al. Dendritic Cell Migration Toward CCL21 Gradient Requires Functional Cx43. *Front Physiol* (2018) 9:288. doi: 10.3389/fphys.2018.00288
35. Corvalán LA, Araya R, Branes MC, Sáez PJ, Kalergis AM, Tobar JA, et al. Injury of Skeletal Muscle and Specific Cytokines Induce the Expression of Gap Junction Channels in Mouse Dendritic Cells. *J Cell Physiol* (2007) 211:649–60. doi: 10.1002/jcp.20971
36. Kronlage M, Song J, Sorokin L, Isfort K, Schwerdtle T, Leipziger J, et al. Autocrine Purinergic Receptor Signaling is Essential for Macrophage Chemotaxis. *Sci Signal* (2010) 3:ra55. doi: 10.1126/scisignal.2000588
37. Davalos D, Grutzendler J, Yang G, Kim JV, Zuo Y, Jung S, et al. ATP Mediates Rapid Microglial Response to Local Brain Injury *In Vivo*. *Nat Neurosci* (2005) 8:752–8. doi: 10.1038/nn1472
38. Fontainhas AM, Wang M, Liang KJ, Chen S, Mettu P, Damani M, et al. Microglial Morphology and Dynamic Behavior is Regulated by Ionotropic Glutamatergic and GABAergic Neurotransmission. *PloS One* (2011) 6: e15973. doi: 10.1371/journal.pone.0015973
39. Garg C, Seo JH, Ramachandran J, Loh JM, Calderon F, Contreras JE. Trovafloxacin Attenuates Neuroinflammation and Improves Outcome After Traumatic Brain Injury in Mice. *J Neuroinflamm* (2018) 15:42. doi: 10.1186/s12974-018-1069-9
40. Eugenin EA, Branes MC, Berman JW, Saez JC. TNF-Alpha Plus IFN-Gamma Induce Connexin43 Expression and Formation of Gap Junctions Between Human Monocytes/Macrophages That Enhance Physiological Responses. *J Immunol* (2003) 170:1320–8. doi: 10.4049/jimmunol.170.3.1320
41. Campwala H, Sexton DW, Crossman DC, Fountain SJ. P2Y(6) Receptor Inhibition Perturbs CCL2-Evoked Signalling in Human Monocytic and Peripheral Blood Mononuclear Cells. *J Cell Sci* (2014) 127:4964–73. doi: 10.1242/jcs.159012
42. Chen Y, Yao Y, Sumi Y, Li A, To UK, Elkhal A, et al. Purinergic Signaling: A Fundamental Mechanism in Neutrophil Activation. *Sci Signal* (2010) 3:ra45. doi: 10.1126/scisignal.2000549
43. Bao Y, Chen Y, Ledderose C, Li L, Junger WG. Pannexin 1 Channels Link Chemoattractant Receptor Signaling to Local Excitation and Global Inhibition Responses at the Front and Back of Polarized Neutrophils. *J Biol Chem* (2013) 288:22650–7. doi: 10.1074/jbc.M113.476283

44. Sarieddine MZ, Scheckenbach KE, Foglia B, Maass K, Garcia I, Kwak BR, et al. Connexin43 Modulates Neutrophil Recruitment to the Lung. *J Cell Mol Med* (2009) 13:4560–70. doi: 10.1111/j.1582-4934.2008.00654.x
45. Wang X, Qin W, Xu X, Xiong Y, Zhang Y, Zhang H, et al. Endotoxin-Induced Autocrine ATP Signaling Inhibits Neutrophil Chemotaxis Through Enhancing Myosin Light Chain Phosphorylation. *Proc Natl Acad Sci USA* (2017) 114:4483–8. doi: 10.1073/pnas.1616752114
46. Poplimont H, Georgantzoglou A, Boulch M, Walker HA, Coombs C, Papaleonidopoulou F, et al. Neutrophil Swarming in Damaged Tissue Is Orchestrated by Connexins and Cooperative Calcium Alarm Signals. *Curr Biol* (2020) 30:2761–76.e2767. doi: 10.1016/j.cub.2020.05.030
47. Medina CB, Chiu YH, Stremska ME, Lucas CD, Poon I, Tung KS, et al. Pannexin 1 Channels Facilitate Communication Between T Cells to Restrict the Severity of Airway Inflammation. *Immunity* (2021) 54:1715–27.e1717. doi: 10.1016/j.immuni.2021.06.014
48. Ledderose C, Liu K, Kondo Y, Slubowski CJ, Dertnig T, Denicolo S, et al. Purinergic P2X4 Receptors and Mitochondrial ATP Production Regulate T Cell Migration. *J Clin Invest* (2018) 128:3583–94. doi: 10.1172/JCI120972
49. Gurusamy M, Tischner D, Shao J, Klatt S, Zukunft S, Bonnavion R, et al. G-Protein-Coupled Receptor P2Y10 Facilitates Chemokine-Induced CD4 T Cell Migration Through Autocrine/Paracrine Mediators. *Nat Commun* (2021). doi: 10.1038/s41467-021-26882-9
50. Hainz N, Wolf S, Beck A, Wagenpfeil S, Tschernig T, Meier C. Probenecid Arrests the Progression of Pronounced Clinical Symptoms in a Mouse Model of Multiple Sclerosis. *Sci Rep* (2017) 7:17214. doi: 10.1038/s41598-017-17517-5
51. Harcha PA, Vargas A, Yi C, Koulakoff AA, Giaume C, Saez JC. Hemichannels Are Required for Amyloid Beta-Peptide-Induced Degranulation and Are Activated in Brain Mast Cells of APPswe/PS1dE9 Mice. *J Neurosci* (2015) 35:9526–38. doi: 10.1523/JNEUROSCI.3686-14.2015
52. Berzat A, Hall A. Cellular Responses to Extracellular Guidance Cues. *EMBO J* (2010) 29:2734–45. doi: 10.1038/emboj.2010.170
53. Thiam HR, Wong SL, Qiu R, Kittisopikul M, Vahabikashi A, Goldman AE, et al. NETosis Proceeds by Cytoskeleton and Endomembrane Disassembly and PAD4-Mediated Chromatin Decondensation and Nuclear Envelope Rupture. *Proc Natl Acad Sci USA* (2020) 117:7326–37. doi: 10.1073/pnas.1909546117
54. Chen Y, Corriden R, Inoue Y, Yip L, Hashiguchi N, Zinkernagel A, et al. ATP Release Guides Neutrophil Chemotaxis *via* P2Y2 and A3 Receptors. *Science* (2006) 314:1792–5. doi: 10.1126/science.1132559
55. Alarcon P, Manosalva C, Quiroga J, Belmar I, Alvarez K, Diaz G, et al. Oleic and Linoleic Acids Induce the Release of Neutrophil Extracellular Traps *via* Pannexin 1-Dependent ATP Release and P2X1 Receptor Activation. *Front Vet Sci* (2020) 7:260. doi: 10.3389/fvets.2020.00260
56. Bao Y, Ledderose C, Graf AF, Brix B, Birsak T, Lee A, et al. mTOR and Differential Activation of Mitochondria Orchestrate Neutrophil Chemotaxis. *J Cell Biol* (2015) 210:1153–64. doi: 10.1083/jcb.201503066
57. Sil P, Hayes CP, Reaves BJ, Breen P, Quinn S, Sokolove J, et al. P2Y6 Receptor Antagonist MRS2578 Inhibits Neutrophil Activation and Aggregated Neutrophil Extracellular Trap Formation Induced by Gout-Associated Monosodium Urate Crystals. *J Immunol* (2017) 198:428–42. doi: 10.4049/jimmunol.1600766
58. Alkayed F, Kashimata M, Koyama N, Hayashi T, Tamura Y, Azuma Y. P2Y11 Purinoceptor Mediates the ATP-Enhanced Chemotactic Response of Rat Neutrophils. *J Pharmacol Sci* (2012) 120:288–95. doi: 10.1254/jphs.12173fp
59. Barrett MO, Sesma JI, Ball CB, Jayasekara PS, Jacobson KA, Lazarowski ER, et al. A Selective High-Affinity Antagonist of the P2Y14 Receptor Inhibits UDP-Glucose-Stimulated Chemotaxis of Human Neutrophils. *Mol Pharmacol* (2013) 84:41–9. doi: 10.1124/mol.113.085654
60. Xu X, Zheng S, Xiong Y, Wang X, Qin W, Zhang H, et al. Adenosine Effectively Restores Endotoxin-Induced Inhibition of Human Neutrophil Chemotaxis *via* A1 Receptor-P38 Pathway. *Inflamm Res* (2017) 66:353–64. doi: 10.1007/s00011-016-1021-3
61. Liu L, Das S, Losert W, Parent CA. Mtorc2 Regulates Neutrophil Chemotaxis in a cAMP- and RhoA-Dependent Fashion. *Dev Cell* (2010) 19:845–57. doi: 10.1016/j.devcel.2010.11.004
62. Rivas-Yanez E, Barrera-Avalos C, Parra-Tello B, Briceno P, Rosemblatt MV, Saavedra-Almarza J, et al. P2X7 Receptor at the Crossroads of T Cell Fate. *Int J Mol Sci* (2020) 21. doi: 10.3390/ijms21144937
63. Schenk U, Westendorf AM, Radaelli E, Casati A, Ferro M, Fumagalli M, et al. Purinergic Control of T Cell Activation by ATP Released Through Pannexin-1 Hemichannels. *Sci Signal* (2008) 1:ra6. doi: 10.1126/scisignal.1160583
64. Woehrle T, Yip L, Elkhal A, Sumi Y, Chen Y, Yao Y, et al. Pannexin-1 Hemichannel-Mediated ATP Release Together With P2X1 and P2X4 Receptors Regulate T-Cell Activation at the Immune Synapse. *Blood* (2010) 116:3475–84. doi: 10.1182/blood-2010-04-277707
65. Shoji KF, Saez PJ, Harcha PA, Aguila HL, Saez JC. Pannexin1 Channels Act Downstream of P2X 7 Receptors in ATP-Induced Murine T-Cell Death. *Channels (Austin)* (2014) 8:142–56. doi: 10.4161/chan.28122
66. Ledderose C, Bromberger S, Slubowski CJ, Sueyoshi K, Aytan D, Shen Y, et al. The Purinergic Receptor P2Y11 Choreographs the Polarization, Mitochondrial Metabolism, and Migration of T Lymphocytes. *Sci Signal* (2020) 13. doi: 10.1126/scisignal.aba3300
67. Campello S, Lacalle RA, Bettella M, Manes S, Scorrano L, Viola A. Orchestration of Lymphocyte Chemotaxis by Mitochondrial Dynamics. *J Exp Med* (2006) 203:2879–86. doi: 10.1084/jem.20061877
68. Vincent P, Collette Y, Marignier R, Vuaillat C, Rogemond V, Davoust N, et al. A Role for the Neuronal Protein Collapsin Response Mediator Protein 2 in T Lymphocyte Polarization and Migration. *J Immunol* (2005) 175:7650–60. doi: 10.4049/jimmunol.175.11.7650
69. De Winde CM, Munday C, Acton ,SE. Molecular Mechanisms of Dendritic Cell Migration in Immunity and Cancer. *Med Microbiol Immunol* (2020) 209:515–29. doi: 10.1007/s00430-020-00680-4
70. Banchereau J, Steinman RM. Dendritic Cells and the Control of Immunity. *Nature* (1998) 392:245–52. doi: 10.1038/32588
71. Cekic C, Linden J. Purinergic Regulation of the Immune System. *Nat Rev Immunol* (2016) 16:177–92. doi: 10.1038/nri.2016.4
72. López X, Palacios-Prado N, Guiza J, Escamilla R, Fernandez P, Vega JL, et al. A Physiologic Rise in Cytoplasmic Calcium Ion Signal Increases Pannexin1 Channel Activity *via* a C-Terminus Phosphorylation by CaMKII. *Proc Natl Acad Sci USA* (2021). doi: 10.1073/pnas.2108967118
73. Khan S, Downing KH, Molloy JE. Architectural Dynamics of CaMKII-Actin Networks. *Biophys J* (2019) 116:104–19. doi: 10.1016/j.bpj.2018.11.006
74. Bretou M, Sáez PJ, Sanseau D, Maurin M, Lankar D, Chabaud M, et al. Lysosome Signaling Controls the Migration of Dendritic Cells. *Sci Immunol* (2017) 2. doi: 10.1126/sciimmunol.aak9573
75. Boyce AKJ, van der Slagt E, Sanchez-Arias JC, Swayen LA. ATP Triggers Macropinocytosis That Internalizes and is Regulated by PANX1. *bioRxiv* (2020) doi. doi: 10.1101/2020.11.19.389072
76. Cina C, Maass K, Theis M, Willecke K, Bechberger JF, Naus CC. Involvement of the Cytoplasmic C-Terminal Domain of Connexin43 in Neuronal Migration. *J Neurosci* (2009) 29:2009–21. doi: 10.1523/JNEUROSCI.5025-08.2009
77. Jakubzick CV, Randolph GJ, Henson PM. Monocyte Differentiation and Antigen-Presenting Functions. *Nat Rev Immunol* (2017) 17:349–62. doi: 10.1038/nri.2017.28
78. Rodjakovic D, Salm L, Beldi G. Function of Connexin-43 in Macrophages. *Int J Mol Sci* (2021) 22. doi: 10.3390/ijms22031412
79. Geissmann F, Gordon S, Hume DA, Mowat AM, Randolph GJ. Unravelling Mononuclear Phagocyte Heterogeneity. *Nat Rev Immunol* (2010) 10:453–60. doi: 10.1038/nri2784
80. Yu C, Roubeix C, Sennlaub F, Saban DR. Microglia *Versus* Monocytes: Distinct Roles in Degenerative Diseases of the Retina. *Trends Neurosci* (2020) 43:433–49. doi: 10.1016/j.tins.2020.03.012
81. Poon IK, Chiu YH, Armstrong AJ, Kinchen JM, Juncadella IJ, Bayliss DA, et al. Unexpected Link Between an Antibiotic, Pannexin Channels and Apoptosis. *Nature* (2014) 507:329–34. doi: 10.1038/nature13147
82. Seo JH, Dalal MS, Calderon F, Contreras JE. Myeloid Pannexin-1 Mediates Acute Leukocyte Infiltration and Leads to Worse Outcomes After Brain Trauma. *J Neuroinflamm* (2020) 17:245. doi: 10.1186/s12974-020-01917-y
83. Shen C, Chen JH, Lee Y, Hassan MM, Kim SJ, Choi EY, et al. mTOR- and SGK-Mediated Connexin 43 Expression Participates in Lipopolysaccharide-Stimulated Macrophage Migration Through the iNOS/Src/FAK Axis. *J Immunol* (2018) 201:2986–97. doi: 10.4049/jimmunol.1700954
84. Cui K, Ardell CL, Podolnikova NP, Yakubenko VP. Distinct Migratory Properties of M1, M2, and Resident Macrophages Are Regulated by

Alphadbeta2 and Alphambeta2 Integrin-Mediated Adhesion. *Front Immunol* (2018) 9:2650. doi: 10.3389/fimmu.2018.02650
85. Lopez-Castejon G, Baroja-Mazo A, Pelegrin P. Novel Macrophage Polarization Model: From Gene Expression to Identification of New Anti-Inflammatory Molecules. *Cell Mol Life Sci* (2011) 68:3095–107. doi: 10.1007/s00018-010-0609-y
86. Chekeni FB, Elliott MR, Sandilos JK, Walk SF, Kinchen JM, Lazarowski ER, et al. Pannexin 1 Channels Mediate 'Find-Me' Signal Release and Membrane Permeability During Apoptosis. *Nature* (2010) 467:863–7. doi: 10.1038/nature09413
87. Xiao F, Waldrop SL, Bronk SF, Gores GJ, Davis LS, Kilic G. Lipoapoptosis Induced by Saturated Free Fatty Acids Stimulates Monocyte Migration: A Novel Role for Pannexin1 in Liver Cells. *Purinergic Signal* (2015) 11:347–59. doi: 10.1007/s11302-015-9456-5
88. Pillon NJ, Li YE, Fink LN, Brozinick JT, Nikolayev A, Kuo MS, et al. Nucleotides Released From Palmitate-Challenged Muscle Cells Through Pannexin-3 Attract Monocytes. *Diabetes* (2014) 63:3815–26. doi: 10.2337/db14-0150
89. Zhang P, Ishikawa M, Rhodes C, Doyle A, Ikeuchi T, Nakamura K, et al. Pannexin-3 Deficiency Delays Skin Wound Healing in Mice Due to Defects in Channel Functionality. *J Invest Dermatol* (2019) 139:909–18. doi: 10.1016/j.jid.2018.08.033
90. Ling EA, Kaur C, Lu J. Origin, Nature, and Some Functional Considerations of Intraventricular Macrophages, With Special Reference to the Epiplexus Cells. *Microsc Res Tech* (1998) 41:43–56. doi: 10.1002/(SICI)1097-0029(19980401)41:1<43::AID-JEMT5>3.0.CO;2-V
91. Maslieieva V, Thompson RJ. A Critical Role for Pannexin-1 in Activation of Innate Immune Cells of the Choroid Plexus. *Channels (Austin)* (2014) 8:131–41. doi: 10.4161/chan.27653
92. Tozzi M, Hansen JB, Novak I. Pannexin-1 Mediated ATP Release in Adipocytes is Sensitive to Glucose and Insulin and Modulates Lipolysis and Macrophage Migration. *Acta Physiol (Oxf)* (2020) 228:e13360. doi: 10.1111/apha.13360
93. Adamson SE, Meher AK, Chiu YH, Sandilos JK, Oberholtzer NP, Walker NN, et al. Pannexin 1 is Required for Full Activation of Insulin-Stimulated Glucose Uptake in Adipocytes. *Mol Metab* (2015) 4:610–8. doi: 10.1016/j.molmet.2015.06.009
94. Huang C, Jacobson K, Schaller MD. MAP Kinases and Cell Migration. *J Cell Sci* (2004) 117:4619–28. doi: 10.1242/jcs.01481
95. Hino N, Rossetti L, Marin-Llaurado A, Aoki K, Trepat X, Matsuda M, et al. ERK-Mediated Mechanochemical Waves Direct Collective Cell Polarization. *Dev Cell* (2020) 53:646–60.e648. doi: 10.1016/j.devcel.2020.05.011
96. López X, Escamilla R, Fernandez P, Duarte Y, Gonzalez-Nilo F, Palacios-Prado N, et al. Stretch-Induced Activation of Pannexin 1 Channels Can Be Prevented by PKA-Dependent Phosphorylation. *Int J Mol Sci* (2020) 21. doi: 10.3390/ijms21239180
97. Lagos-Cabre R, Alvarez A, Kong M, Burgos-Bravo F, Cardenas A, Rojas-Mancilla E, et al. Alphavbeta3 Integrin Regulates Astrocyte Reactivity. *J Neuroinflamm* (2017) 14:194. doi: 10.1186/s12974-017-0968-5
98. Peñuela S, Kelly JJ, Churko JM, Barr KJ, Berger AC, Laird DW. Panx1 Regulates Cellular Properties of Keratinocytes and Dermal Fibroblasts in Skin Development and Wound Healing. *J Invest Dermatol* (2014) 134:2026–35. doi: 10.1038/jid.2014.86
99. Liu H, Yuan M, Yao Y, Wu D, Dong S, Tong X. *In Vitro* Effect of Pannexin 1 Channel on the Invasion and Migration of I-10 Testicular Cancer Cells *via* ERK1/2 Signaling Pathway. *BioMed Pharmacother* (2019) 117:109090. doi: 10.1016/j.biopha.2019.109090
100. Furlow PW, Zhang S, Soong TD, Halberg N, Goodarzi H, Mangrum C, et al. Mechanosensitive Pannexin-1 Channels Mediate Microvascular Metastatic Cell Survival. *Nat Cell Biol* (2015) 17:943–52. doi: 10.1038/ncb3194
101. Nakajima KI, Tatsumi M, Zhao M. An Essential and Synergistic Role of Purinergic Signaling in Guided Migration of Corneal Epithelial Cells in Physiological Electric Fields. *Cell Physiol Biochem* (2019) 52:198–211. doi: 10.33594/000000014
102. Xiang X, Langlois S, St-Pierre ME, Barre JF, Grynspan D, Purgina B, et al. Pannexin 1 Inhibits Rhabdomyosarcoma Progression Through a Mechanism Independent of its Canonical Channel Function. *Oncogenesis* (2018) 7:89. doi: 10.1038/s41389-018-0100-4
103. Xiang X, Langlois S, St-Pierre ME, Blinder A, Charron P, Graber TE, et al. Identification of Pannexin 1-Regulated Genes, Interactome, and Pathways in Rhabdomyosarcoma and its Tumor Inhibitory Interaction With AHNAK. *Oncogene* (2021) 40:1868–83. doi: 10.1038/s41388-020-01623-2
104. Lai CP, Bechberger JF, Thompson RJ, Macvicar BA, Bruzzone R, Naus CC. Tumor-Suppressive Effects of Pannexin 1 in C6 Glioma Cells. *Cancer Res* (2007) 67:1545–54. doi: 10.1158/0008-5472.CAN-06-1396
105. Flores-Munoz C, Maripillan J, Vasquez-Navarrete J, Novoa-Molina J, Ceriani R, Sanchez HA, et al. Restraint of Human Skin Fibroblast Motility, Migration, and Cell Surface Actin Dynamics, by Pannexin 1 and P2X7 Receptor Signaling. *Int J Mol Sci* (2021) 22. doi: 10.3390/ijms22031069
106. Werner S, Krieg T, Smola H. Keratinocyte-Fibroblast Interactions in Wound Healing. *J Invest Dermatol* (2007) 127:998–1008. doi: 10.1038/sj.jid.5700786
107. Russo B, Brembilla NC, Chizzolini C. Interplay Between Keratinocytes and Fibroblasts: A Systematic Review Providing a New Angle for Understanding Skin Fibrotic Disorders. *Front Immunol* (2020) 11:648. doi: 10.3389/fimmu.2020.00648
108. Burnstock G, Knight GE, Greig AV. Purinergic Signaling in Healthy and Diseased Skin. *J Invest Dermatol* (2012) 132:526–46. doi: 10.1038/jid.2011.344
109. Peñuela S, Bhalla R, Gong XQ, Cowan KN, Celetti SJ, Cowan BJ, et al. Pannexin 1 and Pannexin 3 are Glycoproteins That Exhibit Many Distinct Characteristics From the Connexin Family of Gap Junction Proteins. *J Cell Sci* (2007) 120:3772–83. doi: 10.1242/jcs.009514
110. Celetti SJ, Cowan KN, Penuela S, Shao Q, Churko J, Laird DW. Implications of Pannexin 1 and Pannexin 3 for Keratinocyte Differentiation. *J Cell Sci* (2010) 123:1363–72. doi: 10.1242/jcs.056093
111. Pinheiro AR, Paramos-De-Carvalho D, Certal M, Costa MA, Costa C, Magalhaes-Cardoso MT, et al. Histamine Induces ATP Release From Human Subcutaneous Fibroblasts, *via* Pannexin-1 Hemichannels, Leading to Ca2+ Mobilization and Cell Proliferation. *J Biol Chem* (2013) 288:27571–83. doi: 10.1074/jbc.M113.460865
112. Lagos-Cabre R, Burgos-Bravo F, Avalos AM, Leyton ,L. Connexins in Astrocyte Migration. *Front Pharmacol* (2019) 10:1546. doi: 10.3389/fphar.2019.01546
113. Dreyer EB, Leifer D, Heng JE, Mcconnell JE, Gorla M, Levin LA, et al. An Astrocytic Binding Site for Neuronal Thy-1 and its Effect on Neurite Outgrowth. *Proc Natl Acad Sci USA* (1995) 92:11195–9. doi: 10.1073/pnas.92.24.11195
114. Leyton L, Schneider P, Labra CV, Ruegg C, Hetz CA, Quest AF, et al. Thy-1 Binds to Integrin Beta(3) on Astrocytes and Triggers Formation of Focal Contact Sites. *Curr Biol* (2001) 11:1028–38. doi: 10.1016/s0960-9822(01)00262-7
115. Avalos AM, Arthur WT, Schneider P, Quest AF, Burridge K, Leyton L. Aggregation of Integrins and RhoA Activation are Required for Thy-1-Induced Morphological Changes in Astrocytes. *J Biol Chem* (2004) 279:39139–45. doi: 10.1074/jbc.M403439200
116. Kong M, Munoz N, Valdivia A, Alvarez A, Herrera-Molina R, Cardenas A, et al. Thy-1-Mediated Cell-Cell Contact Induces Astrocyte Migration Through the Engagement of Alphavbeta3 Integrin and Syndecan-4. *Biochim Biophys Acta* (2013) 1833:1409–20. doi: 10.1016/j.bbamcr.2013.02.013
117. Henriquez M, Herrera-Molina R, Valdivia A, Alvarez A, Kong M, Munoz N, et al. ATP Release Due to Thy-1-Integrin Binding Induces P2X7-Mediated Calcium Entry Required for Focal Adhesion Formation. *J Cell Sci* (2011) 124:1581–8. doi: 10.1242/jcs.073171
118. Alvarez A, Lagos-Cabre R, Kong M, Cardenas A, Burgos-Bravo F, Schneider P, et al. Integrin-Mediated Transactivation of P2X7R *via* Hemichannel-Dependent ATP Release Stimulates Astrocyte Migration. *Biochim Biophys Acta* (2016) 1863:2175–88. doi: 10.1016/j.bbamcr.2016.05.018
119. Clark AG, Vignjevic DM. Modes of Cancer Cell Invasion and the Role of the Microenvironment. *Curr Opin Cell Biol* (2015) 36:13–22. doi: 10.1016/j.ceb.2015.06.004
120. Vilchez Mercedes SA, Bocci F, Levine H, Onuchic JN, Jolly MK, Wong PK. Decoding Leader Cells in Collective Cancer Invasion. *Nat Rev Cancer* (2021) doi: 10.1038/s41568-021-00376-8
121. Proulx AA, Lin ZX, Naus CC. Transfection of Rhabdomyosarcoma Cells With Connexin43 Induces Myogenic Differentiation. *Cell Growth Differ* (1997) 8:533–40.

122. Peñuela S, Gyenis L, Ablack A, Churko JM, Berger AC, Litchfield DW, et al. Loss of Pannexin 1 Attenuates Melanoma Progression by Reversion to a Melanocytic Phenotype. *J Biol Chem* (2012) 287:29184–93. doi: 10.1074/jbc.M112.377176
123. Brenet M, Martinez S, Perez-Nunez R, Perez LA, Contreras P, Diaz J, et al. Thy-1 (CD90)-Induced Metastatic Cancer Cell Migration and Invasion Are Beta3 Integrin-Dependent and Involve a Ca(2+)/P2X7 Receptor Signaling Axis. *Front Cell Dev Biol* (2020) 8:592442. doi: 10.3389/fcell.2020.592442
124. Abascal F, Zardoya R. LRRC8 Proteins Share a Common Ancestor With Pannexins, and may Form Hexameric Channels Involved in Cell-Cell Communication. *Bioessays* (2012) 34:551–60. doi: 10.1002/bies.201100173
125. Friard J, Corinus A, Cougnon M, Tauc M, Pisani DF, Duranton C, et al. LRRC8/VRAC Channels Exhibit a Noncanonical Permeability to Glutathione, Which Modulates Epithelial-to-Mesenchymal Transition (EMT). *Cell Death Dis* (2019) 10:925. doi: 10.1038/s41419-019-2167-z
126. Weyand CM, Goronzy JJ. Aging of the Immune System. Mechanisms and Therapeutic Targets. *Ann Am Thorac Soc* (2016) 13(Suppl 5):S422–8. doi: 10.1513/AnnalsATS.201602-095AW
127. Raab M, Gentili M, De Belly H, Thiam HR, Vargas P, Jimenez AJ, et al. ESCRT III Repairs Nuclear Envelope Ruptures During Cell Migration to Limit DNA Damage and Cell Death. *Science* (2016) 352:359–62. doi: 10.1126/science.aad7611
128. Agrawal A, Agrawal S, Cao JN, Su H, Osann K, Gupta S. Altered Innate Immune Functioning of Dendritic Cells in Elderly Humans: A Role of Phosphoinositide 3-Kinase-Signaling Pathway. *J Immunol* (2007) 178:6912–22. doi: 10.4049/jimmunol.178.11.6912
129. Nikolich-Zugich J. Ageing and Life-Long Maintenance of T-Cell Subsets in the Face of Latent Persistent Infections. *Nat Rev Immunol* (2008) 8:512–22. doi: 10.1038/nri2318
130. Chen G, Lustig A, Weng NP. T Cell Aging: A Review of the Transcriptional Changes Determined From Genome-Wide Analysis. *Front Immunol* (2013) 4:121. doi: 10.3389/fimmu.2013.00121
131. Turner VM, Mabbott NA. Ageing Adversely Affects the Migration and Function of Marginal Zone B Cells. *Immunology* (2017) 151:349–62. doi: 10.1111/imm.12737
132. Saare M, Tserel L, Haljasmagi L, Taalberg E, Peet N, Eimre M, et al. Monocytes Present Age-Related Changes in Phospholipid Concentration and Decreased Energy Metabolism. *Aging Cell* (2020) 19:e13127. doi: 10.1111/acel.13127
133. Zhang Y, Zhu W, He H, Fan B, Deng R, Hong Y, et al. Macrophage Migration Inhibitory Factor Rejuvenates Aged Human Mesenchymal Stem Cells and Improves Myocardial Repair. *Aging (Albany NY)* (2019) 11:12641–60. doi: 10.18632/aging.102592
134. Damani MR, Zhao L, Fontainhas AM, Amaral J, Fariss RN, Wong WT. Age-Related Alterations in the Dynamic Behavior of Microglia. *Aging Cell* (2011) 10:263–76. doi: 10.1111/j.1474-9726.2010.00660.x
135. Uhl B, Vadlau Y, Zuchtriegel G, Nekolla K, Sharaf K, Gaertner F, et al. Aged Neutrophils Contribute to the First Line of Defense in the Acute Inflammatory Response. *Blood* (2016) 128:2327–37. doi: 10.1182/blood-2016-05-718999
136. Barkaway A, Rolas L, Joulia R, Bodkin J, Lenn T, Owen-Woods C, et al. Age-Related Changes in the Local Milieu of Inflamed Tissues Cause Aberrant Neutrophil Trafficking and Subsequent Remote Organ Damage. *Immunity* (2021) 54:1494–510.e1497. doi: 10.1016/j.immuni.2021.04.025
137. Wenisch C, Patruta S, Daxbock F, Krause R, Horl W. Effect of Age on Human Neutrophil Function. *J Leukoc Biol* (2000) 67:40–5. doi: 10.1002/jlb.67.1.40
138. Butcher SK, Chahal H, Nayak L, Sinclair A, Henriquez NV, Sapey E, et al. Senescence in Innate Immune Responses: Reduced Neutrophil Phagocytic Capacity and CD16 Expression in Elderly Humans. *J Leukoc Biol* (2001) 70:881–6. doi: 10.1189/jlb.70.6.881
139. Brown AD, Close GL, Sharples AP, Stewart CE. Murine Myoblast Migration: Influence of Replicative Ageing and Nutrition. *Biogerontology* (2017) 18:947–64. doi: 10.1007/s10522-017-9735-3
140. Agliari E, Saez PJ, Barra A, Piel M, Vargas P, Castellana M. A Statistical Inference Approach to Reconstruct Intercellular Interactions in Cell Migration Experiments. *Sci Adv* (2020) 6:eaay2103. doi: 10.1126/sciadv.aay2103
141. Buttenschon A, Edelstein-Keshet L. Bridging From Single to Collective Cell Migration: A Review of Models and Links to Experiments. *PloS Comput Biol* (2020) 16:e1008411. doi: 10.1371/journal.pcbi.1008411
142. Tweedy L, Thomason PA, Paschke PI, Martin K, Machesky LM, Zagnoni M, et al. Seeing Around Corners: Cells Solve Mazes and Respond at a Distance Using Attractant Breakdown. *Science* (2020) 369. doi: 10.1126/science.aay9792
143. Jin S, Guerrero-Juarez CF, Zhang L, Chang I, Ramos R, Kuan CH, et al. Inference and Analysis of Cell-Cell Communication Using CellChat. *Nat Commun* (2021) 12:1088. doi: 10.1038/s41467-021-21246-9
144. Sanchez-Arias JC, Candlish RC, van der Slagt E, Swayne LA. Pannexin 1 Regulates Dendritic Protrusion Dynamics in Immature Cortical Neurons. *eNeuro* (2020) 7. doi: 10.1523/ENEURO.0079-20.2020
145. Coste B, Mathur J, Schmidt M, Earley TJ, Ranade S, Petrus MJ, et al. Piezo1 and Piezo2 are Essential Components of Distinct Mechanically Activated Cation Channels. *Science* (2010) 330:55–60. doi: 10.1126/science.1193270
146. Zmurchok C, Collette J, Rajagopal V, Holmes WR. Membrane Tension Can Enhance Adaptation to Maintain Polarity of Migrating Cells. *Biophys J* (2020) 119:1617–29. doi: 10.1016/j.bpj.2020.08.035
147. Adamson SE, Leitinger N. The Role of Pannexin1 in the Induction and Resolution of Inflammation. *FEBS Lett* (2014) 588:1416–22. doi: 10.1016/j.febslet.2014.03.009
148. Giuliani AL, Sarti AC, Di Virgilio F. Extracellular Nucleotides and Nucleosides as Signalling Molecules. *Immunol Lett* (2019) 205:16–24. doi: 10.1016/j.imlet.2018.11.006
149. Montell C. The TRP Superfamily of Cation Channels. *Sci STKE* (2005) 2005: re3. doi: 10.1126/stke.2722005re3
150. Harcha PA, Lopez X, Saez PJ, Fernandez P, Barria I, Martinez AD, et al. Pannexin-1 Channels Are Essential for Mast Cell Degranulation Triggered During Type I Hypersensitivity Reactions. *Front Immunol* (2019) 10:2703. doi: 10.3389/fimmu.2019.02703
151. Lai CP, Bechberger JF, Naus ,CC. Pannexin2 as a Novel Growth Regulator in C6 Glioma Cells. *Oncogene* (2009) 28:4402–8. doi: 10.1038/onc.2009.283
152. O'donnell BL, Penuela S. Pannexin 3 Channels in Health and Disease. *Purinergic Signal* (2021). doi: 10.1007/s11302-021-09805-7
153. Sundara Rajan S, Longhi MP. Dendritic Cells and Adipose Tissue. *Immunology* (2016) 149:353–61. doi: 10.1111/imm.12653

Conflict of Interest: The authors declare that the research was conducted in the absence of any commercial or financial relationships that could be construed as a potential conflict of interest.

Publisher's Note: All claims expressed in this article are solely those of the authors and do not necessarily represent those of their affiliated organizations, or those of the publisher, the editors and the reviewers. Any product that may be evaluated in this article, or claim that may be made by its manufacturer, is not guaranteed or endorsed by the publisher.

frontiers in Immunology

ORIGINAL RESEARCH
published: 17 December 2021
doi: 10.3389/fimmu.2021.680071

GSK3β Interacts With CRMP2 and Notch1 and Controls T-Cell Motility

Mobashar Hussain Urf Turabe Fazil[1†], *Praseetha Prasannan*[1†], *Brandon Han Siang Wong*[1,2], *Amuthavalli Kottaiswamy*[1], *Nur Syazwani Binte Mohamed Salim*[1], *Siu Kwan Sze*[3] *and Navin Kumar Verma*[1*]

[1] Lee Kong Chian School of Medicine, Nanyang Technological University Singapore, Singapore, Singapore, [2] Interdisciplinary Graduate Programme, NTU Institute for Health Technologies (HealthTech NTU), Nanyang Technological University Singapore, Singapore, Singapore, [3] School of Biological Sciences, Nanyang Technological University Singapore, Singapore, Singapore

The trafficking of T-cells through peripheral tissues and into afferent lymphatic vessels is essential for immune surveillance and an adaptive immune response. Glycogen synthase kinase 3β (GSK3β) is a serine/threonine kinase and regulates numerous cell/tissue-specific functions, including cell survival, metabolism, and differentiation. Here, we report a crucial involvement of GSK3β in T-cell motility. Inhibition of GSK3β by CHIR-99021 or siRNA-mediated knockdown augmented the migratory behavior of human T-lymphocytes stimulated *via* an engagement of the T-cell integrin LFA-1 with its ligand ICAM-1. Proteomics and protein network analysis revealed ongoing interactions among GSK3β, the surface receptor Notch1 and the cytoskeletal regulator CRMP2. LFA-1 stimulation in T-cells reduced Notch1-dependent GSK3β activity by inducing phosphorylation at Ser9 and its nuclear translocation accompanied by the cleaved Notch1 intracellular domain and decreased GSK3β-CRMP2 association. LFA-1-induced or pharmacologic inhibition of GSK3β in T-cells diminished CRMP2 phosphorylation at Thr514. Although substantial amounts of CRMP2 were localized to the microtubule-organizing center in resting T-cells, this colocalization of CRMP2 was lost following LFA-1 stimulation. Moreover, the migratory advantage conferred by GSK3β inhibition in T-cells by CHIR-99021 was lost when CRMP2 expression was knocked-down by siRNA-induced gene silencing. We therefore conclude that GSK3β controls T-cell motility through interactions with CRMP2 and Notch1, which has important implications in adaptive immunity, T-cell mediated diseases and LFA-1-targeted therapies.

Keywords: GSK3β, NOTCH1, T-lymphocytes, LFA-1, T-cell migration

OPEN ACCESS

Edited by:
Emmanuel Donnadieu, Institut National de la Santé et de la Recherche Médicale (INSERM), France

Reviewed by:
Jerome Delon, INSERM U1016 Institut Cochin, France
Vincenzo Di Bartolo, Institut Pasteur, France

***Correspondence:**
Navin Kumar Verma
nkverma@ntu.edu.sg

[†]*These authors have contributed equally to this work*

Specialty section:
This article was submitted to Molecular Innate Immunity, a section of the journal Frontiers in Immunology

Received: *13 March 2021*
Accepted: *30 November 2021*
Published: *17 December 2021*

Citation:
Fazil MHUT, Prasannan P, Wong BHS, Kottaiswamy A, Salim NSBM, Sze SK and Verma NK (2021) GSK3β Interacts With CRMP2 and Notch1 and Controls T-Cell Motility. Front. Immunol. 12:680071. doi: 10.3389/fimmu.2021.680071

INTRODUCTION

In a healthy human under physiological conditions, T-lymphocytes continuously recirculate between the peripheral lymphoid tissues *via* the blood and lymphatic systems to perform an active immune surveillance as well as mount an adaptive immune response. Dysregulation of T-cell recruitment can result in impaired adaptive immunity, recurrent infections, chronic inflammation, and a diverse range of autoimmune diseases (1).

T-cell trafficking is mediated by an active engagement of cell surface receptors, cytoskeletal remodeling, and a broad array of signal transduction processes, including activation/deactivation of kinases and phosphatases (2). In particular, the T-cell αLβ2 integrin lymphocyte function-associated antigen-1 (LFA-1; CD11a/CD18) binds to its ligand intercellular adhesion molecule-1 (ICAM-1) expressed on the endothelium, and this adhesive interaction is crucial for T-cell migration and effector functions (3). The molecular machinery and the downstream pathways triggered by LFA-1 attachment to the ICAM-1 facilitating T-cell motility remain unclear.

The glycogen synthase kinase 3 (GSK3) is a ubiquitous constitutively active serine/threonine kinase that exists in two isoforms, GSK3α and GSK3β, and targets over hundred proteins to regulate context-specific cellular functions (4). Initially uncovered as a key enzyme involved in glycogen synthesis, GSK3β is now known to regulate cell cycle, development, survival, metabolism, and inflammation in multiple cell types (5–8). However, GSK3β involvement in T-cell motility is yet to be fully understood.

The functional activities of GSK3β are regulated by its post-translational modifications, nuclear localization, and interactions with other proteins. The phosphorylation of a Ser9 residue in the N-terminus of the GSK3β protein (pGSK3β-S9) by other kinases, such as Akt, phosphatidylinositol-3-kinase (PI3K), and protein kinase C (PKC) isoforms, inactivates GSK3β (4). This, in turn, drives dynamic fluxes of primed substrates contributing to the regulation of cell/tissue-specific functions. We have previously reported that LFA-1/ICAM-1 ligation in human peripheral blood lymphocyte (PBL) T-cells promotes Th1 polarization through a GSK3β-dependent pathway (9). Here, we identify GSK3β-interacting proteins and show that GSK3β interacts with the Notch1 and collapsing response mediator protein 2 (CRMP2) and regulates T-cell motility.

MATERIALS AND METHODS

Human T-Cell Isolation and Culture

Human primary PBL T-cells were isolated from healthy volunteers or leukocyte reduction system (LRS) cones obtained from the Health Sciences Authority (HSA) of Singapore using Lymphoprep™ density gradient medium (STEMCELL Technologies) and centrifugation as described previously (10). All experiments involving human peripheral blood or components were approved by the Nanyang Technological University Singapore Institutional Review Board (IRB-2018-05-034 and IRB-2014-09-007). The human T-cell line HuT78 was obtained from the American Type Culture Collection (ATCC, Manassas, VA) and cultured in Gibco™ RPMI 1640 medium supplemented with 10% fetal bovine serum, 1 mM sodium pyruvate and antibiotics (penicillin 100 units/ml, streptomycin 100 μg/ml) at 37°C and 5% CO_2 as described (11).

Antibodies and Reagents

Anti-GSK3β, anti-pGSK3β-S9, anti-CRMP2, and anti-rabbit antibodies were from Cell Signaling Technology. Anti-pCRMP2-T514 and anti-pericentrin antibodies were from Abcam. Anti-GM130 was from MBL International. IL-2 and stromal cell-derived factor 1 (SDF-1α) were obtained from PeproTech. The GSK3β inhibitor CHIR-99021 was obtained from STEMCELL Technologies. The γ-secretase inhibitor N-[(3,5-difluorophenyl) acetyl]-L-alanyl-2-phenylglycine-1,1-dimethyl ethyl ester (DAPT) was from Merck Millipore. Recombinant human ICAM-1 (rICAM-1) was procured from Sino Biological. Anti-mouse antibody was from Agilent Technologies. Dimethyl sulfoxide (DMSO), poly-l-lysine (PLL), Phalloidin-Alexa Fluor® 647, CellMask™ (Orange), Hoechst-33342, anti-rabbit and anti-mouse fluorescent secondary antibodies, Gibco™ RPMI 1640 and cell culture supplements were purchased from Thermo Fisher Scientific.

LFA-1/ICAM-1-Induced T-Cell Migration

We used our well-characterized T-cell migration *in vitro* model, where primary or cultured T-cells were seeded on rICAM-1-coated plates and cells were allowed to migrate as described previously (12). Briefly, 5 μg/ml anti-human IgG (Fc specific) in sterile phosphate buffered saline (PBS, pH 7.2) was coated on 6- or 96-well tissue culture plates or 18 mm coverslips overnight at 4°C. After washing with PBS, 1 μg/ml rICAM-1 was added into the wells of the plates/coverslips and incubated for another 2 h at 37°C. Wells of the plates/coverslips were washed with PBS before seeding T-cells (20×10^3 cells/well in 96-well plate; 200×10^3 cells/well in 6-well plate) in an activation medium. The activation medium consisted of cell culture medium with added 5 mM $MgCl_2$ and 1.5 mM EGTA.

Live Cell Imaging of LFA-1/ICAM-1-Stimulated Migrating T-Cells

We used an established live cell imaging protocol to quantify T-cell migration by an automated microscopy (13). Briefly, control or pretreated T-cells were stained with CellMask™ and added on an rICAM-1-coated 96-well flat-bottom plate (2×10^4 cell per well) and cells were allowed to migrate as described above. Live cell migration was recorded using an automated microscope IN Cell Analyzer 2200 (GE Healthcare) equipped with temperature and environmental controls. Cell tracking and measurements of distance were performed using the Imaris software (Andor-Bitplane, Zurich).

Real-Time Monitoring of T-Cell Migration in 2D and Through Transwell Membranes

Kinetic monitoring of T-cell migration on rICAM-1-coated 2D surfaces and through transwell membrane towards the chemokine SDF-1α was performed using xCELLigence E-Plate 16 and CIM-Plate 16, respectively, and the Real-Time Cell Analysis (RTCA) instrument (Agilent). The E-Plate 16 plates contain gold microelectrodes embedded in the bottom of each well that can continuously monitor the adhesion and spreading of motile T-cells by automatic measurement of the changes in impedance signals. For T-cell 2D migration assays, bottom surfaces of the E-Plate 16 wells were coated with 1 μg/ml rICAM-1 at 37°C for 2 h. T-cells that have been pre-treated

under various experimental conditions, as indicated in the corresponding figure legends, were added in the wells of the rICAM-1-coated E-Plate 16 (2×10^4 cells/well) in 100 µl activation medium in triplicates. Changes in T-cell migratory phenotypes in 2D, including cell adhesion and spreading, were automatically recorded by impedance measurements using the RTCA system. For transwell migration assays, upper chambers of the CIM-plate 16 plates containing electronically integrated microporous membranes (pore size 8 µm) were coated with 1 µg/ml rICAM-1 at 37°C for 2 h, as describes earlier (14). T-cells that have been pre-treated under various experimental conditions, as indicated in the corresponding figure legends, were loaded in the upper chambers of the CIM-Plate 16 (1×10^5 cells/well) in 100 µl activation medium in triplicates. Cells were allowed to transmigrate through the membrane toward 100 ng/ml SDF-1α-enriched medium in the lower wells at 37°C. T-cells passing through the pores of the rICAM-1-coated membrane were immediately detected by gold electrodes, covering the lower side of the membrane, and quantified by the RTCA system in terms of impedance changes in real-time. The kinetic data (baseline cell index) automatically recorded by the RTCA system over the course of the entire experiment was plotted against time and presented.

siRNA-Induced Knockdown of GSK3β and CRMP2

SMARTpool® siRNA targeted against GSK3β, CRMP2 and non-specific control siRNA (Dharmacon ON-TARGETplus siRNA Reagents, Thermo Fisher Scientific) were used. Actively growing HuT78 and PBL T-cells (1.2×10^6 cells) were mixed with siRNA molecules (100 nM) in the SF Cell Line and P3 Primary Cell 4D-Nucleofector™ X Kit, respectively. Cells were the nucleofected using the 4D-Nucleofector™ system (Lonza) according to the manufacturer's instructions and used for experiments after 72 h.

Co-Immunoprecipitation and Western Immunoblotting

T-cells treated under various experimental conditions were washed with PBS (4°C) and lysed in the cell lysis buffer as described earlier (15). The protein content of the cell lysates was determined by the Bradford protein assay (Bio-Rad). For co-immunoprecipitation assays, whole cell lysates (WCL, 500 µg each) were gently mixed with 3 µg of the target antibody or an isotype control IgG. Protein A/G plus agarose beads (25 µl/sample) were added to the antibody/cell lysate mix and incubated for 4 h at 4°C on a benchtop rotating/rocking shaker. The immune complexes were gently washed with the buffer containing 0.1% Triton X-100, 20 mM HEPES (pH 7.4), 130 mM NaCl, 10% glycerol, 1 mM phenylmethylsulfonyl fluoride, 10 mM sodium fluoride, 2 mM sodium vanadate and a cocktail of protease inhibitors. WCL or immunoprecipitated protein samples were heated in Laemmli sample buffer (95°C for 5 min), separated by gel electrophoresis, and then transferred to a nitrocellulose or PVDF membrane. Membranes were blocked using 5% Blotto or 2.5% bovine serum albumin (BSA) (Thermo Fisher Scientific) in PBS-0.05% Tween 20 for about 1 h at room temperature. Membranes were then incubated with primary antibody overnight at 4°C on a rotating shaker. After three washes, membranes were probed with corresponding HRP-conjugated secondary antibody for 1-2 h at room temperature. After washing, membranes were developed using an enhanced chemiluminescence reagent (Thermo Fisher Scientific) and imaged using ChemiDoc™ Gel Imaging System (Bio-Rad) or light sensitive films.

GSK3β Interactome Analysis by LC-ESI-MS/MS

GSK3β-interacting proteins were co-immunoprecipitated from cellular lysates of resting (unstimulated) or LFA-1/ICAM-1-stumulated migrating T-cells using anti-GSK3β antibody and peptide identification was carried out by LC-MS/MS analysis. Briefly, GSK3β co-immunoprecipitated samples (from 2 mg protein each) were resolved by native gel electrophoresis and the proteins were digested in-gel with trypsin (Promega) after reduction and alkylation. Tryptic peptides were desalted using a C18 SPE cartridge (Waters, Singapore). The peptides were dried, reconstituted with 3% acetonitrile and 0.1% formic acid, and then separated and analysed using a coupled to a Q-Exactive tandem mass spectrometry coupled with Dionex Ultimate™ 3000 RSLCnano system (Thermo Fisher Scientific). Separation was performed on an EASY-Spray™ column (75 µm × 10 cm) packed with PepMap C18 3 µm, 100 Å (Thermo Fisher Scientific) using solvent A (0.1% formic acid) and solvent B (0.1% formic acid in 100% acetonitrile) at flow rate of 300 nL/min with a 60 min gradient. Peptides were then analysed on the Q-Exactive apparatus with the EASY-Spray™ Source (Thermo Fisher Scientific) at an electrospray potential of 1.5 kV. A full MS scan (350–1,600 m/z range) was acquired at a resolution of 70,000 and a maximum ion accumulation time of 100 ms. Dynamic exclusion was set as 30 s. The resolution of the higher energy collisional dissociation spectra was set to 350,00. The automatic gain control settings of the full MS scan and the MS2 scan were 5E6 and 2E5, respectively. The 10 most intense ions above the 2,000-count threshold were selected for fragmentation in higher energy collisional dissociation, with a maximum ion accumulation time of 120 ms. An isolation width of 2 m/z was used for MS2. Single and unassigned charged ions were excluded from MS/MS analysis. For higher energy collisional dissociation, the normalized collision energy was set to 28. The underfill ratio was defined as 0.3%. Raw data files were processed and converted to Mascot generic files format and submitted for database searching against the UniProt Human database with Mascot (v2.4.1, Matrix Science). The criteria used to filter results included 1% false positive threshold, expect value < 0.05 for significant peptide matches and the emPAI score was calculated as per a standard Mascot protein family report. Moreover, identification of peptides required at least two unique peptides under the standard search parameters. The mascot results were exported as.csv files for further analysis in Excel program (Microsoft Singapore Pte Ltd.).

Ingenuity Pathway Analysis (IPA®)

The IPA® software program (Qiagen) is a well-established bioinformatics tool facilitating identification of molecular relationships, mechanisms, and functions through dynamic pathway modelling. An updated repository of biological interactions (Ingenuity® Knowledge Base) is utilized to create functional annotations from individually modelled relationships among proteins, genes, cells etc. We employed IPA® to decipher dynamic molecular changes in GSK3β protein-protein interactions between resting T-cells and LFA-1/ICAM-1-stimulated migrating T-cells. To generate biological networks, protein dataset obtained from Mascot analysis was uploaded onto the IPA® software and IPA® protein networks were created and scored based on a Fisher's exact test, indicating the likelihood of proteins associating into the GSK3β network by random chance. The core analysis was restricted to the immune cells to extract the relationships.

Confocal Microscopy, High Content Imaging and Analysis

T-cells were allowed to migrate on rICAM-1-coated (migrating) or PLL-coated (resting control) coverslips for 2 h and then cells were fixed with 4% (v/v) formaldehyde for 10 min as described (11). After permeabilization using 0.3% Triton X-100 (prepared in PBS) and blocking in 5% BSA, cells were immunostained for selected proteins. Hoechst-33342 was used to stain the nuclei. Fluorescently stained cells on coverslips were then mounted onto clear glass slides with the help of the Fluoromount™ Aqueous Mounting Medium (Sigma-Aldrich). A Zeiss LSM800 Airyscan microscope attached with 405, 488, 561, and 647 nm lasers and a 63X/1.4 numerical aperture (NA) oil immersion objective lens (Carl Zeiss, Inc.) was used for confocal imaging. At least 3 images were acquired under each treatment condition and ZEN lite 2.1 (Carl Zeiss) software was used for image processing, analysis, and presentation. Intensity profiles of selected molecular signals in the confocal images were generated using the ZEN lite 2.1 and were replotted using the GraphPad Prism software. To quantify the colocalization of the CRMP2 and pericentrin proteins, Pearson Correlation Coefficient (PCC) was calculated using the ZEN Black software (Carl Zeiss). Cellular/nuclear location of GSK3β, pGSK3β-S9, and CRMP2 in motile T-cells was quantified by high content imaging and automated analysis. Briefly, T-cells were allowed to migrate on the wells of the rICAM-1-coated 96-well tissue culture plate (2×10^4 cells/per well) for multiple time-points up to 2 h and fixed. Cells were then fluorescently labelled for GSK3β, pGSK3β-S9 or CRMP2 and co-stained with Rhodamine-Phalloidin and Hoechst to demarcate cytoplasmic and nuclear regions. Fluorescently labelled cells were then imaged by an automated microscope IN Cell Analyzer 2200 (GE Healthcare) using 20X objective (6 fields/well). Acquired image-sets containing >500 cells/well were subsequently analyzed cell-by-cell using the IN Cell Investigator software.

Statistical Analysis

The level of statistical significance was computed using one-way analysis of variance (ANOVA) with Dunnett's correction among experimental groups and the t-test using GraphPad Prism (v8.4.3, GraphPad). Difference with $p < 0.05$ was considered as significant.

RESULTS

GSK3β Inhibition Promotes T-Cell Motility

We first investigated the involvement of GSK3β in T-cell migration by real-time monitoring of motile T-cells in the presence of an established GSK3β inhibitor, CHIR-99021, using an automated live cell imaging. CHIR-99021 specifically inhibits GSK3α/β and its IC_{50} concentration is 7-10 nM in cell-free *in vitro* assays (16, 17). The effective inhibitory concentrations of CHIR-99021 in cultured mammalian cells have been reported to be in the range of 3 to 10 μM (18–31). Here we choose to pre-treat T-cells with 5 μM CHIR-99021 for 2 h to inhibit GSK3β in our experiments. Cellular treatment with CHIR-99021 significantly enhanced the migratory behaviour of T-cells following stimulation by LFA-1/ICAM-1 engagement (**Figure 1A** and **Videos 1**, **2** in **Supplementary Material**) without impacting T-cell viability (**Supplementary Figure S1A** in **Supplementary Material**). Quantification of the trajectories taken by motile T-cells over the course of 2 h showed that CHIR-99021-treated T-cells travelled significantly (>20%) longer distance compared to control (**Figure 1B**). GSK3β inhibition significantly increased the chemotactic potential of motile PBL T-cells as analysed by transwell assay using real-time impedance-based measurements (**Figure 1C**). Similarly, siRNA-induced knockdown of GSK3β in HuT78 T-cells (**Figure 1D**) enhanced their migratory action (**Figure 1E**) without impacting cell viability (**Supplementary Figure S1B** in **Supplementary Material**). Notably, CHIR-99021 treatment did not impact the ability of T-cells to proliferate or produce cytokines (IL-2 and IFN-γ) in response to activation *via* the T-cell receptor (**Supplementary Figure S2** in **Supplementary Material**).

GSK3β Interactome in LFA-1-Stimulated Migrating T-Cells Identifies Notch1 and CRMP2 Interactions

We next determined intracellular proteins that interact with endogenous GSK3β in LFA-1-stimulated motile T-cells by co-immunoprecipitation with anti-GSK3β antibody and subsequent mass spectrometry analysis as illustrated in **Figure 2A**. We detected 1,168 unique proteins directly or indirectly pulled down by anti-GSK3β [Mascot protein database search against Human Uniprot protein database, false discovery rate (FDR) ≤1%]. Based on protein abundance exponentially modified Protein Abundance Index (emPAI) scores (32) of GSK3β interactome, 256 candidate proteins were identified to be differentially associated with GSK3β (82 protein IDs with ≥2-fold higher emPAI score and 174 protein IDs with ≥2-fold lower emPAI score in LFA-1/ICAM-1-stimulated migrating T-cells compared to unstimulated resting cells, **Supplementary Table 1**). Of the 256 protein ID's, 243 were "analysis ready" consistent with Ingenuity® Knowledge Base and generated

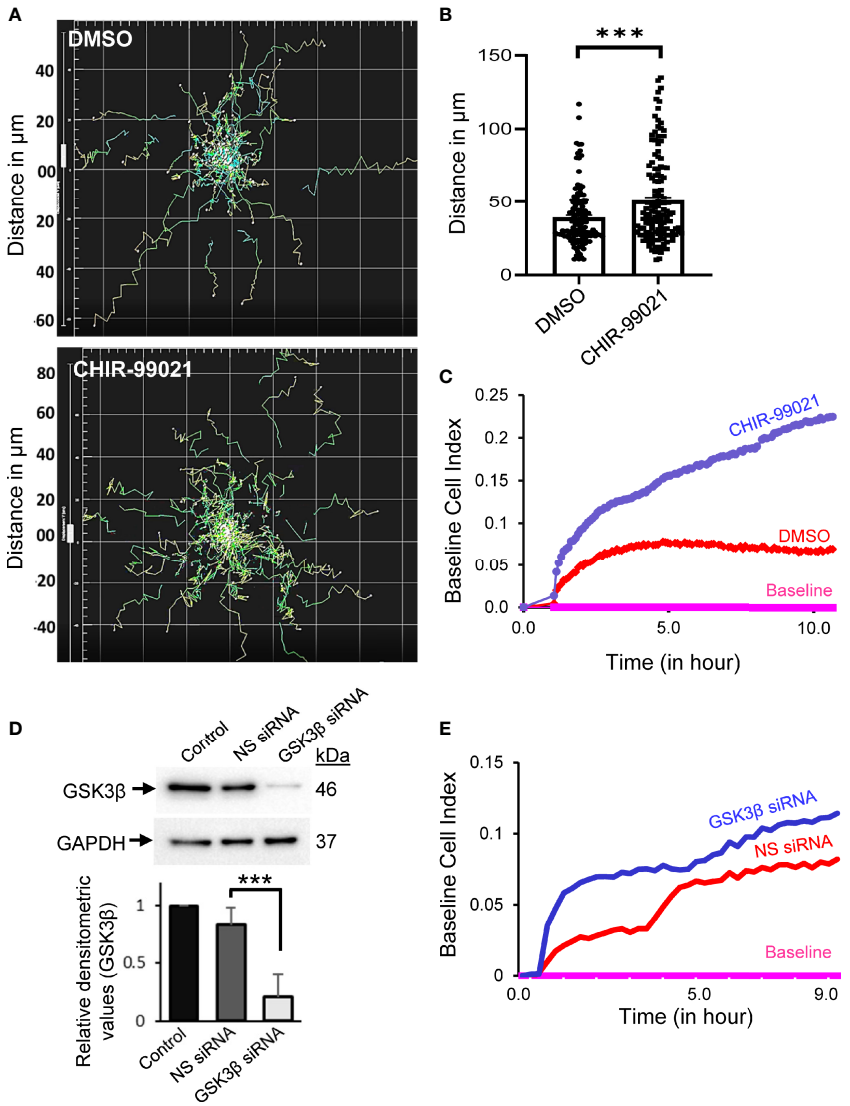

FIGURE 1 | Inhibition or depletion of GSK3β enhances T-cell motility. **(A)** Human primary T-cells were pre-treated with 5 µM CHIR-99021 for 2 h to inhibit GSK3β or DMSO (solvent control). Cells were then allowed to migrate on rICAM-1-coated plate and tracked in live cell microscopy. Spider plots showing the traced tracks of cells are presented. **(B)** Distance travelled by migrating T-cells over a 2-h period in µm. **(C)** Transwell chemotaxis of primary T-cells towards the chemokine SDF-1α, as determined using CIM-Plate 16 and real-time impedance-based measurements by the RTCA instrument. **(D)** HuT78 T-cells were nucleofected with 100 nM siRNA targeting GSK3β or non-specific (*NS*) siRNA. After 72 h, cells were lysed and the expression levels of GSK3β was determined by Western immunoblotting. Blots were re-probed for GAPDH as a loading control. The relative densitometry values for GSK3β were determined and plotted (mean ± SEM). **(E)** Transwell chemotaxis of control (*NS siRNA*) and GSK3β-depleted (*GSK3β siRNA*) HuT78 T-cells towards SDF-1α was determined using CIM-Plate 16 and real-time impedance-based measurements. Baseline was drawn automatically for wells without SDF-1α. Data represent at least three independent experiments. ***$p < 0.001$.

multiple canonical pathways, upstream regulators, associated diseases, and cellular functions. The top diseases and functions associated with the GSK3β interactome included cellular compromise, cellular movement, inflammatory response, and immune cell trafficking. Of the major canonical pathways with a positive Z-score among the protein networks were RhoGDI signaling, sirtuin signaling pathway, hippo signaling and Wnt/β-catenin signaling pathways (**Supplementary Figure S3** in **Supplementary Material**). Four direct interactions of GSK3β identified in the enriched network were *i*) Notch1, *ii*) dihydropyrimidinase-related protein 2 (DPYSL2, also called CRMP2), *iii*) ribosomal protein S6 kinase beta-1 (RPS6KB1), and *iv*) caspase recruitment domain-containing protein 11 (CARD11) (**Figure 2B**). Of note, based on empirical abundance scores, the CRMP2-GSK3β association was more pronounced in resting T-cells in comparison to migrating T-cells.

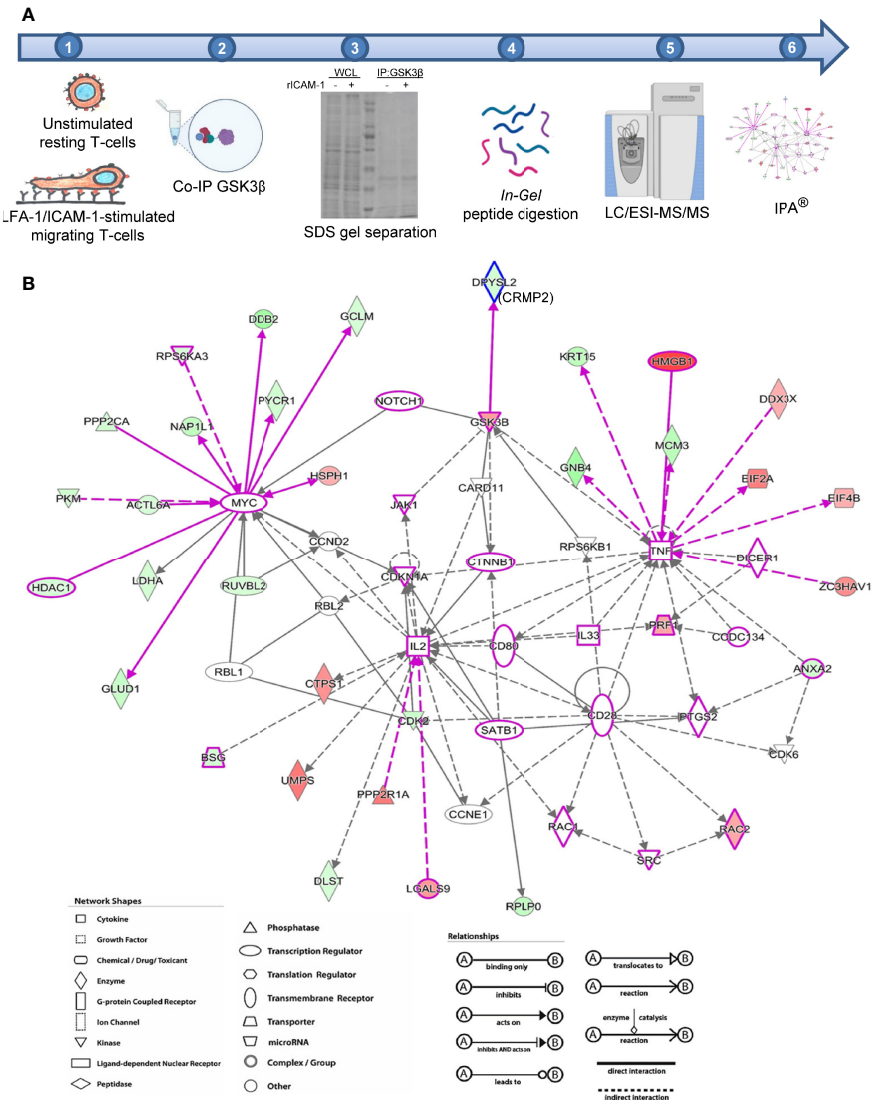

FIGURE 2 | Identification of GSK3β interactome in migrating T-cells. **(A)** Schematic representation of workflow employed in mass spectrometry-based proteomics analysis of GSK3β interacting proteins in human HuT78 T-cells. **(B)** Image output from IPA Ingenuity Knowledge Base indicating statistically probable interactions of GSK3β in LFA-1-stimulated T-cells. Proteins depicted in red are high abundance in migrating T-cells and proteins shown in green are low in abundance, compared to resting T-cells. The protein symbols in purple highlight proteins curated from Ingenuity Knowledge Base with potential roles in cellular movement and modelled relationships among known functional networks in immune cells. The type of proteins, network, shapes, and relationships in IPA are provided in the legends.

GSK3β Interaction With Notch1 and CRMP2 in LFA-1/ICAM-1-Stimulated Motile T-Cells

Concurrent with an increased phosphorylation of GSK3β (pGSK3β-S9) and cleavage of Notch1 intracellular domain (NICD) following LFA-1 stimulation (**Figures 3A, B**), pGSK3β-S9 translocated to the nucleus in LFA-1/ICAM-1-stimulated migrating T-cells (**Figure 3C** and **Supplementary Figure S4** in **Supplementary Material**). The LFA-1-induced translocation of pGSK3β-S9 to the nucleus occurred in a time-dependent manner reaching to maximum in a time-window of 10 to 30 min of stimulation (**Figure 3D**). This pGSK3β-S9 translocation was accompanied with cleaved NICD in motile T-cells (**Figure 3C**). Blocking Notch1 cleavage by the γ-secretase inhibitor DAPT (**Figure 3B**) inhibited LFA-1-induced pGSK3β-S9 phosphorylation (**Figure 3A**) and its nuclear translocation (**Figure 3C**, middle vs lower panels), and reduced T-cell migration (**Figure 3E**).

To comprehend an interaction between GSK3β and CRMP2, T-cells were stimulated to migrate *via* LFA-1/ICAM-1 and lysed. Cellular lysates were then immunoprecipitated using an anti-CRMP2 antibody or IgG (control) and probed for GSK3β and

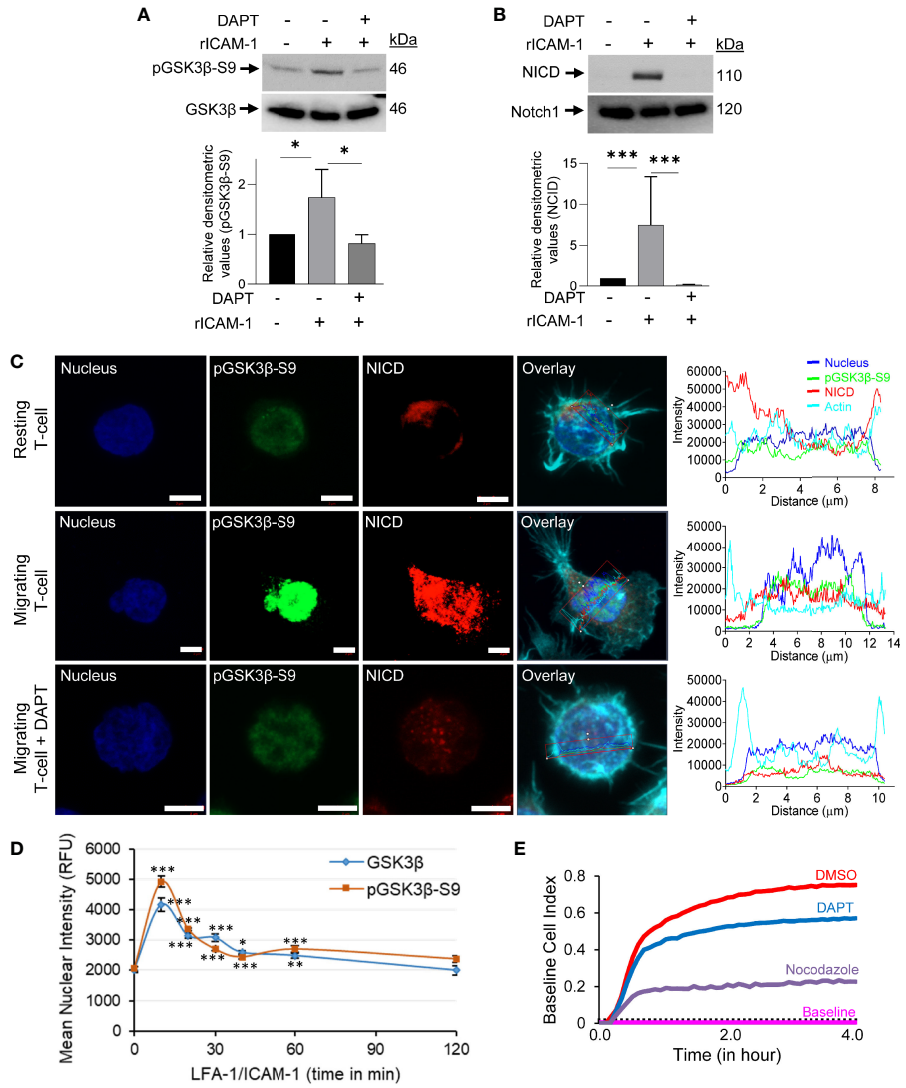

FIGURE 3 | GSK3β-Notch1 interactions in motile T-cells. **(A, B)** Human primary T-cells, untreated or pre-treated with 10 μM DAPT, were stimulated to migrate on rICAM-1-coated plates for 30 min and lysed. Cellular lysates were Western immunoblotted for pGSK3β-S9, GSK3β, NICD and total Notch1. The expression levels of proteins were quantified by determining relative densitometry (mean ± SEM) of pGSK3β-S9/GSK3β and NICD/Notch1. **(C)** Resting and LFA-1-stimulated HuT78 T-cells were immunostained with anti-pGSK3β-S9/Alexa Fluor® 488 (*green*), anti-NICD/Alexa Fluor® 568 (*red*), Phalloidin-Alexa Fluor® 647 (actin, *cyan*) and Hoechst (nucleus, *blue*) and then imaged by confocal laser scanning microscopy, 63X oil objective. Overlay images with intensity profiles (replotted using the GraphPad Prism software) of nucleus, pGSK3β-S9, NICD and actin are shown. Scale bar = 5 μm. **(D)** T-cells (2×10^4 cells/per well) were allowed to migrate on rICAM-1-coated 96-well plate for multiple time-points up to 2 h and fixed. Cells were stained for pGSK3β-S9 or GSK3β and imaged by an automated IN Cell Analyzer 2200 microscope using 20X objective (6 fields/well). Cellular images containing >500 cells/well were subsequently analysed cell-by-cell by the IN Cell Investigator software. **(E)** HuT78 T-cells were pre-treated with 10 μM DAPT, nocodazole (positive control), or DMSO (solvent control) and then allowed to migrate on rICAM-1-coated E-Plate 16. Cell migration was recorded in real-time using impedance-based measurements by the RTCA instrument. Wells without cells were used to automatically draw the baseline. Data represent at least three independent experiments. *$p < 0.05$; **$p < 0.01$; ***$p < 0.001$ compared to corresponding resting T-cells (0 min) control; RFU, relative fluorescent intensity.

CRMP2. Consistent with protein abundance scores from mass spectrometry, immunoblotting revealed a decreased interaction between GSK3β and CRMP2 in LFA-1-stimulated T-cells in comparison to unstimulated resting cells (**Figure 4A**). LFA-1 stimulation resulted in decreased phosphorylation of CRMP2 at the Thr514 residue, which could be partially rescued by DAPT (**Figure 4B**). The decreased phosphorylation of CRMP2 was also evident in T-cells treated with the GSK3β inhibitor CHIR-99021 (**Figure 4C**). While pGSK3β-S9 translocated to the nucleus following LFA-1 stimulation, CRMP2 remained in the cytoplasm (**Figures 4D, E** and **Supplementary Figure S5** in **Supplementary Material**).

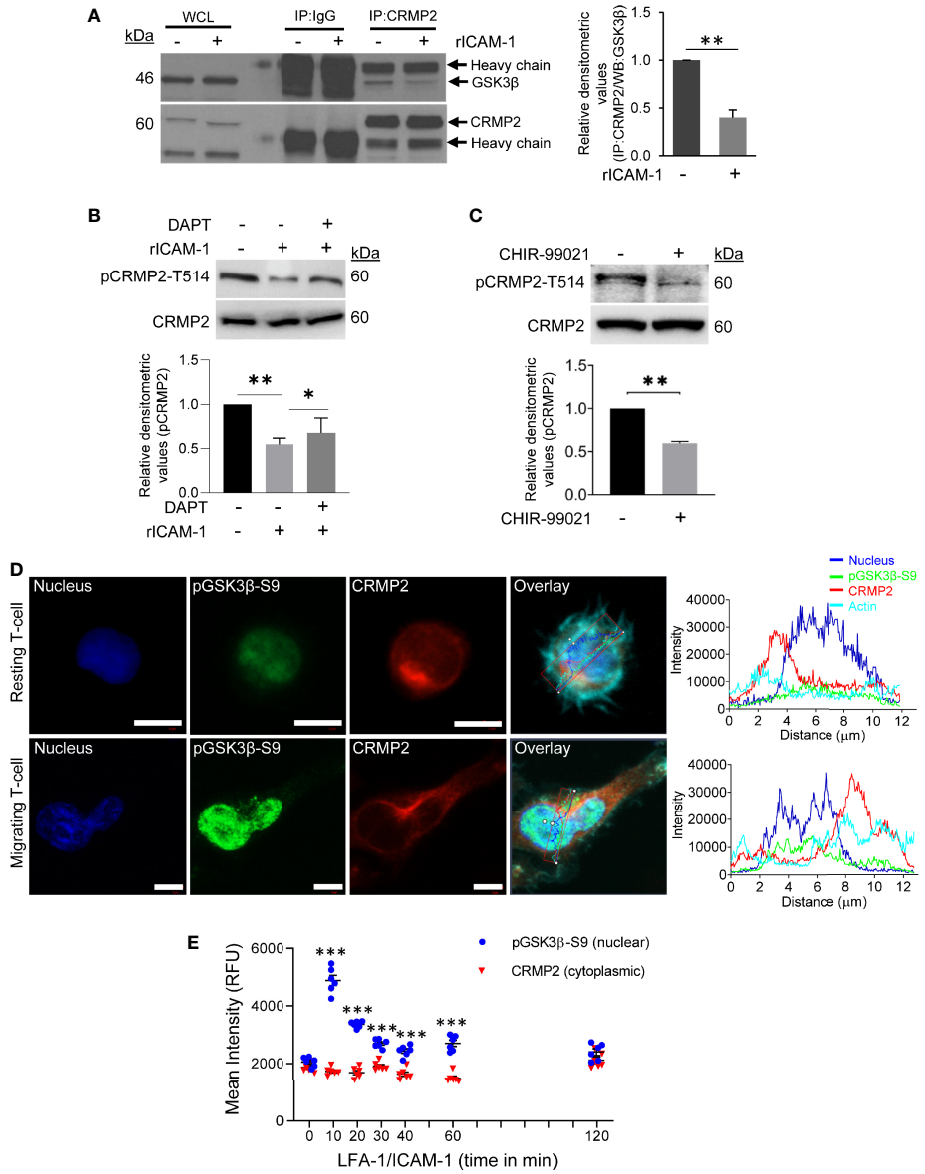

FIGURE 4 | GSK3β-CRMP2 interactions in motile T-cells. **(A)** Human primary T-cells were stimulated to migrate on rICAM-1-coated plates for 30 min and lysed. Cellular lysates from unstimulated or LFA-1/ICAM-1-stimulated T-cells were immunoprecipitated (*IP*) with anti-CRMP2 and Western immunoblotted for GSK3β and CRMP2. The amounts of GSK3β co-precipitating with CRMP2 were quantified by densitometry analysis (mean ± SEM). **(B)** Human primary T-cells, untreated or pre-treated with 10 μM DAPT, were stimulated to migrate on rICAM-1-coated plates for 30 min and lysed. **(C)** Human primary T-cells were treated with 5 μM CHIR-99021 or an equivalent amount of DMSO (solvent control) for 2 h and lysed. Cellular lysates in "B" and "C" were Western immunoblotted for pCRMP2-T514 and total CRMP2. The relative expression levels of pCRMP2-T514 were quantified by densitometry analysis (mean ± SEM). **(D)** Resting and LFA-1-stimulated migrating HuT78 T-cells were immunostained with anti-pGSK3β-S9/Alexa Fluor® 488 (*green*), anti-CRMP2/Alexa Fluor® 568 (*red*), Phalloidin-Alexa Fluor® 647 (actin, *cyan*) and Hoechst (nucleus, *blue*), and then imaged by confocal laser scanning microscopy, 63X oil objective. Overlay images with intensity profiles (replotted using the GraphPad Prism software) of nucleus, pGSK3β-S9, CRMP2 and actin are shown. Scale bar = 5 μm. **(E)** T-cells (2×10^4 cells/per well) were allowed to migrate on rICAM-1-coated 96-well plate for multiple time-points up to 2 h and fixed. Cells were stained for CRMP2 or pGSK3β-S9 and imaged by an automated IN Cell Analyzer 2200 microscope using 20X objective (6 fields/well). Cytoplasmic and nuclear intensities of CRMP2 and pGSK3β-S9, respectively, from >500 cells/well were subsequently analysed cell-by-cell by the IN Cell Investigator software. Each dot represents mean intensity values from >500 cells. Data represent at least three independent experiments. *p < 0.05; **p < 0.01; ***p < 0.001 compared to resting T-cells (0 min) control; RFU, relative fluorescent intensity.

To examine cellular localization of CRMP2 in motile T-cells, we performed confocal microscopy and subsequent image analysis. In resting T-cells, substantial amounts of CRMP2 were localized in close proximity to the microtubule-organizing center (MTOC), as determined by co-staining of cells with pericentrin (an MTOC marker) (**Figures 5A, B**). We used PCC to assess the overall proximity of CRMP2 and MTOC, additional confirmation of colocalization that provides

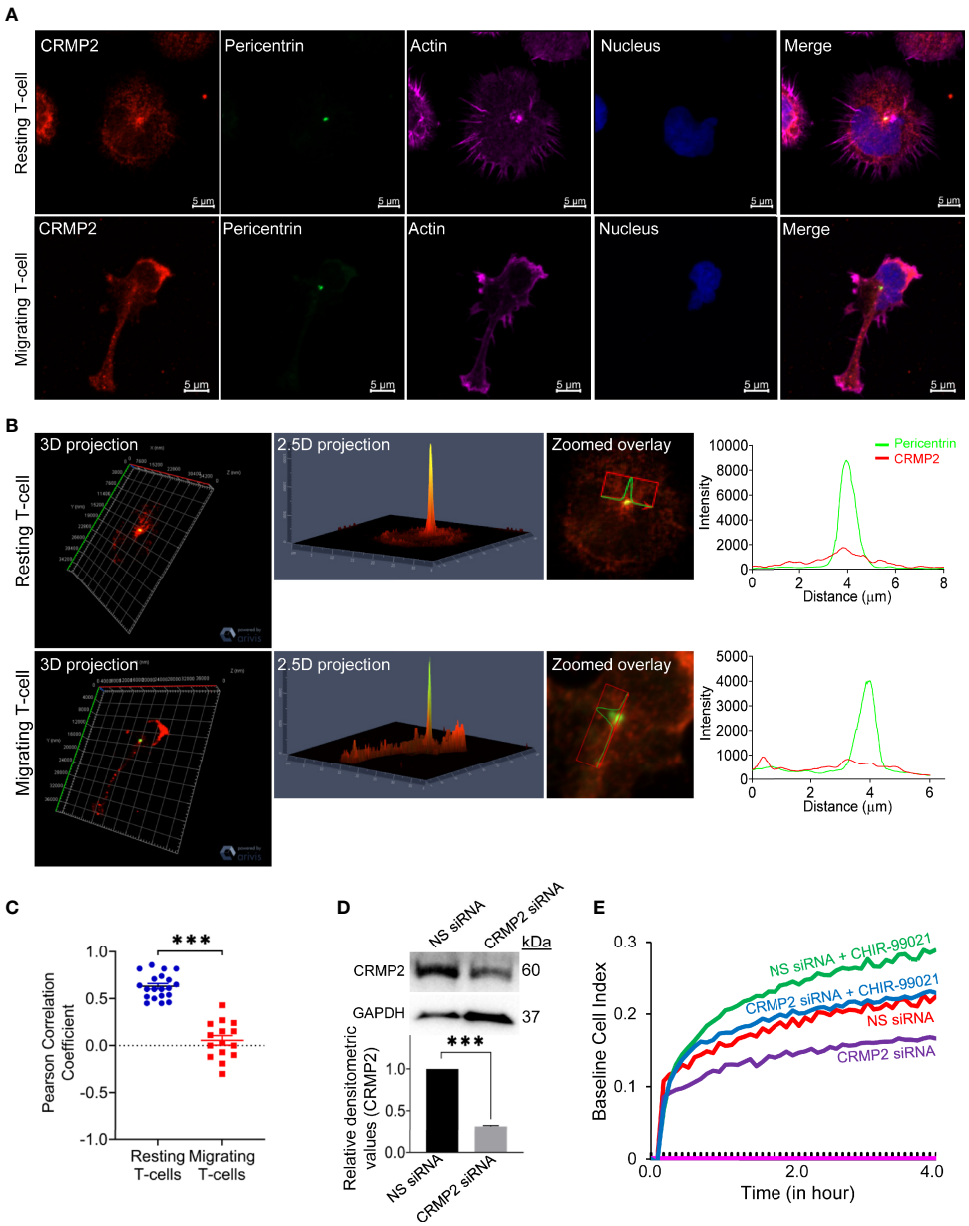

FIGURE 5 | CRMP2 colocalization to the MTOC and the effect of CRMP2 depletion on T-cell motility. **(A)** Resting and LFA-1-stimulated HuT78 T-cells were immunostained with anti-CRMP2/Alexa Fluor® 568 (*red*), anti-pericentrin/Alexa Fluor® 488 (*green*), phalloidin-Alexa Fluor® 647 (actin, *pink*) and Hoechst (nucleus, *blue*). Cells were then imaged by confocal laser scanning microscopy, array scan 63X objective. **(B)** 3D and 2.5D projections, zoomed overlay and intensity profiles (replotted using the GraphPad Prism software) of CRMP2 and pericentrin are shown. **(C)** Pearson Correlation Coefficient between CRMP2 and pericentrin was assessed using Carl Zeiss ZEN Black software. Each dot represents a single T-cell, and the images were taken from at least three independent experiments; n=20 for resting T-cells and n=15 for migrating T-cells; error bar, mean ± SEM. **(D)** PBL T-cells were nucleofected with 100 nM siRNA targeting CRMP2 or non-specific (*NS*) siRNA. After 72 h, cells were lysed, Western immunoblotted and probed for CRMP2. Blots were re-probed for GAPDH as a loading control. Relative densitometry values for CRMP2/GAPDH were determined and plotted (mean ± SEM). **(E)** The control (*NS siRNA*) and CRMP2-depleted (*CRMP2 siRNA*) PBL T-cells were treated with 5 µM CHIR-99021 for 2 h and then allowed to migrate on rICAM-1-coated E-Plate 16 for 4 h. Cell migration was recorded in real-time using impedance-based measurements by the RTCA instrument. Wells without cells were used to automatically draw the baseline. Data represent at least three independent experiments. ***$p < 0.001$.

quantitative values ranging from +1.0 (total positive correlation), 0 (no correlation) to -1.0 (total negative correlation). The mean PCC value for CRMP2 and pericentrin in unstimulated resting T-cells was above 0.5 (**Figure 5C**), indicating a high instance of colocalization. This MTOC colocalization of CRMP2 was lost following LFA-1 stimulation in motile T-cells with the mean PCC value significantly reduced to less than 0.1 (**Figure 5C**), indicating no-to-low colocalization. No colocalization or

containment of CRMP2 with the Golgi was detected in either resting or LFA-1-stimulated T-cells (**Supplementary Figure S6** in **Supplementary Material**). No further change in LFA-1-induced Notch1 cleavage or CRMP2 Thr514 phosphorylation was observed in cells that were pre-incubated with CHIR-99021 (**Supplementary Figure S7** in **Supplementary Material**). Most importantly, the migratory advantage conferred by CHIR-99021 treatment was lost when CRMP2 expression was knocked-down in T-cells (**Figures 5D, E**), indicating that GSK3β inhibition favours CRMP2-dependent T-cell migration. CRMP2-depleted cells exhibited an inhibition of migration compared to control T-cells (**Figure 5E**), implying a crucial involvement of CRMP2 in T-cell motility.

DISCUSSION

The current study demonstrates a crucial involvement of GSK3β in T-cell migration, which is important for T-cells to respond to environmental cues, such as chemokines, in order to mount an effective immune response. We show that selective inhibition or depletion of GSK3β enhances T-cell motility. GSK3β putatively interacts with multiple proteins in the signaling pathways triggered *via* LFA-1/ICAM-1 engagement in motile T-cells. In particular, GSK3β interacts with Notch1 and CRMP2 during the process of T-cell locomotion.

CHIR-99021 is the most selective commercially available ATP-competitive inhibitor of GSK3α/β (16, 17). Cellular treatment with CHIR-99021 significantly increased the rate of migration and chemotaxis in human primary T-lymphocytes. In contrast, a recent study using a different inhibitor of GSK3α/β, SB415286, showed that prolonged (7 days) inhibition of GSK3 in mouse T-cells reduced cell motility in the presence of target cells (EL4-OVA) and decreased the number of cell-to-cell contacts required to induce target killing (33). At the same time, long-term inactivation of GSK-3α/β by SB415286 enhanced the tumor killing potency of the resultant cytolytic mouse T-cells (33, 34). Variable degree of inhibition of GSK3α/β due to inhibitor dose or discrepancies in period of culture could be assumed as the possible explanations for such divergent phenotypes. These variations also suggest a species-specific role of GSK3β in T-cell signaling and functioning. It has also been reported that the biological effects of CHIR-99021 are counteracted by the inhibition of Notch signaling (30).

GSK3β is one of the downstream substrates of the nutrient-sensing kinase, AMP-activated protein kinase (AMPK). This kinase is important in promoting glucose uptake and ATP production to match energy demands in motile T-cells in response to chemokines, such as CCL5 (35). Dynamic interactions among GSK3β, AMPK and β-catenin have been found to be important in controlling metabolic reprogramming, migration, and invasion in anoikis-resistant prostate cancer cells (36). Moreover, in a cultured glioma cell line U-251, GSK3β was shown to interact with Akt and snail and CUX1 pathway and regulate ionizing radiation-induced epithelial-mesenchymal transition as well as migration and invasion (37). In mice, an impaired inducible inactivation of the GSK3β, due to the loss of mDia1 and diminished microtubule dynamics, has been associated with compromised T-cell adhesion, migration, and *in vivo* trafficking (38). A regulatory role of GSK3β in the migration of high-glucose-induced human skin fibroblasts and neural crest lineage in mouse and Xenopus has also been reported (39, 40).

Notch1 is an important substrate for GSK3β (41) and plays a role in T-cell homeostasis and differentiation (42, 43). At the same time, GSK3β functions positively within the Notch pathway and protects the NICD from proteasome-mediated degradation (44). Notch signaling was found to be impaired in GSK3β-null embryonic fibroblasts (44). We have earlier reported GSK3β as an upstream regulator of Notch1 in the LFA-1 signaling pathway leading to T-cell Th1 polarization (9). In the present study, we showed that DAPT, in addition to inhibiting Notch1 cleavage, inhibited LFA-1-induced GSK3β Ser9 phosphorylation and its nuclear translocation. These suggest that GSK3β is also positioned downstream of Notch1 in the LFA-1-induced signaling cascade during the process of T-cell locomotion. We argue that the dynamic and interactive nature of LFA-1-stimulated signaling cascades dictate that downstream signals are in receipt of multiple communications at any given time. T-cell motility represents a net response to these intracellular signals and therefore the pathways mediating LFA-1 responses are frequently integrated. Simultaneous triggering of multiple pathways by LFA-1 stimulation could coincide with GSK3β Ser9 phosphorylation in potentiating Notch-dependent responses. We could also argue that bidirectional interactions exist between GSK3β and Notch pathways. Since GSK3β prefers prior phosphorylation of its substrates (45), NICD is likely to be primed by other kinases that are concurrently activated following LFA-1 stimulation. For example, the cyclin-dependent kinase 8 (Cdk8), Cdk5, and the dual-specificity tyrosine-regulated kinase 2 are known to phosphorylate NICD in various cell types (46–48). Earlier genetic studies using the Drosophila GSK3 ortholog, shaggy, and the rat GSK3 isoforms placed GSK3β downstream of the Notch in the transmission of intracellular signals and upstream of the Notch in the regulation of a cell's ability to communicate (49). These suggest that GSK3β integrates cell's signal transmitting and receiving abilities and that Notch1 exerts its influence on GSK3β, a kinase known to phosphorylate and regulate Notch signals. It would therefore be interesting to explore whether LFA-1 signaling-induced Notch1 cleavage primes subsequent interactions between NICD and pGSK3β-Ser9 or GSK3β Ser9 phosphorylation occurs during interaction with NICD with potential feedback loops that stimulate Notch-1 activity in motile T-cells.

Of the four direct relationships observed in the GSK3β interactome, CARD11 and RPSK6B1 regulate antigen-induced lymphocyte activation and signaling relays involving the mTOR pathway (50, 51). Studies suggest a correlation between GSK3β and mTORC1 in the regulation of energy-reliant transcriptional networks by mitogenic or metabolic signals like PI3K-Akt or ATP (52). In response to chemotactic stimulation, GSK3 directly

phosphorylates RacE-GDP at the Ser192 residue, which controls mTORC2-mediated phosphorylation of Akt and directed cell migration (53). In this context, further exploration of GSK3β interaction with CARD11, RPSK and mTOR pathways would provide vital inputs on energy-dependent mechanisms in T-cell motility. The proteomics database presented in this study thus provides a foundation for more detailed studies to uncover GSK3β involvement in T-cell migration.

CRMP2 (also known as CRMP-62, Ulip2, TOAD-64 and DRP-2), initially reported exclusively in the developing nervous system, plays an important role in specifying axon/dendrite fate, possibly by promoting neurite elongation *via* microtubule assembly. This protein was later found to be expressed in peripheral T-cells and involved in T-cell polarization, recruitment and neuroinflammation (54–57). In particular, the upregulation of CRMP2 expression was recorded in subsets of T-cells bearing early and late activation markers, $CD69^+$ and $HLA\text{-}DR^+$, respectively (55). An involvement of CRMP2 in T-cell migration mediated *via* the chemokine CXCL12 (SDF-1α) and the extracellular signaling protein semaphorin has also been reported earlier (55, 56). In addition, previous studies noted a polarized distribution of CRMP2 at the uropod and its binding to the cytoskeletal protein, vimentin, following CXCL12-induced signaling (55, 56). In the current study, we observed substantial amounts of CRMP2 localized to the MTOC in resting T-cells, which was lost following LFA-1 stimulation in motile T-cells. These findings further confirm a role of CRMP2 in dynamic remodeling of the cytoskeletal systems during T-cell motility.

CRMP2 has been described as a microtubule-associated protein (58) that regulates microtubule dynamics in multiple ways. It associates with α/β-tubulin heterodimers and promotes their transport to the plus end of the growing microtubule (59). It serves as an adaptor to bring together motor proteins (e.g., kinesin-1) and tubulins to promote microtubule elongation (60). It enhances the GTPase activity of the β-tubulin and promotes the polymerization of α/β-tubulin heterodimers on the curved sheets of the microtubule ends (61). As microtubules elongate, CRMP2 moves along the growing plus end to stabilize newly polymerized microtubules (61). The phosphorylation of CRMP2 impedes the binding between CRMP2 and the microtubule (58, 62, 63). In neural cells, sequential phosphorylation of CRMP2 at the C-terminus by several serine/threonine kinases has been shown to be crucial for CRMP2 function (62). For example, Rho-kinase phosphorylates CRMP2 at Thr555 (64, 65) and the Cdk5 kinase phosphorylates CRMP2 at Ser522 (57, 66). Differential phosphorylation of CRMP2 at multiple sites by multiple kinases is thus a crucial regulatory mechanism for the dynamic reorganization of cytoskeleton required for the movement of different cell types. Structural studies have shown that the C-terminus phosphorylation of CRMP2 (*e.g.*, Thr514) confers negative charges adding repulsive forces between the CRMP2 and the E-hook of tubulin, that reduces its tubulin binding affinity and negatively regulates microtubule growth and stability, thus having the opposite effect of unphosphorylated CRMP2 (61, 67). CRMP2 dephosphorylation at Thr514 improves CRMP2 binding and stabilization of microtubules (63). In this regard, it can be inferred that observed decrease in CRMP2 Thr514 phosphorylation following LFA-1 stimulation or GSK3β inhibition by CHIR-99021 treatment promotes microtubule polymerization and facilitates T-cell migration. It would be fascinating to investigate, in future, whether decreased motility of CRMP2-depleted T-cells is due to microtubules being more susceptible to catastrophes in the absence of CRMP2.

In previous studies, Giraudon and colleagues reported CXCL12-induced decrease in CRMP2 phosphorylation at the Thr509/514 residues in motile T-cells (56). They further showed that this decrease in CRMP2 Thr509/514 phosphorylation was mediated *via* the GSK3β kinase (57). In addition, CXCL12 signaling was also found to enhance CRMP2 Tyr479 phosphorylation, a potential target site for the Src-family kinase Yes (56). It has been suggested that initial phosphorylation events in CRMP2 prime this protein for subsequent Thr509/514 phosphorylation by the GSK3β (68). In hippocampal neurons, inactivation of GSK3β by neurotrophin-3 was found to cause CRMP2 dephosphorylation leading to axon elongation and branching (63). Moreover, promotion of axonal regeneration was observed following genetic inhibition of CRMP2 phosphorylation at the Ser522 residue in a mouse model of optic nerve injury (69). Decreased interaction between GSK3β and CRMP2, diminished colocalization of CRMP2 with MTOC, and reduced CRMP2 phosphorylation (pCRMP2-T514) following LFA-1 stimulation and GSK3β inhibition by CHIR-99021 demonstrated in the current study provide a novel regulatory mechanism in T-cell motility.

Heightened CRMP2 expression in T-cell clones derived from patients that were infected with the retrovirus HTLV-1 has been associated with pathological T-lymphocyte CNS infiltration, implicated in virus-induced neuroinflammation (54, 57). The decreased interaction between GSK3β and CRMP2 facilitated by GSK3β Ser9 phosphorylation and NICD-GSK3β nuclear translocation observed in the current study could explain enhanced T-cell infiltration in neuroinflammation due to high levels of active CRMP2. Since multiple priming kinases and phosphatases contribute to differential regulation of CRMP2 by GSK3β (68), it is possible that, in addition to GSK3β, other enzymes are also activated by LFA-1/ICAM-1 cross-linking which phosphorylate/dephosphorylate CRMP2 in motile T-cells. In this context, ongoing interactions among GSK3β, Notch1, and CRMP2 are crucial in the maintenance of polarity and motility in human T-lymphocytes.

In conclusion, we demonstrate that LFA-1-induced Notch1 cleavage, GSK3β interaction with NICD and its inactivation by S9 phosphorylation (pGSK3β-S9), and consequent dephosphorylation of CRMP2 facilitate T-cell migration (**Figure 6**). Our work thus presents a novel mechanism involving GSK3β interaction with CRMP2 and Notch1 in the regulation of T-cell motility. These findings also imply that non-canonical GSK3β signaling plays a crucial role in the rapid response of T-

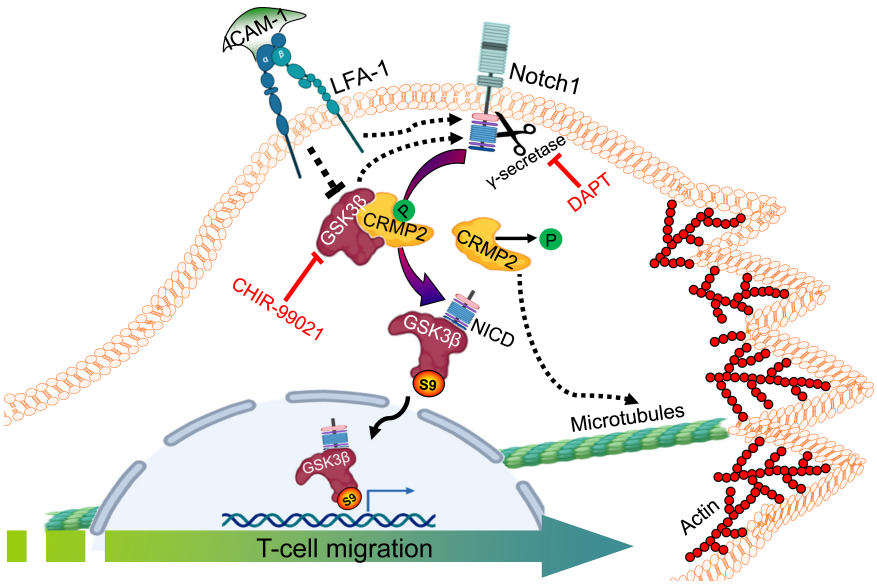

FIGURE 6 | An illustration of GSK3β-Notch1 and GSK3β-CRMP2 interactions in T-cell motility. LFA-1 stimulation-mediated signals in motile T-cells inactivate GSK3β by inducing its Ser9 phosphorylation. pGSK3β-S9 interacts with cleaved NICD and translocates to the nucleus. CRMP2 released from bound GSK3β further coordinates T-cell motility. The image created with BioRender.com.

cells to the extracellular signals. Targeting this multitier signaling interactions may therefore be considered to fine-tune T-cell motility, which has important implications in adaptive immune responses, chronic inflammation, and autoimmunity.

DATA AVAILABILITY STATEMENT

The original contributions presented in the study are included in the article/**Supplementary Material**. Further inquiries can be directed to the corresponding author.

AUTHOR CONTRIBUTIONS

NV conceptualized, designed, and supervised the project. MF, PP, BW, and AK performed experiments and contributed to the preparation of essential materials. NS performed GSK3β high content analysis experiments. MF, PP, and NV interpreted the results and drafted the manuscript. SS performed mass spectrometry and analysis, commented on the experiments, and edited the paper. All authors contributed to the article and approved the submitted version.

FUNDING

This work was supported by the grants from the Singapore Ministry of Education (MOE) Academic Research Fund (AcRF) Tier 1 (2014-T1-001-141 and 2020-T1-001-062) and the National Research Foundation Singapore under its Open Fund Large Collaborative Grant (OFLCG18May-0028) and administered by the Singapore Ministry of Health's National Medical Research Council (NMRC).

ACKNOWLEDGMENTS

Authors acknowledge Professor Dermot Kelleher, the University of British Columbia, Vancouver, Canada for his invaluable support.

SUPPLEMENTARY MATERIAL

The Supplementary Material for this article can be found online at: https://www.frontiersin.org/articles/10.3389/fimmu.2021.680071/full#supplementary-material

REFERENCES

1. von Andrian UH, Mackay CR. T-Cell Function and Migration. Two Sides of the Same Coin. *N Engl J Med* (2000) 343:1020–34. doi: 10.1056/NEJM200010053431407
2. Krummel MF, Bartumeus F, Gérard A. T Cell Migration, Search Strategies and Mechanisms. *Nat Rev Immunol* (2016) 16:193–201. doi: 10.1038/nri.2015.16
3. Verma NK, Kelleher D. Not Just an Adhesion Molecule: LFA-1 Contact Tunes the T Lymphocyte Program. *J Immunol* (2017) 199:1213–21. doi: 10.4049/jimmunol.1700495
4. Cohen P, Frame S. The Renaissance of GSK3. *Nat Rev Mol Cell Biol* (2001) 2:769–76. doi: 10.1038/35096075
5. Hur EM, Zhou FQ. GSK3 Signalling in Neural Development. *Nat Rev Neurosci* (2010) 11:539–51. doi: 10.1038/nrn2870

6. Maurer U, Preiss F, Brauns-Schubert P, Schlicher L, Charvet C. GSK-3 - at the Crossroads of Cell Death and Survival. *J Cell Sci* (2014) 127:1369–78. doi: 10.1242/jcs.138057
7. Cormier KW, Woodgett JR. Recent Advances in Understanding the Cellular Roles of GSK-3. *F1000Res* (2017) 6:F1000 Faculty Rev–167. doi: 10.12688/f1000research.10557.1
8. Beurel E. Regulation of Inflammation and T Cells by Glycogen Synthase Kinase 3: Links to Mood Disorders. *Neuroimmunomodulation* (2014) 21:140–4. doi: 10.1159/000356550
9. Verma NK, Fazil MH, Ong ST, Chalasani ML, Low JH, Kottaiswamy A, et al. LFA-1/ICAM-1 Ligation in Human T Cells Promotes Th1 Polarization Through a GSK3β Signaling-Dependent Notch Pathway. *J Immunol* (2016) 197:108–18. doi: 10.4049/jimmunol.1501264
10. Kizhakeyil A, Ong ST, Fazil MHUT, Chalasani MLS, Prasannan P, Verma NK. Isolation of Human Peripheral Blood T-Lymphocytes. *Methods Mol Biol* (2019) 1930:11–7. doi: 10.1007/978-1-4939-9036-8_2
11. Ong ST, Chalasani MLS, Fazil MHUT, Prasannan P, Kizhakeyil A, Wright GD, et al. Centrosome- and Golgi-Localized Protein Kinase N-Associated Protein Serves as a Docking Platform for Protein Kinase a Signaling and Microtubule Nucleation in Migrating T-Cells. *Front Immunol* (2018) 9:397. doi: 10.3389/fimmu.2018.00397
12. Verma NK, Palapetta SM, Ong ST, Fazil MHUT, Chalasani MLS, Prasannan P, et al. A Laboratory Model to Study T-Cell Motility. *Methods Mol Biol* (2019) 1930:19–23. doi: 10.1007/978-1-4939-9036-8_3
13. Ong ST, Verma NK. Live Cell Imaging and Analysis to Capture T-Cell Motility in Real-Time. *Methods Mol Biol* (2019) 1930:33–40. doi: 10.1007/978-1-4939-9036-8_5
14. Prasannan P, Verma NK. Real-Time Impedance-Based Detection of LFA-1-Stimulated T-Cell Transwell Chemotaxis. *Methods Mol Biol* (2019) 1930:51–7. doi: 10.1007/978-1-4939-9036-8_7
15. Verma NK, Dempsey E, Freeley M, Botting CH, Long A, Kelleher D, et al. Analysis of Dynamic Tyrosine Phosphoproteome in LFA-1 Triggered Migrating T-Cells. *J Cell Physiol* (2011) 226:1489–98. doi: 10.1002/jcp.22478
16. Davies SP, Reddy H, Caivano M, Cohen P. Specificity and Mechanism of Action of Some Commonly Used Protein Kinase Inhibitors. *Biochem J* (2000) 351:95–105. doi: 10.1042/bj3510095
17. Bain J, Plater L, Elliott M, Shpiro N, Hastie CJ, McLauchlan H, et al. The Selectivity of Protein Kinase Inhibitors: A Further Update. *Biochem J* (2007) 408:297–315. doi: 10.1042/BJ20070797
18. Schroeder JH, Bell LS, Janas ML, Turner M. Pharmacological Inhibition of Glycogen Synthase Kinase 3 Regulates T Cell Development *In Vitro*. *PloS One* (2013) 8:e58501. doi: 10.1371/journal.pone.0058501
19. Fan C, Oduk Y, Zhao M, Lou X, Tang Y, Pretorius D, et al. Myocardial Protection by Nanomaterials Formulated With CHIR99021 and FGF1. *JCI Insight* (2020) 5:e132796. doi: 10.1172/jci.insight.132796
20. Sineva GS, Pospelov VA. Inhibition of GSK3beta Enhances Both Adhesive and Signalling Activities of Beta-Catenin in Mouse Embryonic Stem Cells. *Biol Cell* (2010) 102:549–60. doi: 10.1042/BC20100016
21. Wu Y, Liu F, Liu Y, Liu X, Ai Z, Guo Z, et al. GSK3 Inhibitors CHIR99021 and 6-Bromoindirubin-3'-Oxime Inhibit Microrna Maturation in Mouse Embryonic Stem Cells. *Sci Rep* (2015) 5:8666. doi: 10.1038/srep08666
22. Ma Y, Ma M, Sun J, Li W, Li Y, Guo X, et al. CHIR-99021 Regulates Mitochondrial Remodelling *via* β-Catenin Signalling and Mirna Expression During Endodermal Differentiation. *J Cell Sci* (2019) 132:jcs229948. doi: 10.1242/jcs.229948
23. Huang J, Guo X, Li W, Zhang H. Activation of Wnt/β-Catenin Signalling *via* GSK3 Inhibitors Direct Differentiation of Human Adipose Stem Cells Into Functional Hepatocytes. *Sci Rep* (2017) 7:40716. doi: 10.1038/srep40716
24. D'Uva G, Aharonov A, Lauriola M, Kain D, Yahalom-Ronen Y, Carvalho S, et al. ERBB2 Triggers Mammalian Heart Regeneration by Promoting Cardiomyocyte Dedifferentiation and Proliferation. *Nat Cell Biol* (2015) 17:627–38. doi: 10.1038/ncb3149
25. Wang S, Ye L, Li M, Liu J, Jiang C, Hong H, et al. Gsk-3β Inhibitor CHIR-99021 Promotes Proliferation Through Upregulating β-Catenin in Neonatal Atrial Human Cardiomyocytes. *J Cardiovasc Pharmacol* (2016) 68:425–32. doi: 10.1097/FJC.0000000000000429
26. Govarthanan K, Vidyasekar P, Gupta PK, Lenka N, Verma RS. Glycogen Synthase Kinase 3β Inhibitor- CHIR 99021 Augments the Differentiation Potential of Mesenchymal Stem Cells. *Cytotherapy* (2020) 22:91–105. doi: 10.1016/j.jcyt.2019.12.007
27. Fan C, Tang Y, Zhao M, Lou X, Pretorius D, Menasche P, et al. CHIR99021 and Fibroblast Growth Factor 1 Enhance the Regenerative Potency of Human Cardiac Muscle Patch After Myocardial Infarction in Mice. *J Mol Cell Cardiol* (2020) 141:1–10. doi: 10.1016/j.yjmcc.2020.03.003
28. Cheng T, Zhai K, Chang Y, Yao G, He J, Wang F, et al. CHIR99021 Combined With Retinoic Acid Promotes the Differentiation of Primordial Germ Cells From Human Embryonic Stem Cells. *Oncotarget* (2017) 8:7814–26. doi: 10.18632/oncotarget.13958
29. Yoshida Y, Soma T, Matsuzaki T, Kishimoto J. Wnt Activator CHIR99021-Stimulated Human Dermal Papilla Spheroids Contribute to Hair Follicle Formation and Production of Reconstituted Follicle-Enriched Human Skin. *Biochem Biophys Res Commun* (2019) 516:599–605. doi: 10.1016/j.bbrc.2019.06.038
30. Li C, Zhang S, Lu Y, Zhang Y, Wang E, Cui Z. The Roles of Notch3 on the Cell Proliferation and Apoptosis Induced by CHIR99021 in NSCLC Cell Lines: A Functional Link Between Wnt and Notch Signaling Pathways. *PloS One* (2013) 8:e84659. doi: 10.1371/journal.pone.0084659
31. DeJonge RE, Liu XP, Deig CR, Heller S, Koehler KR, Hashino E. Modulation of Wnt Signaling Enhances Inner Ear Organoid Development in 3D Culture. *PloS One* (2016) 11:e0162508. doi: 10.1371/journal.pone.0162508
32. Ishihama Y, Oda Y, Tabata T, Sato T, Nagasu T, Rappsilber J, et al. Exponentially Modified Protein Abundance Index (Empai) for Estimation of Absolute Protein Amount in Proteomics by the Number of Sequenced Peptides Per Protein. *Mol Cell Proteomics* (2005) 4:1265–72. doi: 10.1074/mcp.M500061-MCP200
33. Taylor A, Harker JA, Chanthong K, Stevenson PG, Zuniga EI, Rudd CE. Glycogen Synthase Kinase 3 Inactivation Drives T-Bet-Mediated Downregulation of Co-Receptor PD-1 to Enhance CD8(+) Cytolytic T Cell Responses. *Immunity* (2016) 44:274–86. doi: 10.1016/j.immuni.2016.01.018
34. Taylor A, Rudd CE. Glycogen Synthase Kinase 3 (GSK-3) Controls T-Cell Motility and Interactions With Antigen Presenting Cells. *BMC Res Notes* (2020) 13:163. doi: 10.1186/s13104-020-04971-0
35. Chan O, Burke JD, Gao DF, Fish EN. The Chemokine CCL5 Regulates Glucose Uptake and AMP Kinase Signaling in Activated T Cells to Facilitate Chemotaxis. *J Biol Chem* (2012) 287:29406–16. doi: 10.1074/jbc.M112.348946
36. Zhang P, Song Y, Sun Y, Li X, Chen L, Yang L, et al. Ampk/Gsk3β/β-Catenin Cascade-Triggered Overexpression of CEMIP Promotes Migration and Invasion in Anoikis-Resistant Prostate Cancer Cells by Enhancing Metabolic Reprogramming. *FASEB J* (2018) 32:3924–35. doi: 10.1096/fj.201701078R
37. Fei Y, Xiong Y, Shen X, Zhao Y, Zhu Y, Wang L, et al. Cathepsin L Promotes Ionizing Radiation-Induced U251 Glioma Cell Migration and Invasion Through Regulating the GSK-3β/CUX1 Pathway. *Cell Signal* (2018) 44:62–71. doi: 10.1016/j.cellsig.2018.01.012
38. Dong B, Zhang SS, Gao W, Su H, Chen J, Jin F, et al. Mammalian Diaphanous-Related Formin 1 Regulates GSK3β-Dependent Microtubule Dynamics Required for T Cell Migratory Polarization. *PloS One* (2013) 8:e80500. doi: 10.1371/journal.pone.0080500
39. Wang Y, Zheng X, Wang Q, Zheng M, Pang L. Gsk3β-Ikaros-ANXA4 Signaling Inhibits High-Glucose-Induced Fibroblast Migration. *Biochem Biophys Res Commun* (2020) 531:543–51. doi: 10.1016/j.bbrc.2020.07.142
40. Gonzalez Malagon SG, Lopez Muñoz AM, Doro D, Bolger TG, Poon E, Tucker ER, et al. Glycogen Synthase Kinase 3 Controls Migration of the Neural Crest Lineage in Mouse and Xenopus. *Nat Commun* (2018) 9:1126. doi: 10.1038/s41467-018-03512-5
41. Espinosa L, Inglés-Esteve J, Aguilera C, Bigas A. Phosphorylation by Glycogen Synthase Kinase-3 Beta Down-Regulates Notch Activity, a Link for Notch and Wnt Pathways. *J Biol Chem* (2003) 278:32227–35. doi: 10.1074/jbc.M304001200
42. Brandstadter JD, Maillard I. Notch Signalling in T Cell Homeostasis and Differentiation. *Open Biol* (2019) 9:190187. doi: 10.1098/rsob.190187
43. Eagar TN, Tang Q, Wolfe M, He Y, Pear WS, Bluestone JA, et al. Notch 1 Signaling Regulates Peripheral T Cell Activation. *Immunity* (2004) 20:407. doi: 10.1016/s1074-7613(04)00081-0

44. Foltz DR, Santiago MC, Berechid BE, Nye JS. Glycogen Synthase Kinase-3beta Modulates Notch Signaling and Stability. *Curr Biol* (2002) 12:1006–11. doi: 10.1016/S0960-9822(02)00888-6
45. ter Haar E, Coll JT, Austen DA, Hsiao HM, Swenson L, Jain J. Structure of GSK3beta Reveals a Primed Phosphorylation Mechanism. *Nat Struct Biol* (2001) 8:593–6. doi: 10.1038/89624
46. Fryer CJ, White JB, Jones KA. Mastermind Recruits Cycc : CDK8 to Phosphorylate the Notch ICD and Coordinate Activation With Turnover. *Mol Cell* (2004) 16:509–20. doi: 10.1016/j.molcel.2004.10.014
47. Chu Q, Wang L, Zhang J, Wang W, Wang Y. CDK5 Positively Regulates Notch1 Signaling in Pancreatic Cancer Cells by Phosphorylation. *Cancer Med* (2021) 10:3689–99. doi: 10.1002/cam4.3916
48. Morrugares R, Correa-Sáez A, Moreno R, Garrido-Rodríguez M, Muñoz E, de la Vega L, et al. Phosphorylation-Dependent Regulation of the NOTCH1 Intracellular Domain by Dual-Specificity Tyrosine-Regulated Kinase 2. *Cell Mol Life Sci* (2020) 77:2621–39. doi: 10.1007/s00018-019-03309-9
49. Ruel L, Bourouis M, Heitzler P, Pantesco V, Simpson P. Drosophila Shaggy Kinase and Rat Glycogen Synthase Kinase-3 Have Conserved Activities and Act Downstream of Notch. *Nature* (1993) 362:557–60. doi: 10.1038/362557a0
50. Bedsaul JR, Carter NM, Deibel KE, Hutcherson SM, Jones TA, Wang Z, et al. Mechanisms of Regulated and Dysregulated CARD11 Signaling in Adaptive Immunity and Disease. *Front Immunol* (2018) 9:2105. doi: 10.3389/fimmu.2018.02105
51. Salmond RJ, Emery J, Okkenhaug K, Zamoyska R. MAPK. Phosphatidylinositol 3-Kinase, and Mammalian Target of Rapamycin Pathways Converge at the Level of Ribosomal Protein S6 Phosphorylation to Control Metabolic Signaling in CD8 T Cells. *J Immunol* (2009) 183:7388–97. doi: 10.4049/jimmunol.0902294
52. Bautista SJ, Boras I, Vissa A, Mecica N, Yip CM, Kim PK, et al. Mtor Complex 1 Controls the Nuclear Localization and Function of Glycogen Synthase Kinase 3β. *J Biol Chem* (2018) 293:14723–39. doi: 10.1074/jbc.RA118.002800
53. Senoo H, Kamimura Y, Kimura R, Nakajima A, Sawai S, Sesaki H, et al. Phosphorylated Rho-GDP Directly Activates Mtorc2 Kinase Towards AKT Through Dimerization With Ras-GTP to Regulate Cell Migration. *Nat Cell Biol* (2019) 21:867–78. doi: 10.1038/s41556-019-0348-8
54. Vuaillat C, Varrin-Doyer M, Bernard A, Sagardoy I, Cavagna S, Chounlamountri I, et al. High CRMP2 Expression in Peripheral T Lymphocytes Is Associated With Recruitment to the Brain During Virus-Induced Neuroinflammation. *J Neuroimmunol* (2008) 193:38–51. doi: 10.1016/j.jneuroim.2007.09.033
55. Vincent P, Collette Y, Marignier R, Vuaillat C, Rogemond V, Davoust N, et al. A Role for the Neuronal Protein Collapsin Response Mediator Protein 2 in T Lymphocyte Polarization and Migration. *J Immunol* (2005) 175:7650–60. doi: 10.4049/jimmunol.175.11.7650
56. Varrin-Doyer M, Vincent P, Cavagna S, Auvergnon N, Noraz N, Rogemond V, et al. Phosphorylation of Collapsin Response Mediator Protein 2 on Tyr-479 Regulates CXCL12-Induced T Lymphocyte Migration. *J Biol Chem* (2009) 284:13265–76. doi: 10.1074/jbc.M807664200
57. Varrin-Doyer M, Nicolle A, Marignier R, Cavagna S, Benetollo C, Wattel E, et al. Human T Lymphotropic Virus Type 1 Increases T Lymphocyte Migration by Recruiting the Cytoskeleton Organizer CRMP2. *J Immunol* (2012) 188:1222–33. doi: 10.4049/jimmunol.1101562
58. Lin PC, Chan PM, Hall C, Manser E. Collapsin Response Mediator Proteins (Crmps) Are a New Class of Microtubule-Associated Protein (MAP) That Selectively Interacts With Assembled Microtubules *via* a Taxol-Sensitive Binding Interaction. *J Biol Chem* (2011) 286:41466–78. doi: 10.1074/jbc.M111.283580
59. Fukata Y, Itoh TJ, Kimura T, Ménager C, Nishimura T, Shiromizu T, et al. CRMP-2 Binds to Tubulin Heterodimers to Promote Microtubule Assembly. *Nat Cell Biol* (2002) 4:583–91. doi: 10.1038/ncb825
60. Nakamura F, Ohshima T, Goshima Y. Collapsin Response Mediator Proteins: Their Biological Functions and Pathophysiology in Neuronal Development and Regeneration. *Front Cell Neurosci* (2020) 14:188. doi: 10.3389/fncel.2020.00188
61. Niwa S, Nakamura F, Tomabechi Y, Aoki M, Shigematsu H, Matsumoto T, et al. Structural Basis for CRMP2-Induced Axonal Microtubule Formation. *Sci Rep* (2017) 7:10681. doi: 10.1038/s41598-017-11031-4
62. Uchida Y, Ohshima T, Sasaki Y, Suzuki H, Yanai S, Yamashita N, et al. Semaphorin3A Signalling Is Mediated *via* Sequential Cdk5 and GSK3beta Phosphorylation of CRMP2: Implication of Common Phosphorylating Mechanism Underlying Axon Guidance and Alzheimer's Disease. *Genes Cells* (2005) 10:165–79. doi: 10.1111/j.1365-2443.2005.00827.x
63. Yoshimura T, Kawano Y, Arimura N, Kawabata S, Kikuchi A, Kaibuchi K. Gsk-3β Regulates Phosphorylation of CRMP-2 and Neuronal Polarity. *Cell* (2005) 120:137–49. doi: 10.1016/j.cell.2004.11.012
64. Arimura N, Ménager C, Kawano Y, Yoshimura T, Kawabata S, Hattori A, et al. Phosphorylation by Rho Kinase Regulates CRMP-2 Activity in Growth Cones. *Mol Cell Biol* (2005) 25:9973–84. doi: 10.1128/MCB.25.22.9973-9984.2005
65. Mimura F, Yamagishi S, Arimura N, Fujitani M, Kubo T, Kaibuchi K, et al. Myelin-Associated Glycoprotein Inhibits Microtubule Assembly by a Rho-Kinase-Dependent Mechanism. *J Biol Chem* (2006) 281:15970–9. doi: 10.1074/jbc.M510934200
66. Brittain JM, Wang Y, Eruvwetere O, Khanna R. Cdk5-Mediated Phosphorylation of CRMP-2 Enhances its Interaction With Cav2.2. *FEBS Lett* (2012) 586:3813–8. doi: 10.1016/j.febslet.2012.09.022
67. Sumi T, Imasaki T, Aoki M, Sakai N, Nitta E, Shirouzu M, et al. Structural Insights Into the Altering Function of CRMP2 by Phosphorylation. *Cell Struct Funct* (2018) 43:15–23. doi: 10.1247/csf.17025
68. Cole AR, Causeret F, Yadirgi G, Hastie CJ, McLauchlan H, McManus EJ, et al. Distinct Priming Kinases Contribute to Differential Regulation of Collapsin Response Mediator Proteins by Glycogen Synthase Kinase-3 *In Vivo*. *J Biol Chem* (2006) 281:16591–8. doi: 10.1074/jbc.M513344200
69. Kondo S, Takahashi K, Kinoshita Y, Nagai J, Wakatsuki S, Araki T, et al. Genetic Inhibition of CRMP2 Phosphorylation at Serine 522 Promotes Axonal Regeneration After Optic Nerve Injury. *Sci Rep* (2019) 9:7188. doi: 10.1038/s41598-019-43658-w

Conflict of Interest: The authors declare that the research was conducted in the absence of any commercial or financial relationships that could be construed as a potential conflict of interest.

frontiers in Immunology

MINI REVIEW
published: 10 March 2022
doi: 10.3389/fimmu.2022.733800

Control of Dendritic Cell Function Within the Tumour Microenvironment

*Yukti Hari Gupta**, *Abida Khanom* and *Sophie E. Acton**

Stromal Immunology Laboratory, MRC Laboratory for Molecular Cell Biology, University College London, London, United Kingdom

The tumour microenvironment (TME) presents a major block to anti-tumour immune responses and to effective cancer immunotherapy. The inflammatory mediators such as cytokines, chemokines, growth factors and prostaglandins generated in the TME alter the phenotype and function of dendritic cells (DCs) that are critical for a successful adaptive immune response against the growing tumour. In this mini review we discuss how tumour cells and the surrounding stroma modulate DC maturation and trafficking to impact T cell function. Fibroblastic stroma and the associated extracellular matrix around tumours can also provide physical restrictions to infiltrating DCs and other leukocytes. We discuss interactions between the inflammatory TME and infiltrating immune cell function, exploring how the inflammatory TME affects generation of T cell-driven anti-tumour immunity. We discuss the open question of the relative importance of antigen-presentation site; locally within the TME versus tumour-draining lymph nodes. Addressing these questions will potentially increase immune surveillance and enhance anti-tumour immunity.

Keywords: tumour microenvironment (TME), inflammatory cytokines, dendritic cells, anti-tumour immunity, draining lymph nodes, Tertiary Lymphoid Structures (TLS), immune infiltration

OPEN ACCESS

Edited by:
Jörg Renkawitz, Ludwig Maximilian University of Munich, Germany

Reviewed by:
Christine Moussion, Genentech, Inc., United States
Catherine Hedrick, La Jolla Institute for Immunology (LJI), United States
Toby Lawrence, King's College London, United Kingdom

****Correspondence:***
Yukti Hari Gupta
y.gupta@ucl.ac.uk
Sophie E. Acton
s.acton@ucl.ac.uk

Specialty section:
This article was submitted to Molecular Innate Immunity, a section of the journal Frontiers in Immunology

Received: *30 June 2021*
Accepted: *09 February 2022*
Published: *10 March 2022*

Citation:
Gupta YH, Khanom A and Acton SE (2022) Control of Dendritic Cell Function Within the Tumour Microenvironment. Front. Immunol. 13:733800. doi: 10.3389/fimmu.2022.733800

INTRODUCTION

Anti-tumour immunity is the ability of the body's immune system to recognise and eliminate tumour cells. This phenomenon has the potential to cure cancer even if cells are widely disseminated through multiple metastatic sites and has been harnessed to develop different immunotherapy drugs. With increased understanding of immune surveillance process by innate immune cells and discovery of T cell immune checkpoints, such as PD-1, PD-L1, and CTLA-4; cancer immunotherapy has significantly improved patient survival and quality of life (1–5). Treatments aim to promote successful infiltration and activation of antigen presenting cells and boost T-cells cytotoxic activity to promote anti-tumour immunity. However, despite promising results, not all tumour types or patients respond equally to immunotherapy (6–8). The major reasons for failure of immunotherapy are (1) reduced antigenicity (9–11) and (2) immunosuppressive tumour microenvironment (TME) (12–15). The TME is highly heterogeneous; consisting of tumour cells, stromal cells, extracellular matrix (ECM) and immune cell types including macrophages, dendritic cells, T and B lymphocytes, Natural killer (NK) cells, mast cells, myeloid derived suppressor cells

Abbreviations: APC, Antigen Presenting cells; LNs, Lymph nodes; TDLN, Tumour draining lymph node; TME, Tumour microenvironment; DCs, Dendritic cells; PGE2, Prostaglandin E2; ECM, Extracellular matrix; CAF, Cancer associated fibroblasts; TLS, Tertiary lymphoid structures.

(MDSCs) and neutrophils (16–20). The anti-tumour immune response relies on the antigen presenting cells (APCs) to prime naïve T cells. Tissue resident macrophages can activate T cells locally in the tumour; whereas dendritic cells (DCs), the professional APCs, are thought to migrate into the tumour draining lymph nodes (TDLNs) to prime T cells (21). However, immune surveillance by APCs and T-cell infiltration can be impaired by dynamic changes within the tumour microenvironment such as induction of chemokines, cytokines, growth factors, inflammation, ECM modulators and immune checkpoint proteins (22–27). This review focuses on the immunosuppressive properties of the TME and how these mechanisms alter activation, maturation and trafficking of dendritic cells to enable immune escape and tumour progression.

DC Maturation and DC Gene Signatures in Tumours

DCs are the professional APCs responsible for activation and maintenance of tumour-specific cytotoxicity by T cells (28, 29). Tumour infiltrating conventional DCs (cDC1 and cDC2) scan and phagocytose tumour antigens (30–32); and subsequently migrate to secondary lymphoid tissues to prime naïve CD8+ and CD4+ T cells (33–39). The phenotype and function of highly motile DCs is influenced by co-stimulatory molecules (CD80, CD86), chemokine receptors such as CCR7 and cell adhesion molecules (integrins, ICAM-1 and VCAM-1) (40–43). It has been well established that the interaction between CC chemokine receptor 7 (CCR7) upregulated on activated DCs and its ligand CC chemokine ligand 21 (CCL21) expressed by lymphatic endothelial cells (LECs) is essential for directional DC migration towards the lymph nodes (44–46). Upon entry to the LN, DCs use the C-type lectin CLEC-2 to migrate through the fibroblastic reticular network to reach the paracortex to stimulate the T cells (47–50). Secondary lymphoid tissues are structurally specialised to facilitate effective adaptive immune responses; however, the microenvironment of the tumour-draining lymph nodes (TDLNs) can be immune-suppressed in cancer patients and can display low DC count, defects in DC development, low levels of costimulatory molecules or accumulation of immature T cells (51, 52). DCs evaluated from TDLNs of an immunized B16F10 melanoma-bearing mice showed decreased functionality and expressed higher CD86 and lower CD206 levels (53). Similarly, in a study by Caronni et al., LNs draining lung tumours exhibited DCs with reduced antigen presentation due to downregulation of the SNARE VAMP3 and failed cytokine (IL12 and IFN-I) secretion. They reported lactic acid formation in the TME to be the main cause of DC function impairment (54). In addition, damage-associated molecular patterns (DAMPs) released from dying cells in the TME can also influence dendritic cells and other immune cells by interacting with toll-like receptors (TLRs) contributing to immunosuppressive phenotype (55). Lack of mature, migratory DCs in tumours correlates with poor prognosis in cancer patients and failure of immunotherapies (56–58). Recent development of single cell transcriptome profiling of tumour infiltrating DCs has proven to be a very powerful tool to map tumour-driven immune changes and to design future immune therapies leveraging DC biology. scRNA-seq studies on various human tumours, including non–small cell lung cancer (NSCLC) (59–62), head and neck squamous cell carcinoma (63), hepatocellular carcinoma (64), melanoma (65, 66), cutaneous squamous cell carcinoma (67), colorectal cancer (61, 68), ovarian cancer (61), and breast cancer (61) have identified tissue-specific DC subsets as well as those conserved across cancer types. By comparing tumour infiltrating DC states across various tumour studies, five major DC subsets have been defined that are conserved in most tumour types (69, 70) (**Table 1**). Four major ones are cDC1, cDC2, migratory DC3 (mDC3) and plasmacytoid DC (pDC); and the DC subset (DC5) that were less conserved, mostly contained cDC2 state (CD1C+) but additionally either expressed Langerhans cell-specific markers (CD201, CD1A) or monocyte markers (CD14, CD11b) such as in case of NSCLC (61, 62, 69, 70). DC5 were also referred as inflammatory DCs as these have phenotypic similarities to monocytes but are functionally different due to their cDC2-specific antigen presentation properties (71). On the other hand, classical monocytes (CD14+ CD16-) play a key role in tissue homeostasis and inflammation (72). Like monocytes, inflammatory DCs are also capable of releasing TNF-α and inducible nitric oxide synthase (iNOS) upon pathogen recognition. In addition, there is a subset of cDCs that induce antigen-specific tolerance in dLNs; known as regulatory DCs (DCregs) (73, 74). These are characterized by low MHC expression and therefore weaker antigen presentation capability to effector T cells. Instead, they can induce proliferation of regulatory T cells (Tregs) resulting in immune tolerance. These properties have led the use of DCregs in organ transplantations (75).

Overall cDC2 phenotype is the most abundant, while the other DC subtypes vary in each cancer type (61, 76). Single cell sequencing and clustering analysis have identified transcription factors underlying each DC phenotype, including *BATF3* for cDC1s, *CEBPB* for cDC2s, *NFKB2* for migratory cDCs and *TCF4* for pDCs (61, 77). Another study reports differential expression of costimulatory molecules and immune checkpoints on different DC subsets present in the TME (78). Although these phenomena are tightly regulated, heterogeneity of TME can influence the transcriptional factor activity, expression of costimulatory molecules and hence DC maturation and/or migration (78–82). This new in-depth knowledge of DC gene signatures can facilitate the design of a favourable antitumour response or identification of response biomarkers for targeted therapies (83).

TABLE 1 | Tumour infiltrating DC subsets detected in various human solid tumours – Liver, Ovarian, Lung, Breast and Colorectal (69, 70).

DC subsets	Markers
cDC1	XCR1, CLEC9A, CADM1, CD141, CD103
cDC2	CD11b, SIRPa, CLEC10A, FCER1A, CD1c
mDC3	MARCKS, CCL19, LAMP3, BATF3, CCR7, CD40
pDC	TCf4, CXCR3, LILRA4, CLCEC4C, IRF7
DC5 or inflammatory DCs	CD1c, CD201, CD1A, CD14

TME FACTORS AFFECTING DC DEVELOPMENT IN TUMOURS

Pro- and Anti-Inflammatory Factors

The immunosuppression of tumour-infiltrating DCs can be facilitated by various soluble factors secreted in the TME such as IL-6, IL-10, IDO, M-CSF, transforming growth factor-β1 (TGF-β1), PGE2, VEGF (**Figure 1**) (84–91); although promisingly some of these defects in DC development or function have been proven to be reversible in pre-clinical models and clinical trials (27, 91–94). Mature DC numbers or functions were improved leading to better immune control of the tumour in several mouse models: IL-6 KO mice (95); tumours treated with anti-VEGF antibody (96, 97); and treatment with anti-IL-8 monoclonal antibody (98, 99). On the other hand, pro-inflammatory cytokines such as IFN-α, IL-2, IL-15, IL-21 and GM-CSF are also present in the TME (**Figure 1**) that contribute to enhanced antigen priming, improved DC maturation and increased immune infiltration in tumours (100–103). Therefore, the complex balance of inflammatory signals in the TME is an area of intense research interest but is not trivial to target currently. One of the recent studies on human melanoma reported the correlation of pro-inflammatory cytokine FLT3L production (by NK cells) with abundant intratumoral stimulatory DCs, improved patient responsiveness to anti-PD-1 therapies and better overall survival (104).

The inflammatory factors described above can be derived from tumour cells, immune cells or stromal cells such as fibroblasts surrounding tumour (61, 88, 105, 106). Various subtypes of fibroblasts based on different tissue specific identity, localization, function, transcription factor expression, collagen factors, cancer hallmark genes etc. make up the total tumour mass. CAFs or cancer associated fibroblasts represent a major population in the TME of many solid tumours, however their origin and role in tumour progression is complex and they can generate pro-tumourigenic and anti-tumourigenic secretory factors. Phenotypically and functionally different CAF subtypes based on cell-surface markers such as podoplanin (PDPN), α-smooth muscle actin (αSMA), fibroblast-activated protein (FAP), fibroblast-specific protein-1 (FSP-1/S100A4), THY1 (also known as CD90), and platelet-derived growth factor receptor-α, and β (PDGFRα and PDGFRβ) have been associated with different tumour types, stages and patient survival (107–111). Recently, the ability of CAFs to modulate the immune responses has been discovered and is being explored to improve cancer therapies. CAFs also share some properties with fibroblasts in lymph nodes that already have a well-established role in DC migration (47, 112, 113); and therefore, parallels can be drawn between the two to better understand the DC trafficking in the TME. For example, PDPN present in fibroblasts interacts with CCL21 and promotes CCL21/CCR7 axis mediated DC migration in lymph node. This knowledge was exploited to study the role of PDPN+ CAFs under the influence of hypoxia in tumour progression (114). The study reported PDPN overexpression due to hypoxia in fact favoured invasion of CCR7+ tumour cell into CCL21+ peripheral lymph nodes leading to metastasis (114, 115). Tumours associated with hypoxia are immunosuppressive and lack high expression of CCL21 and therefore therapeutic use of recombinant chemokines (such as CCL21) to stimulate immune cell recognition in tumours is being considered as a novel treatment approach (116, 117). Also, more research is required to understand the transition of a 'normal' fibroblast into an immunosuppressive phenotype such as $S100A4^+$ $PDPN^+$ CAFs as reported in breast cancer patients (109) or into an inflammatory CAF (iCAF) phenotype producing IL-6, IL-10, and IDO (118, 119) linked to poor patient survival. Authors of Fang et al. (118) have shown the role of the urokinase-type plasminogen activator, PLAU in conversion of fibroblasts to iCAFs in esophgeal cancer (118), but much is still unknown about fibroblast differentiation in TME.

TERTIARY LYMPHOID STRUCTURES (TLS)

TLS are established at sites of chronic inflammation and can structurally and functionally resemble secondary lymphoid organs (120–122). Recent studies on murine models of TLS have shown the role of PDPN+ FAP+ immunofibroblasts in driving the development and expansion of TLSs (123, 124). These form part of the TME and can benefit from quick surveillance and locally primed immune response against tumour antigens (**Figure 2**). Occurrence of TLS correlated with high number of mature DCs, strong T-cell infiltration and long-term survival in human primary lung, breast, colorectal, melanoma and other tumours (120, 125–128). However, factors such as TLS location, tumour stage, tumour mutations, treatment history can affect immune cell infiltration and anti-tumour response (128, 129). The cells residing in TLS in tumours are known to express Th1, CD4, CD8, CD31, CD23, FOXP3, chemokines (CCL19, CCL21) and clusters of DC-$Lamp^+$ mature dendritic cells (120, 130, 131) providing an immune-supportive niche (132–134). Typically, TLS at the periphery of the tumour have more organised and distinct DC/T-cell and B-cell zones than intratumoral TLS which contain mostly B cells (133). Future research understanding the immunological features of extratumoral versus intratumoral TLS will be useful to predict responsiveness to immunotherapy and overall survival.

IMMUNE CHECKPOINT GENES

The other group of molecules responsible for causing dysfunction in tumour-infiltrating DCs are immune checkpoint proteins PD-L1, PD-1, ILT2, CTLA4, TIM3 expressed by tumour cells or other immune cells (135–141). As mentioned before, expression of these inhibitory molecules is variable among DC subsets. For example, PD-1 and TIM-3 are mostly expressed on cDC1s; PD-1 expression specifically has been shown to inhibit NF-kB activation which is critical for DC functions including costimulatory molecule expression, antigen presentation and cytokine release leading to T cell inactivation (78, 135, 137, 139, 140). On contrary, ILT2 is expressed on pDCs and cDC2s, but not on cDC1s (78). The central goal of immunotherapies is inhibition of immune checkpoint genes and the expansion of mature cDCs and cytotoxic CD8+ T cells within tumours. It is associated with positive patient outcomes in multiple cancer types when combined with chemotherapy or radiotherapy treatments (28, 135, 142, 143). Despite this, many patients still fail to respond to immune checkpoint blockade. A

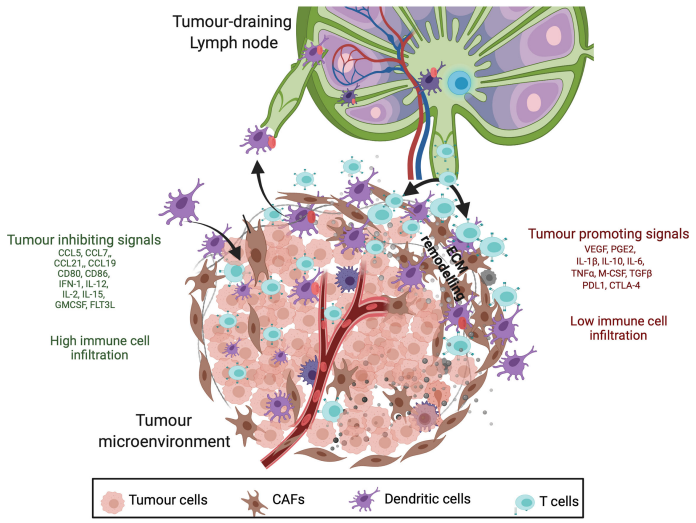

FIGURE 1 | Cancer inhibitory and cancer-promoting signals within the tumour microenvironment (TME). Anti-tumour response is initiated by antigen recognition and trafficking by mature DCs to the tumour draining lymph node (TDLN) which involves upregulation of chemokine receptors (CCR7), MHC class II, co-stimulatory molecules (CD80 and CD86), inflammatory molecules (IL-12, INF-1) and adhesion molecules (ICAM-1) (listed in green). Having said that, immunosuppressive nature of TME secretes tumour promoting inflammatory mediators (listed in red) such as prostaglandin E2, cytokines (IL-10, IL-6, TGFß), chemokines (CXCL1) and growth factors (VEGF) that impede anti-tumour response by altering DC phenotype, T-cell infiltration and ECM remodelling. These differences result in poor surveillance by DCs and lower infiltration of T cells in tumours with immunosuppressive molecules (red).

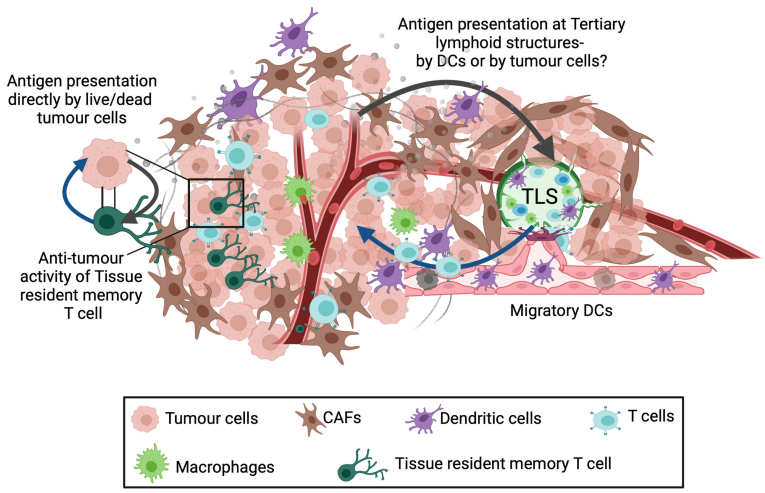

FIGURE 2 | Alternate sites of antigen presentation and T-cell priming. Three different sites for presentation of tumour associated antigens have been described: Tumour draining lymph node (TDLN), Tertiary lymphoid structures (TLS) and Tissue resident memory T cells. A population of memory precursor cells are believed to differentiate into CD103+ tissue resident memory T cells. These cells reside in the tumour and can recognize tumour antigens followed by killing the target tumour cell. In addition, tertiary lymphoid structures (TLS) also present a potential site for T cell priming. TLSs are organised cell aggregates formed within or at tumour margins in response to local inflammation and numerous cell-cell interactions occurring within the TME. Since these contain various immune cell types, TLSs can activate local immune response against the tumour, however the mechanism for T-cell priming within the TLSs is unknown.

better understanding of the role of inflammatory mediators in determining tumour progression will also provide therapeutic avenues to improve immunotherapy outcomes (144–147).

Different labs have reported direct inhibition of pro-tumourigenic inflammation in combination with immune checkpoint blockade as a powerful strategy to improve the patient survival rates (27, 148–150). One such example is the use of aspirin that blocks the COX-2/PGE2 pathway and has shown promising results in preclinical melanoma models (27, 149). Prostaglandin E2 (PGE2), catalysed by the enzyme COX-2 is elevated in many

tumours (151) and plays a role in tumour evasion by directly inhibiting cytotoxic immune responses and subsequently mediates expression of other inflammatory molecules such as CXCL9, CXCL10, CXCR4, CXCL12, IDO1 and interferon (IFN)-γ (27, 144, 148, 150, 152–154). Induction of CXCL12, CXCR4 and IDO1 in tumours have been associated with accumulation of myeloid derived suppressor cells (90, 155). Moreover, direct interaction of EP2/EP4 receptors (present on DCs) with the available PGE2 can modulate DC maturation, metalloprotease-driven DC motility, and immune response in tumours (27, 149, 152, 156–158). Thus, targeting the inflammatory environment of the tumour is important to restore DC function to harvest the full potential of immunotherapy.

LEVERAGING DC BIOLOGY IN CANCER THERAPIES

Anti-tumour immunity relies on cross-presentation of tumour antigens by DCs to elicit a CD8+ T cell response. Among various DC subsets, cDC1s (XCR1+, CD103+) play a critical role in anti-tumour immunity. CLEC9A, (also known as DNGR1) is highly expressed on cDC1s and binds necrotic cell debris and promotes antigen processing in tumours (159–161). One of the reasons for checkpoint blockade failure is poor antigen presentation due to absence of co-stimulatory molecules and therefore modulation of DC function could increase responses to these therapies. One method to address this issue is the development of DC vaccines for cancer treatment, bypassing the need to activate and mature DCs within the tumour. DC-based cancer vaccines work by recruiting ex-vivo generated dendritic cells (or monocyte derived patient DCs) that are genetically engineered, matured, and loaded with tumour-specific antigens (162–164) or by reprogramming endogenous DCs by injecting biomaterial-based scaffolds providing favourable microenvironment for the recruitment of activated DCs (165, 166). An ideal DC vaccine must be able to increase cross-presentation by DCs, express high levels of co-stimulatory molecules, induce tumour-specific T cells with high migratory and cytolytic capabilities. Furthermore, the use of dendritic growth factor Flt3L in combination with checkpoint inhibitors or DC vaccines has improved number of activated intratumoural cDC1s and enhanced anti-tumour immunity to BRAF and checkpoint blockade in preclinical models (167–170).

Presence of co-inhibitory signals (e.g., IL-10, IL-6, PGE2, TGF-β) or absence of co-stimulatory molecules (e.g. CD80 and CD86) can result in inefficient antigen presentation by DCs and poor induction of antigen-specific CD8+T cells. Therefore, inflammatory cytokines secreted by tumour cells and tumour-associated stroma have been identified as promising candidates to potentiate current immunotherapies including immune checkpoint blockade and CAR-T therapy (149, 171–173). Stroma present around most tumours can also magnify inflammation and impede DC phenotype (174–177) and hence manipulating stroma/DC crosstalk in the TME could help improve DC function.

DISCUSSION

It is now established that tumours can exploit their surroundings to create an immunosuppressive microenvironment to control DC function within both the TME and TDLNs (178, 179). These signals including cytokines, chemokines, prostaglandins, growth factors, immune checkpoint genes, etc., may target different DC subsets infiltrating tumours and influence DC maturation, antigen uptake and DC migration (53, 180). Although the success of immunotherapy relies on enhanced T cell activity, activation of tumour-specific T cells cannot be achieved without prior antigen presentation by professional DCs. To overcome immunosuppressive signals, personalized vaccines loaded with patient-derived engineered DCs or delivery of innate stimulus such as TLR3 ligand or a STING agonist to DCs at the tumour site are being developed and have shown promising results (181, 182). Repurposing of existing anti-inflammatory drugs such as aspirin along with DC vaccines or immunotherapies has also been successfully tested in pre-clinical models (149).

This review also addresses the importance of local versus TDLN priming of anti-tumoural T cell responses. Tissue resident memory CD103+ $CD8^+$ T cells residing in the non-lymphoid tissues have shown to provide local immunosurveillance and enhanced immune responses in melanoma, lung and breast tumours (183–187). Moreover, melanoma patients with higher resident T cell population responded better to anti-PD-1 immunotherapy with improved survival (188, 189). However, what is still unclear is how are tissue resident memory $CD8^+$ T cells primed (**Figure 2**) and whether there is a distinct population of DCs required to activate them. Although the exact regulatory mechanisms remain to be explored further, it is hypothesized that crosstalk between tissue resident memory T cells, tumour cells, stromal cells and DCs within the TME potentiate secondary T-cell responses against tumours (**Figure 2**). This also opens discussion on the role of tumour associated tertiary lymphoid structures (TLSs) in intra-tumoural DC maturation; and sourcing T cells and B cells to the tumour (190). Although TLS has been positively correlated with anti-tumour responses, there are still many questions remain to be answered such as TLS composition and TLS induction at tumour site before TLS can be adopted as a predictive tool or as a therapeutic option. Our discussion demonstrates the importance of site of antigen presentation in DC maturation and trafficking which must be exploited therapeutically to enhance immune response against cancer.

AUTHOR CONTRIBUTIONS

YG and SA planned the concept and design of the review. YG and AK collected previous literature on the topic and drafted the article. YG made the figures. SA performed critical revision of the article. YG and SA edited the final version of the article.

FUNDING

This work is funded by Cancer Research UK (Career development fellowship CRUK-A19763 to SA) and Medical Research Council (MC-U12266B).

REFERENCES

1. Esfahani K, Roudaia L, Buhlaiga N, del Rincon SV, Papneja N, Miller WH. A Review of Cancer Immunotherapy: From the Past, to the Present, to the Future. *Curr Oncol* (2020) 27:87–97. doi: 10.3747/co.27.5223
2. Koury J, Lucero M, Cato C, Chang L, Geiger J, Henry D, et al. Immunotherapies: Exploiting the Immune System for Cancer Treatment. *J Immunol Res* (2018) 2018:1–16. doi: 10.1155/2018/9585614
3. Larkin J, Chiarion-Sileni V, Gonzalez R, Grob J-J, Rutkowski P, Lao CD, et al. Five-Year Survival With Combined Nivolumab and Ipilimumab in Advanced Melanoma. *N Engl J Med* (2019) 381:1535–46. doi: 10.1056/NEJMoa1910836
4. Nogrady B. Game-Changing Class of Immunotherapy Drugs Lengthens Melanoma Survival Rates. *Nature* (2020) 580:S14–6. doi: 10.1038/d41586-020-01038-9
5. Zhao B, Zhao H, Zhao J. Efficacy of PD-1/PD-L1 Blockade Monotherapy in Clinical Trials. *Ther Adv Med Oncol* (2020) 12:1–22. doi: 10.1177/1758835920937612
6. Brahmer JR, Tykodi SS, Chow LQM, Hwu W-J, Topalian SL, Hwu P, et al. Safety and Activity of Anti–PD-L1 Antibody in Patients With Advanced Cancer. *N Engl J Med* (2012) 366:2455–65. doi: 10.1056/NEJMoa1200694
7. Haslam A, Prasad V. Estimation of the Percentage of US Patients With Cancer Who Are Eligible for and Respond to Checkpoint Inhibitor Immunotherapy Drugs. *JAMA Network Open* (2019) 2:1–9. doi: 10.1001/jamanetworkopen.2019.2535
8. Royal RE, Levy C, Turner K, Mathur A, Hughes M, Kammula US, et al. Phase 2 Trial of Single Agent Ipilimumab (Anti-CTLA-4) for Locally Advanced or Metastatic Pancreatic Adenocarcinoma. *J Immunother* (2010) 33:828–33. doi: 10.1097/CJI.0b013e3181eec14c
9. Almand B, Resser JR, Lindman B, Nadaf S, Clark JI, Kwon ED, et al. Clinical Significance of Defective Dendritic Cell Differentiation in Cancer. *Clin Cancer Res: An Off J Am Assoc Cancer Res* (2000) 6:1755–66.
10. Balachandran VP, Łuksza M, Zhao JN, Makarov V, Moral JA, Remark R, et al. Identification of Unique Neoantigen Qualities in Long-Term Survivors of Pancreatic Cancer. *Nature* (2017) 551:512–6. doi: 10.1038/nature24462
11. Delp K, Momburg F, Hilmes C, Huber C, Seliger B. Functional Deficiencies of Components of the MHC Class I Antigen Pathway in Human Tumors of Epithelial Origin. *Bone Marrow Transplant* (2000) 25:S88–95. doi: 10.1038/sj.bmt.1702363
12. Bergmann C, Strauss L, Zeidler R, Lang S, Whiteside TL. Expansion of Human T Regulatory Type 1 Cells in the Microenvironment of Cyclooxygenase 2 Overexpressing Head and Neck Squamous Cell Carcinoma. *Cancer Res* (2007) 67:8865–73. doi: 10.1158/0008-5472.CAN-07-0767
13. Ene–Obong A, Clear AJ, Watt J, Wang J, Fatah R, Riches JC, et al. Activated Pancreatic Stellate Cells Sequester CD8+ T Cells to Reduce Their Infiltration of the Juxtatumoral Compartment of Pancreatic Ductal Adenocarcinoma. *Gastroenterology* (2013) 145:1121–32. doi: 10.1053/j.gastro.2013.07.025
14. Feig C, Jones JO, Kraman M, Wells RJB, Deonarine A, Chan DS, et al. Targeting CXCL12 From FAP-Expressing Carcinoma-Associated Fibroblasts Synergizes With Anti-PD-L1 Immunotherapy in Pancreatic Cancer. *Proc Natl Acad Sci* (2013) 110:20212–7. doi: 10.1073/pnas.1320318110
15. Kabacaoglu D, Ciecielski KJ, Ruess DA, Algül H. Immune Checkpoint Inhibition for Pancreatic Ductal Adenocarcinoma: Current Limitations and Future Options. *Front Immunol* (2018) 9:1878. doi: 10.3389/fimmu.2018.01878
16. Chung W, Eum HH, Lee H-O, Lee K-M, Lee H-B, Kim K-T, et al. Single-Cell RNA-Seq Enables Comprehensive Tumour and Immune Cell Profiling in Primary Breast Cancer. *Nat Commun* (2017) 8:1–12. doi: 10.1038/ncomms15081
17. Kojima Y, Acar A, Eaton EN, Mellody KT, Scheel C, Ben-Porath I, et al. Autocrine TGF- and Stromal Cell-Derived Factor-1 (SDF-1) Signaling Drives the Evolution of Tumor-Promoting Mammary Stromal Myofibroblasts. *Proc Natl Acad Sci* (2010) 107:20009–14. doi: 10.1073/pnas.1013805107
18. Medrek C, Pontén F, Jirström K, Leandersson K. The Presence of Tumor Associated Macrophages in Tumor Stroma as a Prognostic Marker for Breast Cancer Patients. *BMC Cancer* (2012) 12:1–9. doi: 10.1186/1471-2407-12-306
19. Smith HA, Kang Y. The Metastasis-Promoting Roles of Tumor-Associated Immune Cells. *J Mol Med* (2013) 91:411–29. doi: 10.1007/s00109-013-1021-5
20. Spaeth EL, Dembinski JL, Sasser AK, Watson K, Klopp A, Hall B, et al. Mesenchymal Stem Cell Transition to Tumor-Associated Fibroblasts Contributes to Fibrovascular Network Expansion and Tumor Progression. *PloS One* (2009) 4:1–11. doi: 10.1371/journal.pone.0004992
21. Ruhland MK, Roberts EW, Cai E, Mujal AM, Marchuk K, Beppler C, et al. Visualizing Synaptic Transfer of Tumor Antigens Among Dendritic Cells. *Cancer Cell* (2020) 37:789–99. doi: 10.1016/j.ccell.2020.05.002
22. Aiello NM, Bajor DL, Norgard RJ, Sahmoud A, Bhagwat N, Pham MN, et al. Metastatic Progression Is Associated With Dynamic Changes in the Local Microenvironment. *Nat Commun* (2016) 7:1–9. doi: 10.1038/ncomms12819
23. Di Blasio S, van Wigcheren GF, Becker A, van Duffelen A, Gorris M, Verrijp K, et al. The Tumour Microenvironment Shapes Dendritic Cell Plasticity in a Human Organotypic Melanoma Culture. *Nat Commun* (2020) 11:1–17. doi: 10.1038/s41467-020-16583-0
24. Oba T, Long MD, Keler T, Marsh HC, Minderman H, Abrams SI, et al. Overcoming Primary and Acquired Resistance to Anti-PD-L1 Therapy by Induction and Activation of Tumor-Residing Cdc1s. *Nat Commun* (2020) 11:1–20. doi: 10.1038/s41467-020-19192-z
25. Poloso NJ, Urquhart P, Nicolaou A, Wang J, Woodward DF. PGE2 Differentially Regulates Monocyte-Derived Dendritic Cell Cytokine Responses Depending on Receptor Usage (EP2/EP4). *Mol Immunol* (2013) 54:284–95. doi: 10.1016/j.molimm.2012.12.010
26. Valenti R, Huber V, Iero M, Filipazzi P, Parmiani G, Rivoltini L. Tumor-Released Microvesicles as Vehicles of Immunosuppression: Figure 1. *Cancer Res* (2007) 67:2912–5. doi: 10.1158/0008-5472.CAN-07-0520
27. Zelenay S, van der Veen AG, Böttcher JP, Snelgrove KJ, Rogers N, Acton SE, et al. Cyclooxygenase-Dependent Tumor Growth Through Evasion of Immunity. *Cell* (2015) 162:1257–70. doi: 10.1016/j.cell.2015.08.015
28. Broz ML, Binnewies M, Boldajipour B, Nelson AE, Pollack JL, Erle DJ, et al. Dissecting the Tumor Myeloid Compartment Reveals Rare Activating Antigen-Presenting Cells Critical for T Cell Immunity. *Cancer Cell* (2014) 26:638–52. doi: 10.1016/j.ccell.2014.09.007
29. Engelhardt JJ, Boldajipour B, Beemiller P, Pandurangi P, Sorensen C, Werb Z, et al. Marginating Dendritic Cells of the Tumor Microenvironment Cross-Present Tumor Antigens and Stably Engage Tumor-Specific T Cells. *Cancer Cell* (2012) 21:402–17. doi: 10.1016/j.ccr.2012.01.008
30. Hildner K, Edelson BT, Purtha WE, Diamond M, Matsushita H, Kohyama M, et al. Batf3 Deficiency Reveals a Critical Role for CD8 + Dendritic Cells in Cytotoxic T Cell Immunity. *Science* (2008) 322:1097–100. doi: 10.1126/science.1164206
31. Nakahara T, Oba J, Shimomura C, Kido-Nakahara M, Furue M. Early Tumor-Infiltrating Dendritic Cells Change Their Characteristics Drastically in Association With Murine Melanoma Progression. *J Invest Dermatol* (2016) 136:146–53. doi: 10.1038/JID.2015.359
32. Theisen DJ, Davidson JT, Briseño CG, Gargaro M, Lauron EJ, Wang Q, et al. WDFY4 Is Required for Cross-Presentation in Response to Viral and Tumor Antigens. *Science* (2018) 362:694–9. doi: 10.1126/science.aat5030
33. Allan RS, Waithman J, Bedoui S, Jones CM, Villadangos JA, Zhan Y, et al. Migratory Dendritic Cells Transfer Antigen to a Lymph Node-Resident Dendritic Cell Population for Efficient CTL Priming. *Immunity* (2006) 25:153–62. doi: 10.1016/j.immuni.2006.04.017
34. Binnewies M, Mujal AM, Pollack JL, Combes AJ, Hardison EA, Barry KC, et al. Unleashing Type-2 Dendritic Cells to Drive Protective Antitumor CD4 + T Cell Immunity. *Cell* (2019) 177:556–71. doi: 10.1016/j.cell.2019.02.005
35. Hirano N, Butler MO, Xia Z, Ansén S, von Bergwelt-Baildon MS, Neuberg D, et al. Engagement of CD83 Ligand Induces Prolonged Expansion of CD8 + T Cells and Preferential Enrichment for Antigen Specificity. *Blood* (2006) 107:1528–36. doi: 10.1182/blood-2005-05-2073
36. Plantinga M, Guilliams M, Vanheerswynghels M, Deswarte K, Branco-Madeira F, Toussaint W, et al. Conventional and Monocyte-Derived CD11b + Dendritic Cells Initiate and Maintain T Helper 2 Cell-Mediated Immunity to House Dust Mite Allergen. *Immunity* (2013) 38:322–35. doi: 10.1016/j.immuni.2012.10.016
37. Pooley JL, Heath WR, Shortman K. Cutting Edge: Intravenous Soluble Antigen Is Presented to CD4 T Cells by CD8 ¯ Dendritic Cells, But Cross-

Presented to CD8 T Cells by CD8 $^{+}$ Dendritic Cells. *J Immunol* (2001) 166:5327–30. doi: 10.4049/jimmunol.166.9.5327
38. Schlitzer A, McGovern N, Teo P, Zelante T, Atarashi K, Low D, et al. IRF4 Transcription Factor-Dependent CD11b+ Dendritic Cells in Human and Mouse Control Mucosal IL-17 Cytokine Responses. *Immunity* (2013) 38:970–83. doi: 10.1016/j.immuni.2013.04.011
39. Steinman RM. Decisions About Dendritic Cells: Past, Present, and Future. *Annu Rev Immunol* (2012) 30:1–22. doi: 10.1146/annurev-immunol-100311-102839
40. Harjunpää H, Llort Asens M, Guenther C, Fagerholm SC. Cell Adhesion Molecules and Their Roles and Regulation in the Immune and Tumor Microenvironment. *Front Immunol* (2019) 10. doi: 10.3389/fimmu.2019.01078
41. Kobayashi D, Endo M, Ochi H, Hojo H, Miyasaka M, Hayasaka H. Regulation of CCR7-Dependent Cell Migration Through CCR7 Homodimer Formation. *Sci Rep* (2017) 7:1–14. doi: 10.1038/s41598-017-09113-4
42. Morrison VL, James MJ, Grzes K, Cook P, Glass DG, Savinko T. Loss of Beta2-Integrin-Mediated Cytoskeletal Linkage Reprogrammes Dendritic Cells to a Mature Migratory Phenotype. *Nat Commun* (2014) 5:1–26. doi: 10.1038/ncomms6359
43. Roberts EW, Broz ML, Binnewies M, Headley MB, Nelson AE, Wolf DM, et al. Critical Role for CD103 +/CD141 + Dendritic Cells Bearing CCR7 for Tumor Antigen Trafficking and Priming of T Cell Immunity in Melanoma. *Cancer Cell* (2016) 30:324–36. doi: 10.1016/j.ccell.2016.06.003
44. Jang MH, Sougawa N, Tanaka T, Hirata T, Hiroi T, Tohya K, et al. CCR7 Is Critically Important for Migration of Dendritic Cells in Intestinal Lamina Propria to Mesenteric Lymph Nodes. *J Immunol* (2006) 176:803–10. doi: 10.4049/jimmunol.176.2.803
45. Russo E, Teijeira A, Vaahtomeri K, Willrodt A-H, Bloch JS, Nitschké M, et al. Intralymphatic CCL21 Promotes Tissue Egress of Dendritic Cells Through Afferent Lymphatic Vessels. *Cell Rep* (2016) 14:1723–34. doi: 10.1016/j.celrep.2016.01.048
46. Vaahtomeri K, Brown M, Hauschild R, de Vries I, Leithner AF, Mehling M, et al. Locally Triggered Release of the Chemokine CCL21 Promotes Dendritic Cell Transmigration Across Lymphatic Endothelia. *Cell Rep* (2017) 19:902–9. doi: 10.1016/j.celrep.2017.04.027
47. Acton SE, Astarita JL, Malhotra D, Lukacs-Kornek V, Franz B, Hess PR, et al. Podoplanin-Rich Stromal Networks Induce Dendritic Cell Motility *via* Activation of the C-Type Lectin Receptor CLEC-2. *Immunity* (2012) 37:276–89. doi: 10.1016/j.immuni.2012.05.022
48. Braun A, Worbs T, Moschovakis GL, Halle S, Hoffmann K, Bölter J, et al. Afferent Lymph–Derived T Cells and DCs Use Different Chemokine Receptor CCR7–dependent Routes for Entry Into the Lymph Node and Intranodal Migration. *Nat Immunol* (2011) 12:879–87. doi: 10.1038/ni.2085
49. Link A, Vogt TK, Favre S, Britschgi MR, Acha-Orbea H, Hinz B, et al. Fibroblastic Reticular Cells in Lymph Nodes Regulate the Homeostasis of Naive T Cells. *Nat Immunol* (2007) 8:1255–65. doi: 10.1038/ni1513
50. Peduto L, Dulauroy S, Lochner M, Späth GF, Morales MA, Cumano A, et al. Inflammation Recapitulates the Ontogeny of Lymphoid Stromal Cells. *J Immunol* (2009) 182:5789–99. doi: 10.4049/jimmunol.0803974
51. Núñez NG, Tosello Boari J, Ramos RN, Richer W, Cagnard N, Anderfuhren CD, et al. Tumor Invasion in Draining Lymph Nodes Is Associated With Treg Accumulation in Breast Cancer Patients. *Nat Commun* (2020) 11:1–15. doi: 10.1038/s41467-020-17046-2
52. Shinde P, Fernandes S, Melinkeri S, Kale V, Limaye L. Compromised Functionality of Monocyte-Derived Dendritic Cells in Multiple Myeloma Patients may Limit Their Use in Cancer Immunotherapy. *Sci Rep* (2018) 8:1–11. doi: 10.1038/s41598-018-23943-w
53. O'Melia MJ, Rohner NA, Manspeaker MP, Francis DM, Kissick HT, Thomas SN. Quality of CD8^{+} T Cell Immunity Evoked in Lymph Nodes Is Compartmentalized by Route of Antigen Transport and Functional in Tumor Context. *Sci Adv* (2020) 6:1–16. doi: 10.1126/sciadv.abd7134
54. Caronni N, Simoncello F, Stafetta F, Guarnaccia C, Ruiz-Moreno JS, Opitz B, et al. Downregulation of Membrane Trafficking Proteins and Lactate Conditioning Determine Loss of Dendritic Cell Function in Lung Cancer. *Cancer Res* (2018) 78:1685–99. doi: 10.1158/0008-5472.CAN-17-1307
55. Wang X, Ji J, Zhang H, Fan Z, Zhang L, Shi L, et al. Stimulation of Dendritic Cells by DAMPs in ALA-PDT Treated SCC Tumor Cells. *Oncotarget* (2015) 6:44688–702. doi: 10.18632/oncotarget.5975
56. Bol KF, Schreibelt G, Rabold K, Wculek SK, Schwarze JK, Dzionek A, et al. The Clinical Application of Cancer Immunotherapy Based on Naturally Circulating Dendritic Cells. *J ImmunoTher Cancer* (2019) 7:1–13. doi: 10.1186/s40425-019-0580-6
57. Spranger S, Luke JJ, Bao R, Zha Y, Hernandez KM, Li Y, et al. Density of Immunogenic Antigens Does Not Explain the Presence or Absence of the T-Cell-Inflamed Tumor Microenvironment in Melanoma. *Proc Natl Acad Sci USA* (2016) 113:7759–68. doi: 10.1073/pnas.1609376113
58. Spranger S, Bao R, Gajewski TF. Melanoma-Intrinsic β-Catenin Signalling Prevents Anti-Tumour Immunity. *Nature* (2015) 523:231–5. doi: 10.1038/nature14404
59. Kim N, Kim HK, Lee K, Hong Y, Cho JH, Choi JW, et al. Single-Cell RNA Sequencing Demonstrates the Molecular and Cellular Reprogramming of Metastatic Lung Adenocarcinoma. *Nat Commun* (2020) 11:1–15. doi: 10.1038/s41467-020-16164-1
60. Maier B, Leader AM, Chen ST, Tung N, Chang C, LeBerichel J, et al. A Conserved Dendritic-Cell Regulatory Program Limits Antitumour Immunity. *Nature* (2020) 580:257–62. doi: 10.1038/s41586-020-2134-y
61. Qian J, Olbrecht S, Boeckx B, Vos H, Laoui D, Etlioglu E, et al. A Pan-Cancer Blueprint of the Heterogeneous Tumor Microenvironment Revealed by Single-Cell Profiling. *Cell Res* (2020) 30:745–62. doi: 10.1038/s41422-020-0355-0
62. Zilionis R, Engblom C, Pfirschke C, Savova V, Zemmour D, Saatcioglu HD, et al. Single-Cell Transcriptomics of Human and Mouse Lung Cancers Reveals Conserved Myeloid Populations Across Individuals and Species. *Immunity* (2019) 50:1317–34. doi: 10.1016/j.immuni.2019.03.009
63. Cillo AR, Kürten CHL, Tabib T, Qi Z, Onkar S, Wang T, et al. Immune Landscape of Viral- and Carcinogen-Driven Head and Neck Cancer. *Immunity* (2020) 52:183–99. doi: 10.1016/j.immuni.2019.11.014
64. Zhang Q, He Y, Luo N, Patel SJ, Han Y, Gao R, et al. Landscape and Dynamics of Single Immune Cells in Hepatocellular Carcinoma. *Cell* (2019) 179:829–45. doi: 10.1016/j.cell.2019.10.003
65. Brown CC, Gudjonson H, Pritykin Y, Deep D, Lavallée V-P, Mendoza A, et al. Transcriptional Basis of Mouse and Human Dendritic Cell Heterogeneity. *Cell* (2019) 179:846–63. doi: 10.1016/j.cell.2019.09.035
66. Nirschl CJ, Suárez-Fariñas M, Izar B, Prakadan S, Dannenfelser R, Tirosh I, et al. Ifnγ-Dependent Tissue-Immune Homeostasis Is Co-Opted in the Tumor Microenvironment. *Cell* (2017) 170:127–41. doi: 10.1016/j.cell.2017.06.016
67. Ji AL, Rubin AJ, Thrane K, Jiang S, Reynolds DL, Meyers RM, et al. Multimodal Analysis of Composition and Spatial Architecture in Human Squamous Cell Carcinoma. *Cell* (2020) 182:497–514. doi: 10.1016/j.cell.2020.05.039
68. Zhang L, Li Z, Skrzypczynska KM, Fang Q, Zhang W, O'Brien SA, et al. Single-Cell Analyses Inform Mechanisms of Myeloid-Targeted Therapies in Colon Cancer. *Cell* (2020) 181. doi: 10.1016/j.cell.2020.03.048
69. Cheng S, Li Z, Gao R, Xing B, Gao Y, Yang Y, et al. A Pan-Cancer Single-Cell Transcriptional Atlas of Tumor Infiltrating Myeloid Cells. *Cell* (2021) 184:792–809. doi: 10.1016/j.cell.2021.01.010
70. Gerhard GM, Bill R, Messemaker M, Klein AM, Pittet MJ. Tumor-Infiltrating Dendritic Cell States Are Conserved Across Solid Human Cancers. *J Exp Med* (2021) 218:1–13. doi: 10.1084/jem.20200264
71. Dutertre C-A, Becht E, Irac SE, Khalilnezhad A, Narang V, Khalilnezhad S, et al. Single-Cell Analysis of Human Mononuclear Phagocytes Reveals Subset-Defining Markers and Identifies Circulating Inflammatory Dendritic Cells. *Immunity* (2019) 51:573–89.e8. doi: 10.1016/j.immuni.2019.08.008
72. Auffray C, Fogg D, Garfa M, Elain G, Join-Lambert O, Kayal S, et al. Monitoring of Blood Vessels and Tissues by a Population of Monocytes With Patrolling Behavior. *Science* (2007) 317:666–70. doi: 10.1126/science.1142883
73. Boldison J, da Rosa LC, Davies J, Wen L, Wong FS. Dendritic Cells License Regulatory B Cells to Produce IL-10 and Mediate Suppression of Antigen-Specific CD8 T Cells. *Cell Mol Immunol* (2020) 17:843–55. doi: 10.1038/s41423-019-0324-z
74. Zhang Q, Fujino M, Iwasaki S, Hirano H, Cai S, Kitajima Y, et al. Generation and Characterization of Regulatory Dendritic Cells Derived From Murine Induced Pluripotent Stem Cells. *Sci Rep* (2015) 4:3979. doi: 10.1038/srep03979

75. Audiger C, Rahman MJ, Yun TJ, Tarbell K, Lesage S. The Importance of Dendritic Cells in Maintaining Immune Tolerance. *J Immunol* (2017) 198:2223–31. doi: 10.4049/jimmunol.1601629
76. del Prete A, Sozio F, Barbazza I, Salvi V, Tiberio L, Laffranchi M, et al. Functional Role of Dendritic Cell Subsets in Cancer Progression and Clinical Implications. *Int J Mol Sci* (2020) 21:1–24. doi: 10.3390/ijms21113930
77. Aibar S, González-Blas CB, Moerman T, Huynh-Thu VA, Imrichova H, Hulselmans G, et al. SCENIC: Single-Cell Regulatory Network Inference and Clustering. *Nat Methods* (2017) 14:7083–6. doi: 10.1038/nmeth.4463
78. Carenza C, Calcaterra F, Oriolo F, di Vito C, Ubezio M, della Porta MG, et al. Costimulatory Molecules and Immune Checkpoints Are Differentially Expressed on Different Subsets of Dendritic Cells. *Front Immunol* (2019) 10. doi: 10.3389/fimmu.2019.01325
79. Hernandez A, Burger M, Blomberg BB, Ross WA, Gaynor JJ, Lindner I, et al. Inhibition of NF-κb During Human Dendritic Cell Differentiation Generates Anergy and Regulatory T-Cell Activity for One But Not Two Human Leukocyte Antigen DR Mismatches. *Hum Immunol* (2007) 68:715–29. doi: 10.1016/j.humimm.2007.05.010
80. Medina BD, Liu M, Vitiello GA, Seifert AM, Zeng S, Bowler T, et al. Oncogenic Kinase Inhibition Limits Batf3-Dependent Dendritic Cell Development and Antitumor Immunity. *J Exp Med* (2019) 216:1359–76. doi: 10.1084/jem.20180660
81. Scholz F, Grau M, Menzel L, Graband A, Zapukhlyak M, Leutz A, et al. The Transcription Factor C/Ebpβ Orchestrates Dendritic Cell Maturation and Functionality Under Homeostatic and Malignant Conditions. *Proc Natl Acad Sci* (2020) 117:26328–39. doi: 10.1073/pnas.2008883117
82. Xiao X, Yang G, Bai P, Gui S, Nyuyen TMB, Mercado-Uribe I, et al. Inhibition of Nuclear Factor-Kappa B Enhances the Tumor Growth of Ovarian Cancer Cell Line Derived From a Low-Grade Papillary Serous Carcinoma in P53-Independent Pathway. *BMC Cancer* (2016) 16:1–13. doi: 10.1186/s12885-016-2617-2
83. Melaiu O, Chierici M, Lucarini V, Jurman G, Conti LA, de Vito R, et al. Cellular and Gene Signatures of Tumor-Infiltrating Dendritic Cells and Natural-Killer Cells Predict Prognosis of Neuroblastoma. *Nat Commun* (2020) 11:1–15. doi: 10.1038/s41467-020-19781-y
84. Brencicova E, Jagger AL, Evans HG, Georgouli M, Laios A, Attard Montalto S, et al. Interleukin-10 and Prostaglandin E2 Have Complementary But Distinct Suppressive Effects on Toll-Like Receptor-Mediated Dendritic Cell Activation in Ovarian Carcinoma. *PloS One* (2017) 12:1–24. doi: 10.1371/journal.pone.0175712
85. Imai K, Minamiya Y, Koyota S, Ito M, Saito H, Sato Y, et al. Inhibition of Dendritic Cell Migration by Transforming Growth Factor-β1 Increases Tumor-Draining Lymph Node Metastasis. *J Exp Clin Cancer Res* (2012) 31:1–9. doi: 10.1186/1756-9966-31-3
86. Llopiz D, Ruiz M, Infante S, Villanueva L, Silva L, Hervas-Stubbs S, et al. IL-10 Expression Defines an Immunosuppressive Dendritic Cell Population Induced by Antitumor Therapeutic Vaccination. *Oncotarget* (2017) 8:2659–71. doi: 10.18632/oncotarget.13736
87. Long J, Hu Z, Xue H, Wang Y, Chen J, Tang F, et al. Vascular Endothelial Growth Factor (VEGF) Impairs the Motility and Immune Function of Human Mature Dendritic Cells Through the VEGF Receptor 2-RhoA-Cofilin1 Pathway. *Cancer Sci* (2019) 110:2357–67. doi: 10.1111/cas.14091
88. Ohno Y, Kitamura H, Takahashi N, Ohtake J, Kaneumi S, Sumida K, et al. IL-6 Down-Regulates HLA Class II Expression and IL-12 Production of Human Dendritic Cells to Impair Activation of Antigen-Specific CD4+ T Cells. *Cancer Immunol Immunother* (2016) 65:193–204. doi: 10.1007/s00262-015-1791-4
89. Tauriello DVF, Palomo-Ponce S, Stork D, Berenguer-Llergo A, Badia-Ramentol J, Iglesias M, et al. Tgfβ Drives Immune Evasion in Genetically Reconstituted Colon Cancer Metastasis. *Nature* (2018) 554:538–43. doi: 10.1038/nature25492
90. Trabanelli S, Lecciso M, Salvestrini V, Cavo M, Očadlíková D , Lemoli RM, et al. PGE $_2$ -Induced IDO1 Inhibits the Capacity of Fully Mature DCs to Elicit an *In Vitro* Antileukemic Immune Response. *J Immunol Res* (2015) 2015:1–10. doi: 10.1155/2015/253191
91. Xu X, Liu X, Long J, Hu Z, Zheng Q, Zhang C, et al. Interleukin-10 Reorganizes the Cytoskeleton of Mature Dendritic Cells Leading to Their Impaired Biophysical Properties and Motilities. *PloS One* (2017) 12:1–15. doi: 10.1371/journal.pone.0172523
92. Ferrara N, Carver-Moore K, Chen H, Dowd M, Lu L, O'Shea KS, et al. Heterozygous Embryonic Lethality Induced by Targeted Inactivation of the VEGF Gene. *Nature* (1996) 380:439–42. doi: 10.1038/380439a0
93. Wakabayashi H, Hamaguchi T, Nagao N, Kato S, Iino T, Nakamura T, et al. Interleukin-6 Receptor Inhibitor Suppresses Bone Metastases in a Breast Cancer Cell Line. *Breast Cancer* (2018) 25:566–74. doi: 10.1007/s12282-018-0853-9
94. Yang J, Yan J, Liu B. Targeting VEGF/VEGFR to Modulate Antitumor Immunity. *Front Immunol* (2018) 9:978. doi: 10.3389/fimmu.2018.00978
95. Park S-J, Nakagawa T, Kitamura H, Atsumi T, Kamon H, Sawa S, et al. IL-6 Regulates *In Vivo* Dendritic Cell Differentiation Through STAT3 Activation. *J Immunol* (2004) 173:3844–54. doi: 10.4049/jimmunol.173.6.3844
96. Gabrilovich DI, Ishida T, Nadaf S, Ohm JE, Carbone DP. Antibodies to Vascular Endothelial Growth Factor Enhance the Efficacy of Cancer Immunotherapy by Improving Endogenous Dendritic Cell Function. *Clin Cancer research : An Off J Am Assoc Cancer Res* (1999) 5:2963–70.
97. Mashima T, Wakatsuki T, Kawata N, Jang M-K, Nagamori A, Yoshida H, et al. Neutralization of the Induced VEGF-A Potentiates the Therapeutic Effect of an Anti-VEGFR2 Antibody on Gastric Cancer *In Vivo*. *Sci Rep* (2021) 11:1–12. doi: 10.1038/s41598-021-94584-9
98. Bilusic M, Heery CR, Collins JM, Donahue RN, Palena C, Madan RA, et al. Phase I Trial of HuMax-IL8 (BMS-986253), an Anti-IL-8 Monoclonal Antibody, in Patients With Metastatic or Unresectable Solid Tumors. *J ImmunoTher Cancer* (2019) 7:1–8. doi: 10.1186/s40425-019-0706-x
99. Feijoó E, Alfaro C, Mazzolini G, Serra P, Peñuelas I, Arina A, et al. Dendritic Cells Delivered Inside Human Carcinomas Are Sequestered by Interleukin-8. *Int J Cancer* (2005) 116:275–81. doi: 10.1002/ijc.21046
100. Cauwels A, van Lint S, Paul F, Garcin G, de Koker S, van Parys A, et al. Delivering Type I Interferon to Dendritic Cells Empowers Tumor Eradication and Immune Combination Treatments. *Cancer Res* (2018) 78:463–74. doi: 10.1158/0008-5472.CAN-17-1980
101. Le DT, Lutz E, Uram JN, Sugar EA, Onners B, Solt S, et al. Evaluation of Ipilimumab in Combination With Allogeneic Pancreatic Tumor Cells Transfected With a GM-CSF Gene in Previously Treated Pancreatic Cancer. *J Immunother* (2013) 36:382–9. doi: 10.1097/CJI.0b013e31829fb7a2
102. Li Y, Bleakley M, Yee C. IL-21 Influences the Frequency, Phenotype, and Affinity of the Antigen-Specific CD8 T Cell Response. *J Immunol* (2005) 175:2261–9. doi: 10.4049/jimmunol.175.4.2261
103. Rhode PR, Egan JO, Xu W, Hong H, Webb GM, Chen X, et al. Comparison of the Superagonist Complex, ALT-803, to IL15 as Cancer Immunotherapeutics in Animal Models. *Cancer Immunol Res* (2016) 4:49–60. doi: 10.1158/2326-6066.CIR-15-0093-T
104. Barry KC, Hsu J, Broz ML, Cueto FJ, Binnewies M, Combes AJ, et al. A Natural Killer–Dendritic Cell Axis Defines Checkpoint Therapy–Responsive Tumor Microenvironments. *Nat Med* (2018) 24:1178–91. doi: 10.1038/s41591-018-0085-8
105. Bai W, Zhang W, Hu B. Vascular Endothelial Growth Factor Suppresses Dendritic Cells Function of Human Prostate Cancer. *OncoTargets Ther* (2018) 11:1267–74. doi: 10.2147/OTT.S161302
106. Cheng J, Deng Y, Yi H, Wang G, Fu B, Chen W, et al. Hepatic Carcinoma-Associated Fibroblasts Induce IDO-Producing Regulatory Dendritic Cells Through IL-6-Mediated STAT3 Activation. *Oncogenesis* (2016) 5:1–8. doi: 10.1038/oncsis.2016.7
107. Costa A, Kieffer Y, Scholer-Dahirel A, Pelon F, Bourachot B, Cardon M, et al. Fibroblast Heterogeneity and Immunosuppressive Environment in Human Breast Cancer. *Cancer Cell* (2018) 33:463–79. doi: 10.1016/j.ccell.2018.01.011
108. Elyada E, Bolisetty M, Laise P, Flynn WF, Courtois ET, Burkhart RA, et al. Cross-Species Single-Cell Analysis of Pancreatic Ductal Adenocarcinoma Reveals Antigen-Presenting Cancer-Associated Fibroblasts. *Cancer Discov* (2019) 9:1102–23. doi: 10.1158/2159-8290.CD-19-0094
109. Friedman G, Levi-Galibov O, David E, Bornstein C, Giladi A, Dadiani M, et al. Cancer-Associated Fibroblast Compositions Change With Breast Cancer Progression Linking the Ratio of S100A4+ and PDPN+ CAFs to Clinical Outcome. *Nat Cancer* (2020) 1:692–708. doi: 10.1101/2020.01.12.903039
110. Rodda LB, Lu E, Bennett ML, Sokol CL, Wang X, Luther SA, et al. Single-Cell RNA Sequencing of Lymph Node Stromal Cells Reveals Niche-Associated Heterogeneity. *Immunity* (2018) 48:1014–28. doi: 10.1016/j.immuni.2018.04.006

111. Song Y-J, Xu Y, Deng C, Zhu X, Fu J, Chen H, et al. Gene Expression Classifier Reveals Prognostic Osteosarcoma Microenvironment Molecular Subtypes. *Front Immunol* (2021) 12:62376. doi: 10.3389/fimmu.2021.623762
112. Acton SE, Farrugia AJ, Astarita JL, Mourão-Sá D, Jenkins RP, Nye E, et al. Dendritic Cells Control Fibroblastic Reticular Network Tension and Lymph Node Expansion. *Nature* (2014) 514:498–502. doi: 10.1038/nature13814
113. Prados A, Onder L, Cheng H-W, Mörbe U, Lütge M, Gil-Cruz C, et al. Fibroblastic Reticular Cell Lineage Convergence in Peyer's Patches Governs Intestinal Immunity. *Nat Immunol* (2021) 22:510–9. doi: 10.1038/s41590-021-00894-5
114. Tejchman A, Lamerant-Fayel N, Jacquinet J-C, Bielawska-Pohl A, Mleczko-Sanecka K, Grillon C, et al. Tumor Hypoxia Modulates Podoplanin/CCL21 Interactions in CCR7+ NK Cell Recruitment and CCR7+ Tumor Cell Mobilization. *Oncotarget* (2017) 8:31876–87. doi: 10.18632/oncotarget.16311
115. Hwang T-L, Lee L-Y, Wang C-C, Liang Y, Huang S-F, Wu C-M. CCL7 and CCL21 Overexpression in Gastric Cancer Is Associated With Lymph Node Metastasis and Poor Prognosis. *World J Gastroenterol* (2012) 18:1249–56. doi: 10.3748/wjg.v18.i11.1249
116. Crola Da Silva C, Lamerant-Fayel N, Paprocka M, Mitterrand M, Gosset D, Dus D, et al. Selective Human Endothelial Cell Activation by Chemokines as a Guide to Cell Homing. *Immunology* (2009) 126:394–404. doi: 10.1111/j.1365-2567.2008.02906.x
117. Lin Y, Sharma S, John M. CCL21 Cancer Immunotherapy. *Cancers* (2014) 6:1098–110. doi: 10.3390/cancers6021098
118. Fang L, Che Y, Zhang C, Huang J, Lei Y, Lu Z, et al. PLAU Directs Conversion of Fibroblasts to Inflammatory Cancer-Associated Fibroblasts, Promoting Esophageal Squamous Cell Carcinoma Progression *via* uPAR/Akt/NF-κb/IL8 Pathway. *Cell Death Discov* (2021) 7:1–14. doi: 10.1038/s41420-021-00410-6
119. Öhlund D, Handly-Santana A, Biffi G, Elyada E, Almeida AS, Ponz-Sarvise M, et al. Distinct Populations of Inflammatory Fibroblasts and Myofibroblasts in Pancreatic Cancer. *J Exp Med* (2017) 214:579–96. doi: 10.1084/jem.20162024
120. Goc J, Germain C, Vo-Bourgais TKD, Lupo A, Klein C, Knockaert S, et al. Dendritic Cells in Tumor-Associated Tertiary Lymphoid Structures Signal a Th1 Cytotoxic Immune Contexture and License the Positive Prognostic Value of Infiltrating CD8+ T Cells. *Cancer Res* (2014) 74:705–15. doi: 10.1158/0008-5472.CAN-13-1342
121. Li Q, Liu X, Wang D, Wang Y, Lu H, Wen S, et al. Prognostic Value of Tertiary Lymphoid Structure and Tumour Infiltrating Lymphocytes in Oral Squamous Cell Carcinoma. *Int J Oral Sci* (2020) 12:1–8. doi: 10.1038/s41368-020-00092-3
122. Salem D, Chelvanambi M, Storkus WJ, Fecek RJ. Cutaneous Melanoma: Mutational Status and Potential Links to Tertiary Lymphoid Structure Formation. *Front Immunol* (2021) 12:629519. doi: 10.3389/fimmu.2021.629519
123. Nayar S, Campos J, Smith CG, Iannizzotto V, Gardner DH, Mourcin F, et al. Immunofibroblasts Are Pivotal Drivers of Tertiary Lymphoid Structure Formation and Local Pathology. *Proc Natl Acad Sci* (2019) 116:13490–7. doi: 10.1073/pnas.1905301116
124. Rodriguez AB, Peske JD, Woods AN, Leick KM, Mauldin IS, Meneveau MO, et al. Immune Mechanisms Orchestrate Tertiary Lymphoid Structures in Tumors *via* Cancer-Associated Fibroblasts. *Cell Rep* (2021) 36:109422. doi: 10.1016/j.celrep.2021.109422
125. Dieu-Nosjean M-C, Antoine M, Danel C, Heudes D, Wislez M, Poulot V, et al. Long-Term Survival for Patients With Non–Small-Cell Lung Cancer With Intratumoral Lymphoid Structures. *J Clin Oncol* (2008) 26:4410–7. doi: 10.1200/JCO.2007.15.0284
126. Figenschau SL, Fismen S, Fenton KA, Fenton C, Mortensen ES. Tertiary Lymphoid Structures Are Associated With Higher Tumor Grade in Primary Operable Breast Cancer Patients. *BMC Cancer* (2015) 15:1–11. doi: 10.1186/s12885-015-1116-1
127. He W, Zhang D, Liu H, Chen T, Xie J, Peng L, et al. The High Level of Tertiary Lymphoid Structure Is Correlated With Superior Survival in Patients With Advanced Gastric Cancer. *Front Oncol* (2020) 10. doi: 10.3389/fonc.2020.00980
128. Jacquelot N, Tellier J, , Nutt SL, Belz GT. Tertiary Lymphoid Structures and B Lymphocytes in Cancer Prognosis and Response to Immunotherapies. *OncoImmunology* (2021) 10(1):1900508. doi: 10.1080/2162402X.2021.1900508
129. Lin L, Hu X, Zhang H, Hu H. Tertiary Lymphoid Organs in Cancer Immunology: Mechanisms and the New Strategy for Immunotherapy. *Front Immunol* (2019) 10:1. doi: 10.3389/fimmu.2019.00001
130. Barone F, Nayar S, Campos J, Cloake T, Withers DR, Toellner K-M, et al. IL-22 Regulates Lymphoid Chemokine Production and Assembly of Tertiary Lymphoid Organs. *Proc Natl Acad Sci* (2015) 112:11024–9. doi: 10.1073/pnas.1503315112
131. Fleige H, Ravens S, Moschovakis GL, Bölter J, Willenzon S, Sutter G, et al. IL-17–Induced CXCL12 Recruits B Cells and Induces Follicle Formation in BALT in the Absence of Differentiated FDCs. *J Exp Med* (2014) 211:643–51. doi: 10.1084/jem.20131737
132. Dieu-Nosjean M-C, Goc J, Giraldo NA, Sautès-Fridman C, Fridman WH. Tertiary Lymphoid Structures in Cancer and Beyond. *Trends Immunol* (2014) 35:571–780. doi: 10.1016/j.it.2014.09.006
133. Engelhard VH, Rodriguez AB, Mauldin IS, Woods AN, Peske JD, Slingluff CL. Immune Cell Infiltration and Tertiary Lymphoid Structures as Determinants of Antitumor Immunity. *J Immunol* (2018) 200:432–42. doi: 10.4049/jimmunol.1701269
134. Sofopoulos M, Fortis SP, Vaxevanis CK, Sotiriadou NN, Arnogiannaki N, Ardavanis A, et al. The Prognostic Significance of Peritumoral Tertiary Lymphoid Structures in Breast Cancer. *Cancer Immunol Immunother* (2019) 68:1733–45. doi: 10.1007/s00262-019-02407-8
135. de Mingo Pulido Á., Gardner A, Hiebler S, Soliman H, Rugo HS, Krummel MF, et al. TIM-3 Regulates CD103+ Dendritic Cell Function and Response to Chemotherapy in Breast Cancer. *Cancer Cell* (2018) 33:60–74. doi: 10.1016/j.ccell.2017.11.019
136. Dixon KO, Tabaka M, Schramm MA, Xiao S, Tang R, Dionne D, et al. TIM-3 Restrains Anti-Tumour Immunity by Regulating Inflammasome Activation. *Nature* (2021) 595:101–6. doi: 10.1038/s41586-021-03626-9
137. Karyampudi L, Lamichhane P, Krempski J, Kalli KR, Behrens MD, Vargas DM, et al. PD-1 Blunts the Function of Ovarian Tumor–Infiltrating Dendritic Cells by Inactivating NF-κb. *Cancer Res* (2016) 76:239–50. doi: 10.1158/0008-5472.CAN-15-0748
138. Oh SA, Wu D-C, Cheung J, Navarro A, Xiong H, Cubas R, et al. PD-L1 Expression by Dendritic Cells Is a Key Regulator of T-Cell Immunity in Cancer. *Nat Cancer* (2020) 1:681–91. doi: 10.1038/s43018-020-0075-x
139. Ouaaz F, Arron J, Zheng Y, Choi Y, Beg AA. Dendritic Cell Development and Survival Require Distinct NF-κb Subunits. *Immunity* (2002) 16:257–70. doi: 10.1016/s1074-7613(02)00272-8
140. Peng Q, Qiu X, Zhang Z, Zhang S, Zhang Y, Liang Y, et al. PD-L1 on Dendritic Cells Attenuates T Cell Activation and Regulates Response to Immune Checkpoint Blockade. *Nat Commun* (2020) 11:1–8. doi: 10.1038/s41467-020-18570-x
141. Wang XB, Fan ZZ, Anton D, Vollenhoven A, Ni ZH, Chen XF, et al. CTLA4 Is Expressed on Mature Dendritic Cells Derived From Human Monocytes and Influences Their Maturation and Antigen Presentation. *BMC Immunol* (2011) 12:1–8. doi: 10.1186/1471-2172-12-1
142. Ruffell B, Chang-Strachan D, Chan V, Rosenbusch A, Ho CMT, Pryer N, et al. Macrophage IL-10 Blocks CD8+ T Cell-Dependent Responses to Chemotherapy by Suppressing IL-12 Expression in Intratumoral Dendritic Cells. *Cancer Cell* (2014) 26:623–37. doi: 10.1016/j.ccell.2014.09.006
143. Sánchez-Paulete AR, Cueto FJ, Martínez-López M, Labiano S, Morales-Kastresana A, Rodríguez-Ruiz ME, et al. Cancer Immunotherapy With Immunomodulatory Anti-CD137 and Anti–PD-1 Monoclonal Antibodies Requires BATF3-Dependent Dendritic Cells. *Cancer Discov* (2016) 6:71–9. doi: 10.1158/1538-7445.AM2016-4908
144. Bonavita E, Bromley CP, Jonsson G, Pelly VS, Sahoo S, Walwyn-Brown K, et al. Antagonistic Inflammatory Phenotypes Dictate Tumor Fate and Response to Immune Checkpoint Blockade. *Immunity* (2020) 53:1215–29. doi: 10.1016/j.immuni.2020.10.020
145. Grivennikov SI, Wang K, Mucida D, Stewart CA, Schnabl B, Jauch D, et al. Adenoma-Linked Barrier Defects and Microbial Products Drive IL-23/IL-17-Mediated Tumour Growth. *Nature* (2012) 491:254–8. doi: 10.1038/nature11465
146. Hu Z, Yang Y, Zhao Y, Huang Y. The Prognostic Value of Cyclooxygenase-2 Expression in Patients With Esophageal Cancer: Evidence From a Meta-Analysis. *OncoTargets Ther* (2017) 10:2893–901. doi: 10.2147/OTT.S134599
147. Shalapour S, Karin M. Pas De Deux: Control of Anti-Tumor Immunity by Cancer-Associated Inflammation. *Immunity* (2019) 51:15–26. doi: 10.1016/j.immuni.2019.06.021

148. Grasso CS, Tsoi J, Onyshchenko M, Abril-Rodriguez G, Ross-Macdonald P, Wind-Rotolo M, et al. Conserved Interferon-γ Signaling Drives Clinical Response to Immune Checkpoint Blockade Therapy in Melanoma. *Cancer Cell* (2020) 38:500–15. doi: 10.1016/j.ccell.2020.08.005
149. Pelly VS, Moeini A, Roelofsen LM, Bonavita E, Bell CR, Hutton C, et al. Anti-Inflammatory Drugs Remodel the Tumor Immune Environment to Enhance Immune Checkpoint Blockade Efficacy. *Cancer Discov* (2021) 11(10):2602–19. doi: 10.1158/2159-8290.CD-20-1815
150. Zelenay S, Reis e Sousa C. Reducing Prostaglandin E_2 Production to Raise Cancer Immunogenicity. *OncoImmunology* (2016) 5:1–3. doi: 10.1080/2162402X.2015.1123370
151. Zhang Y, Tighe S, Zhu Y-T. COX-2 Signaling in the Tumor Microenvironment. *Adv Exp Med Biol* (2020) 1277:87–104. doi: 10.1007/978-3-030-50224-9_6
152. Böttcher JP, Bonavita E, Chakravarty P, Blees H, Cabeza-Cabrerizo M, Sammicheli S, et al. NK Cells Stimulate Recruitment of Cdc1 Into the Tumor Microenvironment Promoting Cancer Immune Control. *Cell* (2018) 172:1022–37. doi: 10.1016/j.cell.2018.01.004
153. Wang D, DuBois RN. The Role of COX-2 in Intestinal Inflammation and Colorectal Cancer. *Oncogene* (2010) 29:781–8. doi: 10.1038/onc.2009.421
154. Zhu Y, Shi C, Zeng L, Liu G, Jiang W, Zhang X, et al. High COX-2 Expression in Cancer-Associated Fibiroblasts Contributes to Poor Survival and Promotes Migration and Invasiveness in Nasopharyngeal Carcinoma. *Mol Carcinogenesis* (2020) 59:265–80. doi: 10.1002/mc.23150
155. Obermajer N, Muthuswamy R, Odunsi K, Edwards RP, Kalinski P. PGE_2-Induced CXCL12 Production and CXCR4 Expression Controls the Accumulation of Human MDSCs in Ovarian Cancer Environment. *Cancer Res* (2011) 71:7463–70. doi: 10.1158/0008-5472.CAN-11-2449
156. Baratelli FE, Heuzé-Vourc'h N, Krysan K, Dohadwala M, Riedl K, Sharma S, et al. Prostaglandin E_2-Dependent Enhancement of Tissue Inhibitors of Metalloproteinases-1 Production Limits Dendritic Cell Migration Through Extracellular Matrix. *J Immunol* (2004) 173:5458–66. doi: 10.4049/jimmunol.173.9.5458
157. Legler DF, Krause P, Scandella E, Singer E, Groettrup M. Prostaglandin E2 Is Generally Required for Human Dendritic Cell Migration and Exerts Its Effect *via* EP2 and EP4 Receptors. *J Immunol* (2006) 176:966–73. doi: 10.4049/jimmunol.176.2.966
158. Yen J-H, Khayrullina T, Ganea D. PGE2-Induced Metalloproteinase-9 is Essential for Dendritic Cell Migration. *Blood* (2008) 111:260–70. doi: 10.1182/blood-2007-05-090613
159. Canton J, Blees H, Henry CM, Buck MD, Schulz O, Rogers NC, et al. The Receptor DNGR-1 Signals for Phagosomal Rupture to Promote Cross-Presentation of Dead-Cell-Associated Antigens. *Nat Immunol* (2021) 22:140–53. doi: 10.1038/s41590-020-00824-x
160. Giampazolias E, Schulz O, Lim KHJ, Rogers NC, Chakravarty P, Srinivasan N, et al. Secreted Gelsolin Inhibits DNGR-1-Dependent Cross-Presentation and Cancer Immunity. *Cell* (2021) 184:4016–31. doi: 10.1016/j.cell.2021.05.021
161. Sancho D, Joffre OP, Keller AM, Rogers NC, Martínez D, Hernanz-Falcón P, et al. Identification of a Dendritic Cell Receptor That Couples Sensing of Necrosis to Immunity. *Nature* (2009) 458:899–903. doi: 10.1038/nature07750
162. Hsu FJ, Benike C, Fagnoni F, Liles TM, Czerwinski D, Taidi B, et al. Vaccination of Patients With B–cell Lymphoma Using Autologous Antigen–Pulsed Dendritic Cells. *Nat Med* (1996) 2:52–8. doi: 10.1038/nm0196-52
163. León B, López-Bravo M, Ardavín C. Monocyte-Derived Dendritic Cells Formed at the Infection Site Control the Induction of Protective T Helper 1 Responses Against Leishmania. *Immunity* (2007) 26:519–31. 10.1016/j.immuni.2007.01.017
164. Palucka AK, Ueno H, Connolly J, Kerneis-Norvell F, Blanck J-P, Johnston DA, et al. Dendritic Cells Loaded With Killed Allogeneic Melanoma Cells can Induce Objective Clinical Responses and MART-1 Specific CD8+ T-Cell Immunity. *J Immunother* (2006) 29:545–57. doi: 10.1097/01.cji.0000211309.90621.8b
165. Dranoff G, Jaffee E, Lazenby A, Golumbek P, Levitsky H, Brose K, et al. Vaccination With Irradiated Tumor Cells Engineered to Secrete Murine Granulocyte-Macrophage Colony-Stimulating Factor Stimulates Potent, Specific, and Long-Lasting Anti-Tumor Immunity. *Proc Natl Acad Sci* (1993) 90:3539–43. doi: 10.1073/pnas.90.8.3539
166. Mach N, Dranoff G. Cytokine-Secreting Tumor Cell Vaccines. *Curr Opin Immunol* (2000) 12:571–5. doi: 10.1016/S0952-7915(00)00144-8
167. Bhardwaj N, Friedlander PA, Pavlick AC, Ernstoff MS, Gastman BR, Hanks BA, et al. Flt3 Ligand Augments Immune Responses to Anti-DEC-205-NY-ESO-1 Vaccine Through Expansion of Dendritic Cell Subsets. *Nat Cancer* (2020) 1:1204–17. doi: 10.1038/s43018-020-00143-y
168. Hammerich L, Marron TU, Upadhyay R, Svensson-Arvelund J, Dhainaut M, Hussein S, et al. Systemic Clinical Tumor Regressions and Potentiation of PD1 Blockade With *in Situ* Vaccination. *Nat Med* (2019) 25:814–24. doi: 10.1038/s41591-019-0410-x
169. Lai J, Mardiana S, House IG, Sek K, Henderson MA, Giuffrida L, et al. Adoptive Cellular Therapy With T Cells Expressing the Dendritic Cell Growth Factor Flt3L Drives Epitope Spreading and Antitumor Immunity. *Nat Immunol* (2020) 21:914–26. doi: 10.1038/s41590-020-0676-7
170. Salmon H, Idoyaga J, Rahman A, Leboeuf M, Remark R, Jordan S, et al. Expansion and Activation of CD103 + Dendritic Cell Progenitors at the Tumor Site Enhances Tumor Responses to Therapeutic PD-L1 and BRAF Inhibition. *Immunity* (2016) 44:924–38. doi: 10.1016/j.immuni.2016.03.012
171. Hou J, Karin M, Sun B. Targeting Cancer-Promoting Inflammation — Have Anti-Inflammatory Therapies Come of Age? *Nat Rev Clin Oncol* (2021) 18:261–79. doi: 10.1038/s41571-020-00459-9
172. Ritter B, Greten FR. Modulating Inflammation for Cancer Therapy. *J Exp Med* (2019) 216. doi: 10.1084/jem.20181739
173. Zappavigna S, Cossu AM, Grimaldi A, Bocchetti M, Ferraro GA, Nicoletti GF, et al. Anti-Inflammatory Drugs as Anticancer Agents. *Int J Mol Sci* (2020) 21:1–29. doi: 10.3390/ijms21072605
174. Chen X, Song E. Turning Foes to Friends: Targeting Cancer-Associated Fibroblasts. *Nat Rev Drug Discov* (2019) 18:99–115. doi: 10.1038/s41573-018-0004-1
175. Kobayashi H, Enomoto A, Woods SL, Burt AD, Takahashi M, Worthley DL. Cancer-Associated Fibroblasts in Gastrointestinal Cancer. *Nat Rev Gastroenterol Hepatol* (2019) 16:282–95. doi: 10.1038/s41575-019-0115-0
176. Liu T, Han C, Wang S, Fang P, Ma Z, Xu L, et al. Cancer-Associated Fibroblasts: An Emerging Target of Anti-Cancer Immunotherapy. *J Hematol Oncol* (2019). doi: 10.1186/s13045-019-0770-1
177. Ziani L, Chouaib S, Thiery J. Alteration of the Antitumor Immune Response by Cancer-Associated Fibroblasts. *Front Immunol* (2018) 9:414. doi: 10.3389/fimmu.2018.00414
178. Wang J-B, Huang X, Li F-R. Impaired Dendritic Cell Functions in Lung Cancer: A Review of Recent Advances and Future Perspectives. *Cancer Commun* (2019) 39(1):43. doi: 10.1186/s40880-019-0387-3
179. Wculek SK, Cueto FJ, Mujal AM, Melero I, Krummel MF, Sancho D. Dendritic Cells in Cancer Immunology and Immunotherapy. *Nat Rev Immunol* (2020) 20(1):7–24. doi: 10.1038/s41577-019-0210-z
180. Martín-Fontecha A, Sebastiani S, Höpken UE, Uguccioni M, Lipp M, Lanzavecchia A, et al. Regulation of Dendritic Cell Migration to the Draining Lymph Node. *J Exp Med* (2003) 198:615–21. doi: 10.1084/jem.20030448
181. Perez CR, de Palma M. Engineering Dendritic Cell Vaccines to Improve Cancer Immunotherapy. *Nat Commun* (2019) 10:1–10. doi: 10.1038/s41467-019-13368-y
182. Ramanjulu JM, Pesiridis GS, Yang J, Concha N, Singhaus R, Zhang S-Y, et al. Design of Amidobenzimidazole STING Receptor Agonists With Systemic Activity. *Nature* (2018) 564:439–43. doi: 10.1038/s41586-018-0705-y
183. Ganesan A-P, Clarke J, Wood O, Garrido-Martin EM, Chee SJ, Mellows T, et al. Tissue-Resident Memory Features Are Linked to the Magnitude of Cytotoxic T Cell Responses in Human Lung Cancer. *Nat Immunol* (2017) 18:940–50. doi: 10.1038/ni.3775
184. Malik BT, Byrne KT, Vella JL, Zhang P, Shabaneh TB, Steinberg SM, et al. Resident Memory T Cells in the Skin Mediate Durable Immunity to Melanoma. *Sci Immunol* (2017) 2.:1–24 doi: 10.1126/sciimmunol.aam6346
185. Park SL, Buzzai A, Rautela J, Hor JL, Hochheiser K, Effern M, et al. Tissue-Resident Memory CD8+ T Cells Promote Melanoma–Immune

Equilibrium in Skin. *Nature* (2019) 565:366–71. doi: 10.1038/s41586-018-0812-9

186. Savas P, Virassamy B, Ye C, Salim A, Mintoff CP, Caramia F, et al. Single-Cell Profiling of Breast Cancer T Cells Reveals a Tissue-Resident Memory Subset Associated With Improved Prognosis. *Nat Med* (2018) 24:986–93. doi: 10.1038/s41591-018-0078-7
187. Schenkel JM, Fraser KA, Beura LK, Pauken KE, Vezys V, Masopust D. Resident Memory CD8 T Cells Trigger Protective Innate and Adaptive Immune Responses. *Science* (2014) 346:98–101. doi: 10.1126/science.1254536
188. Edwards J, Wilmott JS, Madore J, Gide TN, Quek C, Tasker A, et al. CD103 $^{+}$ Tumor-Resident CD8 $^{+}$ T Cells Are Associated With Improved Survival in Immunotherapy-Naïve Melanoma Patients and Expand Significantly During Anti–PD-1 Treatment. *Clin Cancer Res* (2018) 24:3036–45. doi: 10.1158/1078-0432.CCR-17-2257
189. León-Letelier RA, Castro-Medina DI, Badillo-Godinez O, Tepale-Segura A, Huanosta-Murillo E, Aguilar-Flores C, et al. Induction of Progenitor Exhausted Tissue-Resident Memory CD8+ T Cells Upon Salmonella Typhi Porins Adjuvant Immunization Correlates With Melanoma Control and Anti-PD-1 Immunotherapy Cooperation. *Front Immunol* (2020) 11:583382. doi: 10.3389/fimmu.2020.583382
190. Sautès-Fridman C, Petitprez F, Calderaro J, Fridman WH. Tertiary Lymphoid Structures in the Era of Cancer Immunotherapy. *Nat Rev Cancer* (2019) 19:1–21. doi: 10.1038/s41568-019-0144-6

Conflict of Interest: The authors declare that the research was conducted in the absence of any commercial or financial relationships that could be construed as a potential conflict of interest.

Publisher's Note: All claims expressed in this article are solely those of the authors and do not necessarily represent those of their affiliated organizations, or those of the publisher, the editors and the reviewers. Any product that may be evaluated in this article, or claim that may be made by its manufacturer, is not guaranteed or endorsed by the publisher.

Advantages of publishing in Frontiers

OPEN ACCESS
Articles are free to read for greatest visibility and readership

FAST PUBLICATION
Around 90 days from submission to decision

HIGH QUALITY PEER-REVIEW
Rigorous, collaborative, and constructive peer-review

TRANSPARENT PEER-REVIEW
Editors and reviewers acknowledged by name on published articles

Frontiers
Avenue du Tribunal-Fédéral 34
1005 Lausanne | Switzerland

Visit us: www.frontiersin.org
Contact us: frontiersin.org/about/contact

REPRODUCIBILITY OF RESEARCH
Support open data and methods to enhance research reproducibility

DIGITAL PUBLISHING
Articles designed for optimal readership across devices

FOLLOW US
@frontiersin

IMPACT METRICS
Advanced article metrics track visibility across digital media

EXTENSIVE PROMOTION
Marketing and promotion of impactful research

LOOP RESEARCH NETWORK
Our network increases your article's readership